THE UNIVERSITY OF ALBERTA

Design of Shallow Tunnels in Soft Ground

by

Arsenio Negro Jr.

VOLUME III

A THESIS

SUBMITTED TO THE FACULTY OF GRADUATE STUDIES AND RESEARCH

IN PARTIAL FULFILMENT OF THE REQUIREMENTS FOR THE DEGREE

OF Doctor of Philosophy

Department of Civil Engineering

EDMONTON, ALBERTA

SPRING 1988

THE UNIVERSITY OF ALBERTA

Design of Shallow Tunnels in Soft Ground

by

Arsenio Negro Jr.

VOLUME III

A THESIS

SUBMITTED TO THE FACULTY OF GRADUATE STUDIES AND RESEARCH

IN PARTIAL FULFILMENT OF THE REQUIREMENTS FOR THE DEGREE

OF Doctor of Philosophy

Department of Civil Engineering

EDMONTON, ALBERTA

SPRING 1988

closer to F respectively. As the stresses at the opening decrease, the non-linearity of the ground response becomes more pronounced.

Figures 6.48 and 6.49 show that the normalized ground displacements in this case, are not affected much by the amount of stress release. It is noted, however, that the ratio of maximum surface settlement to crown settlement increases slightly (up to 10%) as the stress release is increased (up to 70%). Figure 6.49 also shows that the point of maximum surficial distortion (at about 1.6D off the axis) does not change location with increasing stress release but that the normalized distortion increases slightly.

The last two figures illustrate the format in which all results of the analyses are presented in Appendix C.

Influence of the Tunnel Depth

Figures 6.50 to 6.53 show results of three analyses where the undrained strength ratio $c_u/\gamma D$, was kept constant and equal to 1.25 and the tunnel cover to diameter ratio varied from 1.5 to 6. The NGRC for the crown of a deeper tunnel presents a slightly 'stiffer' response at the early stage of stress release with associated smaller displacements, when compared with a shallower tunnel. This reflects the influence of the proximity of the ground surface, which is also apparent in the springline NGRC, but not at the floor. As the amount of stress release increases the NGRCs become more non-linear. This effect is more pronounced as the tunnel gets deeper. Indeed, ground

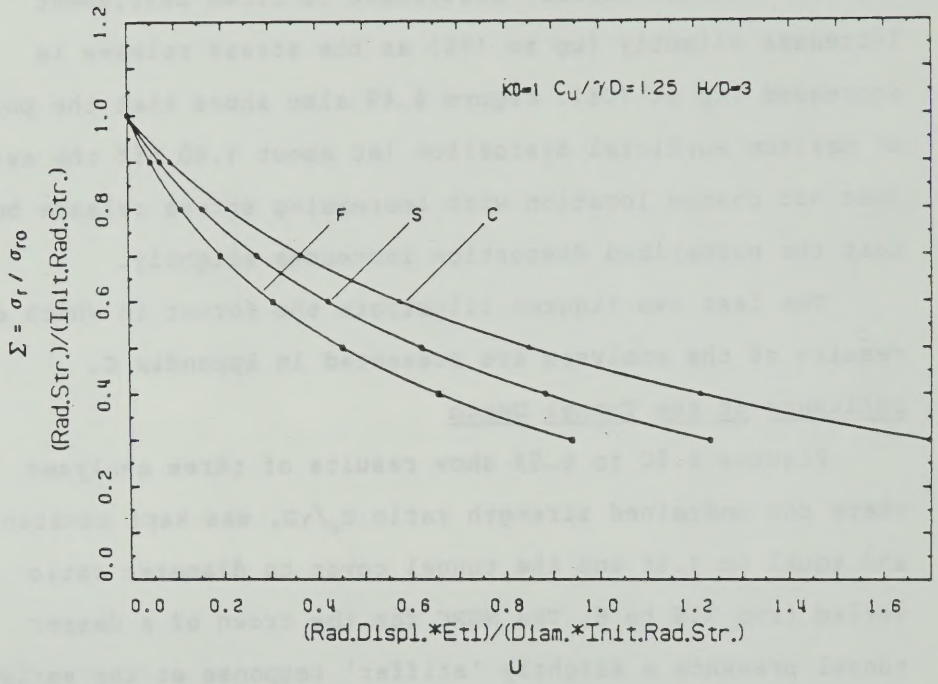

Figure 6.47 Normalized Ground Reaction Curves for H/D=3 and an Undrained Strength Ratio of 1.25

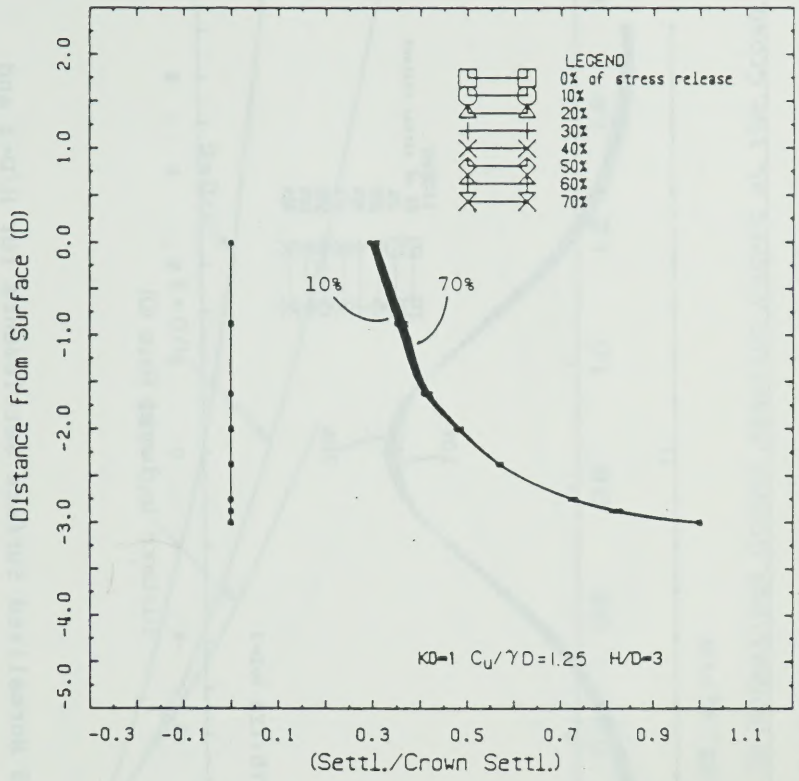

Figure 6.48 Normalized Subsurface Settlements along Tunnel Axis for H/D=3 and an Undrained Strength Ratio of 1.25, Calculated for Increasing Amount of Stress Release

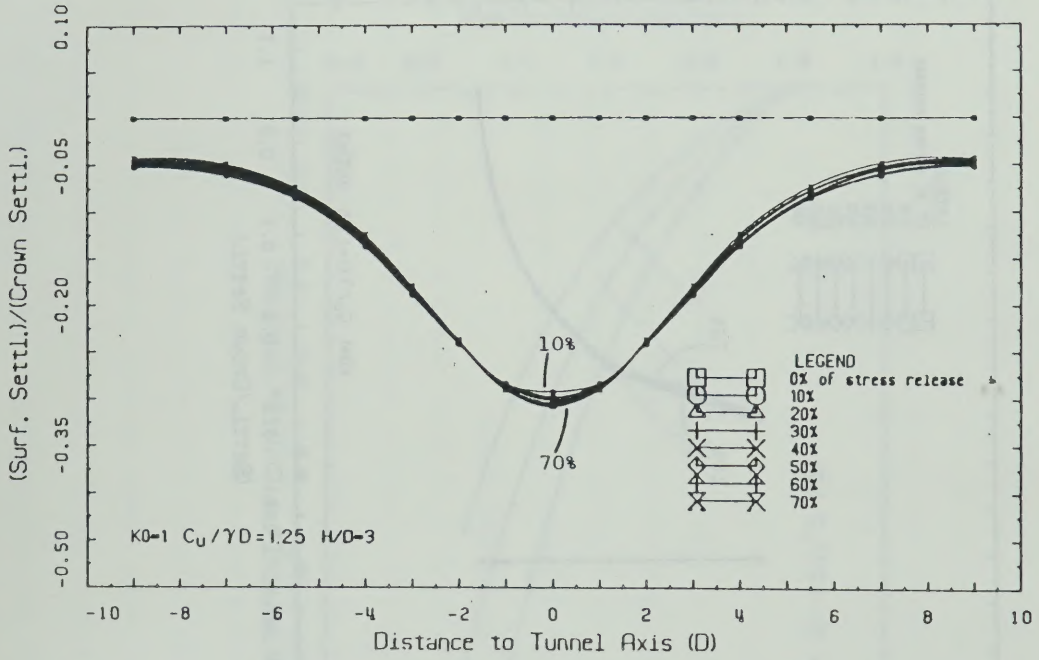

Figure 6.49 Normalized Surface Settlements for H/D=3 and Undrained Strength Ratio of 1.25, Calculated for Increasing Amount of Stress Release

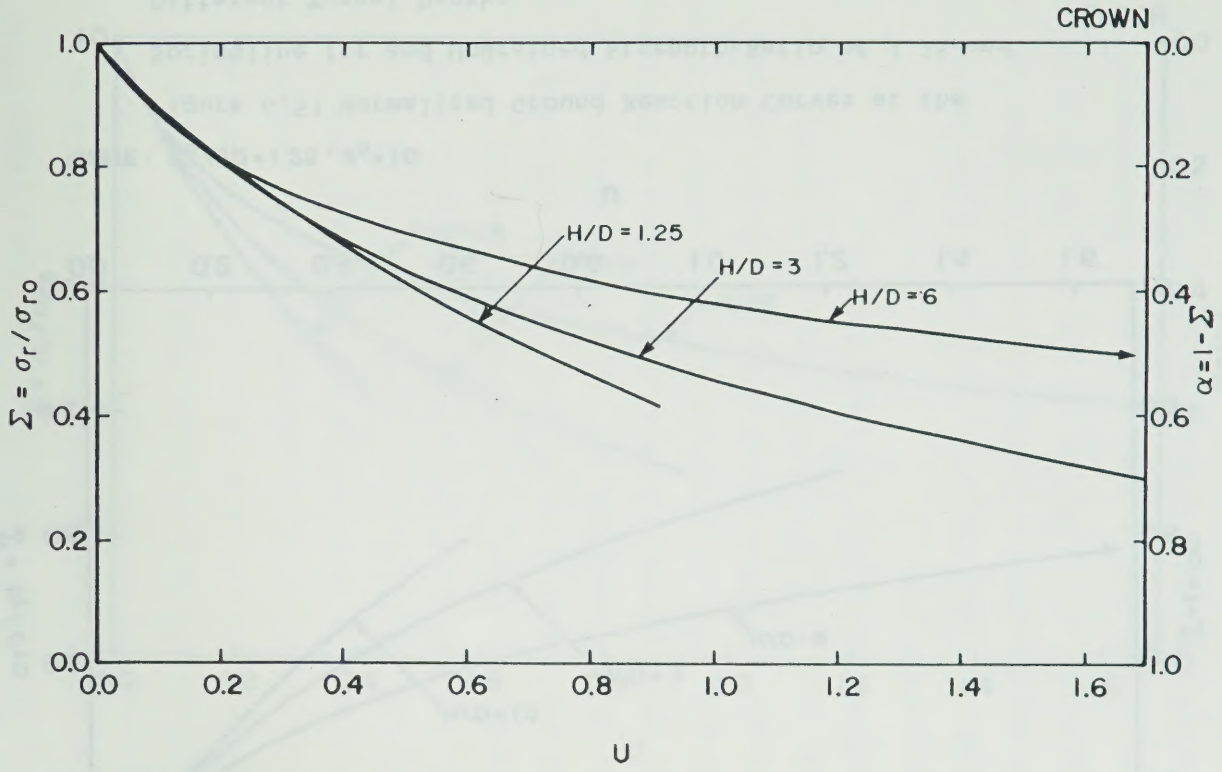

NOTE: $C_u/\gamma D = 1.25$, $K_o = 1.0$

Figure 6.50 Normalized Ground Reaction Curves at the Crown for an Undrained Strength Ratio of 1.25 and Different Tunnel Depths

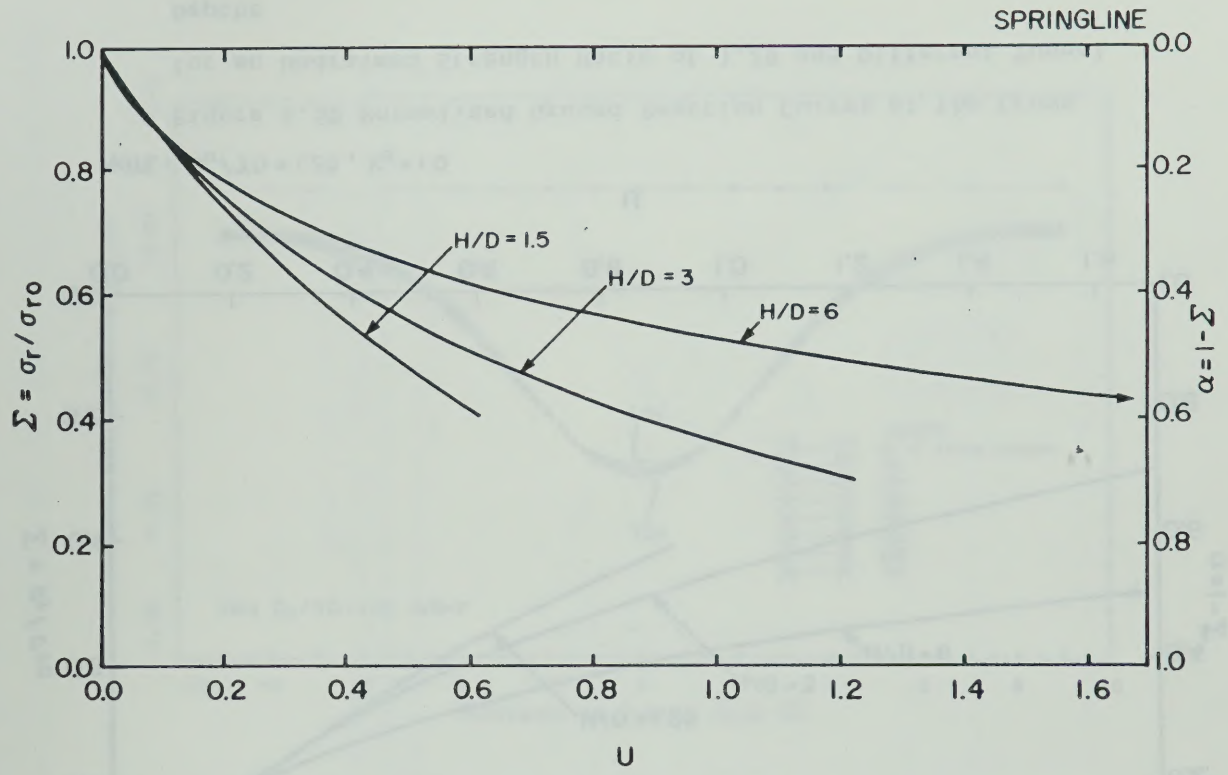

NOTE : $C_u/\gamma D = 1.25$, $K_o = 1.0$

Figure 6.51 Normalized Ground Reaction Curves at the Springline for and Undrained Strength Ratio of 1.25 and Different Tunnel Depths

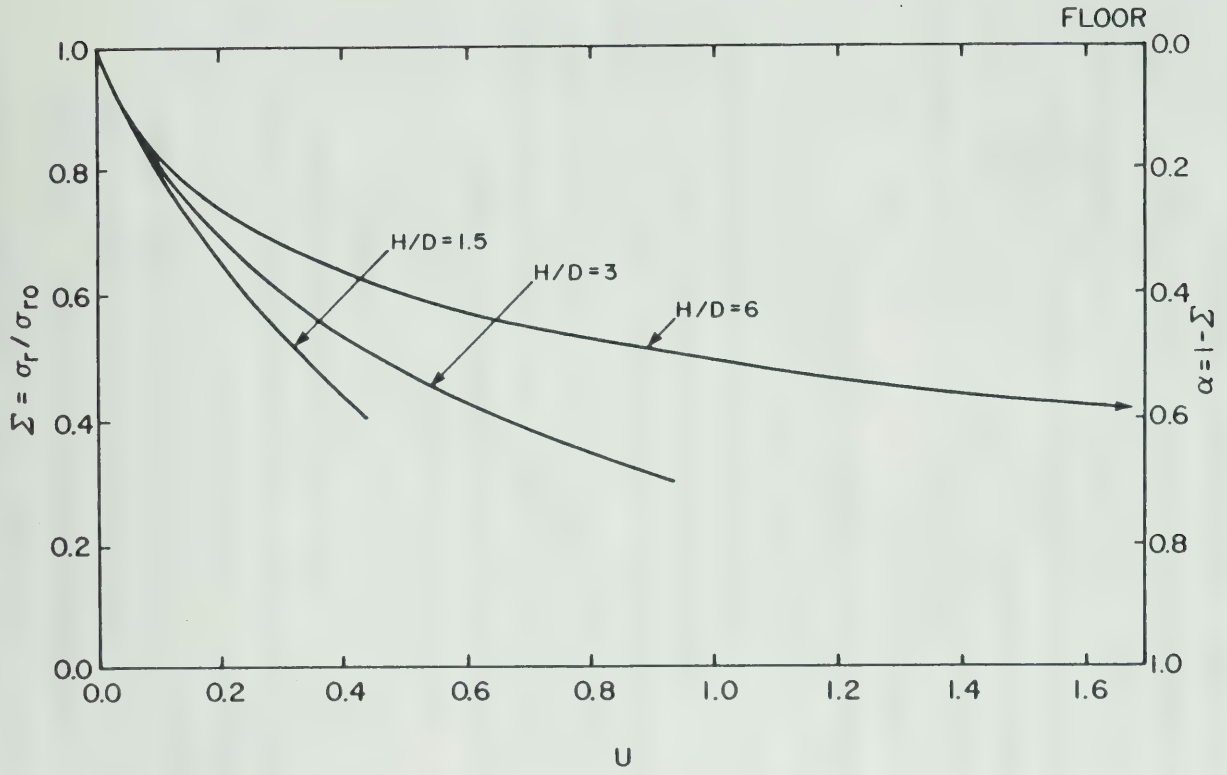

NOTE: $C_u/\gamma D = 1.25$, $K_o = 1.0$

Figure 6.52 Normalized Ground Reaction Curves at the Floor for an Undrained Strength Ratio of 1.25 and Different Tunnel Depths

collapse is approached more rapidly as H/D increases, with the soil undrained strength kept constant.

With respect to the normalized settlements, one notes in Figure 6.53 that the thicker soil cover permits a more rapid attenuation of the ground movements. This leads to the smaller maximum normalized settlement at the surface and the smaller normalized maximum distortion for a given amount of stress release.

Influence of the Undrained Strength Ratio

Figures 6.54 to 6.57 show the results of three analyses, where the relative depth of the tunnel was kept constant (H/D=3) and the undrained strength ratio $c_u/\gamma D$ was varied from 0.625 to 2.5. Clearly as the strength decreases, the larger the displacements are for a given radial stress ratio. A special feature is also apparent in Figures 6.54 to 6.56: the NGRCs for different strengths are nearly homothetic. The centre of similitude of these curves is their origin (σ_r/σ_{ro}=1 and U=0). The coordinates of homothetic points on these curves are defined by the intersections of the latter with arbitrary axes through the centre of similitude (shown by dashed lines). It will be shown in Section 6.4 that if these points were used as reference values and if each curve is transformed into another with coordinates normalized to their respective reference values, then these normalized curves almost coincide. Single curves for each point of the tunnel contour can thus be formulated, regardless of the value of the

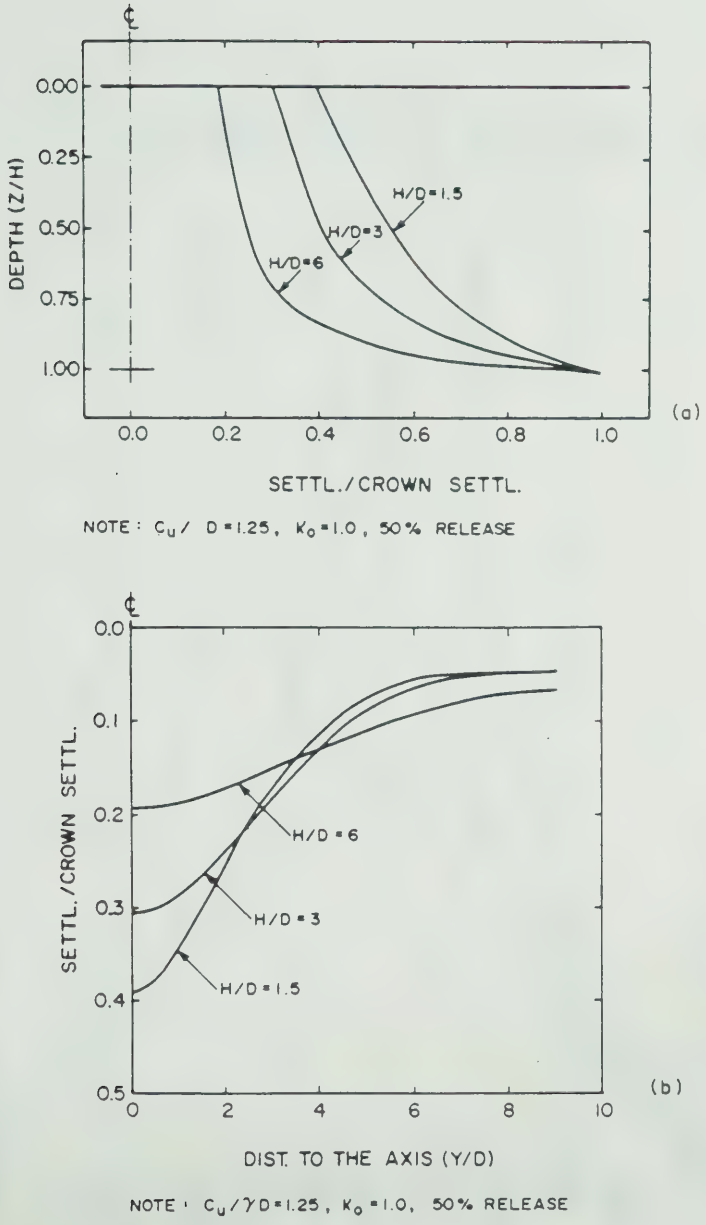

Figure 6.53 Normalized Subsurface and Surface Settlement for an Undrained Strength Ratio of 1.25 and 50% Ground Stress Release, Calculated for Different Tunnel Depths

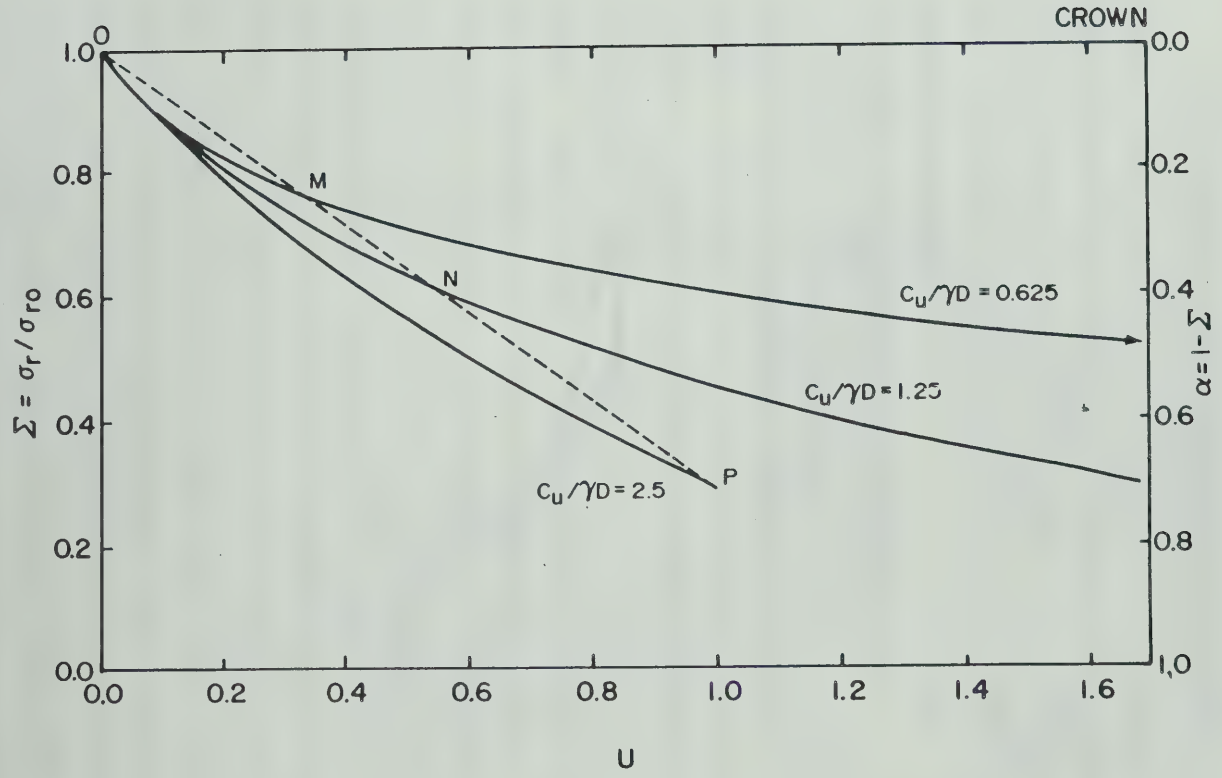

NOTE: $H/D = 3$, $K_o = 1.0$

Figure 6.54 Normalized Ground Reaction Curves of the Crown for H/D=3 and Different Undrained Strength Ratios

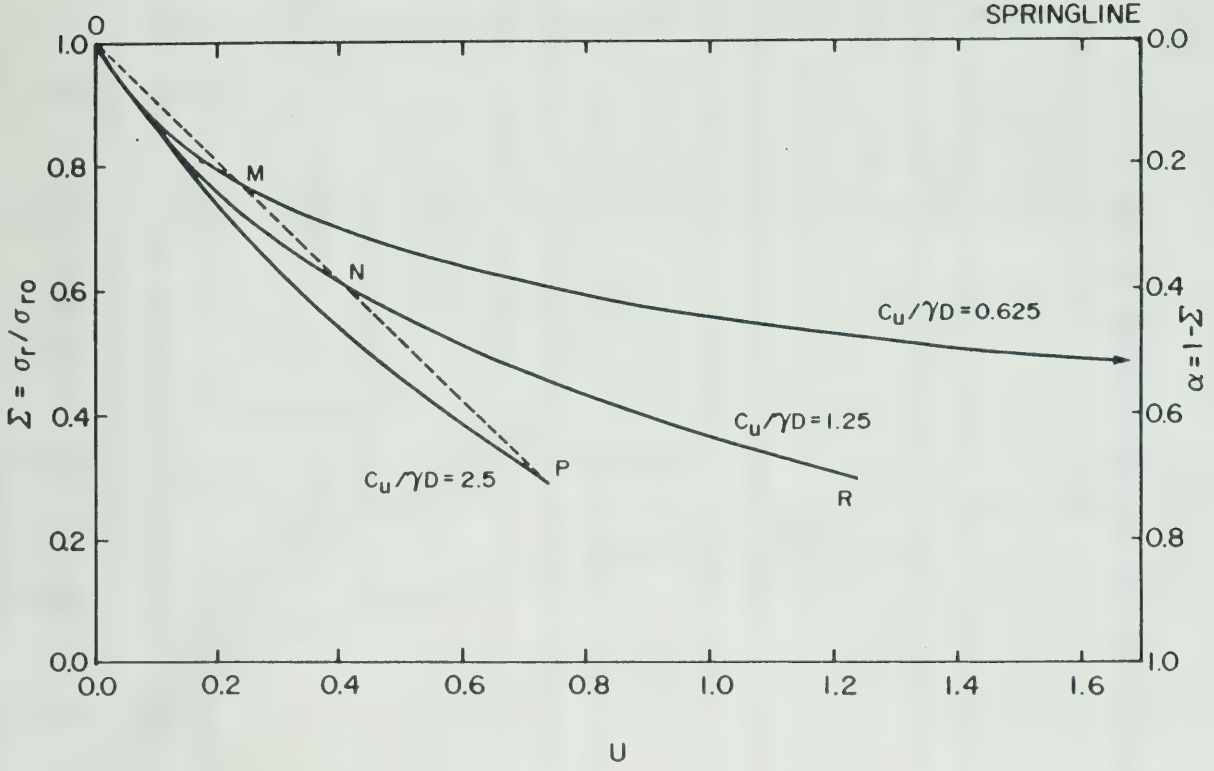

NOTE: $H/D = 3$, $K_o = 1.0$

Figure 6.55 Normalized Ground Reaction Curves of the Springline for H/D=3 and Different Undrained Strength Ratios

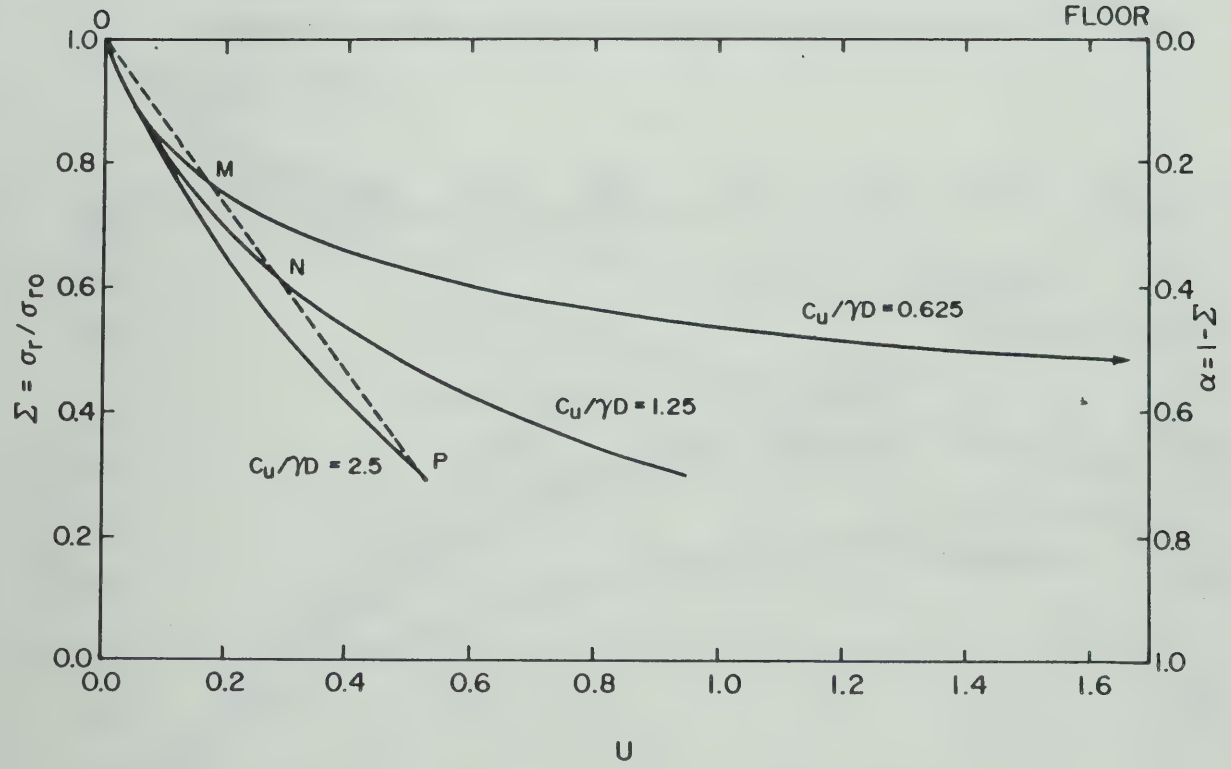

NOTE: $H/D = 3$, $K_o = 1.0$

Figure 6.56 Normalized Ground Reaction Curves of the Floor for H/D=3 and Different Undrained Strength Ratios

undrained strength ratio. This finding will give more generality to the projected solution as will be discussed later.

Figures 6.57(a) and (b) present the distributions of normalized ground settlements at the surface and subsurface for an equal amount of stress release of 50%. As the ground strengths are different in each case, for a fixed radial stress ratio (σ_r/σ_{ro}) the factor of safety against collapse increases as the strength increases. In other words, for the 50% release, the case with lower value of $c_u/\gamma D$ will be closer to collapse (but with an FS greater than unity). Despite this, the distributions of normalized subsurface settlements almost coincide, as shown in Figure 6.57(a). The distributions of surface settlements are also very close to each other. It is apparent, however, that the weaker the soil is (thus, the lower the factor of safety is), the larger the normalized surface distortion is, as expected.

6.3.2.2 Cohesionless Soil Model Results

Effect of the Amount of Stress Release

Figures 6.58 to 6.60 present typical results for a cohesionless soil with $\phi=30°$, $K_o=0.8$ and $H/D=3$. The "stiffness" of the ground can be measured by the derivative of the NGRC. At the springline (Figure 6.58), one notes that the ground softens progressively, as the stress release increases. At the crown and floor, however, during the initial stages of stress reduction, the ground seems to stiffen slightly but below a certain radial stress ratio,

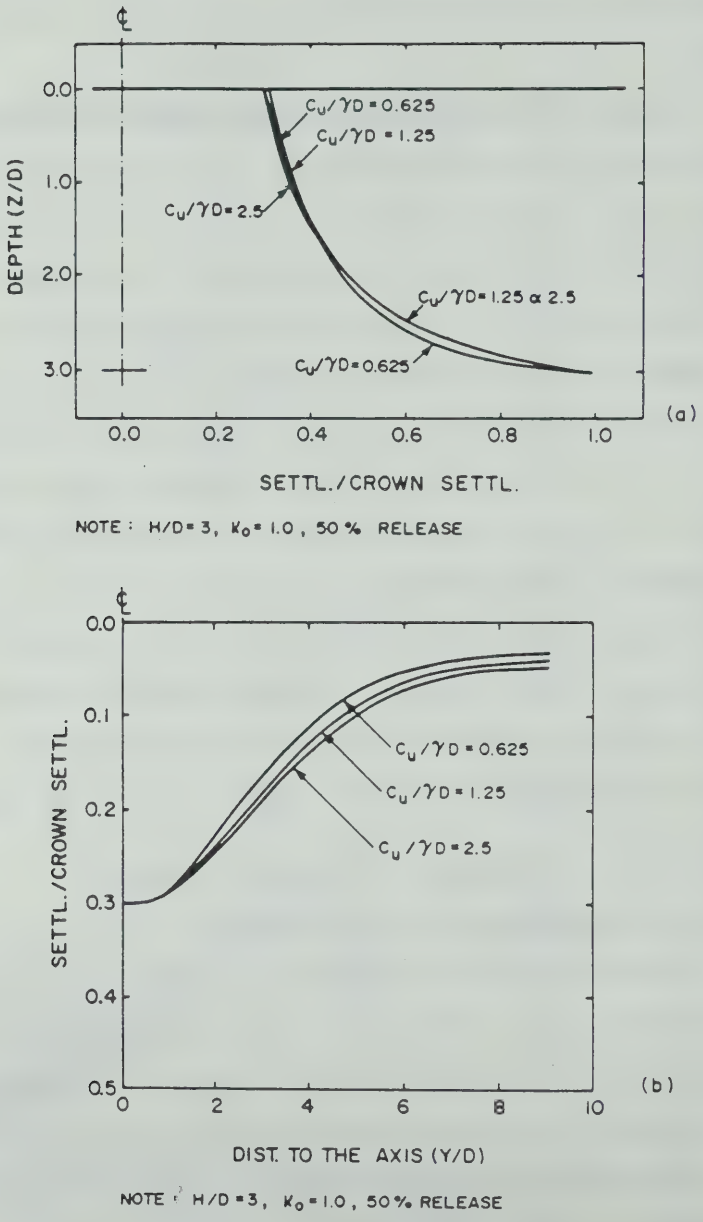

Figure 6.57 Normalized Subsurface and Surface Settlements for H/D=3 and 50% Ground Stress Release, Calculated for Different Undrained Strength Ratios

the response is also that of softening for increasing stress release. That initial stiffening response, was not observed for the frictionless soil, where K_o was set equal to unity. When K_o is less than unity, the ground at the crown or floor initially experiences an increase in the minor principal stress (in the horizontal direction), which leads to an increase in the tangent modulus and thus a stiffer response. After the principal stress directions reverse so that the radial stress becomes the minor principal stress, a progressive softening is also noted at crown and floor.

The distribution of normalized subsurface settlements for the cohesionless soil model seems to be more affected by the amount of stress release, than for the frictionless model. As indicated in Figure 6.59, as the amount of stress release increases, larger normalized settlements are observed. The same effect is noted for the normalized surface settlements, in Figure 6.60, when it is also seen that larger normalized surface distortions are observed for increasing stress reductions.

Influence of the Tunnel Depth

Figures 6.61 and 6.62 present results of analyses for K_o=0.8 and ϕ=30°, carried out for three tunnel depths. As it is noted, the NGRC for the tunnel crown is more sensitive to the relative depth than are the other points of the tunnel contour. In fact, the curves at springline and floor almost coincide. Moreover, as the tunnel gets deeper, the effect of the proximity of the ground surface on the NGRCs of the

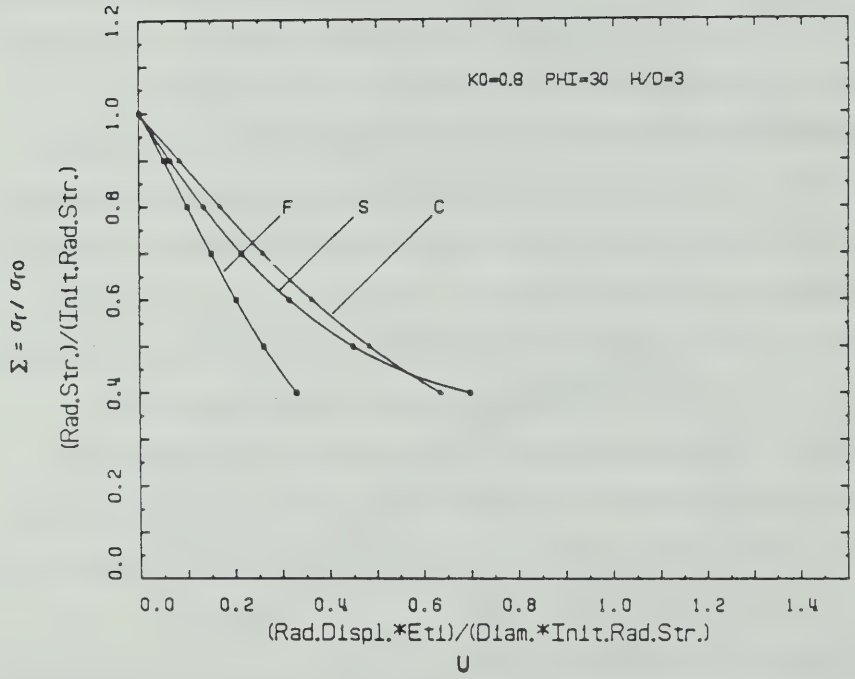

Figure 6.58 Normalized Ground Reaction Curves for H/D=3, K_o=0.8 and ϕ=30°

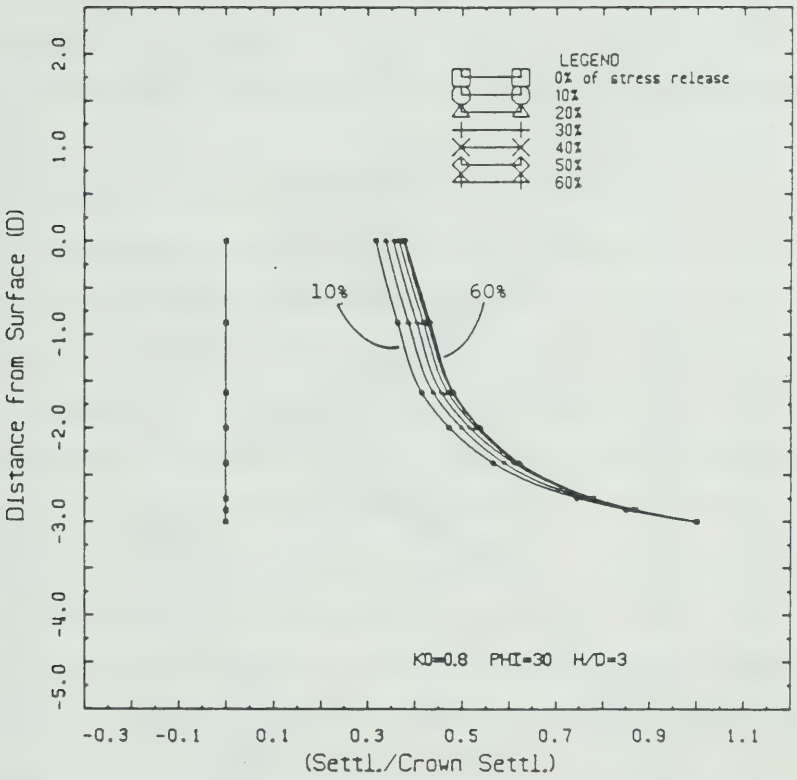

Figure 6.59 Normalized Subsurface Settlements for H/D=3, K_o=0.8 and ϕ=30°, Calculated for Increasing Amount of Stress Release

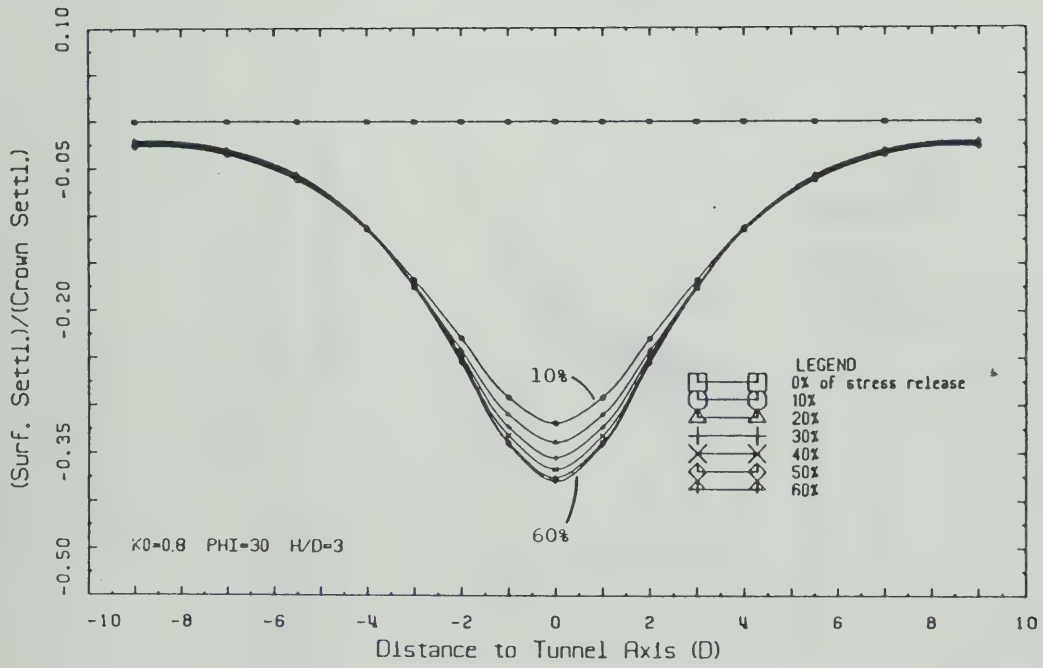

Figure 6.60 Normalized Surface Settlements for H/D=3, K_o=0.8 and ϕ=30°, Calculated for Increasing Amount of Stress Release

crown is reduced and these curves move down and get closer together. This is exactly opposite to the trend noted in the frictionless soil model in which the soil strength was kept constant. In this cohesionless counterpart, the the shear strength increases as the tunnel gets deeper and this explains the noted behaviour. As would be expected when the tunnel gets deeper, the normalized subsurface settlements become smaller as indicated in Figure 6.62(a). These settlements are plotted against the depth ratio z/H (solid lines) and against the depth ratio z/D (dashed curves). The effect of settlement attentuation in the soil cover is perhaps better appreciated through the latter plots. Figure 6.62(b) shows that as the tunnel gets deeper, the normalized surface distortions decrease and the settlement trough gets wider. Recall that the settlements shown in Figure 6.62 correspond to a stress reduction of 50%. Since the friction angle is the same in all cases, the ground strength is higher for deeper tunnels. Thus, for equal stress reduction, the factors of safety are not the same in each case, and are smaller for the shallower tunnel case.

Influence of the Friction Angle

Figures 6.63 to 6.66 present the results of analyses where H/D=3, K_o=0.8 and three values for friction angles were considered (ϕ=20°, 30° and 40°). A stronger non-linear response is noted in the NGRC of the tunnel springline, reflecting that the soil at this point approaches failure earlier than elsewhere around the tunnel. This is consistent

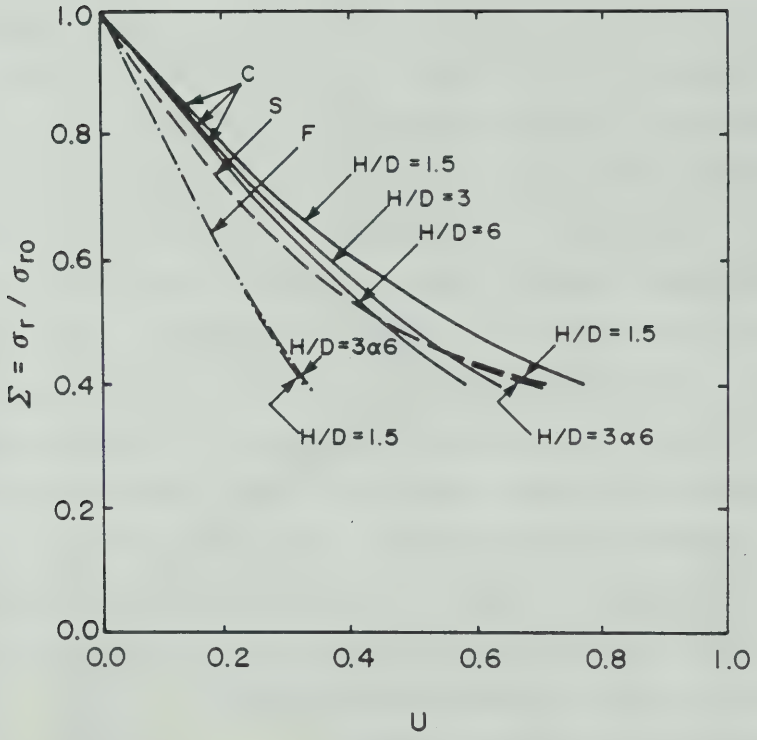

NOTES ;
1. $\phi = 30°$, $K_o = 0.8$
2. C = CROWN , S = SPRINGLINE , F = FLOOR

Figure 6.61 Normalized Ground Reaction Curves for Different Tunnel Depths, Calculated for $\phi=30°$ and $K_o=0.8$

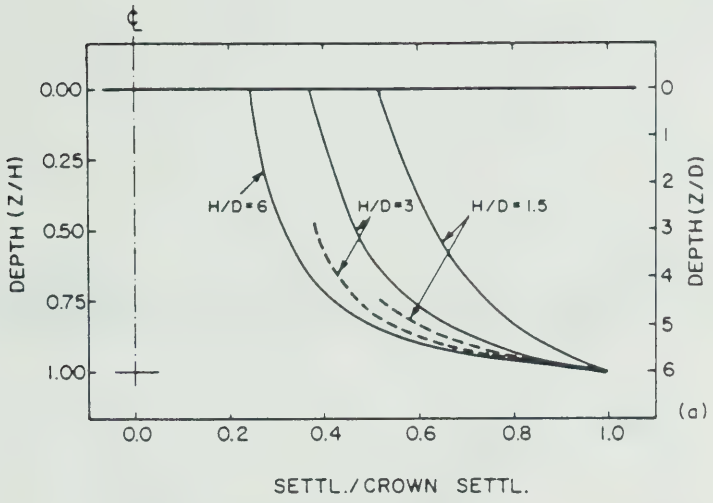

NOTE : $\phi = 30°$, $K_o = 0.8$, 50% RELEASE

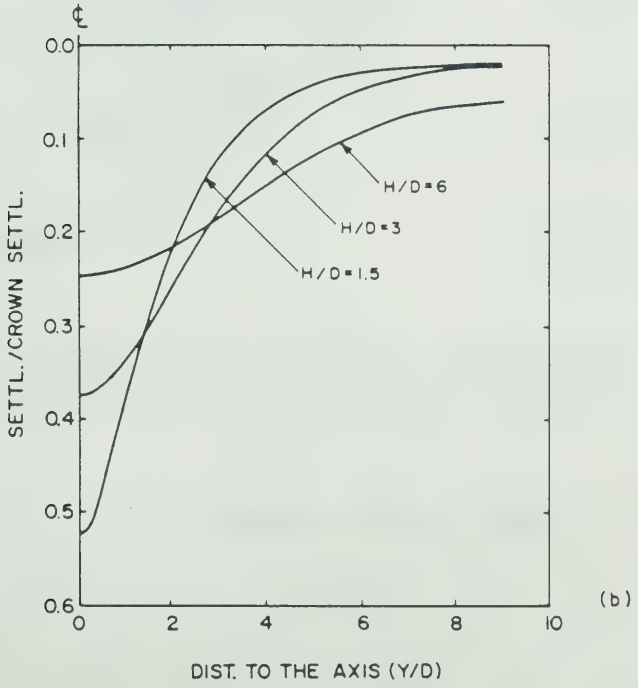

NOTE $\phi = 30°$, $K_o = 0.8$, 50% RELEASE

Figure 6.62 Normalized Subsurface and Surface Settlements for Different Tunnel Depths, Calculated for $\phi=30°$, $K_o=0.8$ and 50% Stress Release

with the selected K_o value which is smaller than unity.

The NGRCs for different friction angles shown in Figures 6.63 to 6.65 were also found to be nearly homothetic, with the centre of similitude at their origin (Σ=1 and U=0). The coordinates of homothetic points on these curves are defined by the intersection of the latter with arbitrary axes through the centre of similitude. It is shown in Section 6.4 that if these points were used as reference values and if each curve is transformed into another with coordinates normalized to their respective reference values, then these normalized curves almost coincide. Single curves for each point of the tunnel contour can thus be formulated independently of the friction angle. This finding will give more generality to the projected solution.

Figure 6.66 presents the distribution of normalized ground settlements at the surface and subsurface, for a stress release of 40%. The noted differences in the settlement distributions can be partly attributed to the differences in shear straining in each case. As the amount of stress release is the same, but the strengths are different, the factor of safety against collapse in each case is different. Correspondingly, the displacement fields should differ. Higher normalized surface distortions are found for decreasing ϕ but the width of the surface settlement trough does not change much.

Influence of the In Situ Stress Ratio

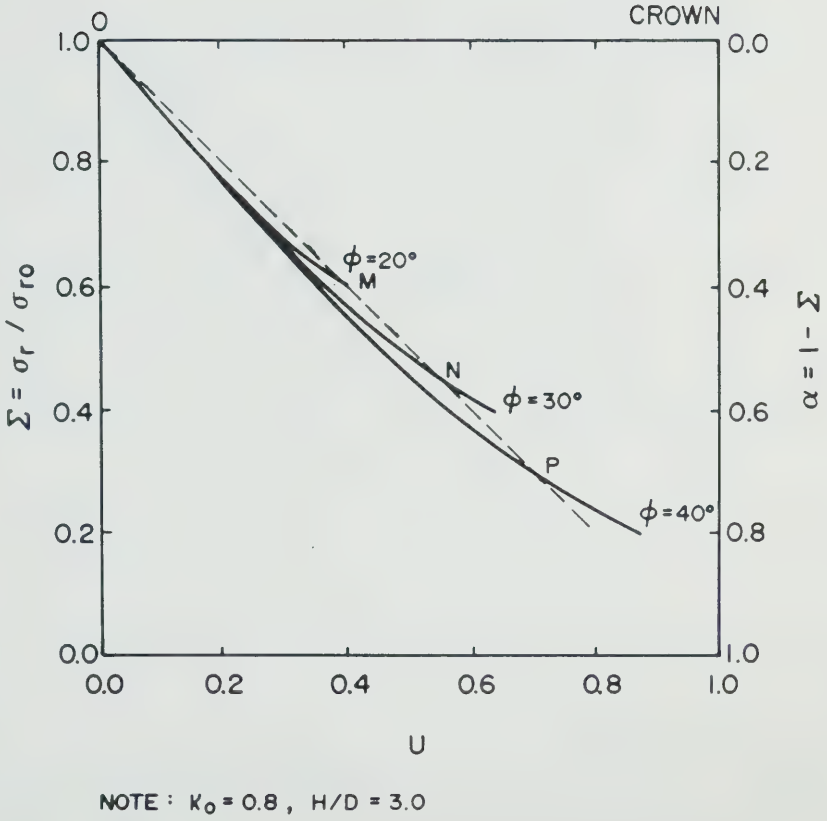

Figure 6.63 Normalized Ground Reaction Curves of the Crown for H/D=3 and K_o=0.8, Calculated for Different Friction Angles

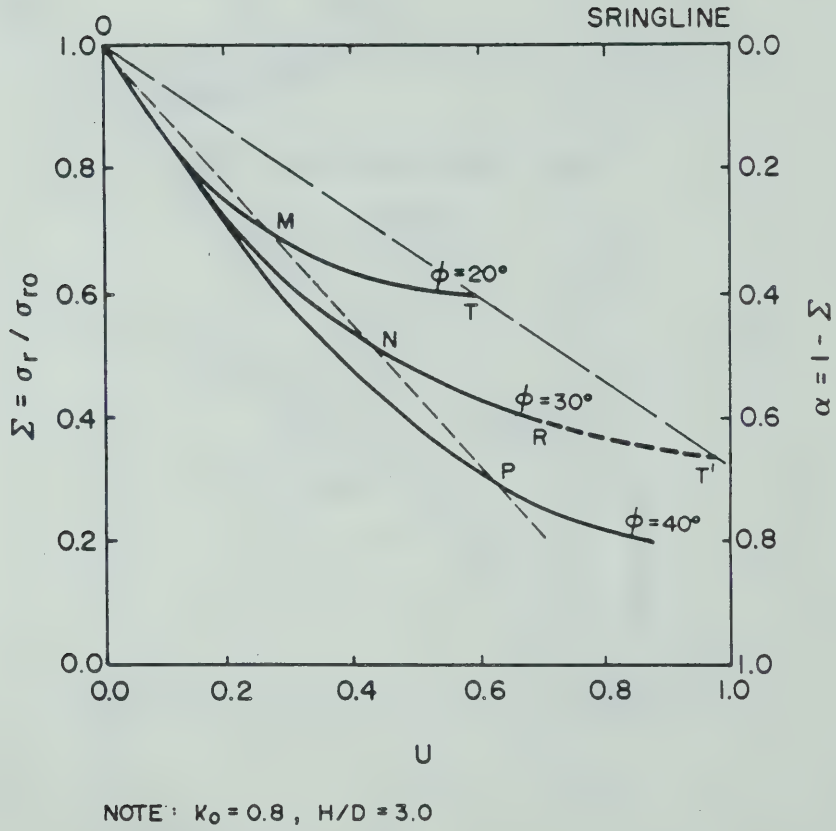

Figure 6.64 Normalized Ground Reaction Curves of the Springline for H/D=3 and K_o=0.8, Calculated for Different Friction Angles

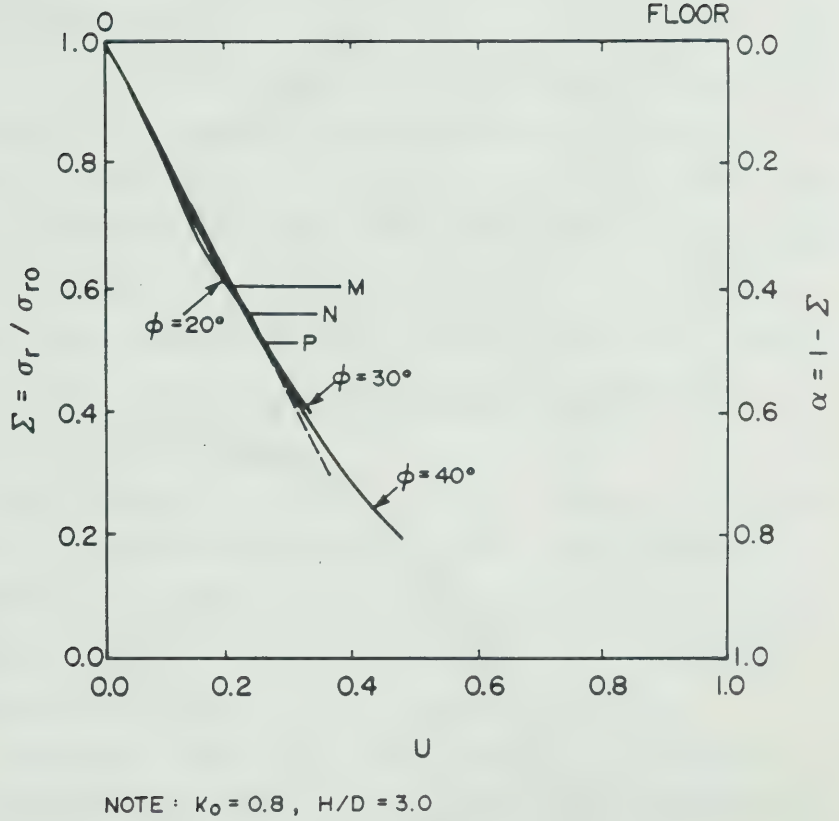

Figure 6.65 Normalized Ground Reaction Curves of the Floor for H/D=3 and K_o=0.8, Calculated for Different Friction Angles

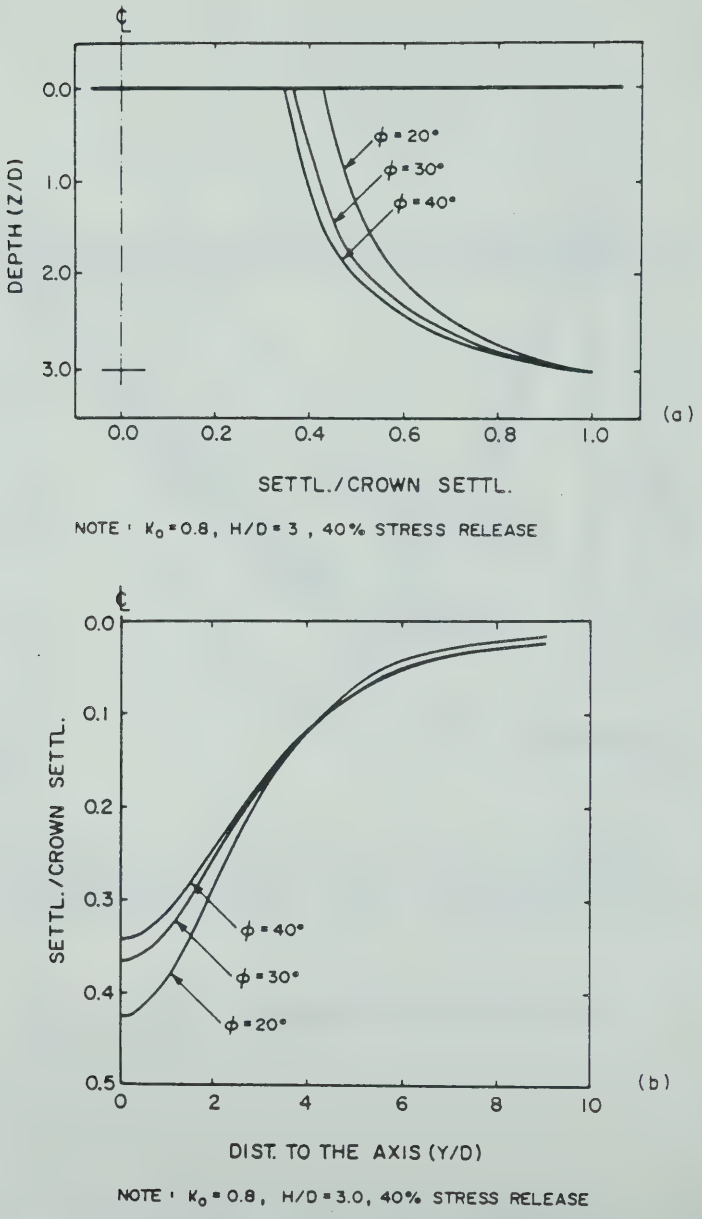

Figure 6.66 Normalized Subsurface and Surface Settlements for H/D=3, K_o=0.8 and 40% Ground Stress Release, Calculated for Different Friction Angles

While for the frictionless soil model, a single value of K_o was considered, in the parametric analyses for the cohesionless model, different K_o values were assumed.

Figures 6.67 to 6.70 present the results of analyses for H/D=3, ϕ=30° and for three in situ stress ratios, (K_o=0.6, 0.8 1.0).

For K_o smaller than unity, soil elements close to the springline undergo local failure before other points at the tunnel contour. This fact is apparent from the NGRCs, which show a more pronounced non-linear aspect at the springline than at elsewhere (Figures 6.67 to 6.69). For K_o equal to unity, soil elements at the springline, crown and floor reach local failure at approximately the same amount of ground stress release.

As noted earlier in this section, when K_o is smaller than unity, the NGRC at the crown and floor, exhibit a 'stiffening' response due to the increase in the minor principal stress in the early stages of the unloading process. This effect is not noted when K_o=1.

Figures 6.70(a) and (b) show the distribution of normalized displacements at the surface and subsurface. It is evident that K_o has a marked influence on the distributions. A lower K_o value promotes a larger maximum normalized settlement, higher normalized surface distortions and a narrower settlement trough. Although the dimensionless displacement U at the crown for K_o=1 is larger than U for K_o smaller than unity, the absolute surface settlement at the

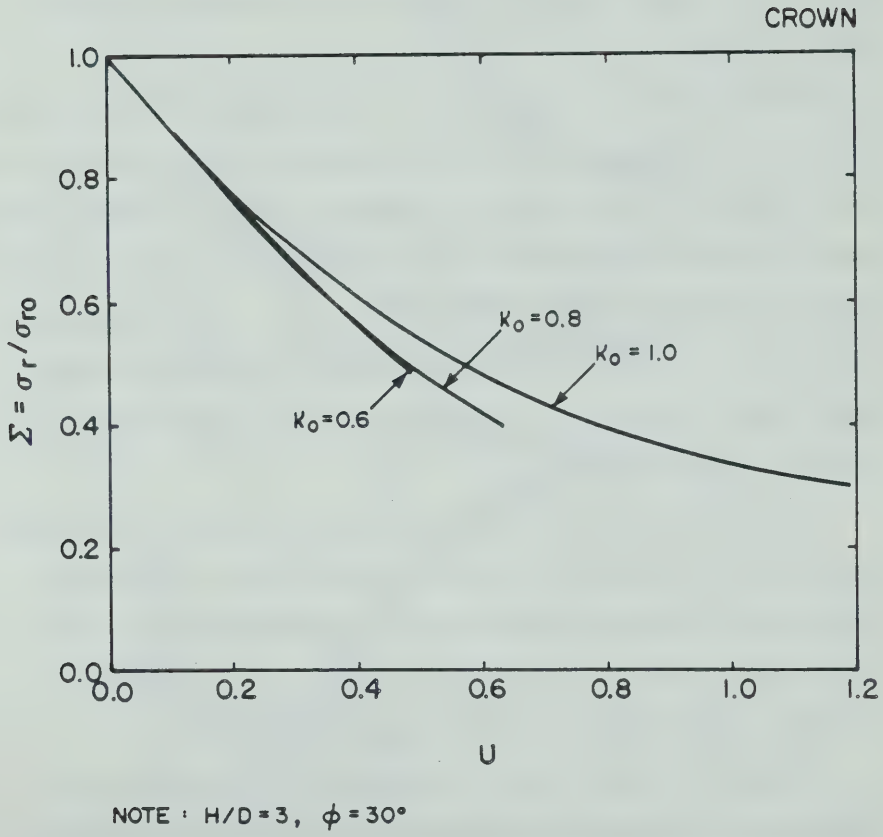

Figure 6.67 Normalized Ground Reaction Curves of the Crown, for H/D=3 and ϕ=30°, Calculated for Different In Situ Stress Ratios

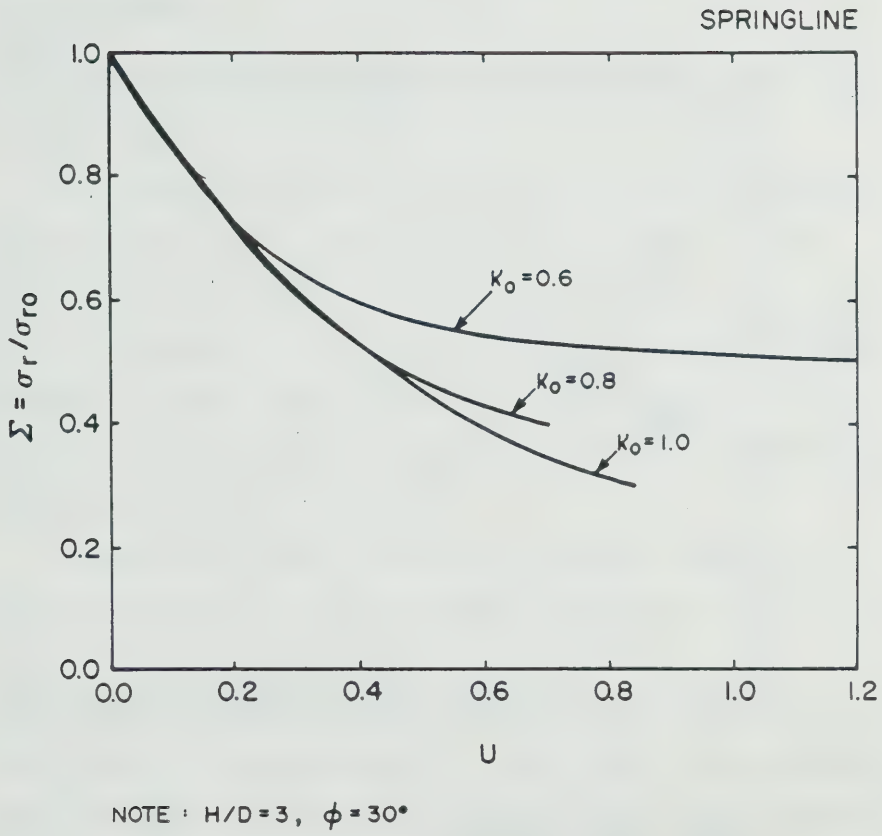

Figure 6.68 Normalized Ground Reaction Curves of the Springline, for H/D=3 and ϕ=30°, Calculated for Different In Situ Stress Ratios

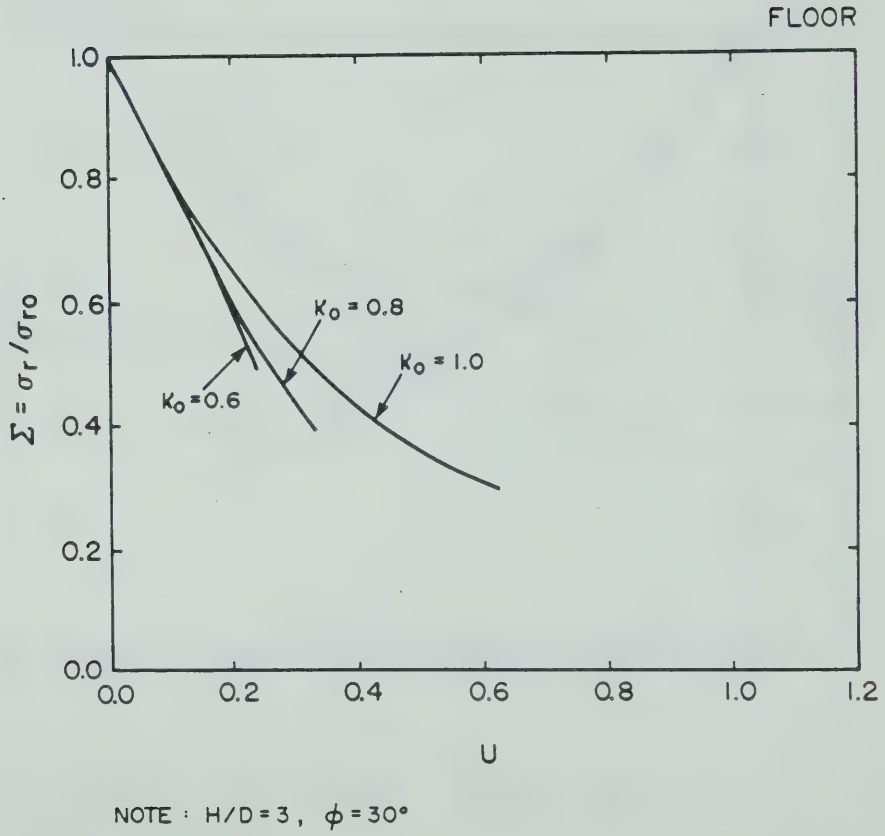

Figure 6.69 Normalized Ground Reaction Curves of the Floor, for H/D=3 and ϕ=30°, Calculated for Different In Situ Stress Ratios

centreline for $K_o<1$ is always larger than that for $K_o=1$, for the same initial tangent modulus and the same amount of stress release. In other words, for K_o decreasing, the average vertical strain in the ground cover above the tunnel axis decreases.

6.3.2.3 Relationships Between Surface and Crown Settlements

The practical interest that exists in relating the crown settlement (u_c) to the surface settlement at the tunnel centreline (S) is derived from the fact that once the former is assessed in some way, the latter could be readily estimated through some relationship. Many authors investigated the subject and proposed different procedures to accomplish this.

Atkinson and Potts (1977:318) proposed simple expressions relating the normalized surface settlement (S/u_c) to the relative depth of cover (H/D) and the soil type. Their expressions were semi-empirically developed from observation of displacements in tunnel model tests, before ground collapse (FS>1). A similar approach was followed by Seneviratne (1979:56) once more using model test results. Ward and Pender (1981:265) explored the subject further and pointed out some of the limitations of the above approaches. Moreover, they discussed the limitations of the S/u_c relationships derived from linear elastic analyses (for instance, Oteo and Sagaseta, 1982:657). Resendiz and Romo (1981:72) developed a relationship through non-linear

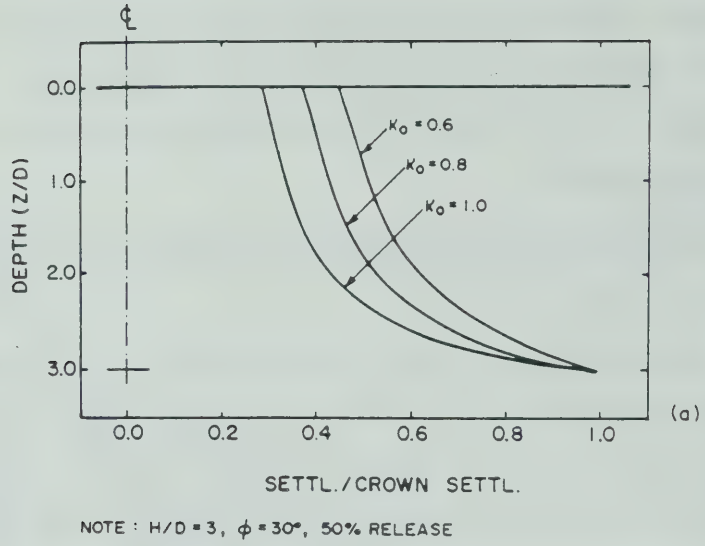

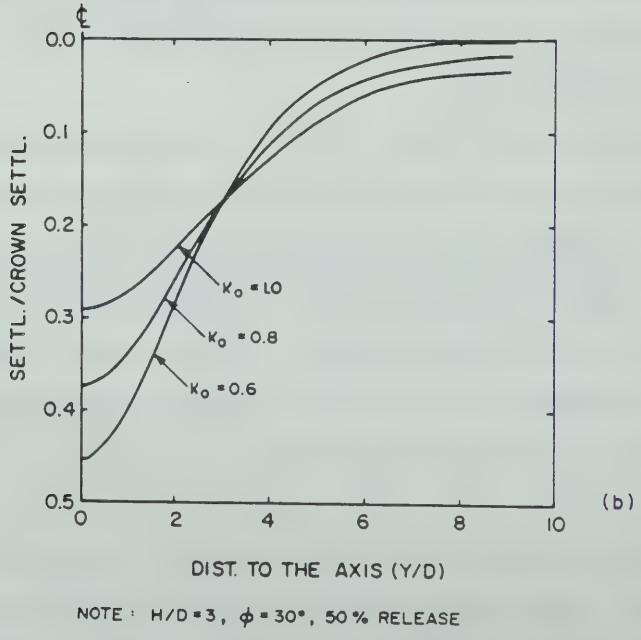

Figure 6.70 Normalized Subsurface and Surface Settlements for H/D=3, ϕ=30° and 50% Ground Stress Release, Calculated for Different In Situ Stress Ratios

elastic numerical modelling and suggested that the normalized surface settlement should be a function of H/D and of the soil strain at failure, as determined in an undrained triaxial test. Wong and Kaiser (1987:331) proposed a conceptual model relating the normalized surface settlement to the amount of stress release allowed. They contended that upon the reduction of ground stresses at the opening, the settlement ratio (S/u_c) remains fairly constant initially, increasing rapidly with yielding and subsequent collapse at which stage it approaches unity.

If general relationships to estimate the S/u_c ratio were to be derived for pre-collapse situations (i.e., for good ground control conditions), and if they were to be based on the two soil models introduced earlier (Sections 6.2.2 and 6.2.3), then they would have to be expressed as:

$$F=f(\frac{S}{u_c},\frac{\sigma_r}{\sigma_{ro}},\frac{H}{D},\ K_o,\ \phi_e) \qquad [6.14]$$

for the cohesionless soil model, and as

$$F=f(\frac{S}{u_c},\frac{\sigma_r}{\sigma_{ro}},\ \frac{H}{D},\ \frac{c_{ue}}{\gamma D}) \qquad [6.15]$$

for the frictionless soil model.

The results of the parametric analyses included in Appendix C could be helpful in establishing these relationships. To assess the role of the dimensionless variables shown in the equations 6.14 and 6.15 on the settlement ratio, it seems worthwhile to examine some of those results. Figure 6.71, for instance, presents how the settlement ratio for the frictionless soil model, varies with the stress ratio Σ, with the undrained strength ratio

and with the tunnel depth. One notes that at the early part of the unloading process and especially for the higher strength soils, the normalized surface settlement is virtually independent of the amount of stress release applied to the opening. Consequently, it does not depend on the factor of safety at pre-collapse stages, despite the pronounced non-linear response one notes even for the stronger soils (see, for instance, Figure 6.54).

The above result is not new as it was noted earlier by Atkinson and Potts (1977:318), through static tunnel model test results in overconsolidated kaolin, performed in Cambridge by Cairncross (1973) and Orr (1976). In these tests, the undrained shear strength ratio ranged from 0.4 to 0.8 and the H/D ratio from 0.35 to 1.2. For deeper tunnels or weaker soils, however, one notes in Figure 6.71 that the normalized surface settlement becomes more affected by the stress ratio, Σ. Therefore, the Atkinson and Potts (1977) conclusion and proposed correlation for the S/u_c ratio is valid only for the conditions they studied (for instance, very shallow tunnels) and cannot be generalized to other situations. Moreover, the linearity between S/u_c and H/D suggested by the Atkinson and Potts (Op.cit.) relationship have not been confirmed by centrifuge model test results obtained later by Mair (1979:127), also in Kaolin with $c_u/\gamma D$ of about 0.38 and larger cover to diameter ratios (up to 3.11).

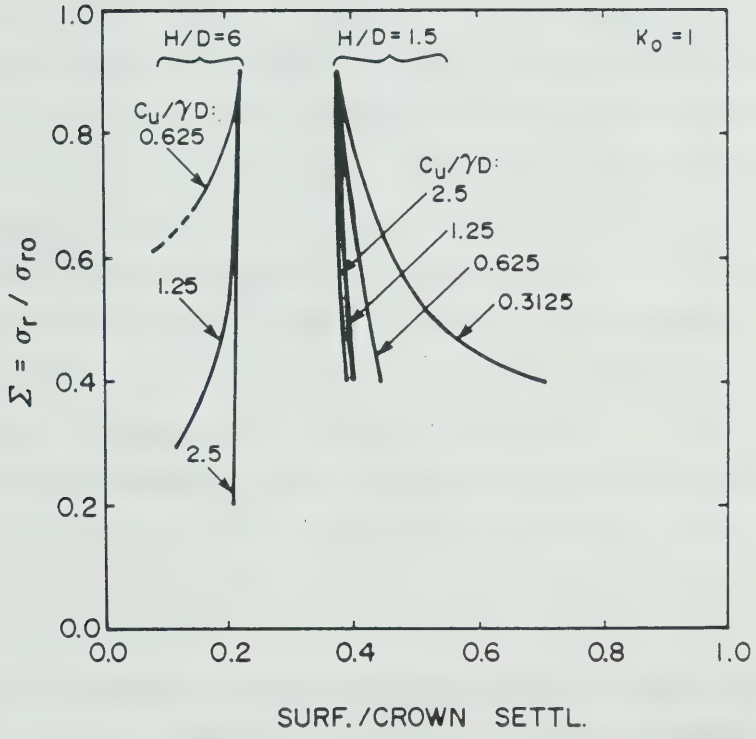

Figure 6.71 Variation of the Maximum Normalized Surface Settlement with the Amount of Stress Release and other Variables, for the Frictionless Soil Model

Another feature that is apparent from Figure 6.71 is that depending on the depth ratio, as ground failure is approached the settlement ratio may either increase or decrease. This seems to reflect the mode of collapse that prevails in shallower or deeper tunnels, with the surface settlement developing at a faster or slower rate compared to the crown settlements. Similar results are found for the cohesionless soil model. These are shown in Figure 6.72 for H/D=3. Once more the normalized surface settlements seem to be unaffected by Σ for small amounts of ground stress release or for larger amounts provided the soil strength is high. Moreover, the influence of the stress ratio K_o now becomes apparent. While for low K_o values, the settlement ratio seems to increase as failure is approached, for higher K_o, that settlement ratio may in fact decrease. The previous criticisms to Atkinson and Pott's (1977) relationship for clays are also applicable for their proposed relations for sand.

The above results indicate that the surface settlement ratio depends on H/D, on the soil strength ($c_u/\gamma D$ or ϕ), on the in situ stress ratio, K_o, and on the amount of stress release allowed (σ_r/σ_{ro}), as is stated by the expressions 6.14 and 6.15. Furthermore they indicate that the S/u_c ratio, regardless of the soil model considered (fully undrained or fully drained), may either increase or decrease with Σ decreasing and ground collapse approaching. Therefore, the conceptual model proposed by Wong and Kaiser

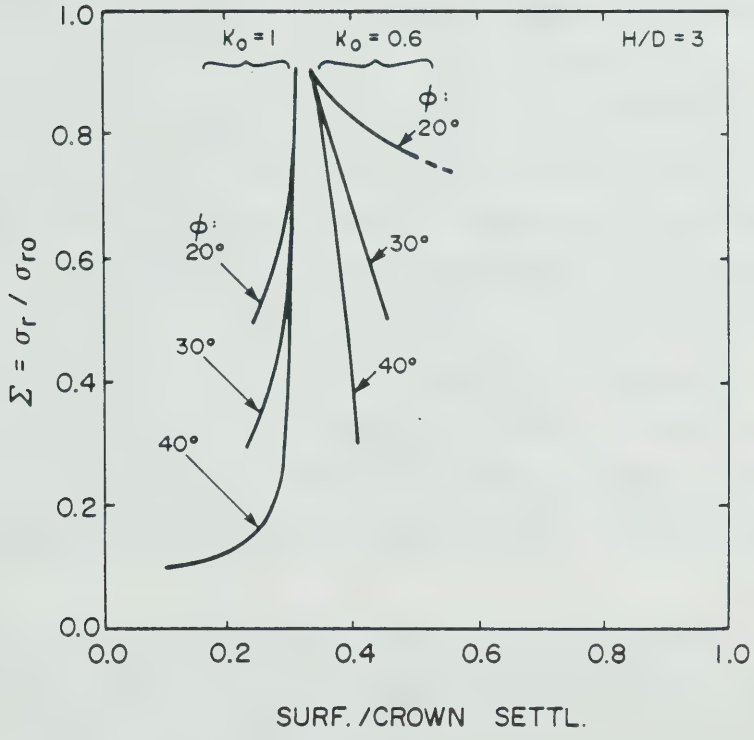

Figure 6.72 Variation of the Maximum Normalized Surface Settlement with the Amount of Stress Release and other Variables, for the Cohesionless Soil Model

(1987:332) is incomplete, as it assumes that in the pre-failure regime, the settlement ratio is always increasing as yielding occurs. In fact, some results by Wong (1986) (not included in Wong and Kaiser, 1987) actually demonstrate the opposite. Wong (1986) studied the subject through finite element modelling using an elasto-plastic stress-strain relationship. For $H/D=2$, $K_o=1.3$ and $\phi=30°$ (analysis ST3 by Wong, 1986:97), the numerical results indicate that the settlement ratio may decrease as the stress ratio Σ decreases. The Wong and Kaiser (1987:333) suggestion that, regardless of the mode of behaviour of the ground defined by its properties, the tunnel depth and the in situ stresses, the settlement ratio S/u_c at collapse becomes unity is yet to be proven. The ratio of settlement increments $\Delta S/\Delta u_c$ may possibly tend toward unity at a complete ground collapse condition but the settlement ratio may not.

To complete the discussion, Figures 6.73 and 6.74 were prepared. They represent graphically the relationship given by the equation 6.15, for the frictionless soil model, and for ground stress releases of 30 and 50% respectively. These amounts of stress reductions in the 2D model could correspond in an actual tunnelling situation, to transverse sections located near the tunnel face and at some distance behind it. Comparing these two figures, one notes that the normalized surface settlement is not very sensitive to the undrained strength ratio, or to the amount of stress

reduction. The settlement ratio is more dependent on the relative tunnel depth. Note also that it has been inferred that as H/D tends toward zero, the settlement ratio should tend towards unity. Observe that in Figure 6.74, the results of Mair's (1979) centrifuge model test in kaolin have been included (tests 2DP and 2DV). The undrained strength ratio of this soil was about 0.34.

Similarly, Figures 6.75 to 6.80 were prepared for the cohesionless soil model. It should be noted that the data referring to the 50% stress release, for ϕ=20°, K_o=0.6 and 0.8 were calculated after a few elements of soil at the springline had failed. As explained, the numerical model was not designed for this condition. However, since the failed zone was limited to a fairly small region next to the springline, it is believed that it had negligible effect on the settlement above the crown. The failed zone extended to no more than D/4 beyond the tunnel contour and up to no more than 45° measured from the horizontal axis towards the crown or floor. The area of failed elements corresponds typically to less than 7% of the tunnel area. The suite of plots shown in the last six figures represents the function given by equation 6.14. They may serve as practical design charts for estimating the settlement ratio, for conditions differing from those considered in the parametric analyses whose results were included in Appendix C.

To illustrate the subject further, Figure 6.81 reproduces data from 28 case histories gathered by Ward and

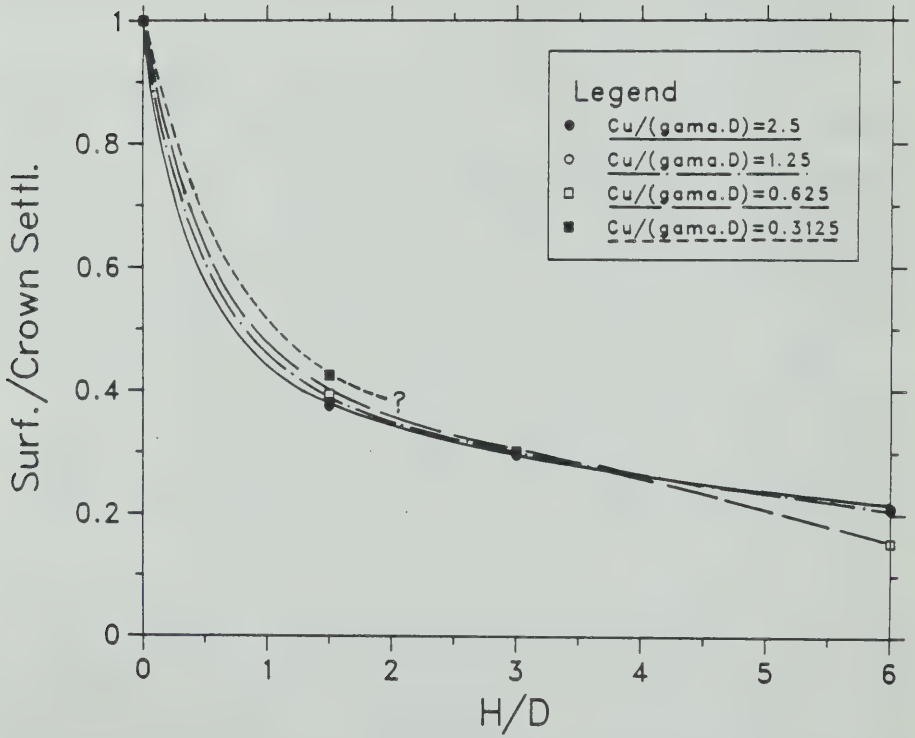

Figure 6.73 Relationships between Normalized Maximum Surface Settlement and Relative Depth of Tunnel, Calculated for the Frictionless Soil Model, for 30% Stress Release

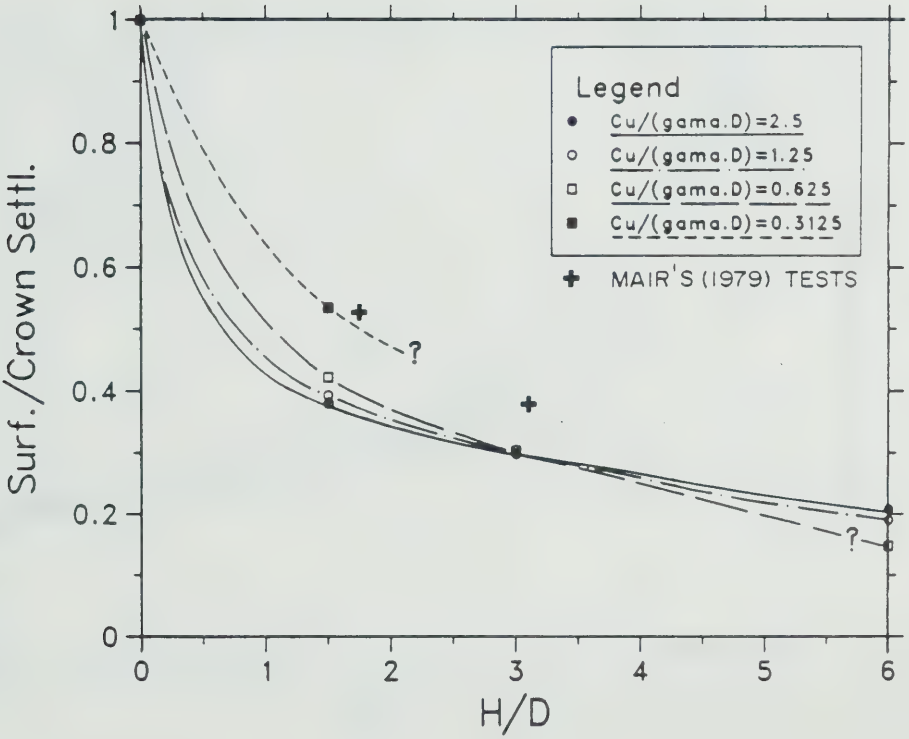

Figure 6.74 Relationships between Normalized Maximum Surface Settlement and Relative Tunnel Depth, Calculated for the Frictionless Soil Model, for 50% Stress Release

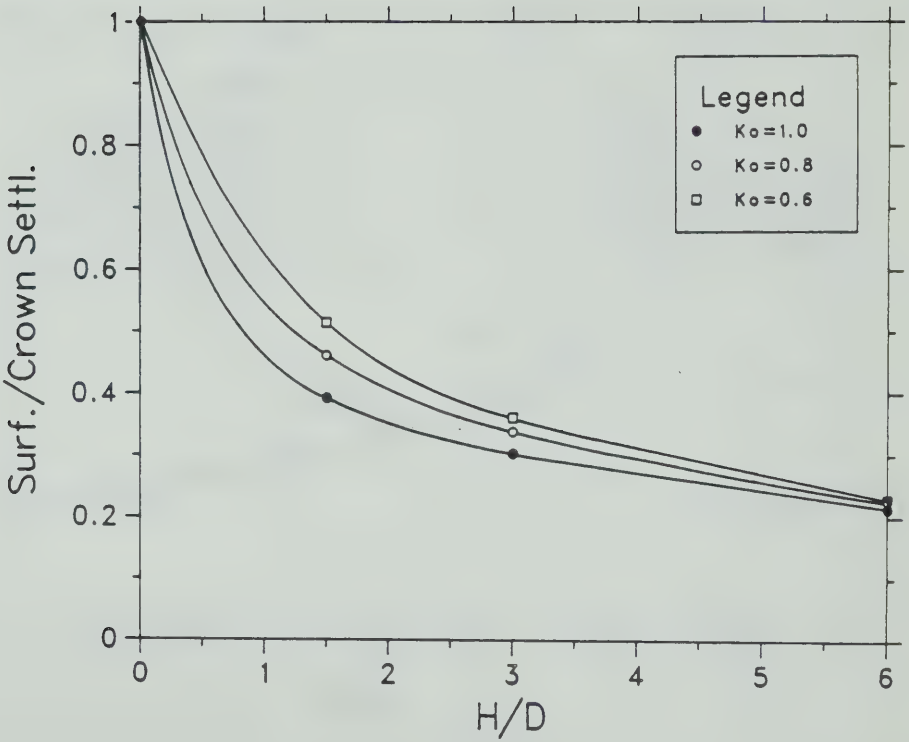

Figure 6.75 Normalized Settlement Ratios for ϕ=40° and 30% Stress Release

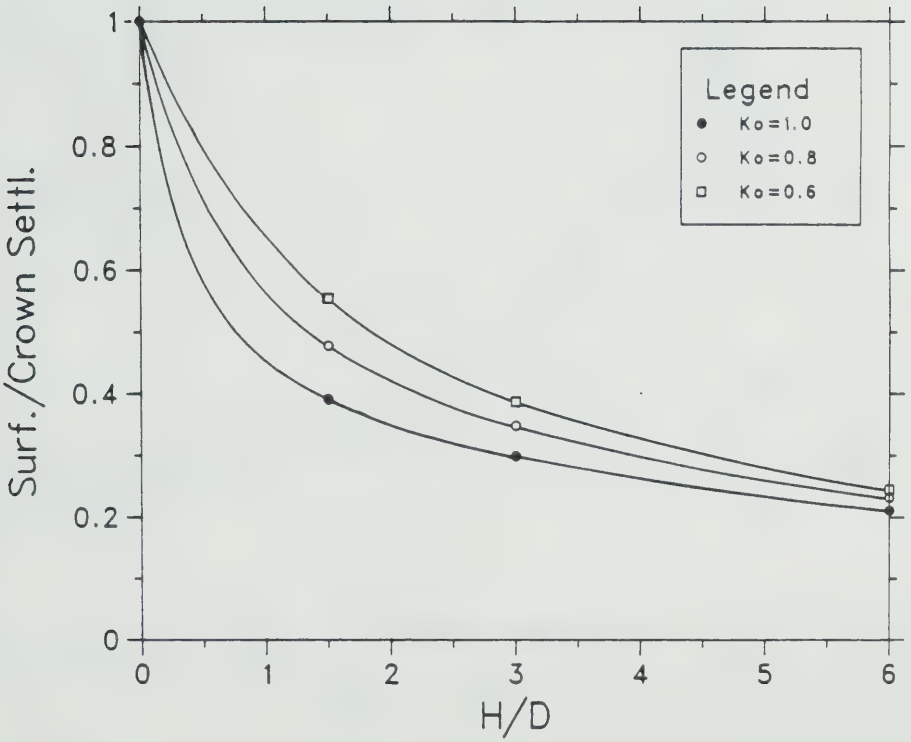

Figure 6.76 Normalized Settlement Ratios for ϕ=40° and 50% Stress Release

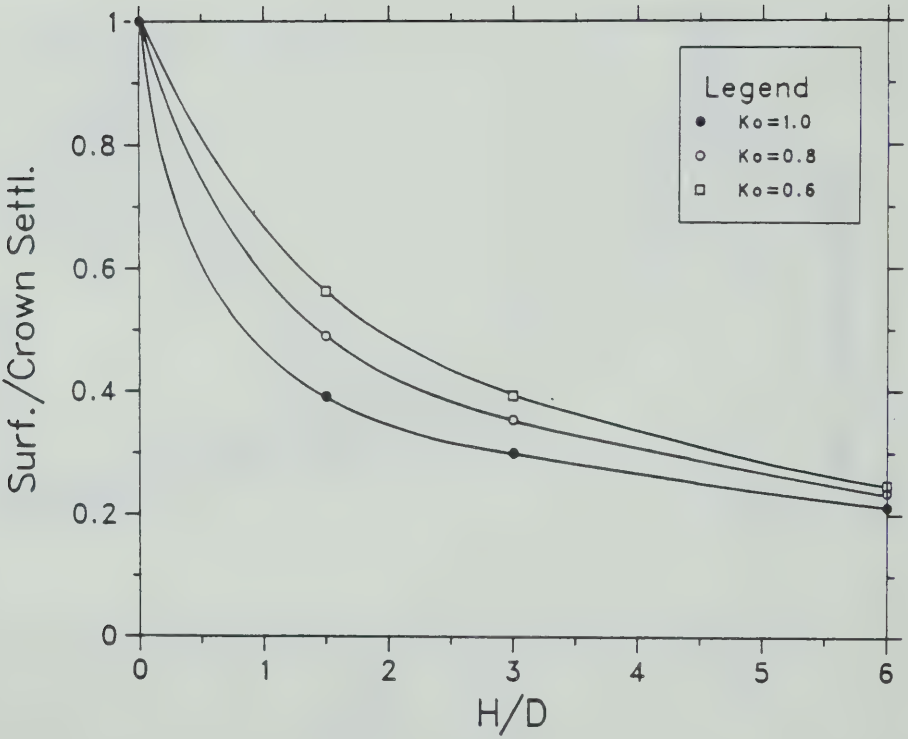

Figure 6.77 Normalized Settlement Ratios for ϕ=30° and 30% Stress Release

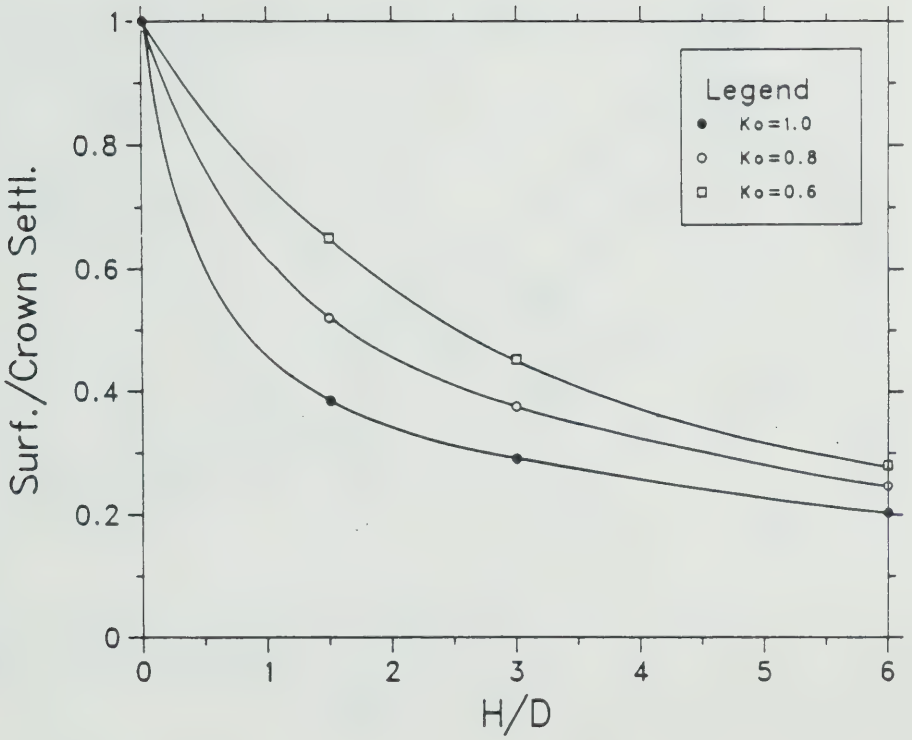

Figure 6.78 Normalized Settlement Ratios for ϕ=30° and 50% Stress Release

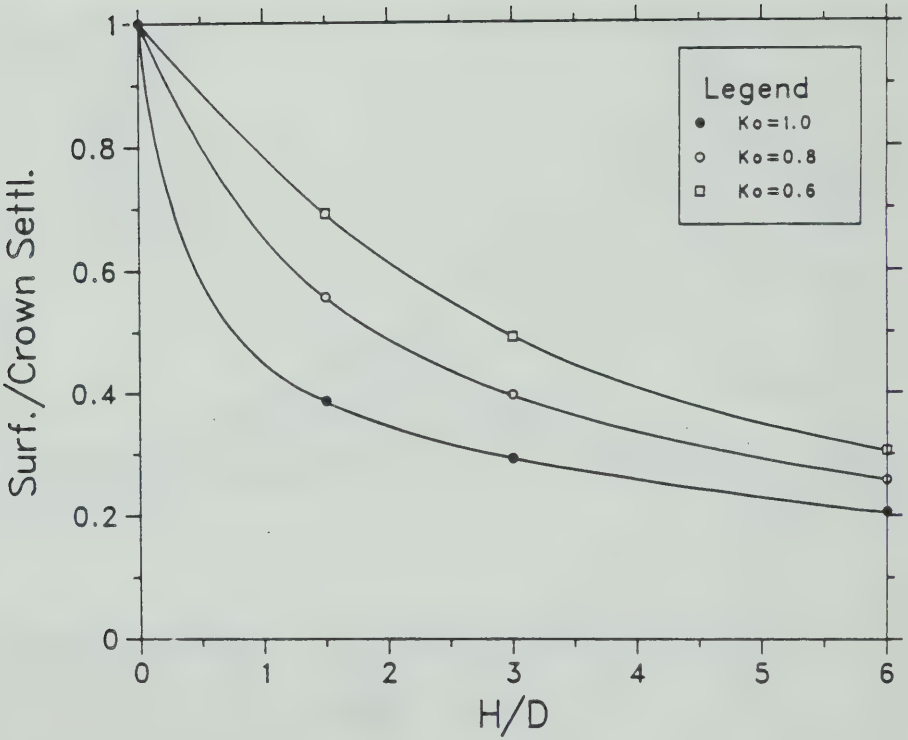

Figure 6.79 Normalized Settlement Ratios for ϕ=20° and 30% Stress Release

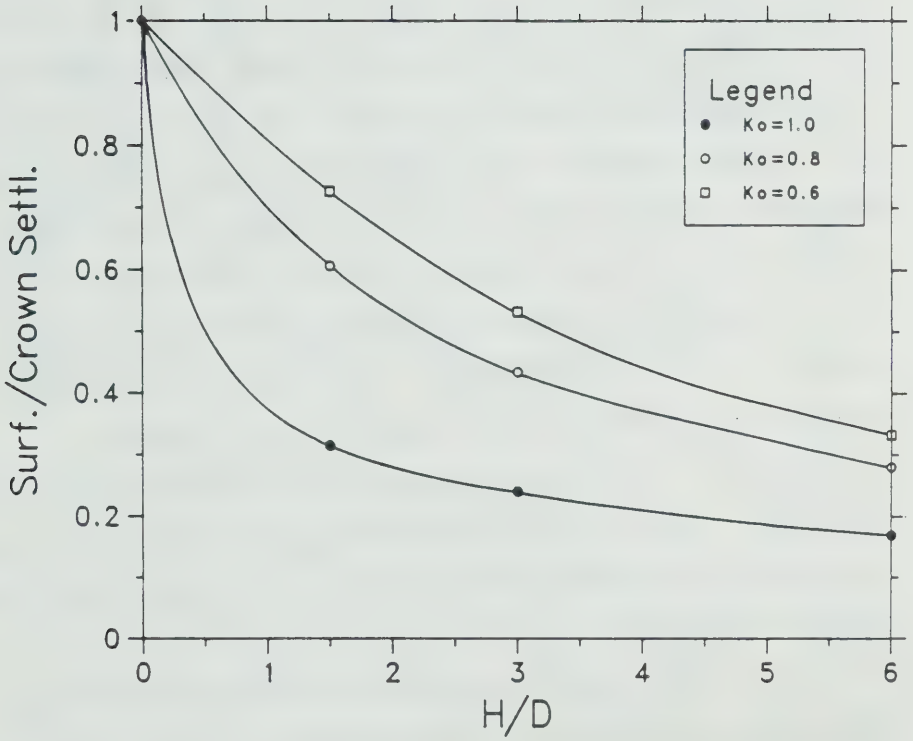

Figure 6.80 Normalized Settlement Ratios for ϕ=20° and 50% Stress Release

Pender (1981:267). It shows the ratios of surface to crown settlements measured by field instrumentation, plotted against the cover to diameter ratio. In most cases, the deep settlement measurements were taken somewhat above the tunnel crown. So, in general, the S/u_c ratio is larger than the actual one. Ward and Pender (Op.cit.) tried to include only short-term displacements, excluding those due to drainage, but it is doubtful whether this has been really achieved. For instance, Cases 17, 18, 24 and 25[16], are respectively, the Mexico Siphon tunnel (see Table 5.31), a tunnel in Buenos Aires, a sewer tunnel in Belfast (see Section 3.3.4.2), and the Thunder Bay tunnel (see Table 5.31 and Section 3.3.4.2) and may have, very possibly, included ground displacement caused by partial drainage and consolidation. In cases like these, one would expect to find settlement ratios larger than those experienced under time independent conditions, as assumed in the present study (see Section 3.3.4.2).

Two extreme curves are superimposed on the Ward and Pender data in Figure 6.81. These were obtained in the present study and correspond to 50% stress release, for a soil with $\phi=20°$ and $K_o=0.6$ and 1.0. It is noted that a large number of cases is bound by those two curves, which also bound a similar set of data collected by Heinz (1984:49) of NATM case histories (not shown). This may not be claimed as

---

[16] For identification of the cases numbered in Figure 6.81, the reader is referred to Table 1 in Ward and Pender, (1981:266, 267).

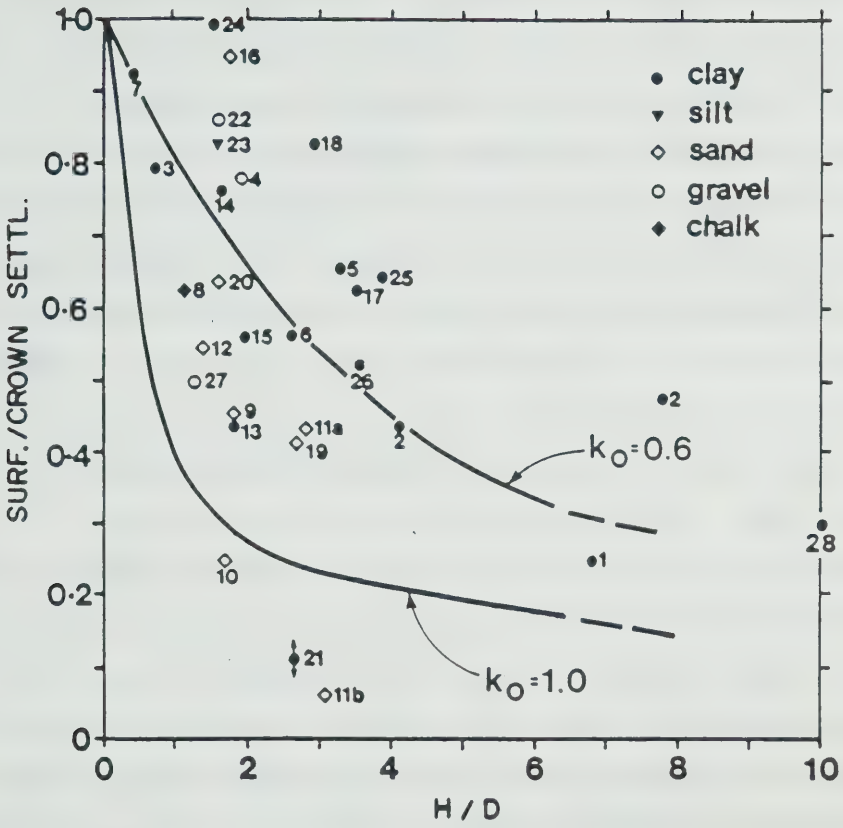

Note: See Ward and Pender (1981:266) for identification of the case histories.

Figure 6.81 Normalized Settlement Ratios Observed in some Case Histories

a proof of the validity of the presently proposed settlement ratios relationships. However, the relationships derived herein may be used to explain the apparently chaotic set of field data shown in Figure 6.81. The scatter of data can possibly be elucidated in terms of differences in K_o, in soil strength and in the amounts of stress release associated with the different case histories.

In Section 5.2.1.2, it was mentioned that a linear elastic finite element back analysis of a shallow tunnel case history could lead to either an overestimate or an underestimate of the maximum surface settlement, whenever a match in the crown displacement is achieved. Conversely, if a match between measured and backcalculated surface settlement is attained, then either an over or an underestimate of the crown settlement may be obtained. The reasons behind these statements are now, perhaps, clearer. In a linear elastic analysis, the surface to crown settlement ratio is always constant, regardless of the amount of stress release. When a non-linear response is taken into account this may not happen, as indicated by the results shown in Figure 6.71 or 6.72, or in the results shown in Appendix C. For a non-linear ground response, the surface to crown settlement ratios can either increase or decrease, with respect to the decreasing stress ratio, Σ. It depends on the type of soil model being considered (the 'undrained' - frictionless soil model, or the 'drained' - cohesionless soil model), on the cover to diameter ratio, on

the in situ stress ratio and on the soil strength. These facts explain the above statements and the comments included in Section 5.2.1.2 regarding Figures 5.6 and 5.7. Note that in Figures 6.71 and 6.72, the starting points at Σ=0.9, for all curves shown (after the first 10% of ground stress release), give the settlement ratios for linear elastic analyses under the conditions considered. The ground response after the first unloading increment, as calculated by the present piecewise elastic numerical solution, is identical to the result a linear elastic analysis would yield.

6.4 Generalization of the Results

6.4.1 Opening Remarks

In this section, an attempt will be made to achieve the objective established in Section 6.1: the development of a general procedure that would allow the ground reaction curves or stress release curves of shallow tunnels to be obtained, without the need of additional finite element analyses.

The parametric analyses that were carrried out allowed those curves to be obtained for certain specific conditions, defined in terms of soil properties (for example, a particular soil strength) or geometry (H/D). In practice, conditions differing from those will normally be found and interpolation between the NGRCs obtained will usually be

required. If some general expression, such as that given by equations 6.11 or 6.12, could be obtained, then the problem would be simplified. Moreover, if some practical situation is found to lie beyond the range of the variables considered, one may attempt an extrapolation of the results of the parametric analyses through these expressions. This could involve some degree of uncertainty and may yield unreliable results, if certain conditions are not fulfilled. Some of these conditions will be discussed later.

The generalization of the NGRC will be developed separately for the frictionless soil model representing an undrained soil response, and for the cohesionless soil model representing a drained soil response.

6.4.2 Frictionless Soil Model

It was anticipated in Section 6.3.2.1 that, for a given cover to diameter ratio, the NGRCs of points of the tunnel contour for different undrained strength ratios, are nearly homothetic. This can be demonstrated taking, for example, the results shown in Figures 6.54 to 6.56. Assume that the origin of the NGRCs, point O, defined by the stress release, $\alpha=1-\Sigma=0$ and the dimensionless displacement $U=0$, is the centre of similitude. Through O, draw an arbitrary axis OP. The point P can be taken, for instance, as the extreme point of the NGRC for $c_u/\gamma D=2.5$. The line OP will intersect the NGRC for $c_u/\gamma D=0.625$ and 1.25 at points M and N. Read the coordinates of points M, N and P. For instance, for the NGRC

of the tunnel crown (Figure 6.54), these coordinates are those shown in Table 6.10. Then use these coordinates as reference values and normalize each of the NGRCs to each corresponding reference value. In other words, replot the results of the numerical analysis with the normalized coordinates a/a_{ref} and U/U_{ref}. If this procedure is applied to the curves for the tunnel crown, Figure 6.54 will be reduced to that shown in Figure 6.82. One notes that the twice normalized ground reaction curves (NNGRC) virtually coincide (Points M, N and P of Figure 6.54 do coincide in Figure 6.82), and it is said that the original NGRCs (Figures 6.54) were nearly homothetic. If they were perfectly homothetic, then they would coincide exactly. Rigorously, this is not the case but, for all practical purposes it can be said that they do coincide.

Moreover, if it is attempted to find out what function fits best the points shown in Figure 6.82, it is soon found that a hyperbola can be quite well adjusted through them. The NNGRC could then be expressed as:

$$a/a_{ref} = (1-\Sigma)/(1-\Sigma_{ref}) = \frac{U/U_{ref}}{a + b\ U/U_{ref}} \qquad [6.16]$$

This function presents two advantages. It has a finite limiting value when U/U_{ref} tends to infinity, as a ground reaction curve should have when a tunnel collapse condition is approached. Secondly, the hyperbola can be transformed into a linear function (see Figure 5.10) and a linear regression analysis can be applied to the transformed normalized points. If this transformation of coordinates is

Position	$C_u/\gamma D$	$\frac{\alpha_{ref}}{1-\Sigma_{ref}}$ =	U_{ref}	$\frac{\alpha_{ref}}{U_{ref}}$	a	b	r
Crown	2.5	0.700	0.9930	0.7049			
	1.25	0.382	0.5419	0.7049	0.6444	0.3253	0.9977
	0.625	0.220	0.3121	0.7049			
Springline	2.5	0.700	0.7290	0.9602			
	1.25	0.382	0.3978	0.9602	0.6575	0.3255	0.9990
	0.625	0.220	0.2291	0.9603			
Floor	2.5	0.700	0.5260	1.3308			
	1.25	0.382	0.2870	1.3308	0.6351	0.3536	0.9999
	0.625	0.220	0.1653	1.3309			

Table 6.10 Parameters used and Obtained in the Reduction of the Twice Normalized Ground Reaction Curves for the Frictionless Soil Model, for H/D=3

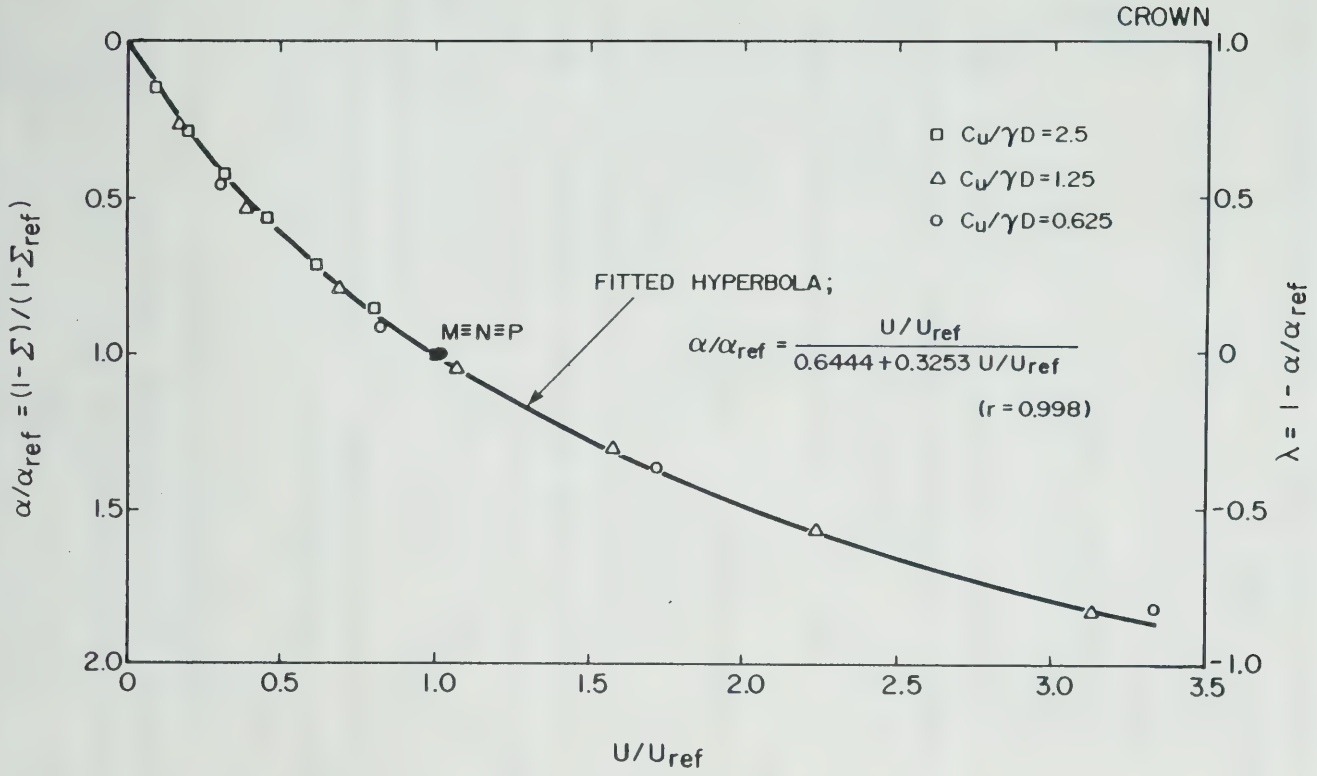

Figure 6.82 Twice Normalized Ground Reaction Curve (NNGRC) for the Crown of a Tunnel with H/D=3, for the Frictionless Soil Model

made and a linear regression is undertaken for the data shown in Figure 6.82, then it is found that the coefficients in equation 6.16 are:

$a = 0.6444$

$b = 0.3253$

and that the correlation coefficient is:

$r = 0.9977$

which is an indication of the goodness of the fit. The fitted hyperbola representing the NNGRC was superimposed on Figure 6.82 and it is seen that the function found for the tunnel crown does fit the transformed numerical results quite well.

If the above process is repeated for the springline and floor curves, then the twice normalized curves shown in Figures 6.83 and 6.84 are obtained. The reference values used for normalizing these curves are also shown in Table 6.10. Note that for each point of the tunnel contour, the ratio a_{ref}/U_{ref} should be constant, as it represents the slope of the selected axis OP used in the transformation process. If the fitted hyperbolae shown in Figures 6.82 to 6.84 are compared, one notes that they come very close together but do not coincide.

If the above procedures are repeated for the other relative tunnel depths considered, then Tables 6.11 and 6.12 are similarly obtained for H/D=1.5 and 6 respectively. In all cases, the correlation coefficient, r, was found to be larger than 0.99, indicating that a good fit was obtained in

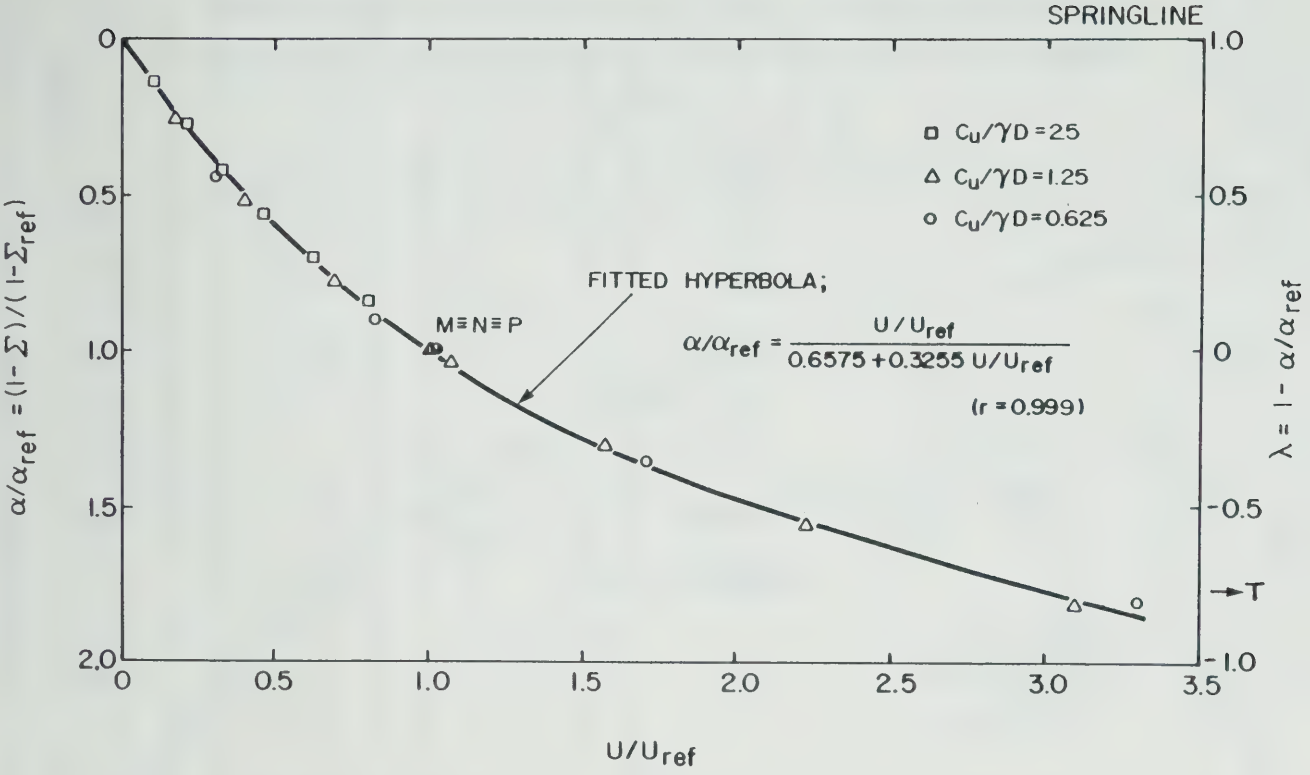

Figure 6.83 Twice Normalized Ground Reaction Curves (NNGRC) for the Springline of a Tunnel with H/D=3, for the Frictionless Soil Model

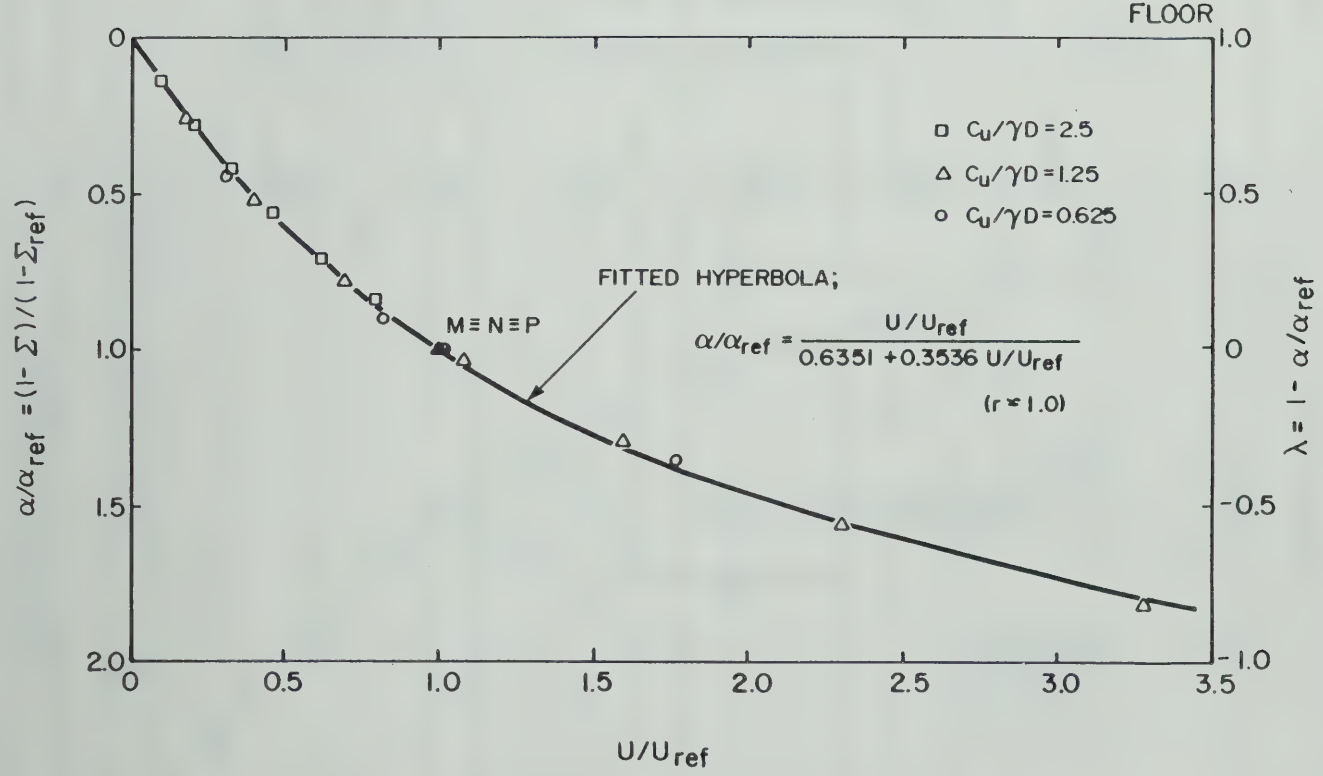

Figure 6.84 Twice Normalized Ground Reaction Curves (NNGRC) for the Floor of a Tunnel with H/D=3, for the Frictionless Soil Model

all situations.

In order to eliminate the arbitrary reference values appearing in equation 6.16, it can be further transformed as below:

$$a = \frac{a_{ref}}{U_{ref}} \cdot \frac{U}{a + b\ U/U_{ref}}$$

Thus:

$$a = 1 - \Sigma = \frac{U}{[a/(a_{ref}/U_{ref})] + [b/a_{ref}].U}$$

or:

$$\Sigma = 1 - \frac{U}{A + B.U} \qquad [6.17]$$

where

$A = a/(a_{ref}/U_{ref})$

$B = b/a_{ref}$

The newly defined parameters can be calculated from Tables 6.10 to 6.12 and thus Table 6.13 is obtained.

The coefficient A is independent of the strength ratio and Figure 6.85 shows how A varies with the relative depth of the tunnel, for three points of the tunnel contour. The coefficient B for each point of the tunnel contour is found to vary with both the soil strength and the tunnel depth. Figures 6.86 to 6.88 summarize these dependencies. In each of these figures, in order to facilitate the interpolation of B for intermediate values of strength or depth ratios, the coefficient B has been plotted against the strength ratio, for constant H/D values (solid lines) and against the depth ratio, for constant $c_u/\gamma D$ values (broken lines).

Equation 6.17 and charts given in Figures 6.85 to 6.88, represent the proposed generalized solution for obtaining

Position	$C_u/\gamma D$	$\alpha_{ref} = 1-\Sigma_{ref}$	U_{ref}	$\frac{\alpha_{ref}}{U_{ref}}$	a	b	r
Crown	2.5	0.600	0.7390	0.8119			
	1.25	0.345	0.4250	0.8118	0.7218	0.2803	0.9936
	0.625	0.219	0.2698	0.8117			
	0.3125	0.152	0.1872	0.8119			
Springline	2.5	0.600	0.5000	1.2000			
	1.25	0.360	0.3000	1.2000	0.7349	0.2693	0.9928
	0.625	0.216	0.1800	1.2000			
	0.3125	0.150	0.1250	1.2000			
Floor	2.5	0.600	0.3520	1.7045			
	1.25	0.3389	0.1988	1.7047	0.7250	0.2693	0.9970
	0.625	0.2087	0.1224	1.7045			
	0.3125	0.1337	0.0784	1.7045			

Table 6.11 Parameters used and Obtained in the Reduction of the Twice Normalized Ground Reaction Curves for the Frictionless Soil Model for H/D=1.5

Position	$C_u/\gamma D$	$\alpha_{ref} = 1-\Sigma_{ref}$	U_{ref}	$\frac{\alpha_{ref}}{U_{ref}}$	a	b	r
Crown	2.5	0.700	1.4470	0.4838			
	1.25	0.382	0.7896	0.4838	0.4540	0.5090	0.9980
	0.625	0.220	0.4548	0.4837			
Springline	2.5	0.700	1.1010	0.6358			
	1.25	0.382	0.6008	0.6358	0.4628	0.4969	0.9969
	0.625	0.220	0.3460	0.6358			
Floor	2.5	0.700	0.8220	0.8516			
	1.25	0.382	0.4486	0.6515	0.4598	0.5322	0.9993
	0.625	0.220	0.2583	0.8517			

Table 6.12 Parameters Used and Obtained in the Reduction of the Twice Normalized Ground Reaction Curves for the Frictionless Soil Model for H/D=6

Position	H/D	$C_u/\gamma D$	$\frac{\alpha_{ref}}{U_{ref}}$	a	$A = \frac{a}{\alpha_{ref}/U_{ref}}$	α_{ref}	b	$B = b/\alpha_{ref}$
Crown	1.5	2.5				0.600		0.4672
		1.25				0.345		0.8125
		0.625	0.8118	0.7218	0.8891	0.219	0.2803	1.2799
		0.3125				0.152		1.8441
	3.0	2.5				0.700		0.4647
		1.25	0.7049	0.6444	0.9142	0.382	0.3253	0.8516
		0.625				0.220		1.4786
	6.0	2.5				0.700		0.7271
		1.25	0.4838	0.4540	0.9384	0.382	0.5090	1.3325
		0.625				0.220		2.3136
Springline	1.5	2.5				0.600		0.4488
		1.25				0.360		0.7481
		0.625	1.2000	0.7349	0.6124	0.216	0.2693	1.2468
		0.3125				0.150		1.7953
	3.0	2.5				0.700		0.4650
		1.25	0.9602	0.6575	0.6848	0.382	0.3255	0.8521
		0.625				0.220		1.4795
	6.0	2.5				0.700		0.7099
		1.25	0.6358	0.4628	0.7279	0.382	0.4969	1.3008
		0.625				0.220		2.2586
Floor	1.5	2.5				0.600		0.4488
		1.25				0.339		0.7946
		0.625	1.70457	0.7250	0.4253	0.209	0.2693	1.2904
		0.3125				0.134		2.0142
	3.0	2.5				0.700		0.5051
		1.25	1.3308	0.6351	0.4772	0.382	0.3536	0.9257
		0.625				0.220		1.6073
	6.0	2.5				0.700		0.7603
		1.25	0.8516	0.4598	0.5399	0.382	0.5322	1.3932
		0.625				0.220		2.4191

Table 6.13 Parameters Obtained in the Reduction of the Twice Normalized Ground Reaction Curves for the Frictionless Soil Model

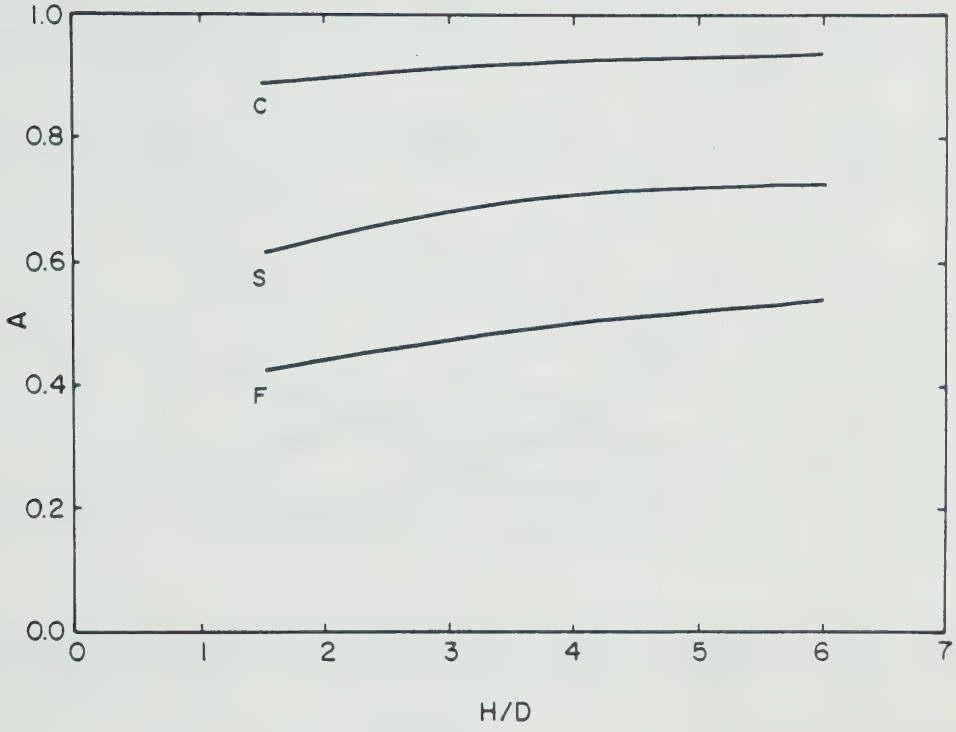

Figure 6.85 Variation of the Coefficient A with Relative Tunnel Depth, for the Frictionless Soil Model

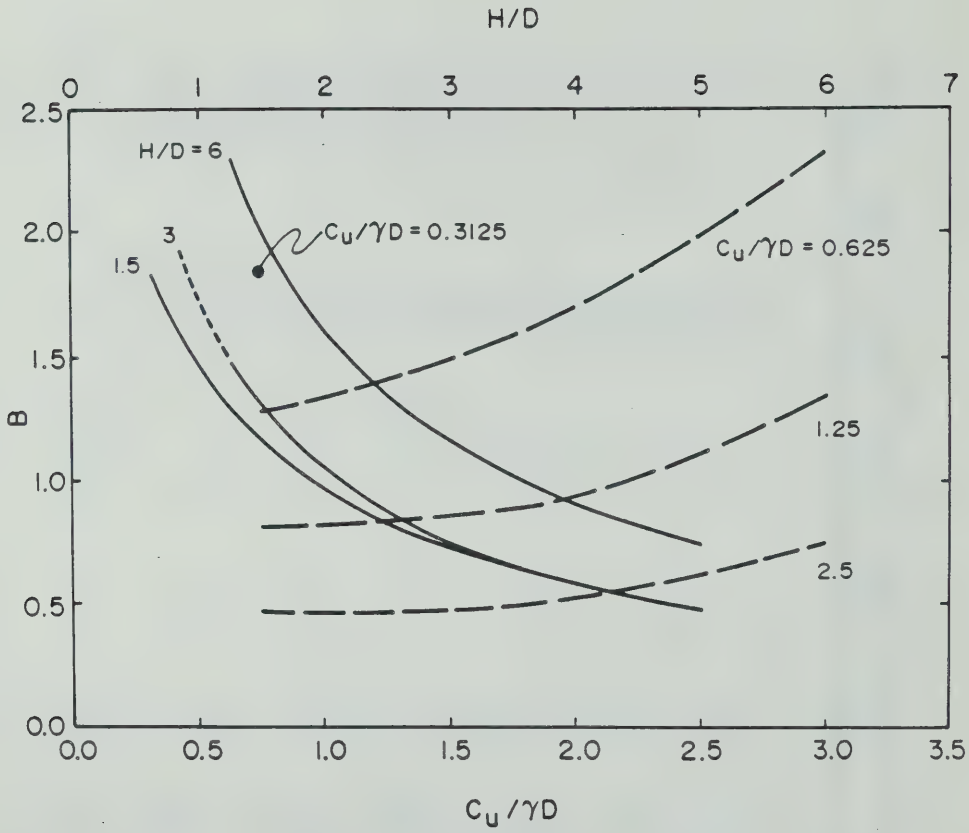

Figure 6.86 Variation of the Coefficient B, for the Tunnel Crown, with Strength and Depth Ratios, Calculated for the Frictionless Soil Model

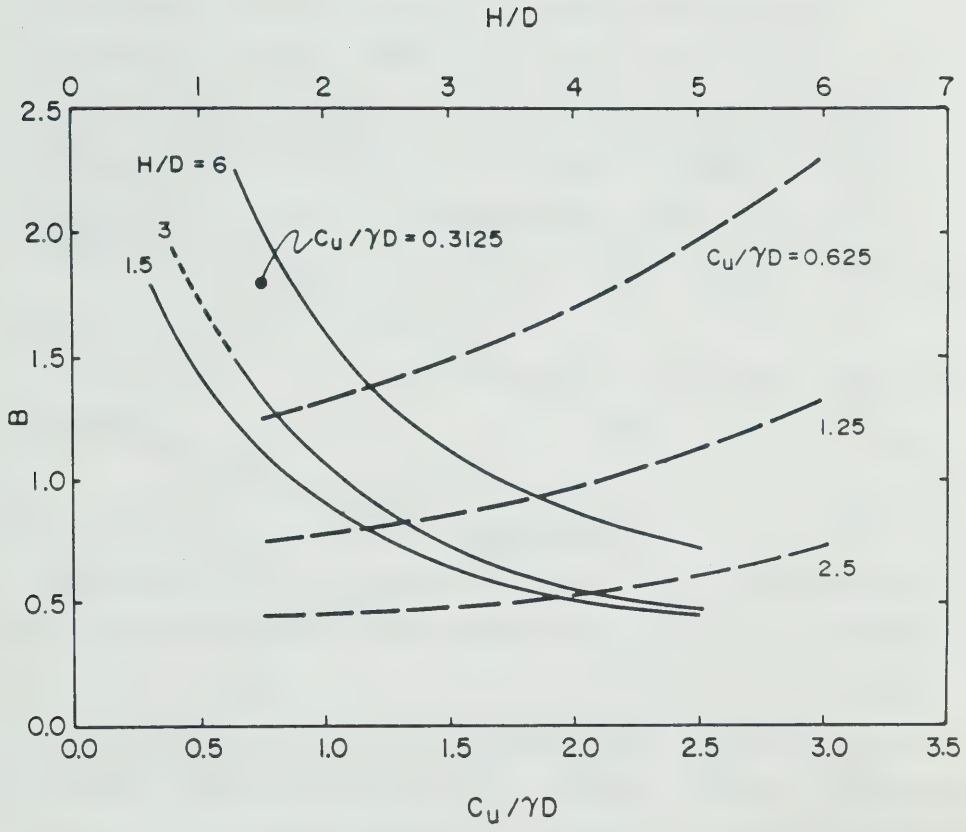

Figure 6.87 Variation of the Coefficient B for the Tunnel Springline, with Strength and Depth Ratios, Calculated for the Frictionless Soil Model

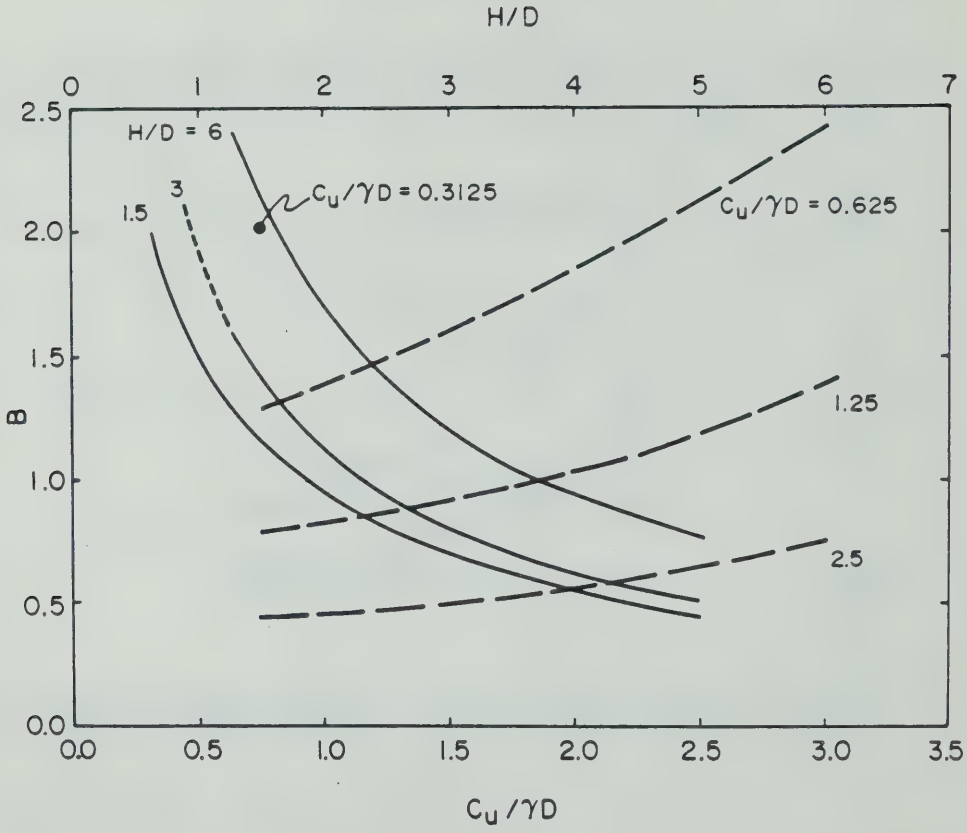

Figure 6.88 Variation of the Coefficient B for the Tunnel Floor, with Strength and Depth Ratios, Calculated for the Frictionless Soil Model

the ground reaction curves for three points on the contour of a shallow tunnel in a soil represented by the frictionless model (equation 6.12). Both coefficients, A and B have some physical meaning. The above solution was designed for applications within the common ranges of variables defined in Section 6.2.5 and its validity is not suggested to hold beyond those ranges. However, it seems interesting to investigate the limits of the solution, in order to assess the physical meaning of the coefficients A and B, in simple qualitative terms.

In the limit for U approaching infinity, equation 6.17 becomes:

$$\Sigma_u = 1 - \frac{1}{B} \qquad [6.18]$$

This would be the limiting stress ratio acting on the opening at a condition of very large radial displacements. One notes that Σ_u does not depend on A, but only on B, which in turn is a function of the soil strength and of the depth of the tunnel. Thus, B is a parameter reflecting the ultimate state of the tunnel at collapse. Since B is related to a limiting stress at tunnel collapse, it should depend on the ground strength and on the tunnel depth, as indicated by any limit analyses solution applied to shallow tunnels.

Moreover, for constant H/D and $c_u/\gamma D$ approaching infinity, Figures 6.86 to 6.88 suggest that B tends towards zero. Under these conditions, for U tending towards infinity, equation 6.18 indicates that Σ_u would tend towards an infinitely large and negative value, which indeed would

be required in such infinitely strong ground to cause its collapse. On the other hand, for H/D constant and $c_u/\gamma D$ tending to zero, Figures 6.86 to 6.88 suggest that B would tend towards infinity. Thus, for U approaching infinity, Σ_u would tend towards unity. This is again a consistent result for an extremely weak ground, which would collapse under any amount of stress release at the opening. A similar result is obtained by making $c_u/\gamma D$ constant and H/D increasing towards infinity. In this case, B would also tend to infinity and Σ_u to unity. The extremely high in situ stress in such a deep tunnel, driven through a soil of finite strength, would lead to collapse for any amount of stress release at the opening.

The coefficient A reflects the in situ stiffness of the ground. The partial derivative function of equation 6.17 is easily found as:

$$\Sigma' = \frac{\delta \Sigma}{\delta U} = \frac{A}{(A+BU)^2} \qquad [6.19]$$

in which the negative sign of the partial derivative has been dropped. For zero displacement, the slope of the NGRC is found to be equal to 1/A. In other words, the coefficient A is inversely proportional to the in situ stiffness of the ground, as reflected by the initial slope of the ground reaction curves at each point of the tunnel contour. As noted in Section 6.3.2.1, and illustrated in Figure 6.47, for a constant in situ tangent modulus profile, the initial slope of the NGRC decreases from the tunnel floor towards the crown. This result reflects the 'stiffening' action of the lower boundary, affecting the floor reaction and the

'softening' action of the free ground surface allowing the ground at the crown to move more freely towards the opening upon the stress release. The initial slope of the springline curve should thus show an intermediate initial slope. Accordingly, the coefficient A should not depend on soil strength, as it indeed does not, but should depend on the position of the ground surface, which is manifested by its dependence on H/D, as shown in Figure 6.85. Furthermore, from the above discussion one would expect to get a larger A for the crown and a smaller one for the floor, as is the case.

Besides supplying components for the prediction of the ground reaction curves, the general solution may also provide a means to estimate the degree of 'softening' of the ground around the tunnel upon the reduction of the in situ stresses. This is particularly relevant in assessing the 'current' ground stiffness to be considered in a ground-lining interaction analyses. As the support is activated after some tunnel closure has developed, the interaction process will be controlled not by the initial ground stiffness, but by that existing at the instant the lining is installed. The effect of the ground 'softening', as a result of unloading, on the ground-lining interaction process was presented and discussed in Section 2.3.5.3.

If the ground-lining interaction analysis is to be performed using a ring-and-spring model, such as reviewed in Section 4.3.2.4, one would need to know, for instance, what

radial spring constant (k_r) should be adopted to account for the non-linear response of the ground and its associated degree of ground 'softening', taking place before the support is activated. Since the stress ratio is $\Sigma=\sigma_r/\sigma_{ro}$ and $U=u_r E_{ti}/\sigma_{ro}.D$, it follows that the partial derivative of Σ is given by:

$$\Sigma' = \frac{\delta\Sigma}{\delta U} = \frac{D}{E_{ti}} \frac{\delta\sigma_r}{\delta u_r}$$

But $\delta\sigma_r/\delta u_r$ is the radial spring constant (k_r) as defined in Section 4.3.2.4. Therefore:

$$k_r = \Sigma' \frac{E_{ti}}{D}$$

Using equation 6.19, one gets:

$$k_r = \frac{A}{(A+BU)^2} \frac{E_{ti}}{D} \qquad [6.20]$$

The above equation would thus solve the posed problem, yielding different spring constants at each point (C, S, F) of the tunnel contour.

Note that if no stress release is allowed and the radial displacements are zero, equation 6.20 would reduce to a linear elastic spring. Therefore:

$$k_{ri} = \frac{1}{A} \frac{E_{ti}}{D} = \frac{1}{2A} \cdot \frac{E_{ti}}{R} \qquad [6.21]$$

It was shown in Section 4.3.2.4 that if a single average radial spring constant ($\bar{k}_r$) is to be considered, as used in most ring-and-spring models, then, for a uniform E_{ti} ground profile:

$$\bar{k}_{ri} = \left(\frac{1}{2A}\right)_{av} \frac{E_{ti}}{R} \simeq \frac{1}{1+\nu} \frac{E_{ti}}{R}$$

thus,

$$A_{av} \simeq \frac{1+\nu}{2}$$

In fact, this approximate equation is confirmed by the results shown in Figure 6.85 or Table 6.13. Depending on H/D, A_{av} is found to vary from 0.635 to 0.734, which is not entirely dissimilar to 0.745 obtained from $(1+\nu)/2$, for ν=0.49, the Poisson's ratio used in the parametric numerical analyses. For H/D increasing, A_{av} gets closer to $(1+\nu)/2$, as it should for a deep tunnel.

If the ground-lining interaction analyses is to be performed using a ring-and-plate model, such as reviewed in Section 4.3.2.3, one would need to know the current tangent Young's modulus of the ground (E_t), at the instant the support is installed. If it is assumed that this modulus is directly proportional to the spring constant (or the slope of the GRC), then:

$$\frac{E_t}{E_{ti}} = \frac{k_r}{k_{ri}}$$

Substituting equations 6.20 and 6.21 into the above, one gets:

$$E_t = \left(\frac{A}{A+BU}\right)^2 . E_{ti} \qquad [6.22]$$

Different current moduli would be found at distinct points around the tunnel contour. The available ring-and-plate solutions normally operate with constant ground modulus[17]. Thus:

$$\bar{E}_t = \left(\frac{A}{A+BU}\right)^2_{av} . \bar{E}_{ti}$$

---

[17] If a numerical ring-and-spring model with discrete beams and springs (see Section 4.3.2.4), is to be used, then different spring constants could be assigned at distinct points of the tunnel contour. This would account for the different degrees of ground 'softening' observed around the opening.

or

$$\bar{E}_t = A_{av} . \bar{\Sigma}' . \bar{E}_{ti} \simeq \frac{1+\nu}{2} \bar{\Sigma}' \bar{E}_{ti}$$

Any of the above expressions can be used to estimate the average current tangent modulus at the instant the support is activated.

It should be pointed out that the current tangent modulus given by equation 6.22 reflects a "weighted" average of all the ground mass affecting the ground response at a certain point of the tunnel contour. Therefore, it is neither equal to the modulus of the soil elements immediately adjacent to the opening nor to that of elements far away. A closer inspection of the results of the parametric analyses, revealed that the moduli given by equation 6.22, for a certain point of the tunnel contour, correspond approximately to the current tangent moduli of elements located radially away from the contour, at distances varying from 0.25D to 0.65D. The magnitude of this distance was found to vary according to the tunnel depth H/D and, to a lesser degree, to the amount of stress release.

As a reasonable approximation, it may be said that the moduli derived from equation 6.22 for the tunnel crown and floor, are nearly equal to the moduli of elements located, respectively, at half diameter above and below the tunnel. The springline modulus also corresponds to the modulus of an element situated at about D/2 radially measured from that point.

As stated earlier the solution presented is strictly valid only within the ranges of the variables considered in the numerical analyses that supplied the data for the generalization. Although apparently unbounded, equation 6.17 may not be valid for large amounts of stress release (or low Σ). Large dimensionless displacements U may involve ground failure. The numerical model used to develop the present solution does not represent this behaviour properly and all data obtained after this event were disregarded in the generalization process. In fact, for large displacements, the solution presented can furnish values of the stress ratio Σ that may violate the failure criteria. This subject will be discussed in Section 6.5.

6.4.3 Cohesionless Soil Model

It was mentioned in Section 6.3.2.2 that for a given cover to diameter ratio, the NGRCs of each point of the tunnel contour, for different friction angles, are nearly homothetic. This can be demonstrated considering, for example, the results shown in Figure 6.63 (crown, K_o=0.8, H/D=3.0). Assume that the origin of the NGRCs, point O, defined by the stress release α=1-Σ=0 and the dimensionless displacement U=0, is the centre of similitude. As for the frictionless soil model (Section 6.4.2), draw through O an arbitrary axis, OP. Point P can be taken, for instance, as the point on the curve for ϕ=40° corresponding to α=0.7 (Σ=0.3). The line OP will intersect the NGRC for ϕ=20° and

30° at points M and N. The coordinates of these points (a_{ref}, U_{ref}) are indicated in Table 6.14. Use these coordinates as reference values and normalize each NGRC in Figure 6.63 to each respective reference value. Replot the numerical results in terms of the normalized coordinates, $1 - a/a_{ref}$ and U/U_{ref}. The curves in Figure 6.63 would thus be transformed into Figure 6.89. The preferred new ordinate variable, λ, is defined as:

$$\lambda = 1 - \frac{a}{a_{ref}} = 1 - \frac{1-\Sigma}{1-\Sigma_{ref}} = \frac{\Sigma-\Sigma_{ref}}{1-\Sigma_{ref}} \qquad [6.23]$$

Note that once the results of the numerical analyses for ϕ=20°, 30° and 40°, are twice normalized as explained, a series of points are obtained and it seems possible to fit a single curve through them. The twice normalized ground reaction curves (NNGRC) are almost coincident (Points M, N and P, of course, coincide), and this confirms that the original NGRCs (Figure 6.63) are nearly homothetic.

Repeating the above process to the NGRCs of the tunnel springline and floor shown in Figures 6.64 and 6.65, then the twice normalized points of the ground reaction curves shown in Figures 6.90 and 6.91, respectively, are obtained. The reference values (points M, N, P in Figures 6.64 and 6.65) used for normalizing the numerical resullts are also shown in Table 6.14. Note that the ratios a_{ref}/U_{ref} shown represent the slope of the arbitrary axes OP used in the reduction process. As was seen for the tunnel crown, the twice normalized points of the springline and floor seem arranged in such a way that a single curve can be well

Position	ϕ (°)	a_{ref}	U_{ref}	$\frac{a_{ref}}{U_{ref}}$	P_1	P_2	P_3	P_4	P_5
Crown	20	0.390	0.3911						
	30	0.540	0.5415	0.9972	0.5055	0.4191	2.8752	3.6904	6.8780
	40	0.700	0.702						
Springline	20	0.290	0.2552						
	30	0.490	0.4312	1.1364	0.4197	0.5380	3.4339	2.6640	14.5739
	40	0.700	0.6160						
Floor	20	0.400	0.1990						
	30	0.440	0.2189	2.0101	0.7328	0.2234	3.8938	-3.9446	15.8681
	40	0.490	0.2438						

Table 6.14 Parameters Used and Obtained in the Reduction of the Twice Normalized Ground Reaction Curves of a Tunnel with H/D=3, for the Cohesionless Soil Model with K_o=0.8

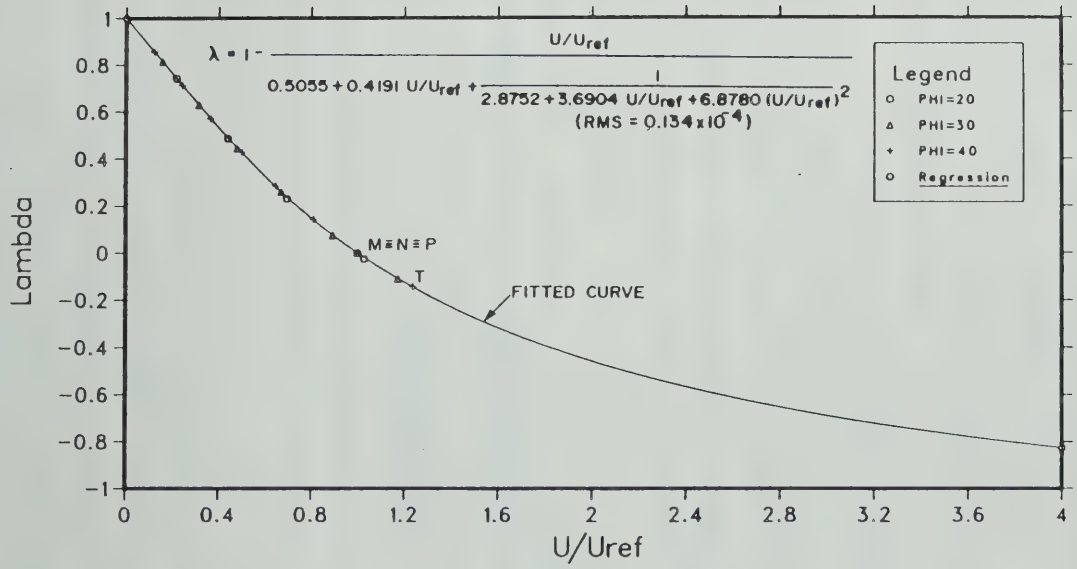

Figure 6.89 Twice Normalized Ground Reaction Curve (NNGRC) for the Crown of a Tunnel with H/D=3, for the Cohesionless Soil Model with K_o=0.8

fitted through them. Some points appear to deviate slightly from the fitted curve, but, for all practical purposes it can be said that all NGRC at different points of the tunnel contour for different friction angles, seem to be very close to homothetic, as single (but distinct) normalized NGRCs can be found for each of these points.

The next step undertaken was to define what function fits best the points shown in the last three figures. Hyperbolae such as were used to fit the data from the frictionless soil model (equation 6.16) did not yield good results. The main reason for this was that this function could not accommodate the apparent inflexion noted in the early part of the curve for the floor (See Figure 6.91) and to a lesser extent, for the crown. It has been mentioned in other sections in this chapter that, when K_o is smaller than unity, elements of the ground at the crown and floor exhibit a stiffening response, resulting from the stress changes that occur at those points (an increase in the minor principal stress). Once the direction of the principal stresses are fully changed, the ground response is again that of softening, as for the springline. A hyperbola could not, therefore, fit this response, as its derivative function is monotonic and does not show a change in sign in its second derivative.

On the other hand, it seemed reasonable to assume that the suitable function should have a definable limit, which is approached monotonically, as in the case of a hyperbola.

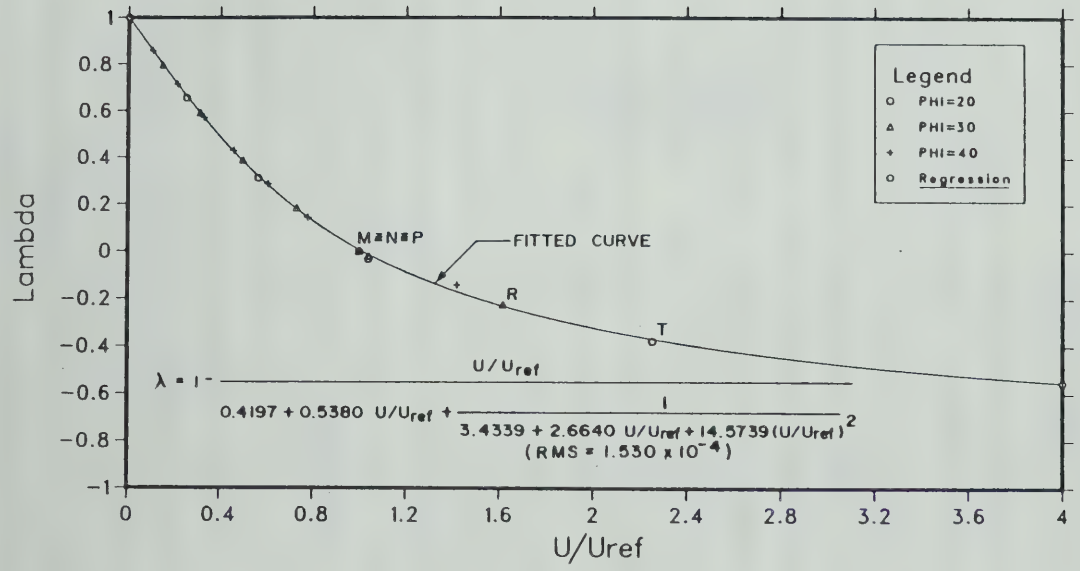

Figure 6.90 Twice Normalized Ground Reaction Curves (NNGRC) for the Springline of a Tunnel with H/D=3, for the Cohesionless Soil Model with K_o=0.8

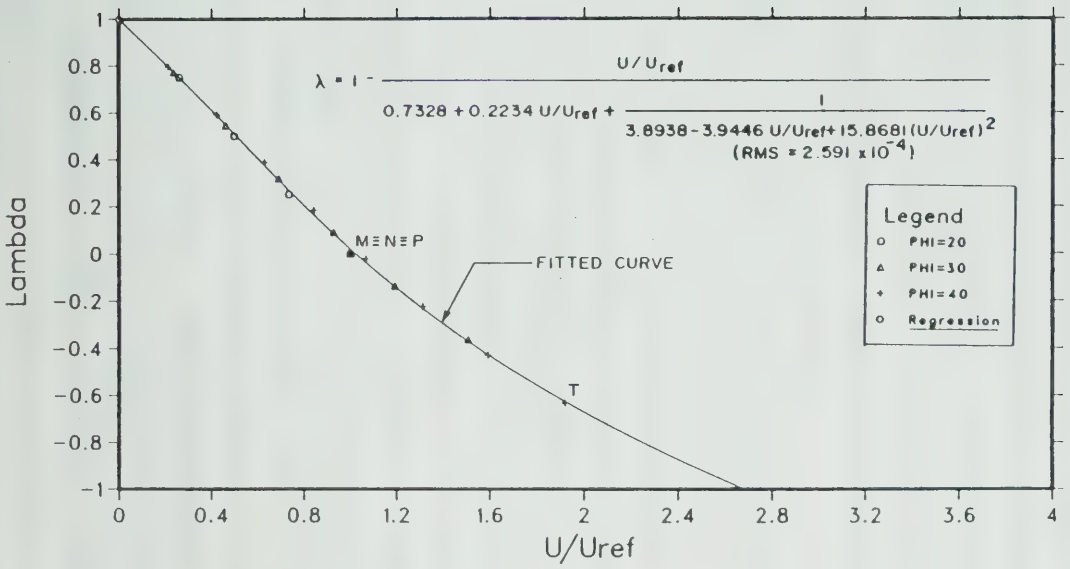

Figure 6.91 Twice Normalized Ground Reaction Curves (NNGRC) for the Floor of a Tunnel with H/D=3, for the Cohesionless Soil Model with K_o=0.8

In other words, it seems reasonable to assume that a collapse radial stress exists at each point of the tunnel contour, which is approached asymptotically upon large displacements.

Moreover, it was decided to select a single function type, that would fit the normalized numerical results found at the three points of the tunnel contour in all of the cases covered in the parametric analyses.

Six types of functions were thoroughly investigated and tested to best fit the requirements. Making $\sigma/\sigma_{ref}=y$ and $U/U_{ref}=x$, these functions were the following:

a) $y = x/(P_1 + P_2x + P_3e^{P_4x}$

b) $y = x/(P_1 + P_2x + P_3e^{P_4+P_5x+P_6x^2}$

c) $y = x/(P_1 + P_2x + P_3(P_4+x)^{P_5}.e^{P_6(P_4+x)})$

d) $y = x/(P_1 + P_2x + (1/(P_3+P_4x)))$

e) $y = x/(P_1 + P_2x + (1/(P_3+P_4x+P_5x^2+P_6x^3)))$

f) $y = x/(P_1 + P_2x + (1/(P_3+P_4x+P_5x^2)))$

To test these functions, a non-linear least-squares regression technique was used, where the unknown parameters, P_i, were allowed to vary, to establish a 'best-fit' through the known pair of data (x,y). This was accomplished using the computer program BMDP3R, Non-linear Regression (Revised Version, October, 1983), which is part of a statistical package developed at the University of California. Besides the data set with the (x,y) pairs, the program requires the function to be described by FORTRAN statements as well as the function partial derivatives of the function with

respect to the parameters, P_i.

Some numerical difficulties were found for certain sets of data (especially for the floor), when applying the program to those functions including exponential terms, a, b and c (floating point overflows and exponential errors). The investigations therefore were concentrated on functions d, e and f above. Visual inspection of the fitted curves on the numerical data revealed that function f was the best fit for all sets of data tested (basically all cases analysed for H/D=1.5).

Besides the visual inspection, a comparative analysis of the quality of the fitting for the different functions can be made through the residual mean square calculated by the program (Torgerson, 1986). This index is defined as:

$$RMS = \frac{\text{Residual Sum of Squares}}{\text{Degrees of Freedom}} = \frac{\Sigma(y - q)^2}{(N-p)}$$

where y is the observed value of the dependent variable, q is the evaluation of the function, N is the total number of samples (x,y) and p is the total number of independent parameters (P_i) in the function. The function fitting the data best would furnish the lowest RMS value. Through this criterion it was confirmed that function f provided the best fitting of the numerical results. Accordingly function f was selected and used to fit all normalized numerical data. This function expresses the twice normalized ground reaction curve as:

$$\lambda = 1 - \frac{a}{a_{ref}} = 1 - \frac{1-\Sigma}{1-\Sigma_{ref}}$$

$$= 1 - \frac{U/U_{ref}}{P_1 + P_2 U/U_{ref} + 1/(P_3 + P_4 U/U_{ref} + P_5 (U/U_{ref})^2} \qquad [6.24]$$

The parameters P_i (i=1,5) for the crown, springline and floor of a tunnel with H/D=3, and K_o=0.8 are shown in Table 6.14, and the equation of the best fitted curves for these points are reproduced in Figures 6.89 to 6.91.

The above procedure was repeated to all cases analysed and the results of these reduction process are summarized in Tables 6.15, 6.16 and 6.17, for K_o=0.6, 0.8 and 1.0 respectively. In all cases ,the RMS varied between 10^{-3} to 10^{-5}. All normalized numerical results and corresponding best fitted curves are included in Appendix D. There is not a reference value for RMS that would allow an assessment of the goodness of fit in absolute terms. The RMS is usually interpreted in relative terms, for comparitive purposes. However, one can appreciate that quite satisfactory fitting was obtained in all cases.

At this stage, one notes that the equations for the NNGRC's have been derived for each point of the tunnel contour, for each H/D and K_o, and are independent of the friction angle. The dependence on ϕ is represented by the different a_{ref} or U_{ref} values associated with each friction angle. But this dependence can be expressed separately. The relationships between the slope of the arbitrary axes a_{ref}/U_{ref} used in the transformation process, and the depth ratio H/D (note that this slope is constant for any ϕ value) can be expressed separately.

Position	H/D	ϕ (°)	α_{ref}	U_{ref}	$\frac{\alpha_{ref}}{U_{ref}}$	P_1	P_2	P_3	P_4	P_5	RMS/10^{-4}
Crown	6	20	0.183	0.1552							
		30	0.365	0.3095	1.1792	0.7863	0.1643	5.8485	-0.9192	15.2721	0.162
		40	0.500	0.4240							
	3	20	0.183	0.1605							
		30	0.365	0.3285	1.1111	0.7592	0.1959	5.5995	-1.8853	18.2108	0.052
		40	0.500	0.4500							
	1.5	20	0.183	0.1856							
		30	0.365	0.3701	0.9862	0.5830	0.3175	2.9017	1.5671	5.6173	0.094
		40	0.500	0.5070							
Springline	6	20	0.130	0.1072							
		30	0.296	0.2267	1.3055	0.3270	0.5378	2.2039	1.3714	4.4509	6.923
		40	0.500	0.3830							
	3	20	0.130	0.1070							
		30	0.296	0.2261	1.3089	0.3262	0.5428	2.3007	1.1162	4.9612	8.026
		40	0.500	0.3820							
	1.5	20	0.130	0.1064							
		30	0.296	0.2250	1.3158	0.3173	0.5517	2.2334	1.0538	5.0694	7.602
		40	0.500	0.3800							
Floor	6	20	0.150	0.0765							
		30	0.210	0.1071	1.9608	0.7550	0.0791	4.2389	-2.7928	4.6785	4.452
		40	0.300	0.1530							
	3	20	0.150	0.0765							
		30	0.210	0.1071	1.9608	0.8201	0.0558	6.3141	-6.6624	8.7052	4.021
		40	0.300	0.1530							
	1.5	20	0.150	0.0770							
		30	0.210	0.1078	1.9481	0.8312	0.0476	6.4333	-5.5703	7.8069	3.749
		40	0.300	0.1540							

Table 6.15 Parameters Used and Obtained in the Reduction of the Twice Normalized Ground Reaction Curves for the Frictionless Soil Model and for K_o=0.6

Position	H/D	ϕ (°)	a_{ref}	U_{ref}	$\frac{a_{ref}}{U_{ref}}$	P_1	P_2	P_3	P_4	P_5	RMS/10^{-4}
Crown	6	20	0.39	0.3655							
		30	0.54	0.5061	1.0671	0.5480	0.3849	3.0527	2.9276	9.9043	0.415
		40	0.70	0.6560							
	3	20	0.39	0.3911							
		30	0.54	0.5415	0.9972	0.5055	0.4191	2.8752	3.6904	6.8780	0.134
		40	0.70	0.7020							
	1.5	20	0.39	0.4350							
		30	0.54	0.6200	0.8589	0.5052	0.4630	3.6081	5.5775	17.3331	0.356
		40	0.70	0.8150							
Springline	6	20	0.29	0.2548							
		30	0.49	0.4305	1.1382	0.4223	0.5317	3.4086	3.2167	12.6102	1.413
		40	0.70	0.6150							
	3	20	0.29	0.2552							
		30	0.49	0.4312	1.1364	0.4197	0.5380	3.4339	2.6640	14.5739	1.530
		40	0.70	0.6160							
	1.5	20	0.29	0.2569							
		30	0.49	0.4340	1.1290	0.4096	0.5500	3.4225	2.1201	15.7848	1.732
		40	0.70	0.6200							
Floor	6	20	0.40	0.1990							
		30	0.44	0.2189	2.0101	0.7230	0.2316	3.5999	-2.8499	14.5303	2.476
		40	0.49	0.2438							
	3	20	0.40	0.1990							
		30	0.44	0.2189	2.0101	0.7328	0.2234	3.8938	-3.9446	15.8681	2.591
		40	0.49	0.2438							
	1.5	20	0.40	0.1980							
		30	0.44	0.2178	2.0202	0.7171	0.2256	3.6040	-2.8964	11.6415	3.048
		40	0.49	0.2426							

Table 6.16 Parameters Used and Obtained in the Reduction of the Twice Normalized Ground Reaction Curves for the Frictionless Soil Model and for K_o=0.8

Position	H/D	ϕ (°)	a_{ref}	U_{ref}	$\frac{a_{ref}}{U_{ref}}$	P_1	P_2	P_3	P_4	P_5	RMS/10^{-4}
Crown	6	20	0.38	0.4418							
		30	0.58	0.6743	0.8602	0.4274	0.5208	4.2706	4.9524	9.1674	0.925
		40	0.80	0.9300							
	3	20	0.38	0.4774							
		30	0.58	0.7286	0.7960	0.4097	0.5446	4.4999	5.3435	10.7461	1.247
		40	0.80	1.0050							
	1.5	20	0.38	0.5700							
		30	0.58	0.8700	0.6667	0.3575	0.6118	5.1904	5.6765	17.2042	2.966
		40	0.80	1.2000							
Springline	6	20	0.38	0.3596							
		30	0.58	0.5488	1.0568	0.4416	0.4977	4.0454	5.6946	6.1024	0.637
		40	0.80	0.7570							
	3	20	0.38	0.3610							
		30	0.58	0.5510	1.0526	0.4484	0.5015	4.6854	3.7948	10.6789	0.803
		40	0.80	0.7600							
	1.5	20	0.38	0.3672							
		30	0.58	0.5604	1.0349	0.4207	0.5227	4.0515	4.5578	8.2557	0.799
		40	0.80	0.7730							
Floor	6	20	0.38	0.2755							
		30	0.58	0.4205	1.3793	0.4323	0.5090	4.0270	5.0692	7.6430	0.741
		40	0.80	0.5800							
	3	20	0.38	0.2707							
		30	0.58	0.4132	1.4035	0.4574	0.4914	4.3206	4.2243	10.4066	0.717
		40	0.80	0.5700							
	1.5	20	0.38	0.2655							
		30	0.58	0.4053	1.4311	0.4258	0.4880	3.2546	4.6773	3.4674	0.454
		40	0.80	0.5590							

Table 6.17 Parameters Used and Obtained in the Reduction of the Twice Normalized Ground Reaction Curves for the Frictionless Soil Model and for K_o=1.0

The same development applied to the frictionless soil model (Section 6.4.2) for assessing the changes in the ground stiffness with the reduction of the in situ stresses can be applied here. The partial derivative of λ with respect to $U/U_{ref}(\lambda')$ can be related to a 'current' ground spring constant (k_r), that could be used in ring-and-spring models to analyse the ground-lining interaction developing once the support is installed, after a certain amount of stress release. Recalling equation 6.23 and the definitions of the stress ratio, $\Sigma=\sigma_r/\sigma_{ro}$, and of the dimensionless displacement, $U=u_r E_{ti}/\sigma_{ro}.D$, it can be demonstrated that:

$$\lambda' = \frac{\delta\lambda}{\delta U/U_{ref}} = \frac{U_{ref}}{a_{ref}} \frac{D}{E_{ti}} \frac{\delta\sigma_r}{\delta u_r}$$

Since $\delta\sigma_r/\delta u_r$ is equal to k_r, then

$$k_r = \frac{a_{ref}}{U_{ref}} \frac{E_{ti}}{D} \lambda' \qquad [6.25]$$

On the other hand, λ' can be obtained by differentiating equation 6.24

$$\lambda' = \frac{\delta\lambda}{\delta U/U_{ref}} = [P_1 + P_2\frac{U}{U_{ref}} + 1/(P_3 + P_4\frac{U}{U_{ref}} + P_5\frac{U^2}{U^2_{ref}})]^{-1} -$$

$$\frac{U}{U_{ref}}.[P_1 + P_2\frac{U}{U_{ref}} + 1/(P_3 + P_4\frac{U}{U_{ref}} + P_5\frac{U^2}{U^2_{ref}})]^{-2} \times$$

$$[P_2 - (P_4 + 2P_5\frac{U}{U_{ref}}).(P_3 + P_4\frac{U}{U_{ref}} + P_5\frac{U}{U_{ref}})^{-2}] \qquad [6.26]$$

in which the negative sign of the derivative has been dropped.

Knowing the parameters, P_i (i=1,5) and the reference values a_{ref} and U_{ref} (Tables 6.15 to 6.17), it is possible to define, using equation 6.24 the amount of stress release a associated with a certain dimensionless displacement U.

Moreover, with equations 6.25 and 6.26, the radial spring constant corresponding to U, can also be determined.

If instead, a ring-and-plate model is to be used for the ground-lining interaction analysis, one would need to know the current tangent modulus of the ground (E_t), rather than the spring constant. If it is assumed that this modulus is directly proportional to the spring constant (or the slope of the GRC), then:

$$\frac{E_t}{E_{ti}}=\frac{k_r}{k_{ri}}$$

and, from equation 6.25:

$$E_t = \frac{\lambda'}{\lambda'_i}.E_{ti} \qquad [6.27]$$

remembering that a_{ref}/U_{ref}, E_{ti} and D are constant for a particular tunnel situation. Note that λ'_i is the derivative of λ for zero stress release at the opening.

Distinct current moduli (or current spring constants) would be found for the crown, springline and floor. The available ring-and-plate models operate with a constant ground modulus. Hence an operational modulus could be considered by averaging the moduli at those points of the tunnel contour (the springline modulus being counted twice). This modulus would then be (for a uniform E_{ti} ground profile):

$$\bar{E}_t = \left[\frac{\lambda'}{\lambda'_i}\right]_{av} E_{ti} \qquad [6.28]$$

The value of the partial derivative of λ for zero stress release, λ'_i, is obtained by setting U=0 in equation 6.26. It represents the initial slope of the NNGRC and therefore is related to the in situ tangent modulus of the

ground. Thus:

$$\lambda'_1 = \frac{1}{P_1 + 1/P_3} \qquad [6.29]$$

The equations furnished above, together with the data summarized in Tables 6.15 to 6.17, represent the proposed solution for obtaining the ground reaction curves or stress release functions for three points of the tunnel contour of a shallow tunnel, in a soil represented by the cohesionless model as indicated by equation 6.11. Although these results could be easily programmed for calculations, it seems convenient to have them presented in form of charts. Accordingly, Figures 6.92 to 6.99 were prepared and represent the complete solution for K_o=0.6. This sequence of charts is described below.

Figure 6.92 furnishes the ratio of α_{ref}/U_{ref} or $(1-\Sigma_{ref})/U_{ref}$ as a function of the relative depth of the tunnel. It was mentioned earlier that this ratio does not depend on ϕ. As it is noted in Table 6.15, the reference values for the amount of stress release, α_{ref} or $(1-\Sigma_{ref})$, were selected for the reduction process in such a way as to make them independent of H/D. They resulted in depending on the friction angle ϕ only. Figure 6.93 shows how that reference value varies with ϕ, expressed here through the function:

$$m-1=\frac{1+\sin\phi}{1-\sin\phi} - 1 = \frac{2\sin\phi}{1-\sin\phi} \qquad [6.30]$$

Note that (m-1) is the ratio of stress difference to minor principal stress at failure that appears in equation 6.2. With Figure 6.92 and 6.93, one can get U_{ref} for K_o=0.6 and

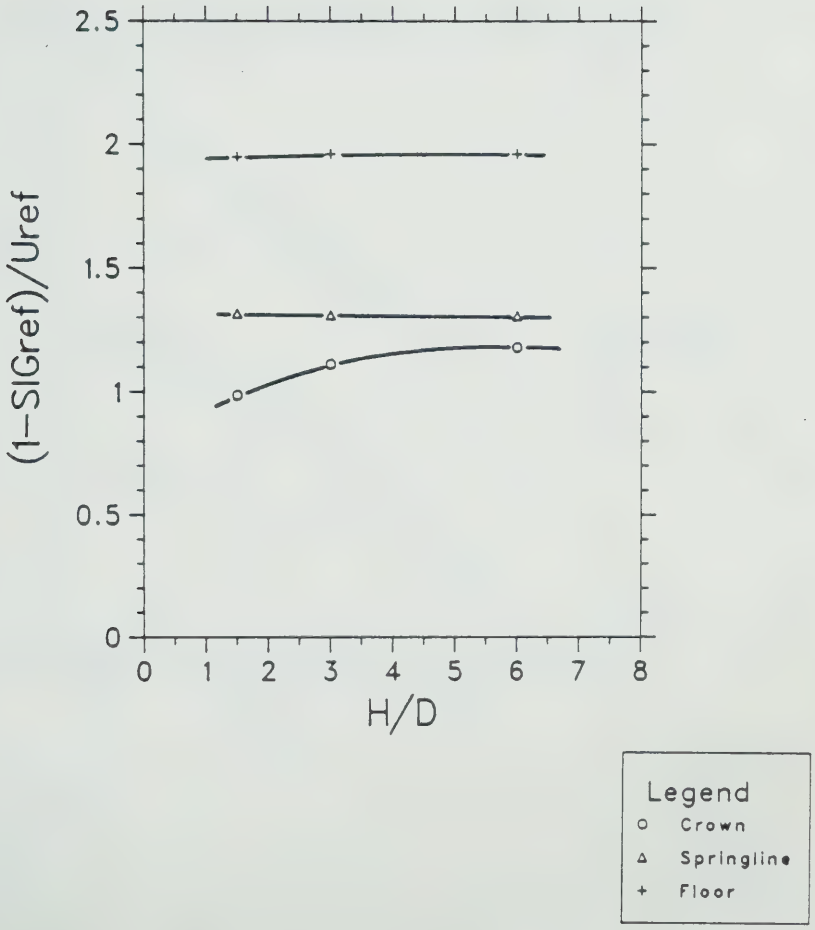

Figure 6.92 Slope of the Arbitrary Axes used to Obtain the NNGRC, Represented as a Function of H/D, for K_o=0.6

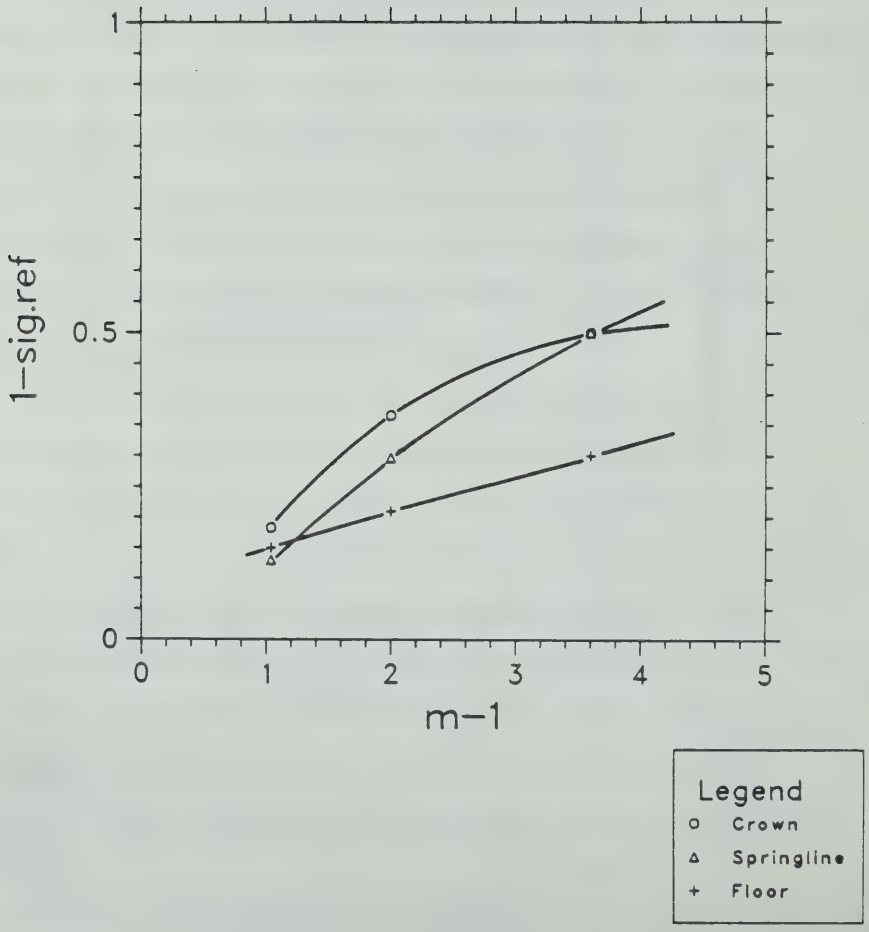

Figure 6.93 Relationships between α_{ref} and the Friction Angle for K_o=0.6

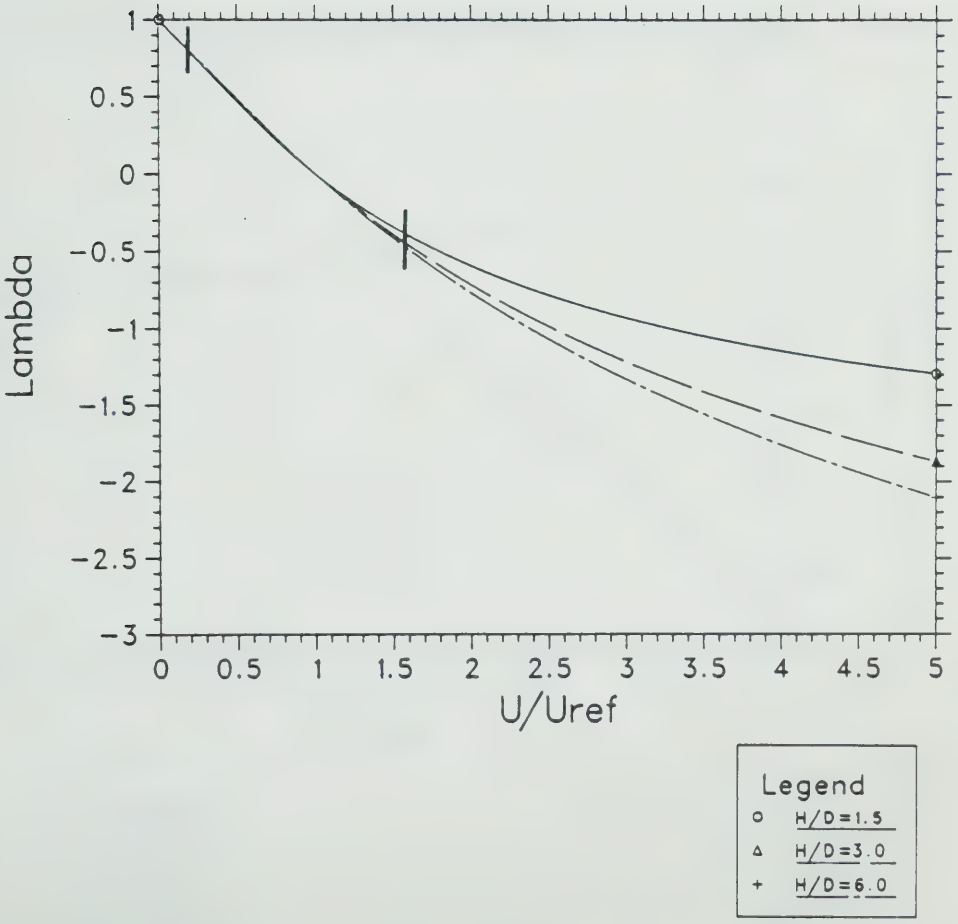

Figure 6.94 Twice Normalized Ground Reaction Curves for Tunnel Crown Calculated for K_o=0.6

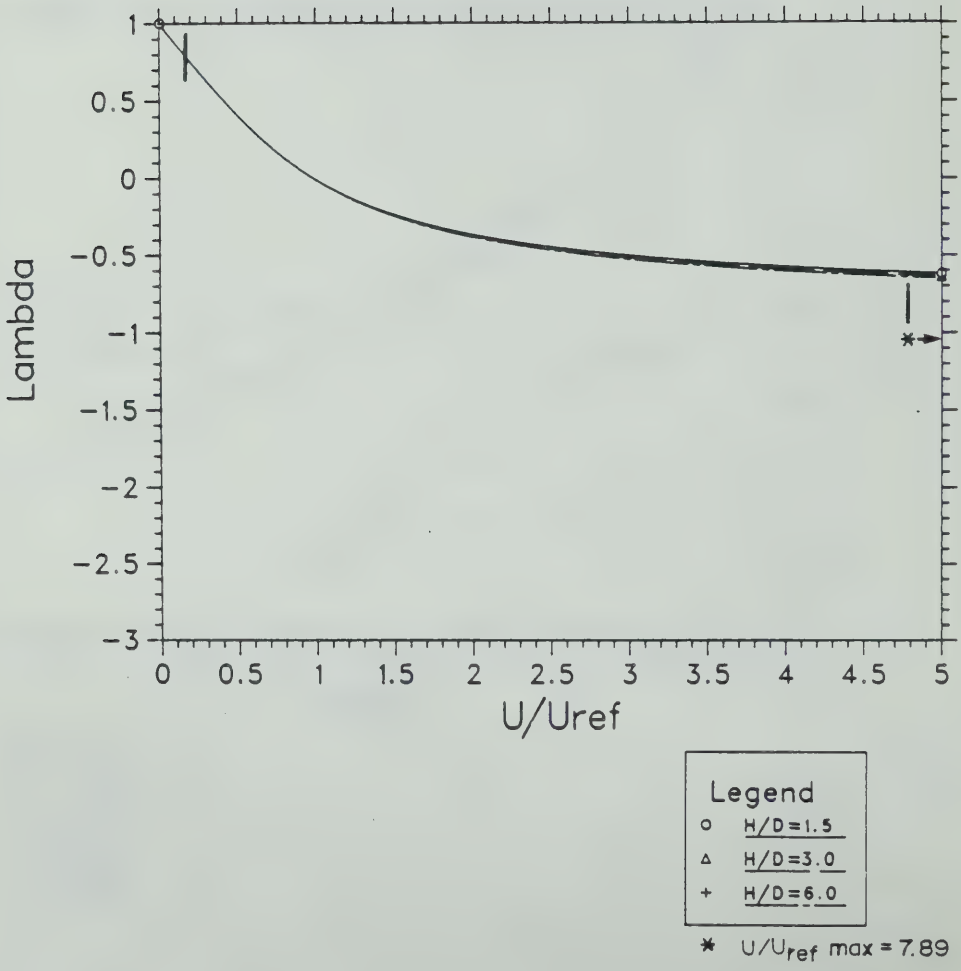

Figure 6.95 Twice Normalized Ground Reaction Curves for the Tunnel Springline, Calculated for K_o=0.6

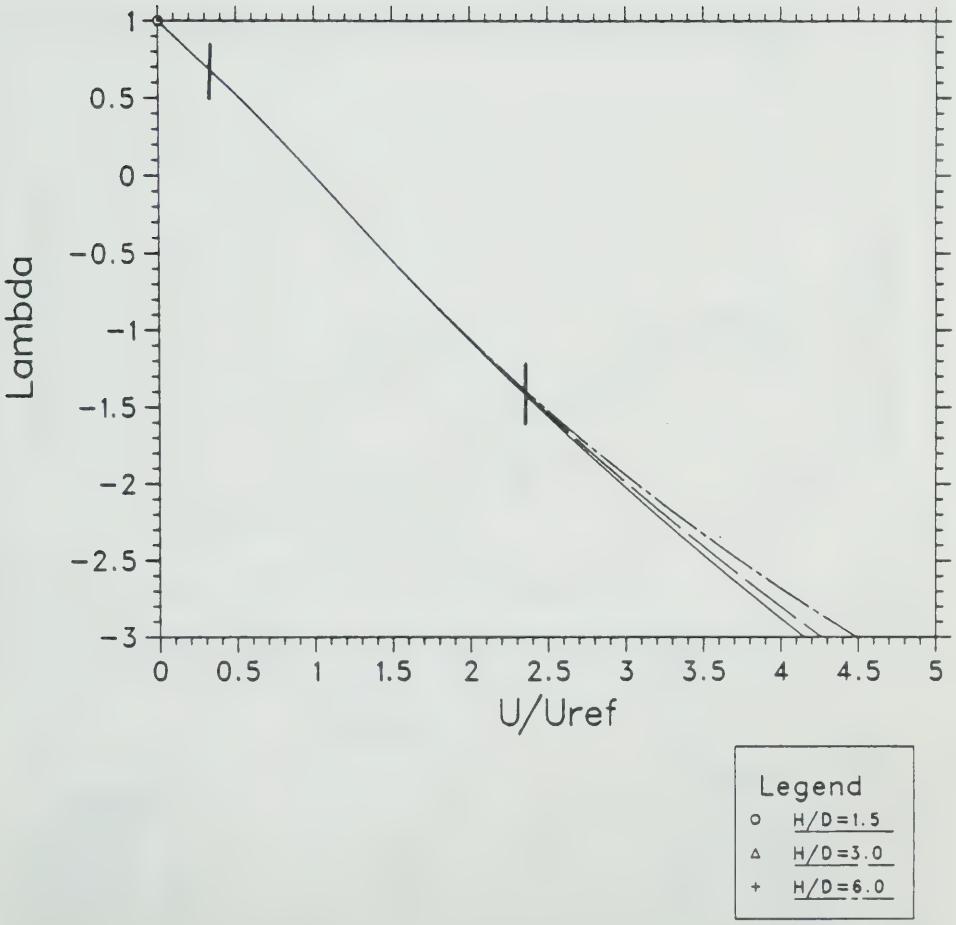

Figure 6.96 Twice Normalized Ground Reaction Curves for the Tunnel Floor, Calculated for K_o=0.6

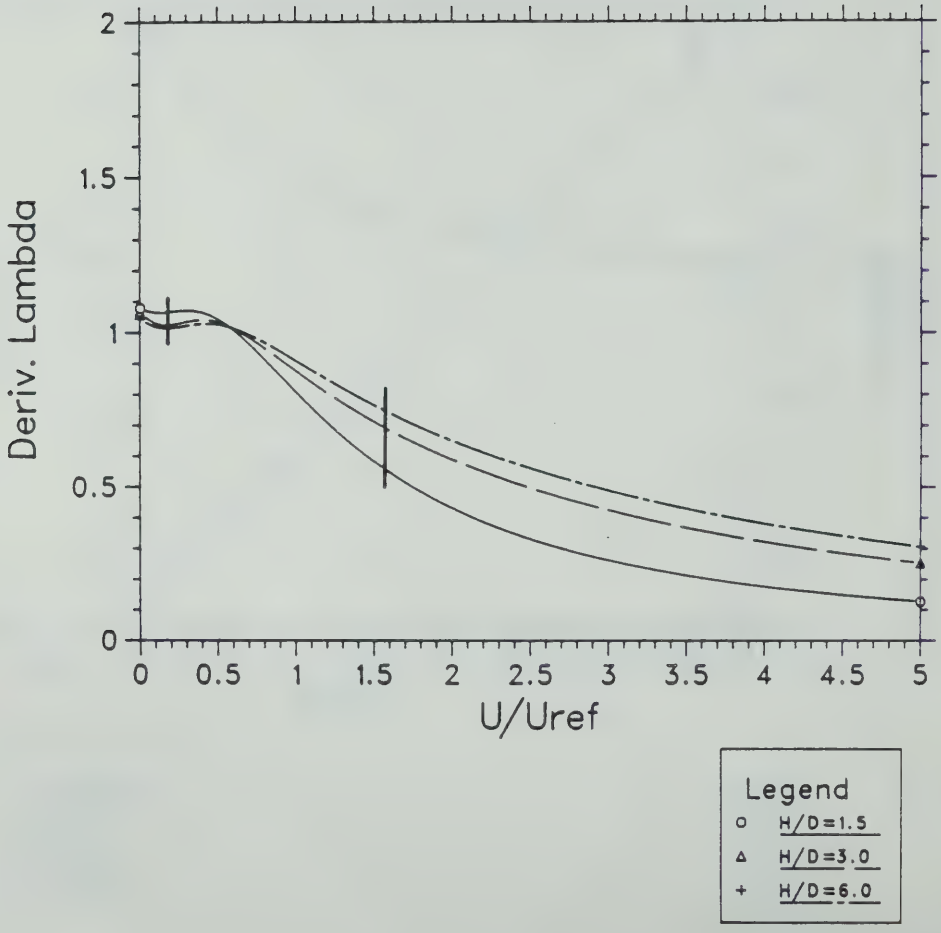

Figure 6.97 Variations of λ' for the Tunnel Crown, Calculated for K_o=0.6

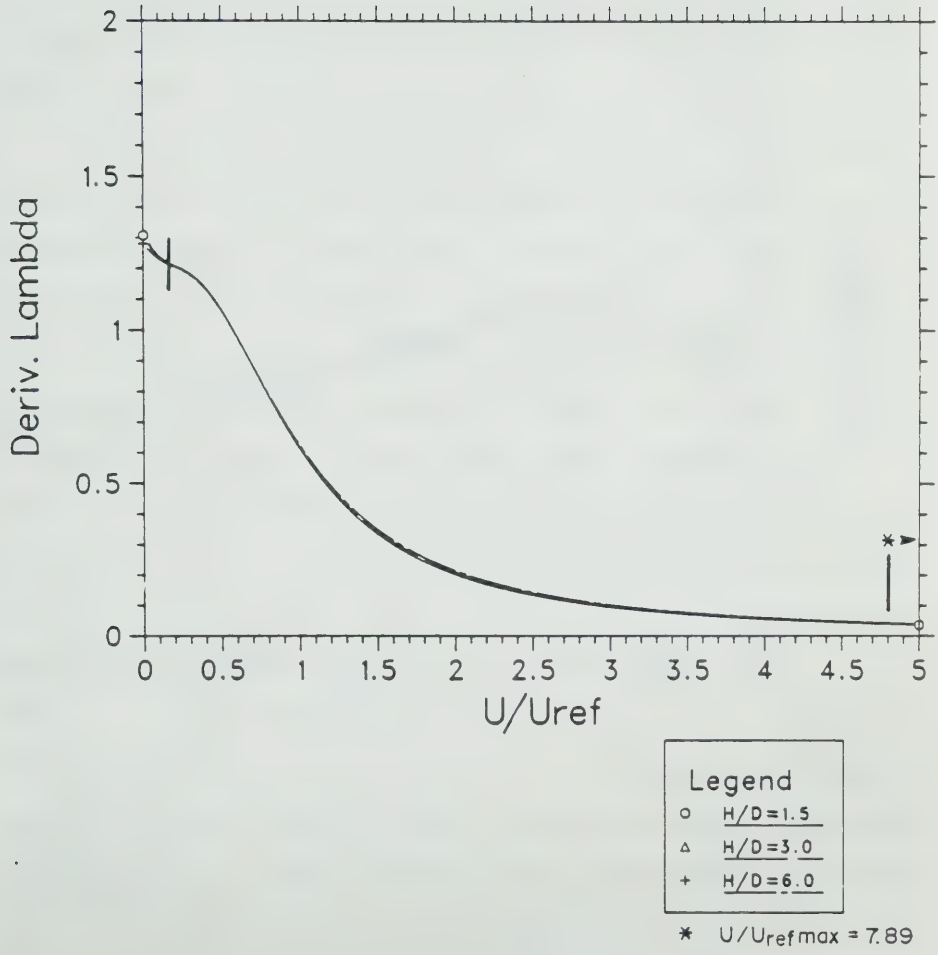

Figure 6.98 Variations of λ' for the Tunnel Springline, Calculated for K_o=0.6

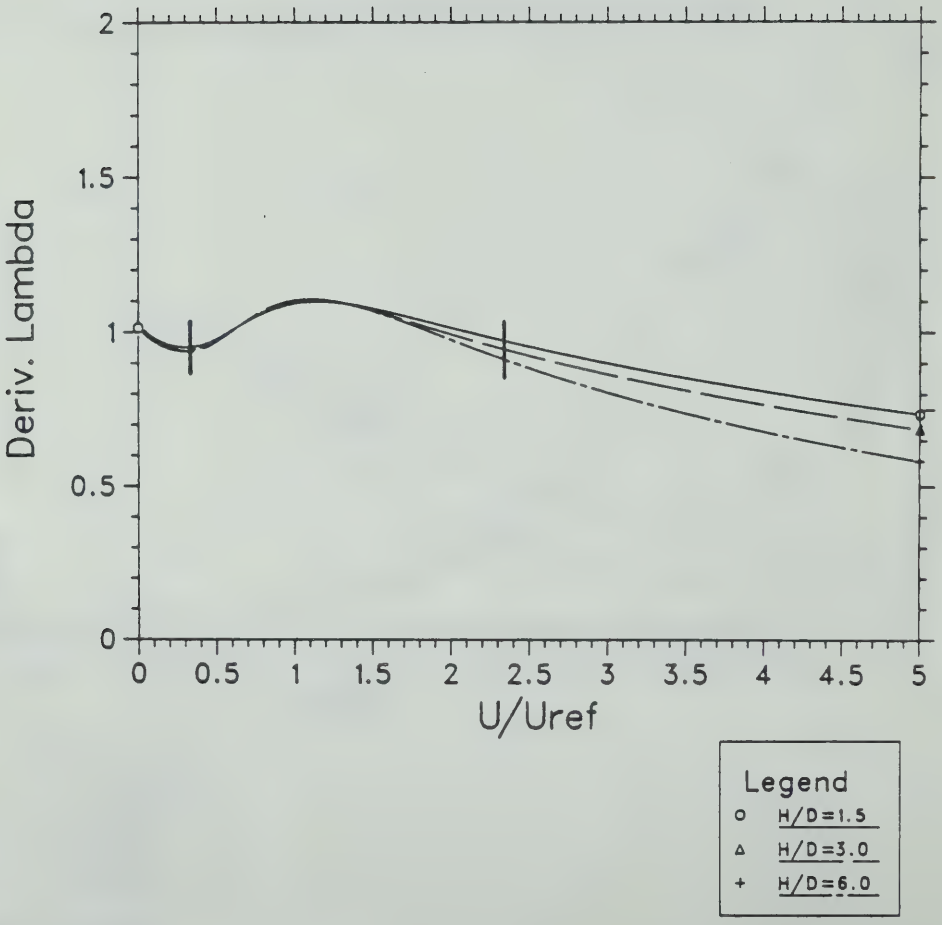

Figure 6.99 Variations of λ' for the Tunnel Floor, Calculated for K_o=0.6

for any H/D and ϕ covered by the parametric analyses.

Figures 6.94 to 6.96 present the twice normalized ground reaction curves (NNGRC) for K_o=0.6, calculated for the tunnel crown, springline and floor, respectively. Note that in each of these figures, the NNGRCs for distinct ratios of H/D have been plotted together. With the exception of the crown, the NNGRC's virtually coincide. This tends to indicate that the effect of H/D is more pronounced at the crown than elsewhere. By understanding this, it seems quite feasible to interpolate data between the curves and to estimate NNGRCs for tunnel depth ratios other that those considered in the parametric analyses. Figure 6.95 indicates that for K_o=0.6, failure at the springline is approached more rapidly for U/U_{ref} increasing than at the other two points of the tunnel contour. The short vertical lines intersecting the NNGRCs in the last three figures delimit the regions where numerical data were available and through which the curves were fitted. The portions of the curves to the right of these regions represent extrapolations of the numerical results. The validity of the functions beyond the region delimited can not be assured. Although the assumption that the fitting functions have always an asymptote and that a good fitting of the numerical results was achieved, there is not the assurance that the extrapolated results can correctly portray the ground behaviour upon large displacements. This subject will be discussed further in the following section.

Figures 6.97 to 6.99 represent equation 6.26 and they provide relationships between the first partial derivative of λ and U/U_{ref}, (λ'), that are needed to assess either the current spring constants through equation 6.25 or the current tangent moduli of the ground through equation 6.27. Note that the values of λ'_i (equation 6.29) can be obtained from these curves by setting U/U_{ref} equal to zero. The last three figures were plotted like the NNGRCs and the same comments made regarding the latter curves are also applicable here. The initial rises in the λ' curves for the crown and floor reflect the 'stiffening' response of the ground noted during the early part of the unloading process.

A similar sequence of charts were prepared for K_o=0.8 (Figures 6.100 to 6.107) and for K_o=1.0 (Figures 6.108 to 6.115). The suite of plots just described represent the proposed generalized solution (equation 6.11) that can be used to estimate both the amount of stress release and the stiffness of the ground after a certain closure of the opening. The solution was formulated in a discrete form for H/D and K_o and this may require interpolation of data for intermediate depth ratios and in situ stress ratio. For instance, this could be done graphically, through the charts given. Figure 6.116, for example, presents a chart for obtaining the initial slope of the NNGRC, λ'_i, for intermediate in situ stress ratios or depth ratios.

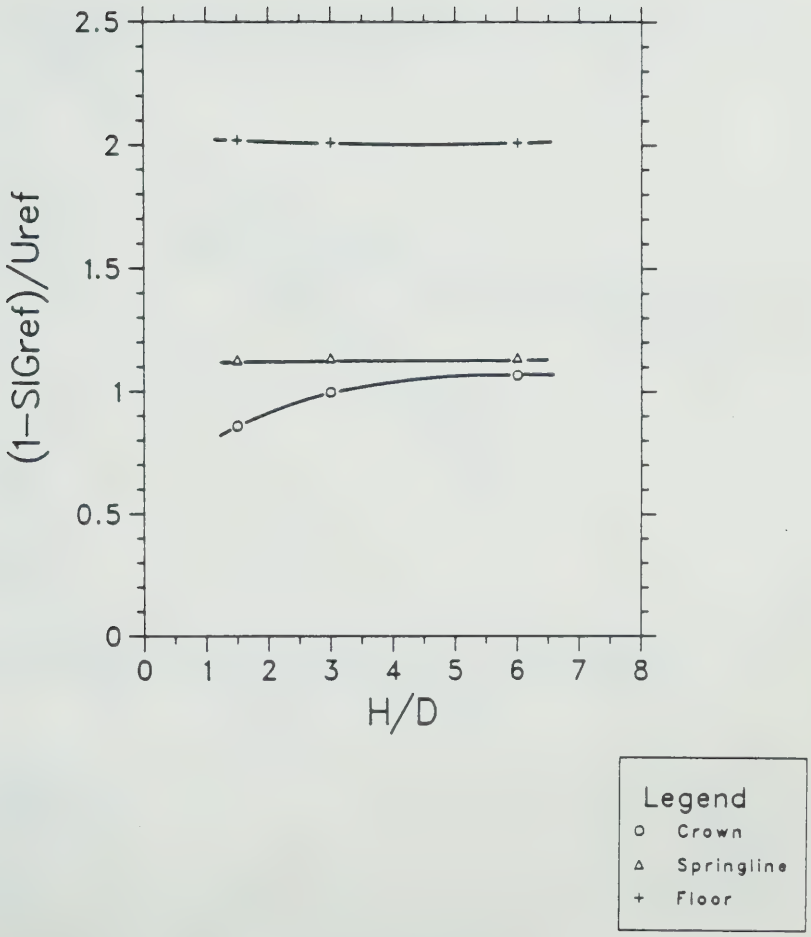

Figure 6.100 Slopes of the Arbitrary Axes used to Obtain the NNGRC Represented as a Function of H/D, for K_o=0.8

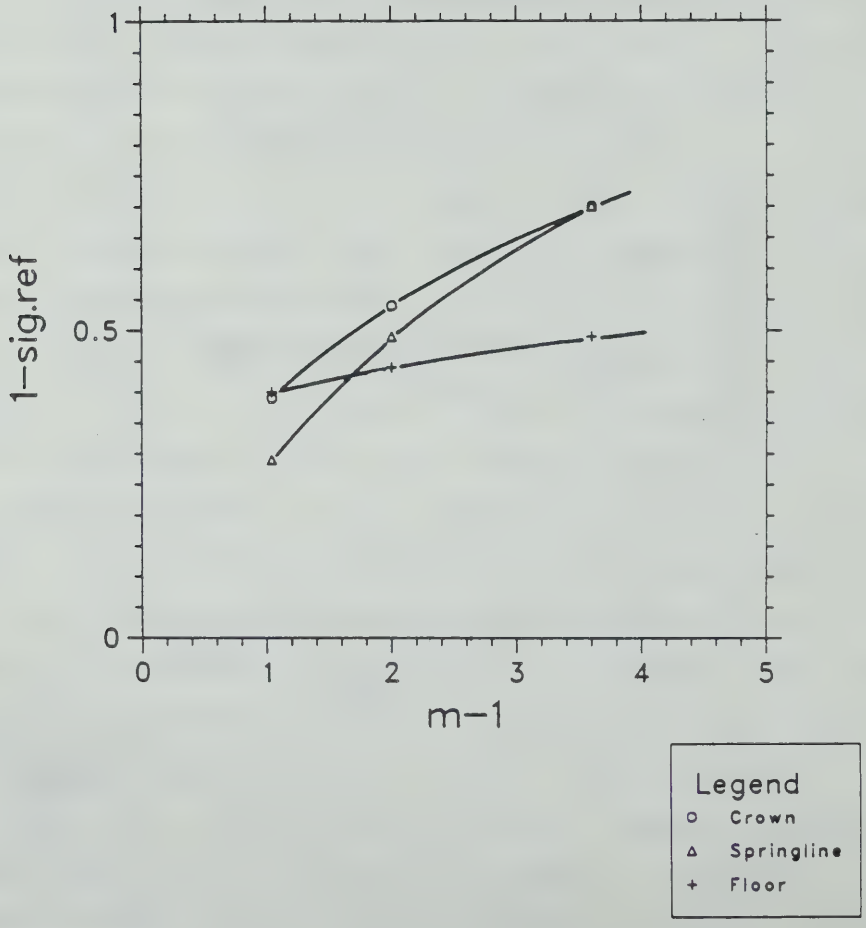

Figure 6.101 Relationships between a_{ref} and the Friction Angle of K_o=0.8

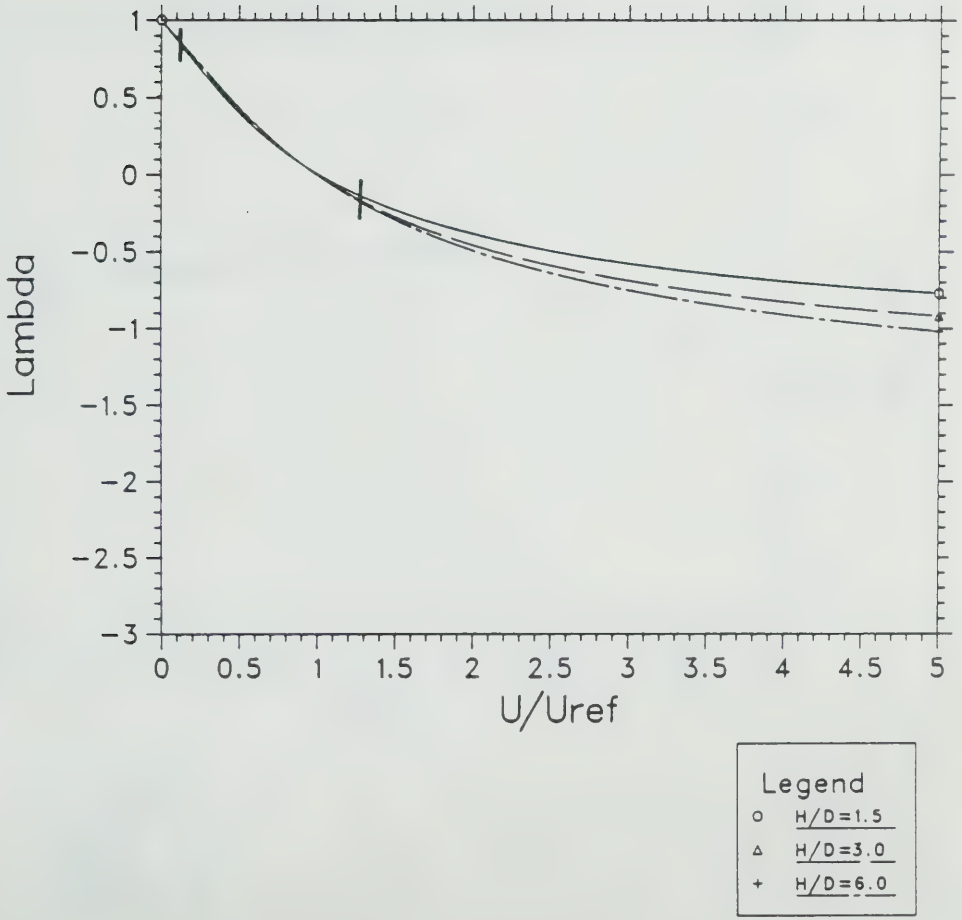

Figure 6.102 NNGRCs for Tunnel Crown, Calculated for K_o=0.8

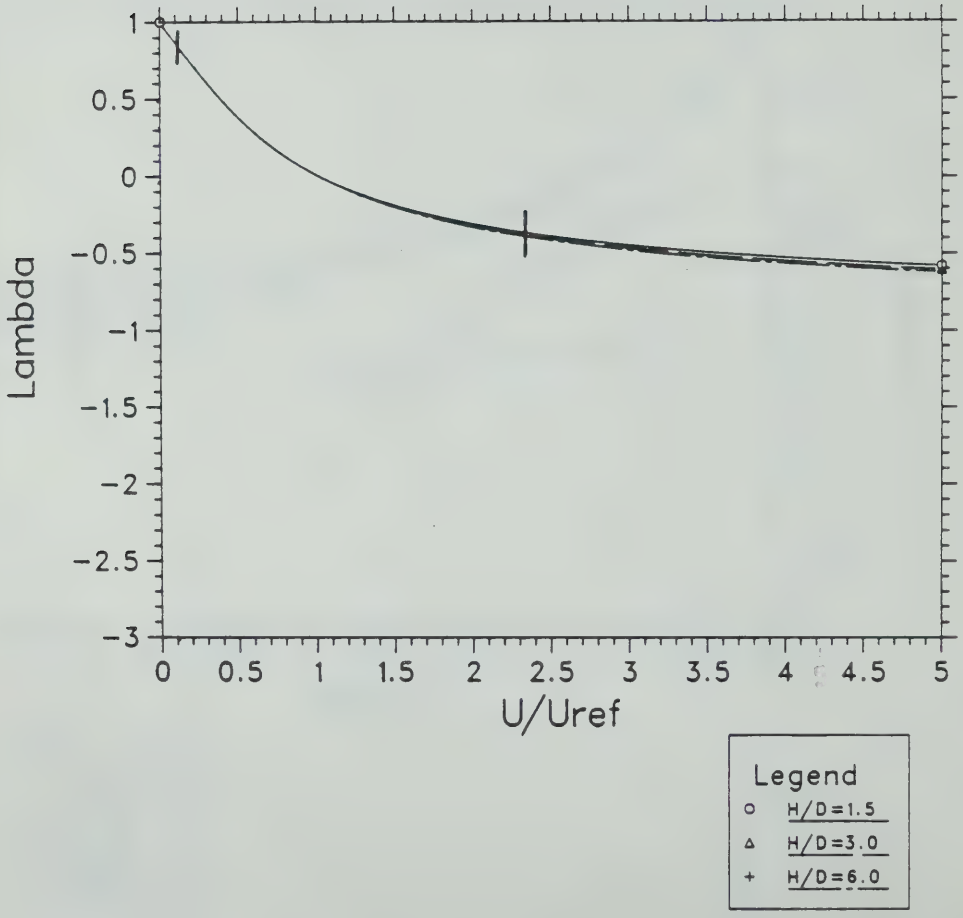

Figure 6.103 NNGRCs for Tunnel Springline, Calculated for K_o=0.8

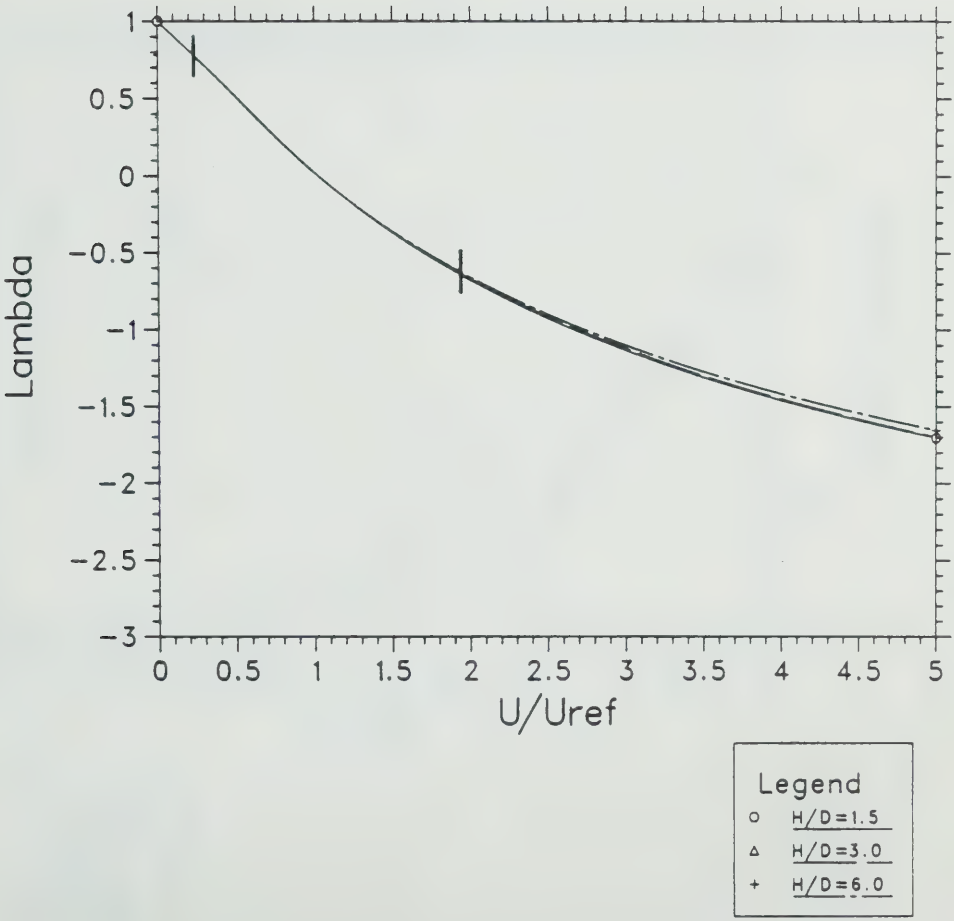

Figure 6.104 NNGRCs for Tunnel Floor, Calculated for K_o=0.8

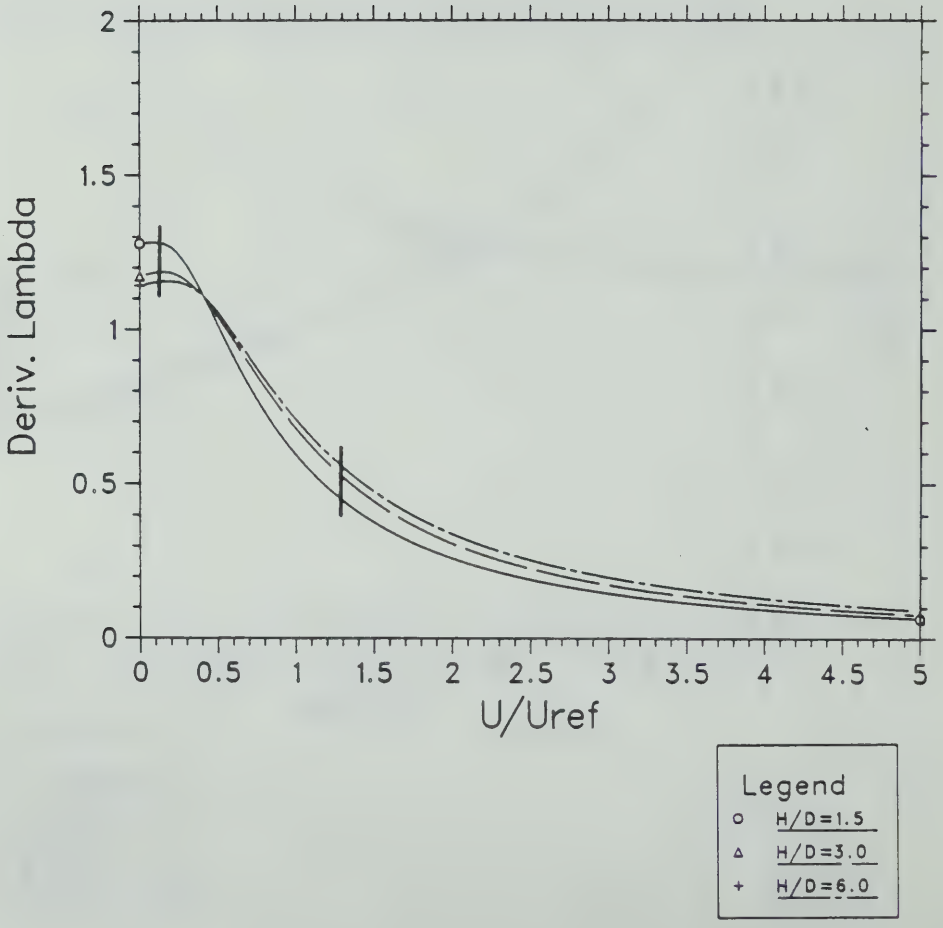

Figure 6.105 Variations of λ' for the Tunnel Crown, Calculated for K_o=0.8

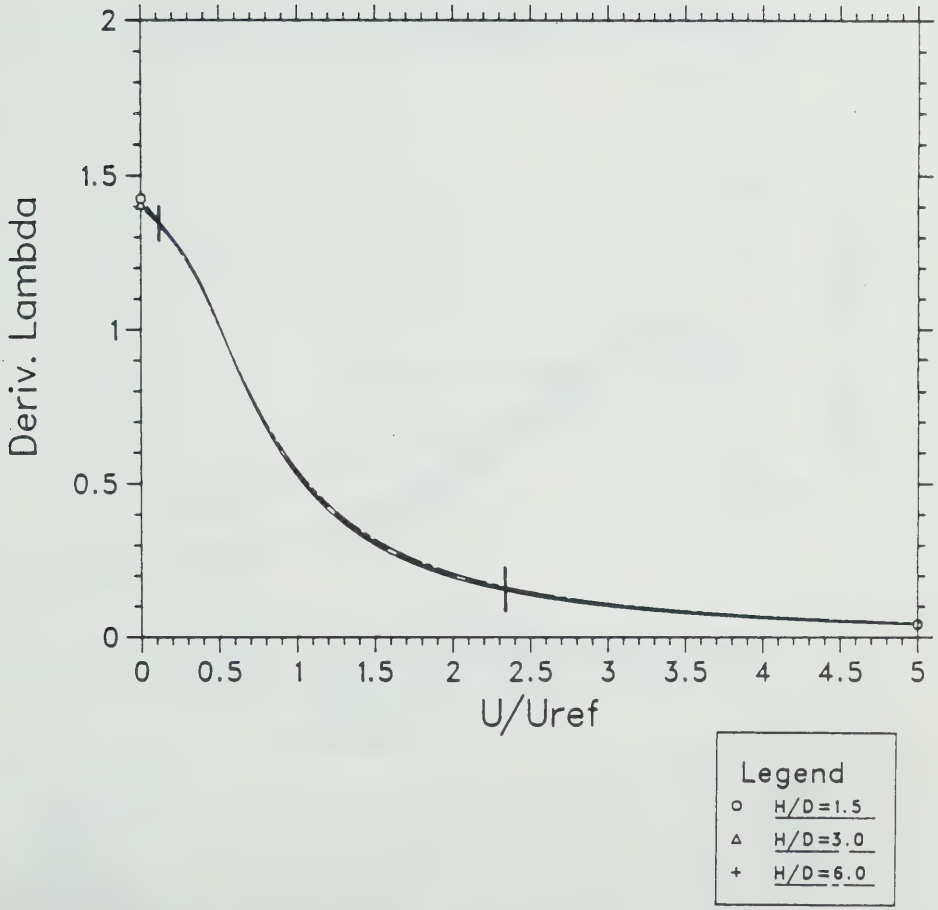

Figure 6.106 Variations of λ' for the Tunnel Springline, Calculated for K_o=0.8

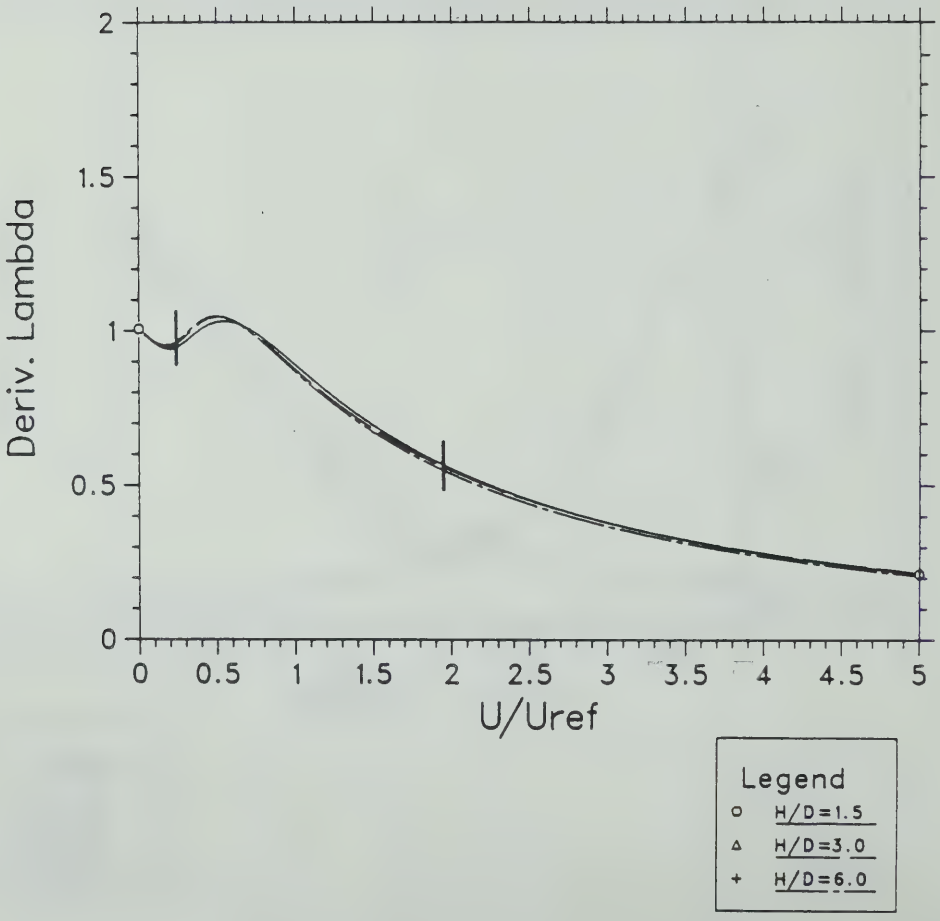

Figure 6.107 Variations of λ' for the Tunnel Floor, Calculated for K_o=0.8

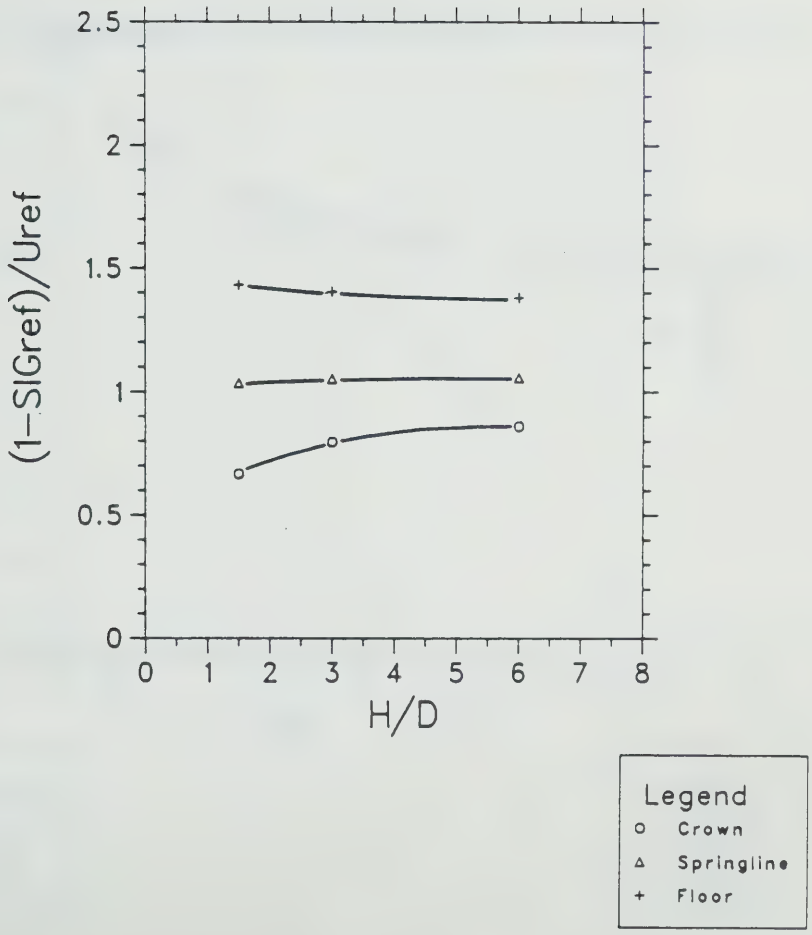

Figure 6.108 Slopes of the Arbitrary Axes used to Obtain the NNGRC Presented as a Function of H/D, for K_o=1.0

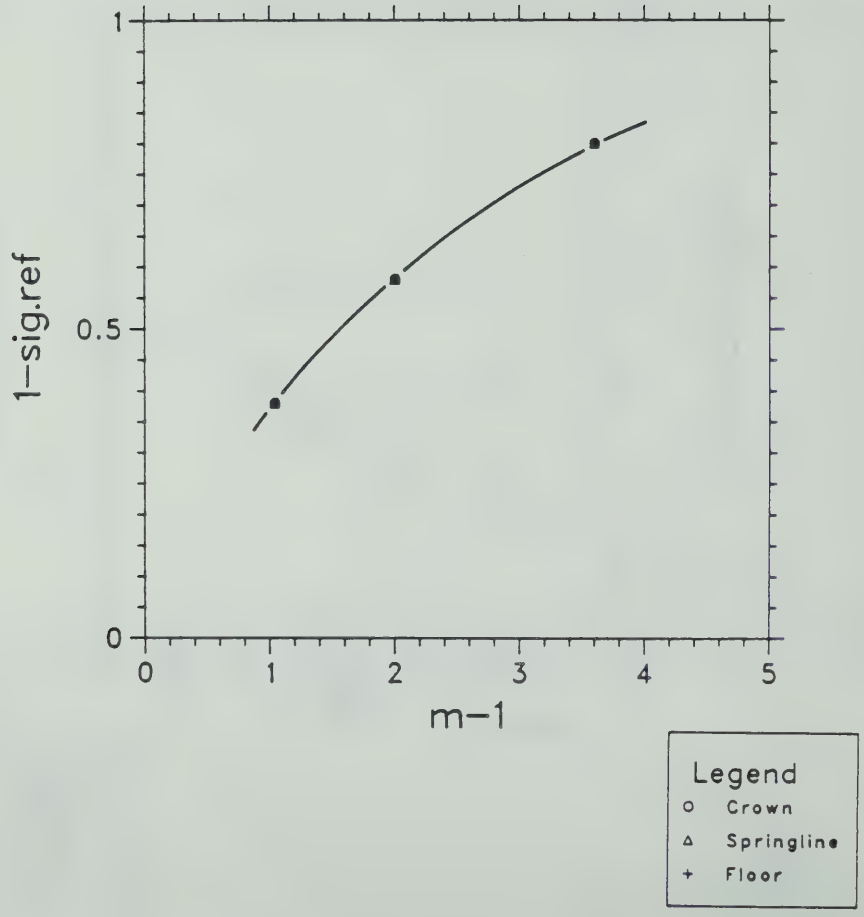

Figure 6.109 Relationships between a_{ref} and the Friction Angle for K_o=1.0

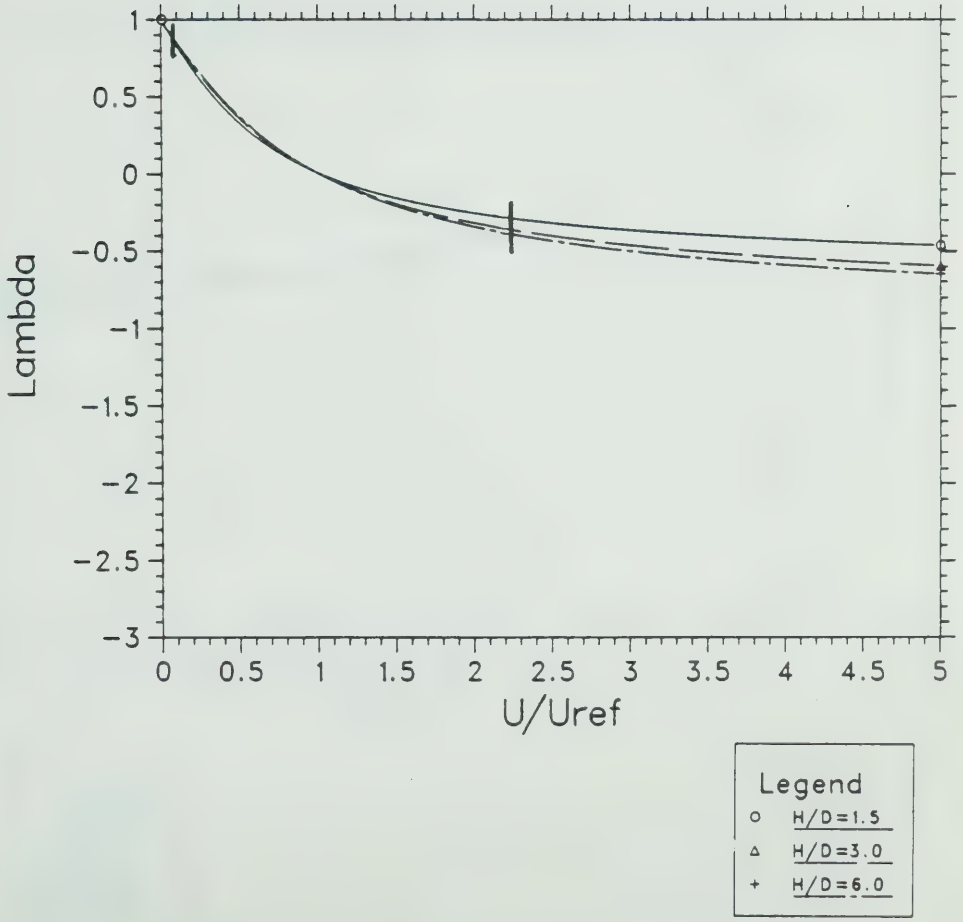

Figure 6.110 NNGRCs for Tunnel Crown, Calculated for K_o=1.0

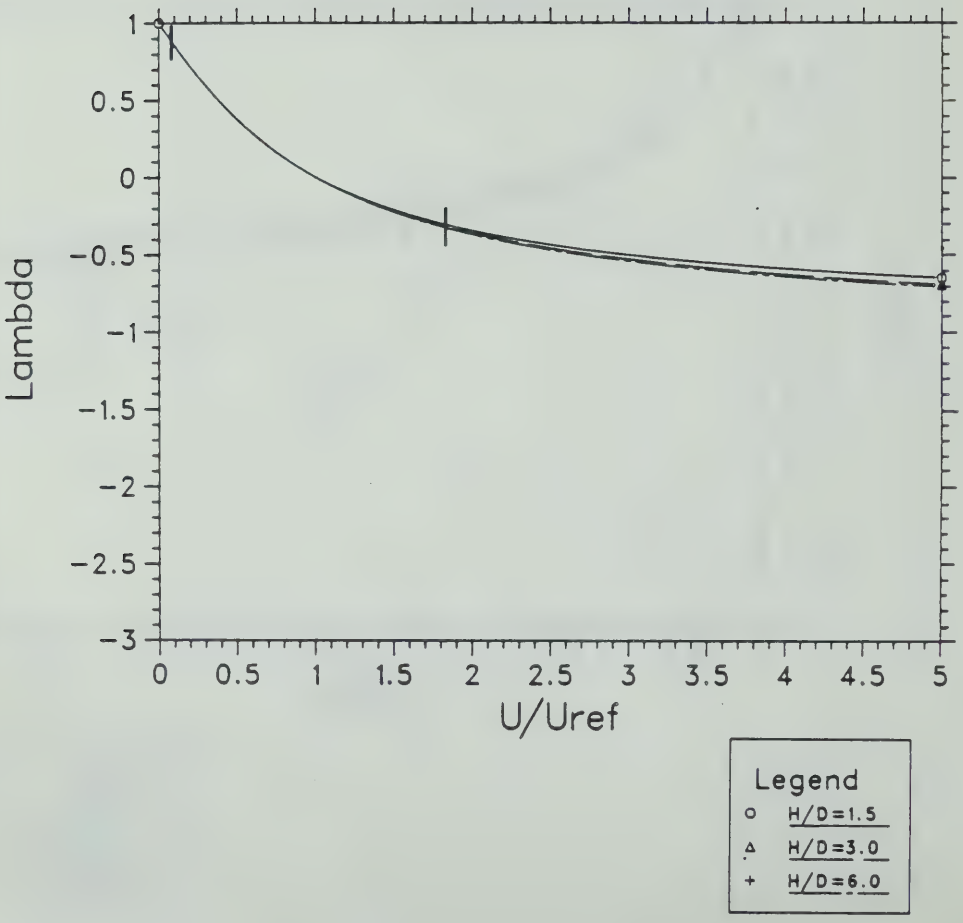

Figure 6.111 NNGRCs for Tunnel Springline, Calculated for K_o=1.0

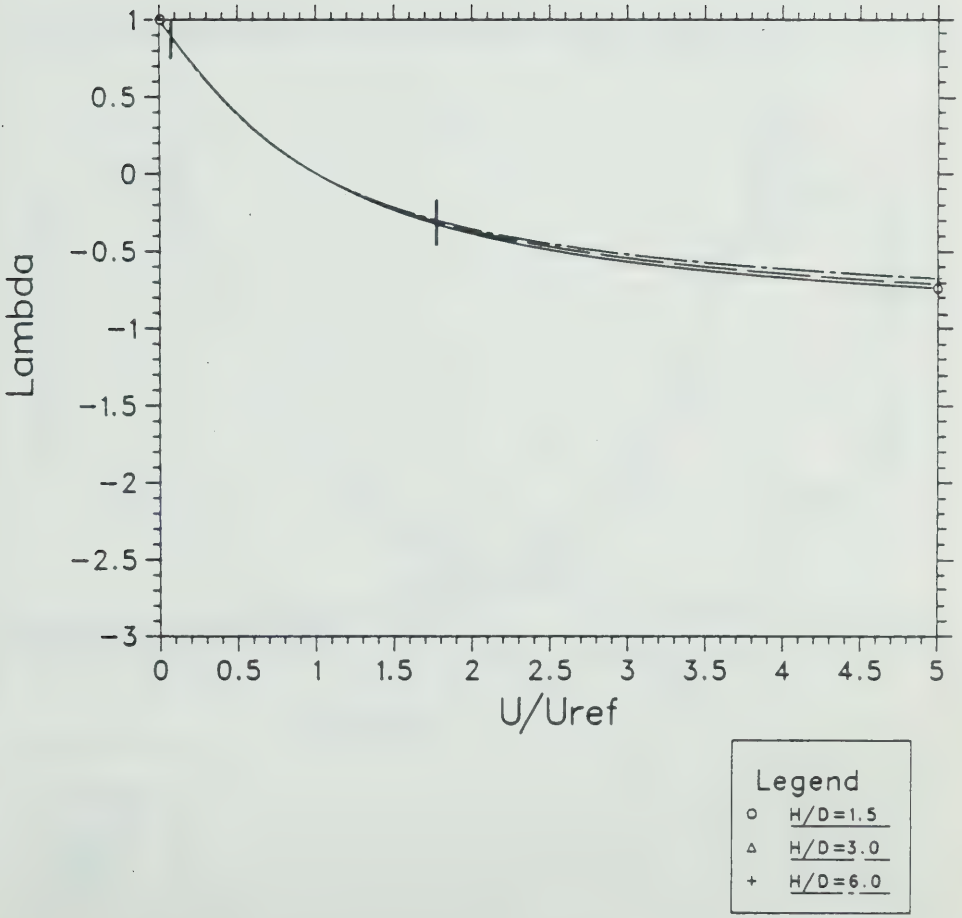

Figure 6.112 NNGRCs for Tunnel Floor, Calculated for K_o=1.0

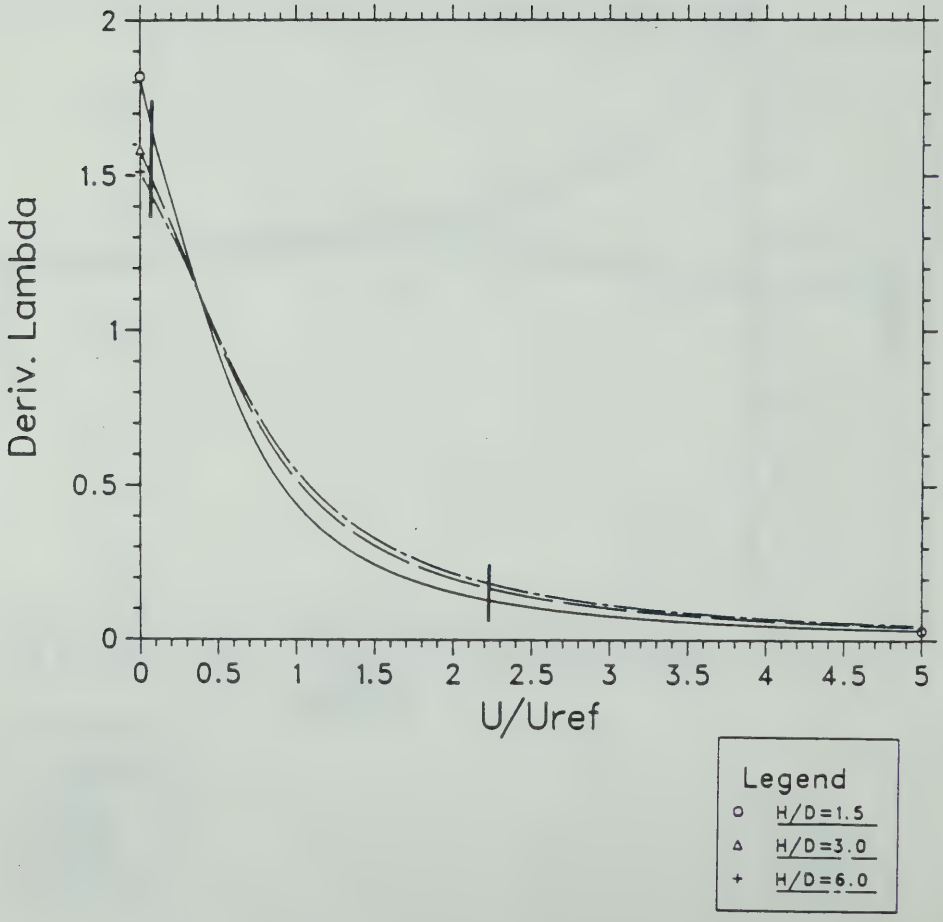

Figure 6.113 Variations of λ' for the Tunnel Crown, Calculated for K_o=1.0

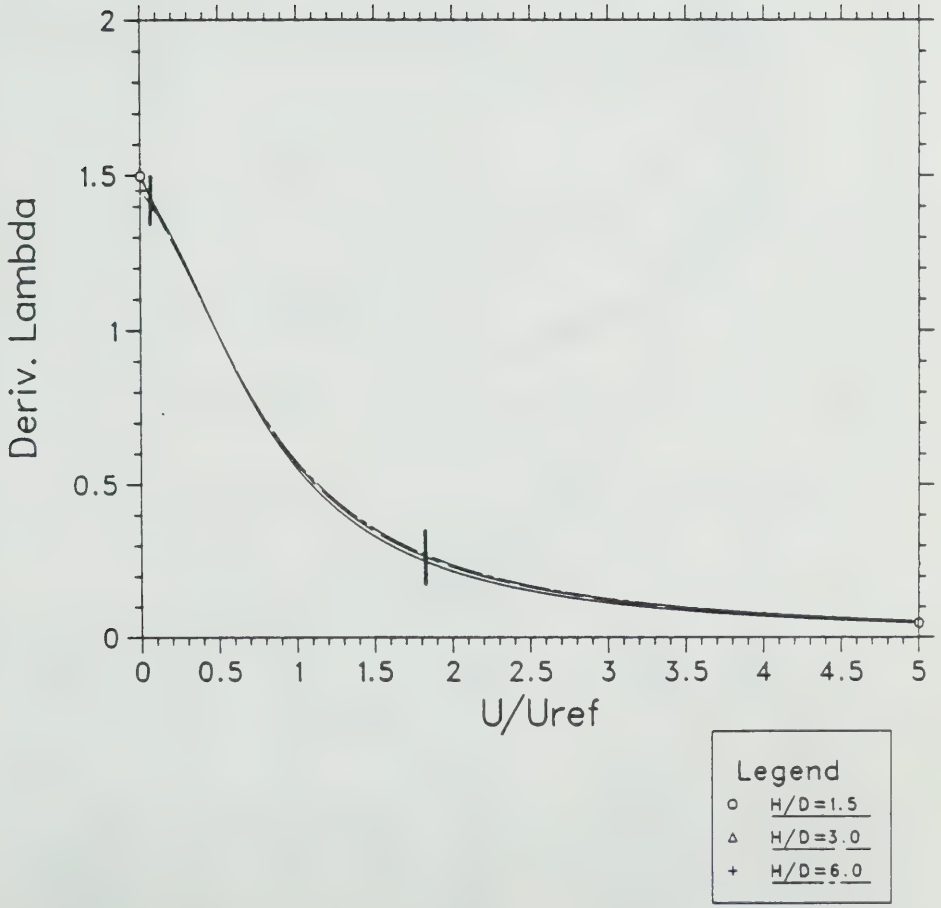

Figure 6.114 Variations of λ' for the Tunnel Springline, Calculated for K_o=1.0

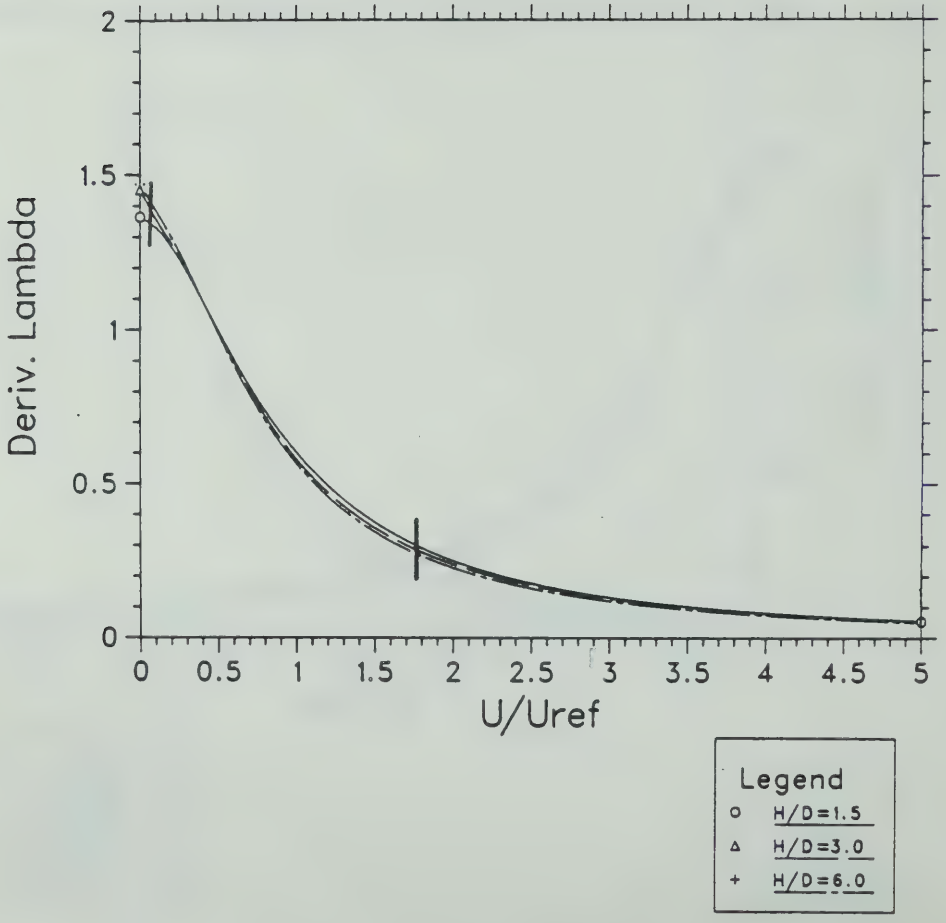

Figure 6.115 Variations of λ' for the Tunnel Floor, Calculated for K_o=1.0

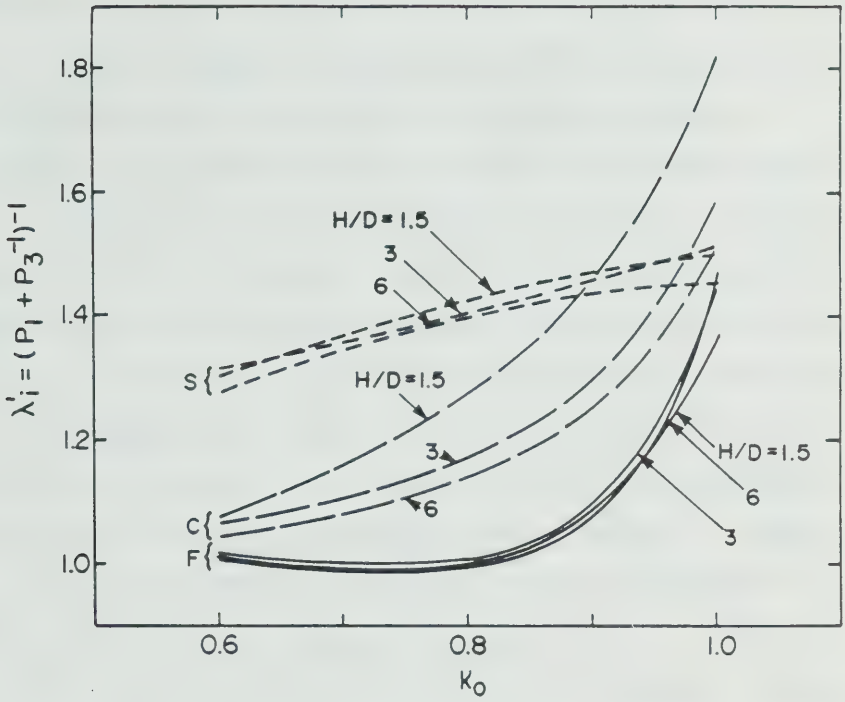

	H/D	λ'_i		
		$K_o = 0.6$	$K_o = 0.8$	$K_o = 1.0$
C	6	1.0446	1.1421	1.5116
	3	1.0663	1.1719	1.5825
	1.5	1.0780	1.2782	1.8176
S	6	1.2808	1.3973	1.4518
	3	1.3143	1.4066	1.5110
	1.5	1.3071	1.4249	1.4981
F	6	1.0092	0.9992	1.4692
	3	1.0210	1.0105	1.4517
	1.5	1.0135	1.0055	1.3641

Figure 6.116 Variations of the Initial Slope of the Twice Normalized Ground Reaction Curves with K_o and H/D

6.5 Limits of the Generalized Solution

6.5.1 Extrapolation of the Numerical Results

It was pointed out earlier that, for the generalization of the parametric analyses results in terms of ground reaction curves, all numerical output after local failure had developed was disregarded (Section 6.3.2). The reasons behind this decision were: a) the numerical model used was not designed to represent this type of behaviour (for instance, the failure criteria can be violated); b) the GRC resulting after local failure of an element or group of elements to which a low tangent modulus is assigned ceases to be homothetic; c) the generalized solution was not intended to cover responses approaching soil failure or ground collapse.

In order to achieve the projected generalization and to find out the functions reprsenting the GRC for the particular soil models investigated (e.g., equations 6.11 and 6.12), some curve fitting techniques were used. The NGRCs were found to be described by equations such as 6.17 and 6.24, obtained by applying non-linear regression techniques to the numerical results of the parametric analyses.

The numerically derived functions that resulted were unbounded and they therefore, may be used to interpolate data between the discrete numerical results of the parametric analyses, and also they may be used for the

extrapolation of these results beyond the range of the data investigated. Although the latter use of these functions was not initially envisaged, it was found that, for practical use and under certain circumstances, some limited extrapolation of data could be required. This may happen when the resulting calculated GRC was "too short" as can be the case in soils with low ϕ and under low K_o, where local failure is attained at small amounts of ground stress release. An approach to this problem could be to accept the onset of global collapse simultaneously with the event of local failure. Accordingly, this would imply a horizontal extension of GRCs at the points of local failure so that very large displacements develop for a certain amount of stress release.

Clearly, this alternative presents an inconvenience: it may be too conservative in terms of ground stress displacement (and thus loads onto the support) and in terms of opening closure. With this problem in mind, it was contemplated that the use of the fitted functions to extrapolate the ground reaction curves could be a more sensible alternative, provided the implications of this operation are fully recognized and caution is exerted in interpreting the extrapolated results.

To illustrate this point, consider the NGRCs shown in Figure 6.58 for H/D=3, ϕ=30° and K_o=0.8. These curves are reproduced in Figure 6.117 by the solid lines OR. R represents the end points of the curves shown in Figure

6.58 and correspond to the numerical results obtained in the last unload increment, prior to the load step at which local failure developed (at an element next to the springline in this particular case). If the NGRCs are extended beyond R, using equation 6.24 and the corresponding parameters found in Table 6.16, the dashed curves shown in Figure 6.117 are obtained. One notes that the extrapolated portions of the NGRCs do not present any significant discontinuity at point R.

By now examining Figure 6.64, we identify point R of the springline NGRC for ϕ=30°, as the end point of this curve for Σ=0.4. This point reappears in the NNGRC shown in Figure 6.90 also as R. Note that, in the latter figure, to the right of R there exists another point (T), which is the end point of the NGRC for ϕ=20° (Figure 6.64). By virtue of the homothety, to this last point there exists a corresponding homothetic point (T') in the NGRC for ϕ=30° which coincides with T in the twice normalized ground reaction curve (Figure 6.90). This point could not be numerically obtained as the unloading increment used was too large. In this particular case, had this increment been about 7% instead of the standard 10%, point T' on the NGRC for ϕ=30° in Figure 6.64 would have been obtained numerically. Regardless of this, it was possible to identify point T' from point T in Figure 6.64, by assuming that the NGRCs are homothetic and by taking the similitude axis OT and defining T' as the intersection of this axis with the

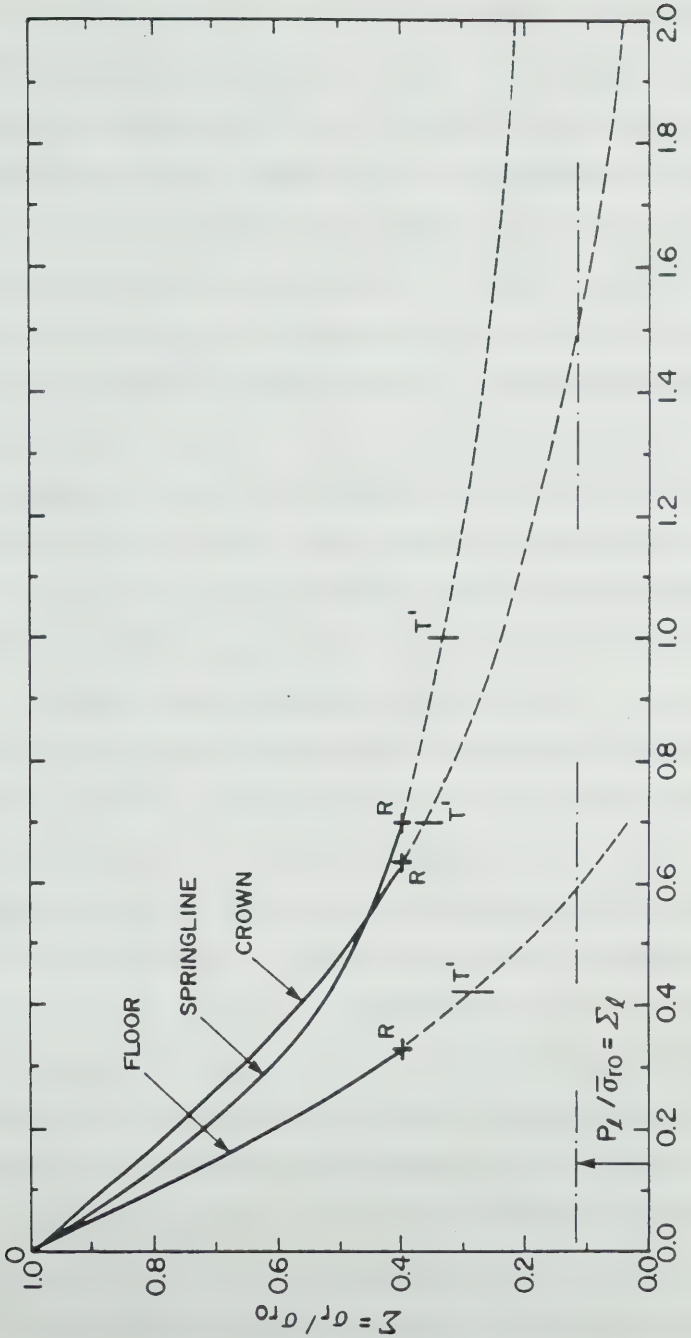

Figure 6.117 Extension of the NGRCs for H/D=3, K_o=0.8 and ϕ=30°

extended NGRC for ϕ=30°.

If the property of homothety can be accepted for the NGRCs of different ϕ values, then the extended portion RT' of the curves in Figure 6.117 are fully admissible. The terminal points T' of the extended NGRCs are easily found through the ratio U/U_{ref} of the extreme rightward point T shown in Figure 6.90, and indicated by the right vertical bar in all λ versus U/U_{ref} curves (Figures 6.94 to 6.96, 6.102 to 6.104 and 6.110 to 6.112). In brief, the results given by these curves up to these points can be used with no restrictions. However, beyond them (to the right of points T' in Figure 6.117), there is not assurance that the relationships between stresses and displacement are correct. In particular, stresses giving stress ratios below $\Sigma_{T'}$ may either violate the failure criteria or may be smaller than the minimum required to maintain stability of the opening. In other words, the stresses given by the extrapolated NGRC beyond T' may not ensure the equilibrium of the system.

Unfortunately, there is no simple way to check if the failure criteria is being locally violated. In fact, one may assess the global stability of the tunnel, to evaluate how close to tunnel collapse one is, when using acting stresses lower than that at T'. A stability calculation may give some indication as to whether or not the acting stresses are high enough to ensure global equilibrium but it will not ensure that local equilibrium is attained. Neither will it guarantee that the failure criteria is not being violated

locally. Consequently, the displacements associated with these stresses are likely to be in error, and are possibly smaller than the correct ones. In spite of these limitations, if one still needs to go beyond T' in Figure 6.117, the least that can be done is to ensure that the factor of safety for the acting stresses is greater than unity.

The discussion just presented referred to the cohesionless soil model but it applies to the frictionless soil model as well. The extension of the NGRCs shown in Figure 6.47 for H/D=3 and $c_u/\gamma D$=1.25 is presented in Figure 6.118. The same notation used before is adopted herein. The extension beyond point R is obtained using equation 6.17 and the corresponding parameters found in Table 6.13 or in Figures 6.85 to 6.88. Similarly the reader is referred to Figures 6.55 and 6.83. Note that in the latter, point T lies outside the figure. The positions of points T' in Figure 6.118 are shown in the inset. The same comments made regarding Figure 6.117 are valid here. The main difference lies in how the points T' are found for the frictionless soil model. As the general solution for this case was presented in a slightly different format, some additional information is needed for establishing T'. This is supplied by Figures 6.119 to 6.121 which provide the values of U_{ref} for different $c_u/\gamma D$ and H/D values. Note that U_{ref} was deliberately chosen as to result in a linear function of the strength ratio. In the inset shown in each of these three

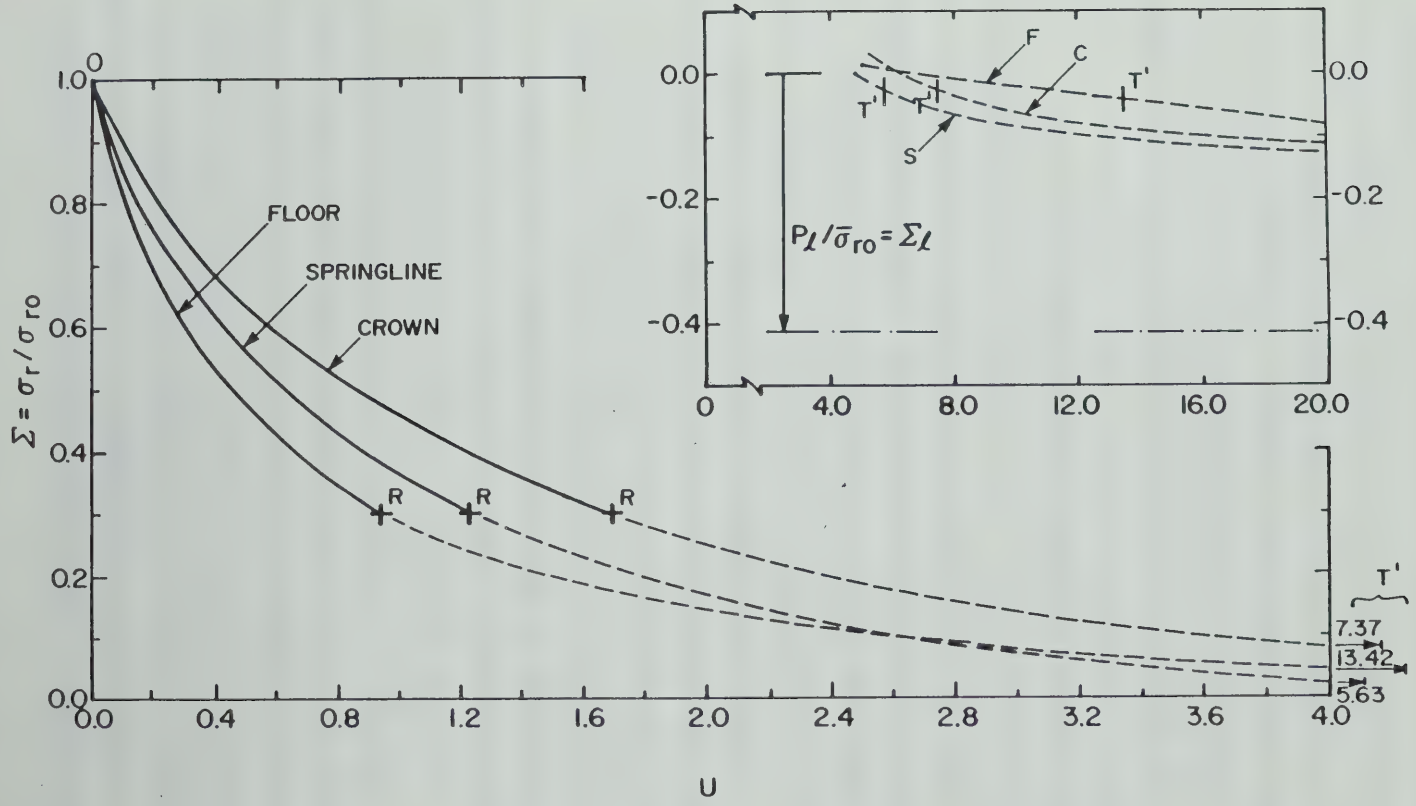

Figure 6.118 Extension of the NGRCs for H/D=3 and $c_u/\gamma D$=1.25

figures, the maximum value of U/U_{ref} calculated for each H/D is also given. This maximum normalized dimensionless displacement corresponds to the terminal point T identified by the vertical bars shown in the NNGRCs for the cohesionless soil.

Another peculiarity found in the results of some analyses with the frictionless soil model was that tensile stresses developed in some elements around the opening, before the development of shear failure. This was noted mainly in the shallower tunnel cases with higher strength ratios. As explained in the introductory remarks to Section 6.3.2, all numerical data output obtained following the development of any tension in the ground was disregarded.

6.5.2 Assessment of the Two-Dimensional Stability

Although not recommended by the reasons exposed in the previous section, if one is forced to use the generalized solutions beyond their terminal points, an assessment of the two-dimensional tunnel stability is required. It should be stressed that this does not secure that the extrapolation is correct, but this evaluation can provide indications of whether or not the calculated stresses for a certain closure of the opening are sufficiently high to keep it stable. Though the excavation stability verification is usually circumscribed to the tunnel face and heading (See Section 4.2.3), in this particular case the two-dimensional stability evaluation also becomes important. The subject was

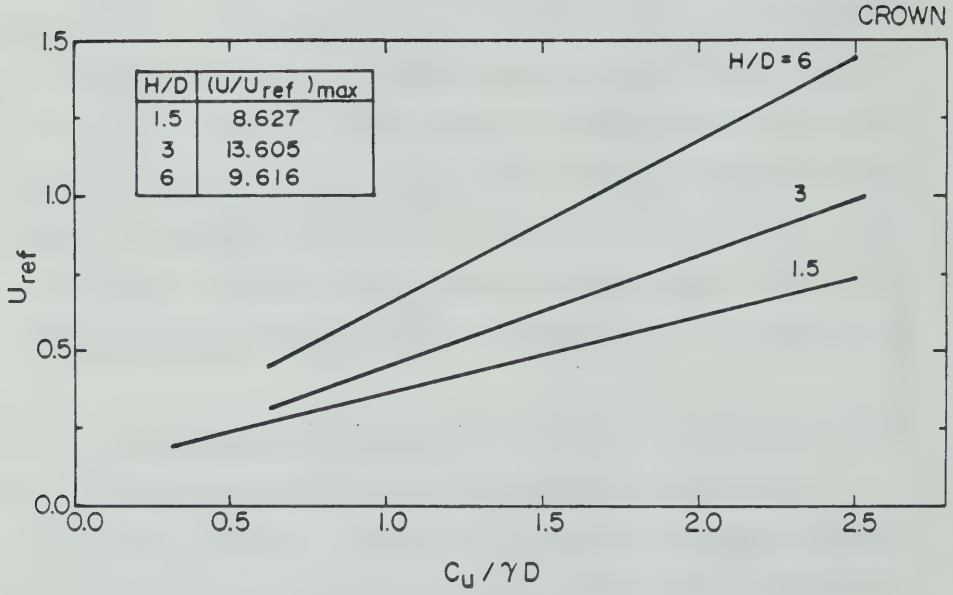

Figure 6.119 Reference Values used for Normalizing the NGRC of the Tunnel Crown for the Frictionless Soil Model and Components to Define the Limiting U of the Fitted Function

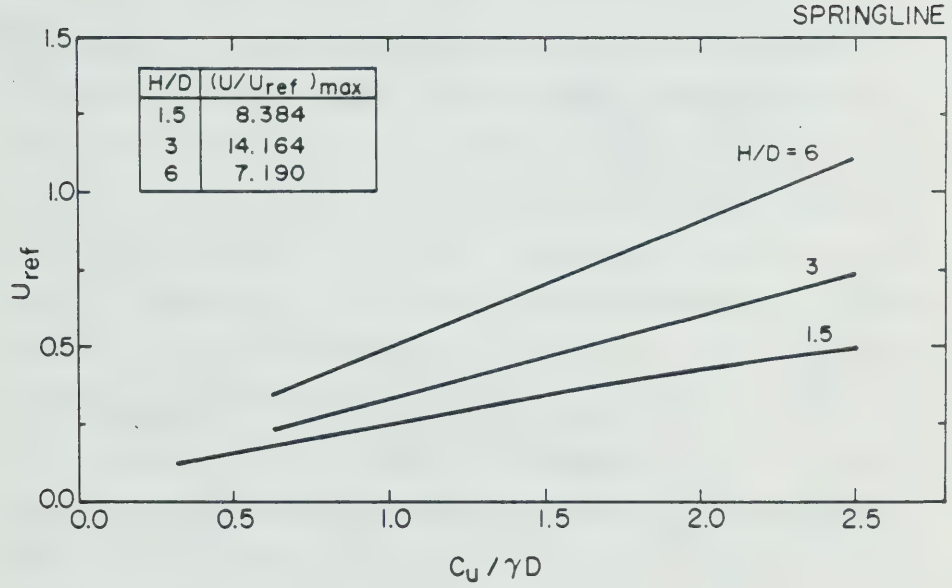

Figure 6.120 Reference Values used for Normalizing the NGRC of the Tunnel Springline for the Frictionless Soil Model and Components to Define the Limiting U of the Fitted Function

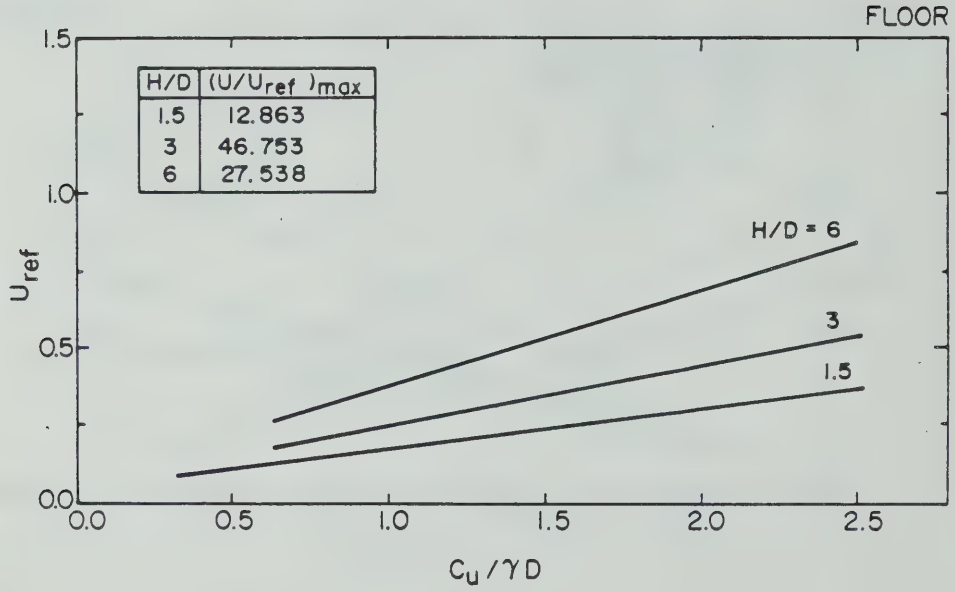

Figure 6.121 Reference Values used for Normalizing the NGRC of the Tunnel Floor for the Frictionless Soil Model and Components to Define the Limiting U of the Fitted Function

discussed and reviewed in different sections of this thesis, especially in Section 4.3.4.

The possibility of violating the boundary or failure conditions in limit equilibrium analyses of the ground mass suggests the use of plasticity solutions. The available plasticity solutions for estimating the two-dimensional stability of a shallow tunnel are based on the Limit Theorems (Lower and Upper Bound). These theorems can be proved for materials with an associated flow rule, where the angle of dilation, ψ, is equal to the friction angle, ϕ. While this assumption provides a good approximation in the case of a saturated soil under undrained loading, in which $\psi=\phi=0$, in general it does not properly represent the actual soil behaviour at ultimate failure under drained loading, when usually ψ is not equal to ϕ. Davis (1968:352) showed that the Upper Bound Theorem can be proved to be correct even for this condition (see also Atkinson, 1981:117). No complete proof of validity of the Lower Bound Theorem was found so far for this condition. There are some indications, however, that it may be valid for ϕ not equal to ψ and $\psi=0$ (for instance, Cox, 1963 - quoted by Davis, 1968:345 and Palmer, 1966).

Davis (1968:346) suggests that while the plastic deformations may strongly depend on the flow rule, the collapse loads may not. Atkinson (1981:118) seems to share this opinion and suggests that the approximate lower bounds calculated for a soil with ψ not equal to ϕ by assuming $\psi=\phi$

are unlikely to exceed the true collapse loads.

An additional aspect of the plasticity solutions is that a unique collapse load is steadily approached, and remains constant at its maximum once collapse is fully developed. This can be proved to hold (Davis, Op.cit.:346) on the condition that the geometry of the problem is not changed significantly. Regarding the tunnel problem, this implies that a unique collapse load can be found provided 'loosening' effects and associated changes in the geometry of the problem does not occur (see Section 3.2.3). In other words, plasticity solutions could be used to approach the stresses associated with point E in Figure 3.8. Beyond it, the changes in geometry would have to be considered in order to investigate the loads associated with point G in Figure 3.8, which lies on the speculated sweeping upward ground reaction curve as discussed in Section 3.2.3. If the displacements are limited as in good ground control tunnelling conditions, which are usually required in urban environments, it will be sufficient to investigate the ground stability on the assumption of uniqueness of the plasticity solution.

The available plasticity solutions to the two-dimensional shallow tunnel problem usually represent the internal stress acting on the circular opening as a uniform pressure which, at ground collapse, is denoted by p_1. An exception to this rule are solutions that assume the cavity being filled by a heavy and non-permeating fluid with a

density equal to the soil density (for instance Caquot, 1934:81, or D'Escatha and Mandel, 1974). In both cases, it is noted that the conditions assumed do not correspond exactly to the loading conditions assumed in the two-dimensional numerical modelling adopted in the present study. As described in Section 5.2.2, in any stage of the unloading process, the tunnel contour is subjected to stresses that correspond to a fraction $\Sigma=1-\alpha$ of the in situ stresses, which can be calculated through the expressions given in Figure 2.14. One notes that while in the plasticity solutions the opening walls are subjected only to normal (radial) stresses, the numerical modelling adopted herein assumes that both normal and shear stresses act on the opening contour, which are equal to $\Sigma\sigma_{ro}$ and $\Sigma\tau_{o}$ respectively, with σ_{ro} and τ_{o} given in Figure 2.14. Even for K=1 (i.e., τ=0), the conditions in the numerical model do not fully correspond to that in the plasticity solution, where the tunnel is assumed to be filled with a fluid with density equal to γ. The latter implies the existance of a pressure gradient across the tunnel, from crown to floor, equal to γ, whereas this gradient is equal to $\Sigma\gamma$ in the numerical model adopted (with Σ smaller than unity).

Even when working in terms of stresses averaged around the tunnel contour, there will always be a non-zero residual shear stress acting on the shallow tunnel walls, whose effect on the limiting tunnel pressure has not been fully assessed. Besides affecting local failure, these shear

stresses may affect the global collapse condition and therefore the limiting tunnel load. For K not equal to 1, they may lead to an increase in p_l. For K=1, p_l may also increase since $\Sigma\gamma$ is less than γ. Increased limiting tunnel pressure implies a smaller factor of safety. defined as (see Chapter 2):

$$FS = \frac{\sigma_o - p_l}{\sigma_o - \sigma_i} \qquad [6.31]$$

where σ_o is the in situ vertical stress at the tunnel axis and σ_i is the current internal stress in the tunnel. As the latter, in the numerical model, varies from point to point of the contour, it seems convenient to define σ_i as the current average radial stress acting on the tunnel profile. Thus:

$$\sigma_i = \Sigma\bar{\sigma}_{ro} \qquad [6.32]$$

where $\bar{\sigma}_{ro}$ is the average in situ radial stress, which is given by:

$$\bar{\sigma}_{ro} = \frac{1+K_o}{2}\gamma(H + \frac{D}{2}) \qquad [6.33]$$

Therefore:

$$FS = \frac{1 - \Sigma_l((1+K_o)/2)}{1 - \Sigma((1+K_o)/2)} = \frac{(1-K_o)/(1+K_o) + a_l}{(1-K_o)/(1+K_o) + a} \qquad [6.34]$$

with Σ_l equal to the ratio $p_l/\bar{\sigma}_{ro}$ and $a_l = 1-\Sigma_l$.

It should be remembered that the collapse pressure given by plasticity solutions is independent of the initial stresses acting in the ground before the tunnel is built and also independent of the sequence in which the stress release is applied to the opening, provided it is steadily increased

during unloading (Davis, 1968:346,347, D'Escatha and Mandel, 1974:46). Hence p_1 does not depend on K_o, although the local failure in the ground during the unloading process does depend on K_o. Note that FS expressed by equation 6.31 or 6.34 is dependent on K_o, not through p_1 but through the current average radial stress acting on the opening contour. Note, moreover, that this definition of FS is approximate since the effect of the shear stresses acting on the contour was disregarded.

Safe estimates of p_1 can possibly be made through solutions developed from applications of the method of characteristics. As it is based on a statically admissible stress field not violating the failure criteria, the solution it provides is a lower bound (theoretically safe) estimate of the exact solution. In other words, the p_1 value estimated is higher than (or equal to) that actually causing the tunnel collapse. On the other hand, an upper bound (unsafe) solution will provide an estimate of p_1 which is lower than (or equal to) the correct value.

If the flow rule is associated, with $\psi=\phi$, then the stress characteristics line coincide with the velocity characteristics (or slip lines). Therefore one can assume that, at collapse, the soil strength is fully mobilized along the slip lines and the safe collapse load can be estimated through the method of characteristics (see, for example, Wu, 1966:215).

For a purely cohesive soil, D'Escatha and Mandel (1974) and Seneviratne (1979:79) (reproduced in Davis et.al., 1980) presented lower bound solutions for the two-dimensional shallow tunnel problem which are shown together in Figure 6.122. The solutions by these authors are intrinsically the same and assume that the opening is supported by a uniform pressure (γ_t=0). They differ slightly (see curves for $c_u/\gamma D$=0.25 and 1.00) because Seneviratne's characteristic net was less refined than D'Escatha and Mandel's. The tunnel contour was divided into 16 equal segments in the former and into 60 in the latter. The D'Escatha and Mandel solution is therefore numerically more accurate. However, it does not provide solutions for the intermediate range of strength ratios which is of considerable practical interest and for this reason, both solutions are reproduced in Figure 6.122.

Also plotted in Figure 6.122 are the results of some two-dimensional centrifuge model tests (Series I) by Mair (1979:121). It can be appreciated that the interpolated plasticity solution provides a very close estimate of the collapse tunnel (internal) pressures observed in the tunnel model tests.

For a cohesive and frictional soil, D'Escatha and Mandel (1974) also presented 'safe' estimates of the collapse tunnel pressure, once more assuming $\psi=\phi$. These are given by the curves shown in Figures 6.123 to 6.126, for ϕ equal to 10° to 40° and different cohesion, c, expressed in terms of the ratio $c/\gamma D$. Again, this solution assumes that

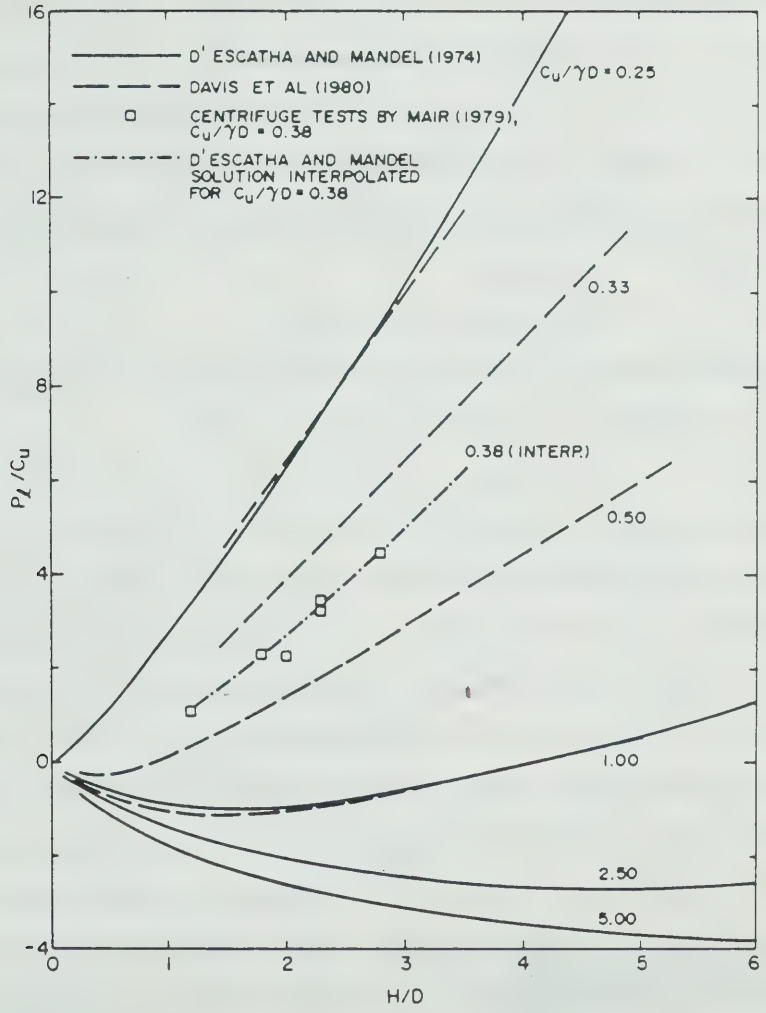

Figure 6.122 Lower Bound Solution for Tunnel Collapse Pressure in a Frictionless Soil

the tunnel walls are submitted to a uniform pressure, p_1.

An upper bound solution for local collapse of a wedge of cohesionless soil at the tunnel crown (See Figure 3.7) can easily be obtained by a work calculation assuming $\psi=\phi$. This solution, which gives a tunnel pressure which is lower than (or equal to) the actual internal pressure at collapse was first proposed by Atkinson et.al., (1975:84) and is given by:

$$\frac{p_1}{\gamma D} = \frac{1}{4\cos\phi}\left[\frac{1}{\tan\phi}+\phi-\frac{\pi}{2}\right] \qquad [6.35]$$

provided that the sides of the wedge do not intersect the ground surface. In other words, provided

$$\frac{H}{D} > \frac{1}{\sin\phi} - 1 \qquad [6.36]$$

Values of the $p_1/\gamma D$ given by equation 6.35 and the restriction given by 6.36 are shown in Figures 6.123 to 6.126 by chaindotted lines. It can be observed that for any ϕ this Upper Bound solution always provides a p_1 value lower than that given by the lower bound solution (for $c/\gamma D=0$).

If the above solutions are compared to results of tunnel model tests carried out under drained conditions, mixed results are obtained. The lower and upper bound solutions are found to bracket the loads associated with local collapse as observed in static tests in sand by Atkinson et.al., (1975:84). However, under some circumstances they do not approximate the collapse pressures found by Seneviratne (1979:64) in drained static tests in normally consolidated kaolin. The lower bound solution given was found to underpredict the observed collapse pressure of

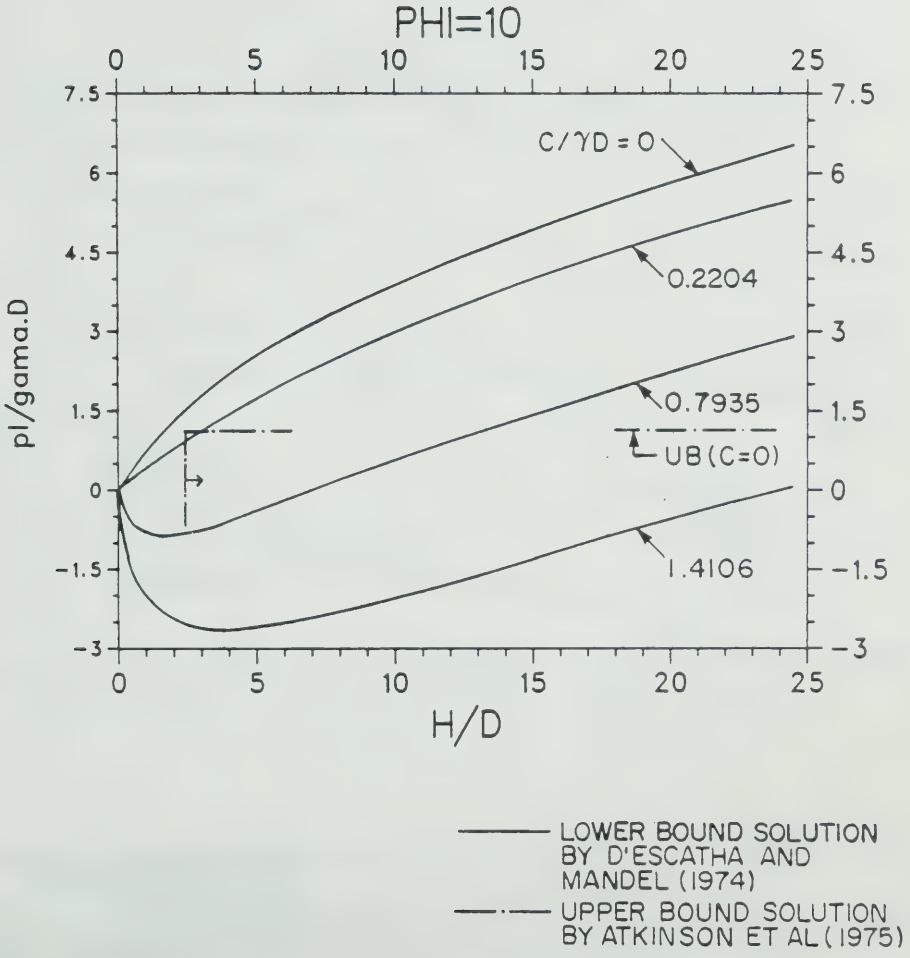

Figure 6.123 Lower and Upper Bound Solutions for Tunnel Collapse Pressu re in a Frictional and Cohesive Soil (ϕ=10°)

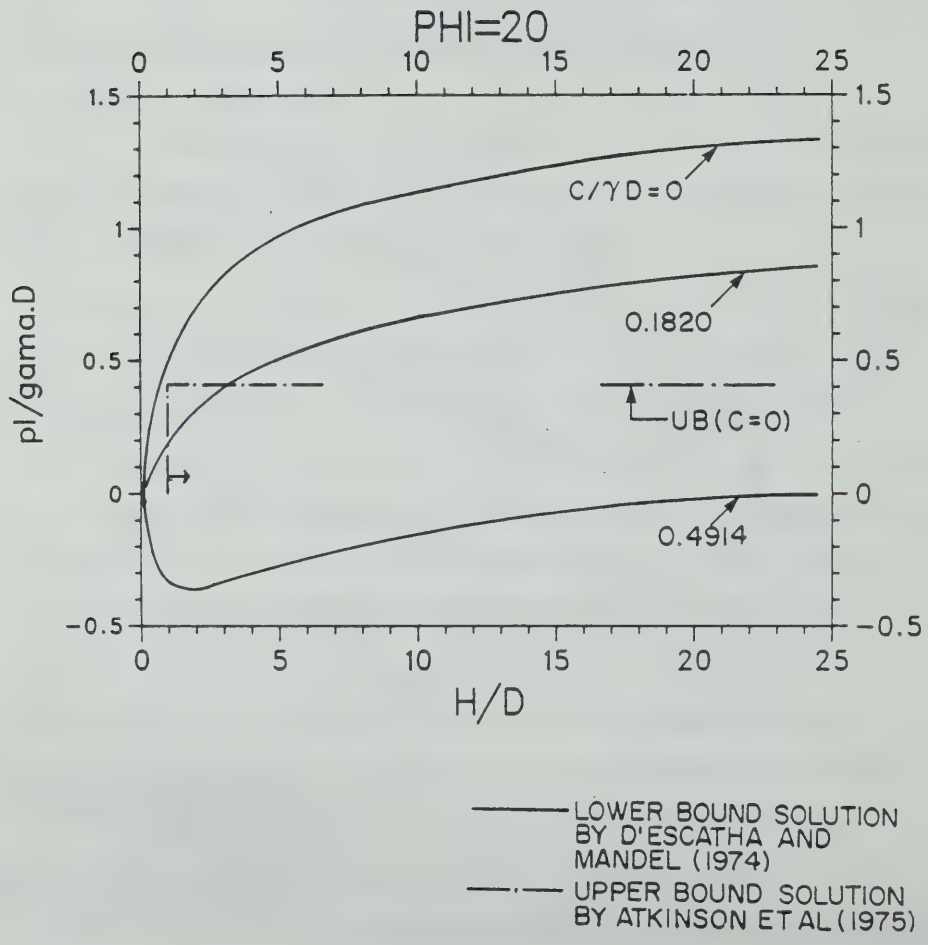

Figure 6.124 Lower and Upper Bound Solutions for Tunnel Collapse Pressure in a Frictional and Cohesive Soil (ϕ=20°)

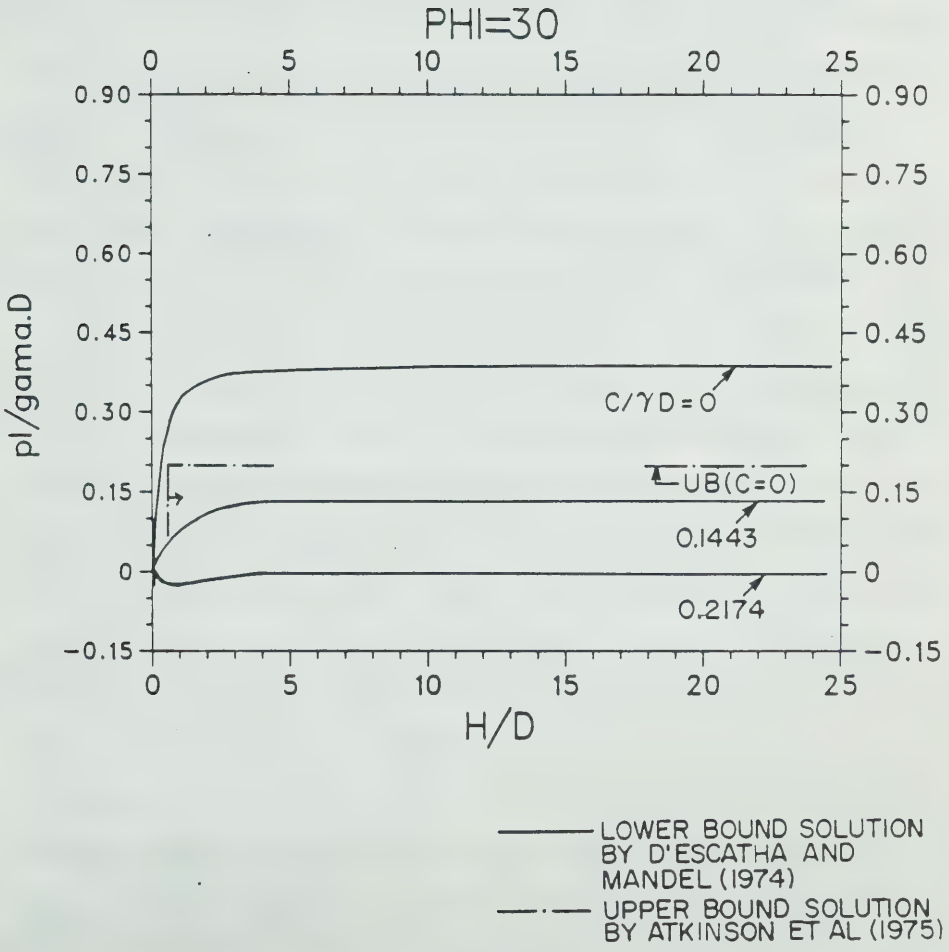

Figure 6.125 Lower and Upper Bound Solutions for Tunnel Collapse Pressure in a Frictional and Cohesive Soil (ϕ=30°)

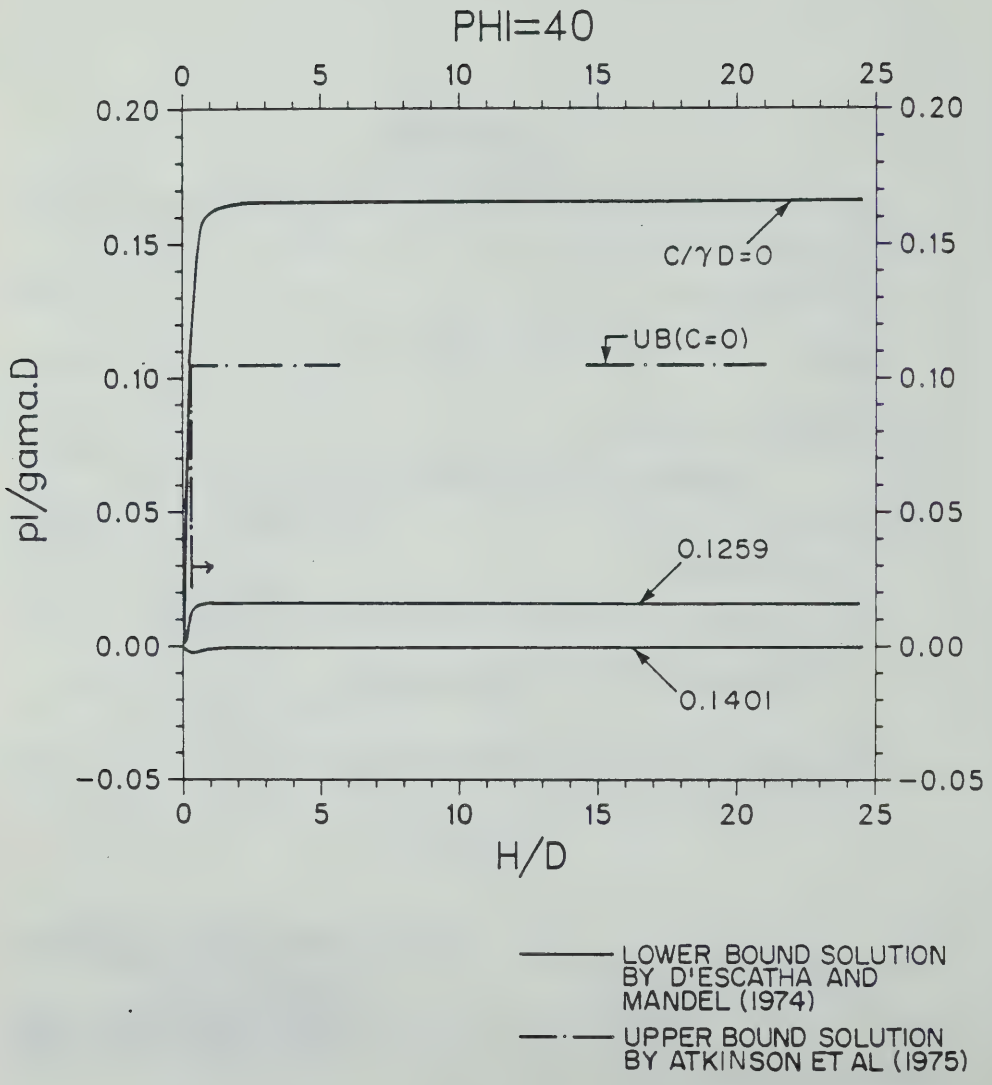

Figure 6.126 Lower and Upper Bound Solutions for Tunnel Collapse Pressure in a Frictional and Cohesive Soil (ϕ=40°)

these tests conducted with small cover to diameter ratios. This may be an indication that, in fact, the solution does not provide 'safe' estimates of the collapse load for materials with a non-associated flow rule behaviour. Another interpretation would be that the deformations in the soil prior to collapse do have an effect on the collapse pressure (see Section 4.3.4). Nevertheless, whatever the reasons are, these findings suggest that caution should be always excercised when using the above solutions, and it is considered good practice to allow as much safety as possible or preferably to avoid any extrapolation of the NGRCs.

If the above lower bound solutions are applied to the conditions assumed in the analyses that led to the results shown in Figure 6.117 and 6.118, the corresponding p_1 and $\Sigma_1=p_1/\bar{\sigma}_{ro}$ are found. These are shown by the chaindotted lines also plotted in these two figures. Those points in the NGRCs below the $\Sigma=\Sigma_1$ line would thus imply stresses acting on the opening smaller than those needed to keep it in a state of limit equilibrium. Note in Figure 6.117 that the dimensionless displacement, U, at the tunnel crown corresponding to $\Sigma=\Sigma_1$ is about U=1.5, which is not dissimilar to the limiting value of U=1.8 suggested in Section 2.3.4.3 for a near collapse situation. Note also that in Figure 6.118 the NGRCs are not intersected by the $\Sigma=\Sigma_1$ line and thus they always give stresses which are higher than those at collapse. This feature is observed for some situations in the generalized solution for the

frictionless soil model, but only when $R_f=1$. When the failure ratio is smaller than unity, the NGRC becomes steeper and the $\Sigma=\Sigma_1$ line may intersect them.

6.6 Summary and Conclusions

The main objective of this chapter was to develop a procedure that would allow the ground reaction or stress release curves of points at the contour of a shallow tunnel to be obtained without the need of finite element analyses. In parallel with this development, it was also attempted to obtain the relevant ground displacements associated with the reduction of the in situ stresses, with the tunnel construction being represented by a two-dimensional simulation.

To achieve these aims, some additional simplifications were introduced into the 2D finite element model presented in Chapter 5. These simplifications led to the establishment of two stress-strain models: the frictionless soil model and the cohesionless soil model. The first would represent the behaviour of a saturated soil under undrained conditions, whereas the second would simulate the drained behaviour of frictional soil without cohesion. Both models originated from the hyperbolic model presented in Section 5.2.2.1. The first was obtained by setting $\phi=0$, $K_o=1$ and by making the Janbu's exponent n equal to zero. The second was obtained by setting both the cohesion, c, and the exponent, n, equal to zero. With these simplifications, it was found that the

resulting stress-strain curves for these two groups of soil present the property of homothety. This property allows the responses of homothetic circular tunnels (tunnels with the same cover to diameter ratio) to be normalized and become represented by a unique response. Unique normalized ground reaction curves (NGRC) are thus found at corresponding points on the contour of homothetic tunnels. Furthermore, unique normalized distributions of ground settlements at the surface and in the subsurface are also found. These findings facilitate the generalization of the numerical results since they become independent of the scale of the problem.

It was shown that the normalized responses calculated for these models are invariant with regard to the unit weight of the soil. It was also demonstrated that the normalized responses calculated for a certain failure ratio R_f are easily extended to different R_f values. This enables the projected solutions to be developed for a fixed R_f value equal to unity. For R_f different from unity, either the undrained strength, c_u, or the friction angle, ϕ, would be transformed into an equivalent strength parameter (c_{ue} or ϕ_e) using equations 6.3 and 6.7. By implementing the equivalent strength parameters an identical solution is obtained.

It was demonstrated that the normalized responses are invariant to the Janbu's modulus K. Both models set Janbu's modulus n equal to zero, therefore assuming that the in situ tangent modulus is constant with depth. This is restrictive since the normalized ground response was shown to be

sensitive to the increase of the in situ modulus with depth, notably at the crown and at the floor. A simple expedient was devised to make the NGRC at those points less sensitive to the modulus increase with depth. It consists of normalizing the displacements at the contour to the in situ stiffness of the ground at points located a half diameter radially away from the tunnel. This artifice provided favourable results and one can approximate the increase of the in situ modulus with depth in both soil models.

The use of the cohesionless soil model for soils in which the cohesive component of strength is not zero was investigated. The normalized ground response was found, of course, to depend on the soil cohesion. By neglecting its influence an unduly conservative ground response may be obtained. To bring the results of the cohesionless soil model closer to the correct one, another approximation was proposed and provided reasonable, yet safe, results. It consists of increasing the friction angle in the cohesionless soil model, so that the in situ strength at the springline elevation is equal to the actual strength, defined in terms of the principal stress difference at failure. The adjusted friction angle to be used in the c=0 model is given by equation 6.10 and is found to depend on the actual c and ϕ values and on the in situ minor principal stress at the tunnel axis elevation.

In order to further reduce the number of variables, the effect of Poisson's ratio on the normalized ground response

was investigated. For the frictionless model, the assumption of a ratio close to 0.5 was justified as representing the behaviour of a saturated soil under undrained conditions. For the cohesionless model, the ground response for two typical values of Poisson's ratio was studied, which lead to the adoption of a Poisson's ratio of 0.4.

After the introduction of the above simplifications, general equations describing the NGRC for the two soil models were presented in terms of dimensionless and independent variables (equations 6.11 and 6.12). Parametric finite element analyses were the modelling tool used to establish the relationships among these variables. It was decided to investigate these relationships within ranges of variables which would include the most common situations found in practice. These ranges were established by investigating 53 case histories of shallow tunnels. Most of these were identified as having been built under good ground control conditions where collapse and pronounced time dependent responses were not entailed. The most typical ranges in situ stress ratios, of cover to diameter ratios and strength parameters (ϕ and $c_u/\gamma D$) were identified. As a consequence of this investigation, the variables for the parametric finite element analyses were finally defined as (H/D=1.5 to 6, ϕ=0 to 40°, $c_u/\gamma D$=0.3125 to 2.5, K_o= 0.6 to 1.0.

Details of the 2D parametric finite element analyses were presented, including the number of unloading increments

used, the assessment of its effect on the numerical results, the finite element mesh design and particularly the effect of the fixed lower boundary. The latter was found to have a significant effect on the numerical output, mainly because of the constant modulus profile assumption. Unrealistic numerical results in terms of the ground settlements and ground reaction curves were obtained depending on its position. In order to select the most convenient location for this boundary a very large number of cases were processed. A distance of 1.5D below floor elevation was selected as being a position close enough to the tunnel invert to minimize excessive ground heave and far enough away to minimize its effect on the stiffness expressed by the ground reaction curves.

The generalization of the parametric analyses data was limited to pre-failure conditions because the numerical model is unable to simulate the soil failure. These results are included in Appendix C and D in compact graphic form, in terms of the distributions of normalized ground surface and subsurface settlements and of the NNGRCs for three points of the tunnel contour.

Some of these results for both soil models were presented and discussed in detail. The influence of each dimensionless variable on the ground response was individually assessed. This included the effects of the amount of stress release, the relative tunnel depth, the undrained strength ratio, the friction angle and the in situ

stress ratio. Conclusions regarding these assessments can be found in specific sections of this chapter. Of particular interest was the normalized ground reaction curves for different strengths (either expressed in terms of $c_u/\gamma D$ or ϕ) that are homothetic with the centre of similitude at their origins (Σ=1 and U=0). Therefore, if the NGRCs are normalized once more, unique twice normalized ground reaction curves (NNGRC) are found irrespective of the soil strength. This finding had a major impact on the generalization of the numerical modelling results, as the projected solution could be extended to soil strengths other than those used in the parametric analyses.

Relationships between surface and crown settlements (S and u_c) were derived from the results of the numerical analyses. These relations were found to depend on the relative tunnel depth (H/D), on the strength parameters ($c_u/\gamma D$ or ϕ) and on the in situ stress ratio. Moreover, it was found to be a function of the amount of stress release allowed. The ratio, S/u_c, was found to either increase or decrease depending on the stress relief, on K_o and on the geometry of the problem. Results obtained by other authors regarding this aspect were critically assessed and previously proposed relationships for the settlement ratio S/u_c were analysed. The relations proposed herein were found to bound field observations, and it is suggested that they could be used to define the maximum surface settlement above a shallow tunnel whenever the crown settlement is assessed.

The results obtained were used to explain the limitations of linear elastic analyses which, when used to back-analyse actual tunnel performances, lead to either over or underestimates of surface settlement, whenever a match in the crown displacements is achieved.

The results of the numerical modelling were further generalized in an attempt to define expressions relating the variables controlling the ground response. Such expressions would allow one to obtain the ground reactions for conditions or variables other than those considered in the modelling stage. It would serve as a tool to furnish the ground reaction curves for any tunnel size, at any intermediate depth, in soils described by any in situ stiffness or strength. This generalization process was undertaken in parallel for both the frictionless and the cohesionless soil models.

A single expression (6.17) relating the radial stress ratio Σ and the radial dimensionless displacement U, with two parameters (A and B), was found to be a good representation of the normalized ground reaction curve for the frictionless soil model. Parameter A was found to depend on the point of the tunnel contour being considered and on the relative tunnel depth. Parameter B was also found to vary around the contour but to a lesser degree, and depends largely on the undrained strength ratio ($c_u/\gamma D$) and the relative depth of the tunnel (H/D). The first parameter was shown to reflect the in situ stiffness of the ground and the

second, the ultimate collapse state of the ground. Charts were prepared, which allow A and B to be estimated for three points of the tunnel contour (crown, springline and floor), for any cover to diameter ratio or any undrained strength ratio.

The partial derivative of the function expressing the NGRC for the frictionless soil model is easily related to the ground stiffness at any stage of the tunnel unloading process. Therefore, it can provide estimates of the 'current' radial spring constant (k_t) for any amount of tunnel closure (equation 6.20). These constants vary from point to point of the tunnel contour, and could be used as input parameters for a ground-lining interaction analysis using conventional ring-and-spring models such as reviewed in Chapter 4.

If instead, ring-and-plate models were to be used for the interaction analysis, the 'current' tangent Young's modulus (E_t) could also be derived from the derivative of the general NGRC function (equation 6.22).

These derivations would enable an approximation of the degree of 'softening' experienced by the ground around a shallow tunnel and the amount of stress release associated with a certain degree of opening closure taking place before the lining is installed or activated. This would serve to improve the approximations for the actual mechanisms involved in the ground-lining interaction process and perhaps lead to better estimates of tunnelling performance.

Even though more difficult, similar reasoning and development were applied to the cohesionless soil model. The homothetic responses of the ground in terms of the NGRC for different friction angles, allowed an additional normalization of the NGRC. The twice normalized ground reaction curves (NNGRC or λ - curves) could then be fitted by a single five parameter function (equation 6.24). Best fit parameters were then found through a non-linear regression technique using a statistical program package, for each point of the tunnel contour, for each cover to diameter ratio and for each in situ stress ratio. The λ curves obtained for each of the three points of the tunnel contour were found to be relatively insensitive to the cover to diameter ratio (except for the tunnel crown) but more sensitive to the in situ stress ratio. The first finding assures that the definition of the ground reaction curves for intermediate H/D values could be easily achieved by data interpolation. Interpolation of data for intermediate in situ stress ratios could also be made, but with a larger degree of uncertainty. Estimates of the ground reaction curves for any tunnel size, depth, soil stiffness, strength, or in situ stress ratio can thus be obtained, either using the basic general expression and appropriate parameters or through the prepared design charts.

Once more, estimates of 'current' radial spring constant (k_r) or 'current' tangent Young's modulus (E_t) could be obtained by partial differentiation of the basic

function giving the NNGRC. Through equations 6.25 to 6.27 the ground stiffness could be assessed for any amount of stress release prior to ground failure, or for any amount of tunnel closure. To facilitate this assessment, a suite of convenient design charts was also prepared and presented. As before, through these derivations, one would be in position to approximately account for the degree of 'softening' and the degree of stress release associated with a given amount of tunnel closure. These factors could be used as input for traditional ground-lining interaction solutions, using either ring-and-spring or ring-and-plate models. Since most of these models operate with a constant spring constant or a constant ground modulus, average stiffness values would have to be estimated from the values found for the crown, springline and floor.

Although the solutions obtained were developed for use within the ranges of variables considered, one may be tempted to use them beyond the ranges of stress release covered by the parametric analyses. In some instances, the NGRC may be "too short" and some limited extrapolation may be needed for certain practical applications. The limits of validity of the solutions were then explored and defined. The terminal points, T, of the functions were identified both for the cohesionless and for the frictionless model solutions. The validity of extrapolations beyond those points cannot be assured, as the corresponding stresses eventually obtained may violate the failure criteria or they

may not be sufficient to keep the opening stable. The associated displacements will likely be in error (possibly smaller than the correct values). The generalized solutions are not recommended beyond their terminal points, but if required, an assessment of the 2D tunnel stability is needed. The limitations of plasticity solutions for this purpose were assessed and discussed. Lower bound solutions such as those by D'Escatha and Mandel (1974) or Davis et.al., (1980) were presented and the shortcomings of their application to the posed problem were discussed. The factor of safety assessed using the collapse tunnel pressures that these solutions provide are interpreted, at best, as a crude estimate of the actual factor of safety. While these solutions seem to operate quite satisfactorily for the frictionless soil model (ϕ_u=0), they may not provide good approximations of the collapse loads in soils under drained conditions (c and ϕ not equal to 0). Unsafe estimates of the collapse tunnel pressure may be obtained. It was then advised to allow as much safety as possible or, preferably, to avoid any extrapolation of the NGRC beyond its terminal point. An additional criteria that could be evoked is the limiting dimensionless crown displacement, U=1.8, derived in Section 2.3.4.3 from observations in tunnel model tests. Recall that above this value a ground collapse condition was noted in the physical models.

A compact generalization of the numerical results in terms of ground settlement, similar to that undertaken for

the ground reaction curves, was not attempted, although it could possibly be implemented. In fact, Resendiz and Romo (1981) succeeded in doing so, using a model similar to the frictionless model used herein. Nevertheless, the charts included in Appendix C, with normalized surface and subsurface settlements, do present sufficient generality for practical use, simply requiring interpolation of results for conditions other than those considered in the parametric analyses. An example of the interpolation procedure required was presented in terms of the relations between the maximum surface and crown settlements discussed earlier.

Finally, the approximate nature of the generalized solution must be emphasized. It reflects the simplifications introduced, the very approximate nature of the numerical model used, of the simplified constitutive models employed, the approximations related to the finite number of increments used to describe the degradation of the soil stiffness in the pre-failure regime, etc. Although these approximations have been introduced with some degree of discernment and judgement, which in turn requires equal consideration when using these solutions, it is important to test them against actual field cases. This is the last step in the development of the projected design procedure. It would include the validation of the proposed method, comparing its results with measured tunnel performance. The proposed method needs to be calibrated by assessing the deviation of predictions and by identifying the reasons for

these deviations. This is the next natural step in the generalization process, following the modelling step just completed in the present Chapter. Accordingly, this will be one of the goals of the next chapter.

However, before this undertaking, an additional and important aspect of the tunnel design should be addressed. This refers to the ground-lining interaction phase of the tunnel construction representation, only briefly discussed in this chapter. The development presented so far attempted to portray the ground response through a 2D representation, up to the instant the support is activated. The first part of the next chapter will present and discuss procedures to represent the interaction process, taking into consideration the main features of the ground response prior to the support installation. With this, a design procedure for shallow tunnels would have been completed.

7. DEVELOPMENT AND VALIDATION OF A DESIGN PROCEDURE

7.1 Introduction

In Chapter 6, an approximate procedure was developed through which relationships between radial stresses and radial displacements at a point of the contour of a shallow tunnel could be obtained without the need of finite element modelling. These relationships, expressed for two idealized soil models in both algebraic and graphic forms, allow the amount of ground stress release in a two-dimensional representation to be determined from the knowledge of the tunnel closure. Other relationships were derived from which the change in the ground stiffness could be assessed by also relating it to the amount of tunnel closure. The first type of relationship expresses the stress transfer, or two-dimensional 'arching' process around a stable opening upon its closure, by a reduction of the stresses acting on its contour. The second portrays the response of the ground, in terms of changes in its stiffness associated with this stress transfer and of the tunnel closure.

Concurrently with these developments, relationships were established between the amount of stress release allowed at the opening and the settlements induced at the ground surface and subsurface. All relations were presented in a non-dimensional and scale independent form to allow generality.

The above derivations assumed that the opening was supported by internal radial and shear stresses which had been gradually and continuously reduced to a fraction Σ of the in situ stresses. This was in order to simulate the ground stress transfer process in an advancing tunnel. A simplification in this simulation process was to disregard the action of an actual lining support (see Sections 2.3.5 and 2.3.6). Both in a simplified 2D representation or in a 3D simulation, it is known that the lining does affect the ground response, as it interacts with the soil by inducing changes in stresses that may alter its stiffness.

In the present chapter the soil-lining interaction will be discussed and a simple model representing the process will be presented and evaluated. The effects of the lining action in the 2D ground response will be addressed. An approximate procedure to account for these effects in the tunnel design will be proposed and evaluated. Within this procedure, the ground stress reduction by arching and the changes in ground stiffness taking place prior to lining activation (in a 2D representation) will be taken into consideration. Subsequently, a complete sequence for design will be proposed, in which the ground settlements and lining loads will be obtained simultaneously. This newly proposed method is verified against results of simulations of shallow tunnels through numerical and physical modelling. Some of the limitations of the proposed procedure will be discussed. Finally, the method will be validated by comparing its

predictive capabilities against observed field performances in some case histories.

7.2 Soil-Lining Interaction

7.2.1 Choice of the Model: Hartmann Solution

The basic aspects of the soil-lining interaction process were discussed in Sections 2.3.5 and 2.3.6. The available models representing this process were reviewed in Section 4.3.2. The most simple lining design methods that take into account the interaction between the ground and the support in the lining loads calculation, are those reviewed in Sections 4.3.2.3 and 4.3.2.4, i.e., the ring-and-plate and the ring-and-spring models, respectively. It was shown in Section 4.4.2.2 that the latter is perhaps the most popular type of statical system used for assessment of lining loads in shallow tunnels. Any of the above models could be used in connection with the design procedure being developed in this thesis. If fact, the ring-and-spring models, with ground reaction represented by discrete springs or bars, could be the most convenient one to be used. These models could allow different ground stiffnesses to be considered at distinct points of the tunnel contour. This would permit, as suggested in Section 2.2, taking into account a 'weakened' or 'softened embedment' condition whenever applicable. Certain criteria would have to be established and tested in order to assign different spring

constants (radial and tangential) for points at intermediate locations between crown, springline and floor.

The effect of such differential degradation of the ground stiffness around the tunnel could not be considered if other soil-lining interaction models were chosen. An averaged ground stiffness would have to be defined, as these models assume a constant modulus of deformation, to represent the linear elastic behaviour of the ground. The accuracy lost with this assumption is in turn compensated by a gain in the compactness of the solution, particularly if a closed form analytical solution is selected. The latter, furthermore, would offer considerable ease in the design procedure since it permits simpler handling of parametric or sensitivity analyses which are sometimes required at initial design stages. Additionally, it is believed that if such an analytical solution could be coupled with the design procedure, the further simplifications it requires would not be discordant with the overall approximate nature of other components in the design procedure.

These aspects lead to favouring a closed form ring-and-plate solution to analyse the soil-lining interaction phase of the design procedure and to serve as a tool for the lining load prediction. The consequences and limitations of this choice will be further discussed in this and in the following sections. A number of options are offered with this choice but by inspecting the solutions reviewed in Section 4.3.2.3, not many are found that would

not introduce further approximations. In fact, Hartmann's (1970,1972) approach is the only one that makes full allowance for the non-uniform stress field existing in a shallow tunnel, which is generated by in situ stress ratios different from unity and by the action of gravity. Therefore, this solution seems to be the most convenient for the problem at hand, in that it partly accounts for one of the features of a shallow tunnel situation: the gravitational stress gradient across the opening. It neglects, however, the effect of the ground surface, since the ground is approximated by an infinite plate subjected to a gravitational stress field. It was shown in Section 2.2 that the effect of the ground surface on the lining response can be considered as neglible for H/D greater than 1.5 but that the influence of the gravity cannot be disregarded in the interaction analysis for most shallow tunnels.

Hartmann's original solution treats both soil and lining as linear elastic, isotropic and homogeneous materials. The opening is assumed to be circular, the ground mass is represented by an infinite plate and the lining by a weightless thin cylindrical shell of constant thickness. The lining is assumed to be installed in the opening before any displacement occurs in the ground. Moreover, lining and ground are assumed to be in full contact, so a non-slip condition at the interface is admitted. More recently (Hartmann, 1986: unpublished report) a full slip solution was derived but will not be discussed herein for reasons

presented in Section 2.3.5.

A zero stress horizontal surface represents the ground surface, so that the principal in situ stresses are vertical (γz) and horizontal ($K\gamma z$), where z is the depth to a point measured from the ground surface, γ is the unit weight of the soil and K is the in situ stress ratio.

The lining is activated by an excavation loading condition (see Section 4.3.2.3). The solution is formulated for both plane strain and plane stress, the former being more relevant to the tunnel problem and is presented herein. The equilibrium and compatibility conditions are formulated in terms of polar coordinates. The internal forces in the lining are computed using Flügge's (1962:134) differential equations relating lining thrust, shear and bending moments to the lining displacements.

The relative stiffness of the lining-ground system is expressed in terms of two coefficients, referred to as the compressibility ($\dot{a}$) and the flexibility (β) ratios. These are defined as:

$$\dot{a}=\frac{E_s A_s(1+\mu)}{E.r_o(1-\mu_s^2)} \qquad [7.1]$$

$$\beta=\frac{E_s I_s(1+\mu)}{E.r_o^3(1-\mu_s^2)} \qquad [7.2]$$

where r_o is the tunnel radius, E, μ and E_s, μ_s are elastic constants for the ground and the support, A_s is the cross sectional area of the lining per unit length of the tunnel (A_s=d=lining thickness) and I_s is the moment of inertia of the support per unit length of the tunnel ($I_s=d^3/12$).

Note that these ratios are related to the corresponding ratios used in the Einstein and Schwartz (1979) derivation (C and F, see Section 2.3.5.2) by:

$$\alpha = \frac{1}{C(1-\mu)}$$

$$\beta = \frac{1}{F(1-\mu)}$$

Typical flexibility and compressibility ratios can be found in Table 7.1. These were calculated using both the Hartmann and Einstein and Schwartz definitions. The ratios were calculated for six soil types and three common lining systems. The assumptions made are given in the table. Note that the deformation moduli given correspond to initial tangent values at a confining stress of 0.1 MPa. As indicated in Section 2.3.5.3, different stiffness ratios would have to be considered if the effect of the global 'softening' of the ground on the decrease of the in situ stresses with tunnel advance, was to be considered.

The notation and conventions used in Hartmann's solution are shown in Figure 7.1. Note that stresses are positive in compression. A summary of the solution is presented in Figure 7.2, where the equations for lining stresses, displacements and internal forces are given. It should be noted that v'_{ro} and $v'_{\phi o}$ given by equations 7.7 and 7.9 are the components of the total radial and tangential displacements, to which the overall heave component v''_{zo} given by equation 7.10, should be added in order to obtain the total lining displacements v_{ro} and $v_{\phi o}$, as shown in equations 7.6 and 7.8. Note moreover, that the heave v''_{zo} is

Soil		Steel ribs and lagging[2]		Precast concrete segments[3]		Shotcrete[4]	
Type	E_t[1] (MPa)	β	F	β	F	β	F
Soft clay	8	0.030	40	0.140	10	0.040	35
Medium clay	25	0.010	125	0.040	30	0.012	110
Stiff clay	100	0.003	500	0.010	120	0.003	450
Loose sand	40	0.007	200	0.030	50	0.008	170
Medium sand	60	0.004	300	0.020	70	0.005	250
Dense sand	120	0.002	600	0.009	150	0.002	550
		$\frac{\dot{\alpha}}{\beta} = \frac{F}{C} \cong 1{,}300$		$\frac{\dot{\alpha}}{\beta} = \frac{F}{C} \simeq 1{,}200$		$\frac{\dot{\alpha}}{\beta} = \frac{F}{C} \simeq 2{,}800$	

Notes:

(1) Typical initial tangent values at a confinement pressure of 0.1 MPa (tunnel at 10 m depth in a soil with $\gamma = 17$ kN/m^3 and $K_0 = 0.7$).

(2) Lagging stiffness disregarded. Influence of joints in β disregarded. Joint compressibility partly accounted. $E_s = 100$ GPa, $d/r_0 = 1.3 \times 10^{-3}$, $I_s/r_0 = 10^{-6}$.

(3) Influence of joints in β disregarded. Joint compressibility partly accounted. $E_s = 10$ GPa, $d/r_0 = 0.1$, $I_s = d^3/12$.

(4) Hardening effect partly accounted. $E_s = 10$ GPa. Presence of ribs or lattice girders disregarded. $d/r_0 = 0.065$, $I_s = d^3/12$.

(5) In all cases $\mu = \mu_s$.

Table 7.1 Typical Relative Stiffness Ratios for Common Linings and Soils

dependent on r_1, which is the radius of an arbitrary circle at which the vertical heave displacement is set equal to zero. If this boundary is located at infinity, an infinite heave would be calculated. Therefore, for practical applications, r_1 is to be chosen according to the position of a stiffer horizon below the tunnel floor or to the location of points below the floor, where no displacements are noted. From what was shown in Table 6.9 (Section 6.3.1.2), the ratio r_o/r_1 is likely to be larger than 1/4 or 1/3. It should be pointed out that the shear force Q_ϕ given by equation 7.13 was not included in Hartmann's original solution, but it could be obtained by differentiating the bending moments ($Q_\phi=(1/r_o)\partial M/\partial\phi$).

Hartmann's solution includes second-order terms that are frequently neglected in similar derivations (for example, see Schwartz and Einstein, 1980:367). The first term in the expression for the bending moments (equation 7.12 in Figure 7.2) represents the influence of the lining perimeter reduction, caused by the action of the thrust forces. A decrease in the lining diameter produces an increase in the lining curvature that leads to bending stresses. These stresses will be present even under an ideal isotropic loading condition ($K=1$ and $z_o >> r_o$). In most cases this term is of small magnitude. The second term in the expression for M_ϕ gives the influence of the overburden stress γz_o on the bending moment and the third describes the influence of the gravitational stress gradient across the

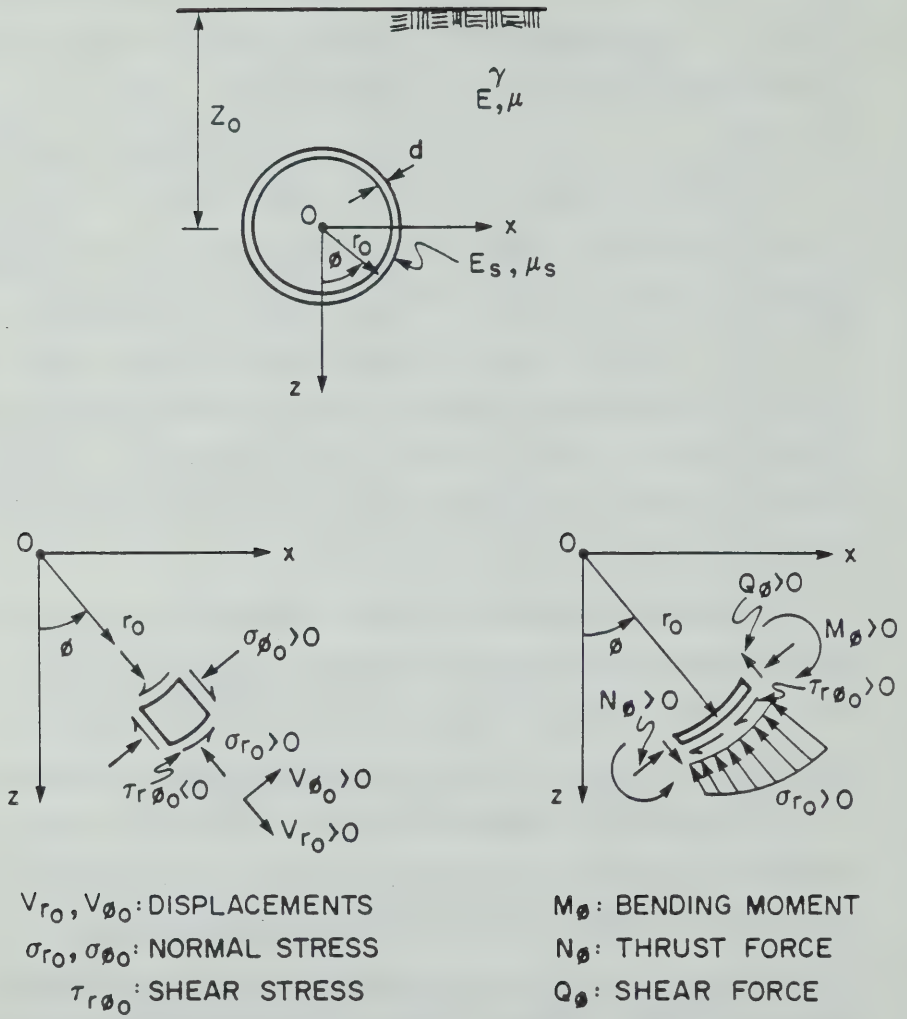

Figure 7.1 Notations and Conventions used in Hartmann's Solution

$$\alpha = \frac{E_s A_s (1+\mu)}{E r_0 (1-\mu_s^2)} \qquad (7.1)$$

$$\beta = \frac{E_s I_s (1+\mu)}{E r_0^3 (1-\mu_s^2)} \qquad (7.2)$$

$$\sigma_{r0} = \frac{(1+K)(\alpha+\beta)}{2(1+\alpha+\beta)} \gamma z_0 + \frac{(1+K)\alpha}{4(1+\alpha)} \gamma r_0 \cos\phi - \frac{(1-K)(3-4\mu)(\alpha-9\beta-12\alpha\beta)}{2\{1+(3-2\mu)\alpha+3[5-6\mu+4(3-4\mu)\alpha]\beta\}} \gamma z_0 \cos(2\phi) - \frac{(1-K)(3-4\mu)(\alpha-32\beta-72\alpha\beta)}{4\{1+(5-4\mu)\alpha+8[7-8\mu+9(3-4\mu)\alpha]\beta\}} \gamma r_0 \cos(3\phi) \qquad (7.3)$$

$$\sigma_{\phi 0} = \frac{(1+K)(2+\alpha+\beta)}{2(1+\alpha+\beta)} \gamma z_0 + \frac{2+\alpha+(K-\mu-\mu\lambda)(4+3\alpha)}{4(1-\mu)(1+\alpha)} \gamma r_0 \cos\phi - \frac{(1-K)\{4+(3+4\mu)\alpha+3[11-12\mu+4(3-4\mu)\alpha]\beta\}}{2\{1+(3-2\mu)\alpha+3[5-6\mu+4(3-4\mu)\alpha]\beta\}} \gamma z_0 \cos(2\phi) - \frac{(1-K)\{4+(5+4\mu)\alpha+8[16-16\mu+9(3-4\mu)\alpha]\beta\}}{4\{1+(5-4\mu)\alpha+8[7-8\mu+9(3-4\mu)\alpha]\beta\}} \gamma r_0 \cos(3\phi) \qquad (7.4)$$

$$\tau_{r\phi 0} = \frac{(1+K)\alpha}{4(1+\alpha)} \gamma r_0 \sin\phi - \frac{(1-K)(3-4\mu)(1+6\beta)\alpha}{1+(3-2\mu)\alpha+3[5-6\mu+4(3-4\mu)\alpha]\beta} \gamma z_0 \sin(2\phi) - \frac{3(1-K)(3-4\mu)(1+24\beta)\alpha}{4\{1+(5-4\mu)\alpha+8[7-8\mu+9(3-4\mu)\alpha]\beta\}} \gamma r_0 \sin(3\phi) \qquad (7.5)$$

$$v_{r0} = v'_{r0} + v''_{z0} \cos\phi \qquad (7.6)$$

$$v'_{r0} = -\frac{1+\mu}{E}\left(\frac{1+K}{2(1+\alpha+\beta)} \gamma z_0 r_0 + \frac{(1+K)}{8(1+\alpha)} \gamma r_0^2 \cos\phi + \frac{(1-K)(3-4\mu)(1+2\alpha)}{2\{1+(3-2\mu)\alpha+3[5-6\mu+4(3-4\mu)\alpha]\beta\}} \gamma z_0 r_0 \cos(2\phi) + \frac{(1-K)(3-4\mu)(1+3\alpha)}{8\{1+(5-4\mu)\alpha+8[7-8\mu-9(3-4\mu)\alpha]\beta\}} \gamma r_0^2 \cos(3\phi)\right) \qquad (7.7)$$

$$v_{\phi 0} = v'_{\phi 0} + v''_{z0} \sin\phi \qquad (7.8)$$

$$v'_{\phi 0} = \frac{1+\mu}{E}\left(-\frac{1+K}{8(1+\alpha)} \gamma r_0^2 \sin\phi + \frac{(1-K)(3-4\mu)(1+\alpha+3\beta)}{2\{1+(3-2\mu)\alpha+3[5-6\mu+4(3-4\mu)\alpha]\beta\}} \gamma z_0 r_0 \sin(2\phi) + \frac{(1-K)(3-4\mu)(1+\alpha+16\beta)}{8\{1+(5-4\mu)\alpha+8[7-8\mu+9(3-4\mu)\alpha]\beta\}} \gamma r_0^2 \sin(3\phi)\right) \qquad (7.9)$$

$$v''_{z0} = \frac{(1+\mu)(3-4\mu)}{4(1-\mu)E} \gamma r_0^2 \ln\frac{r_0}{r_1} \qquad (7.10)$$

$$N_\phi = \frac{(1+K)(\alpha+\beta)}{2(1+\alpha+\beta)} \gamma z_0 r_0 + \frac{(1+K)\alpha}{4(1+\alpha)} \gamma r_0^2 \cos\phi - \frac{(1-K)(3-4\mu)(\alpha+3\beta+12\alpha\beta)}{2\{1+(3-2\mu)\alpha+3[5-6\mu+4(3-4\mu)\alpha]\beta\}} \gamma z_0 r_0 \cos(2\phi) - \frac{(1-K)(3-4\mu)(\alpha+4\beta+36\alpha\beta)}{4\{1+(5-4\mu)\alpha+8[7-8\mu+9(3-4\mu)\alpha]\beta\}} \gamma r_0^2 \cos(3\phi) \qquad (7.11)$$

$$M_\phi = -\frac{(1+K)\beta}{2(1+\alpha+\beta)} \gamma z_0 r_0^2 + \frac{3(1-K)(3-4\mu)(1+2\alpha)\beta}{2\{1+(3-2\mu)\alpha+3[5-6\mu-4(3-4\mu)\alpha]\beta\}} \gamma z_0 r_0^2 \cos(2\phi) + \frac{(1-K)(3-4\mu)(1+3\alpha)\beta}{1+(5-4\mu)\alpha+8[7-8\mu+9(3-4\mu)\alpha]\beta} \gamma r_0^3 \cos(3\phi) \qquad (7.12)$$

$$Q_\phi = -\frac{3(1-K)(3-4\mu)(1+2\alpha)\beta}{\{1+(3-2\mu)\alpha+3[5-6\mu+4(3-4\mu)\alpha]\beta\}} \gamma z_0 r_0 \sin(2\phi) - \frac{3(1-K)(3-4\mu)(1+3\alpha)\beta}{1+(5-4\mu)\alpha+8\{7-8\mu+9(3-4\mu)\alpha]\beta\}} \gamma r_0^2 \sin(3\phi) \qquad (7.13)$$

Figure 7.2 Lining Stresses, Displacements and Internal Forces Given by Hartmann's Solution

opening. Correspondingly, the first and third terms in the expression for N_ϕ (equation 7.11) represents the influence of the overburden stress, while the second and fourth terms describe the influence of the gravity. Moreover, in the latter equation, the first and second terms reflect the effect of the mean normal in situ stress, while the third and fourth terms reflect the effect of the mean in situ stress difference.

Provided the thickness of the lining is small in comparison with the tunnel radius, the second order moments are small. Moreover, if the tunnel is deep (a large z_o/r_o ratio), then Hartmann's solution becomes equivalent to other deep tunnel solutions. In fact, it yields results which are basically identical to Windels (1967), Curtis-Muir Wood (1976), Einstein and Schwartz (1979) and Ahrens et.al., (1982) closed form solutions, as discussed in Section 4.3.2.3. It is simple to show that if the lining is disregarded, (i.e., $\dot{a}=\beta=0$), Hartmann's expression for the tangential stresses at the opening contour reduces to Mindlin's solution for an opening in an infinite plate under gravity with lateral restraint (Mindlin, 1940:1136 - equation 58).

In order to assess the consequences of the infinite plate assumption in Hartmann's solution, a comparison between this solution and the results of a finite element analysis of a shallow tunnel would be required. Unfortunately, the lining representation adopted in the 2D

finite element model presented in Chapter 5 does not permit a direct comparison to be made, particularly regarding bending moments. Ranken (1978), however, performed a few finite element analyses of circular shallow tunnels, whose results can be used for this comparison. Five linear elastic analyses were carried out, for different cover to diameter ratios that varied between 0.5 and 4.5. Details of this study were presented by Ranken (Op.cit.:96) and will not be repeated herein, except for essential information. In all analyses, the in situ stress ratio in the ground was kept constant and equal to 0.5. The ratio of the soil to lining Young's modulus was set equal to 0.0205. The Poisson's ratio of the soil was 0.25 and the lining was 0.1562. The lining thickness was 10% of the tunnel radius. The resulting relative stiffness ratios were $\dot{\alpha}$=6.25 and β=0.0052. As indicated in Table 7.1, these values would be typical for a rib and lagging lined tunnel, in a medium to loose sand. The lining was installed before any release of ground stresses took place. A fixed lower boundary was set up at three diameters below the tunnel floor. A gravitational field stress condition was considered, so the results incorporate both the action of the ground surface and of the in situ stress gradient across the opening. Although both full and no slip conditions were considered for the lining-ground interface, only the results of the latter case will be examined herein.

The solution by Hartmann, as summarized in Figure 7.2, was applied to these cases and some representative results are shown in Figure 7.3. The results of the closed form solution are presented by continuous lines, whereas the numerical results by Ranken are shown by discrete points. In the upper part of Figure 7.3, the calculated thrust forces and bending moments at the crown of the tunnel lining are plotted together. The lower part shows the calculated crown vertical displacement and some diameter changes. All results were conveniently normalized to allow the comparison. Fairly similar results were found at other points of the contour.

Apart from inaccuracies that could be attributed to numerical approximations, the differences in the results by the two approaches can be ascribed to the influence of the ground surface, included in the finite element analyses. As expected, these differences seem to increase as the tunnel becomes shallower. Hartmann's solution seems to furnish results which are either approximately equal to or greater in magnitude than the finite element solution. Moreover, it is noted that both solutions tend to yield very similar results for cover to diameter ratios greater than 1.5. This tends to confirm that the effect of the ground surface on the lining response seems indeed negligible for H/D greater than 1.5 (see Section 2.2). Moreover, even for smaller ratios, the analytical solution seems to furnish results which are greater in magnitude than the numerical solution. Therefore, the Hartmann solution may provide conservative

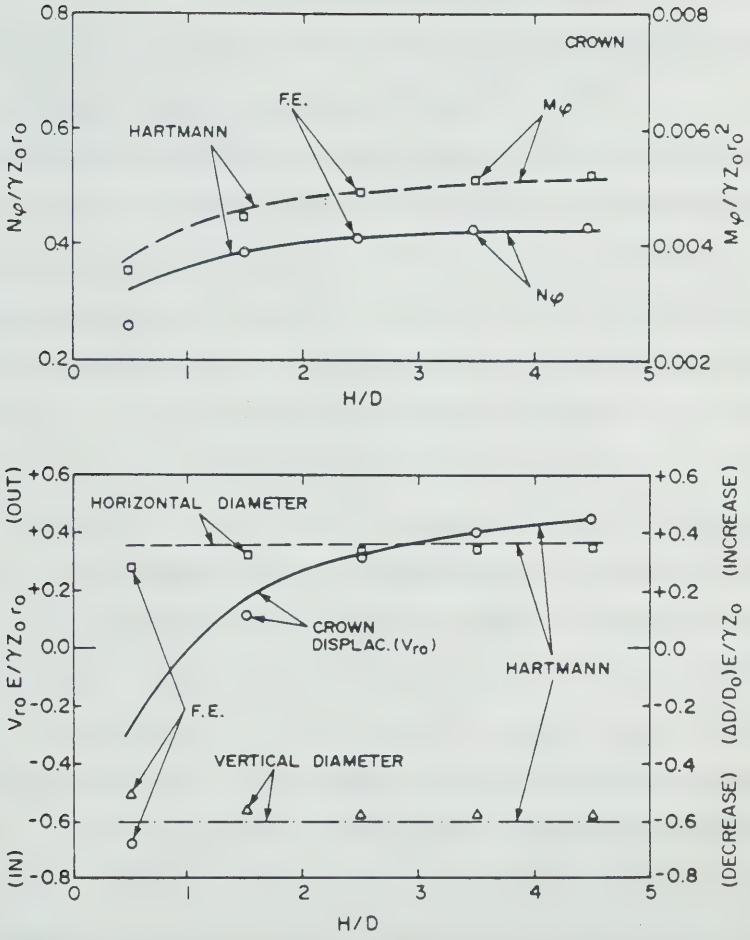

Figure 7.3 Comparison of Lining Responses Calculated for Different Tunnel Depths, with and without Account of the Influence of the Ground Surface

estimates of the lining response for H/D smaller than 1.5. These findings are valid not only for the tunnel crown but for other points of the contour.

The largest discrepancy noted refers to the magnitude of the crown displacement. This result is not surprising since it is the one that involved a larger degree of approximation. As can be noted in Figure 7.2, the radial displacement v_{ro} (equation 7.6) depends on the ground heave v''_{zo} given by equation 7.10. Two approximations are involved in estimating this component of the crown displacement. The first refers to r_1, defined earlier as the radius of an arbitrary circle at which the heave is equal to zero. To simulate the conditions involved in the finite element analyses, r_1 was set equal to 3.5D (thus $r_o/r_1=1/7$), so that such a circle is tangent to the lower boundary of the finite element mesh. This correspondence is, however, not exact and differences in the displacement calculation may result. Secondly, as noticed in equation 7.10, the heave v''_{zo} depends only on the ground modulus E, and is independent of the lining stiffness. Except for the soil to lining modulus ratio, Ranken (1978) did not provide the value of soil modulus used in his analyses. A modulus of 20.09 MPa has been chosen in the present calculation, which may differ from that selected by Ranken.

In summary, it may be concluded that, subject to the assumptions made (notably that of a linear elastic behaviour for soil and lining), Hartmann's solution seems to provide a

good approximation for the two-dimensional ground-lining interaction process, despite not taking the influence of the ground surface into account.

7.2.2 Soil-Lining Interaction Analysis for Delayed Lining Installation in a Non-Linear Ground Mass

Hartmann's solution, like other two-dimensional closed form solutions, assumes the lining to be in place before the excavation loading develops. It was shown in Sections 4.3.2.7 and 5.2.1.1 that there is no rigorous procedure to account for the effects resulting from delaying (in space) the installation of the lining, which involves three-dimensional stress changes in a simpler two-dimensional representation. It was also explained earlier in this thesis why the approximate procedure of the gradual reduction of the in situ stresses around the tunnel was favoured in the present work, to simulate the delayed placement of the lining in a 2D model.

In essence, this approximation mimics the actual stress changes or arching process that leads to smaller ground loads being transferred to the lining as a result of the interaction process within the soil. In Chapter 5 it was shown that, although approximate, this procedure may indeed furnish sensible results in terms of estimates of the tunnel performance.

If Hartmann's solution is to be used to analyse the soil-lining interaction phase of the tunnelling process,

instead of the finite element simulation used in Chapter 5, then that ground load reduction should be introduced into the solution. Provided that in this analysis the lining response, in terms of its loads and displacements, is the only matter of interest, then the reduction of ground loads can be easily implemented. It can be represented by a reduction in the ground stress field, which can be introduced by a reduction in the unit weight of the ground. This in turn, can be related to the amount of stress release (α) taking place up until the instant the support is installed. The reduced unit weight of the soil would then be:

$$\gamma_{red} = \gamma(1-\alpha) = \gamma\Sigma \qquad [7.14]$$

where γ is the actual in situ weight of the ground.

It should be remembered that in the two dimensional representation adopted in this study (see Section 5.2.2.1) which led to the generalized results presented in Chapter 6, the same stress reduction factor is applied uniformly to all points of the tunnel profile and reduces both radial and shear stresses in the same proportion. Due to this assumption, the current stresses acting on the perimeter of the 2D opening after a certain ground stress release α, and immediately before the support installation against the ground of unit weight γ and in situ stress ratio K_o, are exactly equal to the in situ stresses acting on the contour of a tunnel with same geometry, yet to be excavated in an undisturbed ground mass, which has the same in situ stress

ratio K_o but with a reduced unit weight given by equation 7.14. Provided that a linear elastic behaviour can be ensured, the ground-lining response will not depend on the stress and strain changes developing in the ground prior to the support installation. The magnitude of the lining loads and lining displacements furnished by Hartmann's solution, with a field stress reduced through a reduced soil unit weight, will be correct, despite the stress changes and displacements induced within the ground mass being incorrect. The reduced unit weight approximation does not account for the stress changes and displacements induced prior to lining activation. Apparently there is no formal impediment to adapt Hartmann's solution for this new condition, which would explictly include a stress release factor $(1-\Sigma)$ in the derivation, and take into account the stress and strain changes in the ground prior to installing the support. In fact, the Schwartz and Einstein (1980:393) derivation, incorporating a 'soft core' region (see Section 4.3.2.7) that leads to 'pre-support' ground movements is an example of how such a solution could be worked out. Nevertheless, such an undertaking was felt to be out of scope of the present work and therefore was not attempted.

If the non-linear behaviour of the ground is taken into consideration, then the above approach is merely an approximation. The stress changes in the ground prior to the lining installation do have an impact on the ground-lining interaction, as the ground stiffness is inevitably changed.

This point was raised and discussed earlier in Section 2.3.5.3. Moreover, the separate analyses of the pre-support ground response and of the soil-support interaction phase require a superposition of effects for the final equilibrium condition to be found. The validity of such superposition in a non-linear problem is debatable. Furthermore, there is nothing to support a linear elastic interaction analysis in a soil that exhibits a non-linear response. Perhaps the only argument that could be raised in its favour, is that, provided the increments of ground displacements taking place after lining installation are small in comparison with those developing in the finite unloading increment imposed to the ground before that, then the linear elastic approximation may not be entirely discordant with the non-linear, yet piecewise elastic model used herein. But this argument may not be valid under certain practical situations. Therefore, if the linear elastic interaction analysis using Hartmann's solution is used in connection with the design procedure being developed herein, it must be regarded as an approximation whose consequences should be assessed accordingly.

For this end, the numerical analyses described in Section 2.3.5.3 can be helpful. Three analyses were carried out there, with different amounts of ground stress release at the circular opening prior to lining installation: 0%, 40% and 80%. An additional calculation was performed allowing a full stress release. The ground properties were

as given earlier in that section. The soil strength including both frictional and cohesive components and the in situ tangent modulus increasing with depth, were maintained in all analyses. The tunnel with a 4 m diameter and 6.2 m cover was intentionally lined with a very soft and flexible support, so that substantial displacements could develop after its installation. This condition is therefore a critical one in terms of enhancing the effect of the non-linear response of the soil on the ground-lining interaction process. For the reasons exposed in Chapter 5, a fairly thick lining with 0.5 m thickness was used with constant elastic properties, which led to a compressibility ratio α of 0.8 (C=1.8) and a flexibility ratio β of 0.017 (F=86). These were calculated with respect to the in situ elastic modulus of the soil at tunnel axis elevation. Such values could correspond to a flexible and compressible shotcrete lining in a medium clay.

The equilibrium points in terms of radial stresses and radial displacements at crown, springline and floor, as obtained by the finite element analyses, are shown in Figures 7.4, 7.5 and 7.6, respectively. The continuous solid curves shown are the ground reaction curves for these three points, as calculated for a full stress release without installing the lining. The dashed lines link the points representing the equilibrium to the starting point of lining activation. The abscissae of the latter points give the radial closures of the opening when the support was

activated. Unlike the radial displacements that were calculated at nodal points, the radial stresses at equilibrium were obtained by extrapolating the calculated element stresses to the tunnel contour.

Following this, an attempt was made to obtain the equilibrium points (L and E as explained later), using Hartmann's solution coupled with the generalized solution presented in Section 6.4 for obtaining the ground reaction curves. In order to achieve this, a few additional assumptions had to be made and these are discussed in the following.

As stated earlier, the closed form interaction analyses require an assessment of a reduced unit weight, γ_{red}, for the soil. It is necessary to evaluate the ratio of current stress to initial stress (Σ) at tunnel contour when the support is installed, so that γ_{red} can be determined through equation 7.14. If the GRC given by the generalized solution presented in Section 6.4 coincided with the GRC calculated in the finite element analysis, then there would be no need to calculate Σ at lining installation, as it would be equal to that imposed in the analysis. However, since the GRCs do not coincide, as the generalized solution is an approximation of the correct GRC, that need is justified.

To assess Σ, one could assume that the radial displacements at the instant of lining installation are known and equal to those given by the finite element calculation. In a more general case, these displacements

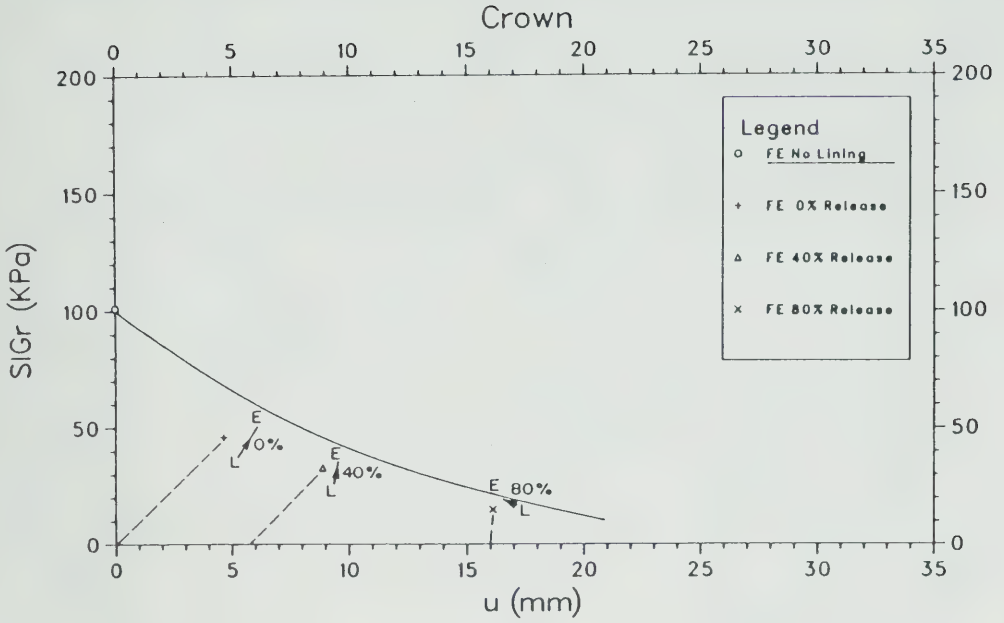

Figure 7.4 Equilibrium Points of the Soil-Lining Interaction at Tunnel Crown

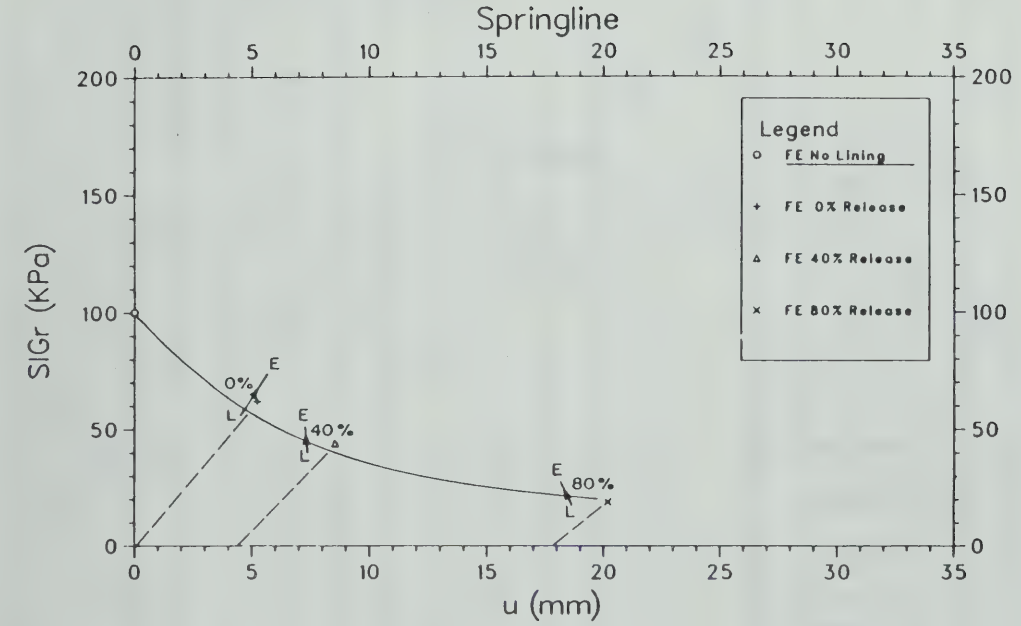

Figure 7.5 Equilibrium Points of the Soil-Lining Interaction at Tunnel Springline

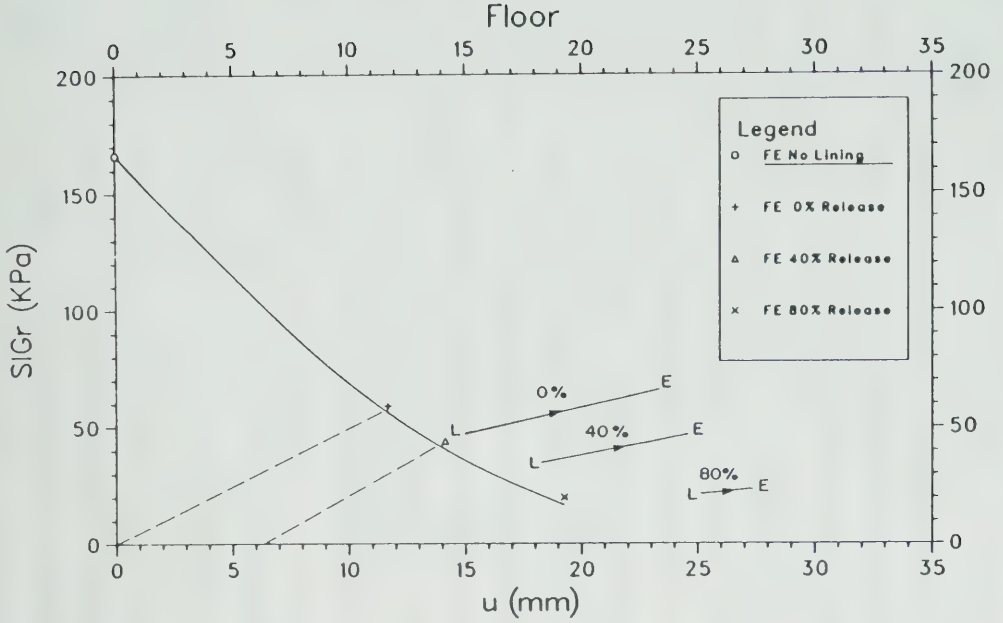

Figure 7.6 Equilibrium Points of the Soil-Lining Interaction at Tunnel Floor

could be estimated by the approximate procedure presented in Section 5.3.5.2 for the assessment of tunnel closure at sections behind the face. With the radial displacements developing before lining installation, it is possible to determine the value of α or Σ at crown (C), springline (S) and floor (F). This is done through the NNGRC or λ curves given by equation 6.24. Before that, however, one has to define $\alpha_{ref}=1-\Sigma_{ref}$, for C, S and F, which is a function of (m-1), which, as indicated by equation 6.30, is a function of the friction angle, ϕ. The friction angle to be used for this purpose is the one obtained after adjusting the actual ϕ to account for the non-zero cohesion, as indicated by equation 6.10. In this case, there is no need to amend the friction angle since the failure ratio, R_{ref}, is equal to one. Otherwise ϕ would have to be adjusted according to equation 6.3. After defining the α_{ref} values, the U_{ref} values should be obtained through the function relating α_{ref}/U_{ref} to H/D. This requires interpolating the reference values between the solutions given by two consecutive K_o curves which bracket the K_o used in the finite element analyses (0.75). Alternatively, one could simply assume the solution set with K_o closer to the required value. This alternative was favoured herein and the reference values for α and U were taken from the solution set for K_o equal to 0.8.

Note also that since a variable in situ modulus profile has been assumed in the numerical analysis, the dimensionless radial displacements U should be normalized to

the in situ tangent moduli of the soil at points located half diameter radially away from the opening profile, as explained in Section 6.2.4.2.

The resulting parameters obtained following the above sequence of calculations are given in Table 7.2. One notes that different Σ ratios are obtained at different points of the tunnel contour, thus a mean Σ should be considered to get γ_{red}, by averaging the calculated ratios (springline being counted twice). For the 40% stress release considered in the finite element analysis, the approximate solution yielded 38.2% for the same radial closure of the opening. For the 80% stress release, the approximate solution furnished 75.4%. In both cases, the calculated amount of stress release for the same radial displacement at lining installation, is slightly smaller than the correct one, indicating that the approximate solution furnishes 'safer' estimates of the current ground stresses at the instant the support is activated.

It should be noted that only for the springline in the 80% stress release case, the generalized solution for the GRC was used beyond its limits, as defined in Section 6.5.1.

In summary, the reduced unit weight of the soil which simulates the reduction of the ground loads for the lining-ground interaction analyses, was obtained through the solution presented in Section 6.4.3. It was assumed that the radial closure is known at the instant the support is activated. The reduced unit weight is calculated directly

GEOMETRY: H = 6.2 m, D = 4.0 m

PROPERTIES: γ = 16 kN/m^3, K_0 = 0.75, ^fC = 39 KPa, ϕ = 21°,
R_f = 1.0, K = 330, n = 0.23, μ = 0.3
Thus:
$(E_{ti})_C$ = 23.53 MPa, $(E_{ti})_S$ = 24.68 MPa,
$(E_{ti})_F$ = 25.22 MPa
And:
ϕ_a = 32.2°, (m - 1) = 2.278

REFERENCES VALUES: H/D = 1.55, K_0 = 0.8 and (m - 1) = 2.278
Thus:

	α_{ref}	α_{ref}/U_{ref}	U_{ref}
C	0.572	0.860	0.665
S	0.528	1.125	0.469
F	0.448	2.020	0.222

REDUCED UNIT WEIGHT:

a. For FE with 0% stress release: $\gamma_{red} = \gamma$ = 16 kN/m^3

b. For FE with 40% stress release:

	u (mm) before lining	U	U/U_{ref}	λ	Σ
C	5.77	0.336	0.505	0.400	0.657
S	4.35	0.267	0.570	0.330	0.646
F	6.35	0.248	1.116	-0.070	0.521

Thus $\bar{\Sigma}$ = 0.618 and $\gamma_{red} = \gamma \bar{\Sigma}$ = 9.88 kN/m^3

c. For FE with 80% stress release:

	u (mm) before lining	U	U/U_{ref}	λ	Σ
C	15.98	0.930	1.399	-0.200	0.314
S	17.91	1.102	2.350	-0.380	0.271
F	15.04	0.570	2.568	-0.950	0.126

Thus $\bar{\Sigma}$ = 0.246 and $\gamma_{red} = \gamma \bar{\Sigma}$ = 3.93 kN/m^3

Table 7.2 Calculation of the Reduced Unit Weight of the Soil for the Lining-Ground Interaction Analyses

from the NNGRC or λ curves.

The other key aspect to be assessed is the ground modulus to be used in the interaction analyses. Had a fairly stiff lining been used, one could use an average modulus calculated at the instant the lining is installed, following the procedures set up in Section 6.4.3 (equation 6.26 and 6.29). The lining presently considered, however, is very deformable and large displacements are thus expected to occur. Therefore, the ground stiffness when the equilibrium with the liner is eventually achieved, is likely to be very different from that at the instant the lining is installed.

Regardless of what ground stiffness is to be considered or how it should be considered, an important assumption has to be made. It will be assumed that the tangent stiffness of the ground is uniquely related to the tunnel radial closure (U), through the derivative function of λ (λ') presented in Section 6.4. In other words, it will be assumed that the ground stiffness does not depend on the action of the lining. This is obviously a simplification which actually may not be correct. It was shown in Section 2.3.5 that the presence of the lining does affect the ground response, as it induced stress changes in the ground which in turn may cause changes in its stiffness. This effect will be disregarded by assuming that the λ' curves are not affected by the interaction between lining and ground.

This assumption also implies that the λ' curves can provide the ground stiffness either upon unloading or

loading. That is to say that the stiffness of the ground can be assessed through these curves both for increasing or decreasing tunnel radial closure. The latter could occur, for instance, at the springline of a lined tunnel squatting and forcing the soil to move outwardly. Note that the fully reversible stress-strain behaviour assumed in the 2D numerical model used in this work (Section 5.2.2.1) does not necessarily ensure the reversibility of behaviour in terms of the λ' curves.

An unstated assumption related to the use of both λ and λ' curves for each point of the tunnel contour, is that they have an independent existence. In other words, the sequence of loading or closure at different points of the opening profile, does not affect the response noted at a particular point of the contour which is always given by a unique λ or λ' curve. It was shown that the twice normalized ground reaction curves were derived from the parametric analyses, where a gradual stress reduction was simulated by applying a uniform amount of stress release (α) at the opening. Thus, the λ and λ' curves were obtained for this particular unloading condition and other unloading sequences could have led to different responses in terms of the λ and λ' curves. Therefore, in using the generalized solution developed, one may disregard the loading condition originally imposed and may operate with the curves for each point of the tunnel contour, as if they were unaffected by responses at other points of the contour. This is equivalent to assuming that

the ground response could be as that given by a series of radial springs, one for each point of the contour but not connected to each other. Obviously this is not true, as the responses expressed in terms of the λ and λ' curves do reflect the interactive responses of all points of the soil mass. The error involved in this assumption will be reduced considerably when the stress ratio, Σ, or tangent stiffness, E_t, obtained independently for each point of the tunnel profile are averaged and single $\bar{\Sigma}$ or $\bar{E}_t$ values are defined.

The idea of using a reduced ground stiffness compatible with the tunnel closure in a non-linear ground mass, for a lining-ground interaction analysis was proposed earlier by Kaiser (1981:265) for uniform stress field conditions. In this case, a simpler approach was favoured by approximating the ground response by a bilinear elastic model.

The average tangent stiffness of the ground at the instant the lining is installed can be readily estimated. With the U/U_{ref} given in Table 7.2, E_t is obtained through the λ' curves (or equation 6.26) and equation 6.27. The tangent moduli caculated for the tunnel crown, springline and floor are then averaged as indicated by equation 6.28. The calculations and results obtained are summarized in Table 7.3. As it is noticed, the delayed installation of the lining in the second finite element calculation (40% stress release) caused a drop in ground stiffness of about 27% and of about 75% in the third analysis (80% stress release).

a. F.E. with 0% stress release

$\lambda' = \lambda'_i \quad \therefore E_t = E_{t_i}$

Thus $\bar{E}_t = (E_{t_i})_C + 2(E_{t_i})_S + (E_{t_i})_F /4 = 24.53$ MPa

b. F.E. with 40% stress release

$E_t = (\lambda'/\lambda'_i) E_{t_i}$

With U/U_{ref} at lining installation (see previous table)

	U/U_{ref}	λ'	λ'_i	E_t (MPa)
C	0.505	1.000	1.278	18.41
S	0.570	0.940	1.425	16.28
F	1.116	0.840	1.006	21.07

Thus $\bar{E}_t = 18.01$ MPa

c. F.E. with 80% stress release

With U/U_{ref} at lining installation (previous table)

	U/U_{ref}	λ'	λ'_i	E_t (MPa)
C	0.930	0.420	1.278	7.73
S	1.102	0.160	1.425	2.77
F	0.570	0.440	1.006	11.04

Thus $\bar{E}_t$: 6.08 MPa

Table 7.3 Calculation of the Reduced Average Ground Stiffness at Lining Installation

At this point, the lining-ground interaction analysis can be performed. For each case (0, 40 and 80% release), the analytical solution summarized in Figure 7.2 was applied, using the data presented in Tables 7.2 and 7.3 as input. The radial stresses at the crown, springline and floor were found from equation 7.3, after calculating the relative stiffness ratios from equations 7.1 and 7.2. These are the equilibrium stresses acting on the lining at those points. The incremental radial displacements at these points resulting from the lining-ground interaction can be calculated from equations 7.6, 7.7 and 7.10. Note that the value of the in situ stress ratio (K_o or K) to be considered, is the value used in the finite element calculations (0.75). The value of r_1 to be used in equation 7.10, for assessment of the ground heave, $v"_{zo}$, as explained in Section 7.2.1, is the distance between the tunnel centre and the lower (fixed) boundary of the finite element mesh. In this case r_1 is equal to 13.5 m. The final (total) radial displacements are obtained by adding the incremental displacements to the displacements that took place before lining installation.

The values of final radial stresses and displacements thus obtained furnish the equilibrium points indicated by letter "L" in Figures 7.4, 7.5 and 7.6. One notes that in almost all cases and at all points of the tunnel contour, the stresses at L are smaller than the radial stresses at equilibrium calculated in the corresponding finite element

analysis. This result is not suprising, as it is a consequence of the criteria used to define the ground stiffness $\bar{E}_t$ adopted in this analysis. It has been assumed that the soil modulus during the lining-ground interaction remained equal to the soil modulus immediately prior to support activation. Since the increments of ground displacements after support installation in this particular case, are quite substantial due to the very compressible lining used, there is also a substantial change in the ground stiffness during the interaction process. Tunnel closure increases during this process and ground stiffness decreases accordingly. Hence at equilibrium the average soil modulus is likely to be appreciably less than that when the support was activated. Therefore, if no allowance is made to account for the additional 'softening' of the ground after the support is installed, then the calculated lining loads will likely be less than the correct ones as the support will be more compressible and more flexible relative to the soil than it should be.

A possibly better and safer assumption regarding the lining loads is to perform the interaction analysis, by assigning the ground its final stiffnesses, defined at the point of equilibrium. This would take into account the additional ground stiffness degradation due to the increment of tunnel closure after the lining is installed. However, this incremental closure is not known beforehand. An iterative procedure would have to be devised to solve the

problem. The lining-ground interaction analysis would be started by assigning the ground a stiffness compatible with the tunnel radial closure at the instant the support is activated, as it was done before. An incremental tunnel closure would then be calculated and a new ground stiffness would thus be estimated. The process would then be repeated until convergence is obtained, when the estimated ground stiffness at equilibrium is equal to the assigned ground stiffness used in the interaction analysis.

This algorithm was applied to the three cases being studied. For the 0% stress release case, five iterations were needed for solution convergence. An average modulus, $\bar{E}_t$ of 13.37 MPa was finally found, which represents 45% additional degradation of the ground stiffness resulting from the lined tunnel incremental closure. For the 40% stress release case, four iterations were needed and the resulting average ground modulus was equal to 9.79 MPa, representing a decrease of about 46% relative to the modulus at lining installation. For the 80% stress release case, only three iterations were needed and the resulting average ground modulus was 4.58 MPa, thus 25% lower than that at support activation.

The resulting equilibrium points found through these calculations are those indicated by letter "E" in Figures 7.4 to 7.6. The reduction in the adopted ground stiffness resulted, as expected, in higher radial stresses than at corresponding points L. More importantly, however, the

equilibrium stresses at E are systematically higher than the equilibrium stresses given by the finite element calculations. This indicates that, the adoption of the ground tangent stiffness calculated for the total tunnel closure at the final equilibrium situation is a safer assumption, though not excessively so, with respect to the ground loads acting on the tunnel. Conservative estimates of bending moments and thrust forces, as well as larger eccentricities are obtained with the latter assumption.

With respect to the radial displacements at equilibrium, mixed results are obtained. At the crown and floor (Figures 7.4 and 7.6), the displacements at both points L and E are larger than those found in the finite element analyses. While at the crown, the movements given by the approximated procedure are not excessively greater than the correct one, at the floor the displacements are substantially overestimated. It seems that this results from an overestimation of the ground heave component calculated by equation 7.10. The heave has been estimated using the same ground modulus used in the interaction analysis. This modulus seems to represent well the soil around the opening which is participating in the lining-ground interaction process. However, it may not approximate the stiffness of the ground below the tunnel, which would be underestimated by the procedure used.

At the springline, the displacements at both points L and E tend to be smaller than that calculated by the finite

element analysis. The degree of underestimation, however is not excessive.

With respect to displacements, those calculated at tunnel crown are of primary importance in the design procedure being developed. This is because all settlements developing above the tunnel are related to the crown displacement, through the normalized settlement distributions. As indicated in Figure 7.4, the approximate method for ground-lining interaction tends to furnish slightly conservative estimates of the crown displacements, which is likely to lead to conservative estimates of surface and subsurface settlements.

The arrows indicated in the last three figures give the directions followed by the equilibrium points, in the proposed analysis, during the iterative calculations. Although depicted as straight vectors, the path from L to E in the iterative analyses is, in fact, a non-linear one.

The above results indicate that, despite the approximate assumptions introduced, a very reasonable estimate of the equilibrium points is possible using the generalized solution developed in Chapter 6, coupled with the closed form solution presented in Section 7.2.1. Moreover, the procedure, derived to account for the delayed installation of a lining in a non-linear elastic ground, seems to furnish safe estimates of lining loads and displacements at the opening which in turn lead to safe estimates of the ground settlements. It should be noted that

the generalized solution for the ground response was used without restrictions and, indeed, at certain points and situations, it was used beyond its limits of strict validity (Section 6.5.1).

For design purposes, it seems preferable to use a ground modulus compatible with the final tunnel closure for the tunnel closure. As this is not known beforehand, a simple algorithm was developed to generate the solution, which is found after 3 to 5 iterations.

In solving the problem at hand, a calculation sequence emerged. This sequence will be summarized and discussed in Section 7.3 as a guideline for practical use. Other sequences or assumptions could have been introduced, and were in fact, attempted with end results that did not differ entirely from those shown. The one presented herein, however, seemed to be the most convenient and easiest for practical use.

There were two basic assumptions in the development of the above solution. Firstly, the effect of the delayed lining installation is accounted for by reducing the ground stress field, through a reduction of the unit weight of the soil. The latter is obtained from an average amount of stress release, calculated using the λ curves (normalized ground reaction curves), for an estimated tunnel closure at the point the support is installed. Secondly, the reduced tangent stiffness of the ground to be considered in the interaction analysis, is that given by the λ' curves or the

derivative of the normalized ground reaction curves. It is assumed that the ground stiffness is uniquely related to the tunnel closure through these curves, which are assumed to be unaffected by the lining action.

7.2.3 Influence of the Lining Presence on the Ground Settlements

The parametric analyses presented in Chapter 6 considered the tunnel to be unlined and, therefore, the resulting normalized settlement distributions shown, for instance, in Figures 6.48, 6.49, 6.59 and 6.60 (see also Appendix C) disregard the influence of a lining on the ground movements. If a fairly rigid lining is installed after a substantial amount of stress release, the increment of ground movements during the soil-lining interaction may not be very significant compared to the magnitude of movements developed in the pre-support phase. Hence, the settlements developing in the pre-support stage will tend to dominate. However, if the lining is flexible or compressible, then the settlement after lining installation can also be significant. This component of the total ground movement is the one affected by the presence of the lining in a two-dimensional tunnel representation.

The results of the finite element analyses discussed in Section 7.2.2 are helpful for the assessment of the lining influence on the ground settlements. The solid curves in Figures 7.7 and 7.8 represent the final distributions of

subsurface and surface settlements, calculated for the cases with ground stress release of 40 and 80% prior to lining installation. The broken curves represent the distributions calculated for an unlined opening, with crown settlements approximately equal to the final crown displacement calculated for the two lined tunnel cases. Since the geometries and soil properties are the same in all cases, the differences between solid and broken curves reflect the influence of the lining on the ground settlements. In the first case, the settlements for the unlined tunnel correspond to a stress release of 55%, to which a crown settlement of 8.97 mm was calculated (against 8.88 mm obtained in the lined case). In the second case, the settlements for the unlined case correspond to a stress release of 80%, and a 16.60 mm crown displacement (compared with 16.10 mm obtained in the corresponding lined case). To obtain a match of crown settlements for the lined and unlined cases, interpolation of displacements between consecutive unloading steps in the unlined case would have been required, but this was not attempted.

For equivalent crown displacements, one notes that the related settlements in both lined cases are smaller than those obtained for the unlined situation. Although the ground surface distortions are not much different for the lined and unlined cases, the latter tend to be marginally higher.

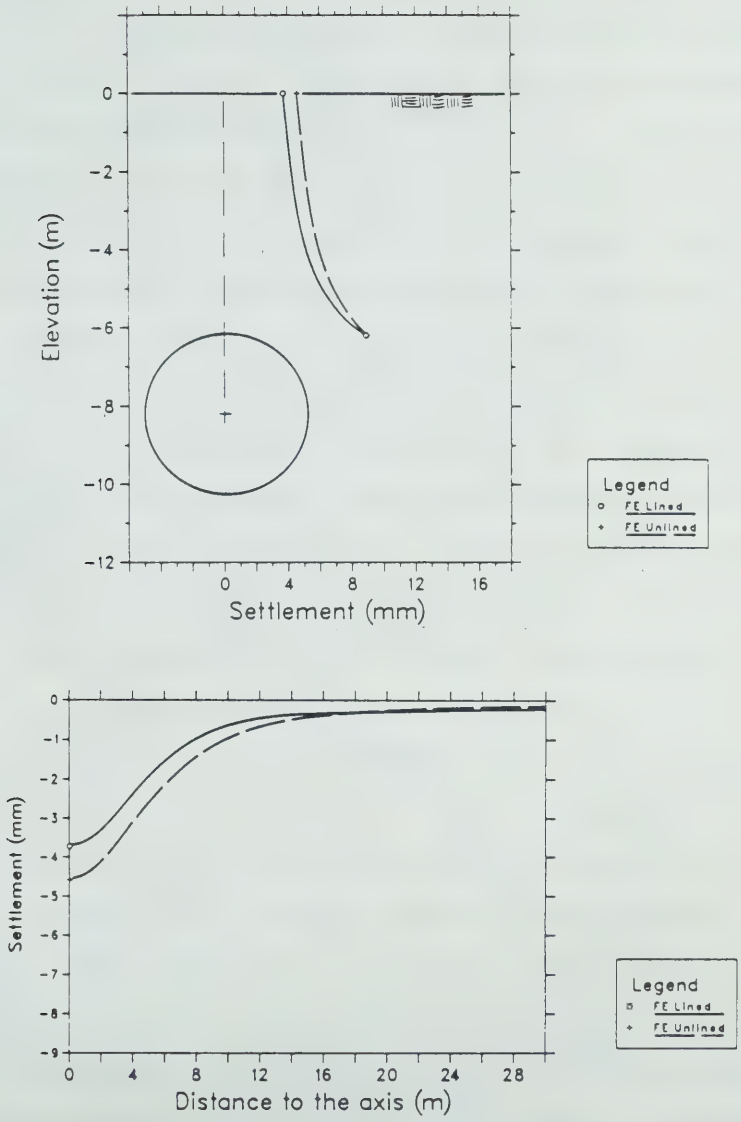

Figure 7.7 Distribution of Final Settlements Calculated for a Tunnel Lined after 40% Stress Release, Compared to the Distributions for an Unlined Tunnel Equal Crown Displacement

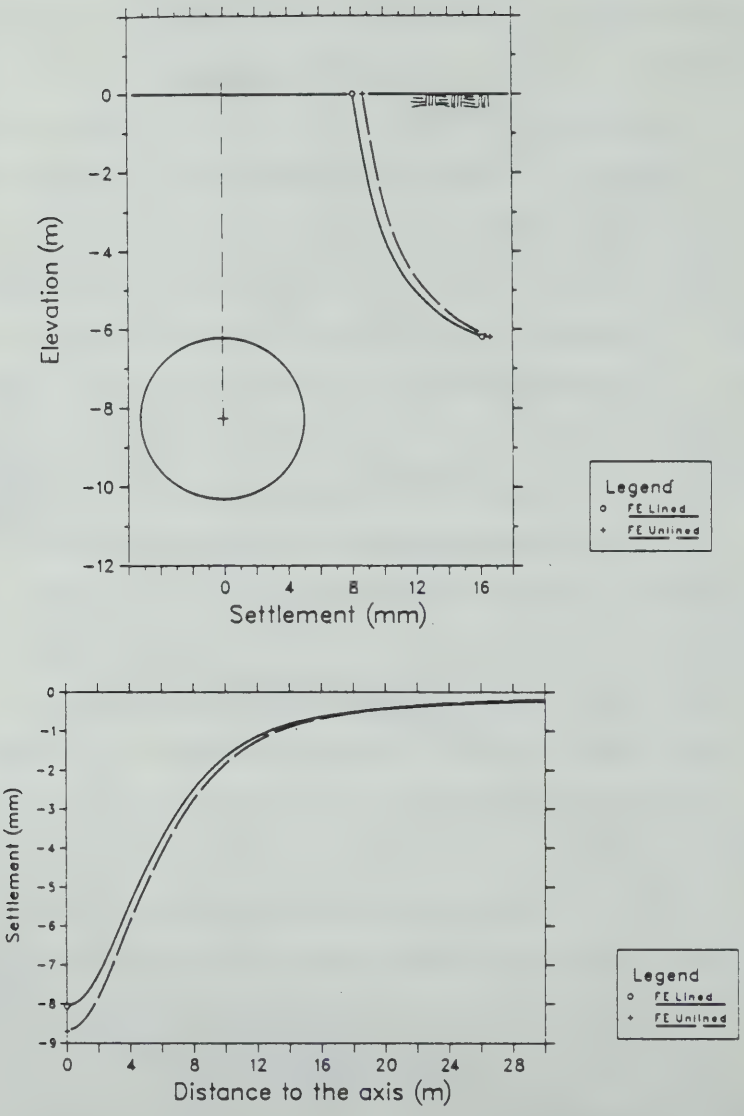

Figure 7.8 Distribution of Final Settlements Calculated for a Tunnel Lined after 80% Stress Release, Compared to the Distributions for an Unlined Tunnel with Equal Crown Displacements

One notes, furthermore, that as the amount of ground stress release before supporting the tunnel increases, the differences in settlements for the lined and unlined cases decrease. The pre-support displacements tend to dominate over the after-support movements as the lining installation is increasingly delayed. The incremental movements after the liner is installed tend to reduce as the ground stress reduction increases, but also as the support becomes stiffer relative to the ground with increasingly delayed installation of the lining. At the instant the lining is installed for the 40% stress release case, the relative stiffness ratios are: β=0.005 and $\dot{\alpha}$=0.96. For the 80% stress release case, they are β=0.015 and $\dot{\alpha}$=2.85. The additional ground softening resulting from the extra 40% ground stress release, caused the same lining to behave three times stiffer.

The presence of a lining inhibits the 'flow' of soil into the tunnel which is unrestrained in the unlined case. Thus, the volume of soil being lost into the opening is reduced. Moreover, if the lining squats, soil elements adjacent to the opening will be pushed outwardly and this may generate an opposing displacement field in the ground.

This mechanism was found to develop for other ground and lining conditions, and it may be said that by neglecting the presence of the lining, a conservative estimate of the ground settlement distributions above the tunnel will normally be found.

Accordingly, the normalized settlement distributions obtained in the parametric analyses and presented in Appendix C, can be used in practice, since it is sufficient to calculate the amount of stress release in the unlined tunnel solution, which causes the same crown settlement obtained in the lining-ground interaction analyses. This amount of stress release is easily obtained from the normalized ground reaction or λ curves defined for the tunnel crown by inputting the calculated dimensionless crown displacement found at equilibrium. As the sets of normalized settlement distributions were obtained for particular values of H/D, K_o, ϕ or $c_u/\gamma D$, and amounts of stress release, some data interpolation may be needed. Alternatively, the sets of data corresponding to the ground properties nearest the actual one are selected and the data interpolation is restricted to finding the normalized settlements for intermediate values of H/D or stress releases.

7.3 Guidelines for Using the Proposed Design Procedure

The purpose of the present section is to suggest and discuss a sequence of steps to be followed when applying the proposed design procedure.

Following the general scope of the present work, emphasis is given to some of the geotechnical aspects of a shallow tunnel design. No attempt is made to address, for instance, the structural design of the lining, although, the output of the present procedure may serve as input for this.

Geological and geotechnical investigations, though playing a paramount role in underground project designs (see, for example, U.S. National Committee on Tunnelling Technology, 1985) are discussed just briefly with reference to what directly concerns the proposed procedure.

Considering the relative simplicity of the procedure, and in spite of its identified limitations which are derived from the assumptions adopted in its development, the proposed method seems to be useful for sensitivity studies. These are frequently performed in feasibility projects and in basic designs, regarding alignment optimization, selection of construction procedures, the assessment of influence of parameter variability, etc. Moreover, its simplicity offers considerable attraction for design reevaluation during tunnel construction, as part of an observational design approach. The method can be applied and calibrated simultaneously with field monitoring, thus serving as an auxiliary tool for design feed-back and for decisions being made during construction. All calculations involved are simple and easy to perform. The entire procedure can be implemented in a small micro-computer.

The guidelines presented herein were developed for the cohesionless soil model described in Chapter 6. However,it can be easily adapted to the frictionless soil model which provides a better representation of the behaviour of saturated soils under undrained loading conditions.

Figure 7.9 shows a flow chart that summarizes the main sequential steps of the proposed procedure for shallow tunnel design. The geometry of the problem is initially assessed. A range of tunnel covers along the alignment is defined or critical sections are selected. If the tunnel contour is non-circular, and provided it does not deviate too much from a circle, the diameter of a circular profile with equal excavation area is defined.

The geological conditions are then assessed. The design procedure was developed for time independent conditions, so it is important to identify the groundwater conditions, soil permeabilities and coefficients of consolidation. The method asks for uniform ground conditions, at least in the subsurface profile from half diameter above to half diameter below the tunnel. One has to verify whether or not ground uniformity can be assumed for this horizon. Mixed face conditions, for instance, cannot be handled by the proposed procedure. Typical ground properties, or their ranges are then defined. If triaxial test results from good quality undisturbed samples are available, the input parameters for the hyperbolic model can be obtained. Undrained or drained parameters are defined according to the type of analyses to be carried out. A profile of an in situ tangent modulus is carefully defined, and possibly adjusted according to available results of in situ tests (for instance, pressuremeter tests). A reliable estimate of the in situ stress conditions is also needed. This is an important issue

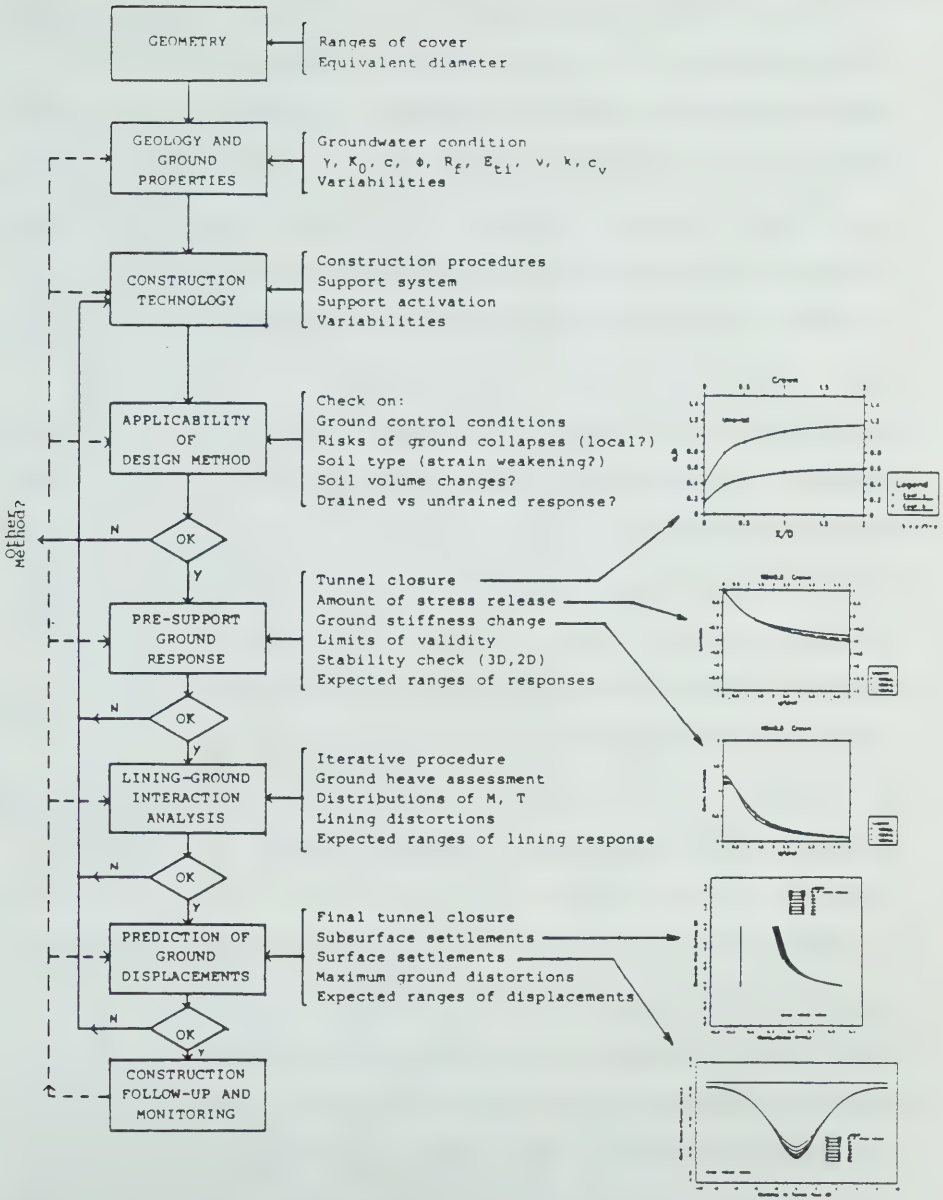

Figure 7.9 Suggested Sequence of Steps for Application of the Proposed Procedure for Shallow Tunnel Design

in the analysis, since both soil and lining performances are very dependent on these conditions. Unfortunately, measurement of K_o in soils is not a simple task. Recent development in push-in stress cells in soft to medium clays have shown promising results (Chan and Morgenstern, 1986). If specific site data is not available, information and field evidence from excavations in nearby areas can provide some help. Additionally, the variability of strength properties, deformation parameters, etc, should be carefully assessed in order to define parameter envelopes. Special attention should be paid to geological features that may likely control local stability conditions. This includes fissures, bedding, sand lenses, etc. Local collapses or cave-ins typify poor ground control conditions under which the present design procedure ceases to be valid. Such occurrences however, can be entirely avoided by appropriate construction techniques or properly chosen construction methods.

Regarding the latter, the design procedure requires a complete knowledge of the method of tunnelling to be undertaken. As originally developed, the present design method is strictly applicable to full face tunnelling, or to tunnelling with minor face excavation staging. In section 7.5, however, the procedure is tested against a few cases that deviate from these conditions. A key issue is the identification of the location where the support is activated and this does not necessarily coincide with the

point of lining assembly, especially in grouted or expanded lining systems. In shotcrete linings, the activation point seems to correspond to the section where the support ring is closed. The proposed method is also strictly valid to good lining-ground contact conditions. While this is normally ensured in shotcrete linings, it may not prevail in some prefabricated linings installed in sections with large overbreaks caused by excessive overcutting or local collapses, or in poorly grouted or backfilled supports. The support characteristics and properties should be defined, and their variability assessed (particularly for a shotcrete support). The expected ranges of lining installation delay also have to be estimated.

The proposed design procedure should be used preferably within its range of applicability, avoiding for instance, extrapolation of results beyond the established limits (see Section 6.5) of the stress release and stiffness reduction normalized curves or corresponding equations (Section 6.4). Accordingly, interpolation of data should be performed within the ranges of variables used in the parametric analyses (Section 6.2.5). Similarly, the estimates of tunnel closure using the approximate solution developed in Chapter 5 should be made having in mind the limitations and restrictions discussed in Sections 5.3.5.2 and 5.3.6.1. Broadly speaking, the method should be used only when good ground conditions are ensured, so that near collapse situations are precluded. A tentative criterion to identify

such situations was set up in Section 2.3.4.3. Results of tunnel model tests indicated that a limiting value for the dimensionless crown displacement associated with near collapse conditions can be defined. Values of U in excess of 1.8 were generally indicative of near collapse conditions in those tests. A good ground control condition would necessarily mean U values at the crown smaller than that figure and possibly less than 1.0. The interpretation of field data in a number of case histories (see Section 5.3.6.1) seemed to confirm the proposed criteria.

The lining-ground interaction analysis used in the proposed design procedure is strictly applicable to good lining-ground contact, as defined in Section 2.3.5. The quality of this contact depends on different factors as discussed in that section. In prefabricated lining systems it depends to a large degree on the size of the space left unfilled behind the support. As suggested in Section 2.3.5.4, the maximum allowable overbreak at the tunnel crown can be calculated from a limiting increment of dimensionless crown displacement, which was estimated to be 0.5 to 0.65.

Moreover, the proposed design procedure is not to be used for soils with stress-strain behaviour departing appreciably from that described by a hyperbolic relationship. Conditions involving appreciable ground volume changes (dilation, consolidation) also cannot be handled by the proposed procedure. The type of analysis to be performed, which can be either undrained or drained, should

be assessed independently, according to the ground profile, soil type, its properties and the construction scheme to be used (lining type, rate of advance, etc). The simplified criteria set up in Section 3.3.4.5 can be helpful for this assessment.

The next step in the design sequence is the evaluation of the pre-support ground response. This requires an estimate of the tunnel closure, which can be made through the procedure developed in Section 5.3.5.2. The dimensionless radial displacements at three points of the tunnel contour can be estimated once the distance (x) behind the face where the support will be activated and the in situ stress ratio K_o are both known. If a drained analysis is made using the cohesionless soil model, then the amount of stress release and the ground stiffness changes at the point the support is activated can be assessed, using the solutions derived in Section 6.4.3 and as explained in Section 7.2.2. Adjustments of the friction angle will be needed for soils with a non-zero cohesive strength component and with failure ratios different from unity. For a variable in situ deformation modulus profile, the radial displacements at the tunnel contour are normalized to the in situ moduli at points located half diameter radially away from the opening, as explained in Section 6.2.4.2. Reference values for the amount of stress release (α_{ref}) and for the dimensionless displacements at tunnel contour (U_{ref}) are found for the particular geometry (H/D), the in situ stress

ratio (K_o) and for the adjusted friction angle (m-1). The reduced unit weight of the soil and reduced ground stiffnesses are found by averaging the stress ratios (Σ) and the current stiffnesses (E_t) at the point where the support is activated. These are obtained through the twice normalized ground reaction curves and their derivative functions λ and λ' curves, see Section 6.4.3).

The three dimensional stability condition of the tunnel is verified, both at the face and at the unsupported heading, through some of the methods discussed in Section 4.3.4. A check of the two-dimensional tunnel stability is also made, using for example, the solutions presented in Section 6.5.2, taking into account the reduction of the ground stress calculated at the point the support is to be activated. Provided the calculated factors of safety are acceptable (greater than or equal to 1.3 to 1.6; see data and discussions on Sections 2.3.4.3 and 4.2.3), the construction procedure is applicable and the proposed design method can be used. Otherwise, changes in the construction method have to be considered or additional ground control procedures, such as those discussed in Section 4.2.3, should be implemented.

Expected ranges of pre-support ground response are thus defined and used as input for the lining-ground interaction analysis. The latter is carried out using the solution presented in Section 7.2.1, following the iterative procedure described in Section 7.2.2. Attention should be

paid to the evaluation of ground heave, which tends to be overestimated by the solution given in Section 7.2.1. Distributions of lining loads are obtained, including bending moments and thrust forces, calculated for the ranges of expected ground responses. They are used in the independent structural design of the lining. Lining loads and distortions are checked for acceptability. Total tunnel closure is calculated and checked if admissible. If the estimated lining-ground response is not acceptable the construction technology has to be reviewed accordingly, and may require changes to the lining system or in the construction procedures.

The total crown displacement is then obtained. The associated amount of stress release is calculated through the λ curve for the tunnel crown, as explained in Section 7.2.3. Finally the subsurface and surface ground settlements are calculated using the distributions of normalized settlements included in Appendix C, and may require some data interpolation. If the calculated ranges of surface and subsurface settlements are not acceptable or if the risk of damage to existing structures is high (see Section 4.2.2), then again, the construction procedures have to be reassessed or additional ground control measures considered.

Finally, during the construction follow up and field monitoring, the anticipated ground and lining performances can be verified. Reasons for possible departures from the predicted behaviour can be assessed and back analysis of

performance can be made, calibrating the proposed procedure to a particular site condition. This feedback process may provide further insight on the tunnelling activities and may help in reevaluating the design and construction, as well as support new decisions to be made.

To facilitate some of the calculations involved in the application of the design sequence described, Figures 7.10 to 7.14 were prepared. As explained earlier, they were developed for applications using the cohesionless soil model, but they can be easily adapted for the frictionless model. The present calculation sheets include the geometry of the problem, the ground properties and the tunnel closure at lining activation (Figure 7.10), reference values used to assess the amount of stress release and the ground stiffness at the section the support is activated (Figure 7.11), the two dimensional ground stability verification and input data for the lining-ground interaction analysis (Figure 7.12), a sheet for the iteration calculations (Figure 7.13) and finally a sheet for the subsurface and settlement calculations (Figure 7.14). For easier reference, some of the equations that are used were reproduced in the calculation sheets.

7.4 An Example of the Use of the Proposed Design Procedure

The Alto da Boa Vista Tunnel built in Sao Paulo, Brazil, is used as an example of the application of the proposed design procedure. This case history was described

1. GEOMETRY

H = [ ] D = [ ] H/D = [ ]

2. GROUND PROPERTIES

γ = [ ] K_o = [ ]

$(\sigma_3)_{axis}$ = [ ] c = [ ] ϕ = [ ] R_f = [ ]

$$\phi_a = \text{arc sin}\left[\frac{1 + (\sigma_3/c)\tan\phi}{1 + (\sigma_3/c)\sec\phi}\right] = [\ ]$$

$$\phi_e = \text{arc sin}\,(1 - R_f + R_f \csc\phi_a)^{-1} = [\ ]$$

$$(m-1) = \frac{2\sin\phi_e}{1-\sin\phi_e} = [\ ]$$

K = [ ] n = [ ] p_a = [ ] μ = [ ]

$$E_{ti} = K p_a \left(\frac{\sigma_3}{p_a}\right)^n \left[1 - \frac{R_f(1-\sin\phi)(\sigma_1-\sigma_3)}{2c\cos\phi + 2\sigma_3\sin\phi}\right]^2$$

Location	σ_3	σ_1	E_{ti}
1/2 D above C at S 1/2 D below F			

3. TUNNEL CLOSURE AT LINING ACTIVATION

X = [ ] X/D = [ ] K_o = [ ] $u_r = (D\sigma_{ro}/E_{ti})U$

Location	U	σ_{ro}	$D\,\sigma_{ro}/E_{ti}$	u_r
C S F				

Figure 7.10 Calculation Sheet with Geometric Ground Properties Data and Tunnel Closure at Lining Activation

4. REFERENCE VALUES

H/D= [ ] K_o= [ ] (m-1)= [ ]

	$1-\Sigma_{ref}=\alpha_{ref}$	α_{ref}/U_{ref}	U_{ref}
C			
S			
F			

5. STRESS RELEASE AND STIFFNESS CHANGE AT LINING ACTIVATION

	U	U/U_{ref}	Beyond Limit?	λ	λ'
C					
S					
F					

STRESSES: $\Sigma = 1-(1-\lambda)\alpha_{ref}$

	$(1-\lambda)$	Σ
C		
S		
F		

$\bar{\Sigma}=(\Sigma_C+2\Sigma_S+\Sigma_F)/4$ = [ ]

$\bar{\alpha} = 1-\bar{\Sigma}$ = [ ]

$\gamma_{red} = \gamma \cdot \bar{\Sigma}$ = [ ]

STIFFNESS: $E_f = (\lambda'/\lambda'_i)\,E_{fi}$

	λ'_i	E_{fi}/λ'_i	E_f
C			
S			
F			

$\bar{E}_f = (E_{fC}+2E_{fS}+E_{fF})/4$ = [ ]

Figure 7.11 Calculation Sheet for Estimates of the Stress Release and Ground Stiffness at the Section the Lining is Activated

6. 2D STABILITY VERIFICATION

$\bar{\alpha}$ = [ ] $\quad \bar{\sigma}_{ro} = \frac{1+K_o}{2}\gamma\,(H+\frac{D}{2})$ = [ ] $\quad \phi$ = [ ] $\quad c/\gamma D$ = [ ] $\quad H/D$ = [ ]

$\therefore P_\ell/\gamma D$ = [ ] $\quad P_\ell$ = [ ] $\quad \alpha_\ell = 1 - P_\ell/\bar{\sigma}_{ro}$ = [ ]

$$FS = \frac{[(1-K_o)/(1+K_o)+\alpha_\ell]}{[(1-K_o)/(1+K_o)+\bar{\alpha}]} = [\ ]$$

7. LINING-GROUND INTERACTION

GEOMETRY : Z_o = [ ] $\quad r_o$ = [ ] $\quad r_i$ = [ ]

SOIL : $\bar{E}_t$ = [ ] $\quad \mu$ = [ ] $\quad \gamma_{red}$ = [ ] $\quad K_o$ = [ ]

LINING : E_s = [ ] $\quad \mu_s$ = [ ] $\quad d$ = [ ] $\quad I_s$ = [ ]

ITERATION No.: _____ $\quad \bar{E}_t$ = [ ] $\quad \dot{\alpha}$ = [ ] $\quad \beta$ = [ ]

	u_r	Δu_r	$u_{rf} = u_r + \Delta u_r + V''_{zo}$	U	U/U_{ref}	λ'	E_t	σ_r
C								
S								
F								

$$V''_{zo} = \frac{(1+\mu)(3-4\mu)}{4(1-\mu)\bar{E}_t}\gamma_{red}\cdot r_o^2 \ell_n \frac{r_o}{r_i} = [\ ] \qquad (\bar{E}_t)_{new} = (E_{tC} + 2E_{tS} + E_{tF})/4 = [\ ]$$

Figure 7.12 Calculation Sheet for 2D Stability Verification and Lining-Ground Interaction Analysis

ITERATION No.: _____ $\bar{E}_f$ = [ ] $\dot{\alpha}$ = [ ] β = [ ]

	u_r	Δu_r	$u_{rf} = u_r + \Delta u_r + v''_{zo}$	U	U/U_{ref}	λ'	E_f	σ_r
C								
S								
F								

v''_{zo} = [ ] $(\bar{E}_f)_{new}$ = [ ]

ITERATION No.: _____ $\bar{E}_f$ = [ ] $\dot{\alpha}$ = [ ] β = [ ]

	u_r	Δu_r	$u_{rf} = u_r + \Delta u_r + v''_{zo}$	U	U/U_{ref}	λ'	E_f	σ_r
C								
S								
F								

v''_{zo} = [ ] $(\bar{E}_f)_{new}$ = [ ]

Figure 7.13 Calculation Sheet for Iterative Analysis of the Lining-Ground Interaction

8. SUBSURFACE SETTLEMENTS

CROWN SETTL. = ____ U/U_{ref} = ____ λ_c = ____ $\alpha_c = (1-\lambda_c)\alpha_{ref}$ = ____

K_o = ____

ϕ = ____

DEPTH Z (m)	Z / H	SETTLEMENT/CROWN SETTL. H/D=	H/D=	H/D=	SETTLEMENT
H=	1.000	1.000	1.000	1.000	

9. SURFACE SETTLEMENTS

α_c = ____

K_o = ____

ϕ = ____

DIST. Y (m)	0.0	
Y/D	0.0	
SETTL./CROWN SETTL. H/D=		MAX. DISTOR.:
H/D=		1:
H/D=		AT:
SETTL.		

Figure 7.14 Calculation Sheet for Subsurface and Surface Settlements

in detail in Section 5.2.4.2, where it was back-analysed through the two-dimensioal finite element model presented in Chapter 5. In the present section, as well as in the following, no attempt will be made to best fit the observed performance. The case history data are used as a design case, where the most likely tunnel response in geotechnical terms, is the matter of interest. For consistency, however, and to allow a comparison with the results of the numerical back-analysis performed earlier, the same parameters then used will be applied here.

The tunnel had a soil cover of 6.2 m and a near circular excavation profile with 3.9 m height and 4 m width. The equivalent diameter of a circular excavation with an equal area is 4 m.

The tunnel was driven above the water table through the variegated silty sand and a drained analysis using effective stress parameters and zero pore pressures is justified. The ground properties and geometric data are reproduced in Figure 7.15. The justifications for using these soil parameters were given in Section 5.2.4.2. An in situ stress ratio of 0.8 was selected in the present analysis (as opposed to the 0.75 ratio back analysed earlier), in order to simplify the application of the generalized solution. Interpolation of data regarding the K_o value was thus eliminated. Note that since the soil cohesion is zero and its failure ratio is equal to one, there is no need to adjust the friction angle using equations 6.3 and 6.10 which

are reproduced in Figure 7.15. The variation of the in situ tangent modulus with depth is given by the last equation in Figure 5.11, using the calculated in situ principal stresses. The in situ modulus at half a tunnel diameter above the crown, at the springline elevation and half a tunnel diameter below the floor are thus calculated and will be used to normalize the radial displacements at the corresponding points of the tunnel contour. The moduli obtained are marginally higher than those used in the numerical back-analysis, as a slightly higher K_o was assumed here. However, they are not discordant with the in situ deformation modulus profile, as obtained through pressuremeter tests (see Figure 5.14).

In a routine design application, ranges of geotechnical parameters, such as those given in Table 5.9 for the variegated soil, would be used instead of the single 'most likely' set of parameters being considered herein.

As described in Section 5.2.4.2, the tunnel construction was performed under good ground control conditions, that were provided both by the favourable ground and by the good construction quality achieved. The shotcrete support and the face excavation were installed in stages. As suggested earlier in different sections of this thesis, it seems reasonable to allow in such a support type, that its activation takes place when the shotcrete ring is closed at the floor. Therefore, the radial closure of the opening, at the point the lining is activated, is calculated at a

1. GEOMETRY

H = 6.2 m D = 4.0 m H/D = 1.55

2. GROUND PROPERTIES

γ = 16 kN/m³ K_o = 0.8

$(\sigma_3)_{axis}$ = 104.12 kPa c = 0 ϕ = 29° R_f = 1.0

$$\phi_a = \text{arc sin}\left[\frac{1 + (\sigma_3/c)\tan\phi}{1 + (\sigma_3/c)\sec\phi}\right] = 29°$$

$$\phi_e = \text{arc sin}\,(1 - R_f + R_f \csc\phi_a)^{-1} = 29°$$

$$(m-1) = \frac{2\sin\phi_e}{1-\sin\phi_e} = 1.882$$

K = 400 n = 0.25 p_a = 101.33 kPa μ = 0.3

$$E_{ti} = K p_a \left(\frac{\sigma_3}{p_a}\right)^n \left[1 - \frac{R_f(1-\sin\phi)(\sigma_1-\sigma_3)}{2c\cos\phi + 2\sigma_3\sin\phi}\right]^2 = 30477.682\,(\sigma_3/101.33)^{0.25}$$

Location	σ_3 kPa	σ_1 kPa	E_{ti} MPa
1/2 D above C	53.76	67.20	26.01
at S	104.32	130.40	30.70
1/2 D below F	154.88	193.60	33.89

av. 30,325

3. TUNNEL CLOSURE AT LINING ACTIVATION

X = 2.6 m X/D = 0.65 K_o = 0.8 $u_r = (D\sigma_{ro}/E_{ti})U$

Location	U	σ_{ro} kPa	$D\sigma_{ro}/E_{ti}$	u_r mm
C	0.587	99.20	0.015255	8.95
S	0.469	104.32	0.013592	6.37
F	0.352	161.60	0.019026	6.70

Figure 7.15 ABV Tunnel - Input Data and Tunnel Closure at Lining Activation

section located 2.6 m behind the heading face (x/D=0.65). Possible variations in the depth of heading advance or distance of lining closure behind the face, would have to be considered in a real design calculation and thus a range of tunnel closures at the lining installation point would have to be considered. For the present, it is sufficient to contemplate the most probable delay of support application in this case history. Being a shotcrete support, the lining-ground condition can be defined as good.

Tunnel closure at crown, springline and floor are estimated using the approximate solution given in Section 5.3.5.2 (Figures 5.94 to 5.96). If the design procedure was being used during construction, the actually observed tunnel closure would possibly be known. The measured radial displacements would, thus, be used instead of the estimated values. As shown in Figure 7.15, the dimensionless crown displacement is smaller than 1.0 and this is consistent with the good ground control conditions met in this case history.

The stress-strain curves of the variegated soil are very closely represented by a hyperbolic relationship. In an actual design activity, the risk of local ground collapse would have to be assessed through a close inspection of the locally occurring geological features and through available stability solutions which can provide the means for assessing the face and unsupported heading stability. In the present analysis this is not needed since the tunnel was already built, and no local or global instability process

was detected during construction. Except for some contraction likely to occur in this soil upon shearing, the overall volume changes expected in this ground were small, and this is partly due to the good ground control conditions implemented. No appreciable volumetric changes associated with changes in the mean normal stresses were expected, partly because the overconsolidated nature of the deposit. For all these reasons, the proposed design method seemed to be fully applicable to the case history considered.

The next step consists of the evaluation of the ground stress release and of the ground stiffness at the point of support activation. The corresponding calculations are shown in Figure 7.16. The solution set for K_o=0.8, summarized in Figures 6.100 to 6.107, is used. With the calculated strength factor (m-1) (Equation 6.30), α_{ref} is obtained from Figure 6.101 and the ratio α_{ref}/U_{ref} is determined through Figure 6.100, for the cover to diameter ratio being considered. The reference dimensionless displacements at the crown, springline and floor are thus obtained. The corresponding ratios U/U_{ref} are then calculated and checked if they are greater than the limiting ratios defined in the solution generalization. In this case, the U/U_{ref} values lie to the left of the terminal points of the fitted function, represented by the right vertical bars in Figures 6.102 to 6.104, and so no data extrapolation is involved. Using the last three figures, the values of λ are obtained and the corresponding stress ratios (Σ) at the crown, springline and

4. REFERENCE VALUES

H/D= 1.55 K_0= 0.8 (m-1)= 1.882

	$1-\Sigma_{ref}=\alpha_{ref}$	α_{ref}/U_{ref}	U_{ref}
C	0.525	0.87	0.603
S	0.465	1.12	0.415
F	0.435	2.02	0.215

5. STRESS RELEASE AND STIFFNESS CHANGE AT LINING ACTIVATION

	U	U/U_{ref}	Beyond Limit?	λ	λ'
C	0.587	0.973	No	0.03	0.62
S	0.469	1.130	No	-0.05	0.45
F	0.362	1.637	No	-0.45	0.65

STRESSES: $\Sigma = 1-(1-\lambda)\alpha_{ref}$

	$(1-\lambda)$	Σ
C	0.97	0.491
S	1.05	0.512
F	1.45	0.369

$\bar{\Sigma}=(\Sigma_C+2\Sigma_S+\Sigma_F)/4$ = 0.471

$\bar{\alpha}=1-\bar{\Sigma}$ = 0.529

$\gamma_{red}=\gamma\cdot\bar{\Sigma}$ = 7.536 kN/m³

STIFFNESS: $E_t=(\lambda'/\lambda'_i)E_{ti}$

	λ'_i	E_{ti}/λ'_i	E_t MPa
C	1.278	20.352	12.618
S	1.425	21.544	9.695
F	1.005	33.721	21.919

$\bar{E}_t=(E_{tC}+2E_{tS}+E_{tF})/4$ = 13.482 MPa

Figure 7.16 ABV Tunnel - Stress Release and Ground Stiffness at Lining Activation

floor are calculated using the definition given by equation 6.23. The stress ratios are averaged and the reduced unit weight of the soil (γ_{red}) is calculated according to the definition given by equation 7.14.

Similarly, the derivative of the twice normalized ground stress release curve (λ') are found, for the calculated U/U_{ref} values at lining installation, using the curves given in Figures 6.105 to 6.107. The current ground moduli are then calculated using equations 6.27 and 6.29 (or Figure 6.116). They are then averaged and E_t is obtained.

It should be noted that since the ratio H/D lies between two values considered in the parametric analyses (1.5 and 3.0), some interpolation of data may be needed to obtain λ and λ'. Since the solutions for those two values lie very close together, a linear interpolation is sufficient. As an alternative, the nearest available solution (H/D=1.5) could be used, as the error involved is insignificant. If the analysis is done through a programmed solution, λ and λ' would be calculated from equations 6.24 and 6.26, using the parameters, P_i, shown in Table 6.16.

One can note from Figure 7.16 that at the section the lining was installed, the ground stress had been reduced by 52.9% and the average ground modulus had been also reduced but by 55.6%. The former ground stress reduction is higher than that found in the back analysis of this case history presented in Section 5.2.4.2 (40%) and also higher than the amount given in Section 5.3.7 (59%). This is because a

slightly higher K_o value has been adopted herein, as well as considering an increased distance between face and point of lining activation (x/D=0.65), and other approximations involved in the proposed calculation method.

A two-dimensional stability check would then be made. This is done here using the lower bound solution presented in Section 6.5.2. For instance, one could say that $\phi \simeq 30°$ and the tunnel collapse pressure, p_1, is obtained from Figure 6.125, with c=0 and H/D=1.55. The factor of safety of the ground is calculated using equation 6.34 and it is found to be about 1.4 (see Figure 7.17). This value is totally acceptable, thus the construction procedure and the proposed design method are applicable.

The next design step is the ground-lining interaction analysis. The values of γ_{ref} and $\bar{E}_t$ are used as input in this analysis. The depth to the tunnel axis is taken as the soil cover plus the half tunnel diameter. The analytical solution assumes the lining thickness to be small. Thus, an average lining radius of 1.95 m (for a shotcrete lining 10 cm thick) is considered. Following the discussions presented in Section 5.2.4.2, a reduced shotcrete modulus of 10 GPa is adopted (instead of the 8.65 GPa modulus back analysed in Section 5.2.4.2). The radius, r_1, of the arbitrary circle at which the vertical ground heave displacement is set equal to zero (see Section 7.2.1), would be chosen as that tangent to a stiffer horizon below the tunnel. According to the description of the local geology (Section 5.2.4.2), it would

6. 2D STABILITY VERIFICATION

$\bar{\alpha}$ = 0.529 $\quad \bar{\sigma}_{ro} = \frac{1+k_o}{2}\gamma(H+\frac{D}{2}) =$ 117.36 kPa $\quad \phi \cong$ 30° $\quad c/\gamma D =$ 0 $\quad H/D =$ 1.55

$\therefore P_l/\gamma D \cong$ 0.35 $\quad P_l =$ 22.4 kPa $\quad \alpha_l = 1 - P_l/\bar{\sigma}_{ro} =$ 0.809

$$FS = \frac{[(1-k_o)/(1+k_o)+\alpha_l]}{[(1-k_o)/(1+k_o)+\bar{\alpha}]} = 1.437$$

7. LINING-GROUND INTERACTION

GEOMETRY : $Z_o =$ 8.15 m $\quad r_o =$ 1.95 m $\quad r_1 =$ 8.15 m tangent to surface

SOIL : $\bar{E}_t =$ 13.482 MPa $\quad \mu =$ 0.3 $\quad \gamma_{red} =$ 7.536 kN/m³ $\quad K_o =$ 0.8

LINING : $E_s =$ 10 GPa $\quad \mu_s =$ 0.25 $\quad d =$ 0.1 m $\quad I_s =$ 8.33.10⁻⁵ m⁴/m

ITERATION No.: 01 $\quad \bar{E}_t =$ 13.482 MPa $\quad \dot{\alpha} =$ 52.745 $\quad \beta =$ 1.156.10⁻²

	u_r mm	Δu_r mm	$u_{rf} = u_r + \Delta u_r + V''_{zo}$	U	U/U$_{ref}$	χ'	E_t MPa	σ_r kPa
C	8.95	1.683	8.093 * (10.633)	0.531 (0.697)	0.881 (1.156)	0.69 (0.52)	14.043 (10.583)	44.24
S	6.37	-1.378	4.992 (4.992)	0.367	0.884	0.62	13.357	57.81
F	6.70	1.847	11.087 (8.547)	0.583 (0.449)	2.712 (2.088)	0.42 (0.53)	14.163 (17.872)	57.14

* No heave between brackets ( )

$$V''_{zo} = \frac{(1+\mu)(3-4\mu)}{4(1-\mu)\bar{E}_t}\gamma_{red}\cdot r_o^2 \ln\frac{r_o}{r_1} = 2.540 \text{ mm} \quad (2<ro)$$

$(\bar{E}_t)_{new} = (E_{1C} + 2E_{1S} + E_{1F})/4 =$ 13.730 MPa ← (13.792)

Figure 7.17 ABV Tunnel - Two Dimensional Stability Calculation and Lining-Ground Interaction

be at 11.85 m. This is however, more than the depth of the tunnel axis, and would likely lead to excessive ground heave. Instead, r_1 is selected so that the arbitrary circle becomes tangent to the ground surface (r_1=8.15 m). The coefficients of relative stiffness can then be calculated (equations 7.1 and 7.2) and are found to be α=52.7 and β=0.0116 (Figure 7.17), which are typical for a shotcrete lining in a medium clay (Table 7.1).

The overall ground heave is calculated using equation 7.10 (Figure 7.2) and it is found to be 2.54 mm (see Figure 7.17). The analysis is conducted using the solution shown in Figure 7.2 (equations 7.3 and 7.7). Increments of radial displacement Δu_r are found. Using equation 7.6, these are added to the heave displacement. The final radial displacements are found after adding those calculated at lining installation (Figure 7.15). New U and U/U_{ref} values are found for the three points of the contour. New λ' and E_t are thus obtained and a new $\bar{E}_t$ is found to be equal to 13.73 MPa, which is to be compared to that formally calculated (13.482 MPa). The new modulus is found to be 1.8% greater than the previous one. A second iteration analysis is thus performed, using the new modulus as input. (Figure 7.18). A new ground heave is calculated and the calculation is repeated. Another $\bar{E}_t$ is found (13.623 MPa), which differs from the old value by less than 0.6%. Therefore, no more iterations are needed. The final radial stresses and displacements are thus found, as shown in Figure 7.18. As

explained in Section 7.3, bending moments and thrust forces in the lining are also obtained in this calculation but are not discussed. Note, moreover, that the normalized final dimensionless displacement (U/U_{ref}) at the tunnel floor exceeded the limit of the fitted λ and λ' functions for this point (see Figures 6.104 and 6.107), unlike at the other points of the tunnel contour. Notwithstanding this, the extrapolation of data at the floor did not impair the quality of the results obtained, as will be seen later.

A total crown settlement of 8.1 mm is obtained, which leads to a U/U_{ref} value of 0.882. Using the λ curves shown in Figure 6.102, it is found that this crown displacement corresponds to λ equal to 0.1 and, therefore, to a stress release at the crown of 47.25%. As recommended in Section 7.2.3, the induced ground settlements are obtained through the results of the parametric analyses (Appendix C) for the unlined tunnel case, considering the amount of stress release ($\simeq$47%) which causes, in the unlined tunnel, the same crown settlement obtained in the lining ground interaction analysis (Figure 7.19).

To obtain the distribution of subsurface settlements, the normalized subsurface settlement plots, such as the one shown in Figure 6.59, are used. The corresponding sets of normalized plots which bracket the case in hand are selected in Appendix C. These are taken as the plots for K_o=0.8 and ϕ=30°, and for H/D=1.5 and 3.0. Curves for these two cover to diameter ratios, for 47% stress release are obtained by

ITERATION No.: 02 $\bar{E}_1$ = 13.730 MPa $\dot{\alpha}$ = 51.793 β = $1.351 \cdot 10^{-2}$

	u_r mm	Δu_r mm	$u_{rf} = u_r + \Delta u_r + v''_{zo}$	U	U/U_{ref}	λ'	E_1 MPa	σ_r kPa
C	8.95	1.658	8.113 (10.606)	0.532 (0.695)	0.882 (1.153)	0.69 (0.52)	14.043 (10.683)	44.21
S	6.37	- 1.352	5.018	0.369	0.889	0.61	13.142	57.80
F	6.70	1.820	11.015 (8.520)	0.579 (0.448)	2.693 (2.084)	0.42 (0.53)	14.163 (17.872)	57.10

v''_{zo} = $(\bar{E}_1)_{new}$ = 13.623 (13.685)

ITERATION No.: $\bar{E}_1$ = $\dot{\alpha}$ = β = $(\bar{E}_1)_{new} \approx \bar{E}_1$ ok

	u_r	Δu_r	$u_{rf} = u_r + \Delta u_r + v''_{zo}$	U	U/U_{ref}	λ'	E_1	σ_r
C								
S								
F								

v''_{zo} = $(\bar{E}_1)_{new}$ =

Figure 7.18 ABV Tunnel - Iterative Calculation for the Lining-Ground Interaction

linear interpolation (see Figure 7.19), from the curves which bracket that amount of stress release (i.e., the 40% and 50% curves). Curves similar to those shown in Figure 6.62(a) are thus obtained. This is followed by another data interpolation, at equal normalized depth to cover ratios (z/H), so that the normalized settlement curve for H/D=1.55 is obtained (see Figures 6.62a and 7.19). The distribution of subsurface settlements is immediately calculated as the crown settlement is known. Note that to find the distribution for the actual friction angle (ϕ=29°), the process would have to be repeated once more for ϕ=20°, and the normalized displacements would have to be interpolated from those found for the 20° and 30° friction angles. It is simpler, as well as sufficient, to select the set of normalized plots for the friction angle which is closer to the actual one, or to assume the angle that leads to a more conservative settlement estimate. The same comments apply to intermediate values of the in situ stress ratio (K_o). The above calculations can be relatively tedious to perform if done manually. However, they can easily be programmed and performed in a small micro-computer.

The distribution of surface settlements are obtained through an identical procedure, except for using the normalized surface settlement plots, such as the one shown in Figure 6.60. Similar interpolation procedures are undertaken, after selecting the sets of normalized plots from Appendix C which bracket the case being investigated.

8. SUBSURFACE SETTLEMENTS

CROWN SETTL. = 8.11 (10.61) U/U_{ref} = 0.882 (1.153) λ_c = 0.1 (-0.075) $\alpha_c = (1-\lambda_c)\alpha_{ref}$ = 0.473 (0.564) 47% (56%)

K_o = 0.8

ϕ = 30°

* No heave between brackets ( )

DEPTH Z (m)	Z/H	SETTLEMENT/CROWN SETTL. H/D = 1.5	H/D = 3.0	H/D = 1.55	mm SETTLEMENT
0	0	0.515 (0.521)	0.375 (0.378)	0.510 (0.516)	4.19 (5.48)
1.862	0.300	0.575 (0.585)	0.422 (0.430)	0.570 (0.580)	4.62 (6.15)
3.044	0.491	0.624 (0.632)	0.460 (0.467)	0.619 (0.627)	5.02 (6.65)
4.568	0.737	0.732 (0.740)	0.580 (0.580)	0.727 (0.735)	5.90 (7.74)
5.080	0.819	0.782 (0.787)	0.642 (0.642)	0.777 (0.782)	6.30 (8.30)
5.613	0.905	0.855 (0.860)	0.765 (0.765)	0.852 (0.857)	6.91 (9.09)
5.982	0.965	0.940 (0.940)	0.873 (0.873)	0.938 (0.938)	7.61 (9.95)
H = 6.20	1.000	1.000	1.000	1.000	8.11 (10.61)

9. SURFACE SETTLEMENTS

α_c = 47% (56%)

K_o = 0.80

ϕ = 30°

DIST. Y (m)		0.0	2.0	4.0	8.0	12.0
Y/D		0.0	0.5	1.0	2.0	3.0
SETTL./CROWN SETTL.	H/D = 1.5	0.515 (0.521)	0.470 (0.475)	0.375 (0.375)	0.220 (0.215)	0.122 (0.117)
	H/D = 3.0	0.375 (0.378)	0.360 (0.365)	0.335 (0.340)	0.254 (0.255)	0.175 (0.175)
	H/D = 1.55	0.510 (0.516)	0.466 (0.471)	0.374 (0.374)	0.221 (0.216)	0.124 (0.119)
SETTL. mm		4.14 (5.48)	3.78 (5.00)	3.03 (3.97)	1.79 (2.30)	1.00 (1.26)

MAX. DISTOR.: 1: 2,000 (1,800)

AT:

Figure 7.19 ABV Tunnel: Subsurface and Surface Settlement Calculations

The interpolations are performed at equal normalized distances to the tunnel axis (Y/D). The resulting calculations are summarized at Figure 7.19, where the calculated maximum surface distortion is also indicated.

If it was only necessary to know the maximum surface settlement, then the above calculations would not be needed. It would be adequate to use the relationships between surface and crown settlements presented in Section 6.3.2.3. For the present case, the solution would be found using the relationships given in Figure 6.77 to 6.80.

The calculations above complete the basic geotechnical design. Obviously, the lining design is an activity in itself, which will not be covered herein. The structural design of the support can, however, make use of the lining internal forces (N_ϕ, M_ϕ, Q_ϕ) calculated through equations 7.11 to 7.13, (Figure 7.2) with the input parameters used in the second and final iteration (Figure 7.18).

It was suggested in Section 7.2.2 that the ground heave as calculated through equation 7.10 tends to be excessive. In fact, Hartmann's solution for this aspect of the shallow tunnel entails an indeterminate degree of approximation, represented by the value of the arbitrary radius r_1. Before a comparison between calculated and measured behaviour is made, it seems convenient to explore the influence of the calculated heave on the overall tunnel response. For this, the calculations presented in Figure 7.17 were repeated, assuming, that v''_{zo} was equal to zero. The resulting

calculations are depicted between parentheses in Figures 7.17 and 7.18. As expected, the total radial displacement at the crown increases, as the floor displacement decreases, while the springline radial displacement remains unchanged. The average ground modulus $\bar{E}_t$, calculated at the end of each iteration, however, does not change by any significant degree. This seems to reflect the compensating effect of the increased crown displacement against the decreased floor heave. As a result, the radial stresses onto the support at equilibrium, do not change significantly. In essence, the effect of the overall ground heave given by equation 7.10 is mostly restricted to the vertical displacements at the floor and crown. Therefore, it should affect the subsurface and surface settlements which are normalized to the crown settlement. Settlement distributions were calculated with the zero heave assumption (not shown in Figure 7.19), and it was found that the amount of stress release in the unlined tunnel solution, which produces the same final crown settlement obtained in the interaction analysis (10.61 mm), was about 56%.

Figure 7.20 presents a comparison between the observed and calculated final subsurface settlements at the ABV tunnel. The calculated ground movements neglecting the heave component given by equation 7.10 are larger than the measured values, showing that this assumption leads to conservative settlement predictions. The calculated settlements including the heave component are, on the other

hand, very much in agreement with the field measurements.

A similar comparison regarding surface settlements is presented in Figure 7.21. Again the zero heave assumption leads to conservative estimates of the surface movements. The larger number of measurements includes a greater scatter of data so that both the heave and the no heave assumptions lead to results are contained well within the measurements.

The calculated and measured radial stresses acting on the lining are shown in Figure 7.22. Note that the calculated stresses are not sensitive to the heave assumption. The proposed design procedure seems to overestimate the ground loads onto the lining, except at the floor, where a good match is obtained. Bearing in mind the known difficulties associated with the installation of contact pressure cells notably at the upper arch of the lining, the agreement between measured and calculated stress seems fairly reasonable.

Finally, Table 7.4 summarizes the comparisons between the measured and calculated performance for the ABV tunnel. Note that the tunnel radial closure at the face was calculated using the approximate solution presented in Section 5.3.5.2 (aspects 3 and 6). The maximum horizontal convergence of the lining (aspect 5) was calculated by discounting the springline movements that took place ahead of the tunnel face (not measured). The total settlement of the lining roof (aspect 8), measured by internal levelling in the field, was calculated by discounting the crown

Performance aspect		Measured[1]	Calculated	
			Heave[2] Included	Heave[3] Excluded
1. Maximum final surface settlement	mm	5.0	4.1	5.4
2. Maximum slope of final settlement trough at surface	-	1:1,300	1:2,000	1:1,800
3. Floor heave at tunnel face	mm	1-1.5[4]	2.2	2.2
4. Final floor heave	mm	5-9[4]	11.0	8.5
5. Maximum horizontal convergence of the lining	mm	0.85	2.7	2.7
6. Crown settlement at tunnel face	mm	1.5[5]	3.9	3.9
7. Final crown settlement	mm	8.0[5]	8.1	10.6
8. Total settlement of lining roof	mm	4-5	4.2	6.7
9. Pressure on lining at the crown	kPa	30	44	44
10. Pressure on lining at springline	kPa	35	58	58
11. Pressure on lining at the floor	kPa	55	57	57

Notes: (1) Average values.
(2) Taking into account the ground heave in the lining-ground interaction analysis.
(3) Disregarding the ground heave in the lining-ground retraction analysis.
(4) Measured at 0.2 m and 1.2 m below tunnel.
(5) At 0.2 m above tunnel.

Table 7.4 Performance at the ABV Tunnel as Measured and as Calculated by the Proposed Procedure

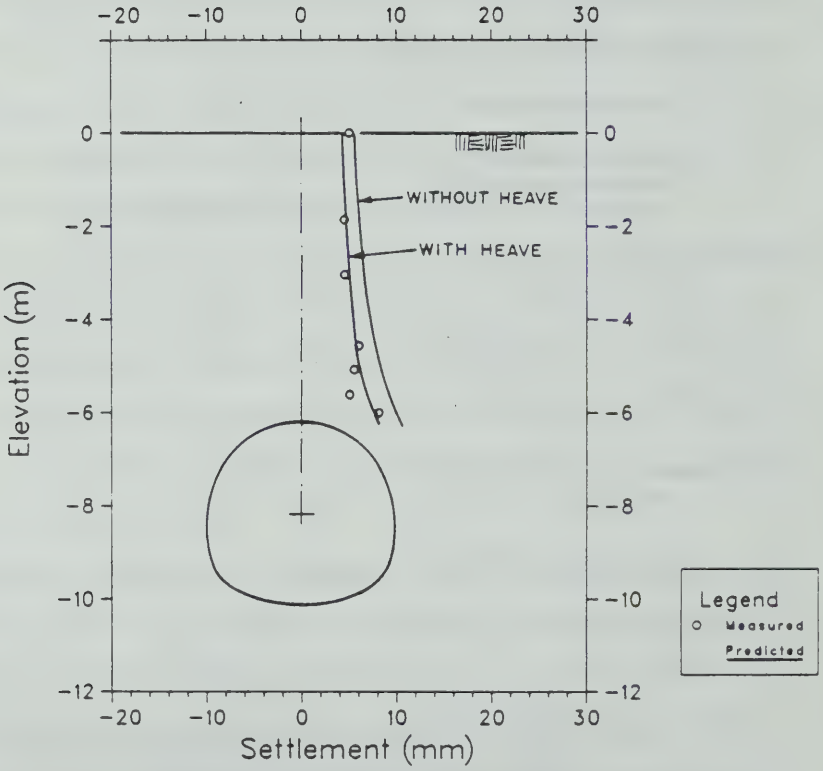

Figure 7.20 Calculated and Measured Final Subsurface Settlements at the ABV Tunnel

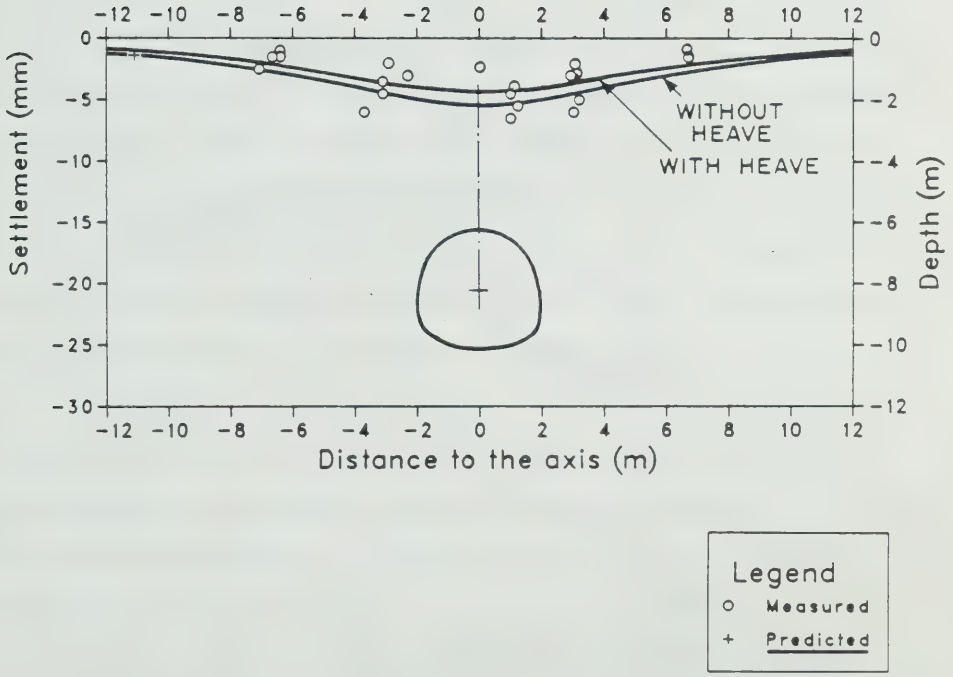

Figure 7.21 Calculated and Measured Final Surface Settlements at the ABV Tunnel

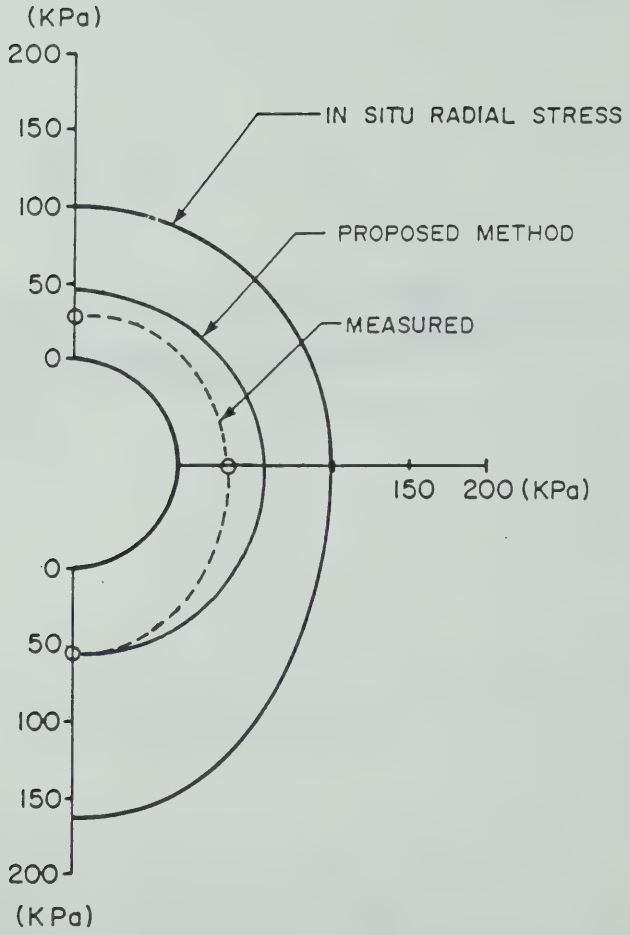

Figure 7.22 Calculated and Measured Radial Stresses on the ABV Tunnel Lining

settlement that also developed ahead of the face.

Regardless of the assumption made with respect to the ground heave, the comparisons shown speak for themselves. If the results of the present calculations are compared with those of the best fit finite element analysis shown in Section 5.2.4.2 (Figure 5.19 to 5.21 and Table 5.12), one may appreciate that they are similar, if not better. In fact, the introduction of a procedure, although approximate, to estimate the tunnel closure prior to lining installation which takes into account the three dimensional nature of the problem, did improve some of the predicted aspects of the performance, particularly aspect numbers 3, 5, 6 and 8, which are those more affected by the 3D nature. On the other hand, the approximations and simplifications introduced in developing the proposed method did not seem to deteriorate the predictions of the remaining aspects.

The time required for someone to use this design procedure for the first time, with the help of a programmable calculator, should not exceed an hour, or less with a microcomputer, provided the input data is fully digested and well defined.

The agreement between calculations and measurements might have been unintentionally biased by the familiarity with this case study that the writer gained earlier through its numerical back analysis. The purpose of the present section was to illustrate the use of the proposed design procedure, more than to validate it. For the latter purpose,

additional comparisons between measured and predicted tunnel performances are needed, and are provided in the next section for a representative range of practical situations.

7.5 Validation of the Proposed Method

7.5.1 Verification Against a Tunnel Model Test

Some tunnel model tests conducted in Cambridge in the seventies, present almost ideal conditions to test the validity of the proposed procedure to estimate the ground response around a tunnel. A number of verification calculations were undertaken using these experimental test results. One of them is presented in this section. It refers to an undrained centrifuge test in kaolin, carried out by Mair (1979), in which the ground reaction curve of the tunnel crown was obtained by simultaneous measurement of the applied internal tunnel pressure and the associated displacements at a point immediately above the crown. The measured ground reaction is compared with that calculated through the procedure proposed herein.

7.5.1.1 Model Test Procedures

The experimental result being focussed on, refers to test 2DP (series II), described by Mair (Op.cit.:62). Very briefly, a plane strain model test was conducted at 75g acceleration in the Cambridge Geotechnical Centrifuge (see Schofield, 1980), using Spestone kaolin as the modelling material. The two dimensional apparatus, housing the model

test, was completely sealed, so that it allowed the modelling of a saturated soil under undrained conditions. A special grease and grease application technique ensured a plane strain condition to be met. A kaolin slurry with a water content twice the liquid limit was placed in the apparatus, and was fully consolidated under a final vertical stress of 171 kPa. After unloading and removing the entire front of the apparatus conveniently tilted back, silvered perspex balls at 10 mm spacing were pressed into the clay surface, as markers for displacement measurements. Pore pressure transducers were also inserted. The model apparatus was then assembled in the centrifuge and an equilibrium stage achieved at 130 r.p.m, which corresponds to 75 g at a 4 m radius. Water was sprayed to the top surface of the model to ensure saturation and a water level coinciding with this surface. After a few hours, pore pressure equilibrium was noted. The gravity scaling factor and model dimensions were such that, at equilibrium, the vertical effective stresses everywhere in the soil were less then the consolidation pressure applied earlier (171 kPa). The kaolin was therefore overconsolidated, with the degree of overconsolidation increasing towards the top surface.

The centrifuge was then stopped, and a circular opening representing the tunnel with a 60 mm diameter, was cut using a specially designed tool. Test 2DP was prepared in such a way that the cover to diameter ratio was equal to 1.67. A greased rubber bag was then inserted into the tunnel. The

centrifuge was restarted and equilibrium conditions restored at 75 g. Concomitant with centrifuge speed build-up, the tunnel internal pressure was steadily increased to maintain it equal to the vertical overburden stress at the tunnel axis. This was ensured by a pressure line connected to the tunnel bag.

Once the design acceleration was reached the centrifuge was kept at constant speed and the tunnel internal pressure immediately reduced in rapid increments, until ground collapse was observed. Simultaneously, photographs of the model were being taken, for each applied internal pressure reduction. The changes in the position of the silvered perspex balls could be monitored through the photographs. Ground strains and displacements could thus be obtained using specially developed techniques and data reduction procedures.

7.5.1.2 Soil Conditions in the Test

If the model is scaled back to gravitational conditions, then the prototype tunnel dimensions are found:

$D = 75 \times 0.06 = 4.5$ m

$H = 1.67\ D = 7.515$ m

The depth of the tunnel axis is equal to 9.675 m.

Through laboratory testing and the measurements taken, Mair (1979) was able to define the profiles of the 'in situ' effective stress, of K_o, OCR and the undrained strength, c_u, with depth. These were shown in Figure 5.17 in Mair (Op.cit.) and are not reproduced here. The overconsolidation

ratio was found to decrease from 5 at half diameter above the tunnel, to 2 at half diameter below it, so that an average OCR would be 2.8 at the tunnel axis elevation. The value of K_o was found to vary from about 1.3 to 0.85 between those two points, and, at axis elevation, K_o was found to be approximately equal to 1.0. Since the 'ground water level' was maintained at the top surface, the resulting in situ total stress ratio also equal to one. The undrained strength varied from 22 to 26 kPa between those two points with an average c_u of 24 kPa at the axis. These values corresponded to the undrained strength of the kaolin in plane-strain extension (Mair, 1979:99,103), consolidated to the effective stress acting at those points.

At tunnel axis elevation and assuming full saturation, the soil water content was found to be about 61%, corresponding to a void ratio of 1.59 and a specific gravity of 2.61. The unit weight of this saturated soil was equal to 16 kN/m^3.

The initial tangent modulus for the kaolin can be estimated from parameters determined by many research workers who investigated this type of soil at Cambridge. According to critical state concepts, the response of a lightly or overconsolidated saturated kaolin under undrained loading, is close to linear elastic, until the stress path reaches the state boundary surface. With the usual Cambridge notation (see Atkinson and Bransby, 1978, for example), the undrained elastic modulus for this soil at stress levels

below yield, is calculated by:

$$E_u = \frac{1+\mu_u}{1+\mu'} E' \qquad [7.15]$$

as the shear modulus of a soil is the same in effective or total stress terms. In this expression, E' and μ' are the Young's modulus and Poisson's ratio in terms of effective stress and μ_u is the undrained Poisson's ratio (0.5). According to Seneviratne (1979:Table 2.1), μ' for this soil is equal to 0.33. The modulus E' can be calculated from the bulk modulus K', through:

$$E' = 3(1-2\mu')K' \qquad [7.16]$$

and K' of an overconsolidated soil can be obtained from the slope k of the swelling curve of a isotropic compression test:

$$K' = \frac{v\ p'}{k} \qquad [7.17]$$

where v is the specific volume (1+e) and p' is the octahedral normal effective stress invariant $((\sigma'_v + 2K_o\sigma'_h)/3)$. The swelling curve of clay in the v x ln(p') representation of the isotropic compression, is approximated by a straight line in the Cam-Clay model. The slope, k, of this line for kaolin was found to vary from 0.04 to 0.06 (Mair, 1979:124). As one is interested in obtaining the initial tangent modulus, the lower k seems to be the most respresentative value.

Combining the equations above one gets:

$$E_u = \frac{1+\mu_u}{1+\mu'}.3.(1-2\mu')\frac{v\ p'}{k} \qquad [7.18]$$

With p' and v calculated at a point half diameter above the tunnel crown, one obtains E_u. Mair (Op.cit.:Figure

5.16a) indicated that the soil water content at this point was equal to 62% and from it, the specific volume can be calculated, and is equal to 2.62. Mair (Op.cit.:Figure 5.17) indicated that p' at this point was about 40 kPa. The undrained Young's modulus is, thus, found to be equal to about 3.0 MPa. This value is the initial tangent modulus that will be used to normalize the displacements at tunnel crown.

A failure ratio, R_f, of about 0.9 is calculated from undrained triaxial test results on this soil, presented by Roscoe and Burland (1968).

7.5.1.3 Predicted and Measured Ground Responses

The generalized solution derived for the frictionless soil model (Section 6.4.2) will be used to estimate the ground reaction curve for the tunnel crown. It should be pointed out that the solution derived for the frictionless soil model does not completely represent the model test condition. In the latter, a uniform pressure was applied inside the tunnel, which was a fraction of the overburden vertical stress at the axis elevation. The derived solution on the other hand, assumes a non-uniform stress applied over the opening contour, which results from the initial gravitational stress field. However, if in both cases, the acting stresses onto the tunnel are normalized to their respective initial values, a comparison between the observed and calculated responses can perhaps be made.

For K_o=1 and ϕ=0, the normalized ground reaction curve is given by equation 6.17:

$$\Sigma = 1 - \frac{U}{A+BU} \qquad [6.17]$$

The coefficient A for the tunnel crown can be obtained from Figure 6.85. For a cover to diameter ratio of 1.67, A is found to be equal to 0.89. The coefficient B, also for the tunnel crown, can be obtained from Figure 6.86. The undrained strength of this soil has to be adjusted, according to equation 6.7, since its failure ratio is less than unity. The equivalent cohesion is thus calculated as $c_{ue} = c_u/R_f \simeq 26.67$ kPa. Therefore, the equivalent undrained strength ratio becomes $c_{ue}/\gamma D$=0.37. In Figure 6.86, B is found to be equal to 1.74. Thus:

$$\Sigma = 1 - \frac{U}{0.89+1.74U} \qquad [7.19]$$

This equation relates the ratio of radial stress at the crown to the normalized crown displacement. In the model test, however, the displacements were not measured exactly at tunnel crown but at some distance above it. From Mair (1979:Figure 5.26), one may suggest that this distance could have been about 20 mm or D/3. The distribution of the normalized subsurface settlements for H/D=1.5 and $c_u/\gamma D$=0.3125, included in Appendix C, shows that at that normalized distance above the crown, the normalized settlement is almost independent of the amount of stress release and is equal to 0.72. For H/D=3, the settlement ratio is about 0.66. Hence for H/D=1.67, it should be 0.713. Thus, the resulting crown settlement (u_c) is equal to 1.402

times the settlement at the displacement marker (u). The normalized crown displacement is:

$$U = \frac{u_c . E_{ti}}{D . \sigma_{ro}}$$

where u_c=1.402u, E_{ti}=3 MPa, D=4.5 m and σ_{ro}=120.24 kPa. Therefore:

$$U \simeq 34.98 \frac{u}{D} \qquad [7.20]$$

Table 7.5 shows the displacement ratios u/D measured at the point above the crown by Mair (1979:Figure 7.8), for different tunnel internal pressure ratios Σ_T. The radial stress ratio, Σ, at the crown was calculated by equation 7.19, for the normalized crown settlement calculated from equation 7.20. The predicted and observed response are shown in Figure 7.23. A certain degree of uncertainty exists in the calculated response, since the exact position of the point where the displacements were measured is not exactly known. Accordingly, the calculations were repeated, assuming now that this point was located at 10 mm above the tunnel crown. The dimensionless crown displacement is then: $U \simeq 30.81\ u/D$.

The ground reaction curve calculated with this assumption is also included in Figure 7.23. One notes that, regardless of the assumption made regarding the position of the marker used for measuring the displacements above the crown, the agreement between predicted and observations is good.

The limiting U beyond which the solution represented by equation 7.19 ceases to be formally valid, can be calculated

Σ_T (1)	u/D (2)	U (3)	Σ (4)
1.000	0	0	1.000
0.800	0.009	0.315	0.781
0.713	0.015	0.525	0.709
0.617	0.036	1.259	0.591
0.513	0.083	2.903	0.511

Notes: (1) Ratio of applied internal pressure in the model test tunnel.
(2) Displacement ratio measured in model test at a point above the crown.
(3) Normalized settlement at the crown.
(4) Predicted radial stress ratio at crown for (3).

Table 7.5 Measured and Calculated Ground Response in the Centrifuge Model Test 2DP by Mair (1979)

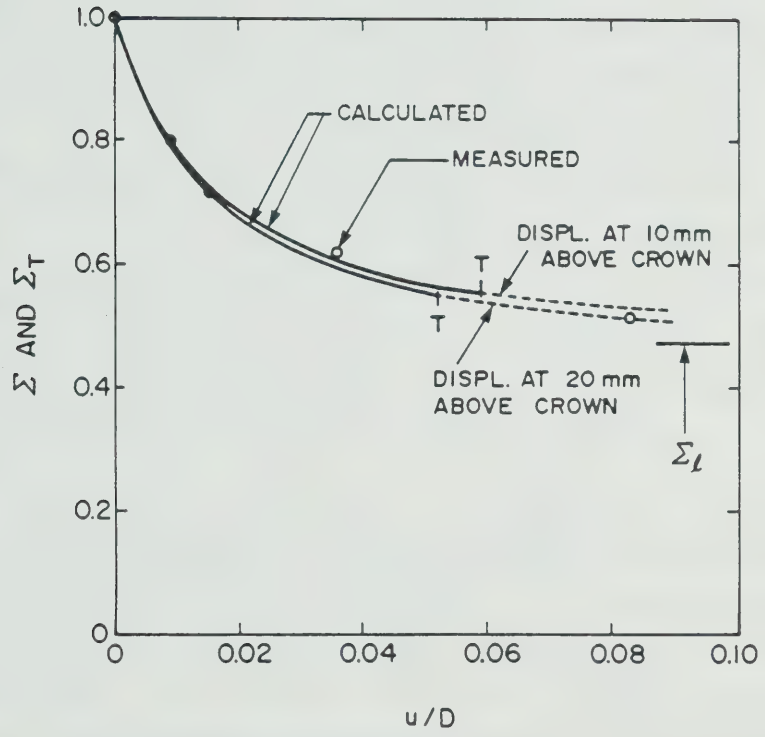

NOTE: TEST 2DP BY MAIR (1979)

Figure 7.23 Measured and Calculated Ground Response at Tunnel Crown for the Centrifuge Model Test

through Figure 6.119. This is found to be equal to 1.812, which corresponds to u/D equal to 0.052 or 0.059, depending on the assumed position of the measuring point (20 mm or 10 mm above the crown respectively). To the right of point T, the dashed curves represent numerical data extrapolation, and nothing ensures that the ground response predicted by the theoretical solution beyond T is correct. Notwithstanding this, the curves bound the experimental observation even beyond their limits.

Figure 7.23 also indicates the ratio of the collapse to initial tunnel pressure, Σ_1. This was calculated through the lower bound solution shown in Figure 6.122. For a strength ratio $c_u/\gamma D=0.33$ (not adjusted) and $H/D=1.67$, the collapse pressure is estimated as 73.2 kPa, while the initial internal pressure applied was equal to the overburden stress at axis elevation, i.e., 154.8 kPa. Hence, Σ_1 resulted in being 0.473, a value that seems to agree with test and calculated results.

Finally, Figure 7.24 compares the measured and calculated surface settlement profiles at two internal pressures (107 and 92 kPa), corresponding to $\Sigma=0.71$ and 0.61. The experimental results were presented by Mair (1979:Figure 5.18) and Mair et.al., (1981:326). The crown displacements were calculated through equation 7.19, and were found to be equal to 0.83×10^{-2} and 4.27×10^{-2} times the opening diameter. The profiles were obtained through the distributions of normalized surface settlements included in

Appendix C, using the procedure given in Section 7.3 and exemplified in Section 7.4. While it provided settlement magnitudes close to those observed, the shape of the settlement troughs furnished by the proposed calculation method did not fully agree with the measurements. This is particularly true for the larger amount of stress release, when Σ gets closer to the collapse stress ratio (0.473). Figure 7.24 shows that the surface distortions are underestimated by the proposed method. This result, however, is not surprising and the reasons behind it were discussed in different occasions in Chapter 5. It was shown there, that this type of result is a common feature in finite element modelling of shallow tunnel behaviour.

7.5.2 Verification Against a Three-Dimensional Finite Element Analysis of a Shallow Tunnel

Katzenbach (1981) performed a fairly refined three dimensional finite element analysis of a shallow tunnel, where the ground was represented by a non-linear elastic stress-strain relationship using the orginal hyperbolic model formulation (Duncan and Chang, 1970). Some results of this study were published by Katzenbach and Breth (1981) and some features of this analysis were reviewed in Section 5.3.3 of this thesis. While in Section 7.5.1, the new design method was verified against an ideal plane strain situation, this finite element analysis may serve to check it against an idealized three-dimensional condition.

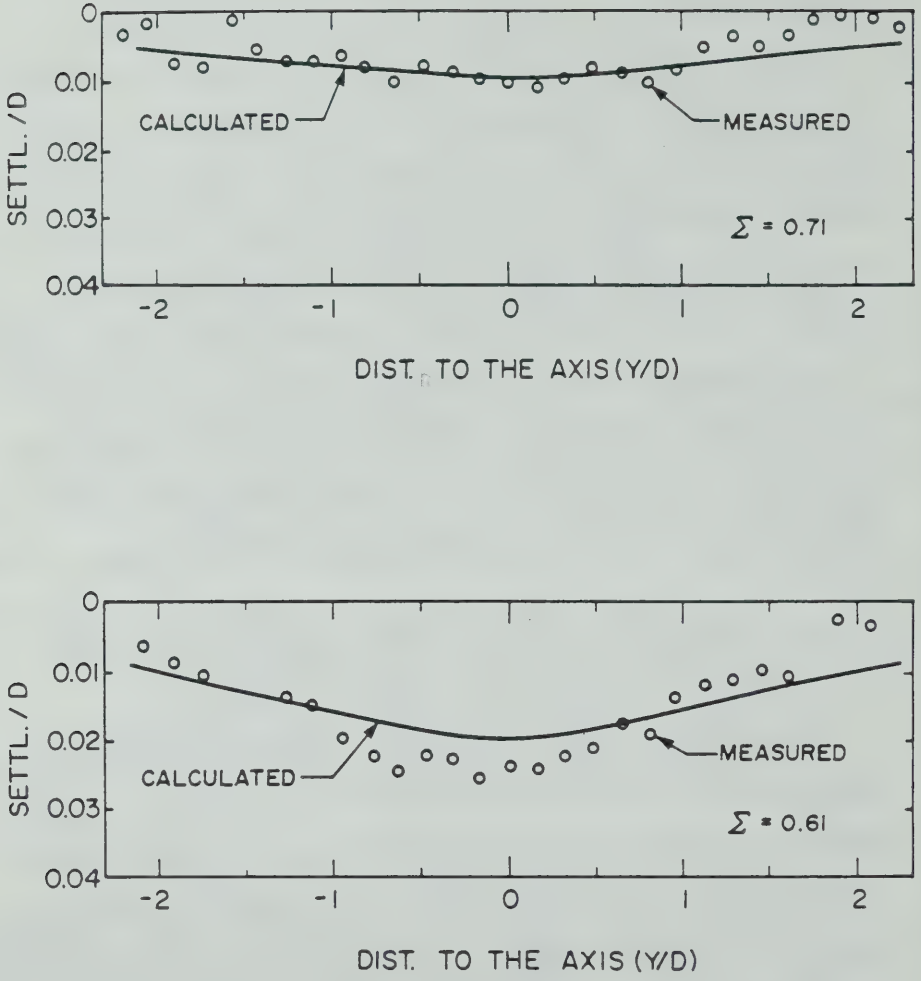

Figure 7.24 Measured and Calculated Surface Settlement Profiles for the Centrifuge Model Test at Two Internal Pressures

In the analysis, the ground mass was assumed to be uniform, with the following parameters: γ=18.5 kN/m^3, K_o=0.8, c=20 kPa, ϕ=20°, R_f=0.9, Janbu's modulus K=225, Janbu's exponent n=0.6, and μ=0.45. The tunnel was assumed to be circular, with an excavated diameter of 6.7 m and with a soil cover of 11.35 m. The support was represented by cylinder, 0.2 m thick, with elastic parameters given by E=12.6 GPa and μ=0.2 (Katzenbach, 1981:39). An incremental construction simulation was performed with a full-face stepwise excavation and delayed support application. Some uncertainty existed in the definition of the distance from the face at which the lining was installed. The reason for it was that, in the numerical simulation, this distance was not kept constant throughout the analysis. When the support ring immediately behind the control section was activated (see LS13 in Katzenbach; Op.cit.:Figure 37b), the distance between its middle point and the vertical tunnel face was 6.25 m. The support ring immediately beyond the control section, on the other hand, was installed at 7.25 m behind the face. For calculation purposes, it will be assumed that lining installation occurred at 1D behind the face.

The proposed calculation method was applied to this problem, using the same parameters and considering the same conditions found in the 3D analyses. At lining activation, the reduced unit weight of the soil was found to be 9.46 kN/m^3, corresponding to about 49% stress release. The averaged soil modulus at this point was calculated to be

9.24 MPa, representing a 68% decrease in the ground stiffness, resulting from the delayed application of the support. The lining-ground interaction was carried out neglecting the overall ground heave developing after lining installation, otherwise calculated by equation 7.10. A final crown settlement of 55.3 mm was obtained, which corresponded to 54.4% stress release at the crown in the 2D unlined tunnel solution.

The distributions of final subsurface settlements along the tunnel axis are compared in Figure 7.25. A fairly good agreement between the results of the 3D finite element analysis and of the proposed calculation method is observed. A good agreement was also found for settlements at sections between the face and the point of lining activation. Poorer agreement was noted for sections at or ahead of the face, where the three-dimensional effects, not fully accounted for in the proposed method, are more pronounced.

In Figure 7.26, the profiles of final surface settlements are compared and, once more a reasonable agreement is noted. The zero settlement noted in the 3D finite element analysis at the furthermost point from the tunnel axis, resulted from the imposed zero displacement condition adopted by Katzenbach (Op.cit.) at the lateral boundary of his finite element mesh. The latter was located closer to the tunnel axis, than was the case in the parametric analyses that generated the present solution.

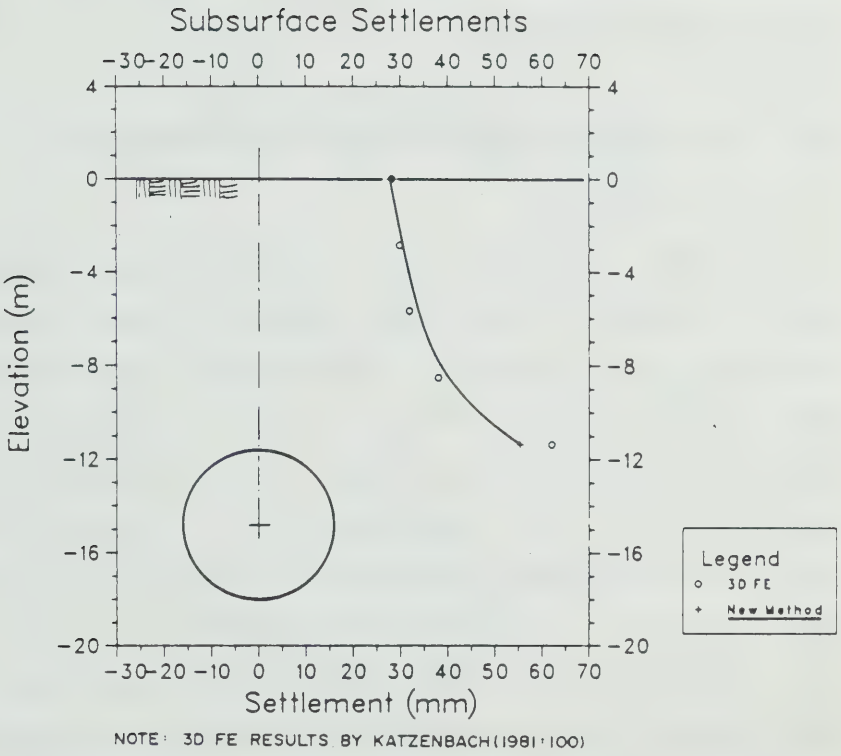

Figure 7.25 Subsurface Settlement Distributions Calculated in a Three-Dimensional Analysis and by the Proposed Method

Unfortunately, Katzenbach (1981) did not present either the resulting ground loads onto the lining or the opening radial displacements. However, the displacements and ground stresses he provided at nodal points and elements located at some distance away from the tunnel contour, seem to be consistent with those presently calculated at the lining-ground interface.

7.5.3 Verification Against Actual Case Histories

7.5.3.1 Foreword

In order to complete the validation of the proposed design procedure, it was tested against a number of case histories. They included both shielded and non-shielded driven tunnels, mainly through fairly firm ground. The case histories were selected according to the availability of adequate or sufficient published field instrumentation data. The comparison between predicted and observed performances was restricted to cases where good ground control conditions were met. Some of these cases, however, included conditions that deviate from those originally covered by the proposed calculation method. These were included to test the applicability of the new method, for practical situations outside its formal range of validity. The calculations were performed without attempting to best fit, or bracket the observed performance. The input parameters were selected by the writer, on the basis of available information and to best represent the most probable conditions found in each

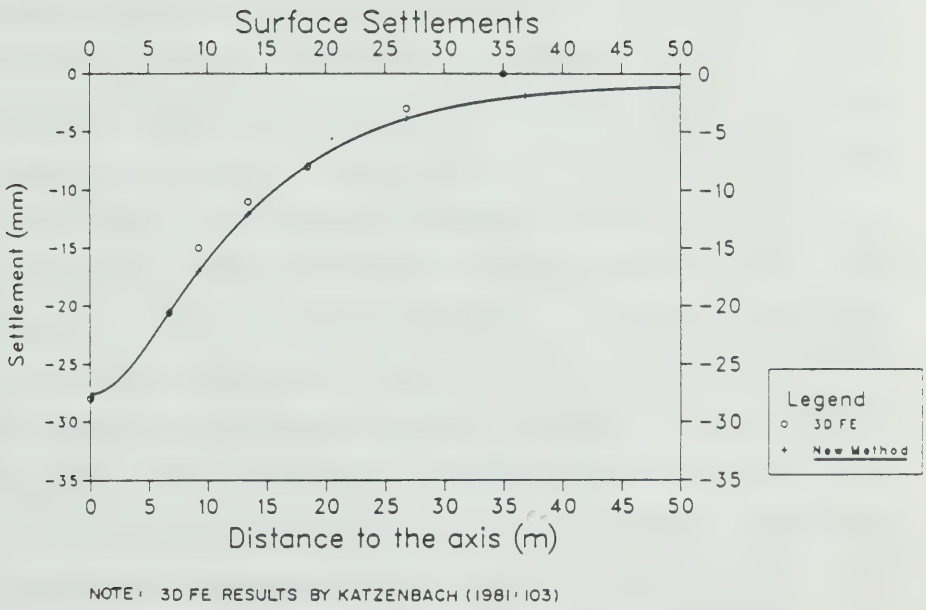

Figure 7.26 Profile of Surface Settlements Calculated in a Three-Dimensional Analysis and by the Proposed Method

case. A general appraisal of the results obtained are included in Section 7.5.4.

7.5.3.2 A Large Shielded Tunnel in Marl: The Frankfurt Baulos 23, Domplatz Tunnel

This case history refers to a subway tunnel built in 1970-1971, north of the Frankfurt Cathedral and described by Chambosse (1972). A twin tunnel system (13.2 m centre to centre) was built, with 6.7 m excavated diameter and cover of 11.8 m. The analysis here is concentrated to the south tunnel which was driven first.

The subsurface soil profile included a 9 m thick surficial layer of quaternary sand and gravel, covering a tertiary clayey marl, locally known as Frankfurt clay. The tunnel was entirely driven through this layer, which is intercepted by occasional limestone bands (up to 2 m thick), which are usually water bearing. The ground water level was originally located at about 5 m below the surface, but it was lowered by an extensive dewatering program, initiated one year before excavation started, so that tunnel construction was undertaken through a fully dewatered ground.

The Frankfurt clay is an overconsolidated fissured soil (CH) which was fairly intensively investigated by laboratory testing at the Univeristy of Darmstadt. Katzenbach (1981) summarized the results of these investigations and prepared a table with typical properties for this clay (also reproduced by Heinz, 1984:239). As input data for the

analysis of this case history, ground parameters equal to the mean between the maximum and minimum properties provided by Katzenbach (Op.cit:Table 4) were selected and are shown in Table 7.6.

An open face shield 6 m long, with working platforms at the face, was used for the construction, which proceeded at a 5 m/day rate of advance. The lining system included a five segment precast concrete ring, 90 cm wide and 35 cm thick with tongue and groove longitudinal joints, which were assembled under the shield tail protection. The fifth segment was a smaller key segment located at 30° from the tunnel floor. The external diameter of the concrete lining was 6.55 m, so that a nominal void space of 7.5 cm had to be filled, all around the ring, once the shield was advanced. Chambosse (1972) did not provide details of the grout filling operation, but it is believed that it took place typically at every second ring installed.

Tunnel construction was carried out under fairly good ground control conditions, with no localized ground collapses or instabilities having been reported. The presence of fissures in the marl could have been a point of concern regarding the applicability of the proposed design procedure. However, recent theoretical and experimental evidence on other fissured overconsolidated soils (Costa-Filho, 1984) seem to suggest that the effect of discontinuities on the pre-failure initial portion of the stress-strain curve is reduced, provided they are (and

Unit weight	γ	kN/m^3	18.5
In situ stress ratio	K_o	-	0.8 (1)
Effective cohesion intercept	c'	kPa	37.5
Effective friction angle	ϕ'	(°)	21.5
Failure ratio	R_f	-	0.8
Janbu's modulus	K	-	175
Janbu's exponent	n	-	0.6
Poisson's ratio	μ	-	0.3 (2)

Notes: (1) Suggested by Katzenbach (1981).,
(2) Adopted value.
(3) All other parameters are mean values calculated from extremes provided by Katzenbach (1981: Table 4).

Table 7.6 Typical Properties of Frankfurt Clay used in the Analysis

remain) closed. A fully drained behaviour was assumed, consistent with the assumption that the ground water level was lowered below the tunnel invert. The ground settlements associated with the changes in pore pressure induced by the dewatering had, in fact, almost stabilized before tunnel construction commenced. Accordingly, both the predictions and measurements, to be presented later, refer only to those additional ground movements caused by the tunnel excavation. Although the Frankfurt clay cover at the instrumented section was a little less than half tunnel diameter, the analysis assumed that the soil profile could be approximated by a uniform layer of marl, and the presence of the limestone bands was disregarded.

An adjusted friction angle of about 30° was found and an average in situ modulus of 21.79 MPa was estimated for this soil. It is uncertain when the lining was brought in full contact with the soil, as the amount of overcutting over the shield as well as the details of the grouting operation were sparse. It was, thus, assumed that lining activation took place at the middle point of the second ring leaving the shield tail and that the soil did not close over the shield body. This results in a distance of 7.35 m behind the face or at about 1.1D. The calculated amount of stress release at this section resulted in being equal to 56% and the current average tangent modulus at this point was estimated as 9.61 MPa. The two-dimensional ground stability verification for this condition furnished a factor of safety

of 1.66, indicating that the opening was stable and the ground far from collapse. The lining-ground interaction analysis was then conducted. No allowance was made for the possible increase in lining flexibility, resulting from the presence of joints. In fact, Muir Wood's (1975) correction for the moment of inertia of a jointed lining is only applicable when more than four equal segments are included. In this case, the fifth segment is the key element, which was much smaller than the others. A Young's modulus of 29.4 GPa was assumed for the lining, as this was the value adopted by Chambosse (1972:77) on the lining measurements data reduction. This modulus is likely to be slightly high, knowing that the longitudinal joints normally increase the compressibility ratio of the support. This is particularly true, for instance, when bitumen strips or neoprene sheets are used as seals, which however, was not the case herein. Had these materials been used, the lining compressibility would have been entirely controlled by their stiffnesses. The flexibility and compressibility ratios defined in Section 7.2.1 were calculated as 0.5 and 468, respectively. The ground heave after the support was activated was assumed to be zero. Only one iteration was needed to define the equilibrium conditions, which reflects the very stiff nature of the lining.

The final crown settlement was estimated as about 59 mm (U=0.657) and the associated amount of stress release at the crown was calculated as 56.7%. The distributions of final

subsurface and surface settlements were immediately obtained and are shown in Figures 7.27 and 7.28. A maximum surface settlement of about 30 mm was calculated. In these figures, field measurements are included for comparison. The settlements due to dewatering prior to the drivage were subtracted from the measurements (Chambosse, Op.cit.:Figure 74). One notes that the predicted settlements agree quite well with the measurements.

The predicted distributions of thrust forces (N_ϕ) and bending moments (M_ϕ) in the three upper segments are shown in Figure 7.29. The notation and sign convention used is that given in Section 7.2.1. The position of the longitudinal joints are indicated by the letter 'J', and the crown and springline by 'C' and 'S', respectively. Unfortunately no load measurements were undertaken in the South tunnel lining. Lining instrumentation was introduced 9 months later in the second driven North tunnel. Thrust forces and bending moments were calculated through strain measurements in seven niches cast in the inner sides of the three upper lining segments. Each niche housed six pairs of steel reference pins, fixed against the niche's transverse wall, so that the strain distributions across the half thickness of the lining could be obtained using a DEMEC type mechanical strain gauge. A linearized stress distribution across the lining thickness was calculated, assuming a Young's modulus of 29.4 MPa, and from it, the thrust forces and bending moments were obtained.

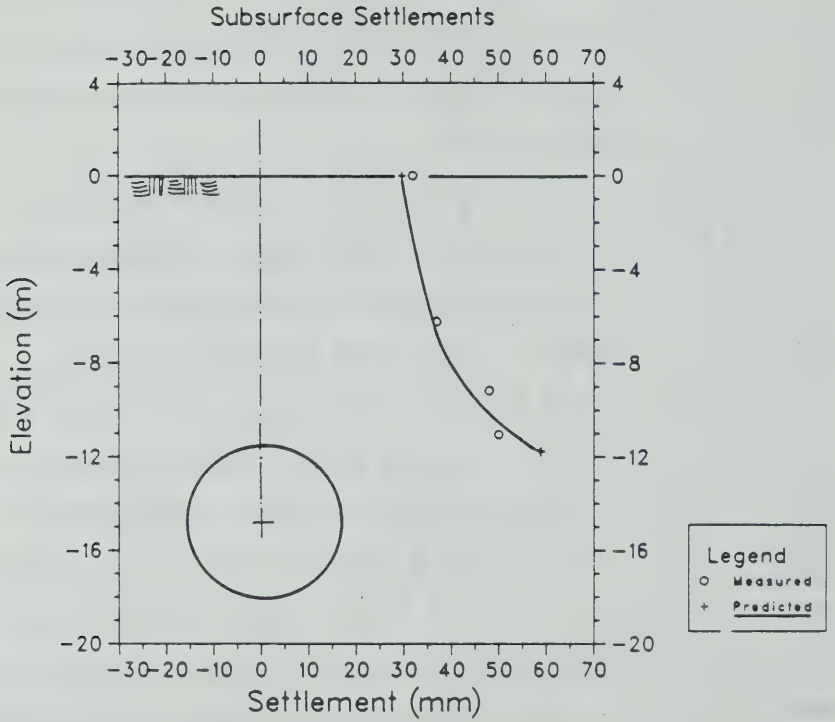

NOTES :
1. SETTLEMENTS CAUSED BY THE FIRST TUNNEL MEASURED AT EXTENSOMETER T4, FROM CHAMBOSSE (1972' FIGURE 19)
2. THE SETTLEMENTS DUE TO GWL LOWERING WERE SUBTRACTED FROM MEASUREMENTS.

Figure 7.27 Measured and Calculated Final Subsurface Settlements over the South Tunnel in the Frankfurt Baulos 23 (Domplatz) Subway

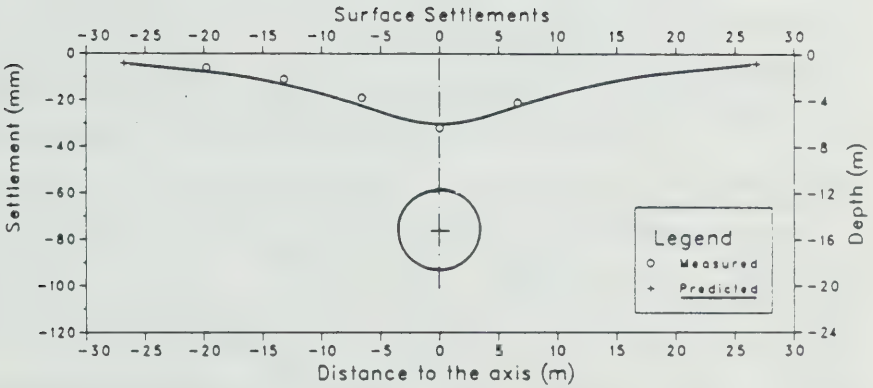

NOTES:
1. MEASUREMENTS AT DOMSTRASSE INSTRUMENTED SECTION AFTER FIRST TUNNEL CONSTRUCTION, FROM CHAMBOSSE (1972, FIGURE 19)
2. THE SETTLEMENTS DUE TO GWL LOWERING WERE SUBTRACTED FROM MEASUREMENTS.

Figure 7.28 Measured and Calculated Final Surface Settlements over the South Tunnel in the Frankfurt Baulos 23 (Domplatz) Subway

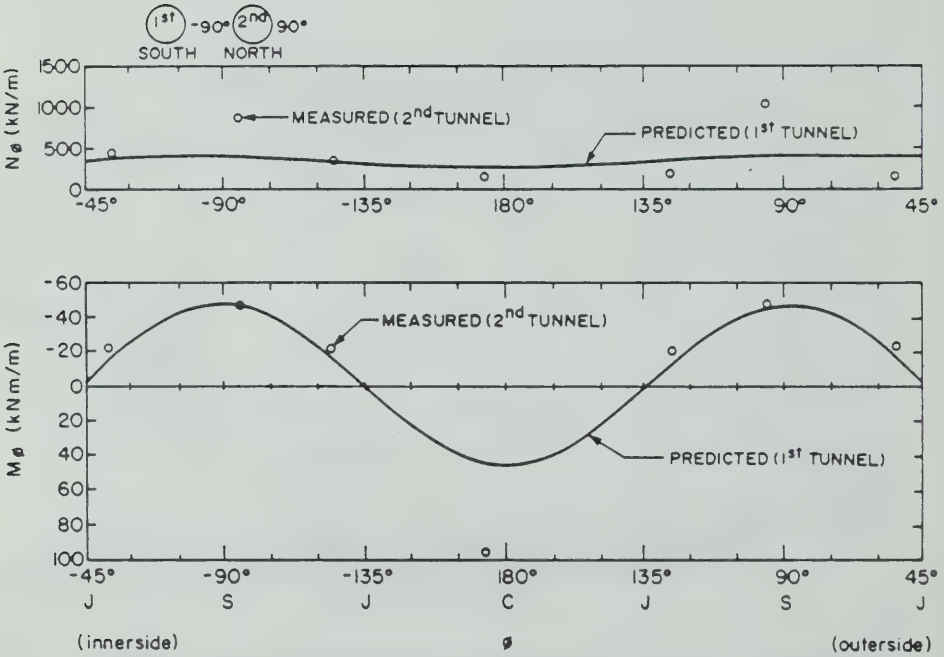

Figure 7.29 Predicted Lining Loads in the South Tunnel (1st driven) Compared to Measurements in the North Tunnel (2nd driven): Frankfurt Baulos 23 (Domplatz) Subway Tunnels

The width of the central soil pillar separating the two tunnels was about one tunnel diameter. The lining measurements taken in the second tunnel were very probably affected by the first tunnel already built. Notwithstanding this, the measurements recorded in the second, are presented together with the lining loads predicted for the first in Figure 7.29. Although an immediate comparison is not formally valid, one notes that the results are not entirely discordant. The differences between predicted and measured loads could be partly attributed to the changes in ground stiffness and in ground stresses induced by the first tunnel construction. The transverse arching process triggered by the first drivage may partly explain the higher thrust forces measured at the springline in the second tunnel, as well as the higher bending moment at the crown. This interpretation is supported, in qualitative terms, by the numerical results obtained by Ranken (1978:219, case C) who studied the lining responses in two parallel tunnels consecutively driven, assuming a linear elastic response for both soil and lining.

The overall agreement between predicted and observed performances in this case history was quite satisfactory, despite no attempt having been made to best fit the observations. In a real design situation, it is believed that the observed performance could have been totally bracketed, had the variabilities of the ground properties and construction operations been taken into consideration.

7.5.3.3 Twin NATM Tunnels in Marl: The Frankfurt Baulos 25, Romerberg Tunnel

This case history refers to a twin subway tunnel built in 1970, at the Romerberg, Frankfurt, that was described by Chambosse (1972), Edeling and Schulz (1972) and Schulz and Edeling (1973). More recently, this case history was reviewed by Heinz (1984:236). It was in this project that the so called New Austrian Tunnelling Method was first used for the construction of an urban tunnel in soil. The two parallel tunnels were advanced simultaneously at a distance of 12.7 m from centre to centre. Each tunnel had a circular profile with a 6.48 m excavated diameter. The soil cover at the instrumented sections was 11.5 m. Although the proposed design procedure was developed for a single and isolated tunnel, it seems interesting to assess the influence of a parallel and simultaneous tunnel construction.

The ground conditions were similar to that found at the Frankfurt Domplatz Tunnel (Section 7.5.3.2), built nearby. The tunnels were entirely driven in the Frankfurt clay marl, which is overlain here by a 4 m thick layer of sand and gravel, which in turn is covered by a 2.5 m thick fill. The marl is also interbedded with limestone bands although thinner than at Domplatz (less than 1 m thick). The clay marl cover at the instrumented section was about 5 m thick. The ground water level, originally located at 4 m depth, was also lowered through deep wells to elevations below the tunnel invert. Dewatering was initiated six months before

tunnel construction started (Chambosse, 1972:48). The ground settlements associated with dewatering had stabilized before construction commenced, so that it was possible to separate these movements from those resulting from the tunnel construction proper. The ground mass, as it appeared during tunnel advance was free of water (Chambosse, Op.cit.:6), so that a drained behaviour could be assumed in the analysis. The relevant ground properties for the Frankfurt clay were already presented in Section 7.5.3.2. The same parameters used for the Domplatz Tunnel will be considered herein.

The simultaneous tunnel construction was carried out with sequential excavation of the face in three stages: heading, bench and invert. The shotcrete lining was also applied in stages, immediately after the ground was exposed. An average rate of advance of 1.2 m/day was achieved. The excavation round length was about 1.2 m, which corresponded to the spacing of light segmented steel ribs, with a channel profile (TH 48, 16.5 kg/m). A steel mesh (Q188) was also incorporated into the support system. The total shotcrete thickness varied between 15 and 18 cm. When the tunnels passed the instrumented section II, the support ring closure at the floor took place typically at 5.7 m behind the face (Edeling and Schulz, 1972:Figure 11). The steel ribs were fixed to the ground by 3 to 4 m long anchors which were found later to have contributed nothing to the opening support (Schulz and Edeling, 1973:251). Tunnel construction was undertaken under good ground control conditions and no

ground instabilities were reported.

The analysis was conducted neglecting the presence of the second tunnel, and assuming a uniform layer of clay marl. An adjusted friction angle of about 30° was found and adopted for the cohesionless soil model. The average in situ tangent modulus was estimated as 21.49 MPa, with the parameters shown in Table 7.6. The lining activation was assumed to have taken place when the shotcrete lining ring was closed at the floor, 5.7 m behind the face. The calculated amount of stress release at this point was 55.5% and the current average tangent ground modulus at this section was estimated as 9.63 MPa. The ground stability verification yielded a factor of safety of 1.67, which confirmed that the opening was stable.

The lining-ground interaction analysis was carried out neglecting the action of the light steel ribs, but considering a nominally increased shotcrete thickness of 20 cm. A lining modulus of 10 GPa was considered as well as a Poisson's ratio of 0.2. The flexibility and compressibility ratios were estimated as 0.03 and 90, respectively, which are typical for a shotcrete lining in a soft to medium clay (see Table 7.1). A single iteration was required to define the equilibrium condition. The ground heave after the support was activated was neglected.

The final crown settlement was estimated as 59.1 mm (U=0.694) and the associated amount of stress release at the crown was calculated as 57.8%. The calculated distributions

of final subsurface and surface settlements are presented in Figures 7.30 and 7.31. Included in these figures are the measured displacements that were caused by the simultaneous construction of the two parallel tunnels. One notes in Figures 7.30 that, while the displacements of points closer to the tunnel are well approximated by the proposed procedure, those at the surface are substantially underestimated. This result was indeed expected, as the prediction did not take into acount the second tunnel construction. Ranken (1978:197) studied the development of surface settlements over twin tunnels built simultaneously, through linear elastic finite element analyses. He showed that the interaction between two shallow tunnels (H/D=1) is small provided the centre to centre distance is greater than 2 diameters. In other words, for this condition, the settlement profile obtained by superimposing two single tunnel settlement distributions is approximately equal to the actual profile from the two parallel tunnels simultaneously built. In the present case history, the tunnels were built at slightly more than two diameters apart. However, unlike the conditions focused on by Ranken (Op.cit.), the tunnels were deeper and the soil response was definitely non-linear. Nevertheless, if the superposition of surface settlements is accepted, then the profile found is that shown in Figure 7.32. One observes now, that a better agreement between measured and predicted responses is attained, at least with regard to the maximum surface

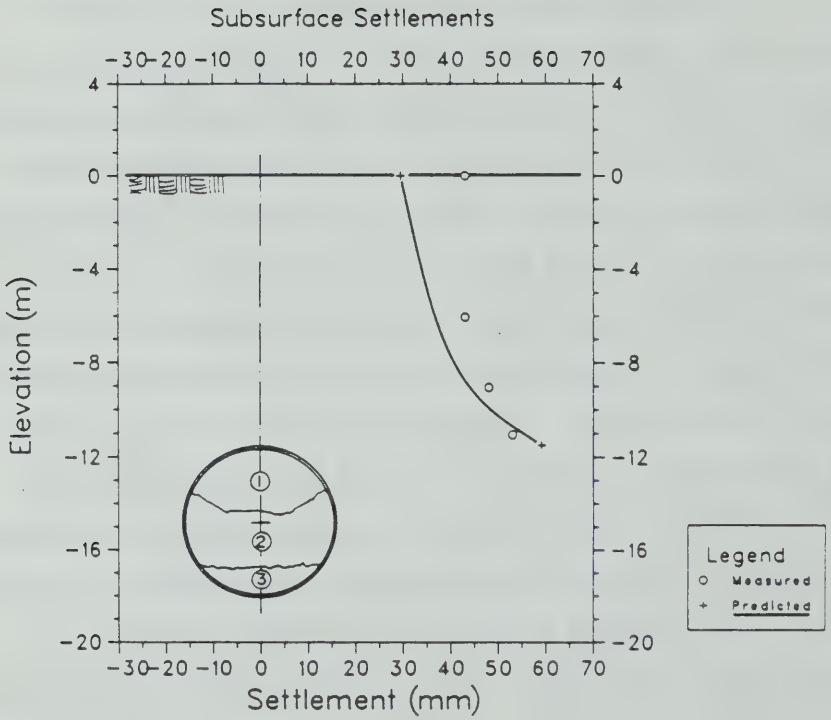

NOTES:
1. MEASUREMENTS AT EXTENSOMETER D2 OVER THE NORTH TUNNEL, AT THE INSTRUMENTED SECTION II, FROM CHAMBOSSE (1972-52)
2. THE SETTLEMENTS DUE TO GWL LOWERING WERE SUBTRACTED FROM MEASUREMENTS.
3. MEASURED SETTLEMENTS CAUSED BY SIMULTANEOUS CONSTRUCTION OF THE TWO PARALLEL TUNNELS.

Figure 7.30 Measured and Calculated Subsurface Settlements over the Frankfurt Baulos 25 (Romerberg) Subway

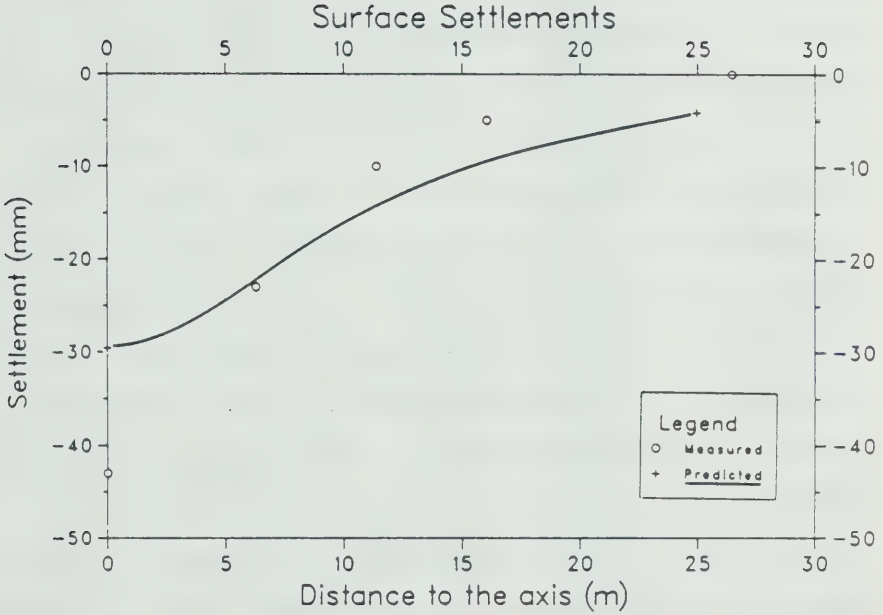

NOTES
1. CALCULATED SETTLEMENTS FOR A SINGLE TUNNEL CONSTRUCTION.
2. MEASUREMENTS AT THE INSTRUMENTED SECTION II, OVER THE SOUTH TUNNEL, FROM CHAMBOSSE (1972 '52)
3. THE SETTLEMENTS DUE TO GWL LOWERING WERE SUBTRACTED FROM MEASUREMENTS.
4. MEASURED SETTLEMENTS CAUSED BY SIMULTANEOUS CONSTRUCTION OF THE TWO PARALLEL TUNNELS.

Figure 7.31 Measured and Calculated Final Surface Settlements at the Frankfurt Baulos 25 (Romerberg) Subway Tunnel

settlements. The maximum surface distortion is however, underestimated by this approximate calculation procedure.

Figure 7.33 presents the calculated and measured radial stresses acting on the upper arch of the shotcrete lining, after equilibrium was achieved. The stresses were measured by Glotzl contact pressure cells (15 x 25 cm). Note that, while the prediction was made for a single tunnel, the measured stresses include the effect of the twin tunnels simultaneous construction. Note, moreover, that the measurements were taken at both tunnels, and for easier comparison, they were plotted together by making the relative position of the measuring points with respect to the central soil pillar to coincide. Accordingly, the measurements at the springlines (S) facing the central pillar (innerside) are plotted together at the +90° position (measured from the floor), whereas those at the outer abutment springlines (outer side) are plotted at the -90° position. The predicted radial stresses seem to be closer to the average stress measured, except at the springlines, where the measured stresses are underestimated, notably at the inner springline, on the pillar side. If it is admitted that the readings are correct, one could speculate that the interaction between the two tunnels forced them to squat more and to mobilize higher radial stress at the springline elevation. This interpretation, however, is not clearly supported by Ranken's (1978:194) numerical results, which suggested that shallow twin tunnels built simultaneously, at

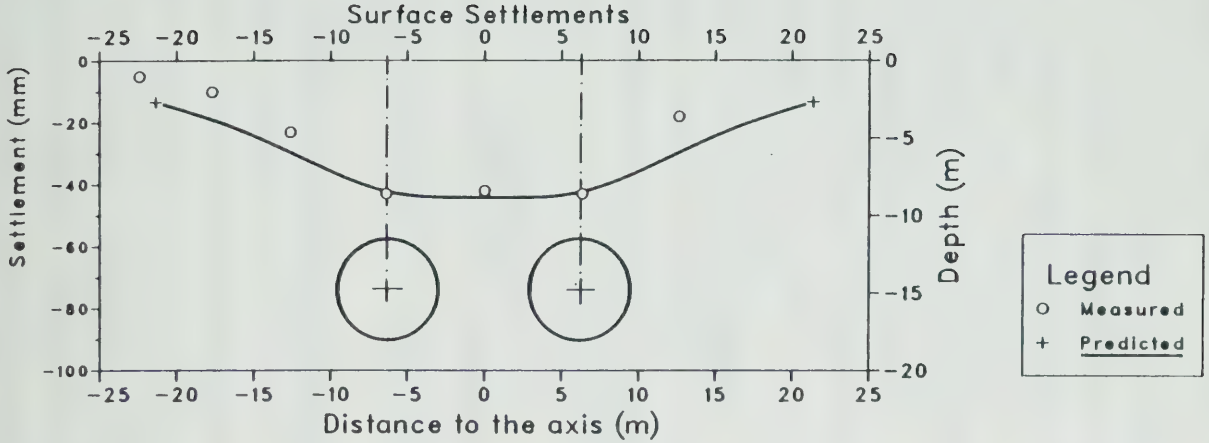

NOTES:

1. CALCULATED SETTLEMENTS OBTAINED BY SUPERPOSITION OF SINGLE TUNNEL PROFILE.
2. MEASUREMENTS AT THE INSTRUMENTED SECTION II, FROM CHAMBOSSE (1972·52)
3. MEASURED SETTLEMENTS CAUSED BY SIMULTANEOUS CONSTRUCTION OF THE TWO PARALLEL TUNNELS, WITH MOVEMENTS DUE TO GWL LOWERING PRIOR TO EXCAVATION DISCOUNTED.

Figure 7.32 Measured and Calculated Final Surface Settlements over Twin Tunnels at the Frankfurt Baulos 25 (Romerberg) Subway

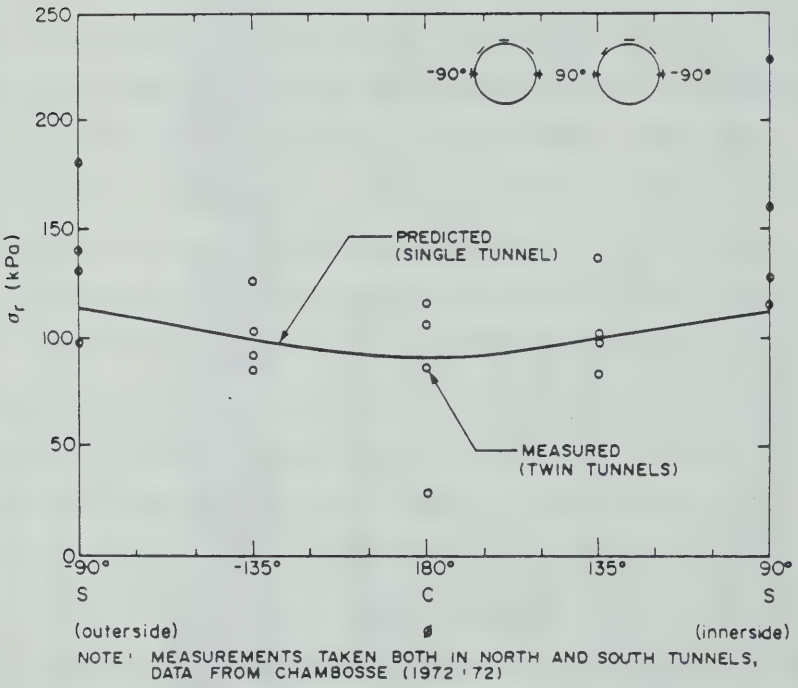

Figure 7.33 Predicted Lining Radial Stresses for Single Tunnel and Measured Stresses in Twin Tunnels at the Frankfurt Baulos 25 (Romerberg) Subway

one diameter apart (centre to centre), exhibit lining loads that do not differ greatly from those for a single tunnel. However, the generality of Ranken's suggestion is debatable, since he assumed linear elastic responses for both soil and liner, and more importantly, he assumed that the linings in both tunnels were installed before soil excavation (no stress relaxation before support application).

A special device, designed by Interfels, installed from the surface, allowed the measurement of horizontal displacements in the ground at the springline elevation, 0.5 m away from the tunnel contour. A maximum horizontal movement towards the opening of about 19.5 mm was measured at Section II, in the outer abutment of the tunnel, just prior to the closure of the shotcrete ring at the invert (Chambosse, 1972:Figure 75). This value is compared with the 31.9 mm of inward radial displacement calculated at the springline of the single tunnel contour at lining installation.

Horizontal diameter changes were also measured in three shotcrete rings in the North Tunnel (Edeling and Schulz, 1972:357). An increase of the horizontal diameter of 12 to 13 mm after completion of the invert was recorded (10.5 to 13 mm according to Chambosse, 1972:66). The lining-ground interaction analysis indicated that this increase amounted to 11.1 mm, which compares favourably with the measurements.

The comparison between calculated and observed performances in this case history should be carefully

interpreted, since the proposed procedure does not account for the interaction of two parallel tunnels. However, one can observe that the resulting calculations are consistent with the observations and that the noted differences could be attributed to the interaction between the tunnels.

7.5.3.4 A Small Shielded Tunnel in Till: The Mississauga (Ontario) Tunnel

This case history refers to a small sewer tunnel, built in 1972 in Mississauga, about 29 km from central Toronto (Ontario), and described by Seychuk (1977) and by DeLory et.al. (1979). The tunnel was bored with a 4.27 m diameter, under a soil cover of 11.5 m at the installed instrumented section.

The soil profile included a 3.5 m superficial layer of recent alluvial sands and gravel, covering a very dense 12.5 m thick, sand-clay till layer. Underneath it, there was another till layer, of 4 m thickness, comprising a dense silty sand. The shale bedrock was found at about 20 m below the surface. The ground water level was about 6 m below the surface before construction started.

According to DeLory et.al. (1979), the tunnel was driven entirely through the very dense upper sand-clay till (SPT in excess of 100), which was found to be a relatively uniform soil, with 20% clay, 36% silt and 44% sand and gravel. The till liquid limit was about 22%, the plastic limit 15% and the natural water content 8%. Its unit weight was 24 kN/m^3 and the in situ effective stress ratio was

estimated as 0.9 to 1.0. The effective friction angle was measured in the laboratory and was found to be 35°. The effective cohesion intercept was not given by those authors, but data from Nipawin and Edmonton Till (Wittebolle, 1983), suggest that it could be greater than 30 kPa. These data also indicated that the failure ratio from drained triaxial tests for this soil may vary from 0.7 to 1.0.

Menard pressuremeter tests carried out in boreholes adjacent to the tunnel gave values of the in situ modulus from 55 to 160 MPa. Assuming that the tests were conducted rapidly and that some disturbance might have been caused by boring, a value of 140 MPa can be taken as typical for the undrained tangent in situ modulus of this till at the tunnel axis elevation. If a drained Poisson's ratio of 0.3 is assumed for the soil, then a drained modulus of about 120 MPa is calculated, provided that (at small strains) the soil behaviour is approximately linear elastic. No details of those tests or of the variation of the pressuremeter moduli with depth are given. It was then assumed that the drained soil modulus varied linearly with the square root of the vertical in situ effective stress (See Lambe and Whitman, 1969:159). In situ drained moduli of 105 and 134 MPa, were therefore estimated at a half diameter above and below the tunnel respectively.

Piezometers installed from the surface above and near the tunnel, showed that there was a lowering of the water pressure near the tunnel after construction. The piezometric

head at the axis elevation, at a point 2.1 m away from the springline decreased from 7 m to 1.4 m or less (DeLory et.al. 1979:193), after the tunnel was built. The original water pressures around the tunnel were not re-established after tunnel completion, which seems to have acted as a drain. If an option had to be made between an undrained and a drained analysis, one could suggest that the observed performance might have been closer to the latter condition rather than to the former. Accordingly, the selected ground parameters, defined in terms of effective stresses, that were considered for the analysis of this case history are those given in Table 7.7.

An open face shield, 5.18 m long, was used for construction. Excavation was by an Alpine miner road header, with the face being undercut some 0.6 to 1.5 m ahead of the shield hood (Seychuck, 1977). The cut profile was about 75 to 100 mm less than the shield outside diameter. The shield shaved off the remaining soil annulus as it was advanced. The rate of advance was about 5 m/day when passing the instrumented section. The primary lining system consisted of steel set rings (H section, 100 x 100 mm) in four segments and concrete planks (75 x 200 x 1200 mm), assembled inside the shield in 1.22 m lengths. As the primary lining emerged from the tail, it rested on the tunnel floor and a space of about 50mm between planks and ground was left at the sides and of about 100 mm at the crown. According to DeLory et.al. (1979:192), this void was filled with pea gravel, and was

Unit weight		γ	kN/m^3	24
In situ stress ratio		K_o	-	1.0 (1)
Effective cohesion intercept		c'	kPa	30 (1)
Effective friction angle		ϕ'	(°)	35°
Failure ratio		R_f	-	0.8 (1)
E_{t_i} (drained)	1/2 D above crown		MPa	105 (2)
	at springline		MPa	120 (2)
	1/2 D below floor		MPa	134 (2)
Poisson's ratio (drained)		μ	-	0.3 (1)

Notes: (1) Assumed value.

(2) Derived from pressuremeter tests.

Table 7.7 Selected Ground Parameters for Drained Analysis of Tunnel in Dense Sand-Clay Till

later grouted with cement. While the filling and grouting operations took place, for most of the tunnel length, at distances greater than 12 m behind the face, at the instrumented section it is estimated that these operations happened after the face had advanced about 7.5 m past the section. It is unlikely that the grout completely filled the gravel voids, particularly at the crown. An excessively robust unreinforced concrete liner, 460 mm thick, was installed about 3 months after passing the instrumented section.

Thanks to the good ground conditions rather than to the quality of the construction, no instability process was observed. The ground response was good, despite some poor construction procedures, such as face undercutting, the use of a long shield or the delay in filling and grouting the void behind the liner, to name a few. The ground drainage caused by the tunnel construction, induced changes in pore pressures which, in itself, may have induced ground displacements. The magnitudes of these were likely to be small, as the till is very dense, has a low void ratio (about 0.22) and a high bulk modulus. The soil volume changes due to consolidation induced by the dewatering were, thus, probably small. Probably the volumetric strains caused by the shear and mean normal stress changes induced by the tunnel excavation were also small. A factor of safety in excess of 1.7 was calculated in the two dimensional ground stability verification, for the instant the support was

activated. From what was shown in Section 2.3.4.4, for this safety level (load factor smaller than 0.6), the volumetric expansion in this soil was probably small.

Since the proposed design procedure does not take into account the consequences of pore water pressure changes, it was conveniently assumed that the ground was entirely dewatered, so that those pressures were equal to zero. However, the in situ ground moduli considered, (Table 7.7) are drained moduli corresponding to effective stress levels existing in situ, prior to dewatering. In other words, the possible gain in stiffness, which results from the increase in the effective stress level that would follow the ground water drawdown (either the hypothetical or the actual one) was neglected.

Having in mind the above discussion and considering the fairly uniform nature of the ground, it was felt that the proposed design procedure could be applied to this case history, and a comparison between the predicted and observed performances could be made. However, as noted above, it should be remembered that the latter may reflect not only the response resulting from the tunnel excavation, but also that resulting from changes in the pore water pressures.

An adjusted friction angle of about 40° was calculated, on account of the cohesive strength component and of the non-unity failure ratio. A certain degree of uncertainty existed regarding when the lining was brought in full contact with the soil. The exact grouting procedures were

not clear, as well as the amount of overcutting over the shield. It was, thus, assumed that lining activation took place 7.5 m behind the face, as mentioned earlier. A smaller distance would have to be considered if the shield had been advanced without an overcutter head. But this is unlikely, since high thrust forces are required to propel the shield in such a strong material, without some overcutting rim. The amount of stress release at lining activation was about 57% and a reduced average tangent modulus of 70.13 MPa was obtained (41% less than the original value).

Although an attempt was made to jack the concrete planks together circumferentially (DeLory et.al., 1979:195) it is very unlikely that they all came in full contact. If a minor gap of 0.5 mm had been left on average between each of the 64 or so planks used, a uniform convergence of more than 10 mm in the lining diameter would be required to put all the planks in full contact with each other. This convergence is an order of magnitude higher than the expected lining convergence. Therefore, it is reasonable to accept that, besides not being able to carry any bending in the plane transverse to the tunnel, the concrete plank lagging was very compressible under uniform transverse loading, and thus unable to carry tangential thrust. If a fully compressible contact between the planks is conceded, then they operate simply by transferring the ground loads in the longitudinal direction, to their supporting ribs. Accordingly, the relative stiffness of the lining would be that given by the

steel ribs at 1.22 m spacing only. Thus, a lining with a moment of inertia of 3.615 x 10^{-6} m^4/m and a cross sectional area of 2.016 x 10^{-3} m^2/m was considered for the lining-ground interaction, with elastic properties of steel (E_s=200 GPa and μ=0.2). The interaction analysis was conducted with the reduced unit weight of the soil and the reduced ground modulus mentioned earlier. Two iterations, in which the ground heave after support activation was neglected, were needed to define the equilibrium condition. An average ground modulus of 60.49 MPa was found for this condition, and the flexibility ratio (β) and compressibility (α) ratios resulted in values of to 1.92x 10^{-3} and 4.44 respectively. As can be observed in Table 7.1, these values are typical for this type of support in dense sand or stiff clay. The ground modulus at equilibrium is roughly half of the in situ modulus value.

The final crown settlement was estimated as about 7.3 mm (U=0.648) and the associated amount of stress release at crown was calculated as 60%. The distributions of the final subsurface and surface settlements were then obtained and are presented in Figures 7.34 and 7.35, together with the results of the field measurement program given by DeLory et.al. (1979:194). Seychuk (1977) made reference to problems regarding survey accuracy and thermal effects affecting the readings. Notwithstanding this, the predicted values broadly conform to the measurements, but it is clear that the maximum surface distortion is underpredicted by the

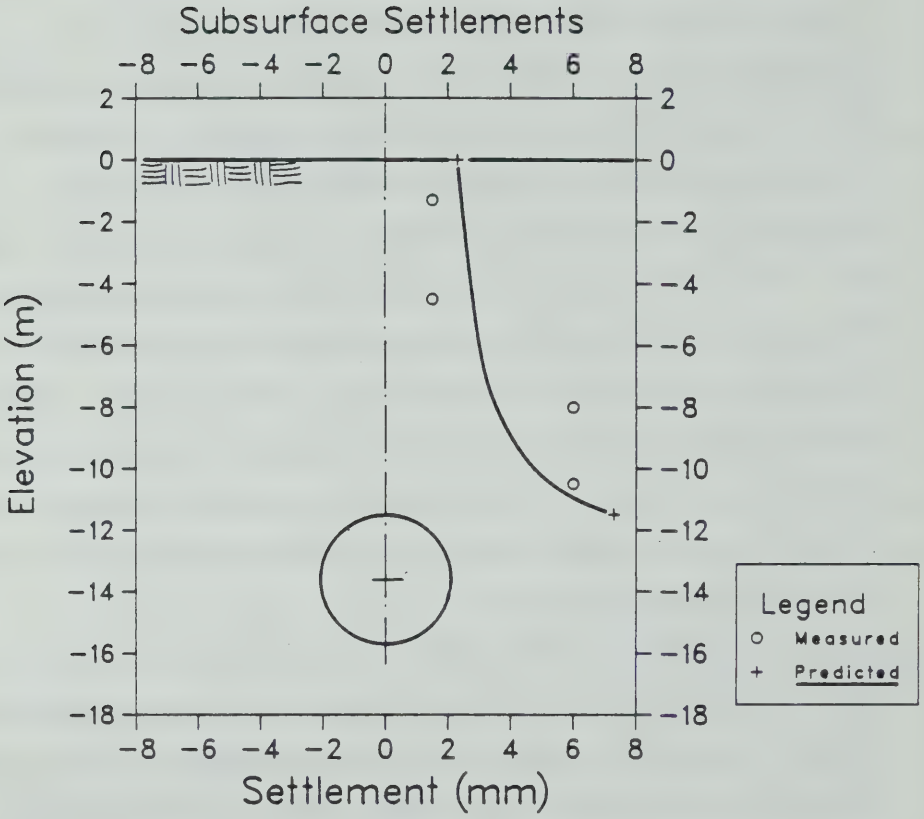

NOTE: MEASUREMENTS RECORDED AT POSITION C (TUNNEL AXIS) BY DELORY ET AL (1979 : 194)

Figure 7.34 Measured and Calculated Final Subsurface Settlements over the Mississauga Sewer Tunnel

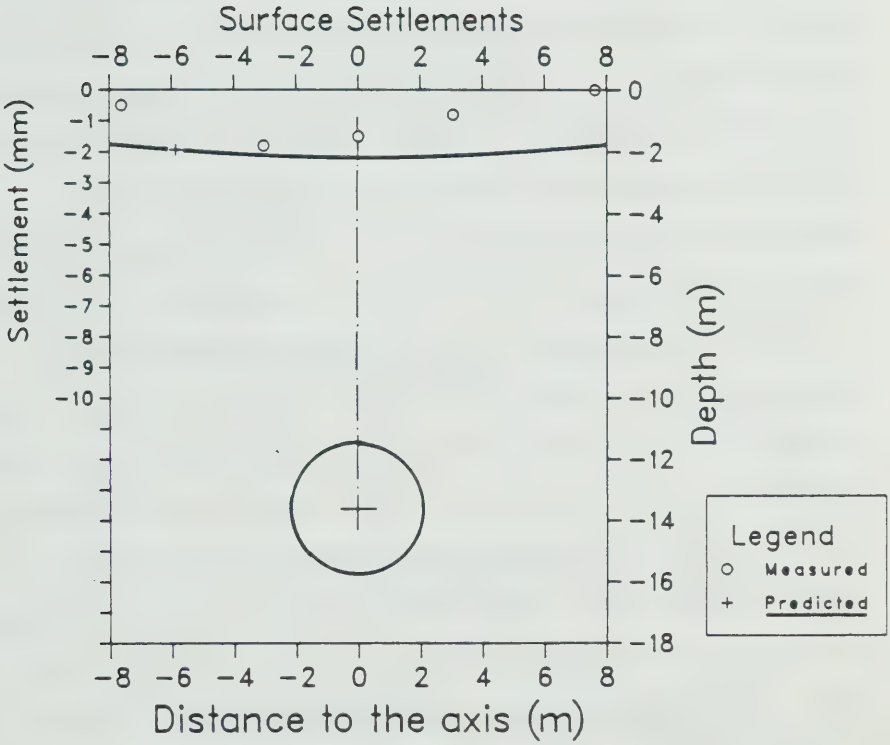

NOTE: MEASUREMENTS PRESENTED BY DELORY ET AL (1979:194)

Figure 7.35 Measured and Calculated Final Surface Settlements over the Mississauga Sewer Tunnel

calculations.

The predicted distribution of radial stress acting upon the lining is shown in Figure 7.36. The measured radial stresses, also shown in this figure, were recorded by 250 mm diameter flat contact cell pressures, installed between the primary lining and the ground. The cells were placed in the void behind the lining and were packed on each face with a soil-bentonite-cement mixture, to fill the space between the soil and support. The mixture was designed to have mechanical properties similar to the surrounding till. Twelve cells were used but one at springline (270°) ceased to operate some time after installation. Four of them installed in the upper arch (three at the crown and one at 45° off) seem to have had faulty installation. As explained by DeLory et.al. (1979:195), "the cells near the crown acted as hard spots taking more than their share of the load". In fact, stresses more than 100% in excess of the overburden stress were recorded in these four cells. Their results are, thus, unreliable and therefore not included in Figure 7.36. The measurements indicated correspond to final long term readings, one year after installation, although they do not differ to any substantial degree, from the short term readings taken a few weeks after the cells were installed (DeLory et.al., Op.cit.:195).

A substantial scatter in the cell pressure measurements is noted, possibly reflecting the effects of the installation procedure adopted. However, if an average

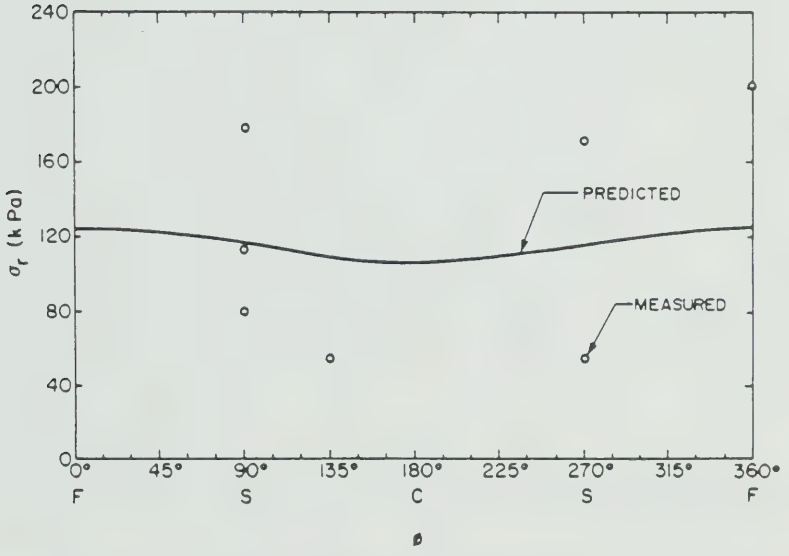

NOTE: LONG TERM MEASUREMENTS BY DE LORY ET AL (1979 [196]). DATA FROM FIVE FAULTY CELLS WERE EXCLUDED.

Figure 7.36 Measured and Predicted Radial Stress Distributions on the Lining of the Mississauga Sewer Tunnel

distribution of radial stresses were to be defined, it would not lie far from the predicted distribution.

A slope indicator was installed at 0.91 m away from the tunnel springline. DeLory et.al., (Op.cit.:Figure 3), presented a plot of radial movements in the ground, at the springline elevation, with tunnel advance. If an average curve is fitted through the points shown in that plot and if the displacements are extrapolated to the tunnel contour following the procedure used in Section 5.3.6.1, one would find that, at the point of lining activation, the radial closure at the springline would have been equal to 6 mm and equal to 7.5 mm at final equilibrium. These values are to be compared with the calculated closures of 6.3 and 7.4 mm respectively. The total increase of about 2.3 mm in the horizontal lining diameter, after its activation (i.e., after grouting), is in agreement with the convergence measurements taken in the field (DeLory et.al. Op.cit.:193).

7.5.3.5 A Large NATM Tunnel in Granular Soil: The Butterberg Tunnel, in Osterode, near Hannover

This case history refers to a large road tunnel built in 1977-1979 in Osterode, about 50 km southeast from Hannover (Germany), that was described by Duddeck et.al., (1979 and 1981). The initial portion of the job, completed earlier in 1975-1976, served as a test tunnel designed to supply information on tunnelling performance for the main tunnel. The investigations carried out in this experimental length were reported by Meister and Wallner (1977). The

tunnel had a non-circular profile of 10.11 m high and 11.70 m wide. The area of excavatiion was about 100 m^3/m, corresponding to an equivalent diameter of 11.5 m. At the main instrumented section the ground cover was 13.6 m.

The ground profile at the instrumented section included a thick Quaternary terrace deposit (Pleistocene Epoch) consisting of a well graded sandy-silty gravel (GM) with a of silt component of 10% and with boulders of diameters up to 1 m. The tunnel, at this section, was entirely driven through this granular soil. Underneath it, some 12 m below the tunnel floor, there was a limestone bedrock. The groundwater level was not identified by the exploratory boreholes drilled down below the tunnel floor. Some local seepage was detected at the portal region, associated with rainfall infiltration. Otherwise the quaternary deposit was water free.

Laboratory and in situ direct shear tests were conducted on the granular soil and showed that the effective shear strength parameters were $c'=20$ kPa and $\phi'=33°$. This soil showed some strength loss after peak, with residual values given by $c'_r=5$ kPa and $\phi'_r=30°$. The soil deformation behaviour was investigated by plate bearing tests in test pits and inside the tunnel. From these tests, an average constrained modulus for the 'intact' material of 330 MPa was estimated (Duddeck et.al., 1979:208). For a Poisson's ratio of 0.3, a Young's modulus of 245 MPa is found for this soil at a depth of about 24 m. If that value is taken as the in

situ tangent modulus, and if it is assumed to be proportional to the square root of the vertical effective stress, in situ moduli of 141 MPa, 217 MPa and 279 MPa are estimated at points located half a diameter above the tunnel crown, at the springline elevation and half a diameter below the tunnel floor, respectively.

The failure ratio (R_f) for this material is not known, but results from triaxial tests on similar materials when compacted (Duncan et.al., 1980), suggest that R_f should be close to 0.7. The unit weight of this soil is 22 kN/m^3 and an in situ stress ratio of 0.5 was suggested by Duddeck et.al. (1979:208). A drained analysis is justified for this case, and the corresponding parameters adopted are summarized in Table 7.8. Peak strength parameters are assumed on the grounds that the soil around the opening was not strained to failure.

The tunnel construction was carried out with the segmented excavation of the face in stages: heading, bench and invert. The bench and invert excavations were undertaken in steps, in such a way that a central core was always left supporting the tunnel face (see Figure 7.37). The heading was advanced in two successive rounds of one metre each. This was followed by a 2 m advance of the bench, floor excavation following this in 4 m sections. An average rate of advance of 2 m/day was maintained during construction. The excavation at the crown was carried out under the protection of short forepoling (1.3 m long).

				(1)
Unit weight		γ	kN/m^3	22
In situ stress ratio		K_o	-	0.5
Effective cohesion intercept		c'	kPa	20 (2)
Effective friction angle		ϕ'	(°)	33 (2)
Failure ratio		R_f	-	0.7 (3)
E_{t_i} (drained)	1/2 D above crown		MPa	141 (4)
	at springline		MPa	217 (4)
	1/2 D below floor		MPa	279 (4)
Poisson's ratio		μ	-	0.3

Notes: (1) Average values provided by Duddeck et al (1979:208).

(2) Peak strength parameter.

(3) Estimated.

(4) Derived from the average constrained modulus from plate bearing tests by Duddeck et al (Op.cit).

Table 7.8 Selected Ground Parameters for Analysis of Tunnel in Well-Graded Sandy-Silty Gravel

The primary lining consisted of a shotcrete layer 30 cm thick, steel wire mesh and light steel ribs at 1 m spacing (GI profile, 130 mm high, 37 kg/m in the instrumented tunnel length). Steel ribs were not installed at tunnel invert. At the instrumented section, the shotcrete ring closure at the floor took place when the face was 9.5 m past the section. This was the distance between the middle point of the shotcrete section at the invert and the heading face (Duddeck et.al., 1979:Figure 16).

A very careful construction procedure was undertaken. The two dimensional ground stability verification at lining closure, furnished a factor of about 1.21, which is, in fact, slightly low. However, no ground instability was observed during construction. Such a low factor of safety may indicate that some shear stress concentration in the ground might have happened. If this is so, the development of some shear dilatancy in this fairly dense granular soil could be expected. The proposed design procedure does not take into account this type of ground response, as well as the effects of some strain weakening that might have also developed around the opening, possibly at the tunnel shoulders. Notwithstanding this, the analysis was carried out neglecting such likely occurrences.

An adjusted friction angle of 41.5° was calculated on account of the cohesive strength component and of the failure ratio different from unity. At lining closure (0.826 D behind the face), the amount of stress release was about

64% and a reduced tangent ground modulus of 115.82 MPa was calculated (46% less than the original average value). In these calculations, the generalized λ and λ' curves for K_o=0.6 were used for simplicity and to avoid the need of extrapolating the numerical results for the selected in situ stress ratio. At lining closure, the U/U_{ref} values for the crown and the springline did not exceed the limits of the fitted solutions. For the floor, however, it was necessary to use the solutions beyond their formal limits.

The lining-ground interaction analysis was carried out neglecting the contribution of the light steel ribs and the shotcrete reinforcement. A lining modulus of 10 GPa was considered, as well as a Poisson's ratio of 0.2. These are the same parameters used for the Romerberg Tunnel (Section 7.5.3.3). Meister and Wallner (1977:930) also used this Young's modulus for the lining in their numerical analysis of this case history. Four iterations, in which the ground heave after support activation was neglected, were needed to obtain the equilibrium condition. An average ground modulus of 144.78 MPa was found for this condition which was higher than that found at lining closure. This modulus increase resulted from the mode of deformation where the lining squatted and pushed the soil outwards at the springline region. The radial confinement increase in this area caused the soil to become locally stiffer and this led to an increase in the average ground modulus, which at equilibrium, was now only 32% lower than the in situ average

value. For this condition, the flexibility (β) and compressibility (α) ratios were found to be about 5 and 0.0012, which are typical for shotcrete linings in dense sand (See Table 7.1).

The final crown settlement was estimated as 22.1 mm (U=0.906) and the associated amount of stress release at the crown was about 70%. The resulting distributions of subsurface and surface settlements were calculated for K_o=0.6 and ϕ=40°, which are not far from the values which that should actually have been considered. An inevitable numerical extrapolation was required regarding the normalized settlements, with respect to the cover to diameter ratio. In this case study, this ratio was equal to 1.183, whereas the parametric numerical results (Appendix C) furnishes distributions for H/D=1.5 and 3.0. A linear extrapolation was made, and the distributions obtained are those shown in Figures 7.37 and 7.38. Included in these figures are the settlements measured in the instrumented section MS3 (Duddeck et.al., 1979:214).

From Figure 7.37, one notes that, although a reasonable agreement was obtained between predictions and measurements, the proposed method underestimated the ground movements close to the tunnel. One could speculate that this is due to the unaccounted for influence of the volumetric expansion of the soil above the tunnel (see Figure 2.9, d and e). Plastic dilation in the ground is known to increase the tunnel convergence, for a given amount of stress release (e.g.,

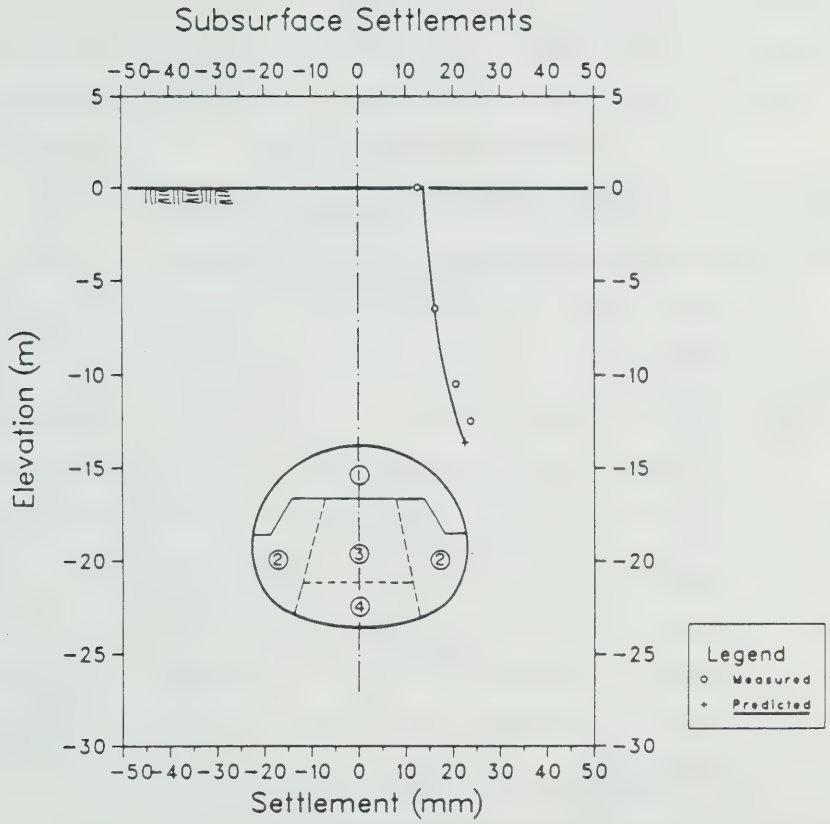

NOTE · MEASUREMENTS AT SECTION MS3, BY DUDDECK ET AL (1979 : 214)

Figure 7.37 Measured and Calculated Final Subsurface Settlements over the Butterberg Tunnel

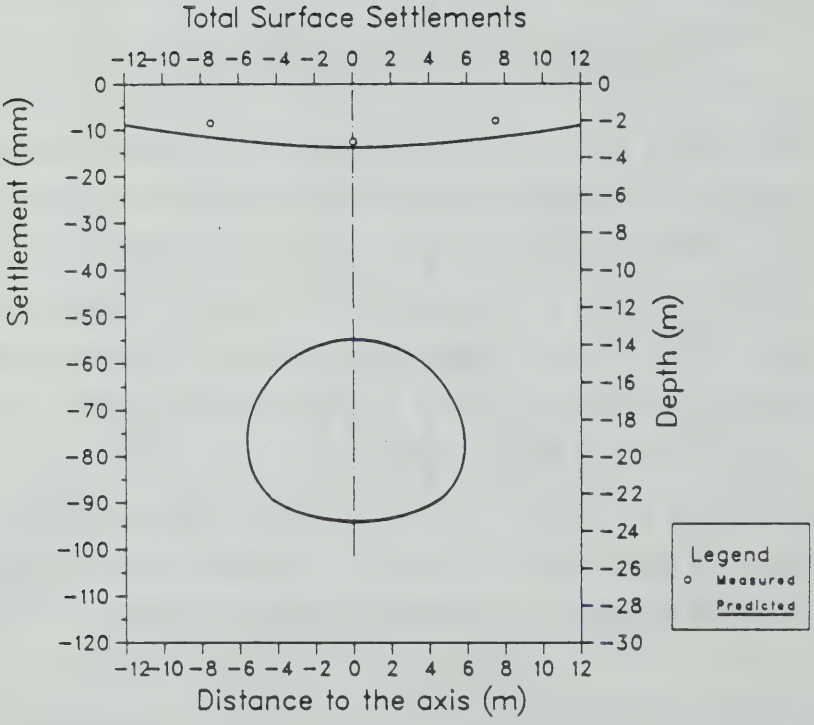

Figure 7.38 Measured and Calculated Final Surface Settlements over the Butterberg Tunnel

Lombardi, 1973, Ladanyi, 1974). The non-circular shape of the tunnel cross section could also be evoked to explain the underestimation of the crown displacements. From Figure 7.38, one notes that the magnitude of the maximum surface settlement observed at surface, was reasonably estimated by the proposed method, but once more the distortions were underestimated.

Predicted and measured radial stress onto the lining are shown in Figure 7.39. The measurements were taken with Maihak pressure cells (Duddeck et.al., 1981:181), but details of their installation were not given. One set of measurements was taken in the experimental tunnel length, while the other was taken during the main tunnel construction under similar conditions. One notes that the shapes of the predicted and measured stress distributions show some sort of broad agreement. However, the predicted stresses are typically twice the stresses measured. Although, it was shown that the proposed method may tend to slightly overestimate the final lining loads (see Section 7.2.2), this fact does not explain the result obtained in this case. Had a smaller shotcrete modulus been assumed a slightly better agreement could have been obtained. A smaller modulus would imply, however, a poorer agreement regarding the lining convergence results. A horizontal diameter increase of 3.96 mm was measured in the field (Duddeck et.al., 1981:180) after the shotcrete ring closure. The predicted increase in the horizontal diameter was 3.74

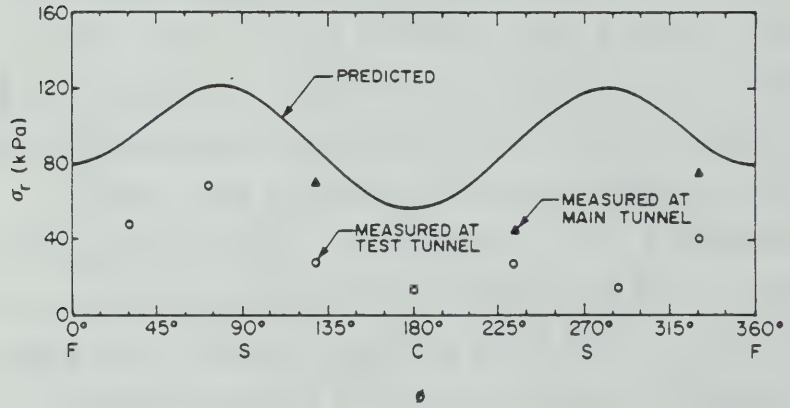

NOTE: MEASUREMENTS BY DUDDECK ET AL (1979: 213 AND 215)

Figure 7.39 Measured and Predicted Radial Stress Distributions on the Shotcrete Lining of the Butterberg Tunnel

mm, which agrees very well with the observed value. Had a 'softer' lining been considered, this agreement would not have been so good.

7.5.3.6 A Large Shield in Till: The Edmonton LRT Tunnel

This case history was described in detail in Section 5.2.4.3, where it was back analysed through the two dimensional finite element model presented in Chapter 5. Basically, the same parameters used in the best fit case were considered in the present analysis.

The tunnel was driven with a 6.172 m diameter under an 8.9 m cover of soil. A uniform till layer was considered with a friction angle of 40° and zero cohesion (R_f=1). For an in situ stress ratio of 0.75, in situ tangent moduli of 45.35 MPa, 65.18 MPa and 80.22 MPa were calculated, at points half a diameter above the crown, at the springline elevation and half a diameter below the tunnel floor, respectively.

Assuming that the lining was activated at one diameter behind the tunnel face, the amount of stress release immediately before liner installation could be calculated. To avoid data interpolation, the λ curve for K_o=0.8 was used for this purpose. The average stress release was about 60% and a reduction of about 43% in the ground modulus was found. The former value is higher than that found in the back analysis presented in Section 5.2.4.3 (50%), which results from the approximation above and from others which are built into the proposed calculation procedure. The two

dimensional ground stability verification at the section the lining was activated furnished a factor of safety of 1.35.

In shielded driven tunnels, it is convenient to check if the soil stood up over the TBM body, in order to assess if the assumed distance between the tunnel face and the section of lining activation is correct. This verification could not be performed in the Domplatz and in the Mississauga tunnel cases, since no information was available regarding the amount of overcutting used. In the LRT tunnel, the ground was bored with a diameter 19 mm larger than the outer diameter of the TBM body (Branco, 1981:23).

By using the approximate solution for tunnel closure presented in Section 5.3.5.2 and the in situ ground moduli estimated earlier, one can calculate the increments of radial displacement at the crown and floor, from the tunnel face to the shield tail. The latter extended to 5.5 m behind the face (0.89D). From this, one finds that the vertical diameter of the bored opening reduced by 14.5 mm from the face to shield tail. This value is less than the clearance provided by the overcutting (19 mm). The reduction in the horizontal diameter was also less than the above clearance. Therefore, one could say that the soil did not close over the shield body. This, in fact, happened whenever the tunnel was bored through uniform till. In some locations, however, (see Section 2.3.5.4), sand pockets were cut at the crown and localized instabilities were observed. Some soil ran into the unsupported heading, over the cutting wheel, and

some soil blocks may have rested over the TBM. But the remainig till mass, otherwise stable, did not come in contact with the TBM body. In other words, in the present case, it is valid to assume that the opening was virtually unsupported until the lining left the shield and was expanded against the opening profile, about one diameter behind the tunnel face.

For the lining-ground interaction analysis, it was assumed that the wooden lagging did not contribute to the lining stiffness. Its action was, thus, limited to longitudinally transferring the ground loads to the steel ribs (E_s=200 GPa, μ_s=0.2, I_s=1.82 x 10^{-5} m^4/m) at 1.22 m spacing. Two iterations were needed to find the equilibrium condition, which yielded an average ground modulus of 34.85 MPa, and relative flexibility (β) and compressibility ($\dot{a}$) lining ratios of 0.0055 and 10.74, respectively (typical for this type of support in stiff clays or medium sands).

The final crown settlement was calculated as 17.5 mm (U=0.754) and the associated amount of ground stress release at the crown was about 65%. The final subsurface settlements could not be measured in this case history, since the magnetic extensometer installed at the tunnel axis was lost when the TBM reached the instrumented section (Branco, 1981:77, 110). Accordingly, only the final surface settlements were calculated and are compared to the measurements in Figure 7.40. Note, however, that while the settlements were measured at points located 3 m below the

surface, the calculated movements refer to points on the actual ground surface. If the calculation method allowed the estimate of settlement distributions in horizontal planes below the surface, a better agreement with the observations would have been found, with a larger maximum displacement and a narrower settlement trough. In fact, the settlement at the tunnel axis, 3 m below surface, was calculated as 9.7 mm, while the actually measured settlement was 9.65 mm. Nevertheless, the agreement between calculations and measurements is reasonable, although it is again noted that the proposed procedure tends to underestimate the ground distortions.

The calculated thrust forces in the steel ribs are shown in Figure 7.41. Thrust forces were measured at rib joints by loads cells, as decribed in Section 5.2.4.3. Note that the calculated and measured thrusts have been reduced for the tunnel unit length, on a 1.22 m rib spacing basis. Note also that the lining self weight was discounted from the readings. The predicted thrusts seem to very closely bound the long term load cell measurements (taken 293 days after installation), while the short term reading (16 days, tunnel face 36.4 m ahead of the instruments) tend to lie below the calculated levels.

In general terms, the tunnel performance predicted herein, agrees well with the back calculated tunnel performance presented in Section 5.2.4.3 using the two dimensional finite element method, as well as with the field

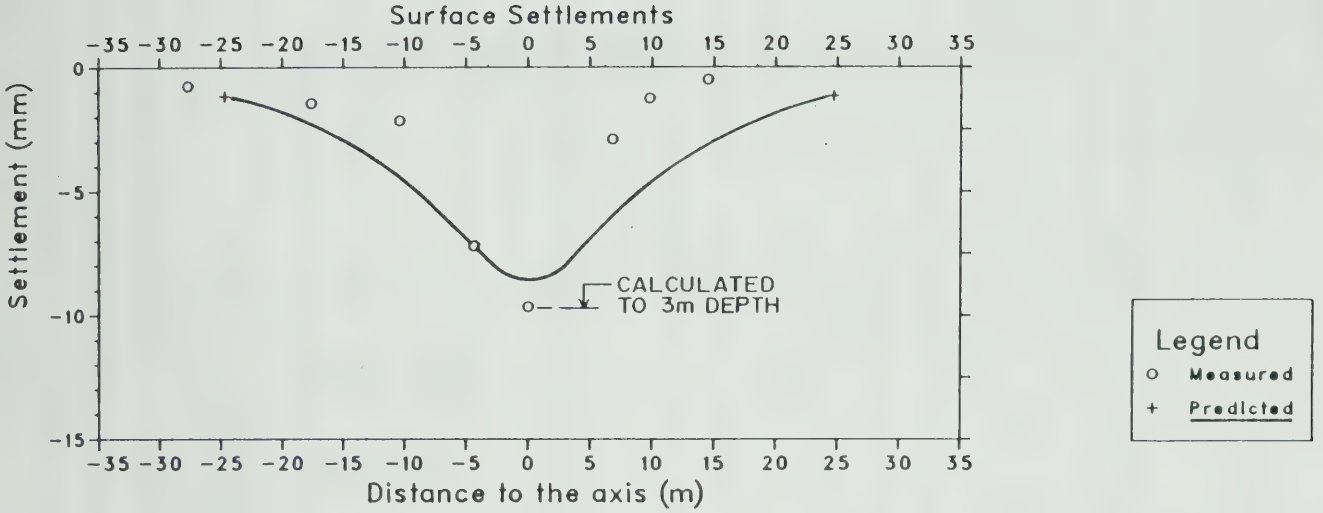

NOTES:

1. MEASUREMENTS TAKEN AT POINTS 3m BELOW SURFACE. CALCULATED SETTLEMENTS AT GROUND SURFACE.
2. FIELD DATA FROM BRANCO (1981:67). READINGS TAKEN WHEN THE TUNNEL FACE WAS 37.6m BEYOND THE INSTRUMENTED SECTION.

Figure 7.40 Measured and Calculated Final Surface Settlements over the Edmonton LRT Tunnel

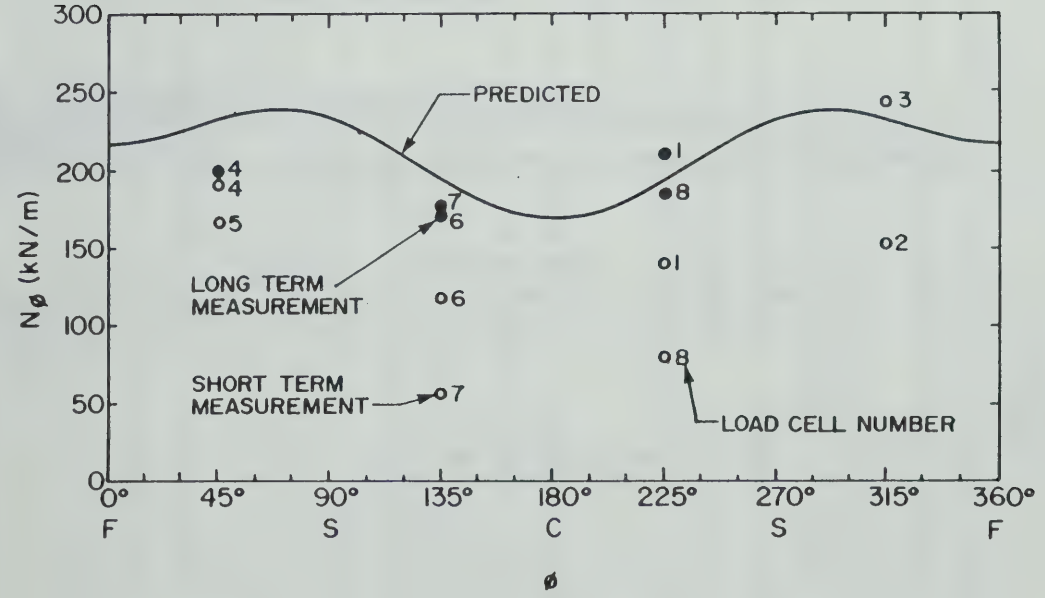

NOTES:
1. FIELD DATA FROM BRANCO (1981:156) AND FROM EISENSTEIN ET AL (1983)
2. SEE OTHER NOTES IN FIG. 5.34

Figure 7.41 Measured and Calculated Thrust Forces on the Edmonton LRT Primary Lining

measurements.

7.5.3.7 An NATM Tunnel in Marl: The Munich U - Bahn - Line 8/1, Baulos 18.2

This case study refers to a subway tunnel built in 1975-1976 in Munich (W. Germany), that was described by Laabmayr and Pacher (1978) and Laabmayr and Weber (1978). Two parallel tunnels were driven consecutively, each one with a near circular cross section, 6.98 m high and 6.32 m wide. The area of excavation of each tunnel was 37.50 m^3/m, corresponding to an equilvalent diameter of 6.91 m. At the instrumented section (MQ4), under the Mathilde Covent (by Mathildenstrasse), the ground cover was 22 m and the tunnels were driven almost 19 m apart (centre to centre), i.e., with a central pillar width of almost 2 diameters. The analysis and instrumentation results to be discussed refer to the first tunnel driven only.

The geological and geotechnical conditions found in Munich, and especially at the site were described by Laabmayr and Pacher (1978), Gebhardt (1980) and Krischke and Weber (1981) and were summarized by Steiner et.al., (1980) and Heinz (1984:267). At the instrumented section, the subsurface profile included a 10 m thick superficial layer of quaternary sands and gravels, underlain by a 7 m thick layer of tertiary dense sand rich in mica (Flinzsande). Below this layer, there was a thick layer of stiff to hard calcareous clay marl (Flinzmergel), also from the Tertiary, which is locally intercepted by other tertiary sand layers.

A perched water table was found at about 15 m below surface, within the upper tertiary sand layer. The other sands layers, within the marl, were found to be saturated and under pressure. A deep dewatering system was installed and operated for more than three months before tunnel construction commenced. The ground settlements due to dewatering had been completely stabilized before the tunnel was driven through the stiff marl, and, during excavation, the ground was found to be almost water-free. A drained analysis could, thus, be considered.

It will be assumed that the ground response was controlled mainly by the marl, although the tunnel cross section was intercepted by a tertiary sand layer between the haunches and the floor. The geotechnical properties of the marl summarized by Steiner et.al. (1980:170) and by Krischke and Weber (1981:11) were used as a basis for the definition of the input parameters for the present analysis (see Table 7.9). A coefficient of earth pressure at rest slightly higher than that suggested by these authors (0.8) has been assumed, perhaps more consistent with the higher overconsolidation of this soil, compared with the Frankfurt marl. No indications were found regarding the variation of the deformation modulus of the Flinzmergel with depth. Accordingly, a constant initial tangent modulus was assumed, corresponding to the upper bound value given by those authors. Since no information was provided regarding the failure ratio, the same R_f used for the Frankfurt marl was

Unit weight	γ	kN/m^3	21
In situ stress ratio	K_o	-	1.0
Effective cohesion intercept	c'	kPa	40
Effective friction angle	ϕ'	(°)	25°
Failure ratio	R_f	-	0.8(2)
Initial tangent modulus	E_{t_i}	MPa	200
Poisson's ratio	μ	-	0.25

Notes: (1) Parameters based on data published by Steiner et al (1980:170) and Krischke and Weber (1981:111).
(2) Assumed equal to that for the Frankfurt marl.

Table 7.9 Selected Parameters for Munich Marl

adopted herein.

The tunnel construction was carried out with the sequential excavation of the face in three stages, heading, bench and invert, with immediate application of shotcrete over the exposed ground. The rate of advance when the tunnel face passed the instrumented section was about 4 m/day. The excavation round length was 1 m at the heading and bench, and 2 m at the invert. The primary lining also included horseshoe shaped segmented steel ribs with a channel profile (TH 21/58), at one metre spacing, which were not closed at the floor. The shotcrete total thickness was 16 cm from crown to haunches, and was increased to 20 cm in the invert. The support ring was closed, at the instrumented section, 7 m behind the face (Laabmayr and Weber, 1978:89). Similarly to the Romerberg Tunnel in Frankfurt, ground anchors were also installed here, but again, their effectiveness in controlling the ground behaviour was questioned (Laabmayr and Weber, Op.cit.:82).

The tunnel construction was undertaken under good ground control conditions, wtih no ground instabilities being reported.

An adjusted friction angle of 31° was calculated. At lining activation the amount of stress release resulted was about 51% and the average ground modulus was 97.69 MPa, which corresponds to a 51% decrease from the in situ value. The 2D ground stability verification at lining closure furnished a factor of safety of 1.91.

The lining-ground interaction analysis was carried out neglecting the action of the steel ribs, and considering a shotcrete lining 0.16 m thick, with a modulus of 10 GPa and a Poisson's ratio 0.2. Two iterations were needed to define the equilibrium condition, neglecting the ground heave after the support was activated. A ground tangent modulus of 79.82 MPa was found at equilibrium, from which flexibility and compressibility ratios of 0.0015 and 7.73 were calculated, respectively.

A final crown settlement of about 9.9 mm was calculated (U=0.616), for which a stress release of about 55% resulted at tunnel crown. At the instrumented section, the surface settlement profile could not be determined due to interference from existing constructions. The ground movements were measured only at two points, as shown in Figure 7.42. Here, only those movements observed during tunnel construction are considered: the displacements due to dewatering were discounted. Figure 7.42 shows also the calculated final subsurface settlement distribution. It seems to agree with the sparse field data available.

Figure 7.43 presents the calculated and measured radial stresses acting around the lining contour. The stresses were measured by Glotzl contact pressure cells and they correspond to the final readings, taken 7 months after the instruments were installed. The measurements indicated some load increase with time. It is not known when the second tunnel was built and therefore, it is not known if these

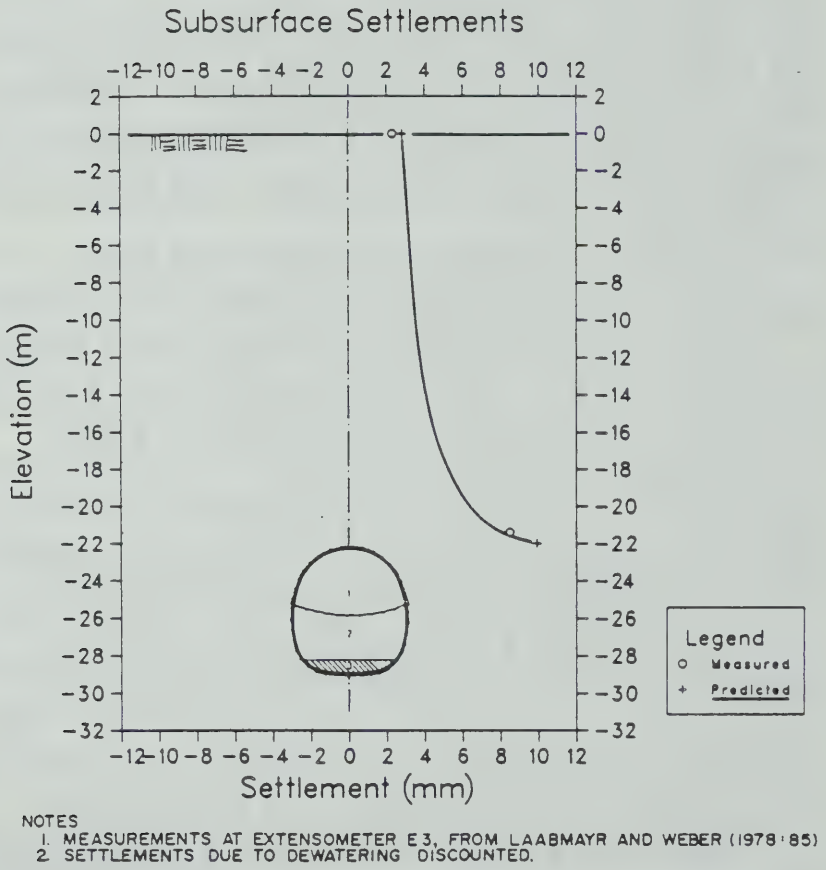

Figure 7.42 Measured and Calculated Final Subsurface Settlements over the Munich Line 8/1 Tunnel

readings were affected by the parallel tunnel construction. If they were, the effect may have not been very pronounced as the second tunnel was built almost three diameters apart from the first one. A substantial scatter was observed in the field data. The predicted stresses tend to bound the measurements.

No convergence measurements were reported at the instrumented section MQ4. However, they were taken at another section (MQ1), some 400 m from MQ4, where not much dissimilar conditions were encountered (Laabmayr and Weber, Op.cit.:81). A fairly uniform lining closure was observed, confirming the in situ stress ratio adopted in the analysis. Horizontal diameter decreases of up to 2.3 to 3.9 mm after the shotcrete ring closure at the floor, were measured at two different convergence bases (H1 and H2). These values compare well with the 3.2 mm horizontal diameter reduction predicted in the lining-ground interaction analysis.

7.5.3.8 An NATM Tunnel Built under Compressed Air: The Munich U-Bahn-Line 5/9, Baulos 7

The present case history refers to a subway tunnel built in the early eighties in Munich (W. Germany), that was described by Baumann et.al. (1985). It represented one of the first experiences in using shotcrete combined with compressed air (Weber, 1984).

Two parallel tunnels were driven consecutively, each one with a near circular cross section, 7.0 m high and 6.5 m wide. The excavation area of each tunnel was 38 m^3/m, which

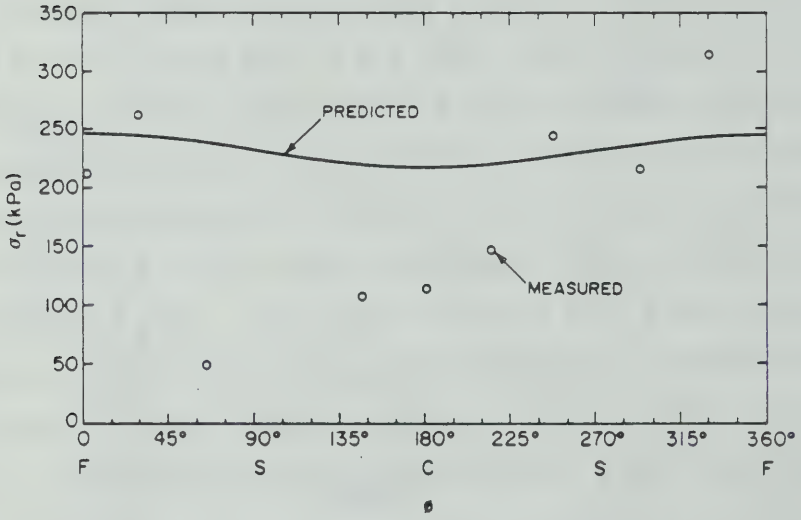

NOTE: MEASURED AT MQ4, TAKEN 7 MONTHS AFTER INSTALLATION (LAABMAYR AND WEBER, 1978: 87)

Figure 7.43 Calculated and Measured Radial Stress Distributions on the Shotcrete Lining of the Munich Line 8/1 Tunnel

corresponds to an equivalent diameter of 6.95 m. At the instrumented section MQ7, located West of the Maximilianeum, not far from the Isar River bank, the ground cover was 20 m and the tunnels were driven about 13 m apart (centre to centre), leaving a central pillar of slightly less than one diameter between the two tunnels. The analysis and instrumentation results to be presented refer to the first tunnel driven only. The second tunnel passed the instrumented section MQ7 4 months after the first tunnel had passed it.

The geological and geotechnical conditions found at this site are similar to that described in Section 7.5.3.7. At the instrumented section, the subsurface profile included a 4.5 m thick superficial layer of quaternary sands and gravels, underlain by a thin marl layer (2.5 m thick). Below it, a 10 m layer of fine to medium dense tertiary sand was found. Underlying this, a thick layer of stiff to hard tertiary marl was encountered, through which the tunnel was driven. The marl cover above the crown was slightly less than half tunnel diameter. At floor elevation the marl was cut by a metre thick sand layer.

A perched water table was found at the quaternary granular soil. Another one was found 15 m below the surface within the thick sand layer. The thinner sand layer below the tunnel was also saturated and under pressure. A compressed air pressure of 60 kPa was used in this section.

For the analysis, it was assumed that the ground response at the crown was controlled by the stiffness of the sand layer located above the tunnel, with an in situ drained modulus estimated as 144 MPa from data presented by Krischke and Weber (1981:111). For the springline and floor, a tangent modulus of 200 MPa was assumed for the stiff marl, as for the U-Bahn-Line 8/1.

Based on data from Krischke and Weber (1981:111) and Steiner et.al., (1980:170), the coefficient of consolidation of the marl was estimated as 2×10^{-2} cm²/s. The likely ground response in terms of pore pressure development, can be estimated through the tentative criterion proposed in Section 3.3.4.5. If the pore pressure changes in the 3 m marl cover were solely caused by the change in the hydraulic boundary condition at the tunnel contour, one could use the criterion given in Figure 3.23. It would then be found that over one week, the marl cover would experience partial consolidation, but over a time span of a month, appreciable consolidation (more than 90%) would have developed. If an average rate of advance of 3 m/day is admitted (Weber, 1984:26), then the 'short term' ground response, corresponding typically to an advance of the face from a section, say, 2D behind the instrumented section, to a point 4D past this section, would take place in a two week time interval. The 'short term' response would thus involve some amount of ground consolidation, and could not be defined as 'undrained'. Accordingly, a drained analysis was favoured,

and the same 'drained' parameters used for the Munich 'Flinzmergel' in Section 7.5.3.7, were adopted presently.

The tunnel construction was similar to that used in the U-Bahn-Line 8/1, except that here the shotcrete ring was closed at a shorter distance from the heading face (5.5 m typically). The minimum shotcrete thickness used was 15 cm, and at some locations it was increased to 18 cm. A single steel mesh (Q188) was laid on the inner side of the shotcrete lining. Lattice girders at one metre spacing were installed instead of steel ribs.

The tunnel construction was carried out under good ground control conditions, and no ground instabilities were reported.

An adjusted friction angle of 31.2° was calculated on account of the cohesive strength component and of the failure ratio equal to 0.8. In calculating the tunnel closure at the instant of lining activation (0.8D behind the face), allowance had to be made regarding the compressed air pressure being applied. To take it approximately into account, the in situ radial stresses at crown, springline and floor were reduced by 60 kPa, the magnitude of the air pressure. This approach was used earlier by Deere et.al. (1969:87). This is equivalent to reducing the soil cover depth by 2.9 m (for a soil unit weight of 21 kN/m^3). In so doing, the amount of stress release at lining activation was about 49% and the mean ground modulus was 95.03 MPa. The latter corresponded to about a 49% decrease of the original

in situ ground modulus. The 2D ground stability verification of lining closure furnished a factor of safety of 2.01.

The lining-ground interaction analysis was carried out neglecting the action of the steel mesh or of the lattice girders. A nominal 16 cm thickness for the lining was considered. As on other occasions, a shotcrete modulus of 10 GPa and a Poisson's ratio of 0.2 were assumed. Two iterations were required to define the equilibrium condition, neglecting the ground heave after support activation. A tangent modulus of 80.18 MPa was found for the ground at equilibrium (about 43% if the in situ value). Flexibility and compressibility ratios of 0.0014 and 7.67 were calculated, respectively.

A final crown settlement of 10.05 mm was calculated (U=0.578), which corresponds to about 52% of the stress release at the tunnel crown. The field instrumentation at section MQ7 did not include the measurement of the subsurface settlements along the tunnel vertical axis. Only surface settlements were measured, as indicated in Figure 7.44. Two measured profiles are indicated, one corresponding to a 'short term' condition (10 days after the face passed the section) and another corresponding to a 'long term' condition (140 days after passage, immediately prior to the second tunnel drivage). Both at the short or long term conditions, the tunnel was being submitted to the same compressed air pressure. The calculated settlement profile is included in Figure 7.44 and one notes that it agrees

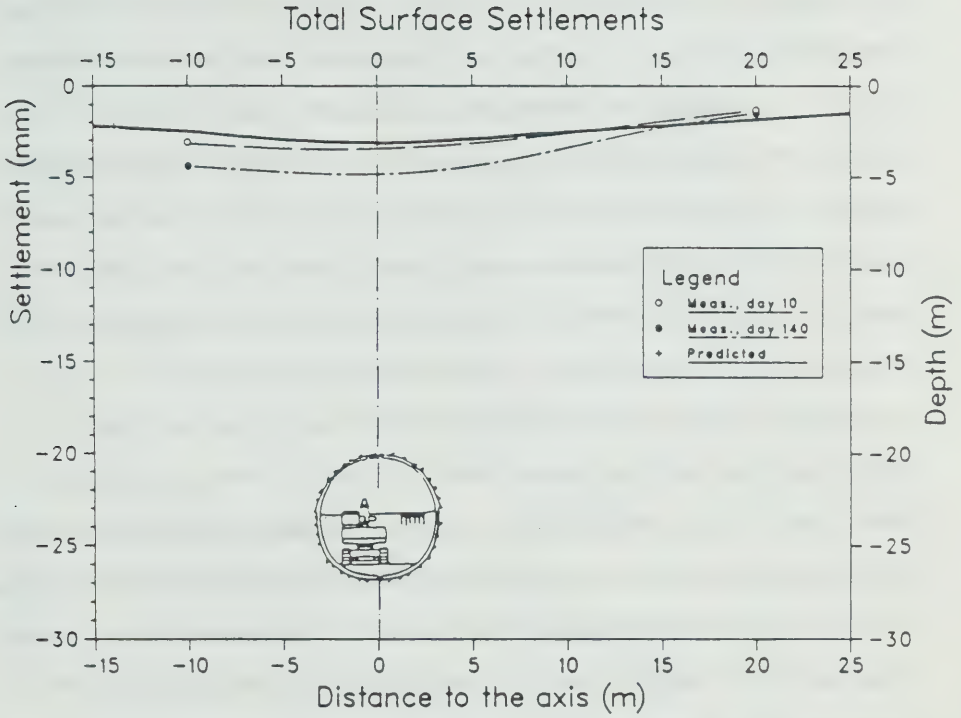

NOTE: MEASUREMENTS AT SECTION MQ7, DATA FROM BAUMANN ET AL (1985: 336)

Figure 7.44 Measured and Calculated Surface Settlements over the Munich Line 5/9 Tunnel

roughly well with the 'short term' profile. This agreement, however, may be claimed as fortuitous, since there is not a complete correspondence between the 'partial consolidation' condition, that may have actually developed in the short term, and the completely drained behaviour (with "zero" pore pressures) assumed in the calculations. On the other hand, it is not unexpected that the measured 'long term' settlements are larger than those calculated. The proposed calculation method does not take into account the ground volume changes and associated consolidation settlements resulting from porewater pressure changes and ground water drainage into the tunnel (see Section 3.3.4.2).

The tunnel convergence was also measured at the instrumented section. Reference points at the springline were installed right at the face, so that the changes in the horizontal tunnel diameter before and after shotcreting the invert could be observed. The radial displacements at the face were calculated using the approximate solution presented in Section 5.3.5.2. The reduction in the horizontal diameter, from a section at the face to the section where the shotcrete lining ring was closed, was thus calculated to be 9.36 mm. This compares favourably with the 10 mm reported by Baumann et.al. (1985:336). After closure of the shotcrete ring, the lining-ground interaction analysis furnished an additional reduction in the horizontal diameter of 2.66 mm, which also agrees well with the 2.5 mm measured.

Specially designed load cells were installed to measure thrust forces and bending moments in the shotcrete lining (Baumann et.al., 1985:450). The measuring system was developed by Philipp Holzmann AG Munchen. Details of this patented measuring gauge were not disclosed. Apparently it consisted of a 2 m long, 0.2 m high and 0.12 m wide steel box, installed at the lining haunches and shoulders, and interrupted the whole shotcrete lining thickness. It is not clear how the system measured the bending moment (or normal force eccentricities). The calculated thrust forces exceeded the forces actually measured both in the short and the long term. As noted in Section 2.3.6.3, a non-uniform thrust force distribution was observed, along the 2 m long embedded gauge. For a given position of the face, the highest thrust force was recorded at the cell end closer to the face. The measured values indicated in Table 7.10 correspond to the mean values provided by Baumann et.al. (1985:336). The eccentricities measured ranged between 1 and 3 cm, while those calculated were one order of magnitude smaller (about 0.06 cm). That could be an indication that the in situ stress ratio is not equal to one, as assumed. But this would be conflicting with the mode of lining deformation, which was well estimated by the calculations. Nothing further can be advanced, as the reliability of these measurements cannot be assessed due to the paucity of the information made available.

Performance aspect	Unit	Calculated	Measured	
			Short Term(2)	Long Term(2)
1. Maximum surface settlement	mm	3.00	3.45	4.9
2. Horizontal diameter change from face to the section the support ring is closed	mm	9.36	10.0	-
3. Final horizontal diameter change of shotcrete lining after invert closure	mm	2.66	-	2.50
4. Thrust force at haunches (45°)	kN/m	693	476	550
5. Thrust force at shoulders (135°)	kN/m	617	305	400

Notes: (1) Measurements at Section MQ7. Data from Baumann et al (1985:336).

(2) Short term: 10 days after the tunnel face passed the section. Long term: 140 days after passage.

Table 7.10 Measured and Calculated Performances at the Munich Line 5/9 Tunnel

7.5.3.9 An NATM Tunnel Driven Through Heterogeneous Ground: The Bochum Baulos A2 Double Track Subway Tunnel

This case history refers to a double track subway tunnel that was described by Jagsch et.al. (1974), by Hofmann (1976) and reviewed by Heinz (1984:69). It was built in 1973 in Bochum (W. Germany) and was one of the first NATM cases with large cross-sectional area built in an urban environment.

The tunnel cross section was non-circular being 8.3 m high and 10.1 m high. It had an excavation area of 64 m^2/m, which corresponds to an equivalent diameter of 9.03 m. At the instrumented section MQI, the ground cover was 12.2 m.

A fairly heterogeneous subsurface profile was found at this site. It included a 7 m thick superficial fill layer, which was the embankment of an existing railway line. Below it there was a sloping layer of a fairly hard chalk-marl about 7 m thick at the tunnel axis. Underlying this, there was a softer sandy-marl, 4 m thick, that rested over a succession of sandstone, shale and coal. The ground water level lay below the tunnel floor. A mixed face condition was thus encountered, with a stiffer marl at crown, a softer marl down below the springline and sedimentary rocks at the floor.

Wittke and Gell (1980:113) presented the geotechnical properties of some of these materials, found however, at a different location (Bochum Baulos B3). While the stiffer marl had an "elastic" modulus of 100 MPa, the softer one had

a modulus of 40 MPa. The proposed calculation method was clearly not designed to be used in such heterogeneous ground conditions. However, it would be interesting to test it under such conditions. A constant in situ tangent modulus of 70 MPa was thus assumed for the entire ground mass. The drained friction angle of these deposits did not vary much and it was assumed to be equal to 25°. The cohesive strength of these materials varied appreciably, within almost one order of magnitude. For the analysis, it was decided to consider the lowest cohesion value, corresponding to that of the softer sandy-marl, which was equal to 64 kPa. An average unit weight of 20 kN/m³ was estimated for the ground mass. No data was available regarding the failure ratio of these materials. An arbitrary value of 0.9 was thus selected. No indications were provided regarding the in situ stress ratio (K_o) in the ground. It is believed that it should not differ much from other marls found in the Frankfurt or in the Munich areas. A stress ratio of 0.8 was thus liberally assumed. Wittke and Gell (Op.cit.:113) suggested that the Poisson's ratio for this soil should be about 0.3.

A very careful construction was carried out, with the face excavated in a variation of the heading-bench-invert scheme, classified as type T3 by Eisenstein et.al., (1985:711). The depth of each excavation round was 0.8 m at the heading and bench and 1.6 m at the invert. A 25 cm thick shotcrete lining was installed as well as steel sets at 0.8 m spacing. The average rate of advance was 2 m/day. The

closure of the shotcrete lining at the floor took place 6.4 m behind the face. Some 3 m long ground anchors were installed to hold in place the steel ribs during their assemblage.

The adjusted friction angle was calculated and was about 35°. At lining closure, a stress release of about 57% was estimated and an average ground modulus of 37.58 MPa was obtained (almost 54% of the assumed in situ value).

The lining-ground interaction analysis was carried out neglecting the steel ribs, and considering a shotcrete modulus of 10 GPa and a Poisson's ratio of 0.2. Two iterations were required to find the equilibrium conditions, neglecting the ground heave after support activation. A 36.31 MPa ground modulus was found at this condition, which enabled the flexibility and compressibility ratios of 0.0057 and 21.24 to be calculated, respectively. These values are typical for shotcrete in stiff clays or medium sands.

A final crown settlement of 22.4 mm resulted (U=0.712), for which a stress release of 60% at the crown was estimated. The calculated final subsurface settlements are compared to those measured (Jagsch et.al., 1974:13) in Figure 7.45. The predicted magnitudes of the ground movements are comparable to the measured but the estimated shape of the settlement distribution does not agree with the observations, which involved less vertical straining. The departure could be attributed to the crude simplifications introduced (e.g. the uniform modulus profile) as well as to

the non-circular shape of the excavation.

Similar results were obtained regarding the surface settlement profile (Figure 7.46). As in other case histories, the surface distortions were underestimated by the proposed calculation method, although the magnitudes of the displacements are closely estimated.

Finally, Figure 7.47 shows the predicted and measured final radial stresses acting on the shotcrete lining. The measurements do not reveal any clear trend. If a mean measured stress distribution could be defined, the calculated radial stress distribution seems to approximate it. The non-circular tunnel contour, as well as the heterogeneity of the ground around the tunnel could partly explain the disagreement between the calculated and observed stress distributions.

7.5.3.10 An NATM Tunnel with Staged Installation of the Lining: The Sao Paulo North Extension Double Track Tunnel

This case study refers to a large subway tunnel built in 1984 in Sao Paulo (Brazil), that was described by Cruz et.al. (1985), Negro et.al. (1985a & b) and by Eisenstein et.al. (1986). The double track tunnel was built with a non-circular cross section, with an area of 76.1 m^2, 8.5 m high and 11.4 m wide (9.84 m equivalent diameter). At the instrumented sections S1-3 and S1-9, the ground cover was about 11.2 m.

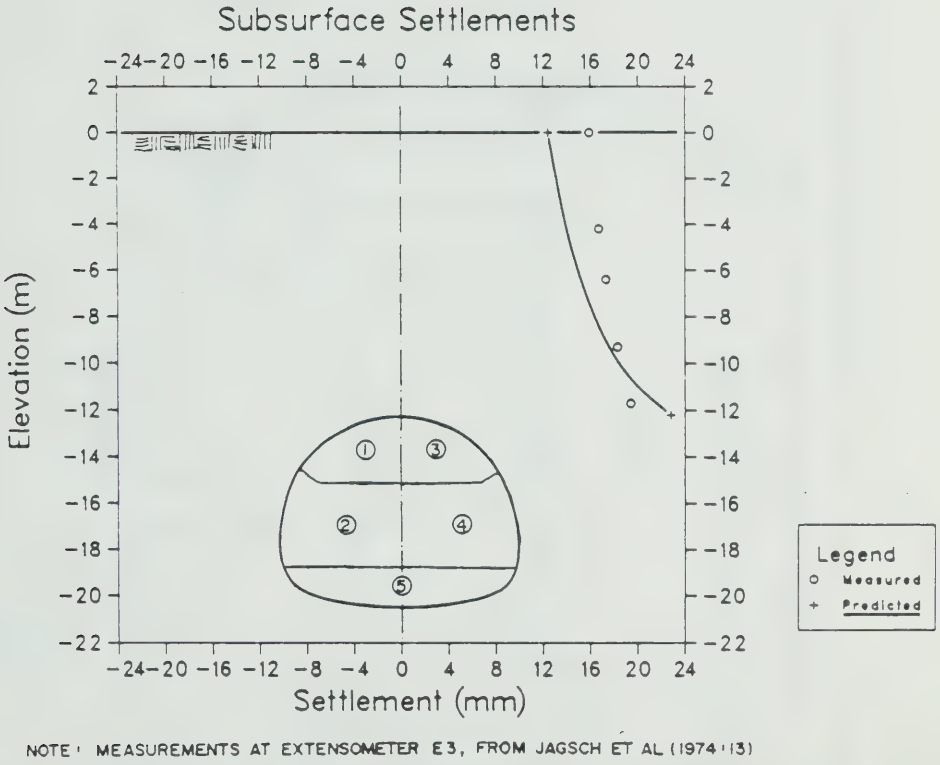

Figure 7.45 Measured and Calculated Final Subsurface Settlements over the Bochum Baulos A2 Tunnel

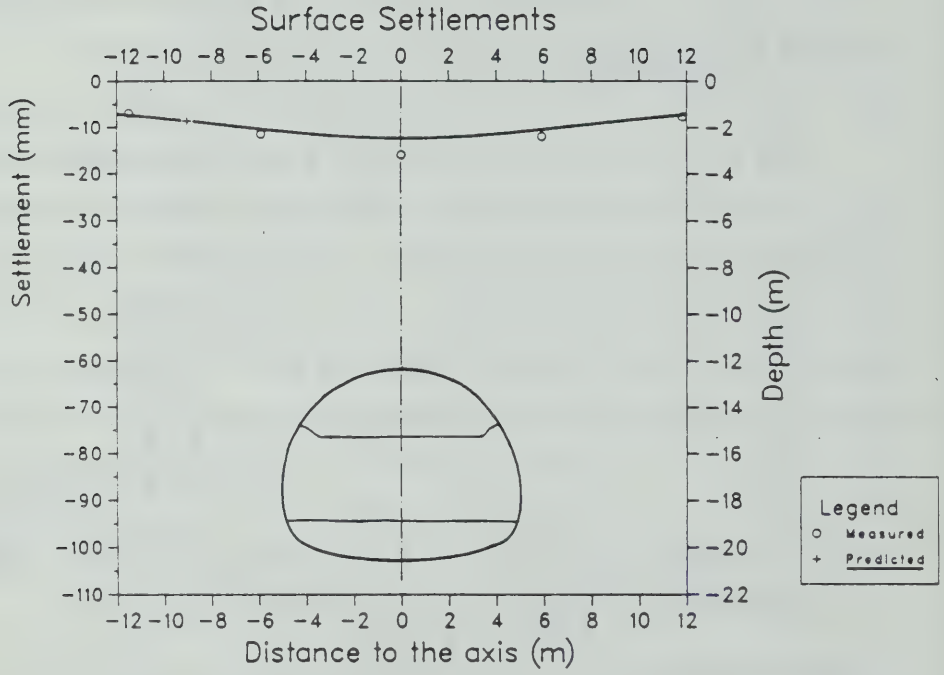

NOTE: MEASUREMENTS AT THE INSTRUMENTED SECTION MQI; DATA FROM JAGSCH ET AL (1978 13)

Figure 7.46 Measured and Calculated Final Surface Settlement Profiles over the Bochum Baulos A2 Tunnel

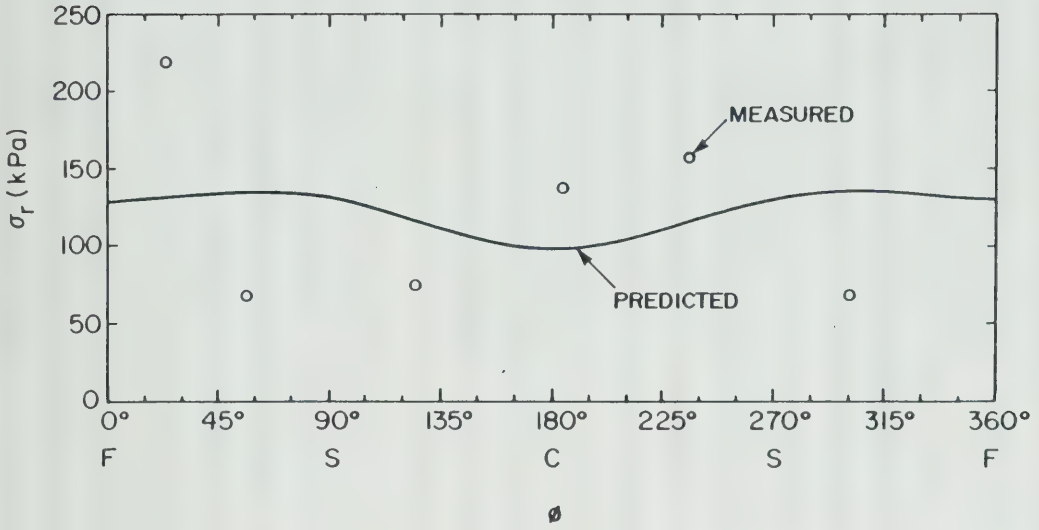

NOTE: MEASUREMENTS AT MQ1; DATA FROM JAGSCH ET AL (1974:13)

Figure 7.47 Calculated and Measured Radial Stress Distributions on the Shotcrete Lining of the Bochum Baulos A2 Tunnel

The tunnel was driven through an overconsolidated stiff and fissured clay layer, about 12 m thick, which is a sediment of the Sao Paulo Tertiary formation. This soil underlay a superficial fine clayey sand layer, about 9 m thick, and overlay a 4 m thick fine clayey sand layer, below the tunnel floor. A perched water table was found 3 m below the surface, in the upper sand layer. The piezometric level in the lower sand layer showed that a nearly uniform pore water pressure distribution with depth existed in the stiff clay layer (in situ pore pressures of about 60 kPa). Some dewatering was undertaken at the portal area, about 80 m away from the measuring section, and caused a 30 kPa reduction in the porewater pressures in the lower aquifer, prior to the tunnel excavation. The settlements associated with this operation were separated from those that developed during tunnel advance.

Negro et.al. (1985:57) showed that the tunnel acted as a drain, and that the 2 to 3 m cover of stiff clay above the crown resulted in being appreciably consolidated from this drainage during the drivage process. Accordingly, in the analysis of this case history, it will be assumed that the ground response was controlled by the drained parameters of these soils. Triaxial tests on the stiff clay furnished a friction angle of 25°, a 3 kPa cohesion and a failure ratio of 0.75. The in situ effective stress ratio of this soil was estimated as 0.9 and an average unit weight of 20 kN/m^3 was determined for this sedimentary deposit. The in situ

(drained) tangent modulus for the stiff clay at the tunnel springline elevation was estimated also from triaxial tests and resulted as 124 MPa. The modulus of the soil located half a diameter above the crown (the fine sand) was estimated as 47 MPa and that half a diameter below the floor (also the fine sand) was 64 MPa.

The tunnel construction was carried out in two main phases: heading excavation with a temporary shotcrete invert and bench excavation. At the instrumented sections, the temporary inverted arch was demolished and bench excavation took place when the heading face was about 19 m past the section. The heading face was always advanced leaving a central supporting ground core. The face was excavated in one metre round depths, and the temporary invert was shotcreted in 2.5 to 3 m lengths. The average distance between the mid-section of the temporary invert being shotcreted and the heading face was 7.7 m at the instrumented section. The depth of bench advance varied between 2.5 and 3 m. The final shotcrete invert was installed immediately after bench excavation.

Besides a 0.25 m thick shotcrete, the support system included two steel wire meshs (4.48 kg/m^2) and polygonal steel sets (I 8") at one metre spacing. The shotcrete lining thickness was increased to 0.40 m, after tunnel completion, and an additional steel mesh included. This tunnel is quoted as being the first subway tunnel in soil where shotcrete was used as the final support. The average excavation progress

was 3 m/day for the heading and 6 m/day for the bench. The overall rate of completed tunnel construction was about 1 m/day.

The conditions involved in this case history, depart considerably from those envisaged for the application of the proposed calculation procedure. The tunnel was driven below the ground water level, with minor dewatering. The tunnel cross-section was non-circular, and, more importantly, the staged application of the lining, with a temporary invert at the heading, respresented a condition not considered in the development of the calculation method.

The analysis was conducted for a circular opening with the same excavated area as in the Bochum case history. The ground parameters were defined for the effective stress levels prior to tunnel construction. However, the stress release at the opening was calculated assuming that the pore pressures were zero in the ground mass, as for the Mississauga tunnel case. To account, at least partly, for the particular sequence of construction, it was assumed that the delay distance of lining activation was equal to the distance between the heading face and the mid point of the temporary invert section (7.7 m), plus the distance between the bench face and the mid point of the final invert section being shotcreted (about 1.4 m). In other words, it was assumed tht the lining deformations developed only after the shotcrete ring was closed at the floor of the completed tunnel section. Although this approximation may lead to

unrealistic estimates of the displacements at sections between the heading face and the bench face, it was felt that it could be reasonable in estimating the final equilibrium condition.

An adjusted friction angle of 30° was calculated. At lining activation, 0.925D behind the face, a ground stress release of about 53% was estimated and an average ground modulus of 36.71 MPa was calculated (almost 60% reduction from the in situ value). The 2D ground stability verification at this instant furnished a factor of safety of 1.35.

The lining-ground interaction was analysed for the completed tunnel section, neglecting the existence of the steel sets and meshes, and considering the 0.25 m shotcrete with a 10 GPa modulus and a Poisson's ratio of 0.2. Two iterations were required to find the equilibrium condition, neglecting the ground heave after support activation.

A final crown settlement of 29.6 mm was calculated (U=0.631), for which at stress release of about 50% resulted at tunnel crown. The comparison between calculated and measured performances was restricted to surface and subsurface settlements, as lining loads were not measured in this case history. While the measured settlements shown in Figures 7.48 and 7.49 do not include the ground movements due to dewatering at the portal areas prior to tunnel excavation, they do include those settlement components resulting from ground drainage and consolidation, which were

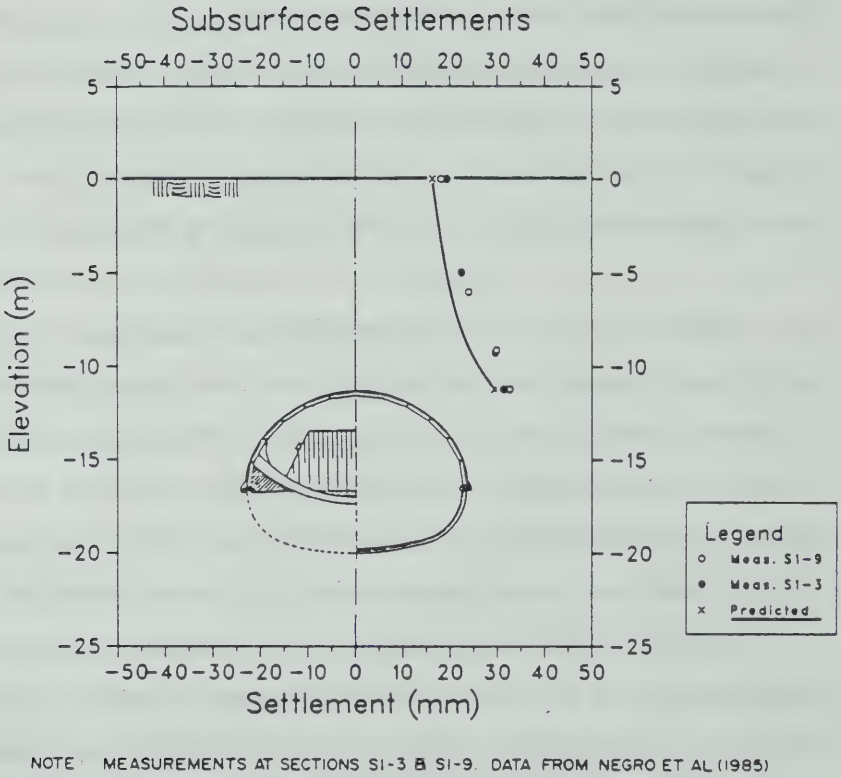

Figure 7.48 Measured and Calculated Final Subsurface Settlements over the Sao Paulo North Extension Tunnel

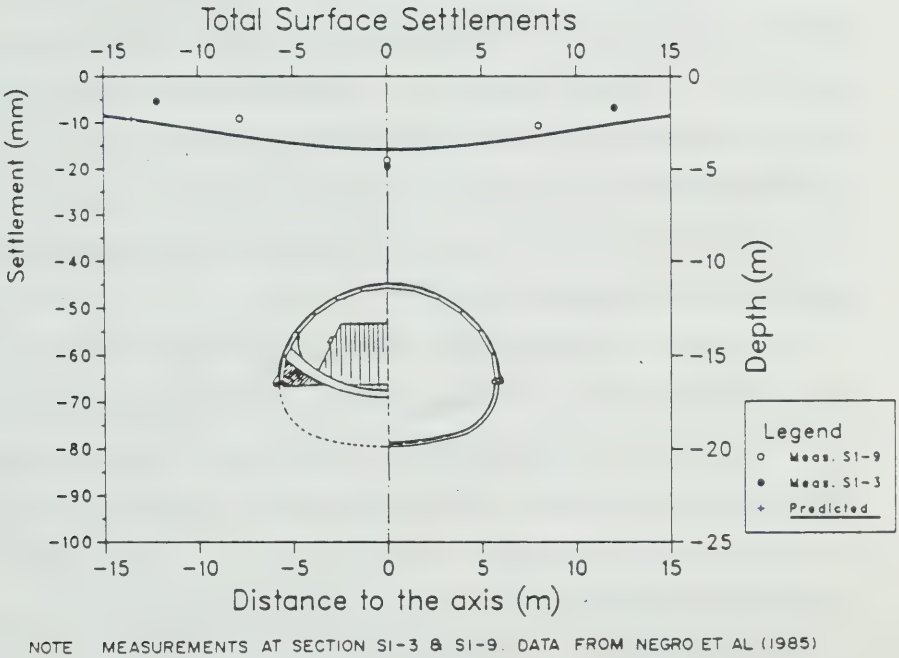

Figure 7.49 Measured and Calculated Final Surface Settlement Profiles over the Sao Paulo North Extension Tunnel

not accounted for in the calculations. As it is noted in those figures, the settlements were underpredicted by this approximate analysis. Also underestimated were the ground surface distortions.

The shape of the cross section of this tunnel deviates considerably from a circular profile. In fact, from all cases investigated, this is the one that presents the lowest opening height to width ratio (h/w=0.746). This can partly explain the underestimation of the magnitude of the crown and of the maximum surface settlement. The former was underpredicted by about 8% and the latter by about 14%, using the calculation, where a circular cross section of equal area was assumed.

In order to assess the influence of the cross section shape on the crown settlement, the solution numerically derived by Negro and Kuwajima (1985) may be of some help. This solution was obtained from 2D linear elastic parametric bounday element analyses of deep unlined tunnels, with cross section shapes similar to the present one. The dimensionless crown displacement is given by:

$$U = 1.058 - 0.179\frac{h}{w} - 0.385K_o \qquad [7.21]$$

where the symbols have the usual meaning. When the height to width ratio is reduced from 1 to 0.746, as in this case, for K_o equal to 0.9, one finds that the crown displacement increases 8.5%. This value is of the same order of magnitude of the underprediction quoted earlier.

7.5.4 Analysis and Interpretation of the Results Obtained

The application of the proposed calculation procedure, to simulate shallow tunnel performance obtained through three-dimensional numerical modelling, through centrifuge model testing and through field observation of full scale prototypes, revealed that it does yield sensible results. With the above exercise, the proposed method was tested and its use exemplified for a variety of conditions that may be found in actual practice.

In only one case, the centrifuge model test, the calculation procedure made use of the frictionless soil solution. In another few cases, although the ground was saturated in situ, the analyses were carried out assuming a fully drained soil behaviour. While in the former, an undrained condition could be assumed, in the latter, evidence showed that partly drained conditions had prevailed, so that the use of the frictional soil solution was preferred.

In the applications of the method to actual tunnel cases, no attempt was made to best fit the observed performances. These tests were not back analyses, since it was assumed that all of the parameters governing the tunnel response were known. Accordingly, these parameters were selected, and in a few cases, assumed, so that they would represent the most probable conditions found in each case. The departures noted in each case study were discussed and tentatively explained. In the present section, a general

appraisal of the results is attempted, with minor references to particular cases.

In some cases, the proposed method was tested to conditions that deviate considerably from those originally set up in the development of the method. As mentioned earlier, some cases investigated (Mississauga, Munich 5/9 and Sao Paulo North Extension) involved constructions below the groundwater level, under partly drained conditions. In these cases, drained ground parameters were estimated for the in situ effective stress conditions. However, the ground stress release and lining-ground interaction analyses were carried out assuming the ground mass was fully drained, with zero pore pressures. Obviously, this does not correspond to reality but it was necessary to use this approximation since the proposed calculation method does not allow an effective stress analysis to be performed with proper consideration of the pore pressure effects. Notwithstanding this, the results obtained with that simplifying assumption compared well with the observed performances. The agreement partly resulted from the fact that, in those cases, the ground was overconsolidated, stiff or dense, and less susceptible to volume changes induced by porewater pressure changes.

In some cases, the method was applied to construction conditions that also departed from those originally admitted. In the Munich 5/9 tunnel, compressed air was used during excavation. In the Sao Paulo North Extension Subway, the tunnel was advanced in stages, using a temporary invert

in the heading excavation, which was later removed. These singular operations were accounted for in the calculations, through simplified, yet conscious approximations. In the former, the ground cover was reduced proportionally to the compressed air pressure. In the latter, the support activation delay was calculated assuming that the first stage lining (with the temporary invert) did not deform: lining activation was assumed to occur only after the invert of the completed tunnel section was installed. In the Romerberg tunnel (Frankfurt), the simultaneous construction of the twin tunnels was partly accounted for by superimposing the settlement solution of single isolated tunnel, and neglecting the interaction between the tunnels, on the assumption they were sufficiently far apart. The approximations introduced in these cases were found to be sufficient to make the calculated performance closer to that observed.

In three cases (Butterberg, Bochum and Sao Paulo North Extension), the tunnel profile deviated considerably from the circular section which was assumed in the development of the calculation method. Some of the noted disagreement in these cases (e.g., the underestimation of final crown settlement) could be attributed to this fact.

Having in mind these peculiarities, the overall results obtained can be better assessed through a table summarizing the analyses conducted (Table 7.11). In all calculation results, the overall ground heave component resulting from

the trend the opening exhibits to 'float' after the lining is activated (equation 7.10), was neglected. Of course, the heave component prior to lining installation is included in the displacement field provided by the proposed method. The reasons and consequences of this assumption were presented and analysed in Section 7.4.

One notes that most of the cases analysed involved fairly favourable ground conditions (stiff or dense soils), and in all of them fair to good construction quality was ensured. In most cases, the tunnel was driven above the in situ water table (A) or above the lowered phreatic surface (LO). In a few cases, discussed earlier, the tunnel was advanced below the groundwater table (B), without dewatering.

In a large number of cases, the tunnel was built following the so called NATM, using shotcrete as the main support element. In all cases, it was assumed that the lining was solely represented by the shotcrete ring activated at the section where it was closed at the floor, and always considering a Young's modulus of 10 GPa and a Poisson's ratio of 0.2. In the shield driven tunnels, steel ribs and lagging or segmented concrete linings were used. The support systems used in the case studies investigated ranged very widely, from very stiff to very flexible. The flexibility ratio, β, was found to vary, in these cases, from about 0.5 to 0.0014. The compressibility ratio $\dot{\alpha}$, on the other hand, varied from about 468 to 4.44. These ranges

Tunnel Case No.	1	2	3	4	5	6	7	8	9	10	11	12
Soil	Clayey-sand	O.C. Kaolin	O.C. Kaolin	Clay Marl	Clay Marl	Till	Sandy Gravel	Till	Hard Marl	Heter. Marl	O.C. Clay	Hard Marl
Water Level	A	B	B	LO	LO	B	A	A	B	A	B	LO
Construction	NATM	Model Test	Model Test	Shield	NATM(a)	Shield	NATM	Shield	NATM-c.air	NATM	NATM	NATM
Lining	Shotcrete	Rubber	Rubber	Segm.concr.	Shotcrete	Ribs&lagg.	Shotcrete	Ribs&lagg.	Shotcrete	Shotcrete	Shotcrete	Shotcrete
β	0.0135	0	0	0.497	0.0303	0.0019	0.0119	0.0055	0.0014	0.0057	0.0042	0.0015
α	51.79	0	0	467.79	89.60	4.44	4.98	10.74	7.67	21.24	18.35	7.73
H/D	1.550	1.670	1.670	1.761	1.775	2.693	1.183	1.442	2.880	1.351	1.138	3.184
Shape	non-circ.	circ.	circ.	circ.	circ.	circ.	non-circ.	circ.	non-circ.	non-circ.	non-circ.	non-circ.
h/w	0.975	1.0	1.0	1.0	1.0	1.0	0.864	1.0	1.077	0.822	0.746	1.104
ϕ_e/Cue:γD	29°/0	0°/0.37	0°/0.37	30°/0	30°/0	40°/0	41.5°/0	40°/0	31.2°/0	35.6°/0	30°/0	31°/0
K_0	0.8	1.0	1.0	0.8	0.8	1.0	0.5	0.75	1.0	0.8	0.9	1.0
Lining activation X/D	0.65			1.10	0.88	1.75	0.826	1.00	0.8	0.7	0.925	1.013
$\bar{\Sigma}$ at L.A.	0.471	(0.710)	(0.610)	0.440	0.445	0.434	0.363	0.383	0.508	0.434	0.471	0.490
$\bar{E}_t/\bar{E}_{ti}$ at L.A	0.445			0.441	0.448	0.586	0.542	0.573	0.511	0.537	0.409	0.488
$\bar{E}_t/\bar{E}_{ti}$ at Equil.	0.449			0.438	0.451	0.505	0.678	0.545	0.431	0.519	0.412	0.399
FS at L.A. [b]	1.437	(1.817)	(1.351)	1.655	1.667	1.767	1.210	1.353	2.010	1.694	1.346	1.910
Extrapolation needed?	Yes	No	No	No	Yes	No	Yes	No	No	No	No	No
Where?	F				F		C,F					
Final U at crown	0.695	0.517	1.065	0.657	0.694	0.648	0.906	0.754	0.578	0.712	0.631	0.616
Surface Settlements												
Max. Magnitude	=	=	=	=	=	=	=	=	=[c]	<	=	=
Max. Distortion	<	<	<	=	=	<	=	<[d]	<	<	<	
Distribution	G	G	R	G	R	P	R	R	G[c]	G	R	
Subsurface Settlements												
Max. Magnitude	=	=	=	=	=	=	=		=	=	=	
Distribution	G			G	P	R	G		P	G	G	
Horiz. Converg. of Liner												
Magnitude	>				=	=	=	>	=			=
Lining Loads												
Aver. Magnitude	>	=	=	=[e]	=	=	>	>	>	=		>
Distribution	R			G[e]	G	R	G	G	G	R		P

Notes: (1) ABV - Sao Paulo
(2) Centrifuge model test (α = 29%)
(3) Centrifuge model test (α = 39%)
(4) Domplatz-Frankfurt
(5) Rom erberg-Frankfurt
(6) Mississauga
(7) Butterberg
(8) Edmonton LRT
(9) Munich 5/9
(10) Bochum
(11) Sao Paulo-North Extension
(12) Munich 8/1

a. Twin tunnels simultaneously driven
b. For actual strength parameters
c. Short term measurement
d. Measurements 3 m below surface
e. Measurements in the 2nd tunnel

Table 7.11 Results of the Application of the Proposed Calculation Procedure to some Case Histories of Shallow Tunnels

entirely cover the spectrum of relative lining stiffness likely to be found in practice (see Table 7.1).

The calculation procedure was tested in tunnels with ratios of cover to diameter ranging from 1.14 to 3.18, and with opening height to width ratio (h/w) ranging from 0.75 to 1.08. The lining activation was assumed to have taken place at 0.65D to 1.75D behind the tunnel face.

The adjusted friction angles of the ground involved varied from 29° to 41.5°. Only in the centrifuge model test a ϕ=0 condition was assumed, and an undrained strength ratio of 0.37 was considered. The in situ stress ratios varied from 0.5 to 1.0.

The calculated amount of ground stress release at lining activation (L.A.) varied from 0.29 to 0.64. Excluding the model tests, the average amount of stress release found in the case histories was 56%. Incidentally, this value compares very favorably with the arbitrary 50% stress reduction proposed by Muir Wood (1975:124) for lining design. At lining activation, it was found that the ratio of average current to in situ tangent ground moduli varied from 0.41 to 0.59. This ratio, at the equilibrium condition, was estimated to vary from 0.40 to 0.68. These findings indicate that for a quick lining-ground interaction analysis, it may be sufficient to assume a 50% reduction in both the ground stresses and in the ground in situ stiffness, provided that the ground control conditions are comparable to those of the present case histories.

The two dimensional stability verifications, at the sections where the linings were activated, yielded factors of safety varying from 1.21 to 2.01, with the median value being about 1.6. It could be said that the proposed calculation method can be successfully applied to predict the performance of a tunnel, whenever this factor of safety is within or above that range. As discussed in Section 2.3.4.3, for this safety range, the ground displacements are small, and high shear strain concentrations in the ground are minimized or avoided. On the other hand, it was shown in Section 2.3.3, that for this range of factors of safety, a non-linear ground response is to be expected. In fact, ground stiffness reductions in the order of 50% were, indeed, calculated in these case histories, despite the good ground control conditions met.

Only in three case histories was there a need to use the extrapolated part of the twice normalized stress release or ground reaction curves. The extrapolation beyond the formal limit of the generalized solution was needed mainly for the tunnel floor. Despite this, the results obtained in these cases were comparable to those where no extrapolation of results was needed.

The final dimensionless crown displacement (U) was found to vary between 0.5 to 1.0, approximately. The latter figure was suggested, in Section 2.3.4.3, as a reasonable bound for crown settlements in tunnels built under good ground control conditions. Thus, quick estimates of the

final crown displacement, under these tunnelling conditions, could be performed assuming U=1.0.

The results of the comparisons between measured and calculated performances are presented in Table 7.11 in simple qualitative terms. The same criteria used to evaluate the prediction of performance by the finite element method (Section 5.2.1.2, Table 5.5) was adopted herein. The calculated value is said to approximately equal the measured value ($\simeq$), whenever the latter is not more than 20% different than the former. Otherwise the calculated value is said greater (>) or smaller (<) than the measured value. The spatial distributions of displacements or loads were arbitrarily defined as good (G), regular (R) or poor(P), after a liberal comparison between prediction and measurements was made. This qualification is likely to be more subjective and may vary among individuals.

A quick inspection of these results reveals that the proposed calculation procedure consistently yielded unsafe estimates of the maximum surface distortion (the maximum slope of the surface settlement trough). For the other performance aspects, the calculation method provided either a good or a safe estimate. If the calculated maximum distortions (γ_c) are plotted against the observed maxima (γ_o), then the results shown in Figure 7.50 would emerge. If the calculated and observed distortions were equal, the points would be accommodated along the full continous line shown. However, the points that were actually obtained were

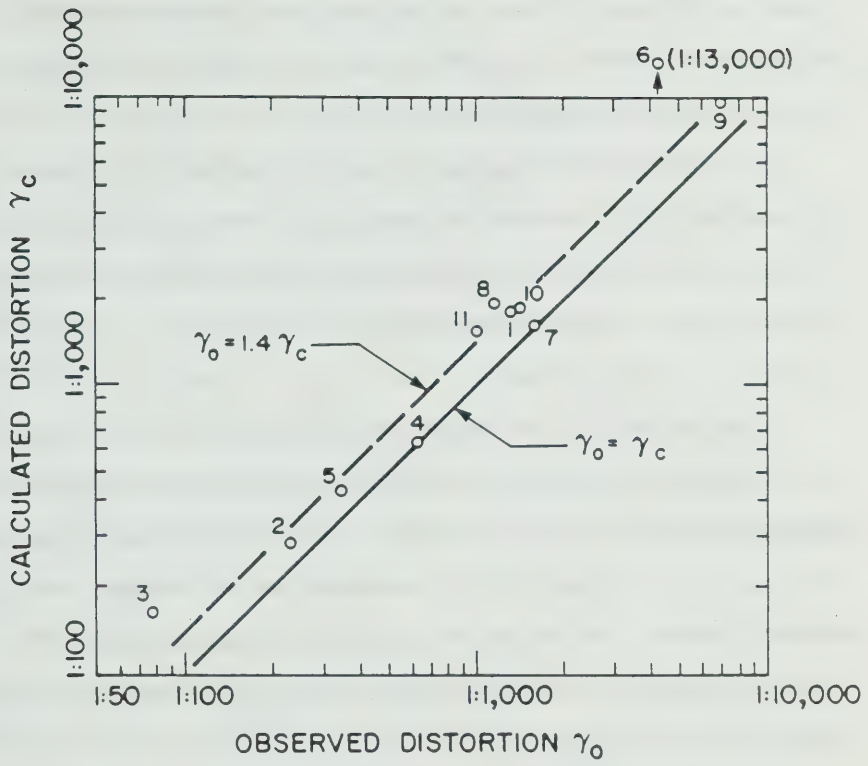

CASE HISTORIES:

1. ABV - SAO PAULO
2. CENTRIFUGE MODEL (α = 29%)
3. CENTRIFUGE MODEL (α = 39%)
4. DOMPLATZ - FRANKFURT
5. ROMERBERG - FRANKFURT
6. MISSISSAUGA
7. BUTTERBERG
8. EDMONTON LRT (γ_0 below surface)
9. MUNICH 5/9 (short term)
10. BOCHUM
11. SAO PAULO - NORTH EXTENSION

Figure 7.50 Calculated Maximum Surface Distortions Compared to the Observed Maxima

found to lie close to the broken line. This line yields observed distortions which are on average, 40% greater than those calculated. This result was not unexpected, as it reflects a common trend shown by most finite element calculations (see Section 5.2.1.2).

In order to compensate for this effect, it seems advisable to introduce an empirical correction into the calculated distortion (γ_c). The corrected distortion (γ_{cc}) would, thus, be obtained through:

$$\gamma_{cc} \simeq 1.4 \ \gamma_c \qquad [7.22]$$

If the above correction was applied to the cases investigated, a better agreement between calculations and observations would be obtained. A possible exception would be case 6 in Figure 7.50. It corresponded to the Mississauga Tunnel, where, as noted in Section 7.5.3.4, some difficulties were experienced in levelling the settlement points in the field.

A pictorial representation of results is given in Figure 7.51. One notes that the calculation method, in the majority of the cases, provided a close estimate of the maximum surface settlement (within a ±20% margin). In only one case (No. 10, Table 7.11), the maximum surface settlement was underestimated. This case (the Bochum Tunnel) involved, however, very peculiar ground conditions (mixed face, heterogeneous profile), that deviates appreciably from the conditions idealized for the application of the calculation method.

The surface distortions were underestimated in 73% of the cases and were never overestimated. In more than half of the cases, the predicted overall distribution of surface settlement was regular or poor. The calculation method tends to furnish settlement troughs which are wider than the observed. This does not seem to be a matter of serious concern, as the theoretical result is safe. Though the criticisms on the use of the error function or normal probability curve are known, it appears that this curve tends to fit actually observed surface settlement profiles better than the distributions proposed by the present calculation method. With this fact in mind, one could suggest a correction on the width of the calculated surface settlement profile, as follows.

The distance (i) between the point of inflexion of the settlement trough and the tunnel axes could be estimated assuming that the maximum surface settlement (S_{max}) is that given by the proposed calculation method, and that the maximum slope of the settlement trough is given by equation 7.22. If the shape of the settlement trough follows a normal probability curve, then:

$$i = 0.606 \frac{S_{max}}{\gamma_{cc}} \qquad [7.23]$$

The width of the settlement trough (w_s) is defined as the distance between the tunnel axis and the point beyond which the settlements are insignificant (i.e., smaller than 4.3% of S_{max}). For a normal probability curve, this point is given by:

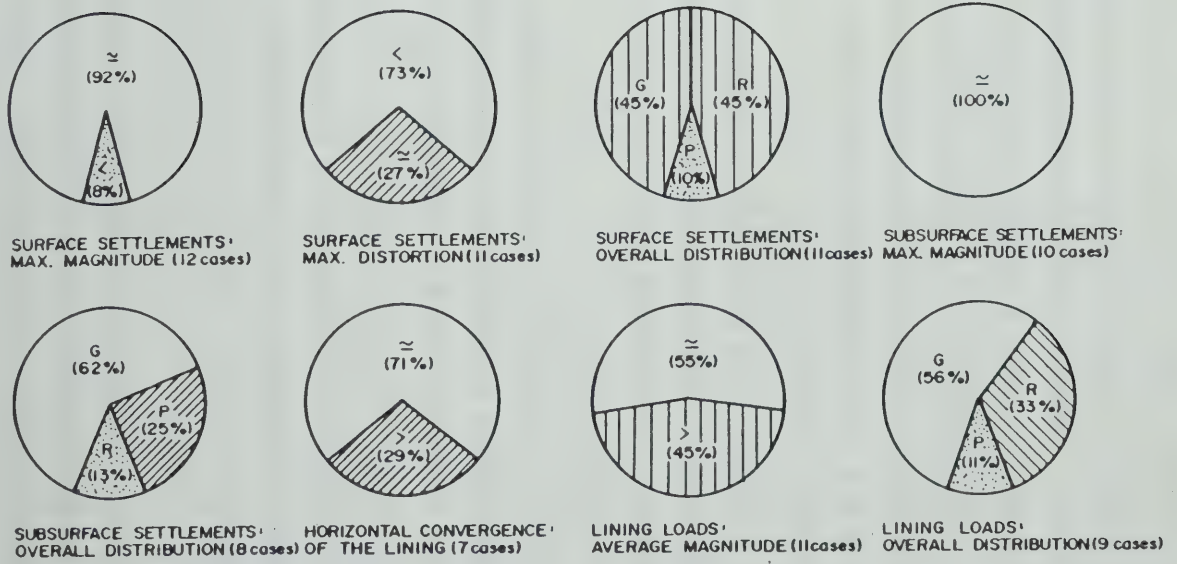

Figure 7.51 Calculated Tunnelling Performance Compared to Field Observations

$$w_s = \sqrt{2\pi}\ i$$

therefore

$$w_s \simeq 1.52 \frac{S_{max}}{\gamma_{sc}} \qquad [7.24]$$

The above semi-empirical correction was tested in the case histories investigated (see Table 7.12) and was shown to give reasonable results. Note that the "measured" trough width is actually an estimated value, based on the measurements available, which in most cases were not extended to a sufficient distance from the tunnel axis to adequately define w_s.

As is also shown in Figure 7.51, the magnitude of the maximum observed subsurface settlement was always closely estimated with the proposed calculation method. The distribution of settlement with depth was good to regular in 75% of the cases. 'Poor' distributions were noted in Case 5 (Table 7.11), which corresponded to twin tunnels simultaneously built and in Case 10, where a heterogeneous ground condition was encountered. For these two particular conditions, it would be expected that the calculated distribution could not compare favourably with the measurements.

Figure 7.51 indicates further, that the horizontal convergence of the lining after its activation was very well estimated in 71% of the cases available. Moreover, the support convergence was never underestimated by the calculation procedure. These results seem to indicate that the assumption that the activation of a shotcrete lining

Case	Tunnel	S_{max}	γ_c	γ_{cc}	w_s	
					Calc.	Meas.
1.	ABV - Sao Paulo	5.4 mm	1:1800	1:1286	10.57 m	10 - 12 m
2.	Centrifuge Test (α = 29%)	8.812 10^{-3}D	1:290	1:207	2.78 D	2.5 - 3 D
3.	Centrifuge Test (α = 39%)	19.68 10^{-3}D	1:167	1:119	3.57 D	2.5 - 2.8 D
4.	Domplatz-Frankfurt	29.4 mm	1:638	1:456	20.37 m	20 - 24 m
5.	Romerberg- Frankfurt	42.5 mm(1)	1:425	1:304	19.61 m(2)	12 - 18 m(2)
6.	Mississauga	2.3 mm	1:13000	1:9286	32.46 m	8 - 11 m
7.	Butterberg	13.9 mm	1:1600	1:1143	24.11 m	20 - 23 m
8.	Edmonton LRT	8.5 mm	1:1933	1:1381	17.92 m(3)	15 - 30 m(4)
9.	Munich 5/9	3.0 mm	1:9756	1:6969	31.78 m	~ 30 m(5)
10.	Bochum	12.2 mm	1:1846	1:1319	24.45 m	20 - 23 m
11.	Sao Paulo - North Extension	16.4 mm	1:1579	1:1097	27.38 m	15 - 19 m

Notes:
(1) Over 1st tunnel driven
(2) Measured on the outer sides of the twin tunnels
(3) At ground surface
(4) 3 m below surface
(5) In short term
(6) γ_{cc} calculated through equation 7.22
(7) w_s calculated through equation 7.24
(8) w_s is the half width of the full surface settlement trough

Table 7.12 Calculated and Measured Widths of the Final Surface Settlement Profiles in Some Case Histories

takes place at the section where it is closed at the tunnel floor, is a reasonable one. Additionally, they tend to confirm that, under this assumption, the arbitrary shotcrete modulus of 10 GPa adopted, combined with the assumption of no contribution of the steel ribs to the relative stiffness of the lining, are also reasonable approximations.

It is difficult to perform an accurate assessment of the ability of the proposed method to estimate lining loads. This is mainly due to the fact that in most cases, contact pressure cells were used to measure the ground loads acting on the support. Depending on the installation procedure, this type of instrument is known to either overestimate or underestimate the actual contact stresses (see, for example, Hanna, 1985:205). A special class of problem arises when pressure cells are used in concrete - soil interfaces, and is related to the heat generated during the setting of fresh concrete (Hanna, Op.cit.:444). Due to these facts, it was decided to compare "average" lining loads, in the hope that the over-reading and the under-reading errors would balance each other. In terms of these qualitatively estimated average lining loads obtained from field measurements, it was noticed (Figure 7.51) that the calculation procedure either matched these loads or overestimated them. Large average load estimates (up to 50%) were noted in the Butterberg and in the Munich 8/1 Tunnels, where Maihak and Glotzl cells were used in the soil-shotcrete contact. This result may be associated with the formation of gaps between

the cell and the concrete after the concrete temperature dropped (the full contact might have been lost at the interface). On the other hand, this effect may have not been present at the Munich 5/9 tunnel, where specially designed load cells were embedded in the shotcrete. Even so, the lining thrusts in this case, were also overestimated by 20 to 50%.

Actually, the proposed calculation procedure was developed in such a way that it may indeed, lead to overestimation of the lining loads. Firstly, as explained in Section 7.2.2, the use of the final equilibrium ground stiffness, defined at the point of equilibrium, will normally lead to higher loads, unless the in situ stress ratio is low and the outward lining displacement at springline is appreciable. This was the case in the Butterberg tunnel, where the overall ground stiffness increased from the instant of lining activation to equilibrium (see Table 7.11). Secondly, if the tunnel closure at the instant of lining activation is large, the combination of the 3D elastic solution for closure estimate, with the 2D non-linear elastic solution for the stress release estimate, may also lead to estimating higher lining loads. With regard to this aspect, an improvement on the closure estimate solution would be beneficial, particularly for cases where the delay in the lining activation is large. For activation at sections more than 1.5D behind the face, the 3D closure solution furnishes radial displacements which

are basically independent of that distance. Hence, for distances greater than 1.5D, the tunnel closure is virtually constant and the resulting amount of stress release is also constant.

In reality, for most soils, the tunnel closure will increase if lining activation is delayed more than 1.5D. The failure of soil elements around the opening will increase the radial displacements and further reduction of the ground stress is attained, before a collapse condition emerges. This additional reduction in the ground stresses cannot be represented by the present calculation procedure, unless another solution for the tunnel closure is developed (including the ground non-linear response) and is coupled to the 2D ground stress release solution. In its present form, the proposed procedure will tend, for these conditions, to estimate smaller tunnel closures and higher lining loads. This limitation of the proposed method was discussed earlier in Section 5.3.7, where the problem was exemplified through the Edmonton Experimental Tunnel case, where the lining was activated at a section more than 2D behind the face. Fortunately, in most cases (See Figure 6.37) and under good ground control conditions, this distance is less than 1.5D.

Also not assessed in the lining load estimate evaluation are the effects of the tunnel shape, and the differential soil stiffness degradation around its contour. It seems interesting to explore these two aspects in future research. The second factor could, perhaps, be investigated

using a ring and spring calculation model, where the spring moduli would vary from point to point along the tunnel profile, according to the stiffness provided by the generalized solution developed in Chapter 6 (the λ' curves, for instance).

Finally, it should be pointed out that the overall results obtained in this chapter with the proposed calculation method, are equivalent to those obtained by the finite element modelling exercises reviewed in Section 5.2.1.2. In fact, if the diagrams shown in Figure 7.51 are compared to those presented in that section, it would be noted that the proposed procedure presented improved results. Using the same point rating criterion referred to in Section 5.2.1.2, to evaluate the quality of the prediction, some of the analyses summarized in Table 7.11 top ranked and none showed results below the average.

7.6 Summary and Conclusions

In this chapter, the soil-lining interaction phase of the shallow tunnel problem was addressed. A simple linear elastic analytical model was selected to study this interaction in a two dimensional representation. The preference towards a ring-and-plate solution was justified, and of these, Hartmann's (1970, 1972) closed form solution was favoured as it is the only one that makes full allowance for the non-uniform stress field existing in a shallow tunnel.

The assumptions involved in the soil-lining interaction solution were described and the main aspects of its derivation were discussed. The relative stiffness of the lining to the ground mass was expressed through two coefficients, the compressibility ratio (α) and the flexibility ratio, (β). Typical values for common linings and soils were given. The closed form solution was presented in an abbreviated form (Figure 7.2) and its significance was assessed.

The selected analytical solution assumes the ground to be represented by an infinite plate under a gravitational stress field. The consequences of this assumption were investigated, by comparing the results of the analytical solution with that obtained from finite element analyses of a shallow tunnel. Since in both cases the action of gravity is included, the differences in the results could be attributed to the influence of the ground surface, if the numerical inaccuracies are ignored. Numerical and analytical solutions were found to yield similar results for cover to diameter ratios greater than 1.5, which confirms the discussions presented in Section 2.2. Moreover, the analytical solution furnished conservative estimates of the lining response for smaller H/D ratios. Some of the discrepancies noted were attributed to the procedure adopted in the analytical solution used to account for the overall ground heave (the trend exhibited by a shallow tunnel to "float").

In order to account for the effects of the delayed lining installation in the soil-lining interaction analysis, the use of the analytical solution had to be adapted. The first effect resulting from a delayed lining activation is the reduction of ground loads and this was introduced through the use of a reduced unit weight for the soil (equation 7.14). Though this artifice may be valid for linear elastic materials, for a non-linear elastic ground it is understood to be an approximation. The second effect, resulting from a delayed support installation, refers to the degradation of the soil stiffness, associated with the tunnel closure developing before the lining is activated.

The reduction in the unit weight of the soil, can be assessed through the twice normalized ground reaction curves (λ curves) derived in Chapter 6, once the radial displacements of the tunnel contour at the instant of lining activation are known.

The degradation of the soil stiffness can be assessed through the derivative functions of the twice normalized ground reaction curves (λ' curves). An important assumption then had to be made: the tangent stiffness of the ground was assumed to be uniquely related to the tunnel radial closure (U), through the derivative functions presented in Section 6.4. The implications of this assumption were assessed and discussed.

To evaluate the ground stress and stiffness reductions associated with the delayed support activation, the twice

normalized support activation, and their derivatives, at different points of the tunnel contour, are assumed to have an independent existence. In other words, the sequence of loading or closure at different points of the opening profile, is assumed to not affect the response noted at any other point of the contour. The approximation involved in this assumption is minimized when the stress ratios (Σ) or the tangent stiffnesses (E_t) obtained indepently for each point of the tunnel profile, are averaged.

To assess the consequences of the preceding simplifying assumptions, the proposed procedures for ground stress and stiffness reductions were tested against the results of 2D non-linear elastic finite element analyses, where different amount of stress release, representing varying degrees of delaying the support activation, were imposed prior to the lining installation. Accordingly, the closed form solution was used, coupled with the generalized solutions for ground reactions derived in Chapter 6. Through these solutions, an average tangent stiffness of the ground, at the instant the lining is installed, could be estimated. This value and the reduced soil unit weight, were used in the lining-ground interaction analysis. The ground loads onto the support at equilibrium, were found to be underestimated by this calculation procedure. This resulted from the assumption that the ground stiffness remains unchanged during the interaction process. The additional soil stiffness degradation, upon further closure of the now lined opening,

would necessarily imply that increased lining loads would exist on the support.

A better and safer assumption would be to assign the ground its stiffness as defined at final equilibrium. This, however, is not known, as the incremental closure of the opening after lining installation is unknown. To solve the problem, an iterative procedure was devised, in which the average ground stiffness is updated after each iteration. The process is repeated until convergence is obtained, which required not more than five iterations. With this algorithm, the calculation procedure was repeated and new ground loads acting on the lining were found. As expected, loads higher than those previously obtained were calculated. More importantly, these resulting ground loads were slightly higher than those given by the finite element analyses. Moreover, the radial displacements of the lining were closely estimated by the approximate analyses, except at the tunnel floor where the displacements were overestimated. This was attributed to an overestimation of the ground heave at points below the tunnel in the analytical approach.

Briefly, the approximate solution developed by coupling the generalized solution for the ground response developed in Chapter 6, with the closed form solution for the lining-soil interaction analysis, furnished reasonable (and safe) estimates of the lining-ground equilibrium condition, both in terms of final stresses acting on the lining as well as final tunnel closure.

The parametric analyses presented in Chapter 6 considered the tunnel to be unlined and, therefore, the resulting normalized settlement distributions disregard the influence of a lining on the ground movements. The influence on ground displacements that a lining has, when installed after allowing some stress release in the ground, was evaluated through the results of the non-linear elastic finite element analyses just discussed. The final settlement distributions obtained for the lined and unlined tunnel cases, were compared by estimating the amount of stress release required in each case to produce the same crown settlement. It was found that the unlined tunnel analysis causing an equal crown displacement, furnished settlement distributions similar to those obtained for the lined cases, and slightly higher settlement magnitudes. In other words, by neglecting the presence of the lining, conservative estimates of the ground settlements above the tunnel are found. Accordingly, the normalized distributions presented in Appendix C, can be used in practice, since it is sufficient to calculate the amount of stress release in the unlined tunnel solution, which causes the same crown settlement obtained in the lining-ground interaction analysis. That amount of stress release is easily obtained through the normalized ground reaction curve for the tunnel crown.

As a result of the above analyses and verifications, a calculation sequence emerged. It was possible to produce a

flow chart, to guide the application of the presently proposed design procedure (Figure 7.9). Its main sequential steps involve:

a) The assessment of the geometric conditions of the problem;

b) The evaluation of the geological and geotechnical aspects involved, including the definition of ground parameters;

c) The assessment of the construction technology to be applied, including details of the support system;

d) The assessment of the applicability of the proposed design procedure, including the anticipation of likely ground conditions to be encountered (risk of collapse, drained or undrained ground responses, soil volume changes, etc);

e) The evaluation of the pre-support ground response (tunnel closure, amount of stress release, ground stiffness change, ground stability verification, etc);

f) The analysis of the lining-ground interaction including the calculation of thrust forces and bending moments, lining distortions, etc;

g) The prediction of the ground movements, including final tunnel closure, subsurface and surface settlements, and maximum ground distortions.

The results obtained in each step, from (e) to (g), should be interpreted accordingly and their acceptability verified. If the results obtained after any step are not acceptable (e.g., unstable pre-support response, excessive

lining loads, excessive ground movements), then the construction technology should be reviewed and modified. If the anticipated tunnel performance is acceptable, then construction follow-up and monitoring are carried out, and the data collected are used for feed-back in each design step, as an on-going process, as part of an observational design approach.

Details of each design step were discussed and analysed. Special attention was given to the formal range of applicability of the proposed calculation method: absence of ground heterogeneities (mixed face conditions, for instance), absence of ground collapse, good lining contact, time independent ground response, limited ground volume changes, etc. Whenever possible, quantitative criteria were proposed to define the conditions for application of the method.

When the proposed method is applied to actual design problems, sensitivity analyses should be undertaken, so that the variability of the ground conditions are assessed, ranges of variation of soil properties are covered and the variabilities of the construction procedure are accounted for. The method can therefore be used in connection with a probabilistic design approach, and expected ranges of ground and lining responses can be defined.

All the calculations involved are simple and easy to program. The entire procedure can be implemented in a small micro-computer, allowing quick on-site re-evaluation of any

design step during the tunnel construction. The method can be applied and calibrated concurrently with field monitoring, thereby serving as an auxiliary tool for decisions being made during construction.

In order to facilitate some of the calculations involved in the application of the design sequence described, a set of calculation sheets was prepared. A complete example of the use of the proposed design procedure was presented. Each design step was covered in detail, for a particular case history (The Alto da Boa Vista Tunnel). The use of the normalized design charts presented in Chapter 6 was exemplified. The lining-ground interaction analysis was conducted using two separate assumptions regarding the overall ground heave taking place after lining installation. Firstly, the ground heave was calculated and incorporated into the method, according to the original formulation of the analytical solution. It was shown that the heave estimate entails an indeterminate degree of approximation, normally leading to an excessive estimation of this ground movement. Secondly, the design procedure was applied assuming that this ground movement component was negligible. It was then shown that the ground heave does not influence the lining loads, but it does affect the radial displacements at floor and crown, and consequently the settlement distribution above the tunnel. A comparison between the calculated settlements using the two assumptions and the ground displacements measured in the field, revealed

that the zero heave assumption leads to slightly conservative estimates of field settlement.

The proposed calculation method was verified against the results of a plane strain centrifuge model test of a shallow tunnel under undrained conditions, carried out by Mair (1979). For that, the frictionless soil model solution, developed in Chapter 6, was used. The calculated responses in terms of the ground reaction curve and surface settlements compared very favourably with the test results. The proposed calculation method proved, however, to furnish progressively poorer predictions of the maximum distortion of the surface settlement trough, as collapse was approached in the test. Nevertheless, as noted in Chapter 5, this result was expected.

The proposed procedure was then compared with the results of a 3D finite element analysis. The latter was carried out by Katzenbach (1981), who used a hyperbolic stress-strain relationship to represent the soil behaviour. Details of the 3D analysis were summarized and the results of the comparison were discussed. Again, the proposed method yielded sensible results which compared very favourably with the 3D analysis results.

Finally, the proposed method was verified against a large number of actual case histories. The latter were selected according to the availability of adequate or sufficient field instrumentation data. Intentionally, the case studies selected always exhibited good ground control

conditions, reflecting either good construction practice and/or good quality ground. Ground instabilities or local collapses were not reported in any of the cases investigated. To test how the method would perform in actual practice required the inclusion of some cases with complex conditions which deviated considerably from those originally set up in the method development. These conditions were represented by tunnelling below the water table with partial consolidation of the soil mass, construction involving the use of compressed air, staged excavation of the tunnel face with a temporary invert in the heading excavation, non-circular tunnel profiles, etc. Additional assumptions and approximations had to be incorporated in order to deal with these distinct features. Despite this, the calculation method yielded sensible results, in terms of both the ground and the lining responses.

It should be remembered that in all applications of the method, no attempt was made to best fit or bound the observed performances. These tests were not back-analyses of case histories, as it was assumed that all parameters and variables governing the tunnel response were known and would represent the most probable conditions found in each case.

The results of the verification tests were put together (Table 7.11) and the overall ability of the proposed calculation procedure to predict actual tunnel performance was generally appraised.

A global inspection of the range of conditions covered in these tests was undertaken. The tests covered both shielded and unshielded tunnel construction, different support systems and lining stiffnesses, a wide range of geometric conditions and a fairly wide range of soil types.

The output revealed that the amount of stress release at lining activation ranged from 29 to 64%, with an average of 56%. This value compares favourably with Muir Wood's (1975:124) arbitrary reduction by 50% of the in situ stress, suggested for lining design. The reduction in the ground stiffness resulting from the ground stress relaxation was found to vary from 32 to 60%. These findings indicate that, for a quick lining-ground interaction analysis, it may be adequate to assume a 50% reduction for both the ground in situ stresses and the in situ (tangent) ground stiffness, provided the ground control conditions are comparable to those found in the cases studied.

The two-dimensional stability verification, at the section where the linings were activated, yielded factors of safety varying from 1.2 to 2.0, with the median value being about 1.6. It was suggested that the proposed calculation procedure seems to provide reasonable predictions of the tunnelling performance, whenever this factor of safety is within or above that range. Tunnel model test results reviewed in Section 2.3.4.3 indicated that, for this range of safety factors, the ground displacements are usually small and that high shear strain concentrations in the

ground are minimized or avoided.

The final dimensionless crown displacement (U) was found to vary between 0.5 and 1.0. The latter figure was suggested, in Section 2.3.4.3, as a reasonable bound for the crown displacement in tunnels built under good ground control conditions. Hence, quick, and possibly, conservative estimates of the final crown displacement under these tunnelling conditions, could be performed by making U=1.0.

The results from the comparisons between calculated and measured performances were presented in simple qualitative terms, following a similar criterion introduced earlier in Section 5.2.1.2. The worst result obtained was related to the maximum ground surface distortions, which were, in more than two-thirds of the cases, unsafely estimated by the proposed calculation procedure. Using the results found, a correction factor was empirically introduced, which indicates that the calculated maximum distortions should be increased by 40%, in order to make them closer to the measured values (see Figure 7.50).

A similar trend was noted regarding the width of the surface settlement profile since the calculation method usually led to troughs wider than the observed. Once more, in order to make the estimated widths closer to the observed, a semi-empirical correction was suggested (equation 7.24). This was tested in the case histories investigated and furnished reasonable results.

The results of this comparative study were then summarized in graphic form (Figure 7.51), where it was shown that the calculation method did furnish good estimates of the maximum surface and subsurface settlements and of the lining convergence. Some difficulties were found in interpreting the results of lining loads. To a large degree, this was due to the fact that most of the lining load measurements were taken with contact pressure cells, and the difficulties associated with this type of instrument are fairly well known. However, it was shown that the proposed calculation procedure, furnished lining loads which either matched the average lining loads measured or overestimated them by up to 50%. Although this figure cannot be taken as definitive, as the accuracy of the measurements can be questioned, especially in shotcrete-soil contact, the noted trend of the calculation method to overestimate lining loads was discussed and explained. Possible improvements on this aspect were discussed and suggestions for future research work on the subject were addressed.

8. CONCLUSIONS

The present research work dealt with the design of shallow tunnels in soil. In an attempt to avoid redundancy, this chapter reviews only the main points and conclusions of the work and the reader is referred to the summaries presented at the end of each chapter for a condensed, yet comprehensive review of all studies undertaken.

The aims of the research were presented in Chapter 1. They included attempts to:

a) identify unsolved or partly solved problems that affect existing practice;

b) more adequately appreciate the mechanisms involved in the soil and in the behaviour of the supporting structures, identifying the controlling parameters, whenever possible;

c) develop procedures to solve these problems and consequently to propose a new design method;

d) summarize the results of the research work in a comprehensive manner and in a way that may be used by the practitioner;

e) validate the results of the research by application o practical problems and defining ranges of validity.

Point (a) above was briefly addressed in Chapter 1 and more thoroughly in Chapter 4. The surveys presented in Chapter 4 revealed that there was no adequate and simple method to couple lining loads and ground settlement predictions. They also revealed that no satisfactory

procedure was available to sensibly account for the effects associated with delaying the activation of the support. These effects are mainly represented by the ground stress relaxation and by the ground stiffness degradation. The importance of such effects seems to be recognized by many. However, since no sensible criteria were available to account for them, the practitioner was compelled to adopt extreme assumptions. Examples of these include the 'full overburden' and partial ground embedment assumptions in lining design, or the assumption of full ground stress release for settlement predictions. With these conflicting assumptions, the design ceases to be an exercise of anticipating the 'most probable' performance, with allowance for adequate safety margins. Instead, it becomes an activity of bounding possible tunnelling performances, which makes the assessment of the safety margins more difficult.

Point (b) was comprehensively addressed in Chapters 2 and 3, where the soil tunnel behaviour was studied through idealizations exemplified by available theoretical and experimental modelling tools and supplemented by observational evidence from prototypes. Through this activity, some of the parameters controlling the behaviour were identified. Soil tunnels in urban environments are designed under requirements that lead to conditions where collapse mechanisms are usually avoided. Accordingly, most of the discussion was confined to the behaviour in pre-collapse stages.

Although urban tunnels are usually designed for and built under 'good ground control' conditions, it was shown that the factor of safety against ground collapse is fairly low, typically 1.2 to 1.7. Moreover, it was shown that for these low safety factors, a non-linear response in terms of ground stress and strain relationships should always be expected. Considerable departures from linear responses were noted in model and prototype behaviour whenever the factor of safety was less than 2 to 3.

A reasonably clear relationship appears to exist between the factor of safety and the dimensionless displacement (U) of the tunnel crown. An interim criterion, based on results of plane section model tunnel tests, was proposed to define a 'good ground control condition', for which the ground movements are generally acceptable and ground collapse is precluded. The test results indicated that near collapse conditions are generally met when U is greater than 1.8 and that values smaller than 1.0 would represent a 'good ground control condition'. Although tentative, this criterion proved to be sensible and to have potential use in practice.

Another tentative criterion was derived from the above. It refers to the limiting dimensionless crown displacement increment for ground movement into a void space behind the lining, which might produce a near collapse ground condition. This dimensionless movement was suggested as equal to 1.0. From this, one may define a maximum crown

overcut in a TBM excavated tunnel. Once more, this is a tentative criterion which may be improved in the future, by further data collation and interpretation and by experimental and theoretical modelling.

It was illustrated that if the overcutting is excessive and the ground displacements are large, 'gravity loads' may act on the lining and that its response may not be predictable. To avoid this condition, a 'good' lining-ground contact should be ensured and ground movements should be limited to levels below those associated with a near collapse stage. A speculative discussion was attempted to analyse the consequences of the development of uncontrolled ground deformations and the associated ground 'loosening' process. A conceptual model was proposed and the need for experimental or theoretical investigations to confirm it, were suggested.

Although of some value at the design stage, the above criteria of limiting displacements may be of little help during construction. For this, a criterion for ground stability assessment in the field was suggested, which is based on the interpretation of longitudinal ground distortions from displacements measurements at points above the tunnel crown.

While the present work focuses on the ground response under time independent conditions, it was felt necessary to analyse the role of groundwater on the ground behaviour. Among others, the effect of pore pressure generation and

dissipation on tunnel stability was addressed for idealized conditions. The difference in the soil response to that observed in other geotechnical structures was explained by the existence of a different intervening parameter: the degree of stress relaxation. Moreover, this analysis illustrated the practical need to identify the ground response in either undrained or drained terms. Examples of how to anticipate these responses were given through approximate criteria derived from simplified theoretical analyses. The need to extend these approaches was suggested.

Another feature studied, still within point (b), was the three-dimensional arching and ground-lining responses associated with the tunnel advance. The stress-displacement responses for points around the tunnel contour were reviewed, as well as some evidence of the three-dimensional stress transfer effects. The role of some of these effects in controlling the tunnel lining design has not been clearly established, for instance, load concentrations or longitudinal bending of the support. Further investigation of these aspects would be of considerable interest, bearing in mind their potential consequences.

After assessing points (a) and (b) described earlier, point (c) was addressed mainly in Chapter 5. To solve this problem, detected in current practice, it was decided to develop an integrated procedure that would allow lining load predictions and settlement estimates taking into account some of the most important factors controlling the tunnel

behaviour. These are:

1. the effect of the relative position of a horizontal and stress free ground surface;
2. the action of gravitational body forces generating a stress gradient in the soil across the tunnel profile;
3. the non-uniformity of the in situ stresses generated by a horizontal to vertical stress ratio different from unity;
4. the non-linear response exhibited by soils in terms of their stress-strain relationships, including the dependence on hydrostatic and deviatoric stress levels;
5. the delayed activation of the lining generating ground movements and associated stress and stiffness changes in the ground, prior to support application;
6. the interactive nature of the load transfer process developed between the soil and the support.

The decision to include these factors in the development of the projected design procedure lies in the fact that they have an important role in most, if not all, shallow tunnel cases. Those factors, that are sometimes influential in one instance but not in others, had to be set aside, and, perhaps studied separately.

Accordingly, in order to render the problem tractable and yet to ensure some generality, it was decided to limit the development to full face excavated circular tunnels, under time independent conditions, in situations not involving ground failure, shear dilatancy and post peak

softening, among others.

The finite element method was selected as an appropriate modelling tool to derive the projected method. A fairly extensive review of previous studies on shallow tunnel modelling using that method was undertaken. Through it, the ability and limitations of this method to portray shallow tunnel performance was critically assessed. This review led to the adoption of a simple two dimensional finite element code developed and tested earlier in this University for analyses of retained excavations. The program was adapted and implemented for the present project, where the soil behaviour is described by a non-linear elastic stress-strain relationship (the hyperbolic model).

Through this program, tunnel construction is represented in stages and the delayed lining installation and associated stress transfers are represented by a partial release of the ground in situ stresses. This two dimensional simulation mimics the three-dimensional stress changes by the introduction of an additional variable, the amount of stress release, α. Three well documented case histories in which good ground control conditions were present, were used to test this numerical solution. It was proved that good estimates of the final displacement field and lining loads are obtained whenever the factor, α, is appropriately selected. Like similar codes, this program seems useful only for the prediction of pre-failure responses. It is evident that there is a need to develop numerical modelling

techniques that portray the ground response for conditions approaching collapse with the formation of shear strain concentrations.

The main limitation of the selected simulation technique is the need for an independent estimate of the amount of stress release taking place before support activation. However, if this stress release was univocally related to the ground displacement, then an estimate of the latter, including the three-dimensional effects of an advancing tunnel, could be sought as an alternative approach to the solution of this problem.

The need to develop a procedure to estimate the amount of tunnel closure at the section at which the support is activated was thus justified and undertaken through parametric three-dimensional finite element analyses. An approximate solution for estimating the closure of an unlined shallow tunnel in an elastic medium was proposed. It allows estimates of radial displacements at three points of the tunnel contour, for different sections at or behind the face. These analyses also allowed simplified solutions to be obtained for estimates of the maximum horizontal displacement of the tunnel face and of the maximum longitudinal distortions for the ground surface and the subsurface ahead of the face.

This approximate method for estimating convergence was used to predict radial displacements for comparison with observed values in a large number of case histories. It was

shown that it can yield sensible results whenever good ground control conditions are specifed and implemented in tunnel construction. Furthermore, it was shown that the method can be successfully applied to NATM construction schemes regardless of the soil type (but provided the face is stable), and to TBM or shielded schemes in firm grounds or even in less stable soils, whenever the overcut is small and the lining is activated in full contact with the ground at a short distace from the face. For conditions different from the above, the simplified method yielded poorer results. Improvements to its predictive capabilities could be attempted in the future by incorporating the non-linear ground behaviour and by accounting for the support installation, both of which are presently neglected.

To validate the proposed approach, the above approximate method was tested against results from the two dimensional modelling of the three case histories studied. By combining the estimates of the radial displacements at the tunnel contour from this method, with ground reaction curves obtained by the two dimensional modelling, reasonable estimates of the amount of stress release at the instant of lining activation were obtained.

The above approach requires the use of a 2D finite element program to generate stress-displacement curves from which it is possible to assess the amount of stress release. The survey of practice presented in Chapter 4 showed that this may represent an inconvenience since this type of

analysis is not always used in routine practice. Accordingly, an attempt was made to develop a procedure which would allow these stress-displacement relationships to be obtained without the need for further finite element analyses. Parallel to this development, an attempt was made to obtain the relevant ground displacement associated with the reduction of the ground stresses, representing the tunnel construction in a two-dimensional simulation.

To achieve these aims, some additional simplifications were introduced into the 2D finite element model presented in Chapter 5. These simplifications led to the establishment in Chapter 6 of two non-linear elastic stress-strain models: the frictionless model representing an undrained soil response, and the cohesionless soil model representing a drained response. These models exhibit stress-strain relationships presenting the property of homothety, which allows these relationships to be normalized into unique stress-strain curves. Moreover, this property causes the response of geometrically homothetic tunnels to become unique when this response is conveniently normalized. These findings facilitated the generalization of results through the similitude they show, as they become independent of the scale of the problem.

Through parametric numerical modelling, the role of each variable affecting the response of unlined tunnels was investigated. Finally, generalized normalized ground reaction curves (NGRC or λ curves) were obtained for points

at the crown, springline and floor of a shallow tunnel, and were presented as equations and charts. The limits of this generalization were identified. The partial derivatives of the NGRC (λ' curves) were related to the ground stiffness at any stage of the tunnel unloading process. The two sets of curves (λ and λ') thus allow estimates of the amount of ground stress relaxation and ground stiffness degradation for any amount of tunnel closure defined by the dimensionless radial displacement, U, taking place at the section where the support is activated. These solutions allowed such estimates to be made for ranges of geometric and geotechnical conditions that were shown to cover most of the cases likely to be encountered in practice. The solutions also permitted some extrapolation of data beyond the ranges of conditions which had been focused on, though considerable care should be taken in this regard.

Parallel with the development of these generalized solutions, normalized subsurface and surface ground displacement distributions were obtained for different amounts of stress relaxation associated with a given amount of tunnel closure.

The soil-lining interaction phase of the shallow tunnel problem was addressed in Chapter 7. Once more, to avoid the need of finite element modelling in the development of the projected design procedure, preference was given to the use of a linear elastic, closed form solution that treats this problem, with full account of the non-uniform stress field

existing in a shallow tunnel, including the effect of gravity. This analytical solution was adapted to take into consideration the effects of the delayed lining installation, represented by the stress relaxation and ground stiffness degradation. These were accounted for through the use of a reduced unit weight of the soil and a reduced ground stiffness, calculated from the normalized ground reaction curves and their derivative functions. The tangent stiffness of the ground was assumed to be uniquely related to the tunnel radial closure. This and other simplifying assumptions were carefully assessed and their consequences evaluated through 2D finite element simulations.

It was demonstrated that adequate and safe estimates of final lining loads and displacements can be obtained by combining the generalized solution for non-linear ground response, with the analytical solution for soil-lining interaction. For this, it is sufficient to estimate the ground stress relaxation prior to lining activation and the ground stiffness at the final lining-ground equilibrium condition. Since the equilibrium condition is not known beforehand, a simple iterative procedure was devised to solve this problem.

The present development could also be of some help, if, alternatively the soil-lining interaction analysis were done through the use of ring - and - spring solutions reviewed in Chapter 4. With them, the non-uniform degradation of the

ground stiffness around the tunnel contour could be taken into consideration.

Regarding the effect of the lining on the ground movements, parametric finite element studies revealed that the unlined tunnel analyses, with a crown displacement equal to the final crown settlement calculated in the lined tunnel case, furnished settlement distribution similar, yet slightly conservative, to those found in the latter case. Thus, the normalized settlement distribution obtained in the parametric analyses can be used for settlement prediction. It is sufficient to calculate the amount of stress release in the unlined tunnel solution, causing the same crown displacement obtained in the lining-ground interaction analysis. This is easily assessed through the generalized ground reaction curves for the tunnel crown.

With these developments, the aims described in point (c), given earlier in this chapter, were fulfilled. The following point, (d), required that the findings accumulated so far be organized in a comprehensive manner to enhance their use in practice. Appropriately, a flow chart was prepared to serve as a guide for using the presently proposed design procedure (Figure 7.9). Each step of the procedure was presented and discussed, with emphasis being given to the assessment of its applicability.

Moreover, to facilitate the calculations involved in the design sequence suggested, a set of calculation sheets was prepared, and an example was worked. It was shown that

all calculations are simple and easy to program, therefore allowing quick on-site re-evaluation of any design step during tunnel construction. Thus, the method can be applied and calibrated simultaneously with field monitoring serving as an auxilary tool for decisions being made during construction. Furthermore, at the design stage, the method allows sensitivity analyses to be undertaken, where the variability of ground conditions, construction procedures, geometric conditions, etc. can be taken into account. Accordingly, the expected ranges of ground and lining responses could be defined. The last point to be addressed, (e), referred to the validation of the proposed design procedure. This was also undertaken in Chapter 7, where the method was verifed against results of plane strain centrifuge model tests of a shallow tunnel. It was also tested against available results of a 3D finite element analysis in which the ground was represented by a hyperbolic stress-strain relationship. In both cases, very favourable results were obtained.

Finally, the proposed method was verifed against a large number of actual case histories. These always involved good ground control conditions, reflected either by good construction quality or simply good ground quality. In order to test the performance of the method in actual practice, some of the case histories included conditions that deviated considerably from those originally set up in the development of the method. These conditions were represented by

tunnelling below the water table with partial consolidation of the soil mass, construction involving the use of compressed air, staged excavation of the tunnel face with a temporary invert in the heading excavation, non-circular tunnel profiles, mixed face conditions. Additional approximations were introduced to account for these distinct features. Despite this, the calculation method yielded sensible results, both in terms of ground and lining responses. Noted discrepancies were duly explained in terms of the limitations of the method.

It should be pointed out that in all applications, no attempt was made to best fit or to bound the observed performances. These tests were not back analyses of prototypes, as it was assumed that all parameters and variables governing the tunnel response were known and supposedly represented the most probable conditions found in each case.

A global assessment of the results obtained was undertaken and the ability of the proposed procedure to predict tunnel performance was carefully investigated (Table 7.11 and Figure 7.51).

This comparative exercise covered both shielded and unshielded tunnels, different support support systems and lining stiffnesses, a wide range of geometric conditions and a fairly wide range of soil types. This study revealed that for a quick lining-ground interaction analysis, it may be sufficient to assume a 50% reduction in the ground in situ

stresses and in the in situ tangent ground stiffness, provided the ground control conditions are comparable to those found in the cases studied.

It was suggested that the proposed calculation method seems to provide reasonable predictions of the tunnel performances, whenever the factor of safety of the ground at the section the support is activated, is within or above the calculated range factors found in these cases (from 1.2 to 2.0). The final dimensionless crown displacement, U, was found to vary between 0.5 and 1.0, and according to the criterion set up earlier in Chapter 2, this confirms that ground control conditions were good and high shear strain concentrations in the ground were minimized or avoided. It was suggested that quick, and possibly, conservative estimates of the final crown displacement under these tunnelling conditions, could therefore be performed by making U=1.0.

Except for the width of the settlement trough or the maximum ground surface distortion, the proposed design procedure yielded performance predictions that either matched or overestimated the observed behaviour. The surface distortions were underestimated in the majority of cases. To compensate for this not unexpected and unsafe trend, a correction factor was empirically introduced. Accordingly, a semi-empirical correction was also suggested for the assessment of the width of the surface settlement profile. In both cases, the proposed corrections improved the

predictions, making them closer to the observed performances.

With this, the aims of the present research project have been fulfilled. Suggestions for future research work have been presented in this chapter and in the summary sections of other chapters. Moreover, it is believed that the present approach could be extended to other conditions not covered by this work, such as twin tunnels and non-circular tunnel profiles.

REFERENCES

Abbiss, C.P., 1986. The effects of damping on the interpretation of geophysical measurements. Geotechnique 36, No. 4, pp. 565-580.

Ahrens, H. 1976. Geometrisch und physikalisch nichtlineare Stabelemente zur Berechnung von Tunnelauskeidungen. Bericht aus dem Institut fur Statik der Technischen Universitat Braunschweig Nr. 76-14, 110p.

Ahrens, H., Lindner, E. and Lux, K.H. 1982. Zur Dimesionierung von Tunnelausbauten nach den Empfehlungen zur Berechnung von Tunneln im Lockergestein (1980). Die Bautechnik, 59, pp. 260-273; 303-311 (see also 'Taschenbuch fur den Tunnelbau' 1983, Verlag Gluckauf, Essen).

Almeida, M.S.S. and Pereira, P.R., 1978. Consideracoes Relativas a aplicacao de elementos finitos a problemas de Escavacoes Subterraneas profundas. Proceedings 6th Brazilian Congress of Soil Mechanics and Foundation Engineering (Rio de Janeiro), pp 1-19.

Amberg, W.A. and Lombardi, G., 1974. Une method de calcul elasto-plastique de l'etat de tension et de deformation autour d'une cavite souterraine. Proceedings 3rd Congress of the International Society for Rock Mechanics (Denver), pp.1055-1060

Amstad, C. and Kovari, K. 1984. Strain monitoring in the subsoil of the Munich subway. Proceedings of the 2nd Conference on Mass Transportation in Asia (Singapore).

Andraskay, E. and Attinger, R., 1979. Behaviour of the prefabricated lining in shield driven tunnels (in German). Proceedings of the 4th International Congress on Rock Mechanics (Montreux), Vol. 2, pp 9-15.

Andraskay, E., Hofmann and Jemelka, p., 1972. Berechnung der Stahlbetontubbinge fur den Heitersbergtunnel, Los West. Schweizerische Bauzeitung, 90 Jahrgang, Heft 36 (September), pp. 864-868.

Atkinson, J.H., 1981. Foundations and slopes, An introduction to applications of critical state soil

mechanics. Halsted Press - John Wiley and Sons, New York, 382 p.

Atkinson, J.H. and Bransby, P.L., 1978. The mechanics of soils, An introduction to critical state soil mechanics. McGraw-Hill Book Co. (U.K.), London, 375 p.

Atkinson, J.H., Brown, E.T. and Potts, D.M., 1975. Collapse of shallow unlined circular tunnels in dense sand. Tunnels and Tunnelling, May, pp. 81-87.

Atkinson, J.H., Brown, E.T. and Potts, D.M., 1977. Ground movement near shallow model tunnels in sand. In Proceedings Conference of Large Ground Movement and Structures. Cardiff, United Kingdom, pp. 372-387.

Atkinson, J.H. and Cairncross, A.M., 1973. Collapse of a shallow tunnel in a Mohr-Coulomb material. Proceedings of the Symposium on the Role of Plasticity in Soil Mechanics, Cambridge, pp. 202-206.

Atkinson, J.H., Cairncross, A.M. and James, R.G., 1974. Model tests on shallow tunnel in sand and clay. Tunnels and Tunnelling, July, pp. 28-32.

Atkinson, J.H. and Mair, R.J., 1981. Soil mechanics aspects of soft ground tunnelling, Ground Engineering (July), pp. 20-26 and 38.

Atkinson, J.H. and Mair, R.J., 1983. Loads on leaking and watertight tunnel linings, sewers and buried pipes due to groundwater. Geotechnique 33, No. 3, pp. 341-344.

Atkinson, J.H., Orr, T.L.L. and Potts, D.M., 1975. Research studies into the behaviour of tunnels and tunnel linings in soft ground . TRRL Supplementary Report 176 UC.

Atkinson, J.H. and Potts, D.M. 1977(a). Subsidence above shallow tunnels in soft ground. Journal of the Geotechnical Engineering Division - American Society of Civil Engineers, Vol. 103, pp.307-325.

Atkinson, J.H. and Potts, D.M., 1977(b). Stability of a shallow circular tunnel in cohesionless soil.

Geotechnique, Vol. 27, No. 2, pp. 203-215.

Atkinson, J.H., Potts, D.M. and Schofield, A.N., 1977. Centrifugal model tests on shallow tunnels in sand. Tunnels and Tunnelling, January, Vol. 9, No.1, pp. 59-64.

Attewell, P., 1977. Ground movements caused by tunnelling in soil. In: Large Ground Movements and Structures (edited by J.D. Geddes), Pentech, London, pp. 812-948.

Attewell, P.B. and Farmer, I.W., 1974(a). Ground deformation resulting from shield tunnelling in London clay. Canadian Geotechnical Journal, Vol. 11, pp. 380-395.

Attewell, P.B. and Farmer, I.W., 1974(b). Ground disturbance caused by shield tunnelling in a stiff overconsolidated clay. Engineering Geology, 8:4, pp. 361-381.

Attewell, P.B. and Farmer, I.W., 1975. Ground settlement above shield driven tunnels in clay. Tunnels and Tunnelling, Vol. 7, No.1, pp. 58-62.

Attewell, P.B. and Woodman, J.P., 1982. Predicting the dynamics of ground settlement and its derivatives caused by tunnelling in soil. Ground Engineering, Vol. 15, No.8, pp. 13-22 and 36.

Attewell, P.B. and Yeates, J., 1984. Tunnelling in soil. In: Ground Movements and their Effects on Structures. Edited by P.B. Attewell and R.K. Taylor (Surrey University Press), pp. 132-215.

Attewell, P.B. and Yeates, J. and Selby, A.R., 1986. Soil movements induced by tunnelling and their effects on pipelines and structures. Blackie and Son (Glasgow), 325 p.

Azevedo, N., 1983. Personal Communication.

Azevedo, N., 1985. Medidas das deformacoes do solo ao redor de tunnel em Shield em Sao Paulo. Anais do 2.° Simposio Sobre Excavacoes Subterraneas - ABGE (Rio de Janerio).

Babendererde, S., 1976. Tunnelvortrieb mit Messerschild und Sprizbetonausbau. Forschung+Praxis (STUVA), Band 19, pp.50-55.

Babendererde, S., 1986. Extruded concrete lining. Proceedings of the International Congress on Large Underground Openings, ITA (Firenze), Vol.I, pp. 607-611.

Baker, W.H., Cording, E.J. and MacPherson, H.H., 1983. Compaction grouting to control ground movements during tunnelling. Underground Space, Vol. 7, pp. 205-212.

Balla, A., 1963. Rock pressure determined from shearing resistance. Proceedings European Conference on Soil Mechanics and Foundation Engineering (Budapest), pp.461-471.

Barla, G. and Ottaviani, M., 1974. Stresses and displacements around two adjacent circular openings near to the ground surface. Proceedings 3rd Congress of the International Society for Rock Mechanics (Denver), Vol. II, part B, pp. 975-980.

Barlow, J.P., 1986. Interpretation of tunnel convergence measurements. M.Sc. Thesis, University of Alberta. 235 p.

Barlow, J.P. and Kaiser, P.K., 1987. Interpretation of tunnel convergence measurements. Proceedings 6th Congress of the International Society for Rock Mechanics (Montreal).

Barratt, D.A. and Tyler, R.G., 1976. Measurements of ground movement and lining behaviour on the London underground at Regents Park. TRRL Laboratory Report 684 (UK).

Bathe, K.J., 1977. Static and dynamic geometric and material nonlinear analysis using ADINA. Report 82448-2, Massachusetts Institute of Technology, 240 p.

Bathe, K.J., 1978. ADINA: A finite element program for automatic dynamic incremental nonlinear analysis. Report 82448-1, Massachusetts Institute of Technology, 385 p.

Baudendistel, M., 1972. Wechselwirkung von Tunnelauskleidung und Gebirge. Veroffentlichungen des Institutes fur Bodenmechanik und Felsmechanik der Universitat Fridericiana, Karlsruhe, Heft 51, 1972. (English translation by BRE, U.K.).

Baudendistel, M., 1973. Zur Bemessung von Tunnelauskleidungen in wenig festem Gebirge. Rock Mechanis, Supplementum 2 (1973), pp.279-312.

Baudendistel, M., 1974. Abschatzung der Seitendruckziffer λ und deren Einfluss auf den Tunnel. Rock Mechanics, Supplementum 3 (1974), pp. 89-96.

Baudendistel, M., 1979. Zum Entwurf von Tunneln mit grossem Ausbruchquerschnitt. Rock Mechanics (Springer, Vienna), Suppl. 8., pp.75-100.

Baudendistel, M., 1984. Die Bedeutung der freien Stutzweite im Tunnelbau. Felsbau 2, Nr.2, pp. 78-83.

Baudendistel, M., 1985. Significance of the unsupported span in tunnelling . Proceedings Tunnelling '85 (Brighton). The Institution of Mining and Metallurgy, pp. 103-109.

Bauernfeind, P., Gartung, E. and Adams, F.J., 1986. Large subway tunnel cross sections at Nuremberg. Proceedings of the International Congress on Large Underground Openings, ITA, (Firenze), Vol. I, pp. 634-643.

Bauernfeind, P., Muller, F. and Muller, L. 1978. Tunnelbau unter historischen Gebauden in Nurnberg. Rock Mechanics (Springer, Vienna), Suppl. 6, pp. 161-192.

Baumann, T., 1985. Messung der Beanspruchung von Tunnelschalen. Bauingenieur 60, pp. 449-454.

Baumann, T., Sulke, B-M. and Trysna, T., 1985. Einsatz von Messung und Rechnung bei Spritzbetonbauweisen im Lockergestein. Bautechnik, 10, pp.330-337 und 11, pp. 368-374.

Belshaw, D.J. and Palmer, J.H.L., 1978. Results of a program of instrumentation involving a precast segmented

concrete-lined tunnel in clay. Canadian Geotechnical Journal, Vol. 15, No.4, November, pp.573-583.

Berest, P. and Nguyen, M.D., 1979. Etude en grandes deformations de la contraction et de l'expansion de cylindres creux de revolution elastoplastiques avec radoucissement. Journal de Mecanique Applique, Vol. 3, No. 4, pp. 463-487.

Berest, P., Nguyen Minh, D. and Panet, M., 1978. Contribution a l'etude de la stabilite d'une cavite souterraine dans un milieu avec radoucissement. Revue Francaise de Geotechnique No. 4 (Juin), pp. 65-72.

Bevington, P.R., 1969. Data reduction and error analysis for physical sciences, McGraw-Hill, 336 p.

Bierbaumer, A., 1913. Die Dimensionerung des Tunnelmauerwerks, Engelmann (Leipzig) (quoted by Steiner and Einstein, 1980).

Bishop, A.W., 1966. The strength of soils as engineering materials. 6th Rankine Lecture, Geotechnique Vol. 16, No. 2, pp.91-128.

Bishop, A.W. and Bjerrum, L., 1960. The relevance of the triaxial test to the solution of stability problems. Proceedings of American Society of Civil Engineers Reseach Conference on Shear Strength of Cohesive Soils (Boulder), pp. 437-501.

Bishop, A.W., Webb, D.L. and Lewin, P.I., 1965. Undisturbed samples of London clay from the Ashford Common shaft; strength-effective stress relationships. Geotechnique, Vol.15, No.1, pp.1-31.

Bishop, A.W. and Wesley, L.D., 1975. A hydraulic triaxial apparatus for controlled stress path testing. Geotechnique, Vol.25, No.4, pp.657-670.

Bjerrum L., and Eide, O., 1956. Stability of strutted excavations in clay. Geotechnique, Vol.6, No.1, pp.32-47.

Blight, G.E., 1986. Pressures exerted by materials stored in silos: part I, coarse materials. Geotechnique 36, No.1, pp.33-46.

Blight, G.E., 1986. Pressures exerted by materials stored in silos: part II, fine powders. Geotechnique, 36, No.1, pp.47-56.

Blindow, F.K., Edeling, H. and Hofmann, H., 1979. Engstenhende tunnel und deren Verschneidungen. Bauingenieur, 54, pp.213-221.

Blindow, F.K. and Wagner, H., 1978. Grenzfalle bei der Anwendung der Neuen Osterreichischen Tunnelbauweise am Beispiel des Pfaffensteiner Tunnels. Forschung+Praxis (Alba, Dusseldorf), 21, pp.30-36.

Boden, J.B. and McCaul, C., 1974. Measurement of ground movements during a bentonite tunnelling experiment. TRRL Laboratory Report 653 (U.K.)

Bolton, M., 1979. A Guide to Soil Mechanics. MacMillan Press. 439p.

Brady, B.H.G. and Brown, E.T., 1985. Rock Mechanics for Underground Mining. George Allen and Unwin (London) 527p.

Branco, P., 1981. Behaviour of a shallow tunnel in till. M.Sc. Thesis, Department of Civil Engineering, University of Alberta, 351p.

Branco, P., 1987. Ph.D. Thesis in prepartion. University of Alberta.

Branco, P. and Eisenstein, Z., 1985. Convergence-confinement method in shallow tunnels. Proceedings of the 11th International Conference on Soil Mechanics and Foundation Engineering, Section 8 (San Francisco).

Brandt, J.R.T., 1985. Behaviour of soil-concrete interfaces. Ph.D. Thesis, University of Alberta, 376 p.

Brebbia, C.A., 1978. The Boundary Element Method for Engineers. Pentech Press, 189p.

Brem, G., 1981. U-Bahnhof Schweizer Platz in Frankfurt am Main: Berechnungs-und Messergebnisse fur die dreischiffige unteridisch aufgefahrene Bahnhofshalle. Forschung+Praxis (Berlin), 27, pp.137-146.

Breth, H. and Chambosse, G., 1975. Settlement behaviour of buildings above tunnels in Frankfurt clay. Proceedings of the Conference on Settlement of Structures, Pentech Press, London, pp.329-336.

Britto, A.M. and Kusakabe, O., 1985. Upperbound mechanisms for undrained axisymmetric problems. Proceedings of the 5th International Conference on Numerical Methods in Geomechanics (Nagoya), pp.1691-1698.

Broms, B., 1978. Subsidence due to seepage to tunnels in rock. Proceedings of the International Conference on Evaluation and Prediction of Subsidence (Pensacola Beach).

Broms, B.B. and Bennermark, H., 1967. Stability of clay at vertical openings. Journal of the Soil Mechanics and Foundaticns Division, American Society of Civil Engineers, Vol.93, pp.71-94.

Brown, E.T., Bray, J.W., Ladanyi, B. and Hoek, E., 1983. Ground response curves for rock tunnels. Journal of Geotechnical Engineering, American Society of Civil Engineers, Vol. 109, pp.15-39. (Discussion with corrections on the original paper in the same journal, January, 1984, pp.140-141.

Bull, A., 1946. Stresses in the linings of shield-driven tunnels. American Society of Civil Engineers, Proceedings, Nov. 1944.

Burland, J.B. and Fourie, A., 1985. The testing of soils under conditions of passive stress relief. Geotechnique, Vol. 35, No.2, pp.193-198.

Burland, J.B. and Wroth, C.P., 1974. Allowable and differential settlements of structures including

drainage and soil-structure interaction. Proceedings of the Conference on Settlement of Structures, Pentech Press, London, pp.611-764.

Burns, J.Q. and Richard, R.M., 1964. Attenuation of stresses for buried cylinders. Proceedings of the Symposium on Soil-Structure Interaction. Tucson, pp. 378-392.

Byrne, P.M. and Eldridge, T.L., 1982. A three parameter dilatant elastic stress-strain model for sand. Proceedings of the International Symposium on Numerical Methods in Geomechanics. (Zurich), pp.73-80.

Byrne, P.M. and Janzen, W., 1984. INCOIL: A computer program for nonlinear analysis of stresses and deformations in oil sand masses. Report to the Alberta Oil Sands Technology and Research Authority, 104p.

Cairncross, A.M., 1973. Deformations around model tunnels in stiff clay. Ph.D. Thesis, Cambridge University.

Calladine, 1969. Engineering Plasticity (U.K.).

Capellari, G. and Ottaviani, M., 1982. Predicted surface settlements due to shield tunnelling with compressed air. Proceedings of the 4th International Conference on Numerical Methods in Geomechanics. (Edmonton), Vol.2, pp.531-536.

Caquot, A., 1934. Equilibre des Massifs a Frottement Interne, Gauthier-Villars (Paris).

Caquot, A. and Kerisel, J., 1956. Traite de Mecanique des Sols. Gauthier-Villars (3^{e} Edition).

Carder, D.R., Ryley, M.D. and Symons, I.F., 1985. Ground movements caused by deep trench construction in Boulder clay and their effect on an adjacent service pipeline. Proceedings of the 3rd International Conference on Ground Movements and Structures (Cardiff), pp.3-23.

Carter, J.P. and Booker, J.R., 1982(a). The analysis of consolidation and creep around a deep circular tunnel in clay. Proceedings of the 4th International Conference on

Numerical Methods in Geomechanics, (Edmonton), Vol.2, pp.537-544.

Carter, J.P. and Booker, J.R., 1982(b). Elastic consolidation around a deep circular tunnel. International Journal for Solids and Structures, Vol.18, No.12, pp.1059-1074.

Carter, J.P. and Booker, J.R., 1983. Creep and consolidation around circular openings in infinite media. International Journal for Solids and Structures, Vol.19, No.8, pp.663-675.

Carter, J.P. and Booker, J.R., 1984. Elastic consolidation around a lined circular tunnel. International Journal for Solids and Structures, Vol.20, No.6, pp.589-698.

Casarin, C., 1977. Soil deformations around tunnel headings in clay. M.Sc. Thesis, Cambridge University.

Casarin, C. and Mair, R., 1981. The assessment of tunnel stability in clay by model tests. Soft-Ground Tunnelling, Failures and Displacements (Ed. D. Resendiz and M.P. Romo), A.A. Balkema (Rotterdam), pp.33-44.

Chambosse, G., 1972. Das Verformungsverhalten des Frankfurter Tons beim Tunnelvortrieb - Berichte uber Messungen in der Frankfurter Innenstadt. Mitteilungen der Versuchsanstalt fur Bodenmechanik und Grundbau der Technischen Hochschule Darmstadt, Heft 10.

Chan, D., 1985. Finite element analysis of strain-softening materials. Ph.D. Thesis. Department of Civil Engineering, University of Alberta, Edmonton, Alberta. 355p.

Chan, A.C.Y. and Morgenstern, N.R., 1986. Measurement of lateral stresses in a lacustrine clay deposit. Proceedings of the 39th Canadian Geotechnical Conference (Ottawa), pp.285-290.

Chandrasekaran, V.S. and King, G.J.W., 1974. Simulation of excavation using finite elements. Journal of the Geotechnical Engineering Division. ASCE GT9, pp.1086-1088.

Chang, C.Y. and Duncan, J.M., 1970. Analysis of soil movement around a deep excavation. Journal of the Soil Mechanics and Foundation Division, ASCE, Vol.96, SM5, pp.1655-1679.

Chen, W.F. and Saleeb, A.F., 1982. Constitutive Equations for Engineering Materials. Volume 1: Elasticity and Modelling. John Wiley & Sons, 580 p.

Christian, J.T., 1982. The application of generalized stress-strain relations. In: Application of Plasticity and Generalized Stress-Strain in Geotechnical Engineering (edited by R.N. Yong and E.T. Selig), American Society of Civil Engineers, pp.182-204.

Christian, J.T. and Wong, I.H., 1973. Errors in simulating excavation in elastic media by finite element. Soils and Foundation, Vol.13, No.1, pp.1-10.

Clayton, C.R.I. and Khatrush, S.A., 1986. A new device for measuring local axial strains on triaxial specimens. Geotechnique, Vol. 36, No. 4, pp.593-597.

Clough, G.W. 1980. Advanced soil and soft rock tunneling technology in Japan. Stanford University Technical Report No. CE-252.

Clough, G.W., 1981. Innovations in tunnel construction and support techniques. Bulletin of the Association of Engineering Geologists, Vol. XVIII, No.2, pp.151-167.

Clough, G.W. and Schmidt, B., 1981. Design and performance of excavations and tunnels in soft clay. In: Soft Clay Engineering (edited by E.W. Brand and R.P. Brenner), Elsevier, pp.569-634.

Clough, C.W., Shirasuna, T. and Finno, R.J., 1985. Finite element analysis of advanced shield tunnelling. Proceedings of the 5th International Conference on Numerical Methods in Geomechanics (Nagoya), pp.1167-1174.

Clough, G.W., Sweeney, B.P. and Finno, R.J., 1983. Measured soil response to EPB shield tunneling. Journal of Geotechnical Engineering Division of the ASCE, Vol. 109,

No. 2, pp.131-149.

Clough, G.W. and Tsui, Y., 1977. Static analysis of earth retaining structures. In: Numerical Methods in Geotechnical Engineering (edited by C.S. Desai and J.T. Christian), McGraw Hill, pp.506-527.

Corbett, I., 1984. Load and displacement variation along a tunnel. M.Sc. Thesis. Department of Civil Engineering, University of Alberta, Edmonton, Alberta, 246p.

Cording, E.J. and Hansmire, W.H., 1975. Displacements around soft ground tunnels. Proceedings of the 5th Pan-American Conference on Soil Mechanics and Foundation Engineering, Buenos Aires, Vol.4, pp.571-633.

Cording, E.J., Hansmire, W.H., MacPherson, H.H., Lenzini, P.H. and Vonderohe, A.P., 1976. Displacement around tunnels in soil. Report DOT-TST 76T-22, National Technical Information Service (Springfield, Virginia).

Cording, E.J., O'Rourke, T.D. and Boscardin, M., 1978. Ground movements and damage to structures. Proceedings of the International Conference on Evaluation and Prediction of Subsidence (Pensacola Beach) pp.516-537.

Costa, F.M., de Mariano, M., Monteiro, J.T. and Kira, Y., 1974. Passagem dos shields sob o Viaduto Boa Vista, observacoes de movimento da Estrutura. Anais do 5.º Congresso Brasileiro de Mecanica dos Solos (Sao Paulo), Vol. I, pp.323-338.

Costa-Filho, L.M., 1980. A laboratory investigation of the small strain behaviour of London Clay. Ph.D. Thesis, University of London.

Costa-Filho, L.M., 1984. A note on the influence of fissures on the deformation characteristics of London clay. Geotechnique, Vol.34, No.2, pp.268-272.

Cox, A.D., 1963. The use of non-associated flow rules in soil plasticity. R.A.R.D.E. Rep (B) 263. (Quoted by Davis, 1968:345).

Craig, R.N. and Muir Wood, A.M., 1978. A review of tunnel lining practice in the United Kingdom. Department of the Environment, Department of Transport, TRRL Supplementary Report 335: Crowthorne, (Transport and Road Research Laboratory).

Crofts, J.E., Menzies, B.K. and Tarzi, A.I., 1977. Lateral displacements of shallow buried pipelines due to adjacent deep trench excavations. Geotechnique, Vol. 27, No.2, pp.161-179.

Crofts, J.E., Menzies, B.K. and Tarzi, A.I., 1978. Discussion: Lateral displacements of shallow buried pipelines due to adjacent deep trench excavations. Geotechnique, Vol.28, No.2, pp.217-220.

Cruz, H.J.V., Couto, J.V.S., Hori, K., Salvoni, J.L. and Ferrari, O.A., 1982. Os tuneis do prolongamento norte - uma primeira avaliacao do NATM em area urbana. Proceedings 'Simposio sobre Escavacoes Subterraneas', Rio de Janeiro, published by ABGE - Brazilian Association of Engineering Geology), pp.297-316.

Cruz, H.J.V., Hori, K., Ferrari, O.A. and Ferreira, A.A., 1985. A construcao em NATM e em area urbana, de um tunel de grande secao - O tunel de Via dupla do Prolongamento Norte. Proceedings of the 2nd Symposium on Underground Excavation (ABGE), Vol. 1, pp.391-411 (Rio de Janeiro).

Curtis, D.J., 1974. Visco-elastic tunnel analysis. Tunnels and Tunnelling. November, pp.38-39.

Curtis, D.J., 1976. The circular tunnel in elastic ground. Discussion. Geotechnique, Vol.26, pp.231-237.

Daemen, J.J., 1975. Tunnel support loading by rock failure. Ph.D. Thesis. Department of Civil Engineering, University of Minnesota, Minnesota.

Daemen, J.J. and Fairhurst, C., 1970. Influence of failed rock properties in tunnel stability. 12th Symposium on Rock Mechanics. Rolla, Missouri, pp.855-875.

Daemen, J.J. and Fairhurst, C., 1972. Rock failure and tunnel support loading. Proceedings of the International

Symposium on Underground Openings, Lucerne, pp.356-369.

Dar, S.M. and Bates, R.C., 1974. Stress analysis of hollow cylindrical inclusions. Journal of the Geotechnical Engineering Division, ASCE, Vol.100, No. GT2, February, pp.123-138.

Davis, E.H., 1968. Theories of soil plasticity and the failure of soil masses. Soil Mechanics: Selected Topics. Ed. Lee, I.K., pp.341-380, Butterworth.

Davis, E.H., Gunn, M.J., Mair, R.J. and Seneviratne, H.N., 1980. The stability of shallow tunnels and underground openings in cohesive material. Geotechnique 30, No.4, pp.397-416.

Deere, D., Peck, R.B., Monsees, J.E. and Schmidt, B., 1969. Design of tunnel liners and support systems, Report No. PB-183799 (NTIS - National Technical Information Service, U.S. Department of Commerce, Springfield, VA 22161).

DeLory, F.A., Crawford, A.M. and Gibson, M.E.M., 1979. Measurements on a tunnel lining in very dense till. Canadian Geotechnical Journal, Vol.16, pp.190-199.

Desai, C.S. and Abel, J.F., 1972. Introduction to the Finite Element Method. A numerical method for engineering analysis. van Nostrand Reinhold Comp., New York.

Descoeudres, F., 1974. Analyse tridimensionelle de la stabilite d'un tunnel au voisinage du front de taille dans une roche elasto-plastic. Proceedings 3rd. Congress of the International Society for Rock Mechanics, Denver, Vol.II-B, pp. 1130-1135.

Detournay, E. and Fairhurst, C., 1982. Generalization of the ground reaction curve concept. Proceedings of the U.S.A. Rock Mechanics Symposium, pp. 924-934.

DGEG - Deutsche Gesellschaft fur Erd- und Grundbau e.V. 1979. Empfehlungen fur den Felsbau Untertage. In; Taschenbuch fur den Tunnelbau 1980. Verlag Gluckauf Essen, pp. 157-239.

Dickin, E.A. and King, G.J.W., 1982. The behaviour of hyperbolic stress-strain models in triaxial and plane strain compression. Proceedings of the International Symposium on Numerical Models in Geomechanics (Zurich), pp.303-311.

Diniz, R.A.D.C., 1978. Schnittgrossen in kreisformigen und elliptischen Tunnelwandungen aus Beton. Dissertation, TU Munchen, Nov.

Dodge, C.W., 1972. Euclidean geometry and transformations. Addison-Wesley Publishing Company, 295 p.

Domaschuk, L. and Valliappan, P., 1975. Nonlinear settlement analysis by finite element. Journal of the Geotechnical Engineering Division, ASCE, Vol.101, No. GT7, pp.601-614.

Domaschuk, L. and Wade, N.H., 1969. A study of bulk and shear moduli of sand. Journal of the Soil Mechanics and Foundations Division, ASCE, Vol. 95, No. SM2, pp. 561-581.

Duddeck, H., 1972. Zu den Berechnungsmethoden und zur Sicherheit von Tunnelbauten. Bauingenier 47. H.2, pp.43-52.

Duddeck, H., 1973. Schildvorgetriebene Tunnel, Entwicklungstendenzen in Forschung and Ausfuhrung. Rock Mechanics, Supplementum 2, pp.257-278.

Duddeck, H., 1980(a). Empfehlungen zur Berechnung von Tunneln im Lockergestein (1980). Die Bautechnik, 10, pp.349-356.

Duddeck, H., 1980(b). On the basic requirements for applying the Convergence Confinement Method. Underground Space, Vol.4, No.4, pp.241-247.

Duddeck, H., 1981, Views on structural design models for tunnelling. Synopsis of answers to a questionnaire (ITA). Advances in Tunnelling Technology and Subsurface Use. Vol.2, No.3, pp.155-228.

Duddeck, H. and Erdmann, J., 1982. Structural design models for tunnels. Proceedings, Tunnelling '82 (edited by M.J. Jones), The Institution of Mining and Metallurgy, London, pp. 83-91.

Duddeck, H. and Erdmann, J., 1985. On structural design models for tunnels in soft soil. Underground Space, Vol.9, pp.246-259.

Duddeck, H., Meister, D., Werner, E., Schlegel, R. and Theurer, M., 1979. Road tunnel in very soft soil in terrace deposits in the Harz Mountains, Germany. Tunnelling '79, pp.205-215.

Duddeck, H., Meister, D., Werner, E., Schlegel, R. and Theurer, M., 1981. Strassen-Tunnel Butterberg in Osterode/Harz. Bauingenieur, 56, pp.175-185.

Duddeck, H. and Stading, A., 1985. Entwurfskonzept und Realitat beim Standsicherheitsnachweis von Tunneln im deutschen Mittelgebirge. Proceedings of STUVA Meeting, (Hannover).

Duncan, J.M., 1979. Behaviour and design of long-span metal culverts. Journal of the Geotechnical Engineering Division, ASCE, Vol. 105, No. GT3, pp.399-418.

Duncan, J.M., 1980(a). Strains predicted using hyperbolic stress-strain relationships. Proceedings of the Workshop on Limit Equilibrium, Plasticity and Generalized Stress-Strain in Geotechnical Engineering (McGill University), pp.245-253.

Duncan, J.M., 1980(b). Hyperbolic stress-strain relationships. Proceedings of the Workshop on Limit Equilibrium, Plasticity and Generalized Stress-Strain in Geotechnical Engineering (McGill University) pp.443-460. (comments on pp.333-335).

Duncan, J.M., Byrne, P., Wong, K.S. and Mabry, P., 1980. Strength, stress-strain and bulk modulus parameters for finite element analysis of stresses and movements in soil masses. Report UCB/GT/80-01, University of California, Berkeley, 77p.

Duncan, J.M. and Chang, C.V., 1970. Nonlinear analysis of stress and strain in soils. Journal of the Soil Mechanics and Foundations Division. American Society of Civil Engineers, Vol.96, pp.1629-1653.

Duncan, J.M. and Chang, C.V., 1972. Discussion closure of "Nonlinear analysis of stress and strain in soils". Journal of the Soil Mechanics and Foundation Division. American Society of Civil Engineers, Vol.98, No.SM5, pp.495-498.

Dyer, M., Jamiolkowski, M. and Lancellota, R., 1986. Experimental soil engineering and models for geomechanics. Proceedings of the 2nd International Symposium on Numerical Models in Geomechancis (Ghent), pp.873-906.

Dysli, M. and Fontana, A., 1982. Deformations around the excavations in clayey soil. Proceedings International Symposium on Numerical Methods in Geomechanics, Zurich, September, pp.634-642.

Ebaid, G.S. and Hammad, M.E., 1978. Aspects of circular tunnel design. Tunnels and Tunnelling (July), pp.59-63.

Edeling, H. and Schulz, W., 1972. Die Neue Osterreichische Tunnelbauweise im Frankfurter U-Bahnbau. Der Bauingenieur, 47, pp.351-362. (English translation by BRE, UK).

Eden, W.J. and Bozosuk, M., 1969. Earth pressures on Ottawa outfall sewer tunnel. Canadian Geotechnical Journal, 6, pp.17-32.

Egger, P., 1974. Gebirgsdruck im Tunnelbau und stuzwirkung der Ortsbrust bei Uberschreiten der Gebirgsfestigkeit. Proceedings of the 3rd Congress of the International Society for Rock Mechanics. (Denver), pp.1007-1011.

Egger, P., 1980. Deformations at the face of the heading and determination of the cohesion of the rock mass. Underground Space, Vol.4, No.4, pp.313-318.

Eigenbrod, K.D., 1975. Analysis of the pore pressure changes following the excavation of a slope. Canadian

Geotechnical Journal, 12, pp.429-440.

Einstein, H.H., Azzouz, A.S., Schwartz, C.W. and Steiner, W., 1979. Improved design of tunnel supports: Executive summary. Report UMTA-MA-06-0100-79-15. NTIS (Springfield, Virginia) 49p.

Einstein, H.H., and Schwartz, C.W., 1979. Simplified analysis for tunnel supports. Journal of the Geotechnical Engineering Division, American Society of Civil Engineers, V. 106, pp.499-518 (Discussion with corrections on the original paper in the same journal, July, 1980, pp.835-838).

Eisenstein, Z., 1974. Application of finite element method to analysis of earth dams. State-of-the art-report, Proceedings of the 1st Brazilian Seminar on Applications of Finite Element Method in Soil Mechanics (Rio de Janerio), pp. 457-528.

Eisenstein, Z., 1982. The contribution of numerical analysis to design of shallow tunnels. Proceedings, International Symposium on Numerical Models in Geomechanics, Zurich, pp. 135-165.

Eisenstein, Z. and Branco, P., 1985. Observational method applied to ground control at the Edmonton LRT Tunnel. Canadian Tunnelling (TAC), pp.51-65.

Eisenstein, Z., El-Nahhas and Thomson, S., 1981(a). Pressure-displacement relations in two systems of tunnel lining. Soft Ground Tunnelling, Failures and Displacements (Ed. D. Resendiz and M.P. Romo) A.A. Balkema (Rotterdam), pp.85-94.

Eisenstein, Z., El-Nahhas, F. and Thomson, S., 1981(b). Strain field around a tunnel in stiff soil. Proceedings, 10th International Conference on Soil Mechanics and Foundation Engineering (Stockholm), Vol.1, pp.283-288.

Eisenstein, Z., Heinz, H. and Negro, A., 1984. On three-dimensional ground response to tunnelling. Proceedings, Geotech' 84, American Society of Civil Engineers (edited by K.Y. Lo), pp.107-127.

Eisenstein, Z., Heinz, Jr., H. and Negro, A., 1986. Multiple excavation schemes for large openings in soft ground. Proceedings, International Congress on Large Underground Openings (Firenze), Vol. 1, pp.710-719.

Eisenstein, Z., Kulak, G.L., MacGregor, J.G. and Thomson, S., 1977. Report on geotechnical and construction performance of the twin tunnels. Unpublished report prepared for the City of Edmonton Engineering Department. Edmonton, Alberta, 77p.

Eisenstein, Z. and Medeiros, L.V., 1983. A deep retaining structure in till and sand. Part II: Performance and analysis. Canadian Geotechnical Journal, Vol.20, pp.131-140.

Eisenstein, Z. and Morrison, N.A., 1973. Prediction of foundation deformation in Edmonton using an in situ pressure probe. Canadian Geotechnical Journal, Vol.10, pp.193-210.

Eisenstein, Z. and Negro, A., 1985(a). Excavations and tunnels in tropical lateritic and saprolitic soils. General Report for Session 5, 1st International Conference on Geomechanics in Tropical Lateritic and Saporlitic Soils (Brasilia), Vol.3, pp.299-333.

Eisenstein, Z. and Negro, A., 1985(b). Comprehensive design method for shallow tunnels. ITA/AITES, International Conference, Underground Structures in Urban Area, Prague, Czechoslavakia, pp.7-20.

Eisenstein, Z. and Thomson, S., 1978. Geotechnical performance of a tunnel in till. Canadian Geotechnical Journal, Vol.15, pp.332-345.

Eisenstein, Z., Thomson, S. and Branco, P., 1983. South LRT extension, Jasper Avenue twin tunnel, instrumentation test section at 102nd Street, Part II: Northbound Tunnel. Report submitted to LRT Project Office, Edmonton Transit, The City of Edmonton.

Elmer, H., 1980. Zusammenhang zwischen Bauverfahren und geringstmoglichen setzungen beim Bau eines doppelgleisigen Stadtbahntunnels in Mulheim a.d. Ruhr. Forschung+Praxis (Koln), 23, pp.160-165.

El-Nahhas, F., 1980. The behaviour of tunnels in stiff soils. Ph.D. Thesis, Department of Civil Engineering, University of Alberta, 305p.

Engelbreth, K., 1961. Correspondence to Tunnel stress analysis. Geotechnique 11, pp.246-248.

Erdmann, J., 1983. Vergleich ebener und Entwicklung raumlicher Berechnungsverfahren fur Tunnel. Bericht Nr. 83-40, Institut fur Statik der Technischen Universitat Braunschweig, 220p.

Erdmann, J. and Duddeck, H., 1983. Statik der Tunnel im Lockergestein-Vergleich der Berechnungsmodelle. Bauingenieur, 58 Jahrgang, pp.407-414.

Erdmann, J. and Duddeck, H., 1984. Stress-displacement fields at the face of rock tunnels. Proceedings, 1st Latin-American Congress of Underground Construction -ITA (Caracas), Vol.I, pp.177-183.

D'Escatha, Y. and Mandel, J., 1974. Stabilite d'une galerie peu profonde en terrain meuble. Revue de L'Industrie Minerale (Special Issue), Avril, pp.45-53.

Evgin, E. and Eisenstein, Z., 1985. Performance of an elastoplastic model. Canadian Geotechnical Journal, Vol. 22, No. 2, pp.177-185.

Evison, S., 1987. M.Sc. Thesis in preparation. University of Alberta.

Ewoldsen, H.M., 1968. The near surface tunnel in a gravitating medium. Proceedings of the 10th Symposium of Rock Mechanics, University of Texas, p.677-698.

Fenner, R., 1938. Untersuchungen zur Erkenntnis des Gebirgsdrucks. Gluckauf Berg- und Huttenmannische Zeitschrift 74, Nr. 32, 681-695, Nr.33, 705-715.

Fitzpatrick, L., Kulhawy, F.H and O'Rourke, T.D., 1981. Flow patterns around tunnels and their use in evaluating construction problems. Soft-Ground Tunnelling, Failures and Displacements (Ed. D. Resendiz and M.P. Romo), A.A.

Balkema (Rotterdam), pp. 95-103.

Fleck, H., and Sklivanos, S., 1978. Statische Berechnung gebetteter Hohlraumaussteifungen (Auskleidungen) bei Berucksichtigung einer tangentialen Bettungmodulwirkund und Vergleich mit Ergebnissen nach der Kontinuumstheorie. Forschung Ing.-Wessen 44 (1978), Heft 4, 101-136, VDI Dusseldorf pp. 149-156.

Fleck, H. and Sonntag, G., 1977. Statische Berechnung gebetteter Hohlraumskleidungen mit einem ortsveranderlichen, last-und verformungsabhangigen Bettungsmodul aus der Method der Finite Elemente. Die Bautechnik 5, pp.149-156.

Fleck, H. and Sonntag, G., 1978. Ermittlung der Biegung von Hohlraumassteifungen (Auskleidungen) aus den Krummungsanderungen der Ausbruchkontur. Bauingenieur 53, Heft 12, pp.471-478.

Flugge, W., 1962. Statik und Dynamik der Schalen, 3. Auflage. Springer-Verlag (Berlin), 292 p.

Focht, J.A. and O'Neill, M.W., 1985. Piles and other deep foundations. Proceedings of the 11th International Conference on Soil Mechanics and Foundation Engineering (San Francisco), 4, pp.187-209.

da Fontoura, S.A.B. and Barbosa, M.C., 1985. Superficial settlements caused by a small diameter tunnel excavated in a residual sandy soil (in Portuguese). Geotecnia (Lisbon), pp. 67-87.

Fourie, A.B., Potts, D.M. and Jardine, R.J., 1986. The determination of appropriate soil stiffness parameters for use in finite element analyses of geotechnical problems. Proceedings of the 2nd International Symposium on Numerical Models in Geomechanics (Ghent), pp. 227-235.

Fredriksson, B. and Mackerle, J., 1983. Stuctural Mechanics Finite Element Computer Programs. Advanced Engineering Corp. (Sweden), Box 3044, S-580 03 Linkoping.

Fujita, K., 1982. Prediction of surface settlements caused

by shield tunnelling. Proc. Conferencia Internacional de Mecanica de Suelos (Sociedade Mexicana de Mecanica de Suelos), Vol.1, pp. 239-246.

Gais, W.H., Harpf, R. and Herg, M., 1985. Hohlraumsicherung beim Nurnberger U-Bahnbau - Messergebmisse zum Tragverhalten, Forschung + Praxis, 29 (STUVA), pp. 196-201.

Gais, W.H., Harpf, R. and Herg, M., 1986. Langzeitige Lastentwiklung in der Auskleidung von Tunneln in Spritzbetonbauweise: Beispeil U-Bahn Munchen. In: Forschung + Praxis (Alba, Dusseldorf), 30, pp. 59-68.

Garcia Gonzalez, J.M., Escario, V., Moya, F.J., Oteo, C.S. and Sagaseta, C., 1984. The Madrid subway extension and its associated geotechnical problems. Proceedings of the 1st Latinamerican Congress of Underground Construction (ITA Caracas), Vol.I, pp. 209-224.

Gartung, E. and Bauernfeind, P., 1977. Subway tunnel at Nurnberg - Predicted and measured deformations. Proceedings of the International Symposium on Field Measurements in Rock Mechanics (Zurich), pp. 473-483.

Gartung, E. and Bauernfeind, P., 1983. Construction of adjacent tubes by NATM. Proceedings, 5th Congress of the International Society for Rock Mechanics, Melbourne, D 163-166 (reprint).

Gartung, E., Bauernfeind, P. and Bianchini, J.C., 1979. Three-dimensional finite element method study of a subway tunnel in Nurnberg. Proceedings, Rapid Excavation and Tunnelling Conference. Atlanta, Vol. 1, pp. 773-789.

Gaudin, B., Folacci, J.P., Panet, M. and Salva, L., 1981. Soutenement d'une Galerie dans le Marnes du Cenomanien. Proceedings 10th International Conference on Soil Mechanics and Foundation Engineering (Stockholm), Vol. 1, pp.293-296.

Gebhardt, P., 1980. Hydrogeologische und geotechnische Probleme bei Planung und Bau der U-Bahn-Linie 8/1. In; U-Bahn fur Munchen, U-Bahn Linie 8/1 (published by U-Bahn-Referat Munchen), pp.65-87.

Gesta, P., Kerisel, J., Londe, P., Louis, C. and Panet, M., 1980. Tunnel stability by Convergence-Confinement Method. Underground Space, Vol. 4, pp. 225-232.

Ghaboussi, J. and Gioda, G., 1977. On the time dependent effects in advancing tunnels. International Journal for Numerical and Analytical Methods in Geomechanics, Vol.1, pp.249-271.

Ghaboussi, J., Hansmire, W.H., Parker, H.W. and Kim, K.J., 1983. Finite element simulation of tunnelling over subways. Journal of Geotechnical Engineering (ASCE), Vol.109, No.3, pp.318-334.

Ghaboussi, J. and Karshenas, M., 1977. On the finite element analysis of certain material nonlinearities in geomechanics. Proceedings of the International Conference on Finite Elements in Nonlinear Solids and Structural Mechanics (Norway) (quoted by Ghaboussi et.al., 1978:191).

Ghaboussi, J. and Pecknold, D.A., 1984. Incremental finite element analysis of geometrically altered structures. International Journal for Numerical Methods in Engineering, Vol.20, pp.2051-2064.

Ghaboussi, J. and Ranken, R., 1974. Tunnel design considerations: Analysis of medium-support interaction. Report FRA - ORD and D75-24, NTIS (Springfield, Virginia).

Ghaboussi, J. and Ranken, R.E., 1981. Finite element simulation of underground construction. Proceedings, Symposium on Implementation of Computer Procedures and Stress-Strain Laws in Geotechnical Engineering (Chicago), pp.253-265.

Ghaboussi, J., Ranken, R.E. and Karshenas, M., 1978. Analysis of subsidence over soft ground tunnels. Proceedings of the International Conference on Evaluation and Prediction of Subsidence (Pensacola Beach), pp. 182-196.

Gibson, R.E. and Anderson, W.F., 1961. In situ measurement of soil properties with the pressuremeter. Civil Engineering Public Works Rev. (London), Vol.56, No.5,

pp.615-620.

Gioda, G., 1985. Some remarks on back analysis and characterization problems in geomechanics. Proceedings of the 5th International Conference on Numerical Methods in Geomechanics (Nagoya), pp.47-61.

Gioda, G. and Jurina, L., 1981. Identification of earth pressure on tunnel liners. Proceedings of the 10th International Conference on Soil Mechanics and Foundation Engineering (Stockholm), Vol.1, pp.301-304.

Glossop, N.H., 1978. Ground movements caused by tunnelling in soft soils. Ph.D. Thesis, University of Durham.

Glossop, N.H. and Farmer, I.W., 1979. Settlement associated with removal of compressed air pressure during tunnelling in alluvial clay. Geotechnique 29, No.1, pp.67-72.

Gopalakrishnayya, A.V., 1973. Analysis of cracking of earth dams. Ph.D. Thesis, The University of Alberta.

Guatteri, G., Teixeira, A.H. and Martins, A., 1986. Solution of stability problems in tunnelling by the CCP method. Proceedings of the International Congress on Large Underground Openings - ITA (Firenze), Vol.II, pp.190-197.

Gunn, M.J., 1977. The use of the finite element method for the design of tunnels in soft ground. Cambridge University Engineering Department Supplementary Research Report to the Director of the Transport and Road Research Laboratory.

Gunn, M.J., 1984. The deformation of ground near tunnels and trenches. Cambridge Univeristy Engineering Department Research Report to the Director of the Transport and Road Research Laboratory.

Gunn, M.J. and Taylor, R.N., 1985. Discussion of Atkinsonn and Mair. Geotechnique 35, No.1, pp.73-75.

Hain, H. and Horst, H., 1970. Spannungstheorie 1. and 2.

Ordnung fur beliebige Tunnelquerschnitte unter Berucksichtigung der einseitigen Bettungswirkung des Bodens. Strasse Brucke Tunnel 22, Heft 4, pp.85-94.

Hain, H. and Horst, H., 1971. Gultigekeitsgrenzen der Theorie 2. Ordnung bei der Berechnung kreisformiger Tunnelquerschnitte. Strasse Brucke Tunnel 23, Heft 3, pp 64-68.

Hain, H. and Horst, H., 1974. Zur Frage der radialen und tangentialen Bettung schildvorgetriebener Tunnel. Strasse Brucke Tunnel 26, Heft 1, pp. 12-20.

Hanafy, E.A. and Emery, J.J., 1980. Advancing face simulation of tunnel excavations and lining placement. Proceedings of the Underground Rock Engineering, 13th Canadian Rock Mechanics Symposium, CIM Special Volume 22, pp. 119-125.

Hanafy, E.A. and Emery, J.J., 1982. Three-dimensional simulation of tunnel excavation in squeezing ground. Proceedings of the 4th International Conference on Numerical Methods in Geomechnics (Edmonton), Vol.3, pp. 1203-1209.

Handy, R.L., 1985. The arch in soil arching. Journal of Geotechnical Engineering Division, ASCE, Vol. 111, No.3, pp.302-319.

Hanna, T.H., 1985. Field Instrumentation in Geotechnical Engineering. Transtech Publications (Germany), 843 p.

Hansmire, W., 1975. Field measurements of ground displacements about a tunnel in soil. Ph.D. Thesis, University of Illinois at Urbana-Champaign. 334p.

Hansmire, W.H., 1984. Example analysis for circular tunnel lining. Proceedings, Geotech '84, ASCE. (Ed. by K.Y. Lo), pp.30-45.

Hansmire, W.H. and Cording, E.J., 1985. Soil tunnel test section: Case history summary. Journal of the Geotechnical Engineering Division. American Society of Civil Engineers, Vol. 111, No. 11, pp. 1301-1320.

Hansmire, W.H., Parker, H.W., Ghaboussi, J., Casey, E.F. and Lentell, R.L., 1981. Effects of shield tunnelling over subways. Proceedings, 3rd Rapid Excavation and Tunnelling Conference (San Francisco), Vol. 1, pp.254-27 6.

Hanya, T., 1977. Ground movements due to construction of shields-driven tunnel. Proceedings, 9th International Conference on Soil Mechanics and Foundation Engineering (Tokyo), Case History Volume, pp.759-790.

Hardy Associates. 1980. City of Winnipeg, Tunnel Instrumentation Project. Geotechnical Consideration. Year 1 Report for the City of Winnipeg, Waterworks Waste and Disposal Division (December).

Hartmann, F., 1970. Elastizitatstheorie des ausgekleideten Tunnelhohlraumes und des eingebohrten kreisformigen Rohres. Strasse Brucke Tunnel 22 (1970), Heft 8, 209-215, Heft 9, 241-246, und Jg. 24 (1972), Heft 1, 13-20, Heft 2, 39-45.

Hartmann, F., 1985. Einfache Berechnung uberschutteter, kreisformiger Rohre von beliebiger Steifigkeit Elastizitatstheorie des uberschutteten Rohres. Bautechnik, 62, Heft 7, pp.224-235.

Hartmann, F., 1986. Personal Communication.

Heilbrunner, J., Gais, W.H., Herg, M., 1981. Neue Messergebnisse zum Tragverhalten von Verbaubogen und Spritzbeton bein der Hohlraumsicherung im U-Bahnbau. Forschung + Praxis (STUVA - Berlin), pp.129-136.

Henkel, D.J., 1960. The relationship between the effective stresses and water content in saturated clays. Geotechnique, Vol.10, p.41.

Heinz, H., 1984. Applications of the New Austrian Tunnelling Method in urban areas. M.Sc. Thesis. Department of Civil Engineering, University of Alberta, Edmonton, 320 p.

Heinz, H., 1987. Ph.D. Thesis in preparation. University of Alberta.

Henry, K., 1974. Grangemouth tunnel sewer. Tunnels and Tunnelling (January)., pp.25 and 29.

Hereth, A., 1979. Der Pfaffensteiner Tunnel in Regensburg. Rock Mechanics (Springer, Vienna), 12, pp.47-60.

Herzog, M., 1985. Die Setzungsmulde uber Seicht liegenden Tunneln. Bautechnik, 11, pp.375-377.

Hewett, B. and Johannesson, S., 1922. Shield and Compressed Air Tunnelling. McGraw Hill, New York.

Ho, S.K., 1980. An investigation into the behaviour of shallow tunnels in elastic soils. B.Eng.Sc. Report, Faculty of Engineering Science, University of Western Ontario.

Hocking, G., 1976. Three-dimensional elastic stress distribution around the flat end of a cylindrical cavity. International Journal of Rock Mechanics, Mining Sciences and Geomechanical Abstracts. Vol. 13, No. 12, pp. 331-337.

Hoeg, K., 1968. Stresses against underground structural cylinders. Journal of the Soil Mechanics and Foundation Engineering Division. ASCE, Vol. 94, No. SM4, July, pp. 833-858.

Hoek, E. and Brown, E.T., 1980. Underground excavations in rock. 1st ed., The Institution of Mining and Metallurgy, London, 527 p.

Hofmann, H., 1976. Progonose und Kontrolle der Verformungen und Spannungen im Tunnelbau. Forschung+Praxis (Alba, Dusseldorf), 19, pp.94-100.

Holmsen, G., 1953. Regional settlements caused by a subway tunnel in Oslo. Proceedings of the 3rd International Conference on Soil Mechanics and Foundation Engineering (Zurich), Vol. I, pp. 381-383.

Horiuchi, Y., Kudo, T., Tashiro, M. and Kimura, K., 1986. A shallow tunnel enlarged in diluvial sand. Proceedings of the International Congress on Large Underground Openings

- ITA (Firenze), Vol. I, pp.752-760.

Howe, M., 1982. Damage control for distribution systems. Gas Engineering and Management. Journal of Institution of Gas Engineers (London), Vol. 22, Oct., pp. 377-399.

Howland, A.F., 1981. The prediction of the settlement above soft ground tunnels by considering the groundwater response with the aid of flow net constructions. Proceedings of the 2nd International Conference on Ground Movements and Structures (Cardiff), pp. 345-358.

Hoyaux, B. and Ladanyi, B., 1970. Gravitational stress field around a tunnel in soft ground. Canadian Geotechnical Journal, Vol. 7, No. 1, pp. 54-61.

Hubbard, H.W., Potts, D.M., Miller, D. and Burland, J.B., 1984. Design of the retaining walls for the M25 cut and cover tunnel at Bell Common tunnel. Geotechnique 34, No.4, pp. 495-512.

Hughes, J.M.O. and Ervin, M.C., 1980. Development of a high pressure pressuremeter for determining the engineering properties of soft to medium strength rocks. Proceedings of the 3rd Australia and New Zealand Geomechanics Conference, (Wellington).

Hughes, J.M.O., Wroth, C.P. and Windle, D., 1977. Pressuremeter tests in sands. Geotechnique, Vol. 27, No. 4, pp.455-477.

Hungr, O., 1985. Discussion of Atkinson and Mair, Geotechnique 35, No. 1, p73.

Hutchinson, D.E., 1982. Effect of construction procedure on shaft and tunnel performance. M.Sc. Thesis, Department of Civil Engineering, University of Alberta.

Imaki, J., Masumoto, H., Ueda, S., Amano, M. and Kurihara, H., 1984. Execution of large cross section tunnel by New Austrian Tunnelling Method in sandy soil with small cover. Proceedings of the 1st Latinamerican Congress of Underground Constructions (ITA, Caracas), Vol. I, pp. 503-508.

Ishihara, K., 1970. Relations between process of cutting and uniqueness of solution. Soils and Foundation, Vol. X, No. 3, pp. 50-65.

Ito, T. and Hisatake, M., 1981. Analytical study of NATM. Proceedings of the 10th International Conference on Soil Mechanics and Foundation Engineering (Stockholm), Vol. 1, pp. 311-314.

Ito, T. and Hisatake, M., 1982. Three-dimensional surface subsidence caused by tunnel driving. Proceedings of the 4th International Conference on Numerical Methods in Geomechanics (Edmonton), Vol. 2, pp.551-559.

Jagsch, D., Muller, L. and Hereth, A., 1974. Bericht uber die Messungen und Messergebnisse beim Bau der Stadtbahn Bachum Los A2. Interfels Messtechnik Information, pp. 11-13.

Jamiolkowski, M., Ladd, C.C., Germaine, J.T. and Lancellotta, R., 1985. New developments in field and laboratory testing of soils. Proceedings of the 11th International Conference on Soil Mechanics and Foundation Engineering (San Francisco), Vol. 1, pp. 57-153.

Janbu, N., 1963. Soil compressibility as determined by oedometer and triaxial tests. European Conference on Soil Mechanics and Foundation Engineering, Wiesbaden, Germany, Vol. 1, pp.19-25.

Jardine, R.J., Fourie, A., Maswoswe, J. and Burland, J.B., 1985. Field and laboratory measurements of soil stiffness. Proceedings of the 11th International Conference on Soil Mechanics and Foundation Engineering (San Francisco), Vol. 2, pp. 511-514.

Jardine, R.J., Potts, D.M., Fourie, A.B. and Burland, J.B., 1986. Studies of the influence of non-linear stress-strain characteristics in soil-structure interaction. Geotechnique, Vol. 36, No. 3, pp. 377-396.

Jardine, R.J., Symes, N.J. and Burland, J.B., 1984. The measurement of soil stiffness in the triaxial apparatus. Geotechnique. Vol. 34, No. 3, pp. 323-340.

Jeffrey, G.B., 1920. Plane stress and plane strain in bipolar coordinates. Transaction of the Royal Society, London, Series A, Vol.221, pp. 265-293.

Johnston, P.R., 1981. Finite element consolidation analyses of tunnel behaviour in clay. Ph.D. Dissertation, Stanford University, 224p.

Johnston, P.R. and Clough, G.W., 1983. Development of a design technology for ground support for tunnels in soil. Volume I: Time-dependent response due to consolidation in clays. Report UMTA-MA-06-0100-82-1, NTIS (Springfield, Virginia), 218p.

De Jong, J. and Harris, M.C., 1971. Settlements of two multistory buildings in Edmonton. Canadian Geotechnical Journal, 8, pp. 217-235.

Kaiser, P.K., 1981. A new concept to evaluate tunnel performance - influence of excavation procedure. Proceedings of the 22nd U.S. Rock Mechanics Symposium, (Boston), pp. 264-271.

Kaiser, P.K., 1982. Proposal for new design approach. In: Course Notes for Design and Construction of Tunnels and Shafts (Chapter 3), Department of Civil Engineering, University of Alberta.

Kaiser, P.K., 1985. Rational assessment of tunnel liner capacity. Proceedings of the 5th Annual Canadian Tunnelling Conference (Montreal).

Kaiser, P.K. and Barlow, J.P., 1986. Rational assessment of tunnel liner capacity. Canadian Tunnelling Canadien, pp. 31-44.

Kaiser, P.K. and Hutchinson, D.E., 1982. Effects of construction procedures on tunnel performance. Proceedings of the 4th International Conference on Numerical Methods in Geomechanics, 2, pp.516-569.

Karlsrud, K. and Sander, L., 1978. Subsidence problems caused by rock-tunnelling in Oslo. Proceedings of the International Conference on Evaluation and Prediction of Subsidence (Pensacola Beach), pp. 197-213.

Karshenas, M., 1979. Modeling and finite element analysis of soil behaviour. Ph.D. Thesis. University of Illinois at Urbana-Champaign. 279 p.

Kasali, G. and Clough,G.W., 1983. Development of a design technology for ground support for tunnels in soil. Volume II: Three-dimensional finite element analysis of advanced and conventional shield tunneling. Report UMTA-MA-06-0100-82-2 NTIS (Springfield, Virginia), 218 p.

Kastner, H., 1949. Uber den echten Gebirgsdruck beim Bau tiefliegender Tunnel. Osterr. Bauzeitschr., 10-11 (Quoted by Szechy, 1973:176).

Kastner, H., 1971. Statik des Tunnel und Stollenbaues. Springer Berlin.

Kathol, C.P. and McPherson, R.A., 1975. Urban geology of Edmonton. Alberta Research Council, Bulletin 32, 61p.

Katzenbach, R., 1981. Entwicklungstendenzen beim Bau und der Berechnung oberflachennaher Tunnel in bebautem Stadtgebiet. Mitteilungen der Versuchsanstalt fur Bodenmechnik und Grundbau der Technischen Hochschule Darmstadt, Heft 24.

Katzenbach, R., 1985. The influence of soil strength and water load to the safety of tunnel driving. Proceedings of the 5th International Conference on Numerical Methods in Geomechanics (Nagoya), pp. 1207-1213.

Katzenbach, R., and Breth, H., 1981. Nonlinear 3-D analysis for NATM in Frankfurt clay. Proceedings of the 10th International Conference on Soil Mechanics and Foundation Engineering, Stockholm, Vol. 1, pp. 315-318.

Katzenbach, R., and Breth, H., 1983. Zur Standsicherheit oberflachennaher Tunnel. Bauingenieur, 58, pp. 201-207.

Kawamoto, T. and Okuzono, K., 1977. Analysis of ground surface settlement due to shallow shield tunnels. International Journal for Numerical and Analytical Methods in Geomechanics, Vol. 1, No. 3, pp.271-281.

Kenney, T.C. and Uddin, S., 1974. Critical period for stability of an excvated slope in clay soil. Canadian Geotechnical Journal, 11, pp. 620-623.

Kerisel, J., 1975. Old structures in relation to soil conditions. 15th Rankine Lecture. Geotechnique 25, No. 3, pp. 433-483.

Kerisel, J., 1980. Commentary on the General Report. In: Analysis of tunnel stability by the Convergence-Confinement Method. Translation of the Proceedings of the Paris Conference, Underground Space, Vol. 4, No. 4, pp. 233-239.

Kimura, T., and Mair, R.J., 1981. Centrifugal testing of model tunnels in soft clay. Proceedings of the 10th International Conference on Soil Mechanics and Foundation Engineering (Stockholm), Vol. 1, pp. 319-322.

Kirsch, G., 1898. Die Theorie der Elasticitat und die Bedurfnisse der Festigkeitslehre. Zeitschrift des Vereines Deutscher Ingenieure, 42:29, 1.

Kochen, R. and Negro, A., 1985. Analise da Ruptura do tunel Oeste. Prolongamento da Linha Norte-Sul do Metro de Sao Paulo. Report MD-1.20.00.00/6G9-204 to Cia. Metro de Sao Paulo.

Kochen, R., Negro, A., Heinz, Jr., H. and Rottmann, E., 1985. Finite element simulations of underground excavations. Proceedings of the 2nd Symposium on Underground Excavations (ABGE) (in Portuguese), Vol. 1, pp. 195-217 (Rio de Janeiro).

Kocken, R., Negro, A., Hori, K., Ferrari, O. and Maffei, C., 1987. Longitudinal displacements induced by the excavation of a shallow tunnel. Proceedings of the International Conference on Soil Structure Interactions (Paris, May'87), pp.405-411.

Koenz, P. and Garbe, L., 1986. Railway tunnel construction under the old city of Zurich. Proceedings of the International Congress on Large Underground Openings - ITA (Firenze), Vol. I, pp. 761-770.

Kommerell, O., 1912 and 1940. Statische Berechnung von Tunnelmauerwerk. Grundlagen und Anwendung auf die wichtigsten Belastungsfalle. Ernst u. Sohn, Berlin 1940.

Kondner, R.L., 1963. Hyperbolic stress-strain response: cohesive soils. Journal of the Soil Mechanics and Foundation Division, ASCE, Vol. 89, SM 1, 115-143.

Kondner, R.L. and Zelasko, J.S., 1963. A hyperbolic stress-strain formulation for sands. Proceedings of the 2nd Panamerican Conference on Soil Mechanics and Foundation Engineering, Vol. 1, Brasil, pp. 289-324.

Kovari, K., 1977. The elasto-plastic analysis in the design practice of underground openings. Finite Elements in Geomechanics, Wiley, 377-412.

Kovari, K., Hagendorn, H. and Fritz, P. 1976. Parametric studies as a design aid in tunnelling. Proceedings of the 2nd International Conference on Numerical Methods in Geomechanics (Virginia), Vol. II, pp. 773-790.

Krischke, A. and Weber, J., 1981. Erfahrungen bei der Erstellung grosser Tunnelquerschnitte in Teilvortrieben beim Munchener U-Bahn-Bau. Rock Mechanics (Springer, Vienna), Suppl. 11, pp. 107-126.

Kuesel, T.R., 1986. Principles of tunnel lining design. Tunnelling Technology Newsletter, U.S. National Committee on Tunnelling Technology, No. 53, pp. 1-8.

Kulhawy, F.H., 1974. Finite element modeling criteria for underground openings in rock. International Journal of Rock Mechanics and Mining Sciences and Geomechanics Abstracts, Vol. 11, pp. 465-472.

Kulhawy, F.H., 1975. Stresses and displacements around openings in homogeneous rock. International Journal of Rock Mechanics and Mining Sciences and Geomechanics Abstracts, Vol. 12, pp. 43-57.

Kulhawy, F.H., 1977. Embankments and excavations. In: Numerical Methods in Geotechnical Engineering (edited by C.S. Desai and J.T. Christian), McGraw Hill, pp. 528-555.

Kulhawy, F.H. and Duncan, J.M., 1972. Stresses and movements in Oroville Dam. Journal of the Soil Mechanics and Foundations Divisions, ASCE, Vol. 98, No. SM7, pp. 653-665.

Kupper, A.M.A.G., 1983. Caracteristicas Tensao x Deformacao x Resistencia de Uma Amostra da Argila Vermelha do Terciario de Sao Paulo. M.Sc. Thesis. Catholic University, Rio de Janeiro.

Kusakabe, O., Kimura, T., Ohta, A., Takagi, N. and Nishio, N., 1985. Centrifige model tests on the influence of axisymmetric excavation on buried pipes. Proceedings of the 3rd International Conference on Ground Movements and Structures (Cardiff), pp. 113-128.

Kyrou, K., 1980. The effect of trench excavations induced ground movements on adjacent buried pipelines. Ph.D. Thesis, Department of Civil Engineering, University of Surrey, (U.K.) (quoted by Rumsey and Dorling, 1985).

Kyrou, K. and Kalteziotis, N.A., 1985. The effect of trenching on adjacent pipelines. Proceedings of the 11th International Conference on Soil Mechanics and Foundation Engineering (San Francisco), Vol. 3, pp. 1657-1660.

Laabmayr, F. and Pacher, F., 1978. Projekt Sondervorschlag U-Bahn Linie 8/1 Los 9/18.2. In: Moderner Tunnelbau bei der Munchner U-Bahn, Springer (edited by H. Lessmann), pp. 29-53.

Laabmayr, F., Swoboda, G., 1979. Zusammenhang zwischen elektronischer Berechnung und Messung, Stand der Entwicklung fur seichtliegende Tunnel. Rock Mechanics, Suppl. 8, 29-42.

Laabmayr, F., and Weber, J., 1978. Messungen, Auswertung und ihre Bedeutung. In: Moderner Tunnelbau bei der Munchner U-Bahn, Springer, (edited by H. Lessmann), pp. 73-96.

Ladanyi, B., 1966. Short term behaviour of clay around a circular tunnel. Universite Laval, Departement de Genie Civil, Rapport S-8.

Ladanyi, B., 1974. Use of long-term strength concept in the determination of ground pressure on tunnel linings. Proceedings of the 3rd International Congress on Rock Mechanics, (Denver), Vol. 2B, pp. 1150-1156.

Ladanyi, B., 1980. Direct determination of ground pressures on tunnel lining in non-linear viscoelastic rock. 13th Canadian Rock Mechanics Symposium, CIM Special Volume 22, Canadian Institute of Mining and Metallurgy. pp. 126-132.

Ladanyi, B., 1982. Issues in rock mechanics: A personal view. Conference Keynote Address. Proceedings of the 23rd Symposium on Rock Mechanics (Berkeley), pp.3-14.

Ladanyi, B. and Hoyaux, B., 1969. A study of the trap-door problem in a granular mass. Canadian Geotechnical Journal, 6, pp. 1-14.

Lambe, T.W., 1973. Predictions in soil engineering. 13th Rankine Lecture, Geotechnique 23, pp. 149-202.

Lambe, T.W. and Whitman, R.W., 1969. Soil Mechanics, John Wiley & Sons, New York, 553 p.

Larnach, W.J. and Wood, L.A., 1972. The effect of soil-structure interaction on settlements. Proceedings of the International Symposium on Computer-Aided Structural Design (Coventry), pp. G1. 1- G1. 13.

Ledesma, A., Gens, A., and Alonso, E.E., 1986. Identification of parameters in a tunnel excavation problem. Proceedings of the 2nd International Symposium on Numerical Models in Geomechanics (Ghent), pp. 333-344.

Limanov, I.A., 1957. Surface settlements in Cambrian clay due to tunnel construction (in Russian). Inst. Inzh. Zhelezn. Transport (Leningrad) - quoted by Szechy (1973:1045)

Lo, K.Y, Leonards, G.A. and Yuen, C., 1977. Interpretation and significance of anisotropic deformation behaviour of soft clay. Norwegian Geotechnical Institute Report No. 117 (Oslo, Norway) (quoted by Ng and Lo, 1985:380).

Lo, K.Y., Ng, M.C. and Rowe, R.K., 1984. Predicting settlement due to tunnelling in clay. Tunnelling in Soil and Rock. Geotech '84 (ASCE)/ pp. 46-75.

Lo, K.Y. and Rowe, R.K., 1982. Prediction of ground subsidence due to tunnelling in clays. Research Report GEOT-10-82 for NRC of Canada, Faculty of Engineering Science, Univeristy of Western Ontario, 353 p.

Lombardi, G., 1970. The influence of rock characteristics on the stability of rock cavitities. Tunnels and Tunnelling, Vol. 2, pp. 104-109.

Lombardi, G., 1972. Diskussionsbeitrag zum Thema 2. Proceedings Internationales Symposium fur Untertagbau (Luzern), pp. 370-378.

Lombardi, G., 1973. Dimensioning of tunnel linings with regards to constructional procedure. Tunnels and Tunnelling, Vol. 5, pp. 340 -351.

Lombardi, G., 1974. The problems of tunnel supports. Proceedings of the 3rd Congress of the International Society for Rock Mechancis (Denver), Vol. III, pp. 109-113.

Lombardi, G., 1980. Some comments on the Convergence-Confinement Method. Underground Space, Vol. 4, No. 4, pp. 249-258.

Lombardi, G. and Amberg, W., 1979. L'Influence de la Methode de Construction sur l'Equilibre final d'un Tunnel. Proceedings, 4th Congress of the International Society for Rock Mechanics, Montreux, Vol. 1, pp. 475-484.

Loudon, P.A., 1967. Some deformation characteristics of kaolin. Ph.D. Thesis, Cambridge University.

Lunardi, P. and Louis, C., 1985. Methodes de presoutenement et pre-etanchement pour le travaux en souterrain. Proceedings of the International Symposium in Tunnelling in Soft and Water-Bearing Grounds. AFTES, Lyon, A.A. Balkema (Rotterdam), pp. 119-124.

Lunardi, P., Mongilardi, E., Tornaghi, R., 1986. Il preconsolidamento mediante jet-grouting nella realizzazione di opere in Sotteraneo. Proceedings of the International Congress on Large Underground Openings -ITA (Firenze), Vol. II, pp. 601-612.

Maffei, C.E.M., 1982. Analise dos modelos calculo de Suportes e Revestimentos. Anais do Simposio Sobre Escavacoes Subterraneas (ABGE - Rio de Janeiro). pp.157-184.

Maidl, B., 1984. Handbuch des Tunnel - und Stollenbaus. Band I: Konstruktionen und Verfahren. Verlag Gluckauf GmbH, 423 p.

Mair, R.J., 1977. Behaviour of tunnels in soft ground. CUED - Soils Report to TRRL (September), University of Cambridge.

Mair, R.J., 1979. Centrifugal modelling of tunnel construction in soft clay. Ph.D. Dissertation, Cambridge University.

Mair, R.J., Gunn, M.J. and O'Reilly, M.P., 1981. Ground movements around shallow tunnels in soft clay. Proceedings of the 10th International Conference on Soil Mechanics and Foundation Engineering (Stockholm), Vol. 1, pp. 323-328.

Mandel, J. and Halphen, B., 1974. Stabilite d'une cavite spherique souterraine. Proceedings of the 3rd Congress of the International Society for Rock Mechanics (Denver), Vol. II, Part B, pp. 1028-1032.

Marsland, A., 1972. The shear strength of stiff fissured clays. In: Stress-Strain Behaviour of Soils. Roscoe Memorial Symposium, Cambridge (edited by R.H.G. Parry), pp. 59-68.

Marsland, A. and Randolph, M.F., 1977. Comparisons of the results from pressuremeter tests and large in situ plate tests in London clay. Geotechnique, Vol. 27, No. 2, pp. 217-243,

Massa, E.M., 1981. Projeto e construcao do Tunel de

Mangueira. Metro do Rio de Janeiro. Special Publication of the Brazilian Association of Soil Mechanics (ABMS - Rio de Janeiro), 43 p.

Massad, F., 1974. Caracteristicas geotecnicas das argilas porosas vermelhas de Sao Paulo. Proceedings of the 5th Brazilian Congress on Soil Mechanics and Foundation Engineering (Sao Paulo), Vol. 2, pp.131-144.

Massad, F., 1980. Caracteristicas e propriedades geotecnicas de alguns solos da Bacis de Sao Paulo. Anais de Mesa Redonda Aspectos Geologico e Geotecnicos da Bacia Sedimentar de Sao Paulo (ABGE - SBG), Sao Paulo - IPT, pp. 53-93.

Massad, F., 1981(a). O problema do coeficiente de empuxo em repouso dos solos terciarios da cidade de Sao Paulo. Proceedings, Simposio Brasileiro de Solos Tropicais em Engenharia (published by ABMS - Brazilian Society for Soil Mechanics), pp. 91-101.

Massad, F., 1981(b). Resultados de Investigacao Laboratorial sobre a deformabilidade de alguns solos terciarios da cidade de Sao Paulo. (Laboratory investigation on the deformability of some Sao Paulo city Tertiary Soils). Proceedings, Brazilian Symposium on Tropical Soils in Engineering (Rio de Janeiro), pp. 66-90.

Massad, F., Niyama, S. and Aleoni, N.A.O., 1981. Analise de provas de cargas horizontais em tubuloes executados num solo lateritico. Proceedings 'Symposio Brasileiro de Solos Tropicais em Engenharia' (ABMS), pp.668-682.

Matheson, D.S., 1970. A tunnel roof failure in till. Canadian Geotechnical Journal, 7, pp. 313-317.

Matsuzaki, S., Yamada, K. and Tanaka, H., 1986. An example of observational construction for risk reduction against existing underground structures in shield tunnelling. Proceedings of the International Congress on Large Underground Openings - ITA (Firenze), Vol. II, pp. 630-639.

May, R.W. and Thomson, S., 1978. The geology and geotechnical properties of till and related deposits in the Edmonton, Alberta, area. Canadian Geotechnical

Journal, Vol. 15, pp. 362-370.

Mayne, P.W. and Kulhawy, F.H., 1982. K_o-OCR relationships in soil. Journal of the Geotechnical Engineering Division, American Society of Civil Engineers, Vol. 108, June, pp. 851-872.

Medeiros, L.V., 1979. Deep excavations in stiff soils. Ph.D. Thesis. Department of Civil Engineering, University of Alberta.

Medeiros, L.V and Eisenstein, Z., 1983. A deep retaining structure in till and sand. Part I: Stress path effects. Canadian Geotechnical Journal. Vol. 20, No. 1, pp. 120-130.

Medeiros, L.V., El-Nahhas, F., Smith, L.B. and Eisenstein, Z., 1982. Modelling of the construction of an underground station. Proceedings of the 4th International Conference on Numerical Methods in Geomechanics (Edmonton), Vol. 2, pp. 929-934.

Meister, D. and Wallner, M., 1977. Instrumentation of a tunnel in extremely bad ground and interpretation of the measurements. Proceedings, International Symposium on Field Measurements in Rock Mechanics, Zurich (edited by K. Kovari), pp. 919-933.

de Mello, V.F.B., 1969. Foundations of buildings in clay. Proceedings of the 7th International Conference on Soil Mechanics and Foundation Engineering, State-of-the-Art Volume (Mexico), pp. 49-136.

de Mello, V.F.B., 1977, Reflections on design decisions of practical significance to embankment dams. Geotechnique 27, No. 3, pp. 279-355.

de Mello, V.F.B., 1981. Proposed bases for collating experiences for urban tunneling design. Proceedings of the Syposium on Tunnelling and Deep Excavations in Soils, Sao Paulo, (published by ABMS - Brazilian Society for Soil Mechanics), pp. 197-23

de Mello, V.F.B. and Sozio, L.E. 1983. Proposed bases for collating experiences for urban tunneling design (in

Portuguese). Course Lecture Note, Department of Civil Engineering, PUC, (Rio de Janeiro).

Menzies, B.K., Sutton, H. and Davies, R.E., 1977. A new system for automatically simulating K_o consolidation and K_o swelling in the conventional triaxial cell. Geotechnique, Vol. 27, pp. 593-596.

Mettier, K., 1979. Messungen und Ergebnisse bei der Anwendung des Gefrierverfahrens im Tunnelbau. Mitteilungen der Schweizenschen Gelleschaft fur Boden und Felsmechanik , No. 100. pp. 53-59.

Migliacci, A., Campagna, D., Levati, S., Riva, P. and Curzio, A.Q., 1986. Le gallerie scavate in terreno cementato. Analisi Strutturali e sperimentzioni. Proceedings of the International Congress on Large Underground Openings - ITA (Firenze), Vol. I, pp. 804-813.

Mindlin, R.D., 1938. Gravitational stresses in bipolar coordinates. Proceedings of the 5th International Congress of Applied Mechanics (Cambridge, MA), pp. 112-116.

Mindlin, R.D., 1939. Stress distribution around a tunnel. Proceedings of the American Society of Civil Engineers, Vol. 65, pp. 619-642. Also in 1940, Trans. ASCE, Vol. 105, pp. 1117-1153.

Mohraz, B., Hendron, A.J., Ranken. R.E. and Salem, M.H., 1975. Liner medium interaction in tunnels. Journal of the Construction Division, American Society of Civil Engineers, Vol. 101, No. CO1, March, pp. 127-141.

Morgan, H.D., 1961. A contribution to the analysis of stress in a circular tunnel. Geotechnique, Vol. 11, pp. 37-46.

Morgenstern, N.R., 1975. Stress-strain relationships for soils in practice. Proceedings of the 5th Panamerican Conference on Soil Mechanics and Foundation Engineering (Buenos Aires), Vol. 1, pp. 1-41.

Morgenstern, N.R. and Eisenstein, Z., 1970. Methods of estimating lateral loads and deformations. Proceedings

of the ASCE Specialty Conference on Lateral Stresses and Retaining Structures, Cornell University, pp. 51-102.

Morgenstern, N.R. and Tchalenko, J.S., 1967. Microscopic structures in kaolin subjected to direct shear. Geotechnique, Vol. 17, pp. 309-328.

Morgenstern, N.R. and Thomson, S., 1971. Comparative observations of the use of the Pitcher sampler in stiff clay. ASTM Special Technical Publication 483, pp. 180-191.

Muhlhaus, H.B., 1983. Critical geometry and material parameters of shallow tunnels. Proceedings of the 5th Congress of the International Society for Rock Mechanics (Melbourne), Vol. I, pp. C263-C268.

Muhlhaus, H.B., 1985. Lower Bound Solutions for Circular Tunnels in Two and Three Dimensions. Rock Mechanics and Rock Engineering, 18, pp. 37-52.

Muir Wood, A.M., 1969. Contribution to discussion. Proceedings of the 7th International Conference on Soil Mechanics and Foundation Engineering (Mexico), Vol. 3, pp. 363-365.

Muir Wood, A.M., 1975, The circular tunnel in elastic ground. Geotechnique, Vol. 25, pp. 115-127.

Muir Wood, A.M. and Gibb, F.R., 1971. Design and construction of the cargo tunnel at Heathrow, London. Proceedings ICE, Vol. 48 (Jan), pp. 11-34. Discussion: Proceedings ICE, Vol. 50 (Oct.), pp. 187-201.

Muller, L. 1977. The use of deformation measurements in dimensioning the lining of subway tunnels. Proceedings of the International Symposium on Field Measurements in Rock Mechanics (Zurich), pp. 451-471.

Muller, L. 1978. Removing misconception on the NATM. Tunnels and Tunnelling, October, pp. 29-32.

Muller, L., 1979. Die Bedeutung der Ringschlusslange und der Ringschlusszeit im Tunnelbau. Proceedings of the 4th

Congress of the International Society for Rock Mechanics (Montreux), Vol. 1, pp. 511-519.

Muller, L., Sauer, G. and Chambosse, G., 1977. Berechnungen, Modellversuche und in situ Messungen bei einem bergmannischen Vortrieb im tonigen Untergrund. Bauingenieur 52, Heft 1, pp. 1-8.

Mullins, W.W., 1977. Stochastic modeling of gravity induced particulate flow. In: Probability Theory and Reliability Analysis in Geotechnical Engineering. Ed. D.A. Grivas (Rensselaer Polytechnic Institute, New York), pp. 36-51.

Murayama, S. and Matsuoka, H., 1969. On the settlement of granular media casued by local yielding in the media. Proceedings of the Japan Society of Civil Engineers (in Japanese), 172, pp. 31-41.

Murray, D.W., 1971. Simple two dimensional finite element program - constant strain triangle. Internal Note. Department of Civil Engineering, The University of Alberta.

Myer, L.R., Brekke, T.L., Dare, C.T., Dill, R.B. and Korbin, G.E., 1981. An investigation of stand-up time of tunnels in squeezing ground. Proceedings of the Rapid Tunneling Excavation Conference (San Francisco), Vol. 2, pp. 1415-1433.

McBean, R.J. and Harries, D.A., 1970. The development of high-speed soft ground tunnelling pre-cast concrete segments and tunnelling machines. Proceedings of the South African Conference on Tunnelling (Johannesburg), pp. 129-134.

McCaul, C.,1978. Settlements caused by tunnelling in weak ground at Stockton-on-Tees. Department of the Environment, Department of Transport, TRRL Supplementary Report 383: Crowthorne, 1978 (Transport and Road Research Laboratory). Also Tunnels and Tunnelling (November, 1978), pp. 63-67.

McCaul, C., Dobson, C., Cooper, I., and Spencer, I.M., 1983. Ground movements caused by tunnelling in loose fill. TRRL Supplementary Report 781 (Crowthorne, U.K.).

McCaul, C., Morgan, J.M. and Boden, J.B., 1976. Measurement of ground movement due to excavation of a shallow tunnel in Lower Chalk. TRRL Supplementary Report 199UC (U.K.).

Nadarajah, V., 1973. Stress-strain properties of lightly overconsolidated clays. Ph.D. Thesis. Cambridge University.

Nath, P., 1983. Trench excavation effects on adjacent buried pipes: finite element study. Journal of Geotechnical Engineering (ASCE), Vol. 109, No. 11, pp. 1399-1415.

Negro, A., 1979. Quality of construction and tunnelling behaviour. Unpublished contribution to the Specialty Session on Tunnels in Soft Ground - 6th Panamerican Conference on Soil Mechanics and Foundation Engineering, Lima.

Negro, A., 1981. Computer program manual: Tunnel excavation. Internal Note. Department of Civil Engineering. The University of Alberta (November)

Negro, A., 1983. Soil tunnels: Construction procedures and induced ground displacements. Journal of Engineering. FAAP, Sao Paulo, Vol. 2, n.3, pp. 14-23 (in Portuguese).

Negro, A., 1984. Avaliacao do sistema Mecanizado de construcao de Tuneis da ETESCO. Report to ETESCO S.A. Comercio e Construcoes (Novembro).

Negro, A. and Eisenstein, Z., 1981. Ground control techniques compared in three Brazilian water tunnels. Tunnels and Tunnelling, Oct., pp. 11-14, Nov., pp.52-54, Dec. pp. 48-50.

Negro, A., Eisenstein, Z. and Heinz, Jr., H., 1985. Three-dimensional displacements at the face of shallow tunnels (in Portuguese). Proceedings of the 2nd Symposium on Underground Excavation (ABGE), Vol. 1, pp. 270-286 (Rio de Janeiro).

Negro, A., Eisenstein, Z. and Heinz, Jr., H. 1986. Prediction of radial displacements at the face of shallow tunnels. Proceedings of the 2nd International Conference on Numerical Models in Geomechanics (Ghent),

pp. 837-843.

Negro, A., Heinz, Jr., H. and Eisenstein, Z., 1984. Urban tunnels with large cross section (in Portuguese). Solos e Rochas, Vol. 7, pp. 7-29.

Negro, A. and Kochen, R., 1985. Discussion on Session III, Underground Construction and Building Foundations (in Portuguese). Proceedings of the Symposium on Special Foundations (ABMS/FAAP), Vol. II, pp. 115-120. (Sao Paulo, Sept.).

Negro, A., Kochen, R. and Rottmann, E., 1985. Analise da Instrumentacao de Campo e Avaliacao do comportamento: Tunnel Duplo. Prolongamento da Linha Norte Sul do Metro de Sao Paulo. Report MD-1.20.00.002/6G9 - 205 to Cia Metro de Sao Paulo.

Negro, A. and Kuwajima, F., 1985. Prediction of displacements around underground caverns (in Portuguese). Proceedings of the 2nd Symposium on Underground Excavations (ABGE), Vol. 1, pp. 234-249 (Rio de Janeiro).

Newmark, N.M., 1964. The basis of current criteria for the design of underground protective construction. Proceedings of the Symposium on Soil-Structure Interaction (Tuscon), pp. 1-24.

Ng, R.M.C., 1984. Ground reaction and behaviour of tunnels in soft clays. Ph.D. Thesis. University of Western Ontario.

Ng, R.M.C. and Lo, K.Y., 1985. The measurements of soil parameters relevant to tunnelling in clays. Canadian Geotechnical Journal, 22, pp. 375-391.

Ng, R.M.C, Lo, K.Y., and Rowe, R.K., 1986. Analysis of field performance - the Thunder Bay tunnel. Canadian Geotechnical Journal, 23, pp. 30-50.

Nguyen Minh, D., 1986. Modeles Rheologigues pour l'anlyse du comportement differe des galeries profonds. Proceedings of the International Congress on Large Underground Openings - ITA (Firenze), Vol. II, pp. 659-666.

Nguyen Minh, D. and Berest, P., 1977. Contraction d'une sphere creuse elastoplastique avec radouscissement. Journal de Mecanique Appliquee, Vol. 1, No. 1, pp. 85-109.

Nguyen Minh, D. and Berest, P., 1979. Etude de la stabilite des cavites souterraines avec un modele de comportement elastoplastique radoucissant. Proceedings of the 4th Congress of the International Society for Rock Mechanics (Montreux), Vol. I, pp. 249-256.

Nishiwaki, S., 1984. Measures for reinforcing ground in tunnel in sandy strata with small overburden. Proceedings of the 1st Latinamerican Congress of Underground Constructions - ITA (Caracas), Vol. I, pp. 457-466.

Niwa, Y., Kobayashi, S. and Fukui, T., 1979. Stress and displacements around an advancing face of a tunnel. Proceedings of the 4th Congress of the International Society for Rock Mechanics (Montreux), Vol. I, pp. 703-710.

Novak, J., 1984. Use of extruded concrete in subway tunnels. Proceedings of the 1st Latinamerican Congress of Underground Constructions - ITA (Caracas), Vol. I, pp. 425-429.

Ohnishi, Y., Nishagaki, Y., Kishimoto, H. and Tanaka, Y., 1982. Analysis of advancing tunnel by 2-dimensional F.E.M. Proceedings of the 4th International Conference on Numerical Methods in Geomechanics (Edmonton), Vol. 2, pp. 571-578.

Ohta, H., Kitamura, H., Itoh, M. and Katsumata, M., 1985. Ground movement due to advance of two shield tunnels. Proceedings of the 5th International Conference on Numerical Methods in Geomechanics (Nagoya), pp. 1161-1166.

Oliveira, M. and Ferreira, A.A., 1982. Consolidacao de Solo aluvionar mole: relato de um tratamento por injecao de cimento para escavacao de de tunel urbano na cidade de Sao Paulo. Anais do Simposio sobre Escavacao Subterraneas (Rio de Janeiro), Vol. 1, pp. 335-353.

OMTC 1976. Tunnelling Technology: an appraisal of the State-of-the-Art for applications to transit systems. Published by Ontario Ministry of Transportation and Communications, Toronto, 166p.

O'Reilly, M.P., Roxborough, F.F. and Hignett, H.J., 1976. Programme of laboratory, pilot and full-scale experiments in tunnel boring. Proceedings Tunnelling '76 (U.K.), pp. 287-299.

O'Reilly, M.P., Ryley, M.D., Barratt, D.A. and Johnson, P.E., 1981. Comparison of settlements resulting from three methods of tunnelling in loose cohesionless soil. Proceedings of the 2nd International Conference on Ground Movements and Structures (Cardiff), pp. 359-376.

O'Rourke, T.D., 1978. Discussion:Lateral displacement of shallow buried pipelines due to adjacent deep trench excavations. Geotechnique, Vol. 28, No. 2, pp. 214-216.

O'Rourke, T.D., Cording, E.J. and Boscardin, M., 1978. Damage to brick-bearing wall structures caused by adjacent braced cuts and tunnels. Proceedings of the Conference on Large Ground Movements and Structures (Cardiff), pp. 647-671.

O'Rourke, T.D. et.al., 1984. Guidelines for Tunnel Lining Design. Prepared by the UTRC Technical Committee on Tunnel Lining Design. ASCE Geotechnical Engineering Division. 82 p.

Orr, T.L.L., 1976. The behaviour of lined and unlined model tunnels in stiff clay. Ph.D. Thesis. Cambridge University.

Orr, T.L.L., Atkinson, J.H. and Wroth, C.P., 1978. Finite element calculations for the deformation around model tunnels. Computer Methods in Tunnel Design. Institution of Civil Engineers (London), pp. 121-144.

Oteo, C.S. and Moya, J.F., 1979. Estimation of the soil parameters of Madrid in relation to tunnel construction. Proceedings of the 7th European Conference on Soil Mechanics and Foundation Engineering (Brighton), Vol. 3, pp. 239-247.

Oteo, C.S. and Sagaseta, C., 1982. Prediction of settlements due to underground openings. Proceedings of the International Symposium on Numerical Models in Geomechanics (Zurich), September, pp. 653-659.

Palmer, A.C., 1966. A limit theorem for materials with non-associated flow rules, Journal de Mecanique, 5(2), 217-22.

Palmer, J.H.L. and Belshaw, D.J., 1979. Long-term performance of a machine-bored tunnel with use of an unreinforced, precast, segmented concrete lining in soft clay. Proceedings of the 2nd International Symposium Tunnelling '79 (IMM, London), pp. 165-178.

Palmer, J.H.L. and Belshaw, D.J., 1980. Deformations and pore pressures in the vicinity of a precast, segmented, concrete-lined tunnel in clay. Canadian Geotechnical Journal, Vol. 17, pp. 174-184.

Panet, M., 1976. Stabilite et Soutenement des tunnels. La mechanique des roches appliquee aux ouvrages du Genie Civil, Chapitre IX, pp.143-168. L'Ecole Nationale des Ponts et Chausses.

Panet, M. and Guellec, P. 1974. Contribution to the problem of the design of tunnel support behind the face. Proceedings, Third Congress, International Society for Rock Mechanics, Denver, Vol. 2, Part B, pp. 1163-1168. (in French).

Panet, M. and Guenot, A. 1982. Analysis of convergence behind the face of a tunnel. Tunnelling 1982, the Institution of Mining and Mettallurgy, pp. 197-204.

Paul, S.L., Hendron, A.J., Cording, E.J., Sgouros, G.E. and Saha, P.K., 1983. Design recommendations for concrete tunnel linings. Volume II: Summary of research and proposed recommendations. Report UMTA-MA-06-0100 83-3. National Technical Information Service, Springfield, Virginia, 22161.

Peck, R.B., 1969. Deep excavations and tunnelling in soft ground. Proceedings, 7th International Conference on Soil Mechanics and Foundation Engineering, Mexico, State-of-the-Art Vol., pp. 225-290.

Peck, R.B., 1981. Weathered rock portion of the Wilson Tunnel, Honolulu. Soft-Ground Tunnelling, Failures and Displacements (Ed. D. Resendiz and M.P. Romo), A.A. Balkema (Rotterdam), pp. 13-22.

Peck, R.B., Deere, D.U. and Capacete, J.L., 1956. Discussion on Skempton and MacDonald. Proceedings, Institution of Civil Engineers. Part II, Vol. 5, p. 778.

Peck, R.B., Hendron, A.J. and Mohraz, B., 1972. State-of-the-Art of soft grond tunnelling. Proceedings, 1st North American Rapid Excavation and Tunnelling Conference, Vol. 1, pp. 259-286.

Pelli, F., 1987. Near Face Behaviour of Deep Tunnels in Rock. Ph.D. Thesis, University of Alberta, 406p.

Pelli, F., Kaiser, P.K. and Morgenstern, N.R., 1986. Three-dimensional simulation of rock-liner interaction near tunnel face. Proceedings NUMOG II, Numerical Models in Geomechanics (Ghent).

Pender, M.J., 1980(a). Elastic solutions for a deep circular tunnel. Geotechnique, Vol. 30, pp. 216-222.

Pender, M.J., 1980(b). Simplified analysis for tunnel. Discussions. ASCE, GT7, p. 833-835.

Pender, M.J., 1980(c). Discussion of "Stress path method: second edition". Journal of the Geotechnical Engineering Division, ASCE, Vol. 106, No. GT9, pp. 1068-1071, September.

Penman, A.D.M., 1986. On the embankment dam. 26th Rankine Lecture. Geotechnique, Vol. 36, No. 3, pp. 301-348.

Penman, A.D.M. and Charles, J.A., 1974. Measuring movements of embankment dams. Proceedings, Symposium on Field Instrumentation in Geotechnical Engineering, Butterworths, pp. 341-358.

Pierau, B., 1981. Tunnelbemessung unter Berucksichtigung der raumlichen Spannungs-Verformungszustande an der Ortsbrust. Publication of the 'Institut fur Grundbau,

Bodenmechanik, Felsmechanik und Verkehrswasserbau der. R.W. Technische Hochschule Aachen, Heft 9, 182 p.

Pierau, B., 1982. Tunnel design with respect to the three-dimensional state of stresses and displacements around the temporary face. Proceedings, 4th International Conference on Numerical Methods in Geomechanics, Edmonton, (edited by Z. Eisenstein), Vol. 3, pp. 1221-1231.

Polshin, D.E. and Tokar, R.A., 1957. Maximum allowable non-uniform settlement of structures. Proceedings, 4th International Conference on Soil Mechanics and Foundation Engineering, (London), Vol. 1, pp. 402-405.

Potts, D.M., 1976. Behaviour of lined and unlined tunnels in sand. Ph.D. Thesis. Cambridge University.

Potts, D.M. and Burland, J.B., 1983. A numerical investigation of the retaining walls of the Bell Common tunnel. TRRL Supplementary Report 783 (U.K.).

Poulos, H.G., 1982. Simplicity a desirable end-point of geotechnical research. Ground Engineering, pp. 2 and 6.

Poulos, H.G. and Davis, E.H., 1980. Pile foundation analysis and design. John Wiley and Sons (New York), 397 p.

Prevost, J.H., 1980. Constitutive theory for soil. Proceedings of the Workshop on Limit Equilibrium, Plasticity and Generalized Stress-Strain in Geotechnical Engineering (McGill University), pp.745-814.

Ranken, R.E., 1978. Analysis of ground liner interaction for tunnels. Ph.D. Thesis. Univeristy of Illinois (Urbana-Champaign), 427 p.

Ranken, R.E. and Ghaboussi, J., 1975. Tunnel design considerations: analyses of stresses and deformations around advancing tunnels. Report UILU-ENG75-2016 (NTIS - National Technical Information Service, U.S. Department of Commerce, Springfield, VA 22161).

Read, H.E. and Hegemier, G.A., 1984. Strain softening of

rock, soil and concrete. A review article. Mechanics of Materials 3, pp. 271-294.

Rebull, P.M., 1972. Earth responses in soft ground tunnelling. Proceedings, Specialty Conference on Performance of Earth and Earth Supported Structures. (Lafayette), Vol. 1, Part 2., pp.1517-1535.

Resendiz, D., 1979. Full-scale observation, numerical modeling, and generalization in soil mechanics. Opening Lecture at the International Symposium on Soil Mechancis (Oaxaca), Publication E-37, Universidad Nacional Autonoma de Mexico.

Resendiz, D. and Romo, M.P., 1972. Analysis of embankement deformations. ASCE Specialty Conference on Performance of Earth and Earth-Supported Structures, Vol. 1, Part 1, pp. 817-836.

Resendiz, D. and Romo, M.P., 1981. Settlements upon soft-ground tunneling: theoretical solution. Soft-Ground Tunneling - Failures and Displacements. Edited by D. Resendiz and M.P. Romo (A.A. Balkema), pp. 65-74.

Reyes, S.F. and Deere, D.U., 1966. Elastic-plastic analysis of underground openings by the finite element method. Proceedings, 1st Congress International Society of Rock Mechanics, Lisbon 1966, Vol. II, pp. 477-483.

Ritter, W., 1879. Die statik der tunnelgewolbe. Springer, Berlin (quoted by Steiner and Einstein, 1980:37).

Rocha, M., 1975. Rock Mechanics in Underground Projects (in Portuguese). Lecture Notes, EPUSP (Sao Paulo).

Rodriguez, L.B., Ruelas, S.A. and Frausto, L.G., 1983. Movimientos presentados durante la excavacion de un tunel con escudo. Proceedings of the 7th Panamerican Conference on Soil Mechanics and Foundation Engineering (Vancouver), Vol. I, pp.425-437.

Rodiguez Roa, F., 1981. Some considerations for tunnel design. Proceedings, 10th International Conference on Soil Mechanics and Foundation Engineering (Stockholm), Vol. 1, pp. 353-356.

Romo, M.P. and Diaz, C.M., 1981. Face stability and ground settlement in shield tunnelling. Proceedings, 10th International Conference on Soil Mechanics and Foundation Engineering. Vol. 1, pp. 357-360.

Romo, M.P. and Resendiz, D., 1982. Observed and computed settlements in a case of soft-ground tunnelling. Proceedings, 4th International Conference on Numerical Methods in Geomechanics. (Edmonton), Vol. 2, pp. 597-604.

Roscoe, K.H., 1970. The influence of strains in soil mechanics. Geotechnique 20, No. 2, pp. 129-170.

Roscoe, K.H. and Burland, J.B., 1968. On the generalized stress-strain behaviour of 'wet' clay. Engineering Plasticity, Eds. J. Heyman and F.A. Leckie, Cambridge University Press, pp. 535-609.

Rowe, R.K., 1986. The prediction of deformations caused by soft ground tunnelling - Recent trends. Canadian Tunnelling.

Rowe, R.K. and Kack, G.J., 1983. A theoretical examination of the settlements induced by tunnelling: four case histories. Canadian Geotechnical Journal, 20, pp. 299-314.

Rowe, R.K., Lo, K.Y. and Kack, G.J., 1981. The prediction of subsidence above shallow tunnels in soft soil. Proceedings, Symposium on Implementation of Computer Procedures and Stress-Strain Laws in Geotechnical Engineering (Chicago), pp.266-280.

Rowe, R.K., Lo, K.Y. and Kack, G.J., 1983. A method of estimating surface settlement above tunnels constructed in soft ground. Canadian Geotechnical Journal, 20, pp. 11-22.

Rozsa, L., 1963. Die Bemessung kreisformiger Tunnelwundungen aus prafabrizierten Stahlbetonelementen nach dem Verfahren der Grenzbelastungen. Bauingenieur 38, Heft 11, pp. 434-441.

Rumsey, P.B. and Dorling, C., 1985. The prediction of ground

movement and induced pipe strain caused by trench excavation. Proceedings, 3rd International Conference on Ground Movements and Structures (Cardiff), pp. 24-49.

Ryley, M.D., Johnson, P.E., O'Reilly, M.P. and Barrat, D.A., 1980. Measurements of ground movements around three tunnels in loose cohesionless soil. TRRL Laboratory Report 938 (Crowthorne, U.K.).

Saenz, J.T. and Utesa, L.V., 1971. Settlement around shield driven tunnels (in Spanish). Proceedings, 4th Panamerican Conference on Soil Mechanics and Foundation Engineering (Puerto Rico), Vol. II, pp. 225-241.

Sagaseta, C., 1973. Estado tenso-deformacional alredor de un tunel excavado en un medio elasto-plastico, con special consideracion de la influencia del proceso construtivo. Ph.D. Thesis. Escuela Tecnica Superior de Ingenieros de Caminos, Canales y Puertos de Madrid.

Sagaseta, C., Moya, J.F. and Oteo, C.S., 1981. Estimation of ground subsidence over urban tunnels. Proceedings of the 2nd International Conference on Ground Movements and Structures (Cardiff), pp. 331-344.

Sagaseta, C. and Oteo, C., 1974. Analisis Teorico de la Subsidencia Originada por la Excavacion de Tuneles. Proceedings, 1er Simposic Nacional Sobre Tuneles (Madrid), II-10, pp. 1-10, discussion pp. 76-79.

Sakurai, S., 1970. Stability of tunnel in viscoelastic-plastic medium. Proceedings, 2nd Congress of the International Society for Rock Mechanics (Beograd), pp. 521-529.

Sakurai, S., 1981. Direct strain evaluation technique in construction of underground openiong. Proceedings, 22nd US Symposium on Rock Mechanics: Rock Mechanics from Research to Application (MIT), pp. 278-282.

Sakurai, S., Yamamoto, Y., 1976. A numerical analysis of the maximum earth pressure acting on tunnel lining. Proceedings, 2nd International Conference on Numerical Methods in Geomechanics (Blacksburg), Vol. II, pp. 821-833.

Samarasekera, L., 1987. Ph.D. Thesis in preparation. University of Alberta.

Sasanabe, M., Matsubara, H. and Nakao, T., 1986. Planning and results of large diameter tunnel driven by soil plasticizing shield. Chichibu section of Nagoya Municipal Subway. Proceedings, International Congress on Large Underground Openings - ITA (Firenze), Vol. I, pp. 925-932.

Sauer, G. and Jonuscheit, P. 1976. Krafteumlagerung in der Zwischenwand eines Doppelrohrentunnels in Zuge eines Synchronvortriebes. Rock Mechanics (Springer, Vienna), 8, pp. 1-22.

Sauer, G. and Sharma, B., 1977. A system for stress measurement in constructions in rock. Proceedings, International Symposium on Field Measurements in Rock Mechanics (edited by K. Kovari), Zurich, Vol. 1, pp. 317-329.

Schikora, K., 1982. Calculation model and measuring results for a double tunnel with low overburden in quarternary soil. Tunnel ('STUVA - Studiengesellschaft fur unterirdische Verkehrsanlagen' - Cologne 3/82, pp. 153-161.

Schikora, K., 1983. Double tunnel in the Munich underground. Tunnel (STUVA - Cologne), 2/83, pp. 71-79.

Schikora, K., 1984. Plane and spatial finite element calculations in tunnelling. Tunnel (STUVA - Cologne), 3/84, pp. 158-161.

Schikora, K. and Fink, T., 1982. Berechnungsmethoden moderner bergmannischer Bauweisen beim U-Bahn-Bau. Bauingenieur 57, pp.193-198.

Schmid, H., 1926. Statische Probleme des Tunnel - und Druckstollenbaues und ihre gegenseitigen Beziehungen, Springer, Berlin Wien 1926.

Schmidt, B., 1969. Settlements and ground movements associated with tunneling in soil. Ph.D. Thesis. University of Illinois at Urbana-Champaign.

Schmidt, B. 1970. Gravitational stress field around a tunnel in soft ground: Discussion. Canadian Geotechnical Journal, Vol. 7, pp. 346-348.

Schmidt, B., 1984. Tunnel lining design - do the theory work?, Proceedings, 4th Australia - New Zealand Conference on Geomechanics, (Perth), May.

Schmidt, B. and Sousa Pinto, 1983. Geotechnical engineering for transportation structures - general report. Proceedings, 7th Panamerican Conference on Soil Mechanics and Foundation Engineering, (Vancouver), Vol. III, pp. 1001-1034.

Schmitter, J.M. and Moreno, A.F., 1983. Tunel con Deformaciones Excesivas. Proceedings, 7th Panamerican Conference on Soil Mechanics and Foundation Engineering (Vancouver), pp. 401-411.

Schneebeli, G., 1957. Une analogie mecanique pour l'etude de la stabilite des ouvrages en terre a deux dimensions. Proceedings 4th International Conference on Soil Mechanics and Foundation Engineering (London), Vol. II, pp. 228-232.

Schofield, A.N., 1980. Cambridge geotechnical centrifuge operations. Geotechnique, Vol. 30, No. 3, pp. 227-268.

Schulz, W. and Edeling, H., 1973. Die Neue Osterreichische Tunnelbauweise beim U-Bahnbau in Frankfurt am Main. Rock Mechanics (Springer, Vienna), Supplement 2, pp. 243-256.

Schulze, H., and Duddeck, H., 1964(a). Statische Berechnung schildvorgetriebener Tunnel. Festschrift "Beton- und Monierbau AG 1889-1964", Dusseldorf, pp. 87-114.

Schulze, H., and Duddeck, H., 1964(b). Spannungen in Schildvorgetriebenen Tunneln. Beton-und Stahlbetonbau (Berlin), Heft 8, 59 Jahrgang, pp. 169-175.

Schwartz, C.W., Azzouz, A.S. and Einstein, H.H., 1980. Improved design of tunnel supports: Vol. 2 - Aspects of Yielding in ground-structure interaction. Report UMTA-MA-06-0100-80-5, NTIS, U.S. Department of Commerce, Springfield, VA 22161.

Schwartz, C.W. and Einstein, H.H., 1980. Improved design of tunnel supports: Vol. 1 - Simplified analysis for ground structure interaction in tunnelling. Report UMTA-MA-06-0100-80-4 (NTIS - National Technical Information Service, U.S. Department of Commerce, Springfield, VA 22161).

Selby, S.M., 1970. Handbook of tables for mathematics (4th edition), Publisher: The Chemical Rubber Co. (Ohio).

Semprich, S., 1980. Berechnung der Spannungen und Verformungen im Bereich der Ortsbrust von Tunnelbauwerken im Fels. Veroff. D. Inst. f. Grundbau, Bodenmechanik, Felsmechanik und Verkehrswasserbau der RWTH Aachen, Heft 8.

Seneviratne, H.N., 1979. Deformations and pore-pressures around model tunnels in soft clay. Ph.D. Thesis. University of Cambridge.

Seychuk, J.L., 1977. Discussion presented to 30th Canadian Geotechnical Conference.

Sgouros, G.E., 1982. Structural behaviour and design implications of concrete tunnel linings based on model tests and parameter studies. Ph.D. Thesis, University of Illinois at Urbana-Champaign., 385 p.

Simondi, S., Negro, A. and Kuperman, S., 1982. The use of shotcrete as secondary lining of a urban tunnel through soil (in Portuguese). Proceedings, Symposium on Concrete for Foundation and Underground Structures (Brazilian Concrete Institute), pp. 42-68, Sao Paulo.

Sizer, K.E., 1976. The determinations and interpretation of ground movements caused by shield tunnelling in silt alluvium at Willington Quay, North-East England. M.Sc. Thesis. University of Durham.

Skempton, A.W., 1951. The bearing capacity of clays. Building Research Congress, England.

Skempton, A.W., 1954. The pore-pressure coefficients A and B. Geotechique, Vol. 4, pp. 143-147.

Skempton, A.W., 1961. Horizontal stresses in overconsolidated Eocene clay. Proceedings, 5th International Conference on Soil Mechanics and Foundation Engineering (Paris), Vol. 1, pp. 351-357.

Skempton, A.W., 1964. Long-term stability of clay slopes. 4th Rankine Lecture, Geotechnique, 14, pp. 77-101.

Skempton, A.W., 1977. Slope stability of cuttings in Brown London Clay. Proceedings, 9th International Conference on Soil Mechanics and Foundation Engineering (Tokyo), pp. 261-269.

Skempton, A.W. and MacDonald, D.H., 1956. Allowable settlement of buildings. Proceedings of the Institute of Civil Engineers, Part III, Vol. 5, pp. 727-768.

Sketchley, C.J., 1973. The behaviour of kaolin in plane strain. Ph.D. Thesis, Cambridge University.

Sonntag, G. and Fleck, H., 1973. Ahnlichkeitsgerechte kohasionslose Modellboden fur Modellversuche an Hohlraumauskleidungen. Strasse Brucke Tunnel, 25 Jahrung, Heft 4, pp. 85-90.

Sonntag, G. and Fleck, H., 1976. Zum Bettungsmodul bei Tunnelauskleidungen. Ingenieur - Archiv 45, pp. 269-273.

Sousa Pinto, C. and Massad, F., 1972. Caracteristicas dos solos variegados da cidade de Sao Paulo. Publicacao No. 984, Instituto de Pesquisas Tecnologicas, Sao Paulo, 31 p.

Sozio, L.E., 1978. Settlements in a Sao Paulo shield tunnel. Tunnels and Tunnelling (September), pp. 53-55.

Steiner, W. and Einstein, H.H., 1980. Improved design of tunnel supports: Volume 5 - Empirical methods in rock tunneling - review and recommendations. Report UMTA-MA-06-0100-80-8, NTIS (National Technical Information Service), U.S. Department of Commerce, Springfield, VA 22161.

Steiner, W., Einstein, H.H. and Azzouz, A., 1980. Improved

design of tunnel supports: Vol. 4 - Tunnel practices in Austria and Germany. Report UMTA-MA-06-0100-80-7, NTIS (National Technical Information Service), U.S. Department of Commerce, Springfield, VA 22161.

Stini, J., 1950. Tunnelbaugeologie. Springer (Vienna). (quoted by Steiner and Einstein, 1980).

Strobl, B., 1986. NATM under compressed air - geomechanical aspects and numerical modelling. Proceedings, International Congress on Large Underground Openings, ITA (Firenze), Vol. II, pp. 686-692.

Stroh, D. and Chambosse, G., 1973. Messungen und Setzungsursachen beim Tunnelvortrieb im Frankfurter Ton. Strasse Brucke Tunnel, Heft 2, pp. 38-42.

Sulem, J., Panet, M. and Guenot, A., 1987(a). Closure analysis in deep tunnels, International Journal of Rock Mechanics, Mining Sciences and Geomechanics Abstract, Vol. 24, No. 3, pp. 145-154.

Sulem, J., Panet, M. and Guenot, A., 1987(b). An analytical solution for time-dependent displacements in a circular tunnel. International Journal of Rock Mechanics, Mining Sciences and Geomechanics Abstract, Vol. 24, No. 3, pp. 155-164.

Sungur, T., 1984. A modern design for tunnel lining. Tunnels and Tunnelling, November, pp. 21-22.

Sweet, A.L. and Bogdanoff, A.L., 1965. Stochastic model for predicting subsidence. Journal of the Engineering Mechanics Division, A.S.C.E., EM 2, pp. 21-45.

Swoboda, G., 1979. Finite element analysis of the New Austrian Tunnelling Method (NATM). Proceedings, 3rd International Conference on Numerical Methods in Geomechanics, Aachen (edited by W. Wittke), Vol. 2, pp. 581-586.

Swoboda, G., 1982. Special problems during the geomechanical analysis of tunnels. Proceedings, 4th International Conference on Numerical Methods in Geomechanics (Edmonton), Vol. 2, pp. 605-609.

Swoboda, G., 1985. Interpretation of field measurements under consideration of the three-dimensional state of stress, the viscoelasticity of shotcrete, and viscoplastic behaviour of rock. Proceedings, 5th International Conference on Numerical Methods in Geomechanics (Nagoya), pp. 1651-1658.

Swoboda, G. and Laabmayr, F., 1978. Beitrag zur Wieterentwicklung der Berechnung flachliegender Tunnelbauten im Lockergestein. In: Moderner Tunnelbau bei der Munchner U-Bahn, Springer, (edited by H. Lessmann), pp. 55-71.

Symons, I.F., 1978. Discussion: Lateral displacement of shallow buried pipelines due to adjacent deep trench excavations. Geotechnique, Vol. 28, No. 2, pp. 212-214.

Szechy, K., 1973. The art of tunnelling. 2nd English Edition. Akademiai Kiado, Budapest, 1097p.

Takagi, N., Shimamura, K. and Nishio, N., 1985. Buried pipe responses to adjacent ground movements associated with tunnelling and excavations. Proceedings of the 3rd International Conference on Ground Movements and Structures (Cardiff), pp. 97-112.

Takemoto, T., Ryoke, K. and Teramoto, T., 1977. Creep behaviour of soft ground tunnel. Proceedings, International Symposium on Field Measurements in Rock Mechanics (Zurich), pp. 669-682.

Tan, D.Y., 1977. Finite element analysis and design of chemically stabilized tunnels. Ph.D. Thesis. Stanford University.

Tan, D.Y. and Clough, G.W., 1980. Ground control for shallow tunnels by soil grouting. Journal of the Geotechnical Engineering Division, American Society of Civil Engineers, Vol. 106, No. GT9, pp.1037-1057.

Tarzi, A.I., Menzies, B.K. and Crofts, J.E., 1979. Bending of jointed pipelines in laterally deforming soil. Geotechnique, Vol. 29, No. 2, pp. 203-206.

Taylor, R.N., 1980. Modelling of tunnel failure in silt.

CUED/D - Soils Report TR81 (University of Cambridge).

Taylor, R.N., 1984. Ground movements associated with tunnels and trenches. Ph.D. Thesis. Cambridge University. (quoted by Gunn, 1984).

Terzaghi, K., 1936. Stress distribution in dry and in saturated sand above a yielding trap-door. 1st International Conference on Soil Mechanics and Foundation Engineering, Vol. 1, pp. 307-311.

Terzaghi, K., 1942. Shield tunnels of the Chicago subway. Journal of the Boston Society of Civil Engineers, Vol. 29, pp. 163-210.

Terzaghi, K., 1943(a). Theoretical Soil Mechanics. John Wiley and Sons, Inc., New York.

Terzaghi, K., 1943(b). Liner-plate tunnels on the Chicago (Ill.) subway. Transactions of the American Society of Civil Engineers, 108, pp. 970-1007.

Terzaghi, K., 1946. Rock defects and loads on tunnel supports. In: Rock Tunneling with Steel Supports (Ed. by R.V. Proctor and T.L. White), pp. 17-102.

Terzaghi, K., 1956. Discussion on Skempton and MacDonald. Proceedings, Institution of Civil Engineers. Part II, Vol. 5, p.775.

Thomson, S., 1969. A summary of laboratory results on Lake Edmonton clay. Internal Note SM2, (April 24), Department of Civil Engineering, University of Alberta.

Thomson, S., Martin, R.L., and Eisenstein, Z., 1982. Soft zones in the glacial till in downtown Edmonton. Canadian Geotechnical Journal, Vol. 19, pp. 175-180.

Thurber Consultants Ltd., 1980. South LRT Extension, Geotechnical Report No. 5, In situ pressuremeter tests, 104th and 107th street stations, Unpublished report to Edmonton Transit.

Thurber Consultants Ltd., 1982. South LRT Extension. Geotechnical Report No. 14, Tunnel section, instrumentation test section at 105th street. Report submitted to LRT Project. Edmonton Transit (February 4).

Togerson, R., 1986. Personal Communication.

Uriel, S. and Oteo, C.S., 1979. Measurements in an experimental tunnel bored in the Sevilla Blue Marls and recommendations for the subway design. Proceedings, 4th Congress of the International Society for Rock Mechanics (Montreux), pp. 697-703.

Vaid, Y.P., 1985. Effect of consolidation history and stress path on hyperbolic stress-strain relations. Canadian Geotechnical Journal, Vol. 22, pp.172-176.

Van Dillen, D. and Fellner, R.W., 1979. A two-dimensional finite element technique for modeling rock/structure interaction of a lined underground opening. Proceedings, 20th U.S. Symposium on Rock Mechanics (Austin), pp. 251-258.

Van Sin Jan, M.L. and Cording, E.J., 1984. Ground and lining behaviour of shallow underground rock chambers for the Washington D.C. subway. Proceedings of a Symposium on Design and Performance of Underground Excavations (Cambridge, U.K.) pp. 415-422.

Vardoulakis, I.G., 1986. Stability and bifurcation in geomechanics. Notes of a short course. University of Alberta. (June 2 to 6).

Vardoulakis, I.G., Graf, B. and Gudehus, G., 1981. Trap-door problem with dry sand: a statical approach based upon model test kinematics. International Journal for Numerical and Analytical Methods in Geomechanics, Vol. 5, pp.57-78.

Vasishth, V., 1986. Mount Baker Ridge Tunnel. Proceedings, International Congress on Large Underground Openings - ITA (Firenze), Vol. I, pp. 579-587.

Vaughan, P.R., 1974. Embankment dams. Course notes. Imperial College, Department of Civil Engineering, University of

London.

Vaughan, P.R. and Walbancke, H.J., 1973. Pore pressure changes and the delayed failure of cutting slopes in overconsolidated clay. Geotechnique 23, No. 4, pp. 531-539.

Verruijt, A., 1976. Non-linear elastic approximations of the behaviour of soils. Proceedings, 2nd International Conference on Numerical Methods in Geomechanics (Virginia), Vol. III, pp. 1321-1328.

Verski, A., Cesar, S.E.D.M. and Ibri, I.A., 1985. Observacao da interacao solo-estrutura atraves da instrumentacao de uma secao tipica do interceptor Tiete do Sistema SANEGRAN. Proceedings of the 2nd Symposium on Underground Excavation (ABGE), Vol. 1, pp. 475-492.

Vesic, A.S. and Clough, G.W., 1968. Behaviour of granular materials under high stresses. Journal of the Soil Mechanics and Foundations Division, ASCE, Vol. 94, No. SM3, pp.661-688.

Voellmy, A., 1937. Eingebettete Rohre. Leemann u. Co., Zurich Leipzig.

Wanniger, R., 1979. New Austrian Tunnelling Method and finite elements. Proceedings, 3rd International Conference on Numerical Methods in Geomechanics, Aachen (edited by W. Wittke), Vol. 2, pp. 587-597.

Wanniger, R. and Breth, H., 1978. Moglichkeiten und Grenzen numerischer Rechenverfahren im Grundbau. Bauingenieur, 53, Heft 12, pp. 465-470.

Ward, W.H., 1956. Discussion on Skempton and MacDonald. Proceedings of the Institution of Civil Engineers, Part III, Vol. 5, pp. 782.

Ward, W.H., 1969. Discussion in Main Session 4. Proceedings, 7th International Conference on Soil Mechanics and Foundation Engineering (Mexico), Vol. 3, pp. 320-325.

Ward, W.H., 1978. Ground supports for tunnels in weak rock.

18th Rankine Lecture. Geotechnique, Vol. 28, pp. 133-171.

Ward, W.H., Coats, D.J., and Tedd, P. 1976. Performance of tunnel support systems in the Four Fathom Mudstone. Tunnelling '76, London, March, pp. 329-340, Discussion, pp. 348-367.

Ward, W.H. and Pender, M.J., 1981. Tunnelling in soft ground. General report, Session 2, 10th International Conference on Soil Mechanics and Foundation Engineering, Stockholm, Vol. 4, pp. 261-275.

Watanabe, T., 1984. Several cases of large size slurry shield tunnelling in heterogeneous soils. Proceedings, 1st Latinamerican Congress of Underground Constructions - ITA (Caracas), Vol. I, pp. 329-337.

Weber, J., 1984. Experience using compressed air drivage and shotcreting. Tunnel 1/84, pp. 16-27.

Wilson, A.H., 1981. Stress and stability in coal ribsides and pillars. Proceedings, 1st Annual Conference on Ground Control in Mining (West Virginia University), pp. 1-12. Quoted by Brady and Brown (1985:374).

Windels, R., 1966. Spannungstheorie zweiter Ordnung fur den teilweise gebetteten Kreisring. Bautechnik 43, Heft 8, pp. 265-274.

Windels, R., 1967. Kreisring im elastischen Kontinuum. Bauingenieur 42. Jahrgang, Heft 12, pp. 429-439.

Winter, H., 1982. Similarity technique for numerical methods in geomechanics. Proceedings, 4th International Conference on Numerical Methods in Geomechanics (Edmonton), Vol. 3, pp. 1073-1080.

Wittebolle, R.J., 1983. The influence of microfabric on the engineering properties of glacial tills. M.Sc. Thesis. University of Alberta.

Wittebolle, R.J., 1987. Personal Communication.

Wittke, W., 1977(a). Static analysis for underground openings in jointed rock. Numerical Methods in Geotechnical Engineering (Ed. by C.S. Desai and J.T. Christian), McGraw Hill, pp. 589-638.

Wittke, W., 1977(b). New design concept for underground openings in rock. Finite Elements in Geomechanics (Ed. by G. Gudehus), John Wiley and Sons, pp. 413-478.

Wittke, W., Carl, L. and Semprich, S., 1974. Felsmessungen als Grundlage fur den Entwurf einer Tunnelauskleidung. Interfels Messtechnik Information, pp. 3-11.

Wittke, W., Feiser, J. and Krieger, J., 1986. Stability analysis of an advanced vault excavation with unlined invert according to the finite element method. International Journal for Numerical and Analytical Methods in Geomechanics, Vol. 10, pp. 259-281.

Wittke, W. and Gell, K., 1980. Raumliche Standsicherheitsuntersuchungen fur einem oberflachennachen Tunnelabschnitt des Bauloses B3 der Stadtbahn Bochum. Geotechnik, Heft 3, pp. 111-119.

Wittke, W., and Pierau, B., 1976. Stability analysis of tunnels in jointed rock. Proceedings, 2nd International Conference on Numerical Methods in Geomechancis, Blacksburg, Vol. III, pp. 1401-1418.

Wittke, W. and Semprich, S., 1974. Messungen als felsmechanische Grundlage beim Entwurf eines Stollens. Discussion in the Proceedings of the 3rd Congress of the International Society for Rock Mechanics (Denver), Vol. III, pp. 121-123.

Wong, R.C.K., 1986. Design and performance evaluation of tunnels and shafts. Ph.D. Thesis. University of Alberta. 308 p.

Wong, R.C.K. and Kaiser, P.K., 1986. Ground behaviour near soft ground tunnels. Proceedings, International Congress on Large Underground Openings (Firenze), Vol. I, pp. 942-951.

Wong, R.C.K. and Kaiser, P.K., 1987. Prediction of ground

movements above shallow tunnels. Proceedings of the International Symposium on Prediction and Performance in Geotechnical Engineering (Calgary), pp. 329-343.

Wroth, C.P. and Houlsby, G.T., 1985. Soil Mechanics - Property characterization and analysis procedures. Proceedings, 11th International Conference on Soil Mechanics and Foundation Engineering (San Francisco), Vol. 1, pp. 1-55.

Wroth, C.P. and Hughes, J.M.O. (1974). Development of a special instrument for the in situ measurement of the strength and stiffness of soils. Proceedings, Engineering Foundation Conference on Subsurface Exploration for Underground Excavations and Heavy Construction, N.E. College, Henniker, (New Hampshire), pp. 295-311.

Yamaguti, S., 1929. On the stresses around a horizontal circular hole in a gravitating elastic solic. Journal of the Civil Engineering Society of Japan, Vol. 15, pp. 291-303. Quoted by Mindlin, 1940:1118).

Yeates, J., 1985. The response of buried pipelines to ground movements caused by tunnelling in soil. Proceedings, 3rd International Conference on Ground Movements and Structures (Cardiff), pp. 129-144.

Yoshida, K., Kondoh, H., Kibe, T., and Takasaki, H., 1986. Tunnelling work in sandy-gravel stratum in urban area. Countermeasures and its results against environmental problems. Proceedings, International Congress on Large Underground Openings -ITA (Firenze), Vol. I, pp. 952-958.

Yoshikoshi, W., Watanab, O. and Takagi, N., 1978. Prediction of ground settlements associated with shield tunnelling. Soils and Foundations, Vol. 18, No. 4, pp. 47-59.

Zagottis, D.L. 1981. An application of finite element non-linear plane analysis to tunnel decision. Proceedings, Symposium on Implementation of Computer Programs and Stress-Strain Laws in Geotechnical Engineering (Chicago), pp. 281-290.

Zienkiewicz, O.C., 1983. The Finite Element Method, Third

Edition. McGraw Hill, London.

APPENDIX A - RESULTS OF 3-D FINITE ELEMENT ANALYSES

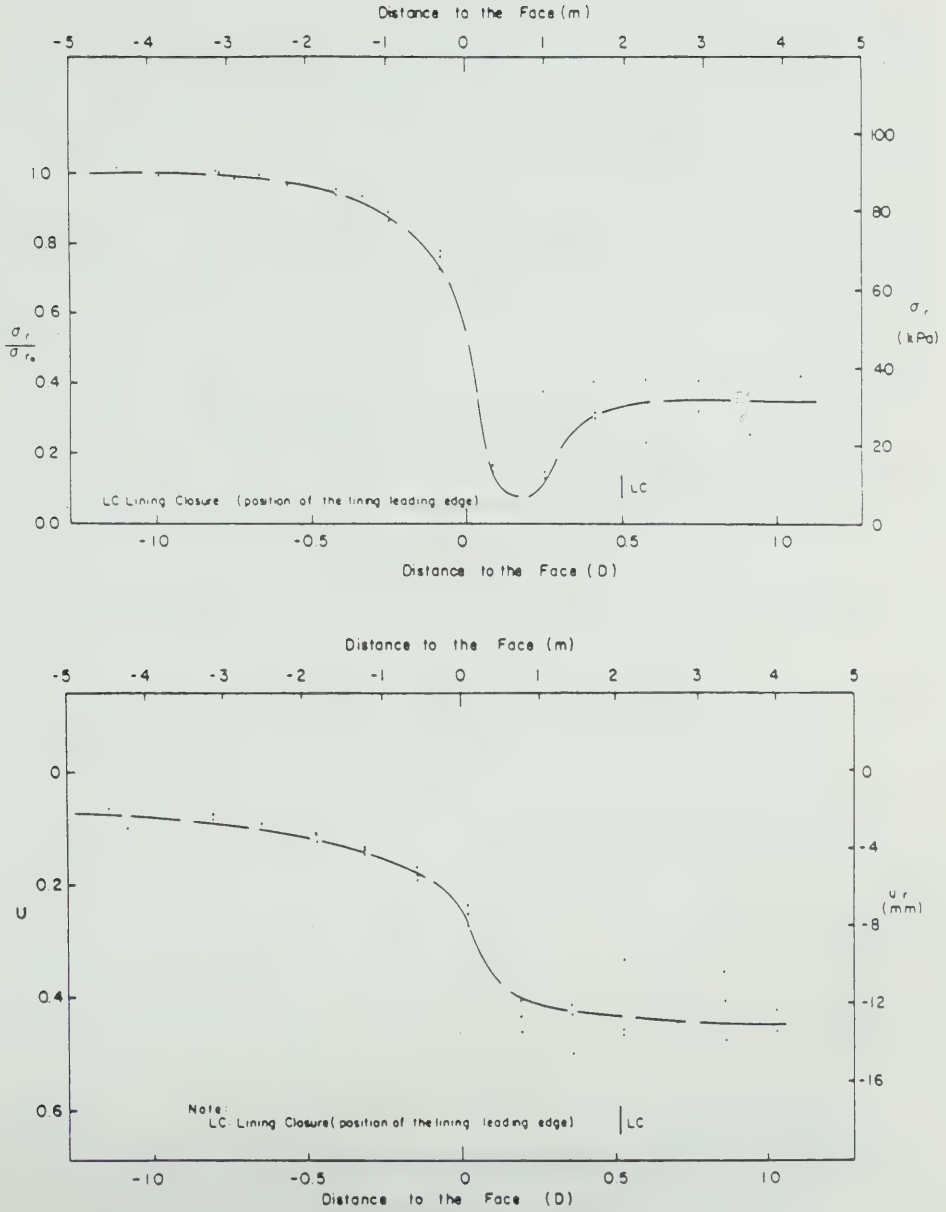

Figure A.1 Radial Stresses and Displacements at the Crown Elevation (L/D=1/2)

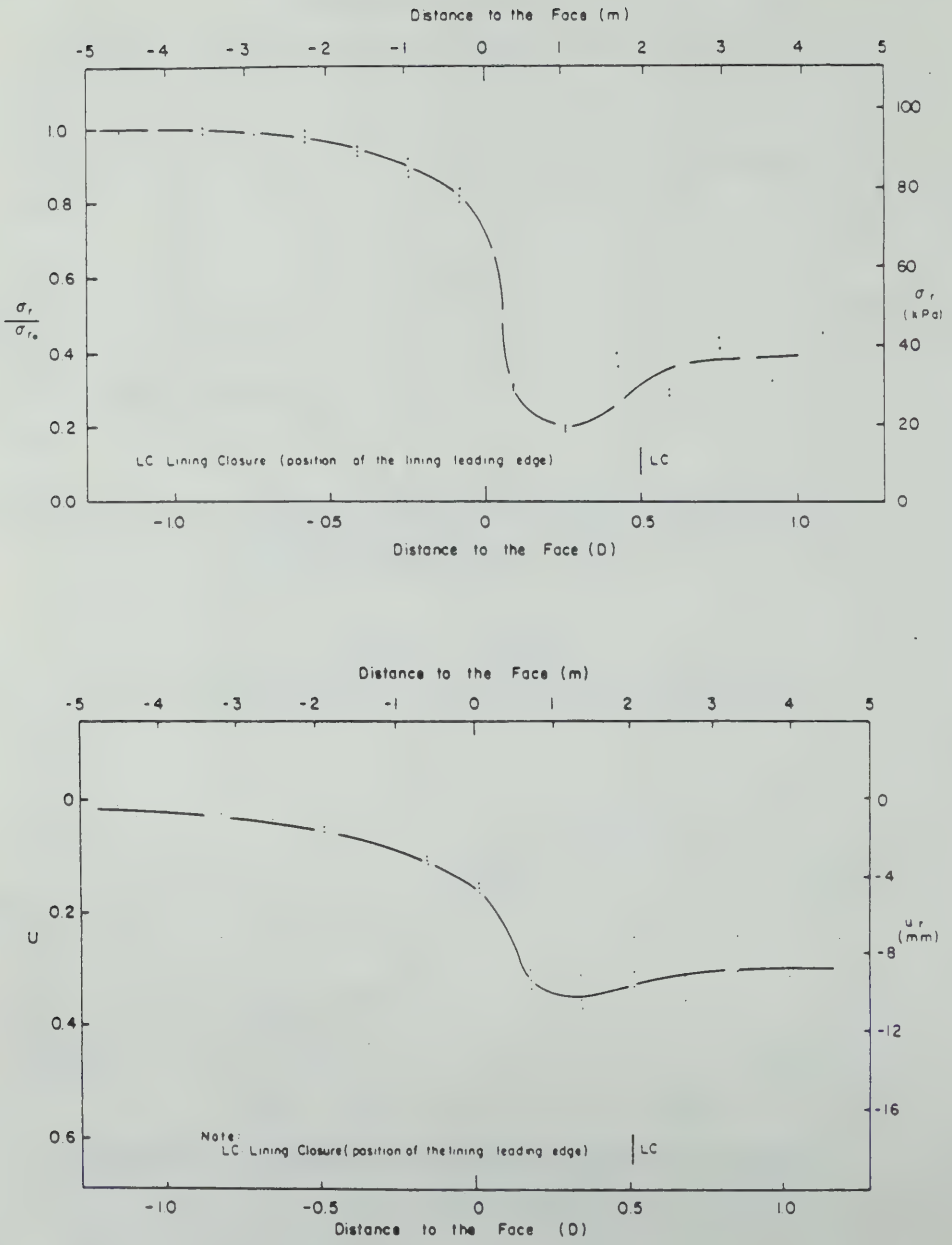

Figure A.2 Radial Stresses and Displacements at the Springline Elevation (L/D=1/2)

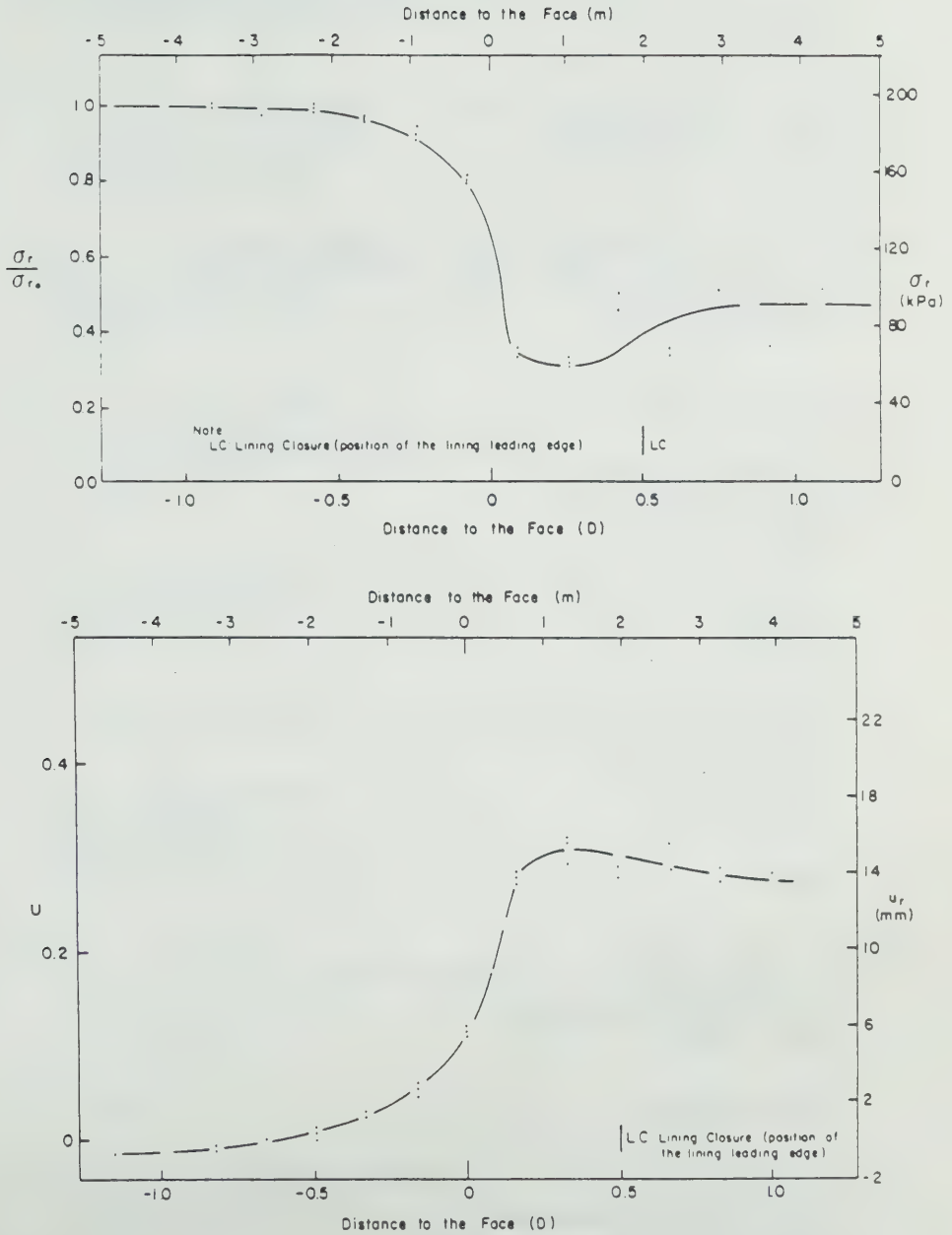

Figure A.3 Radial Stresses and Displacements at the Floor Elevation (L/D=1/2)

APPENDIX B - LIST OF RESPONDENTS TO THE QUESTIONNAIRE

AUSTRIA

1. Prof. Franz Pacher and Mr. N. Ayaydin
   Franz Josef-Strasse 3
   A-5020 Salzburg

2. Mr. Klaus Mussger and Mr. G. Schicktanz
   c/o Geoconsult Consulting Engineers
   Sterneckstrasse 55
   A-5020 Salzburg

CZECHOSLOVAKIA

3. Mr. Josef Novak
   Vodni stavby, o.p.
   Delnicka 12
   Praha 7

ENGLAND

4. Mr. D. Buckley
   c/o Sir William Halcrow and Partners Ltd.
   Vineyard House
   44 Brook Green
   London W6 7BY

FRANCE

5. Mr. Marc Panet
   c/o Simecsol
   115 Rue Saint Dominique
   75007 Paris

WEST GERMANY

6. Dr. T. Baumann
   c/o Philip Holzmann AG
   Herzog-Heinrich-Strasse 20-22
   8000 Munchen 2

7. Prof. Heinz Duddeck

Consulting Engineer
Greifwaldstrasse 38
3300 Braunschweig

8. Dr. Fritz Hartmann
Consulting Engineer
Bahnhofstrasse 39
2248 Hemmingstedt

9. Dr. S. Babendererde
c/o Hochtief AG
Rellinghauser Strasse 53-57
4300 Essen

10. Dr. F. Blennemann
c/o Studiengesellschaft STUVA
Mathias-Bruggen-Strasse 41
5000 Koln 30

11. Mr. J. Weber
c/o U-Bahn-Referat
Viktualienmarkt 13
8000 Munchen 2

HUNGARY

12. Dr. Laszlo Rozsa
c/o UVATERV
Jozsef Attila u. 8
1051 Budapest

13. Mr. G. Greschik
c/o FTV Consulting Engineers
Reviczky utca 4
1088 Budapest

SPAIN

14. Mr. J.M. Gutierrez Manjon
Cardinal Belluga 21
28028 Madrid

15. Dr. C. Sagaseta
c/o E.T.S. Ingenieros de Caminos

Avda. de Los Castros, s/n
39005 Santander

SWITZERLAND

16. Dr. E. Andraskay
c/o Basler and Hofmann AG
Forchstrasse 395
8029 Zurich

CANADA

17. Mr. D.J. Phelps and Dr. J.R.T. Brandt
c/o UMA Engineering
17007-107 Avenue
Edmonton, Alberta
T5S 1G3

18. Mr. E.W. Brooker
c/o EBA Engineering
14535-118 Avenue
Edmonton, Alberta
T5R 0B9

19. Mr. John Yan Egmond
c/o Trow Ltd.
1595 Clarke Blvd.
Brampton, Ontario
L6T 4V1

20. Mr. M. Walia
10180 - Shellbridgeway
Richmond, British Columbia
V6X 2W7

USA

21. Dr. Birger Schmidt
c/o Parsons Brinckerhoff
1625 Van Ness Avenue
San Francisco,
California, 94109

22. Dr. Gerard Sauer

Consultant Engineer
11403 Orchard Green CT.
Reston (Washington, D.C.)
Virginia, 22090

23. Mohamad Irshad
c/o DeLeuw, Cather and Co.
600 Fifth Street, NW
Washington, D.C., 20001

24. Dr. D.R. McCreath
c/o Golder Associates Inc.
4104 148th Avenue, NE
Redmond
Washington, 98052

MEXICO

25. Mr. J. Schmitter
c/o Solum S.A. de C.V.
Rio Becerra 27 5.° Piso
Col. Napoles
03810 Mexico, DF.

BRAZIL

26. Mr. Claudio Casarin
c/o THEMAG Engenharia Ltda.
Rua Beija Flor 34, Vilage 1
Lagoa da Conceicao
88000 Florianopolis, S.C.

27. Dr. Carlos Eduardo Moreira Maffei
Consulting Engineer
Al. Austria, 772, Alphaville Residencial I
06400 Barueri, SP

28. Mr. Mosze Gitelman and Mr. Roberto Kochen
c/o Figueiredo Ferraz Ltda.
Rua Conde de Iraja, 118
04118 Sao Paulo, SP

29. Messrs. Hamilton G. de Oliveira, Alexandre Verski and
Sergio E.D.M. Cesar
c/o Hidroservice (MS)

Rua Afonso Celso, 235
04119 Sao Paulo, SP

30. Mr. Luis E. Sozio
c/o Promon Engenharia
A.V. Juscelino Kubitschek 1830, 5°
04543 Sao Paulo

VENEZUELA

31. Mr. Roberto Centeno Werner
Consulting Engineer, Metro de Caracas
Avenida Sojo, Quinta Chichi
El Rosal
Caracas 106

EGYPT

32. Mr. M.E. Abdel Salam
National Authority for Tunnels
56 Riad Street
Elmohandiseen
Cairo

JAPAN

33. Mr. Yoshio Mitarashi
c/o Kumagai Gumi Co. Ltd.
Institute of Construction Technology
17-1, Tsukudo-CHO, Shinjuku-Ku
Tokyo, 162

34. Dr. Keiichi Fujita
c/o Hazama-Gumi, Ltd.
2-5-8, Kita-Aoyama
Minato-Ku
Tokyo 107

APPENDIX C - NORMALIZED GROUND SETTLEMENTS

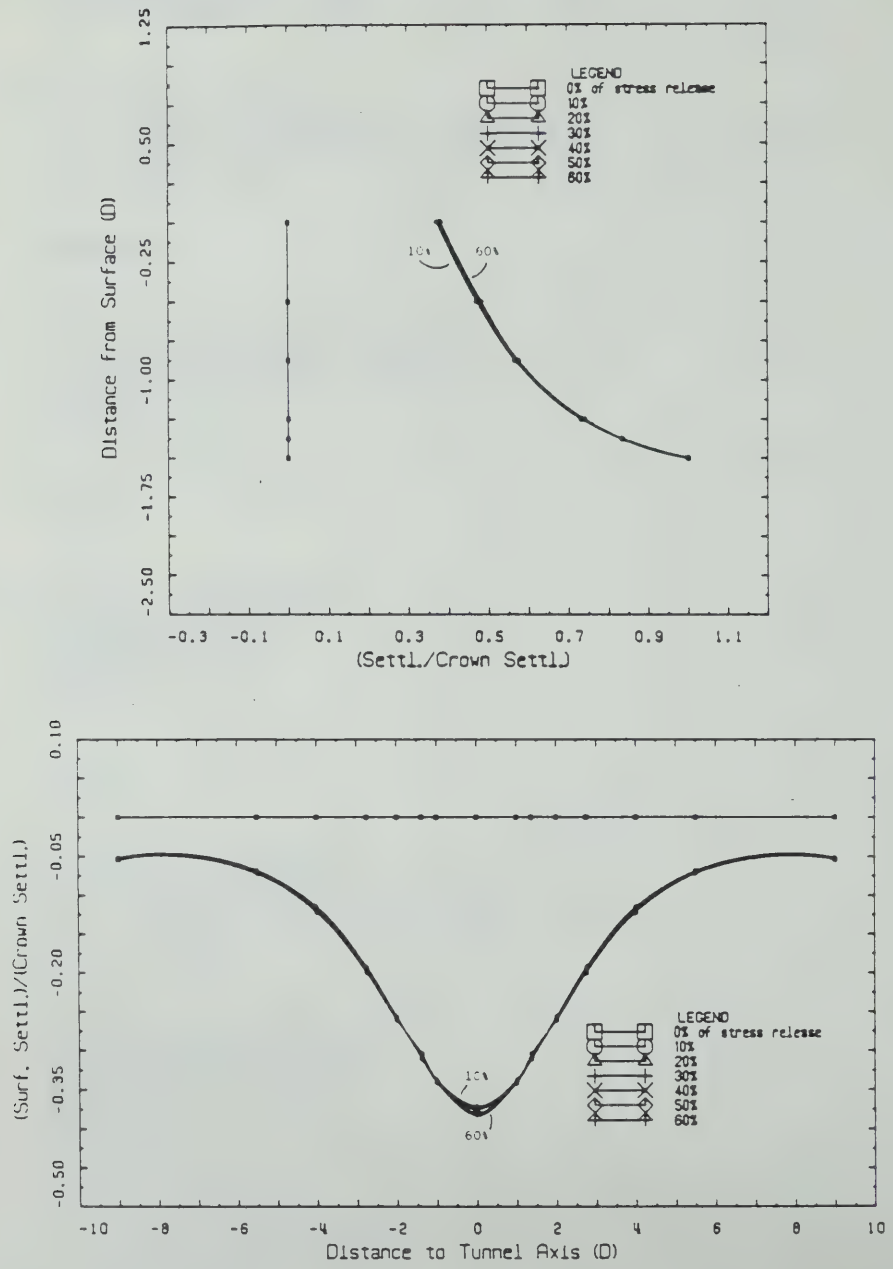

Figure C.1 Normalized Settlements: $K_o=1$, $c_u/\gamma D=2.5$, $H/D=1.5$

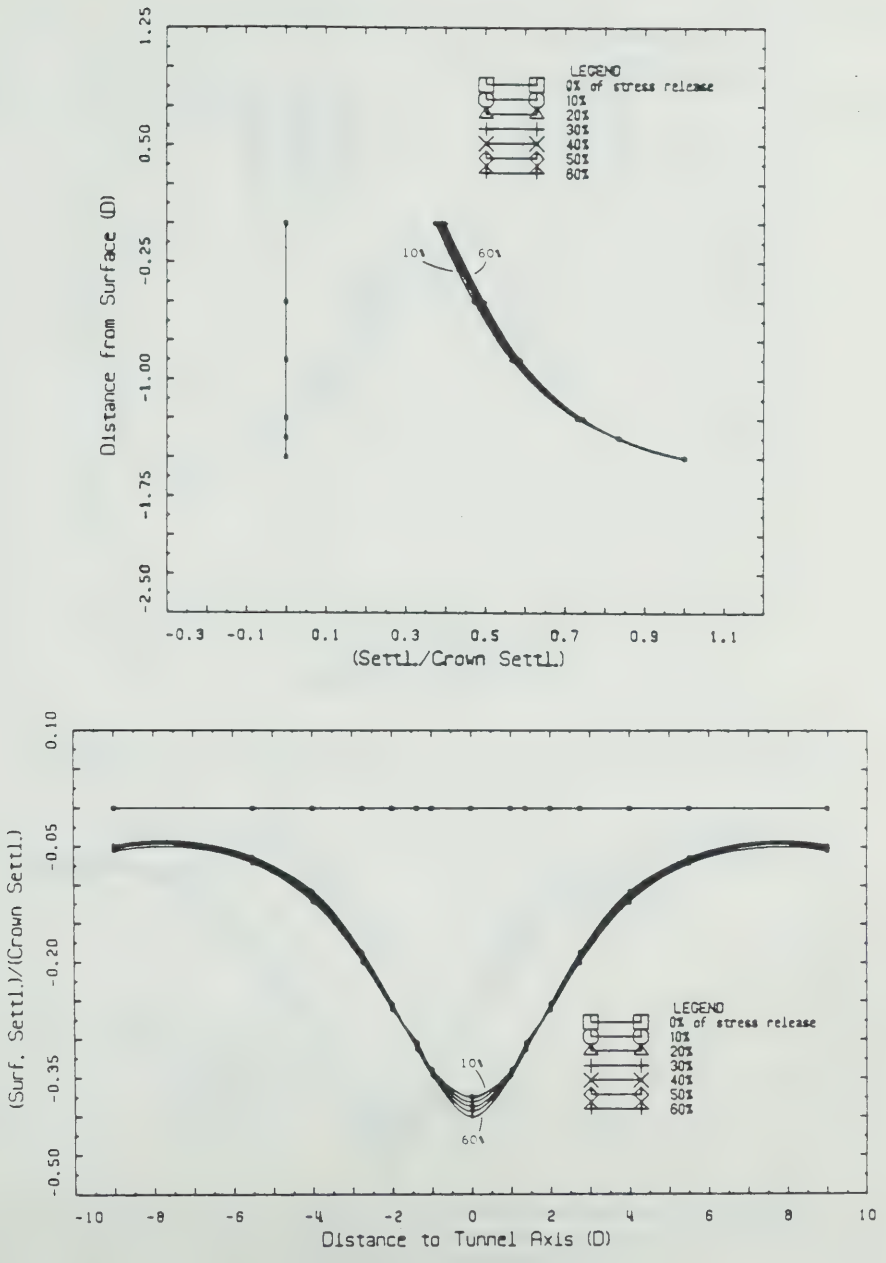

Figure C.2 Normalized Settlements: $K_o=1$, $c_u/\gamma D=1.25$, $H/D=1.5$

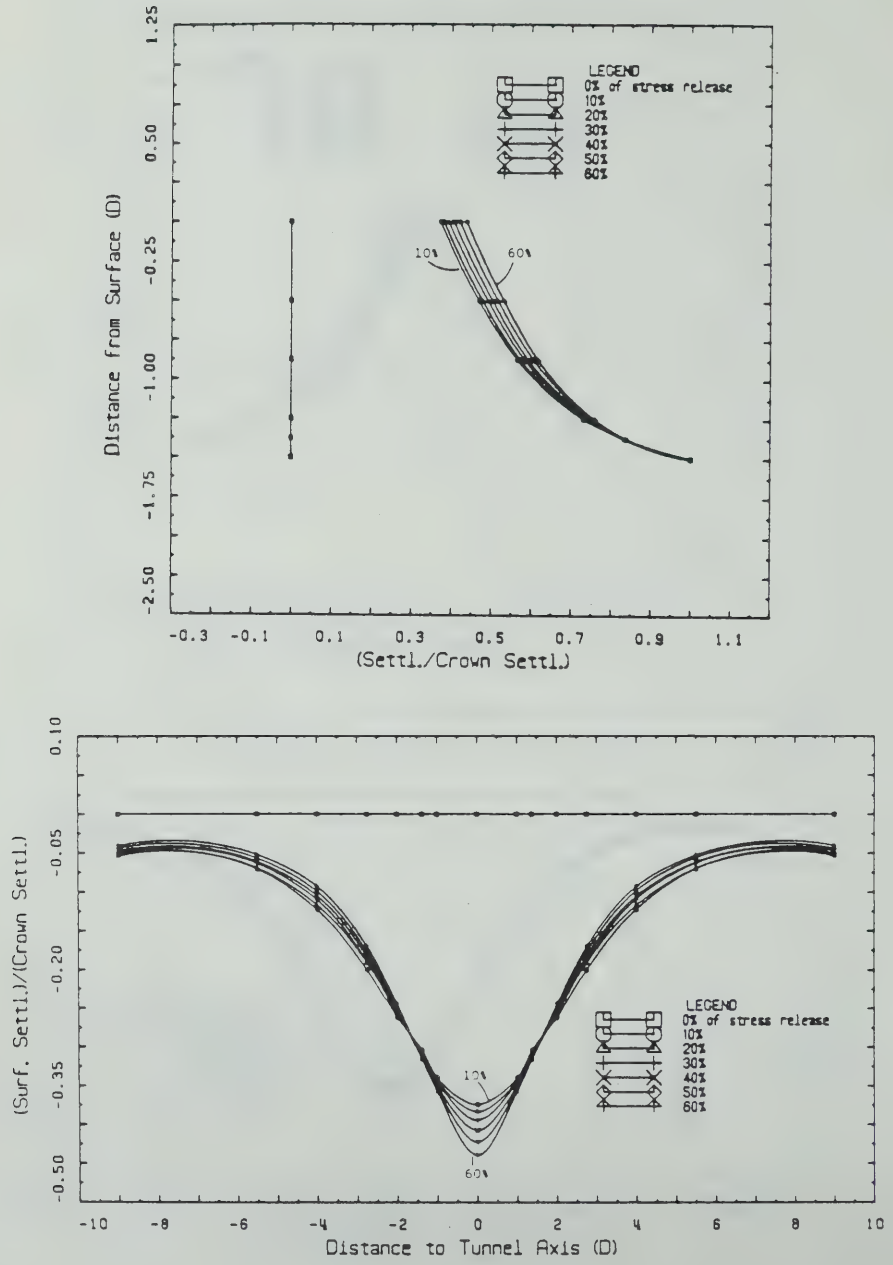

Figure C.3 Normalized Settlements: $K_o=1$, $c_u/\gamma D=0.625$, $H/D=1.5$

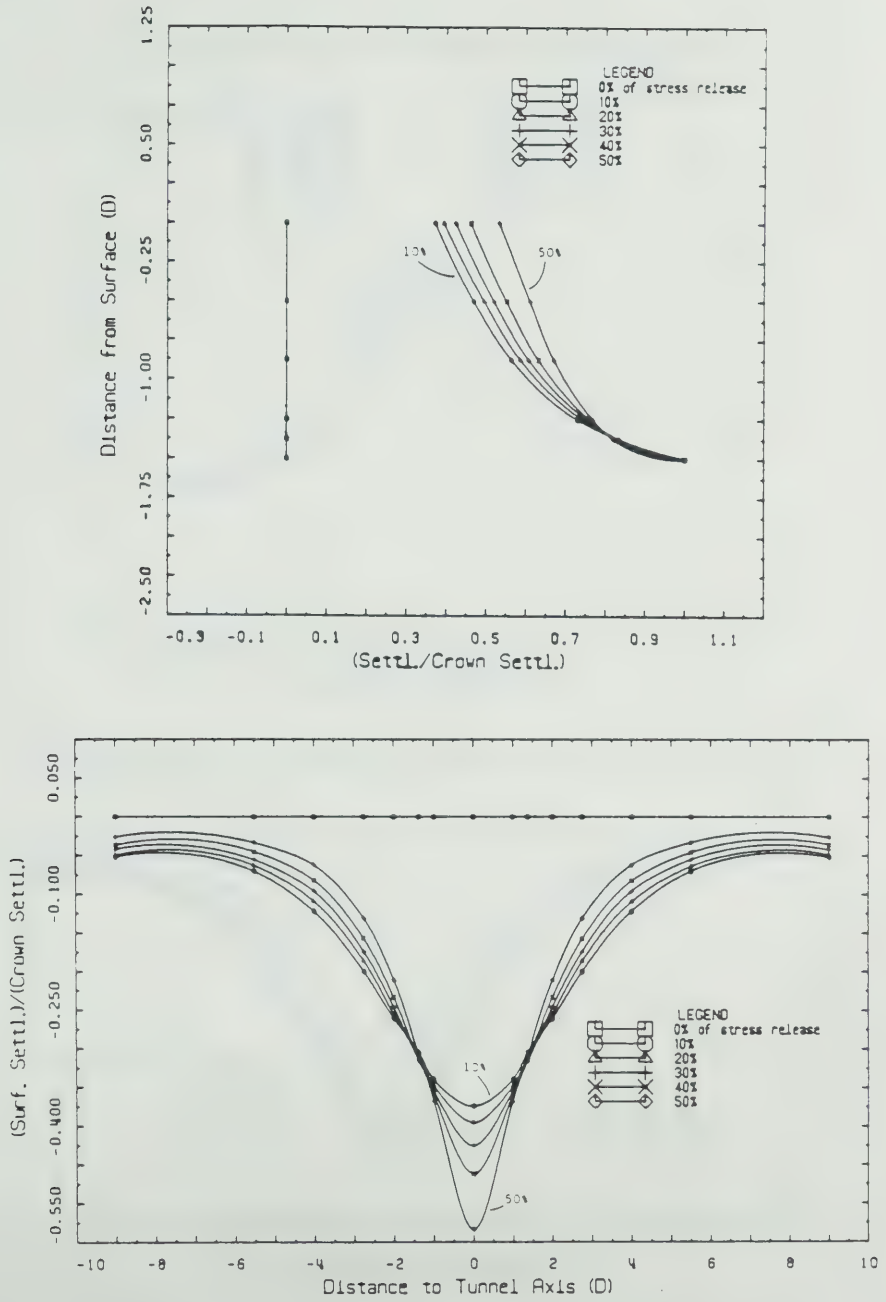

Figure C.4 Normalized Settlements: K_o=1, $c_u/\gamma D$=0.3125, H/D=1.5

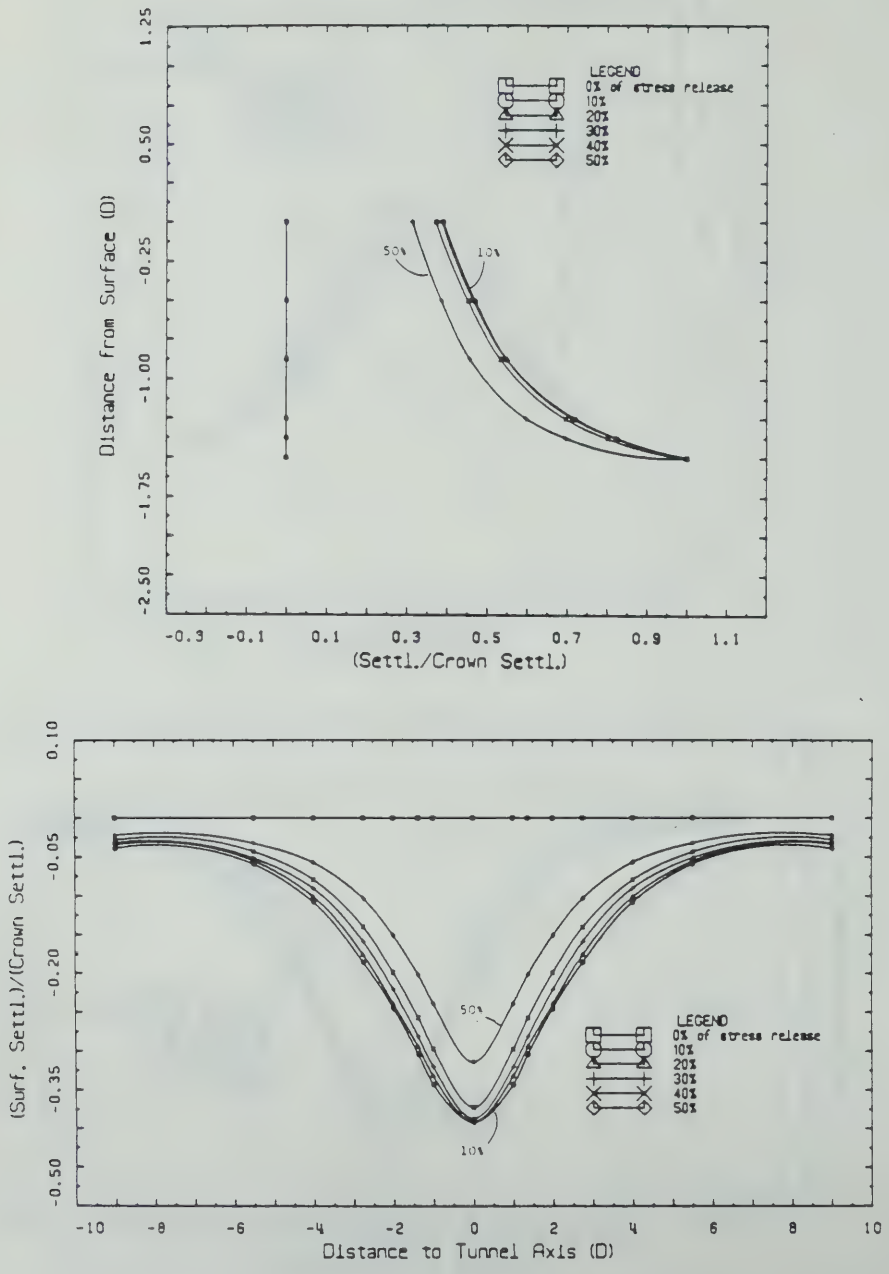

Figure C.5 Normalized Settlements: K_o=1, ϕ=20°, H/D=1.5

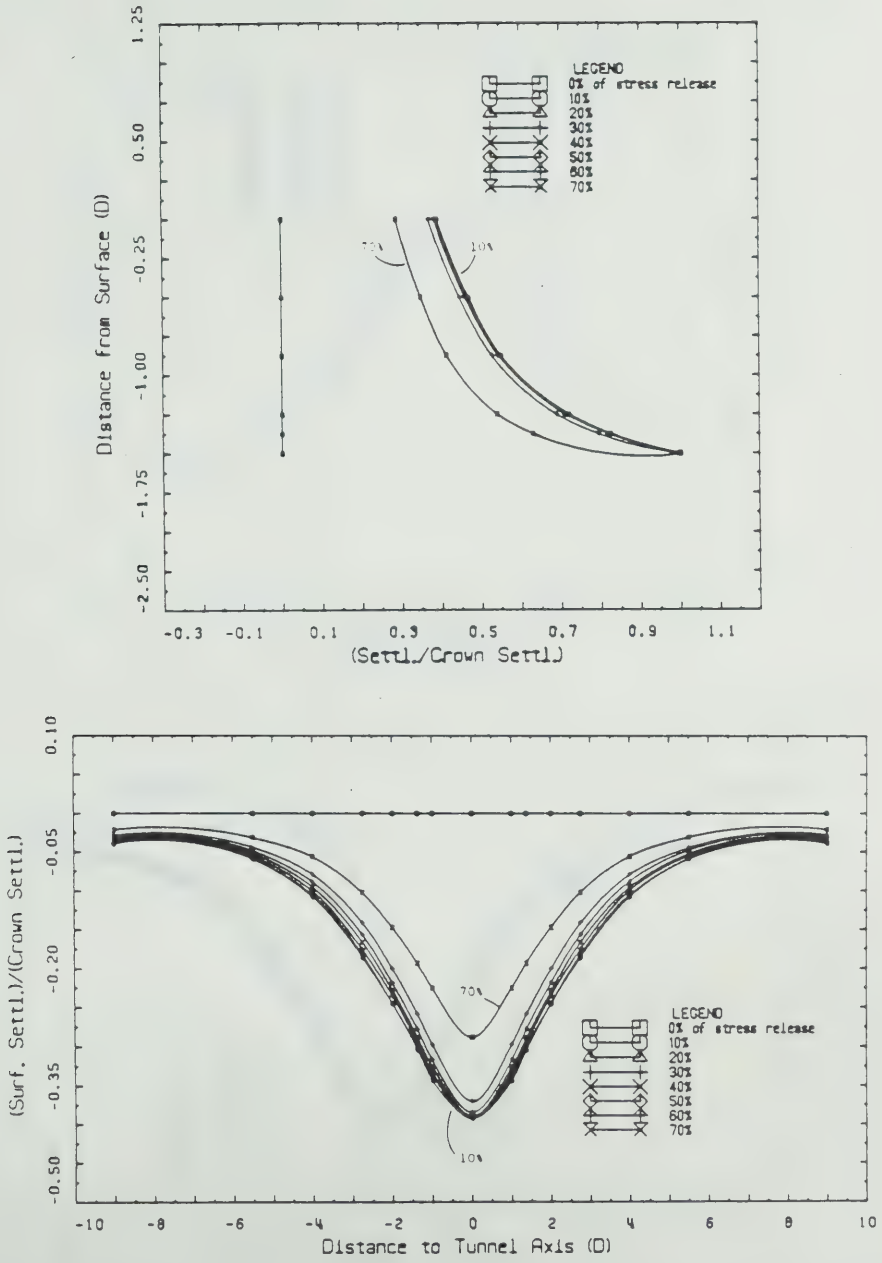

Figure C.6 Normalized Settlements: K_o=1, ϕ=30°, H/D=1.5

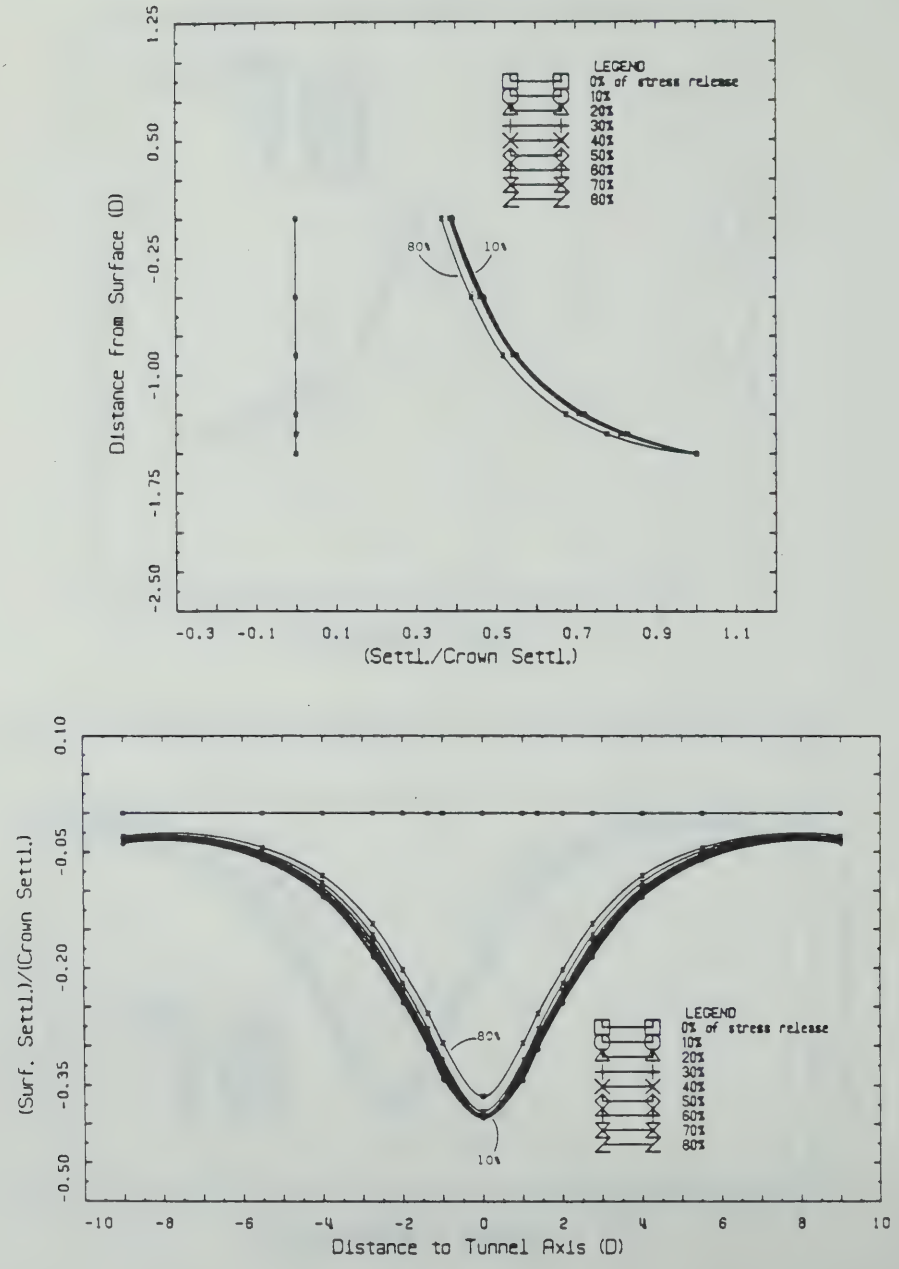

Figure C.7 Normalized Settlements: K_o=1, ϕ=40°, H/D=1.5

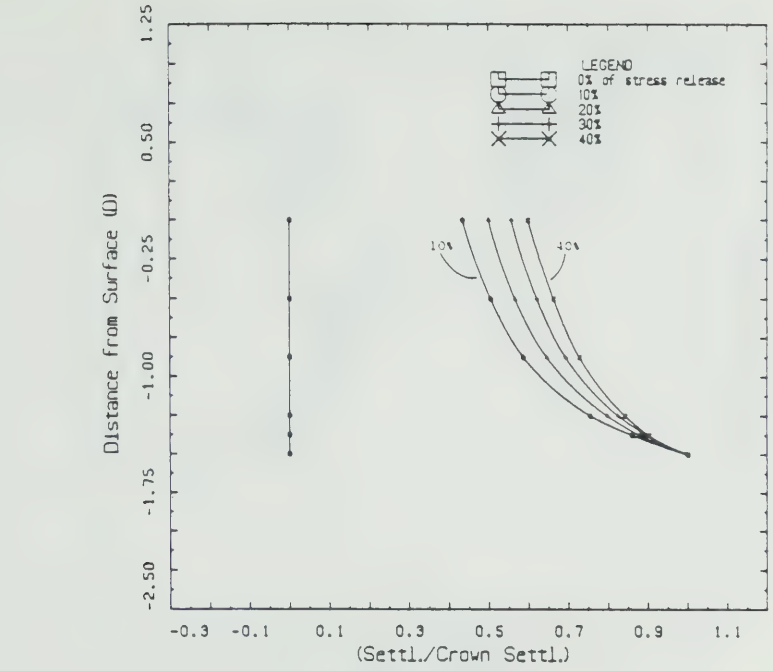

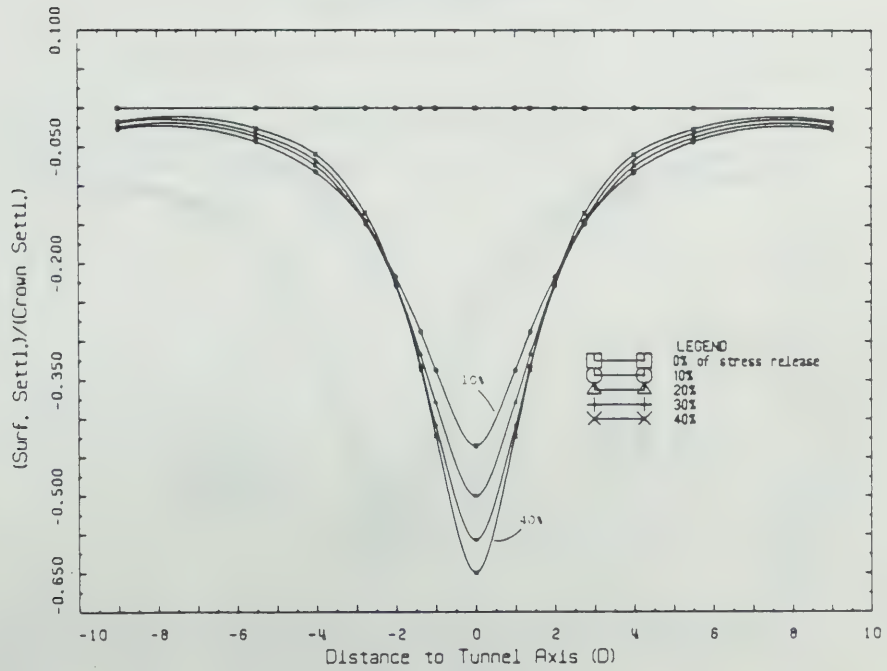

Figure C.8 Normalized Settlements: K_o=0.8, ϕ=20°, H/D=1.5

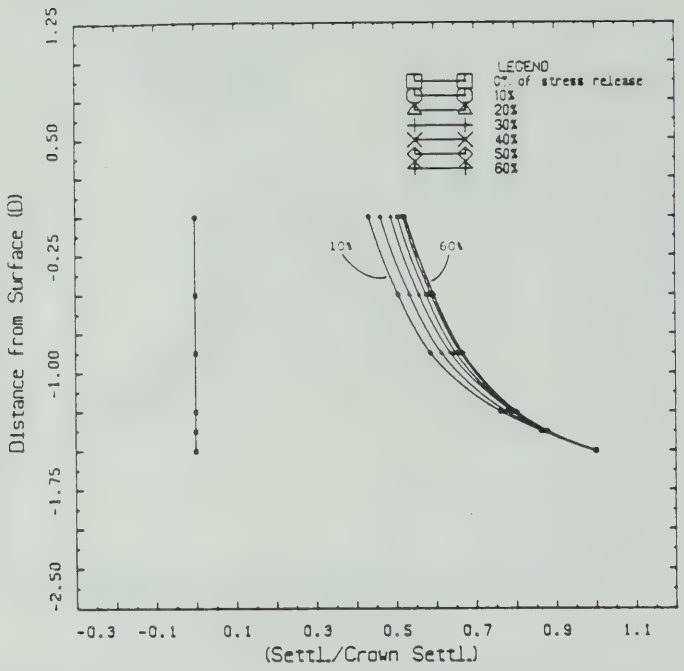

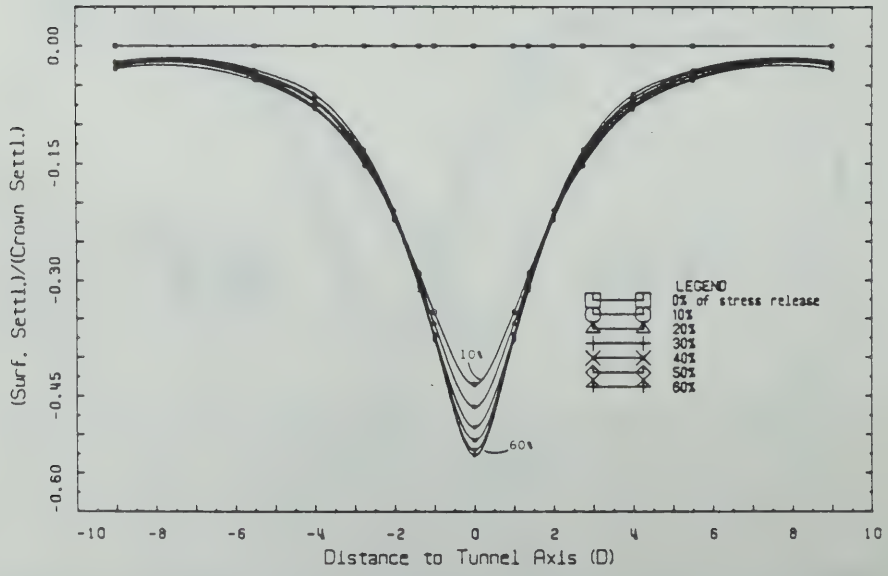

Figure C.9 Normalized Settlements: K_o=0.8, ϕ=30°, H/D=1.5

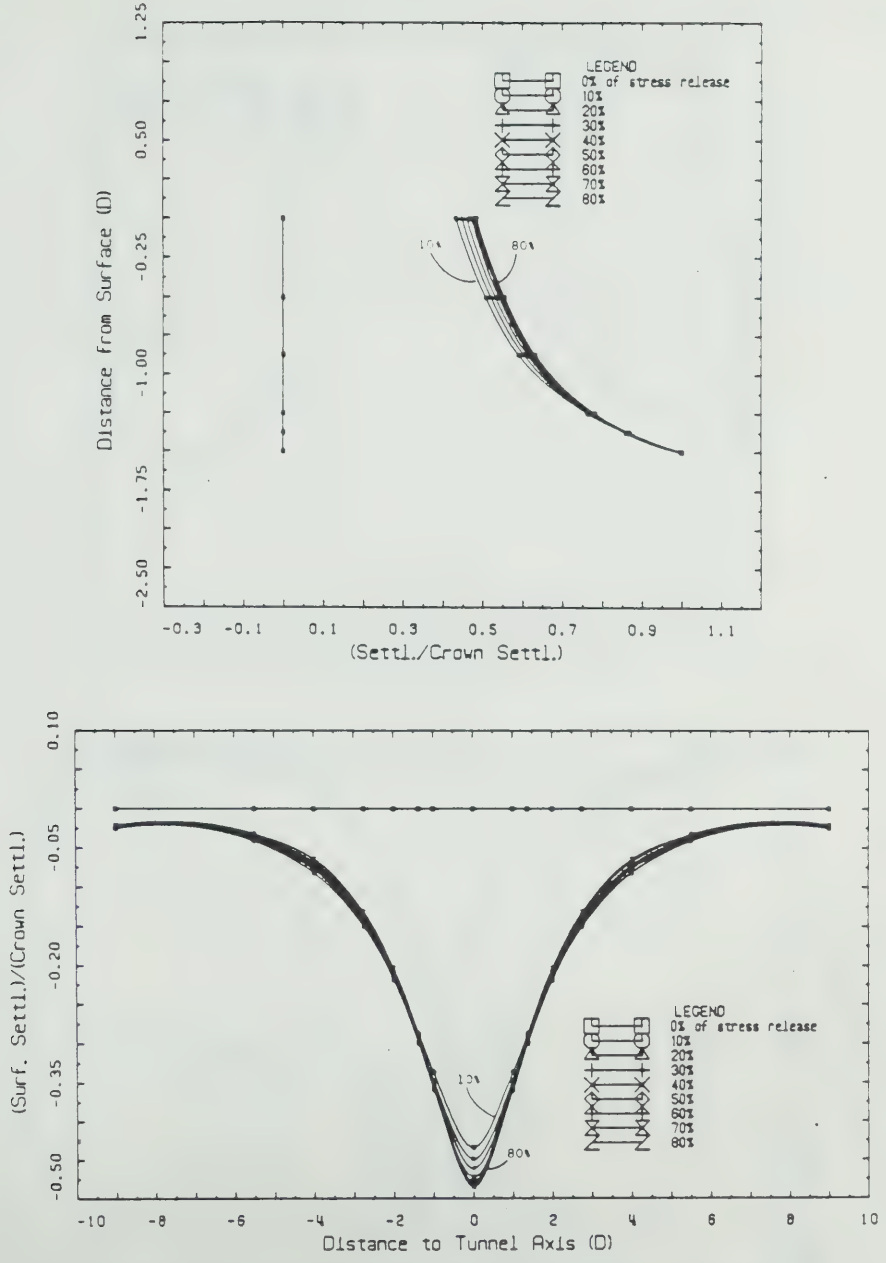

Figure C.10 Normalized Settlements: K_o=0.8, ϕ=40°, H/D=1.5

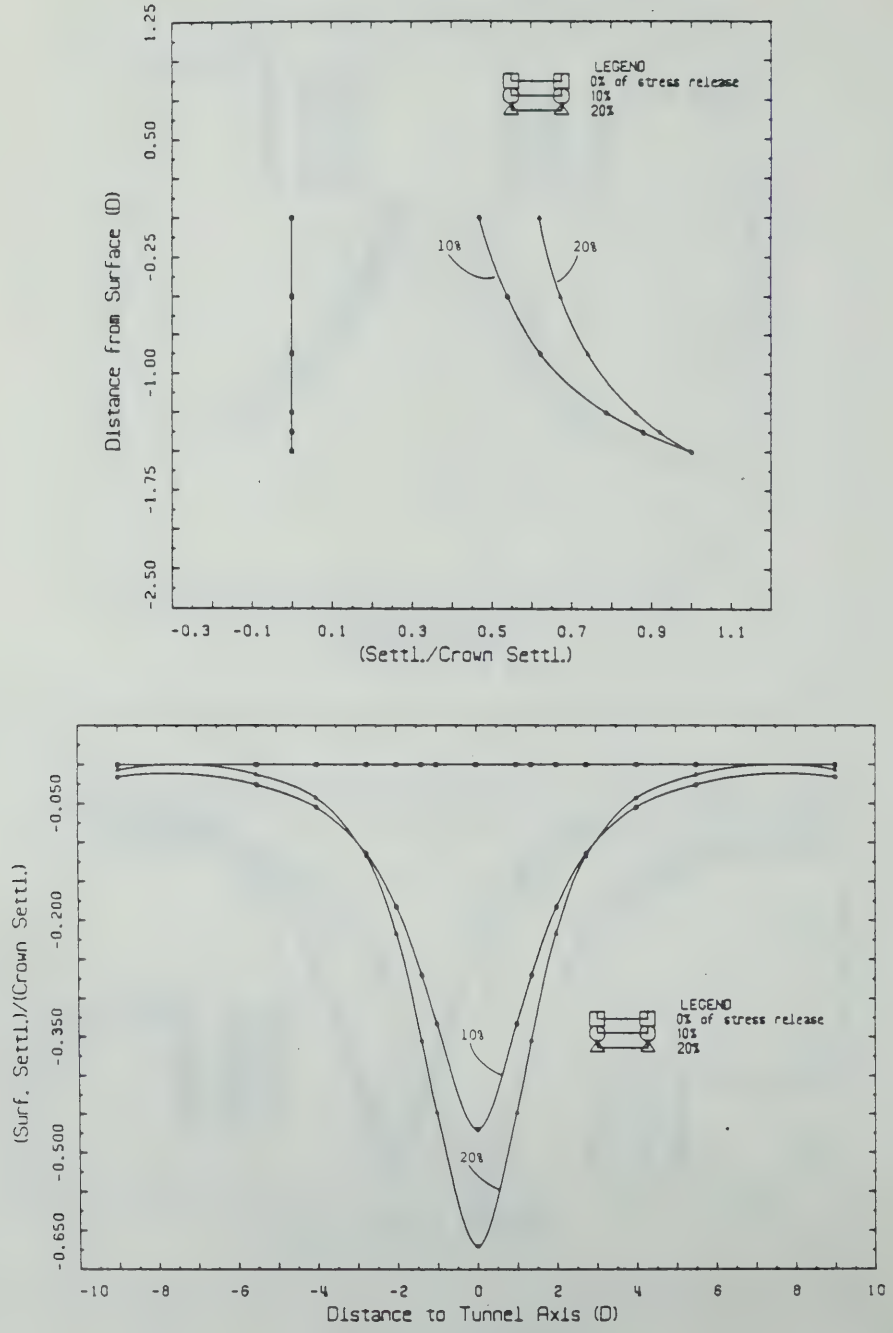

Figure C.11 Normalized Settlements: K_o=0.6, ϕ=20°, H/D=1.5

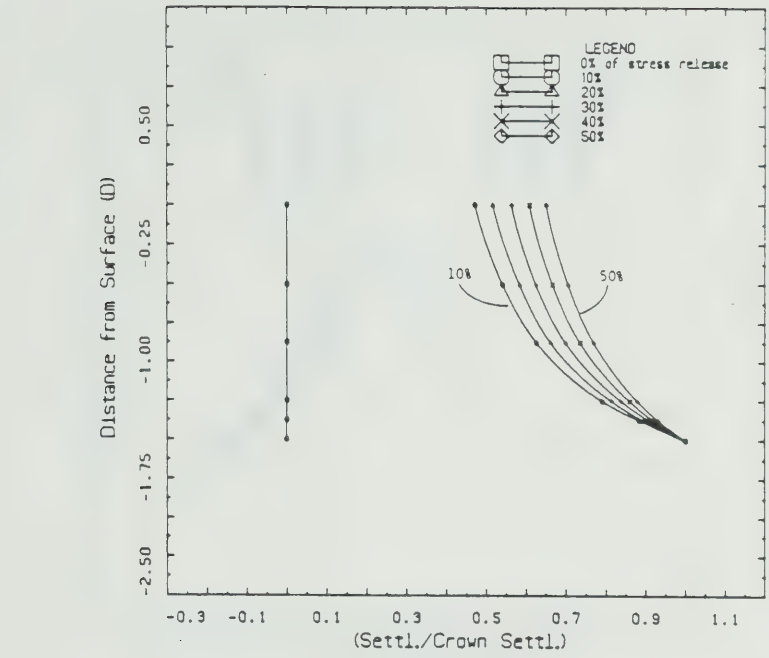

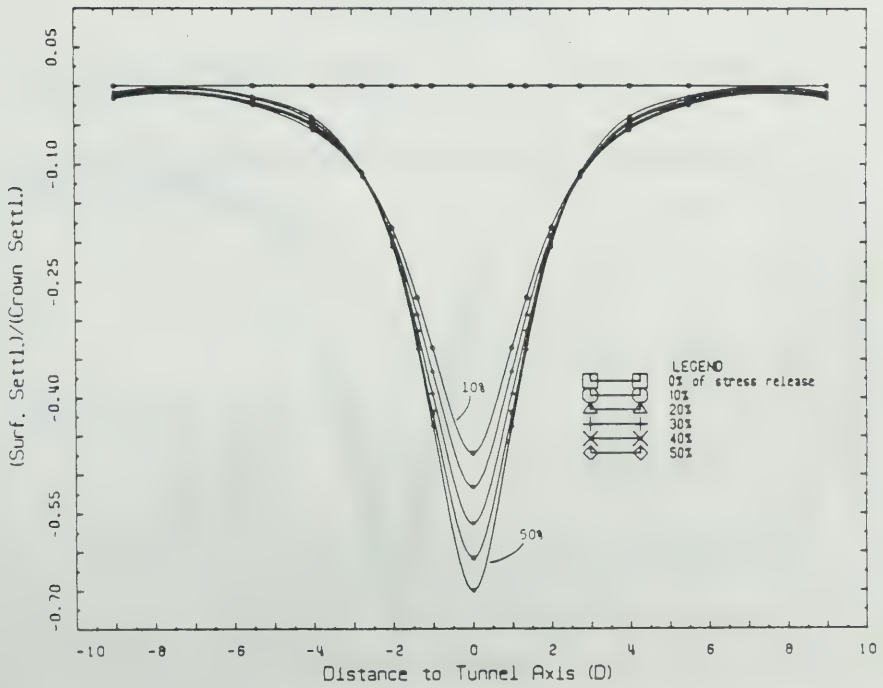

Figure C.12 Normalized Settlements: K_o=0.6, ϕ=30°, H/D=1.5

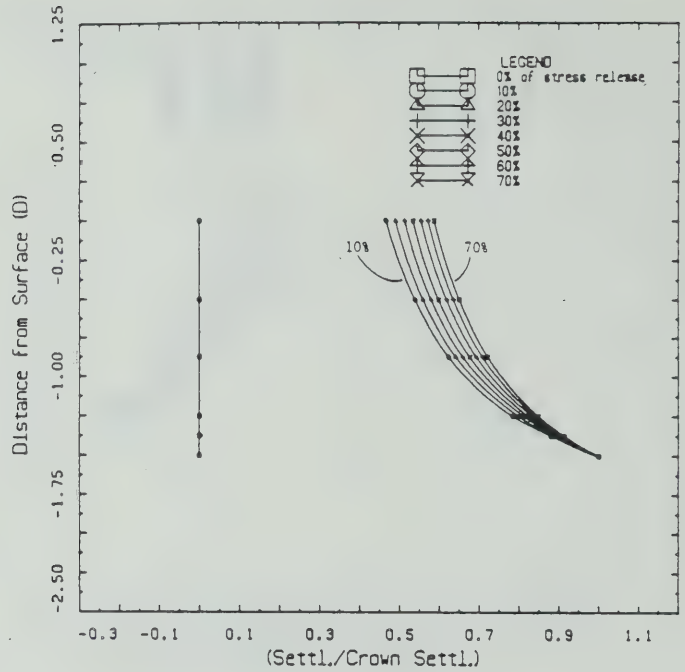

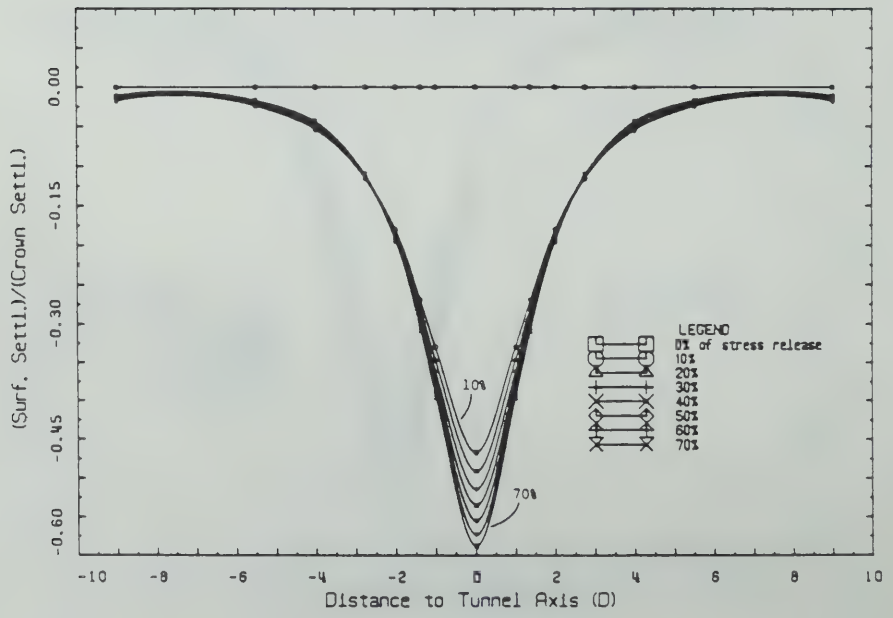

Figure C.13 Normalized Settlements: K_o=0.6, ϕ=40°, H/D=1.5

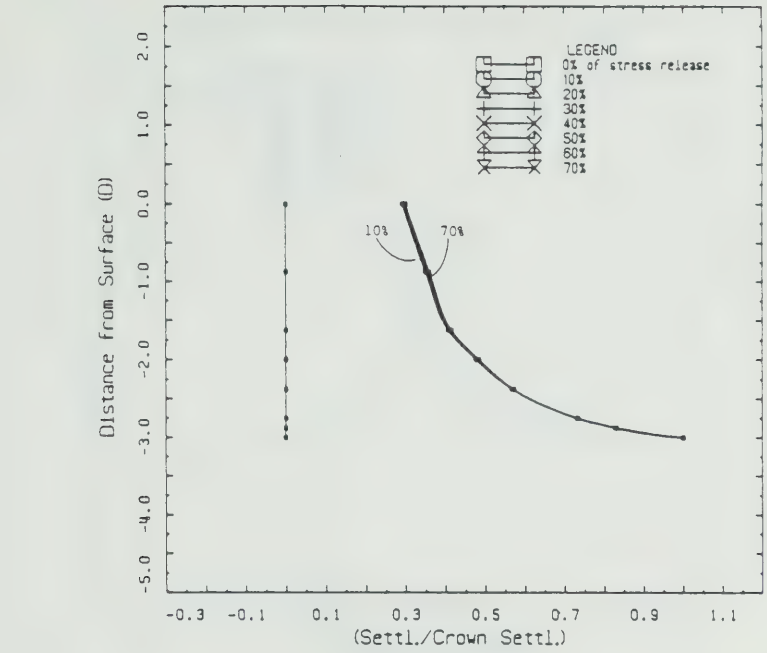

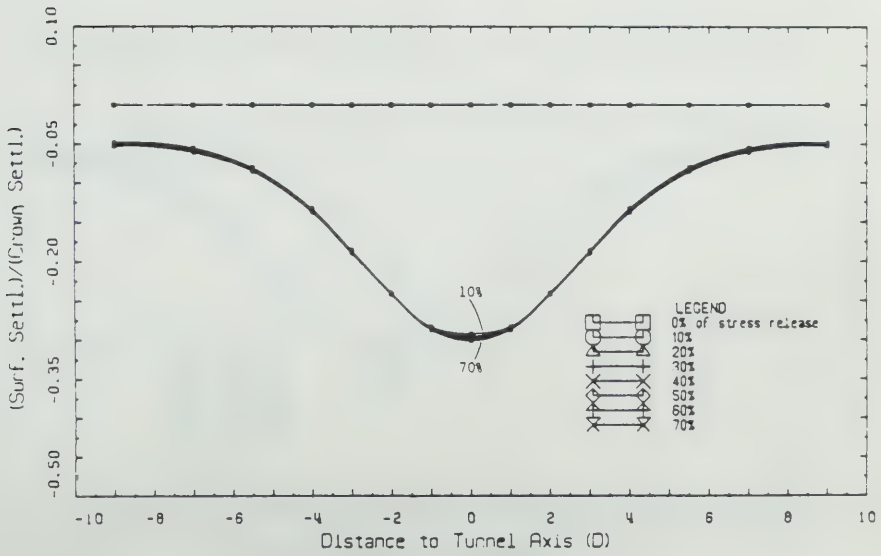

Figure C.14 Normalized Settlements: K_o=1, $c_u/\gamma D$=2.5, H/D=3

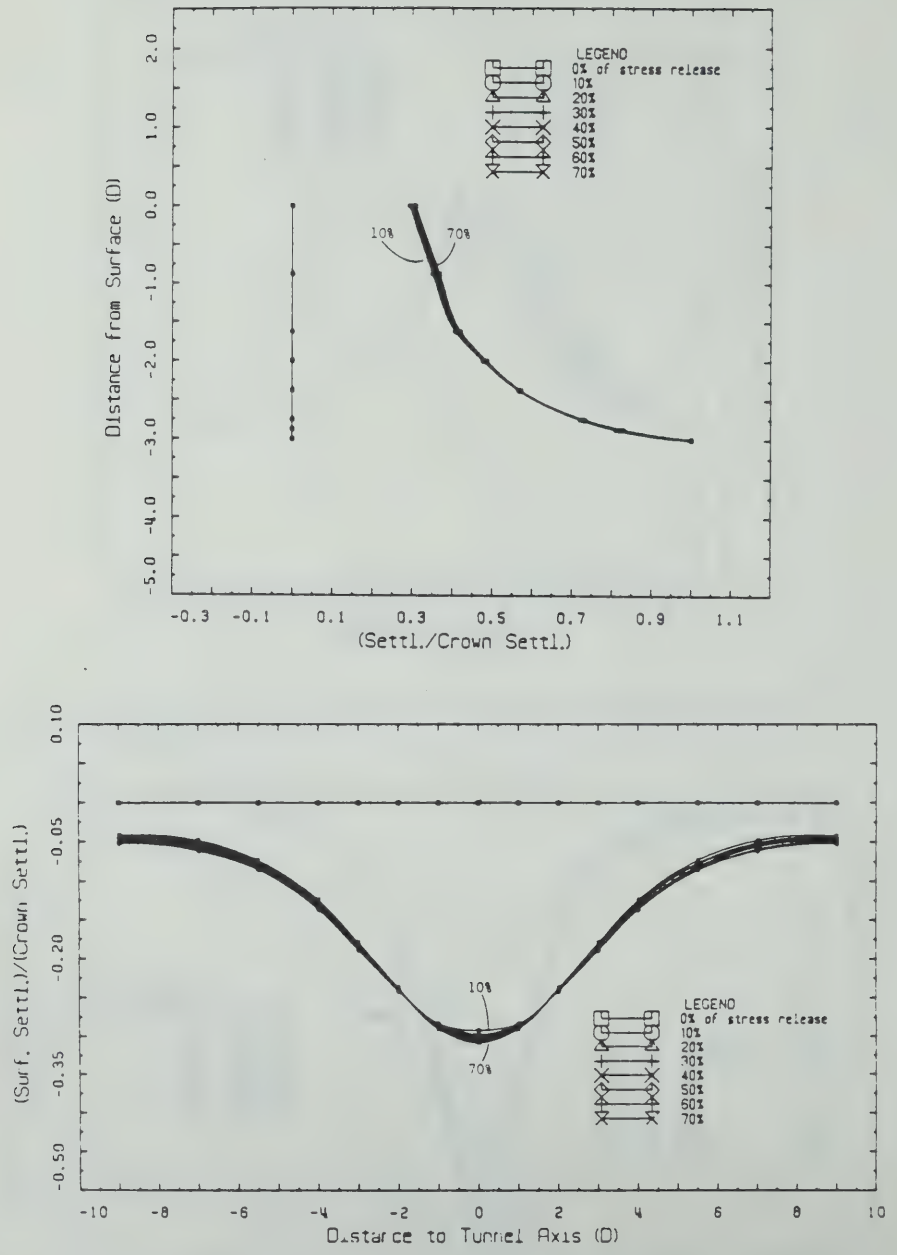

Figure C.15 Normalized Settlements: K_o=1, $c_u/\gamma D$=1.25, H/D=3

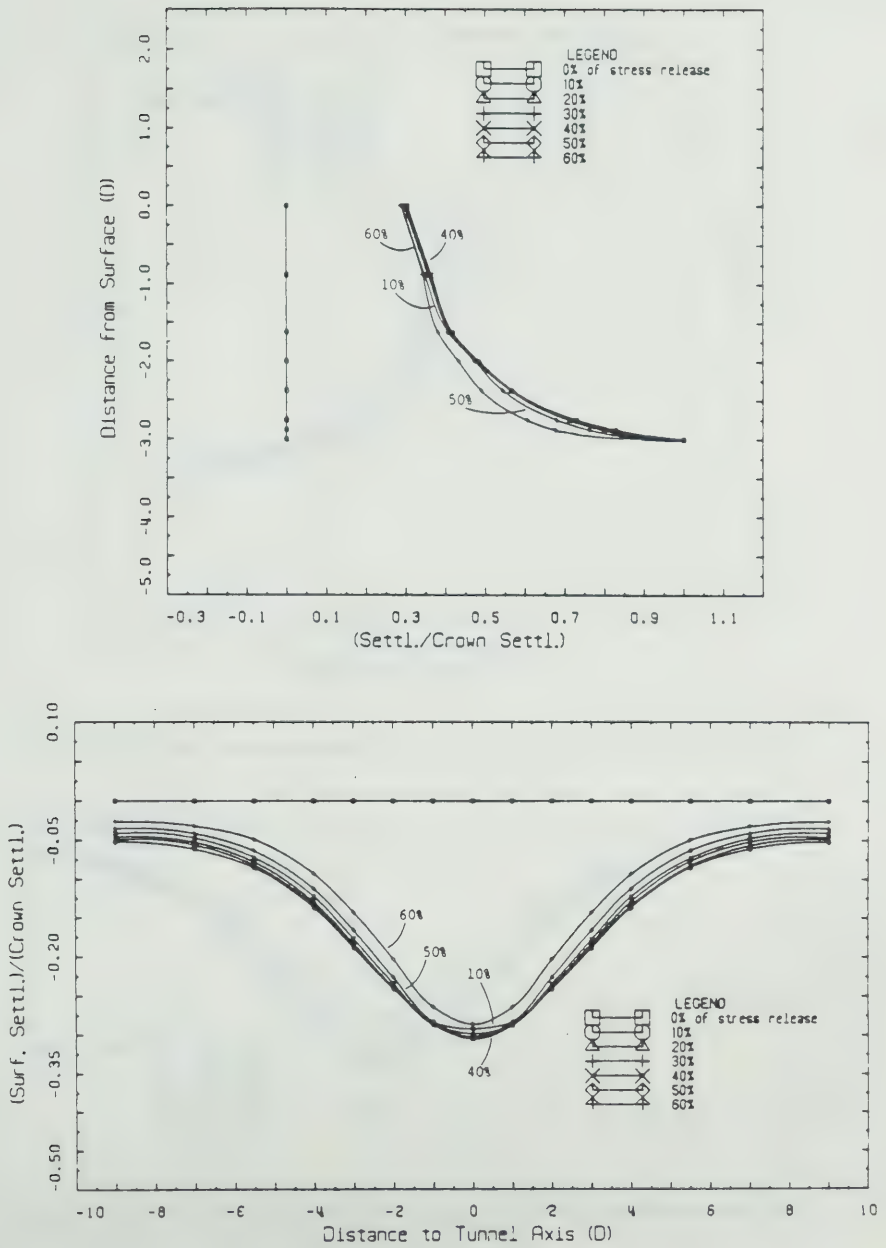

Figure C.16 Normalized Settlements: $K_o=1$, $c_u/\gamma D=0.625$, $H/D=3$

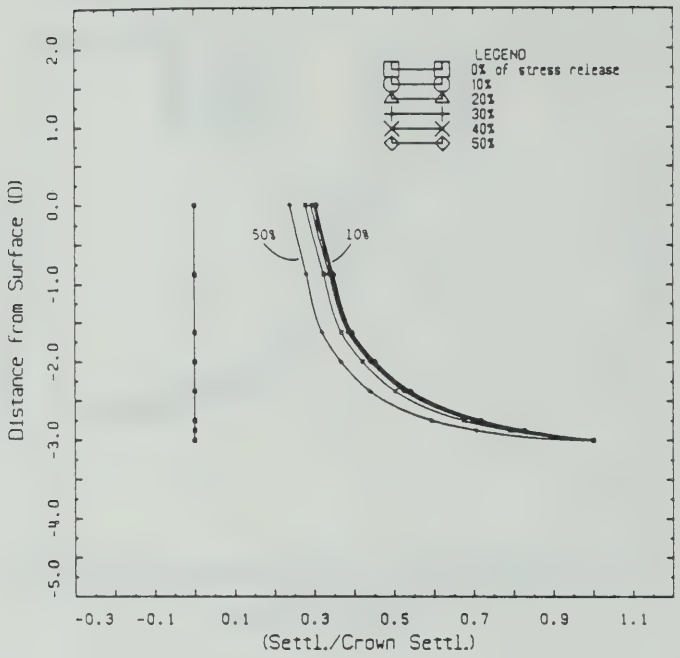

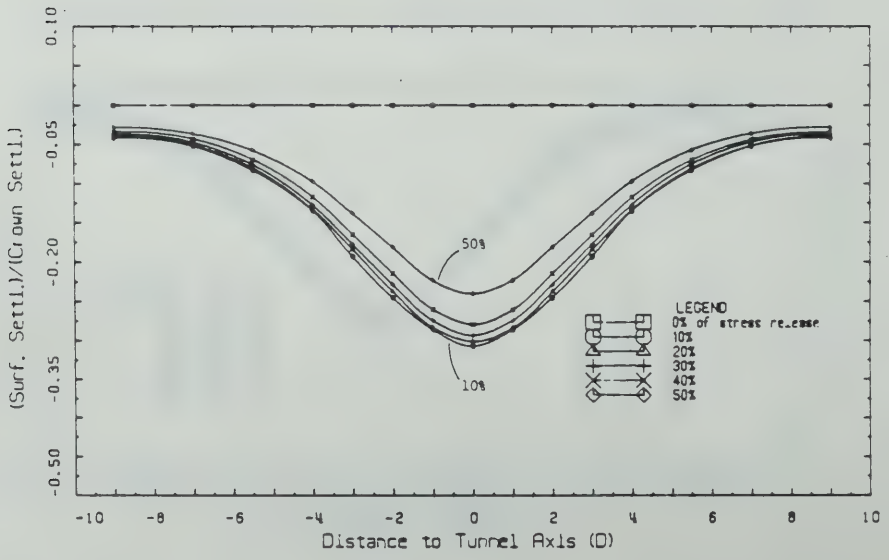

Figure C.17 Normalized Settlements: K_o=1, ϕ=20°, H/D=3

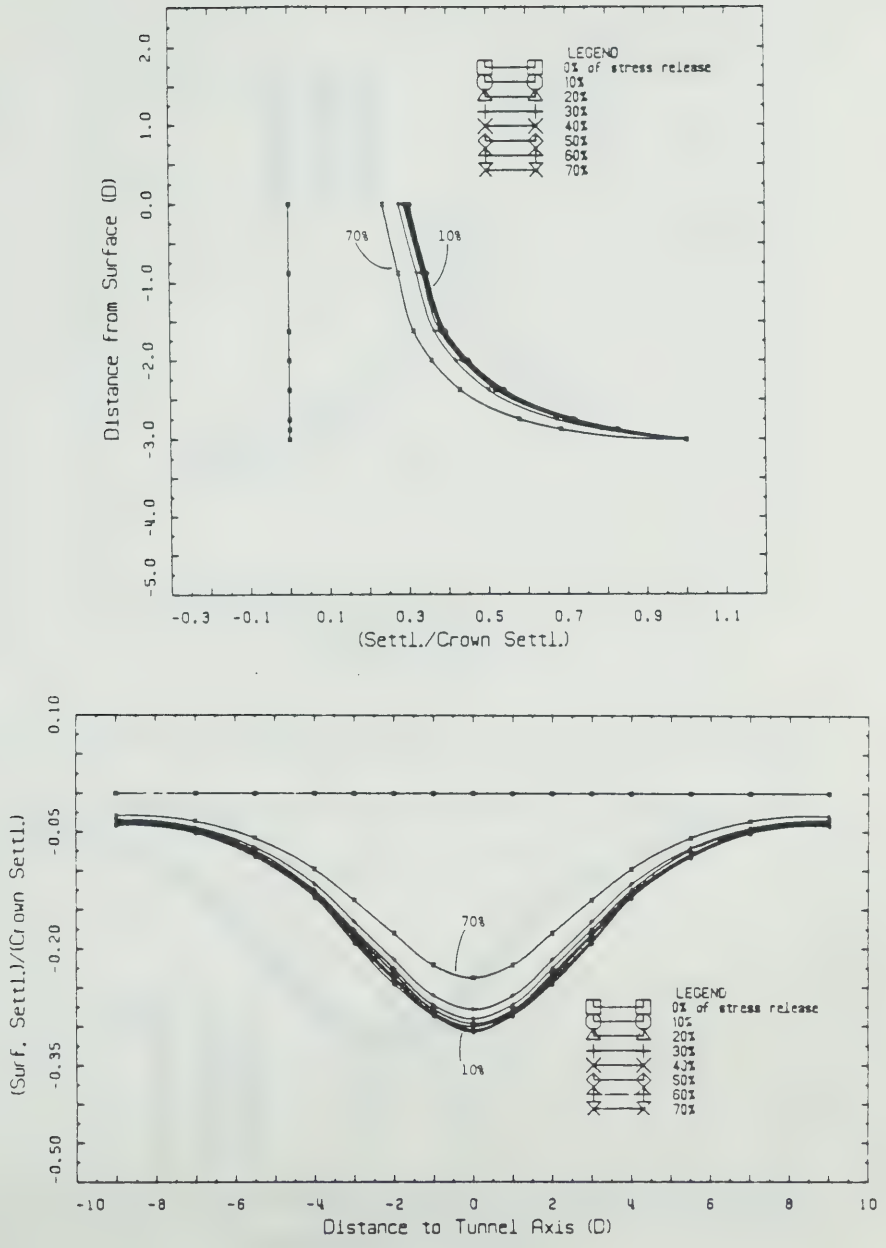

Figure C.18 Normalized Settlements: $K_o=1$, $\phi=30°$, H/D=3

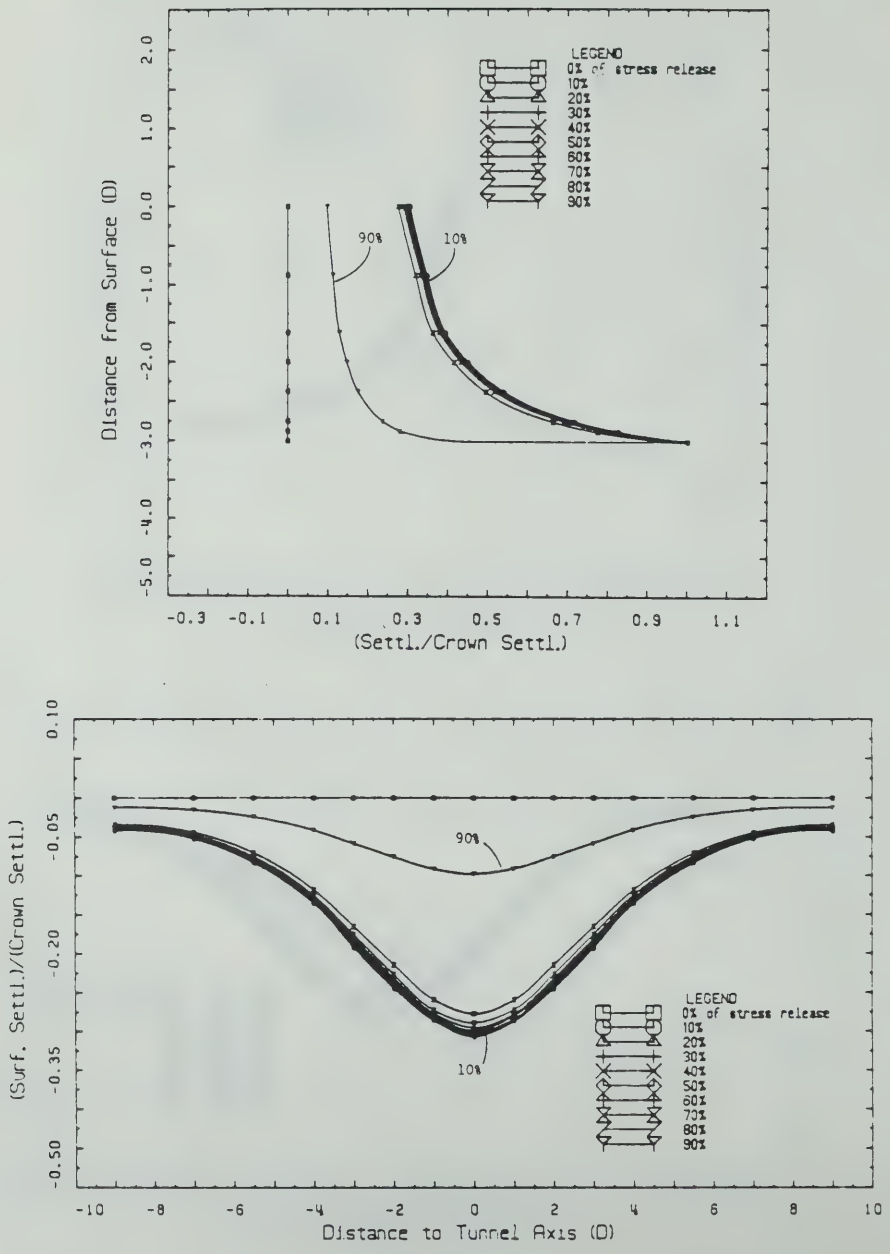

Figure C.19 Normalized Settlements: K_o=1, ϕ=40°, H/D=3

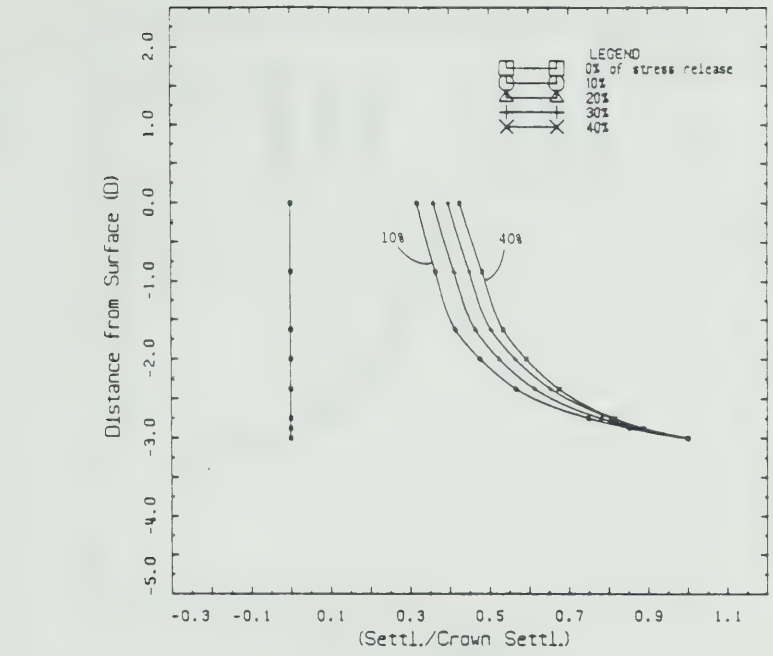

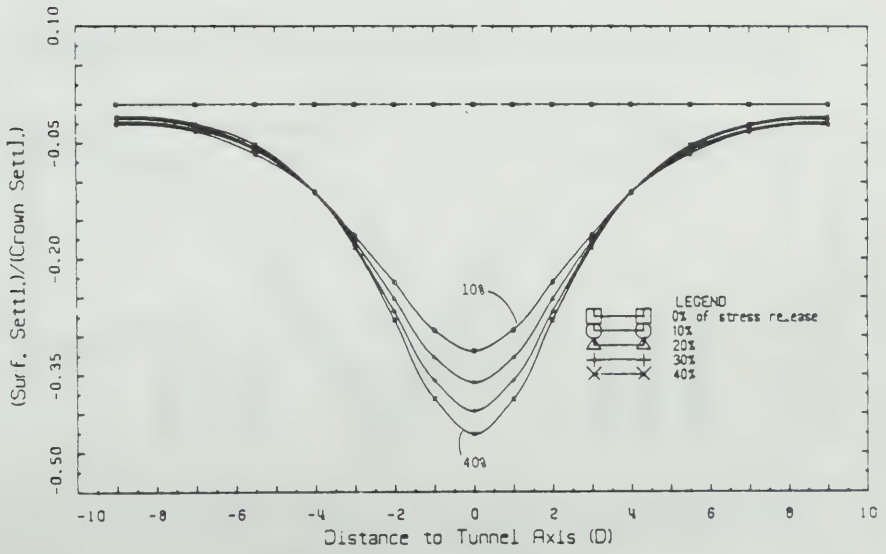

Figure C.20 Normalized Settlements: K_o=0.8, ϕ=20°, H/D=3

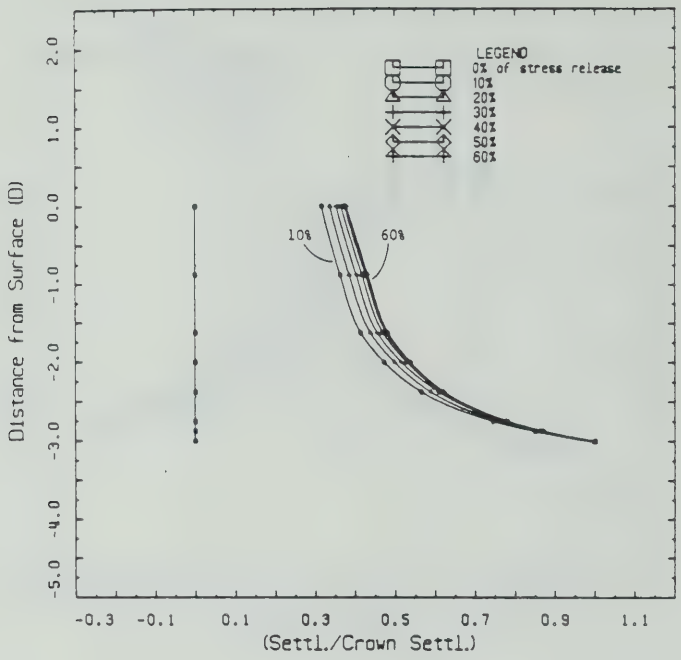

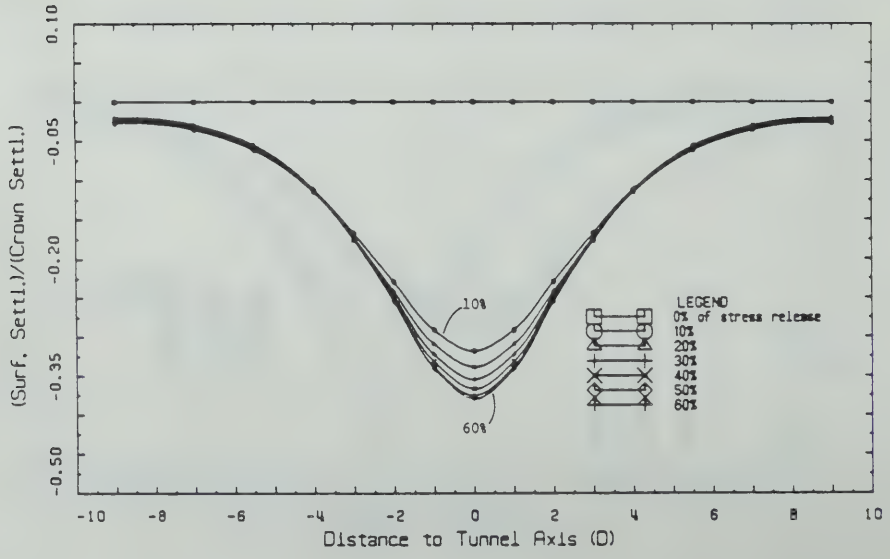

Figure C.21 Normalized Settlements: K_o=0.8, ϕ=30°, H/D=3

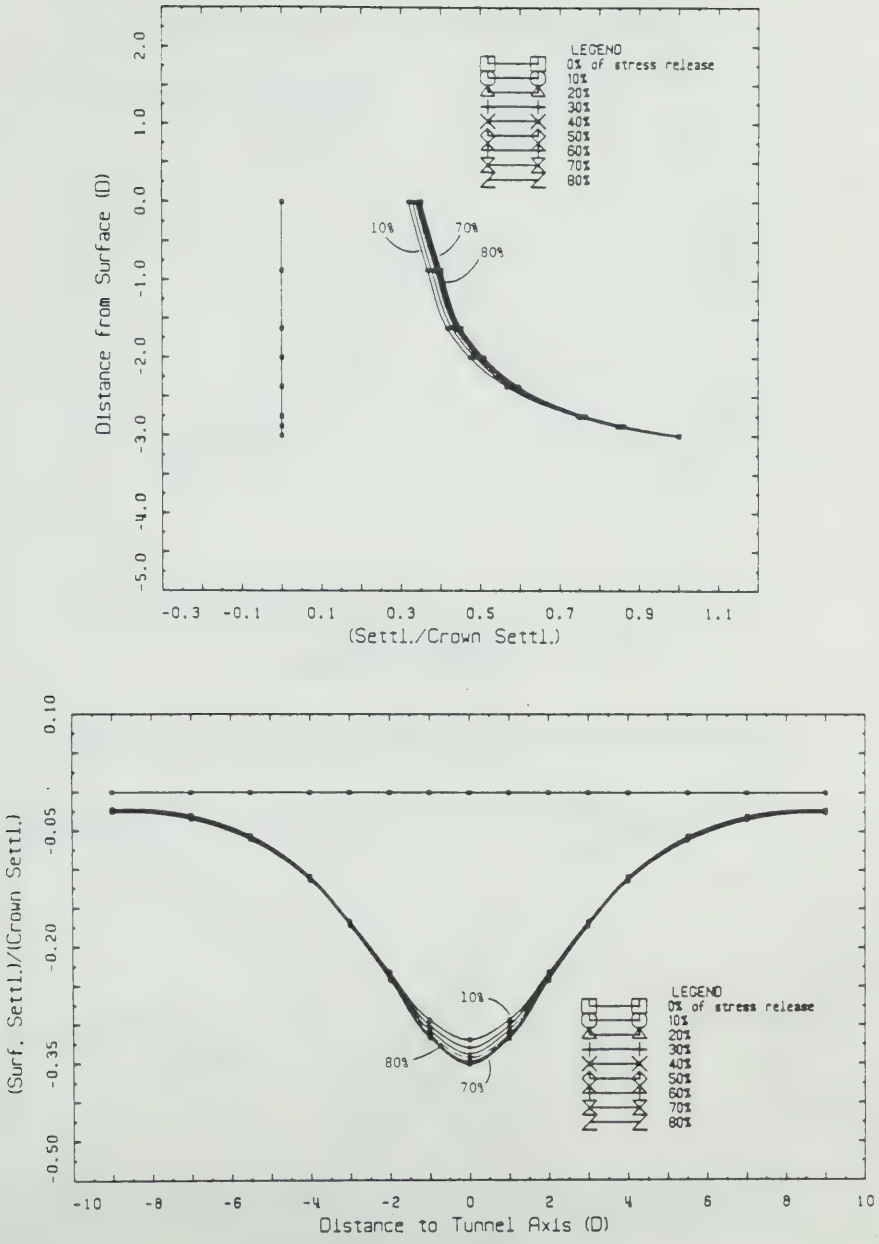

Figure C.22 Normalized Settlements: K_o=0.8, ϕ=40°, H/D=3

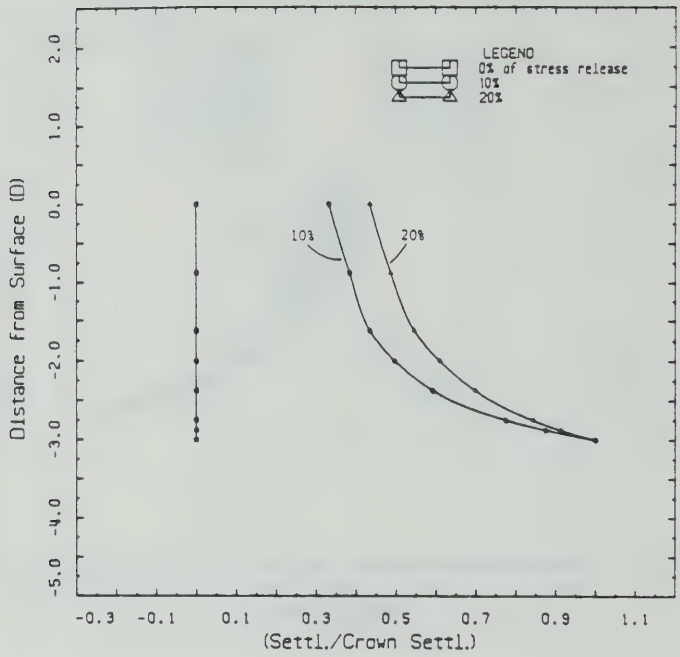

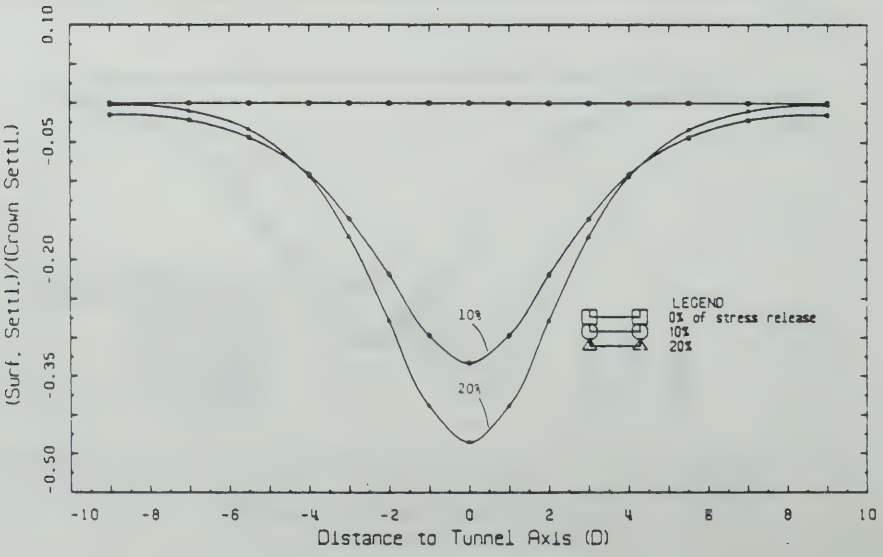

Figure C.23 Normalized Settlements: K_o=0.6, ϕ=20°, H/D=3

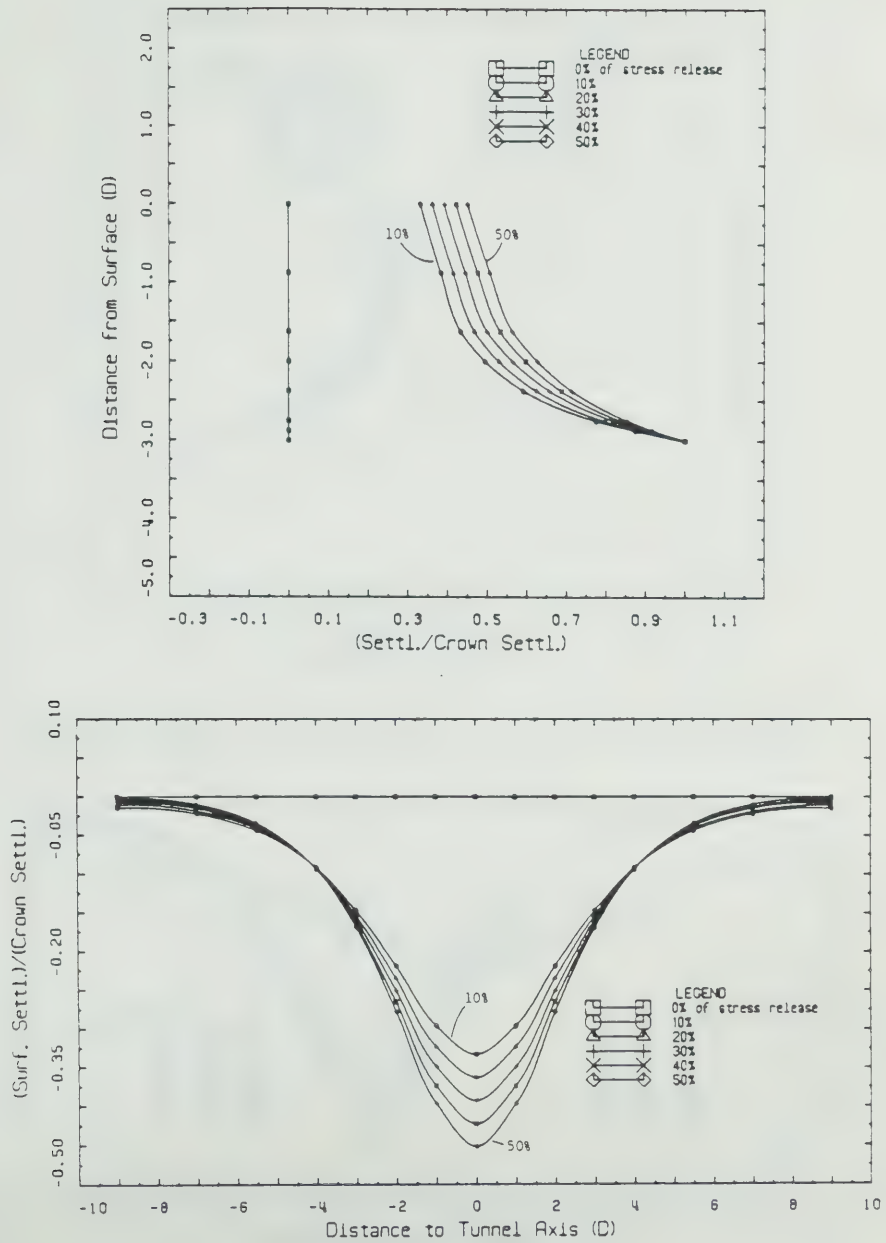

Figure C.24 Normalized Settlements: K_o=0.6, ϕ=30°, H/D=3

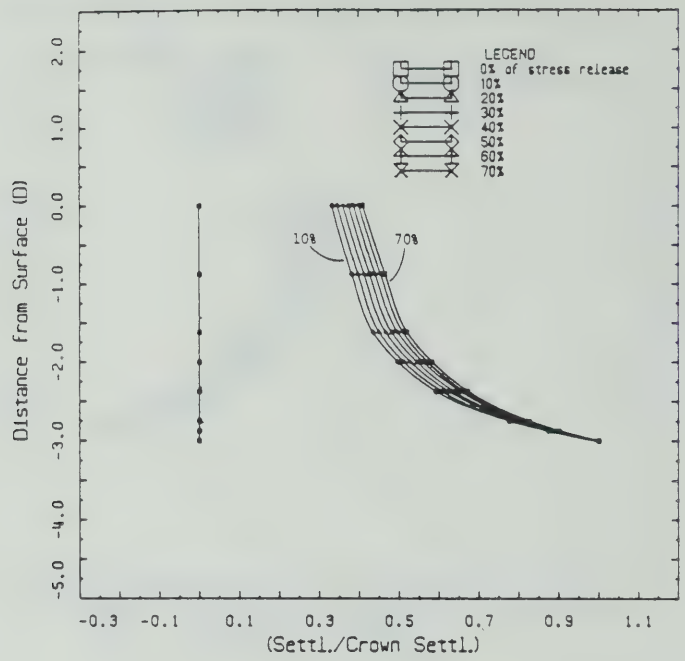

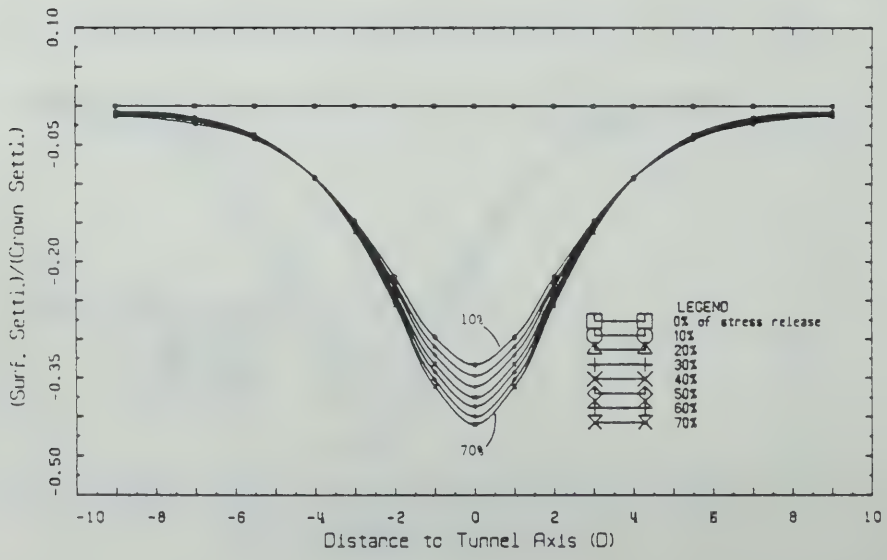

Figure C.25 Normalized Settlements: K_o=0.6, ϕ=40°, H/D=3

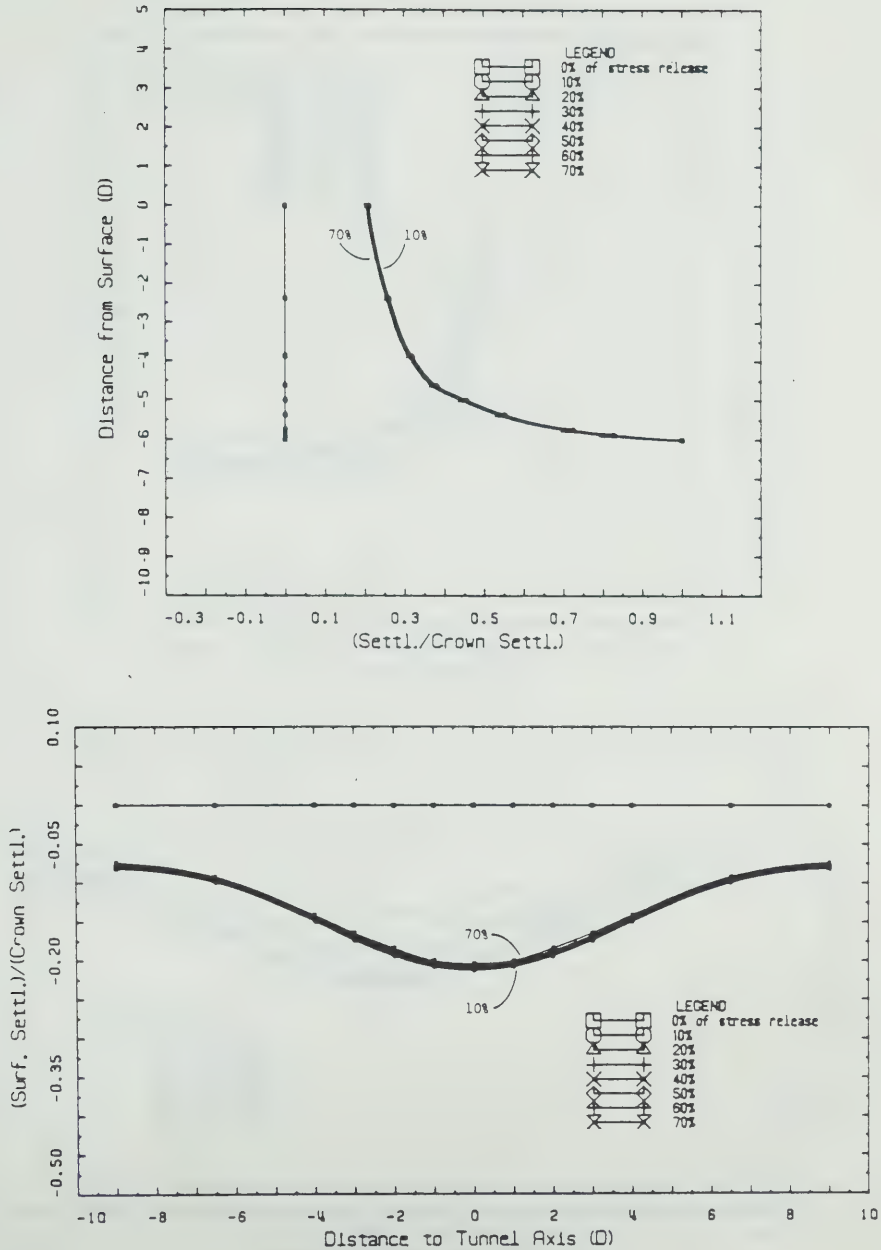

Figure C.26 Normalized Settlements: K_o=1, $c_u/\gamma D$=2.5, H/D=6

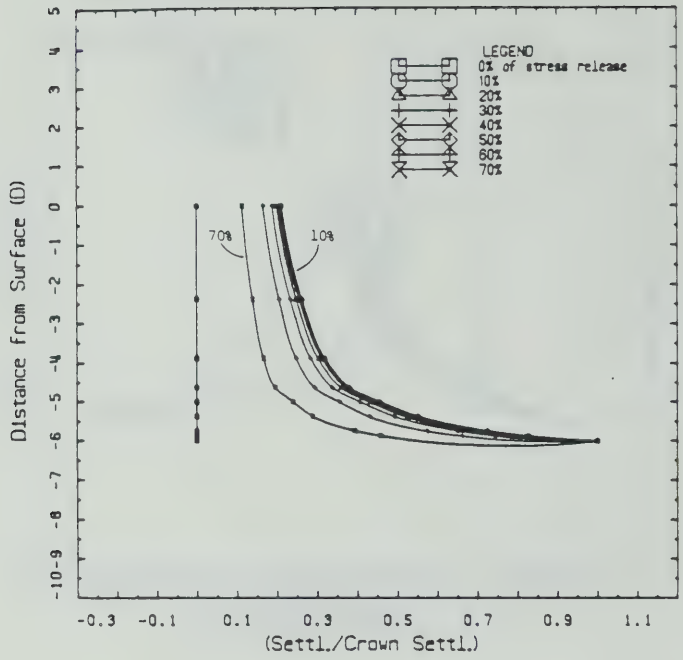

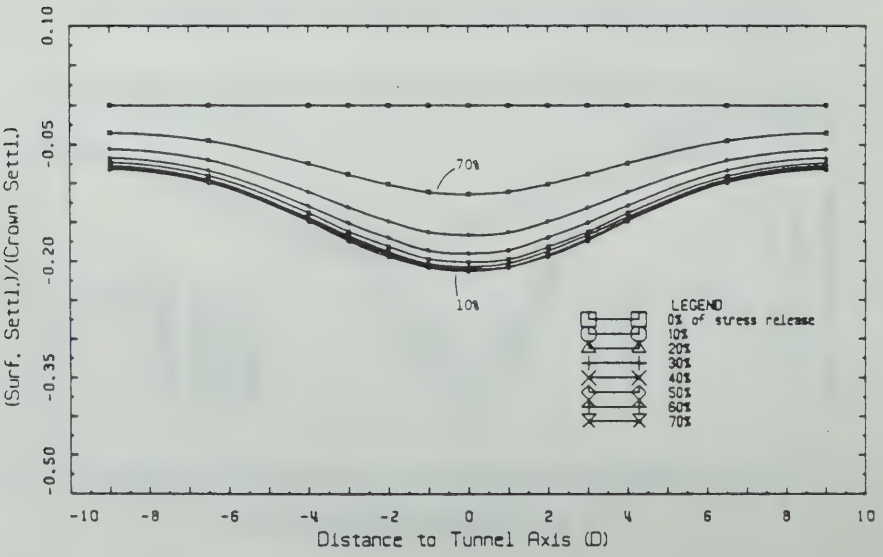

Figure C.27 Normalized Settlements: K_o=1, $c_u/\gamma D$=1.25, H/D=6

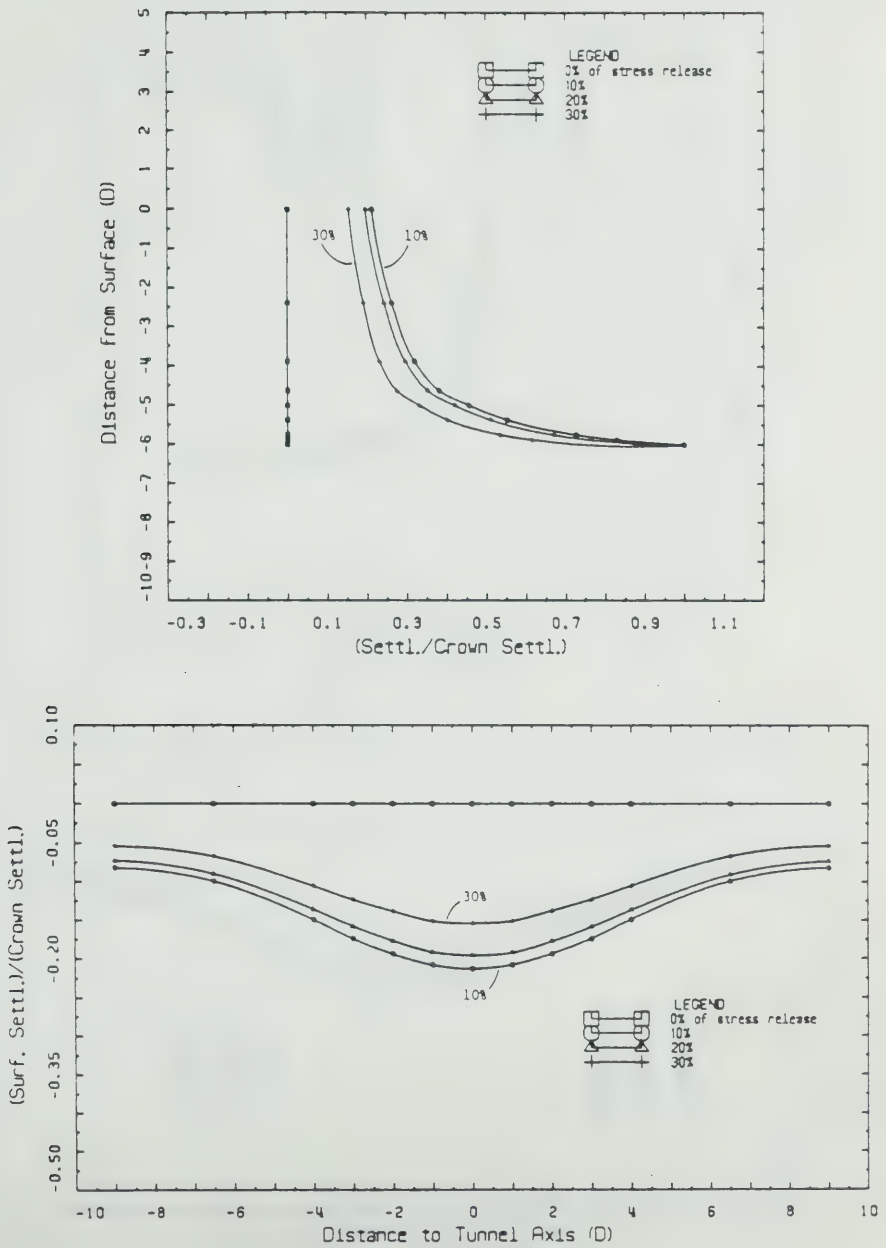

Figure C.28 Normalized Settlements: K_o=1, $c_u/\gamma D$=0.625, H/D=6

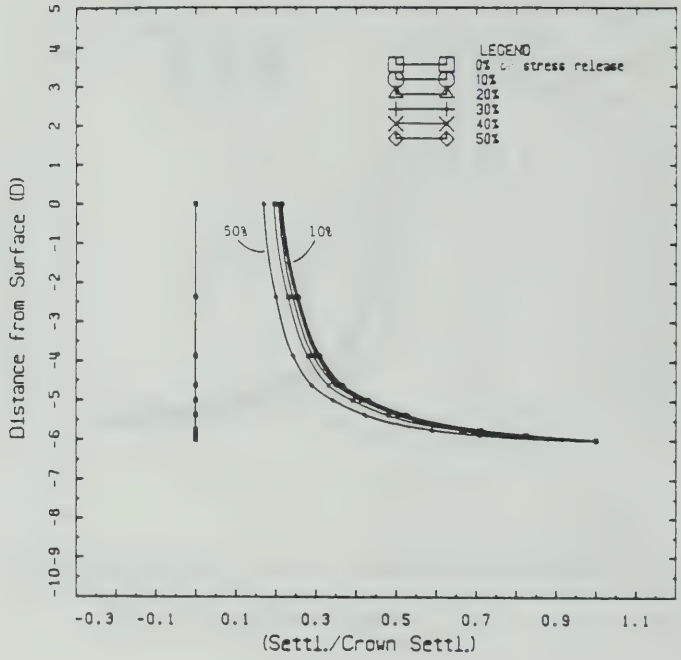

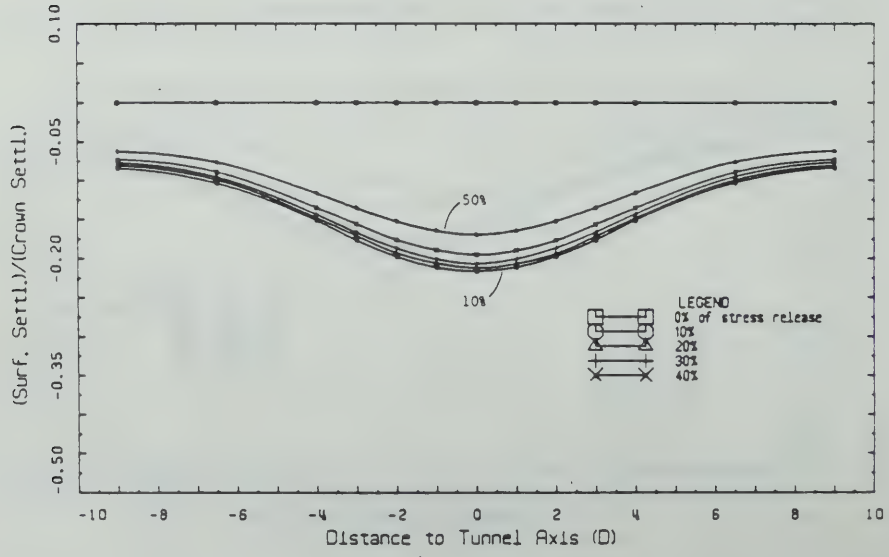

Figure C.29 Normalized Settlements: $K_o=1$, $\phi=20°$, H/D=6

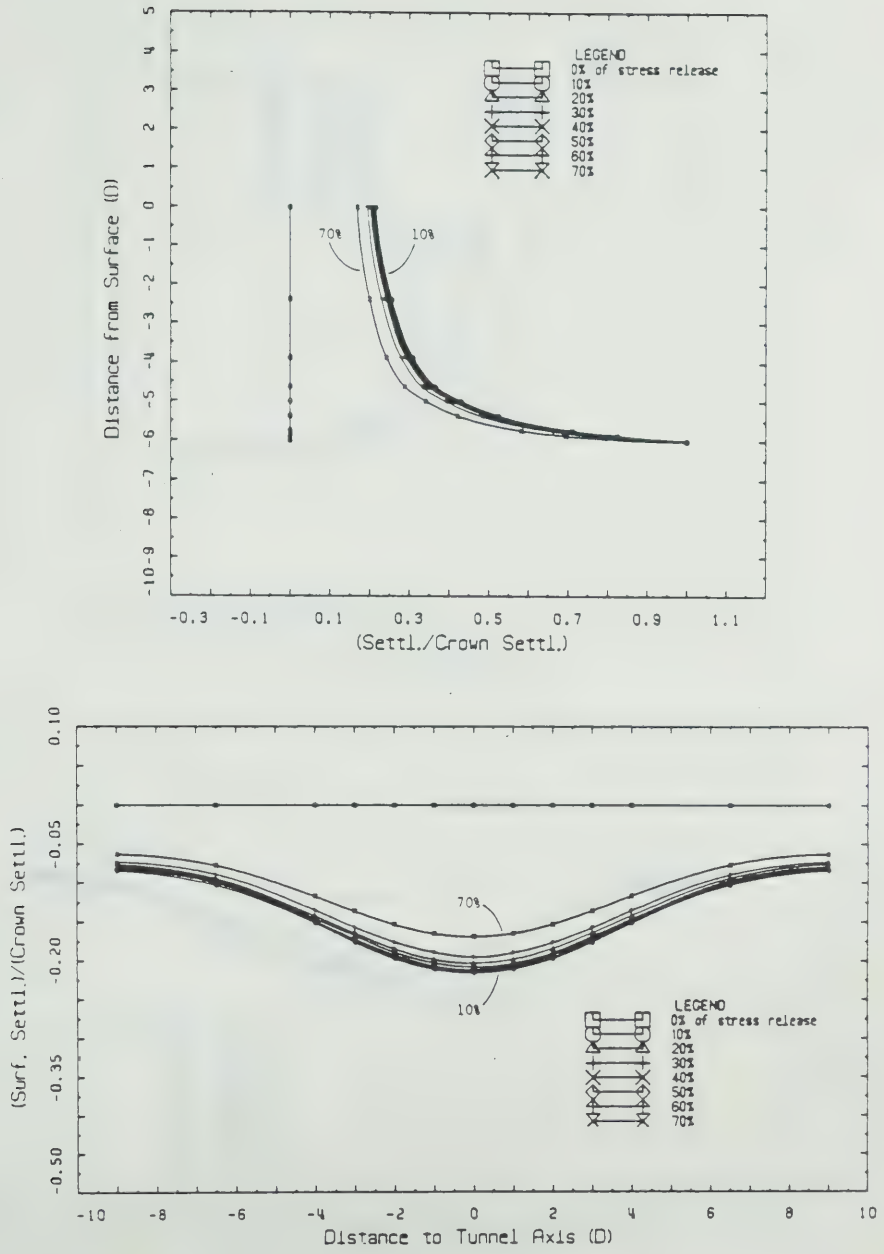

Figure C.30 Normalized Settlements: K_o=1, ϕ=30°, H/D=6

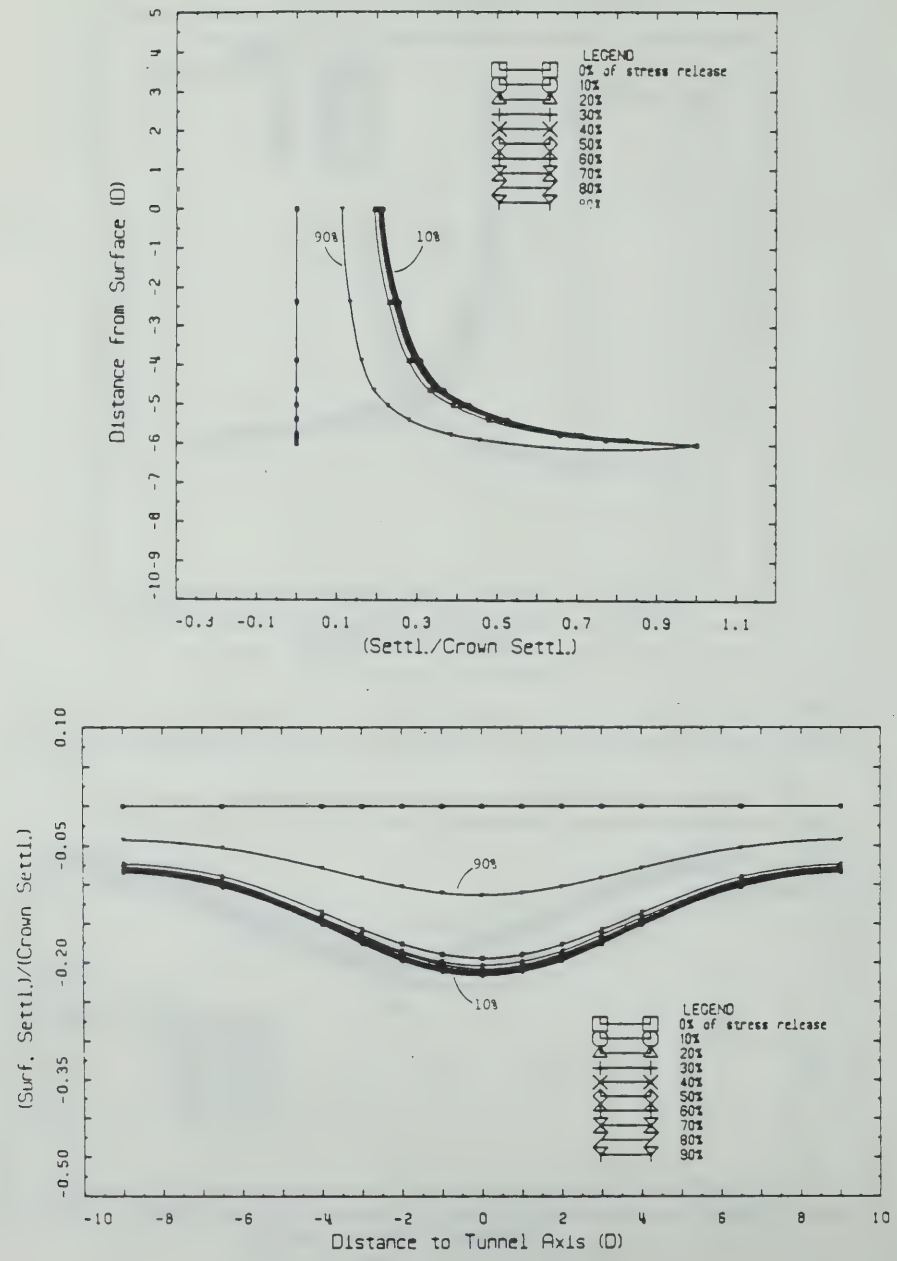

Figure C.31 Normalized Settlements: K_o=1, ϕ=40°, H/D=6

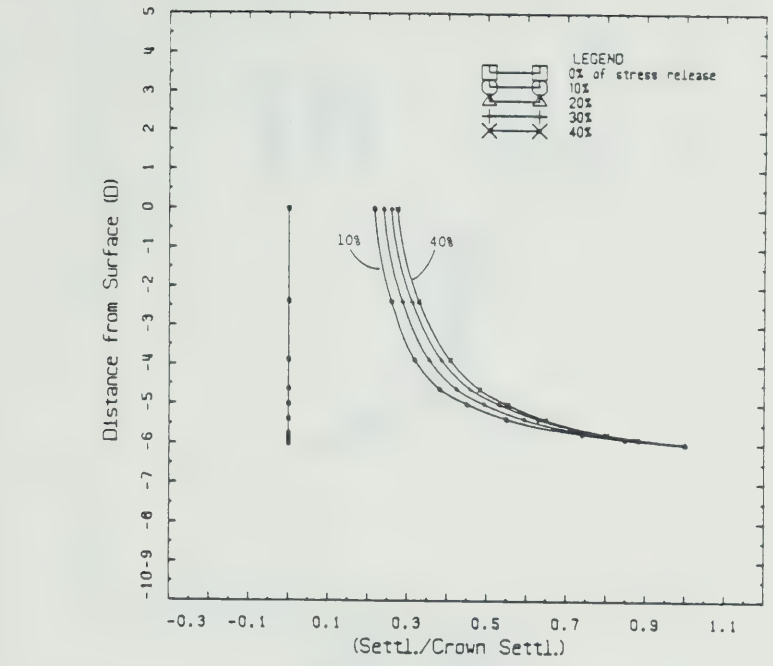

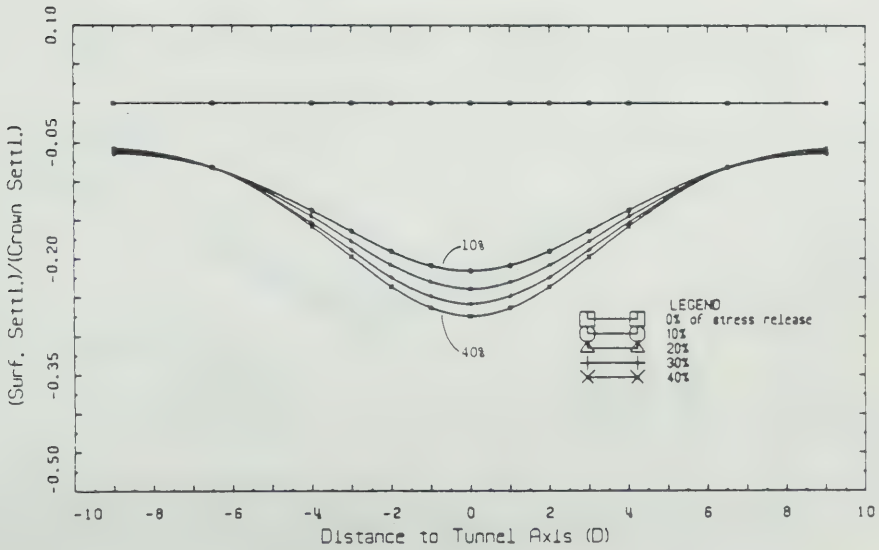

Figure C.32 Normalized Settlements: K_o=0.8, ϕ=20°, H/D=6

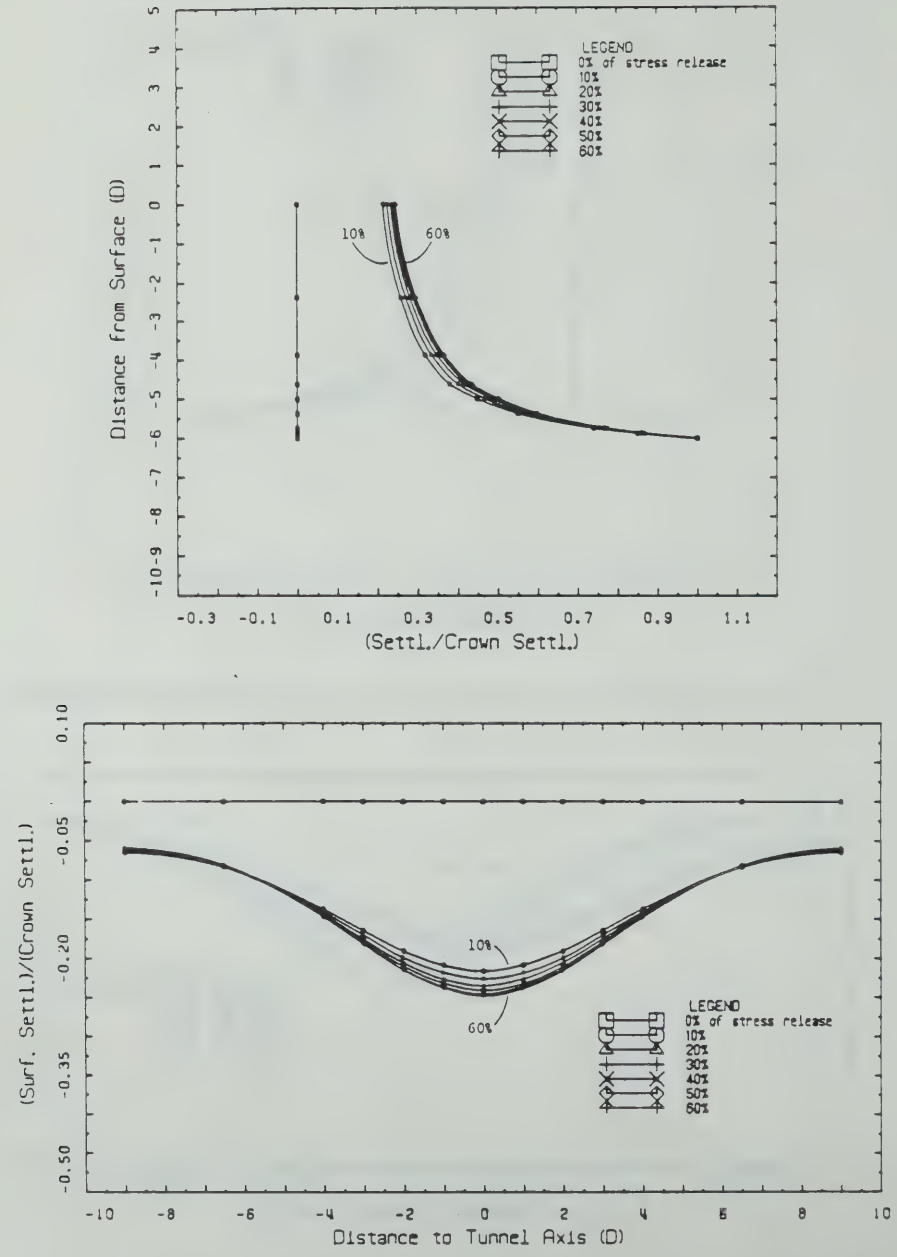

Figure C.33 Normalized Settlements: K_o=0.8, ϕ=30°, H/D=6

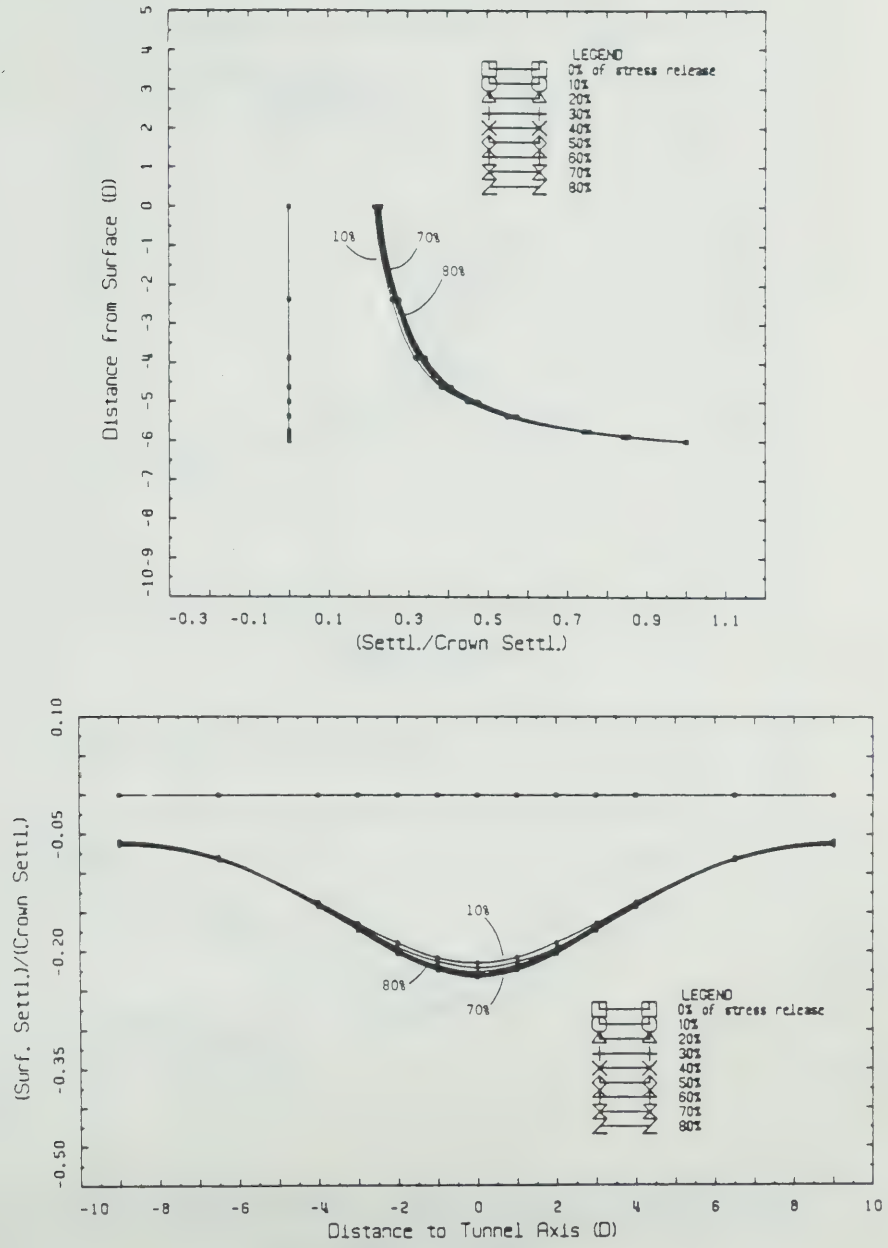

Figure C.34 Normalized Settlements: K_o=0.8, ϕ=40°, H/D=6

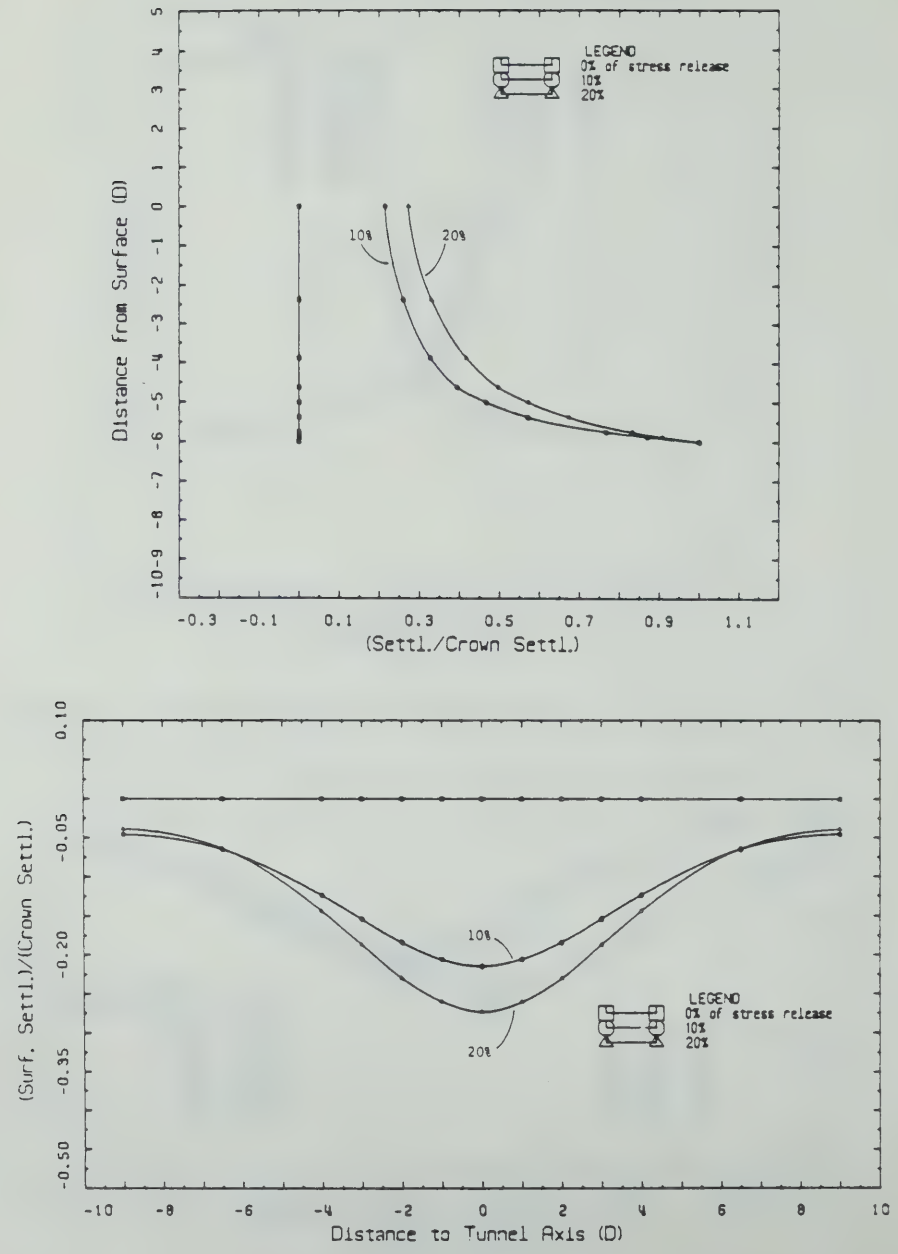

Figure C.35 Normalized Settlements: K_o=0.6, ϕ=20°, H/D=6

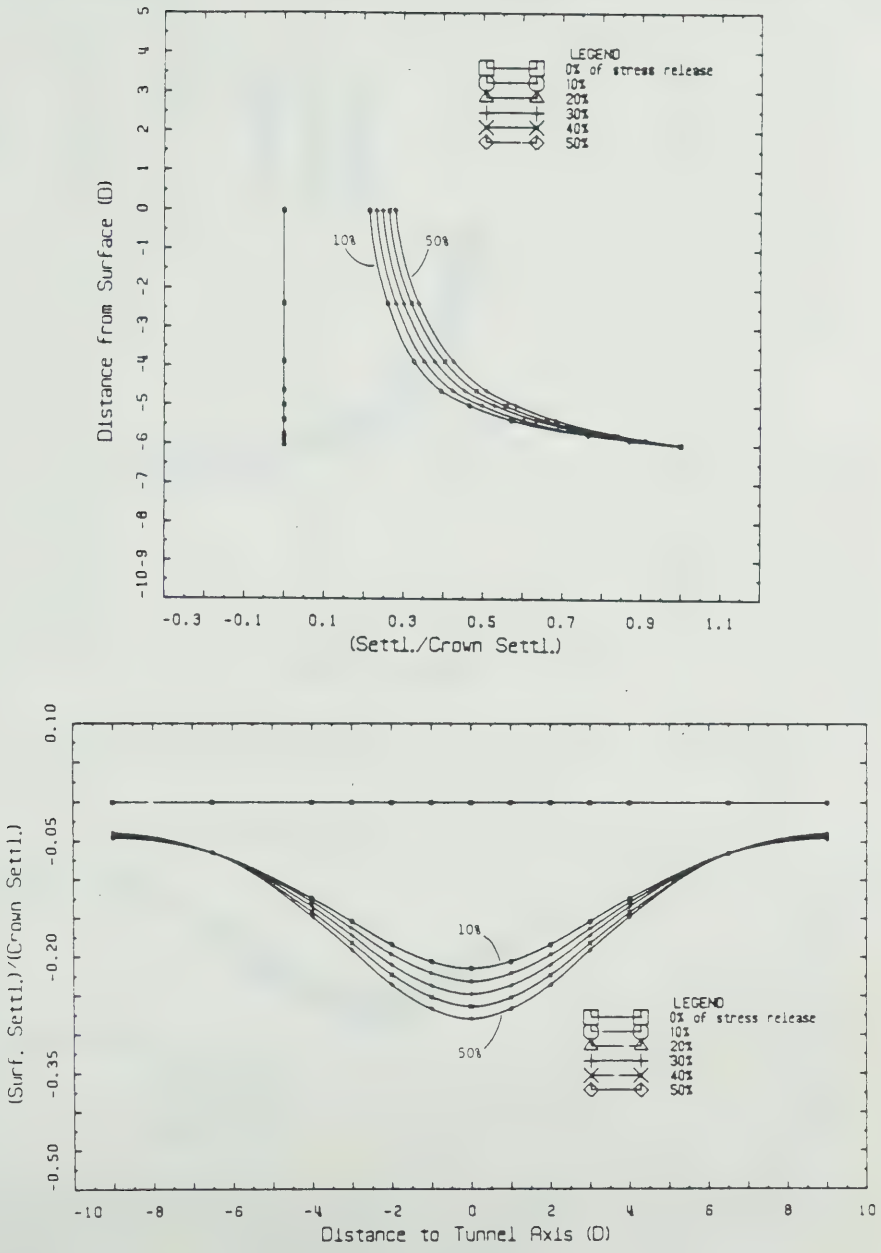

Figure C.36 Normalized Settlements: K_o=0.6, ϕ=30°, H/D=6

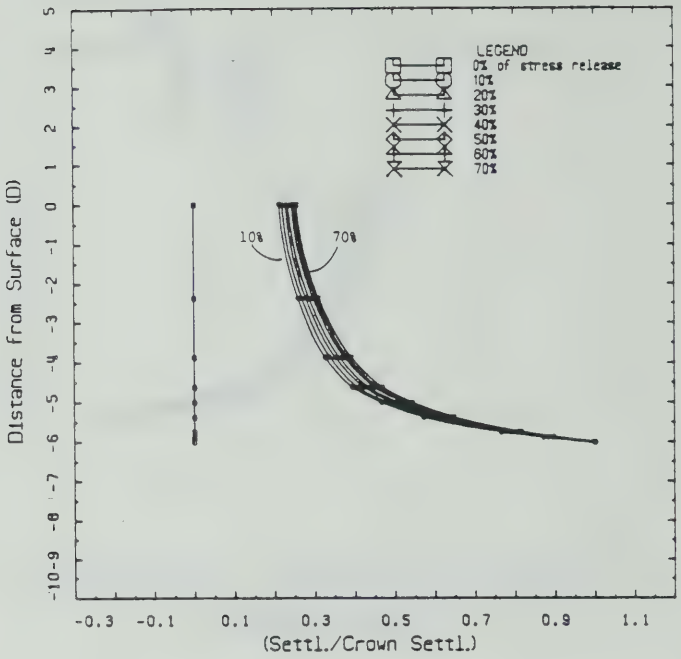

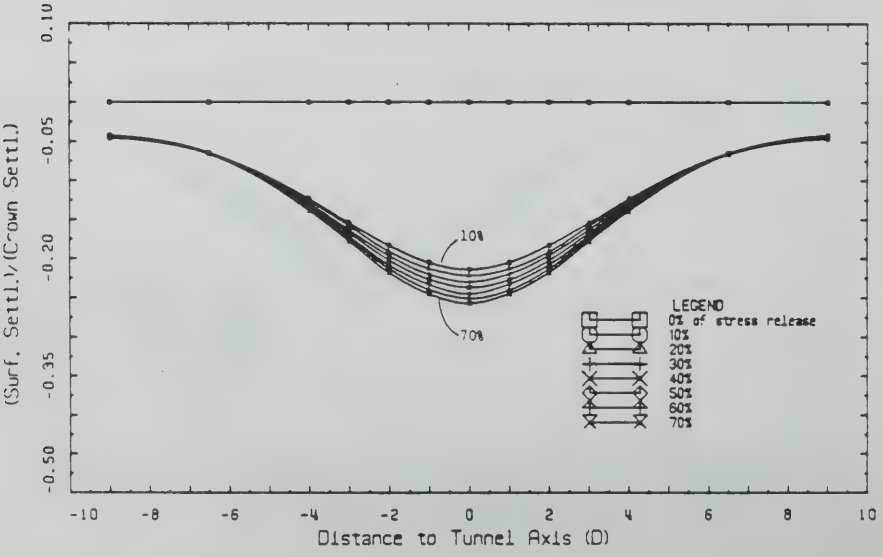

Figure C.37 Normalized Settlements: K_o=0.6, ϕ=40°, H/D=6

APPENDIX D - TWICE NORMALIZED GROUND REACTION CURVES

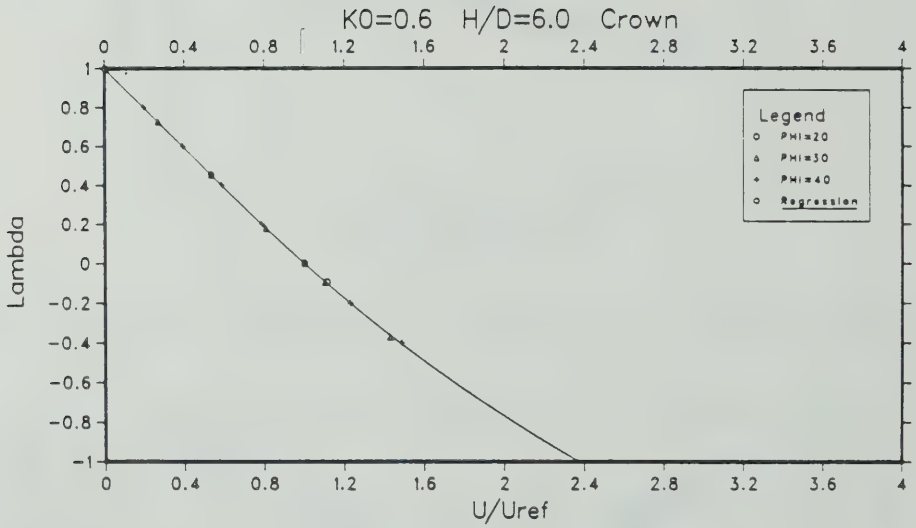

Figure D.1 NNGRC for Crown, K_o= 0.6, H/D=6

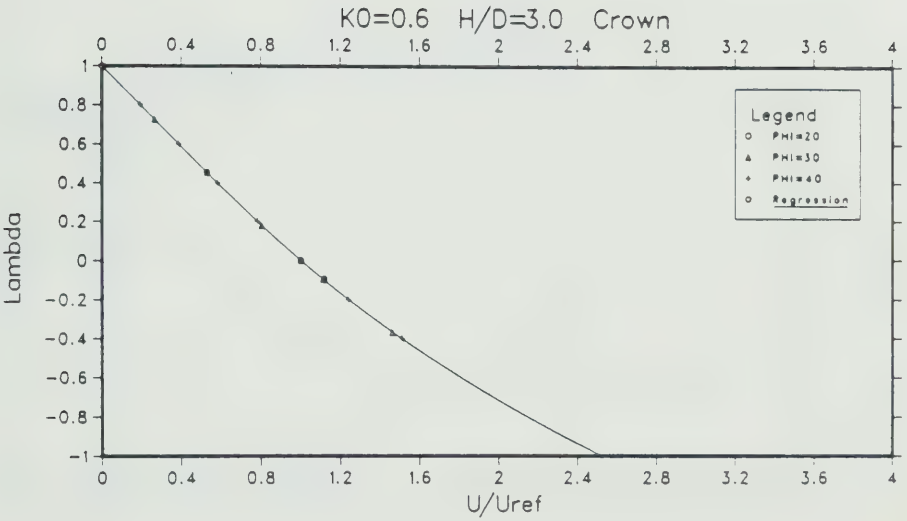

Figure D.2 NNGRC for Crown, K_o= 0.6, H/D=3

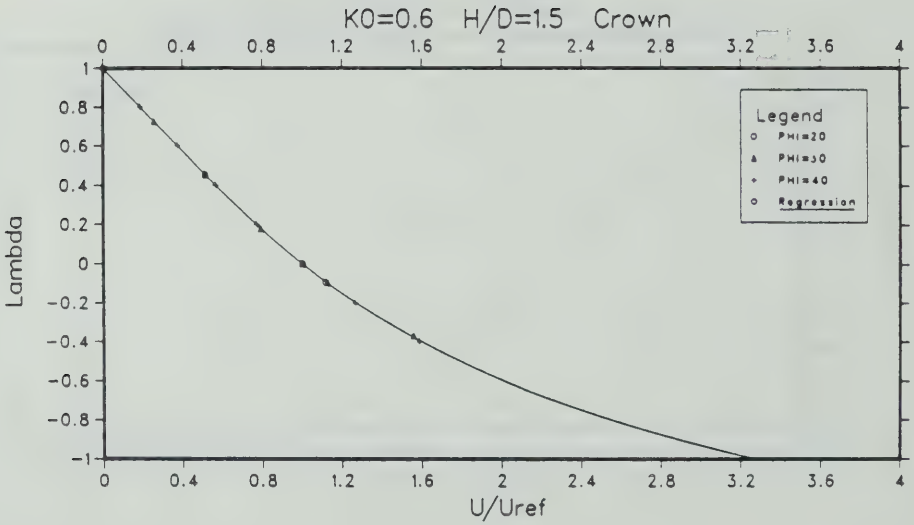

Figure D.3 NNGRC for Crown, K_o= 0.6, H/D=1.5

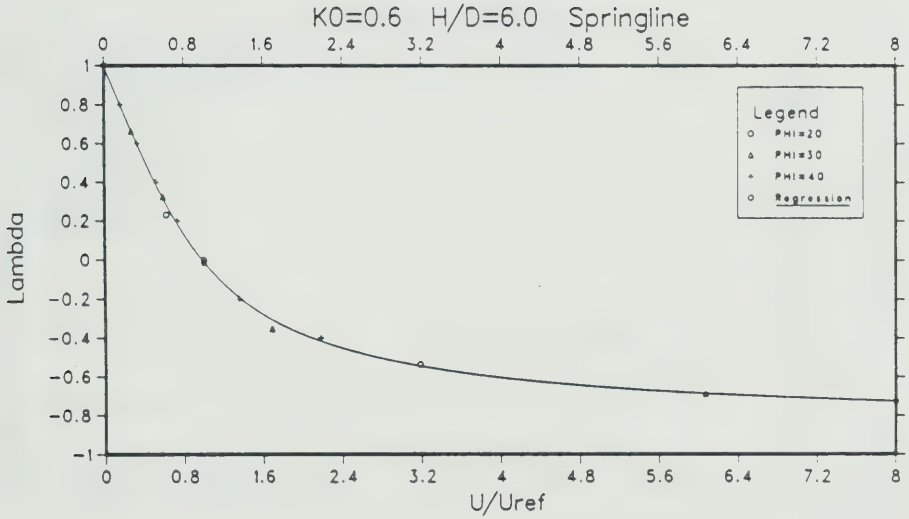

Figure D.4 NNGRC for Springline, K_o= 0.6, H/D=6

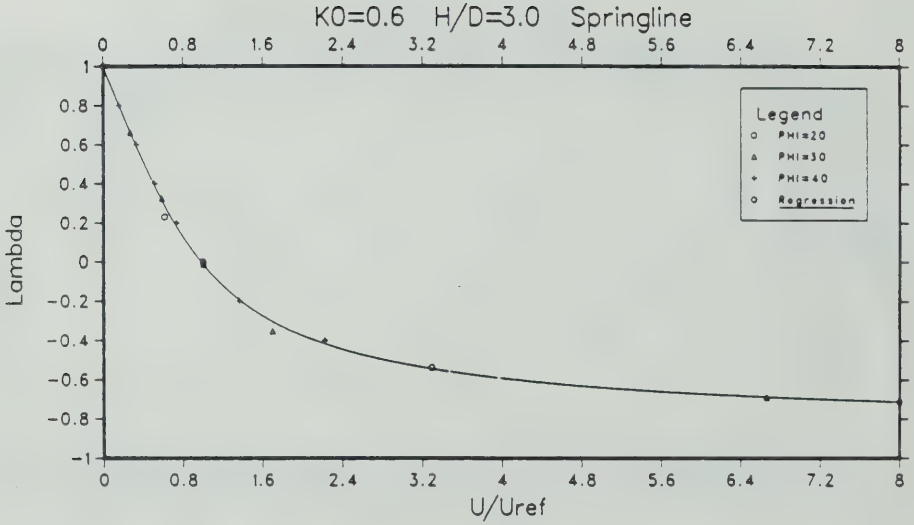

Figure D.5 NNGRC for Springline, K_o= 0.6, H/D=3

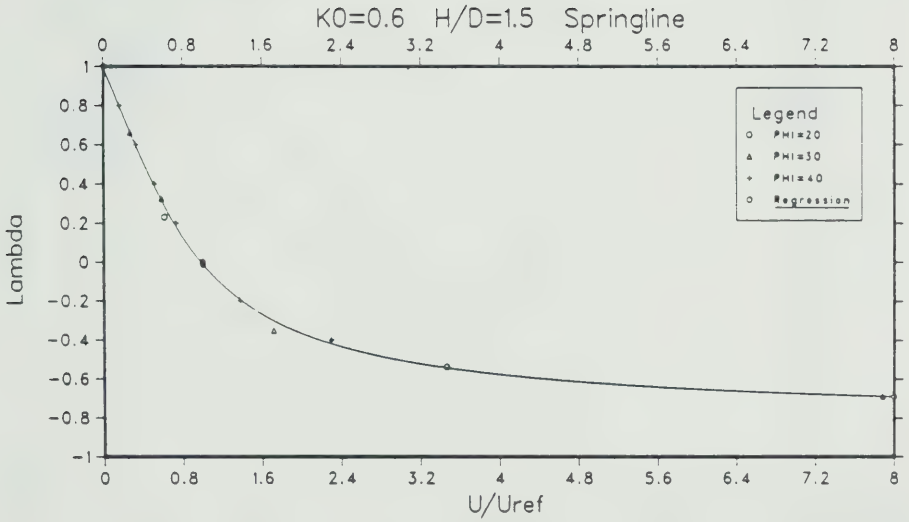

Figure D.6 NNGRC for Springline, K_o= 0.6, H/D=1.5

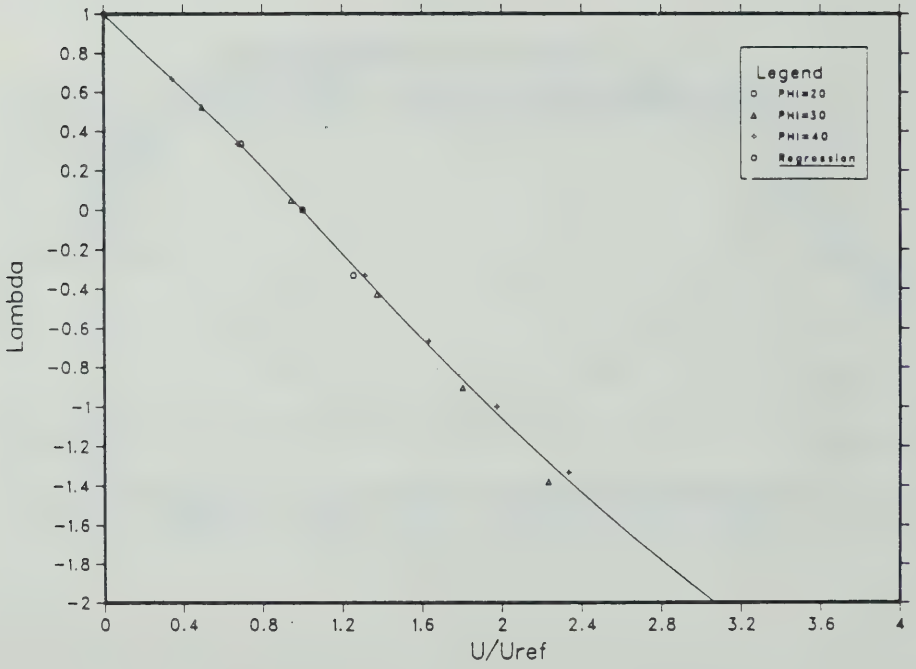

Figure D.7 NNGRC for Floor, K_o= 0.6, H/D=6

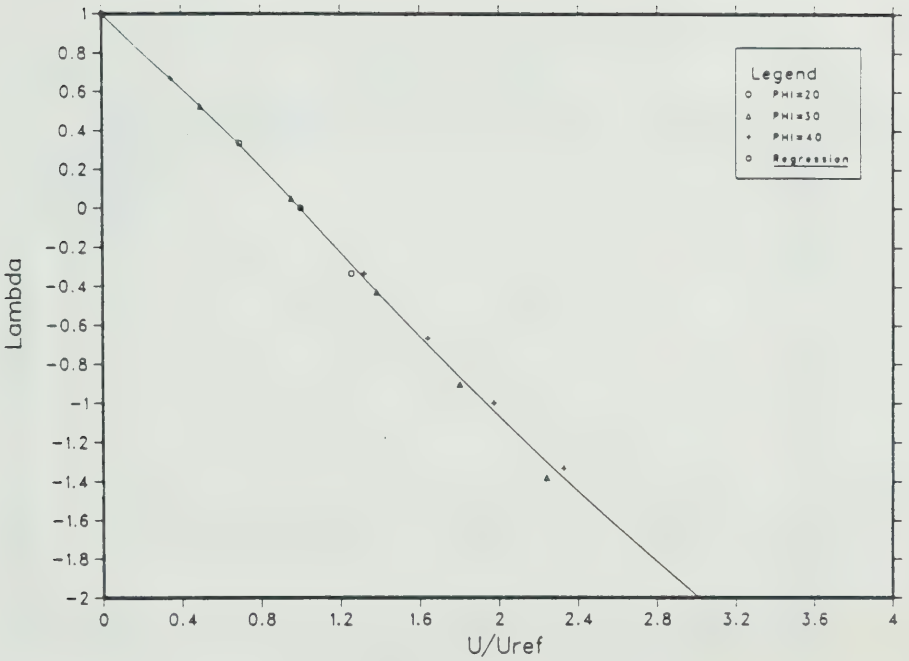

Figure D.8 NNGRC for Floor, K_o= 0.6, H/D=3

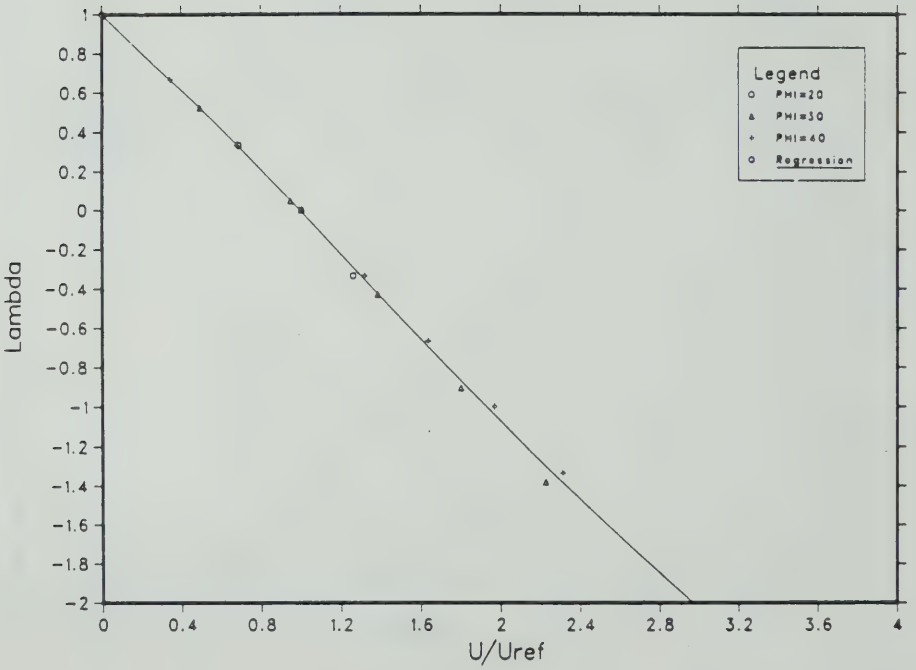

Figure D.9 NNGRC for Floor, K_o= 0.6, H/D=1.5

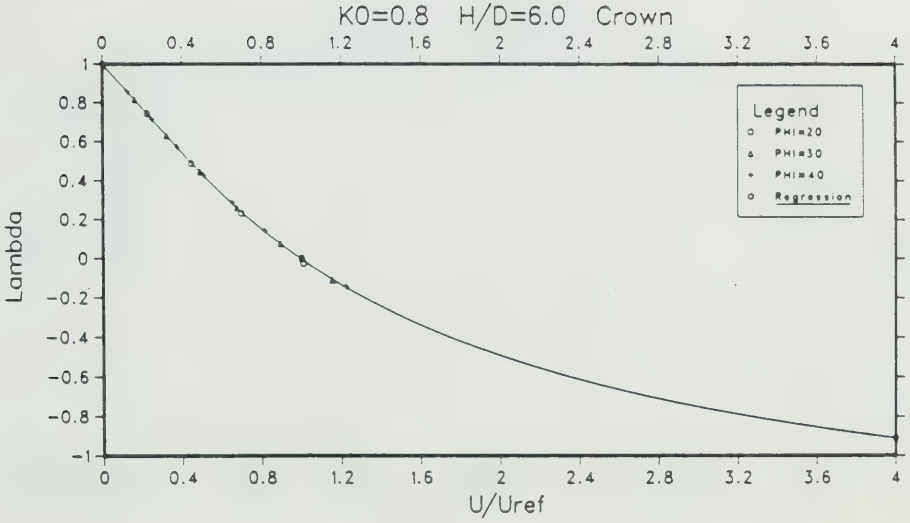

Figure D.10 NNGRC for Crown, K_o= 0.8, H/D=6

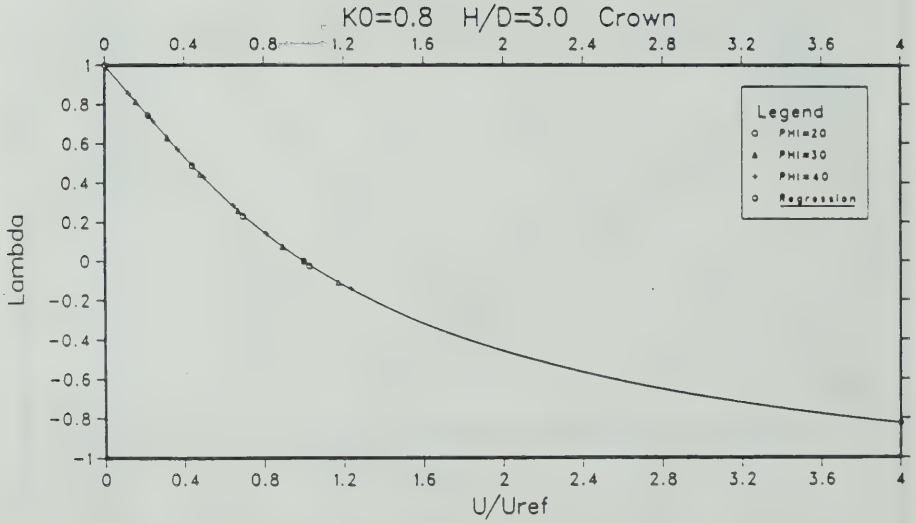

Figure D.11 NNGRC for Crown, K_o= 0.8, H/D=3

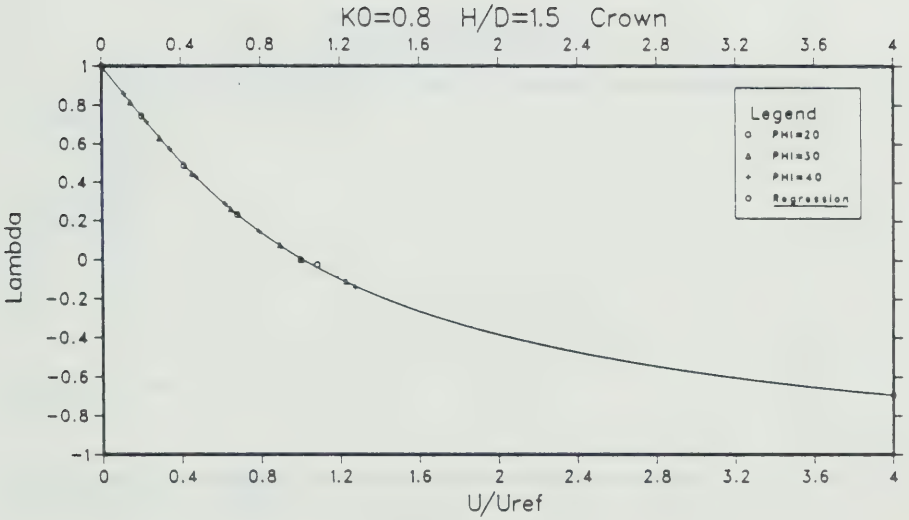

Figure D.12 NNGRC for Crown, K_o= 0.8, H/D=1.5

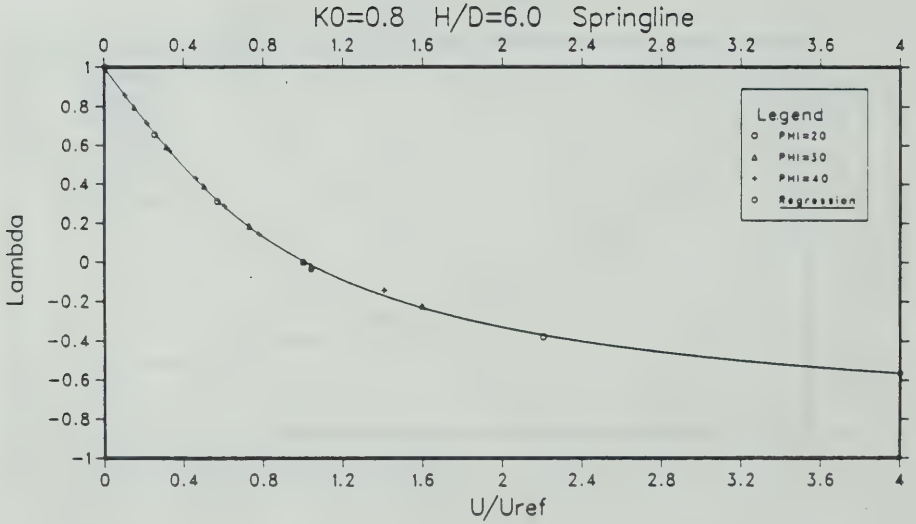

Figure D.13 NNGRC for Springline, K_o= 0.8, H/D=6

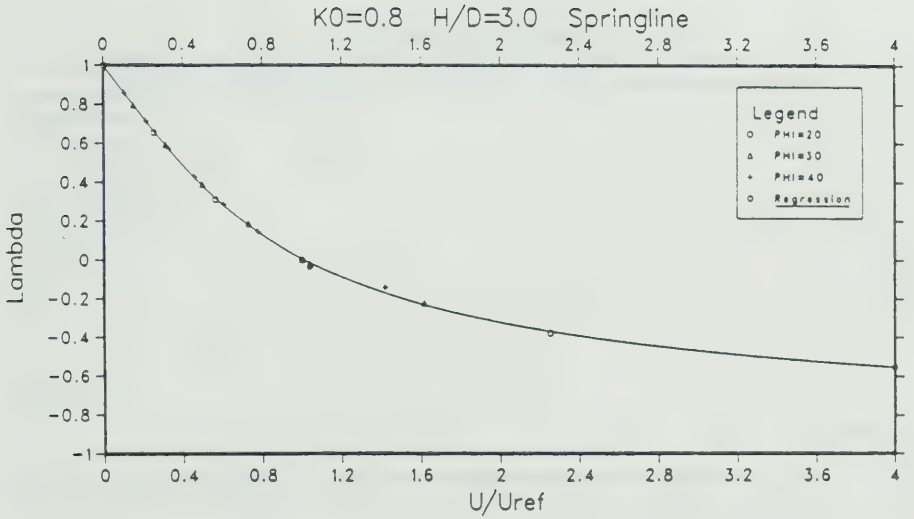

Figure D.14 NNGRC for Springline, K_o= 0.8, H/D=3

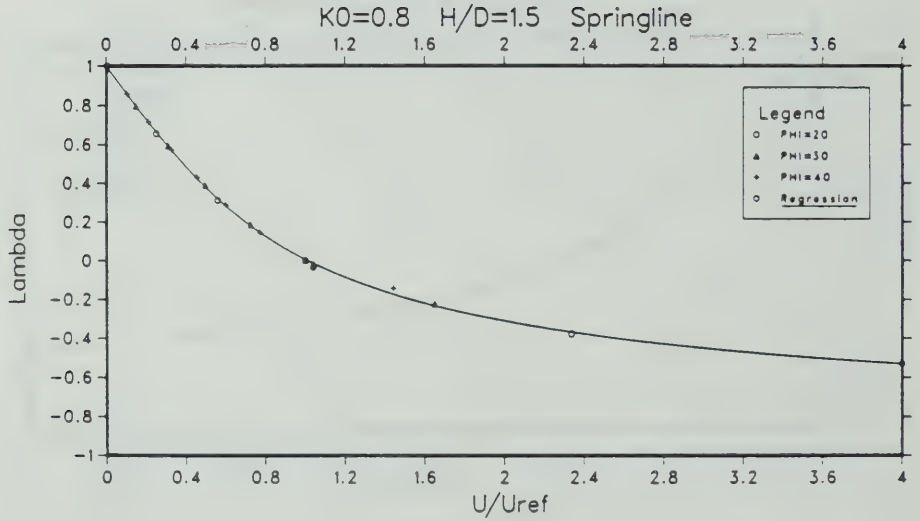

Figure D.15 NNGRC for Springline, K_o= 0.8, H/D=1.5

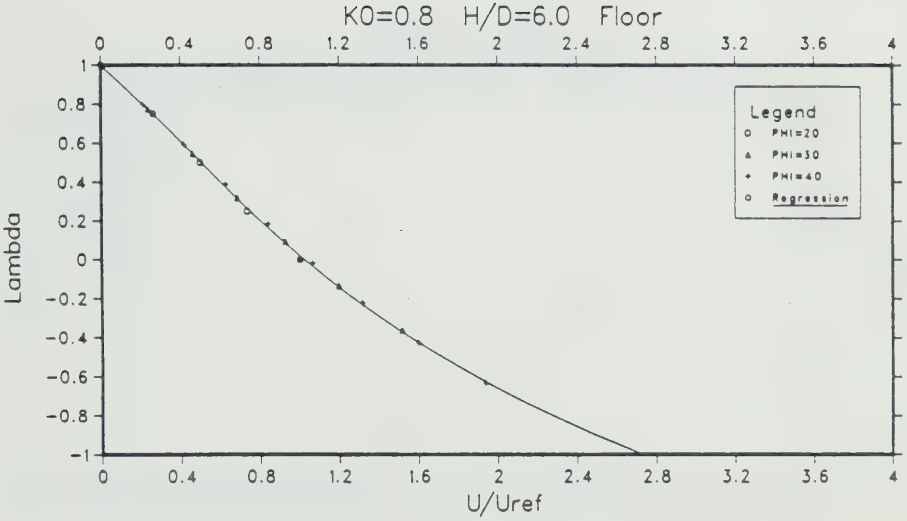

Figure D.16 NNGRC for Floor, K_o= 0.8, H/D=6

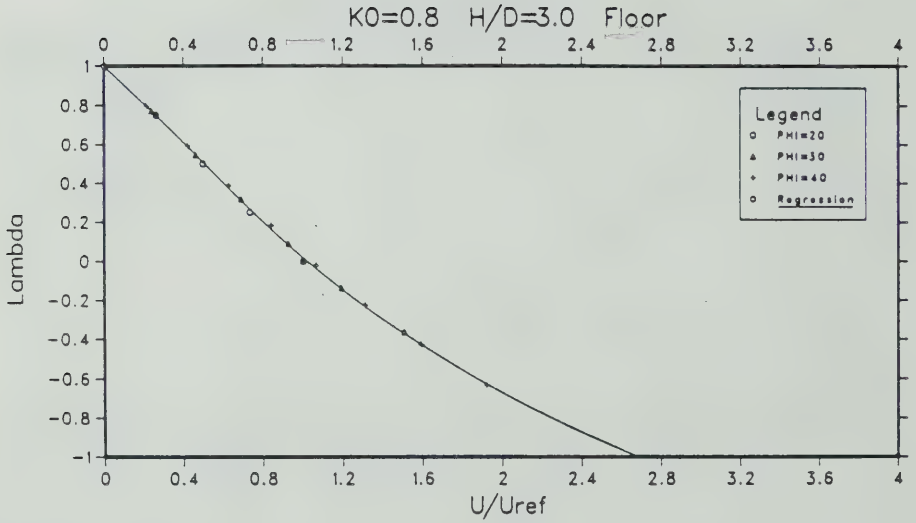

Figure D.17 NNGRC for Floor, K_o= 0.8, H/D=3

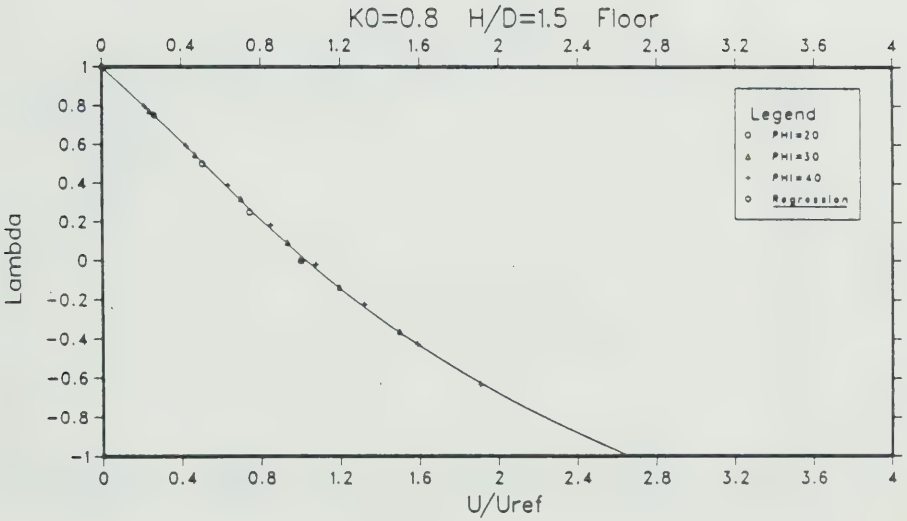

Figure D.18 NNGRC for Floor, K_o= 0.8, H/D=1.5

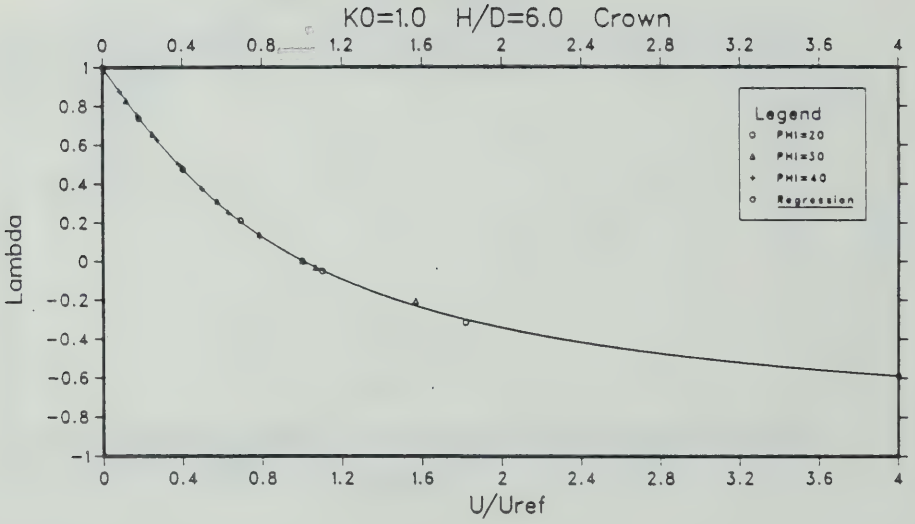

Figure D.19 NNGRC for Crown, K_o= 1.0, H/D=6

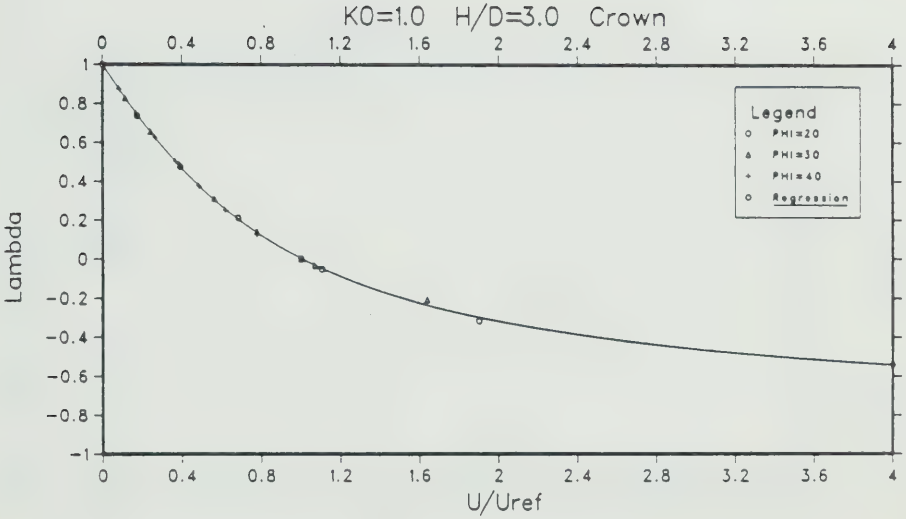

Figure D.20 NNGRC for Crown, K_o= 1.0, H/D=3

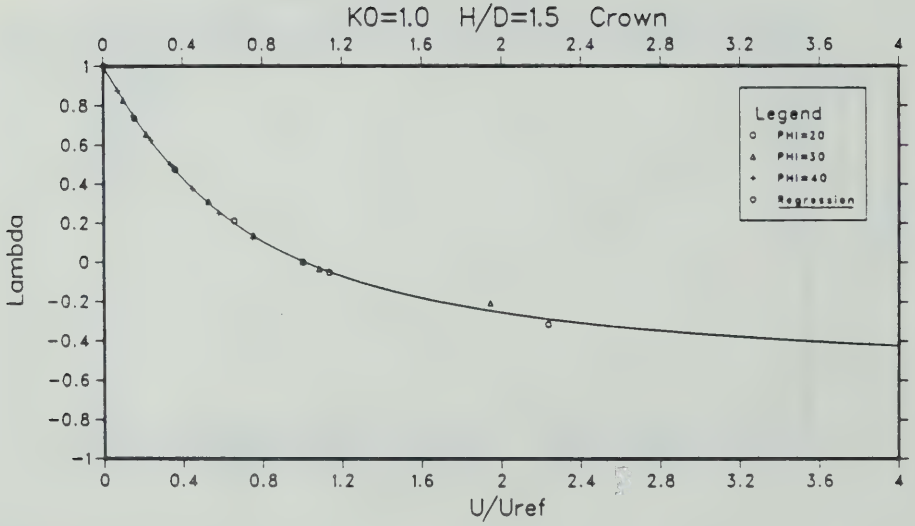

Figure D.21 NNGRC for Crown, K_o= 1.0, H/D=1.5

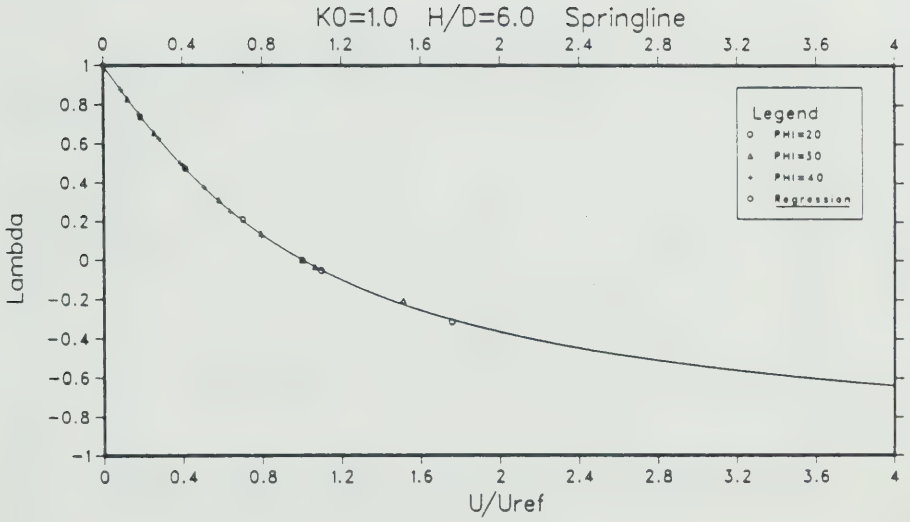

Figure D.22 NNGRC for Springline, K_o= 1.0, H/D=6

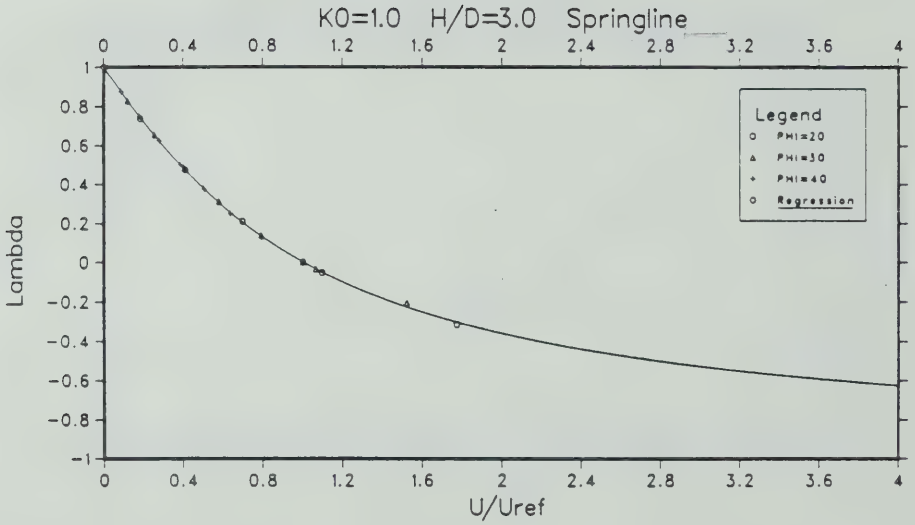

Figure D.23 NNGRC for Springline, K_o= 1.0, H/D=3

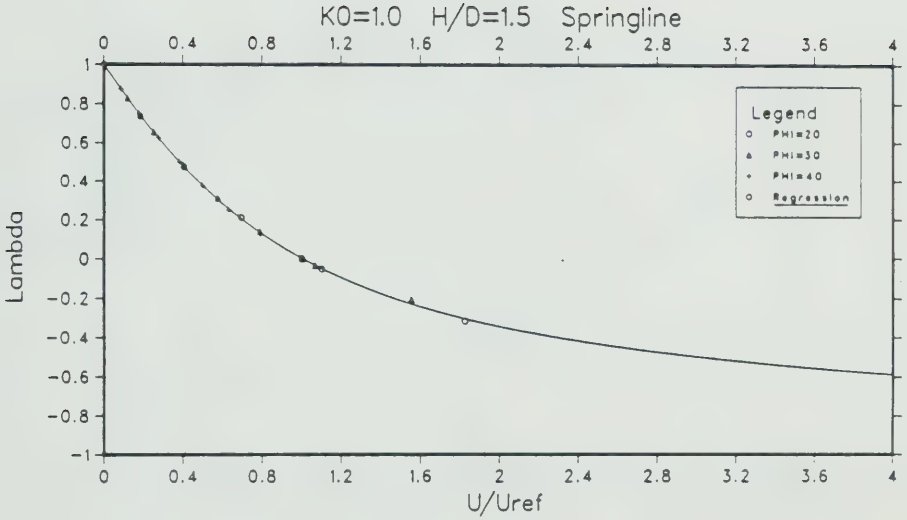

Figure D.24 NNGRC for Springline, K_o= 1.0, H/D=1.5

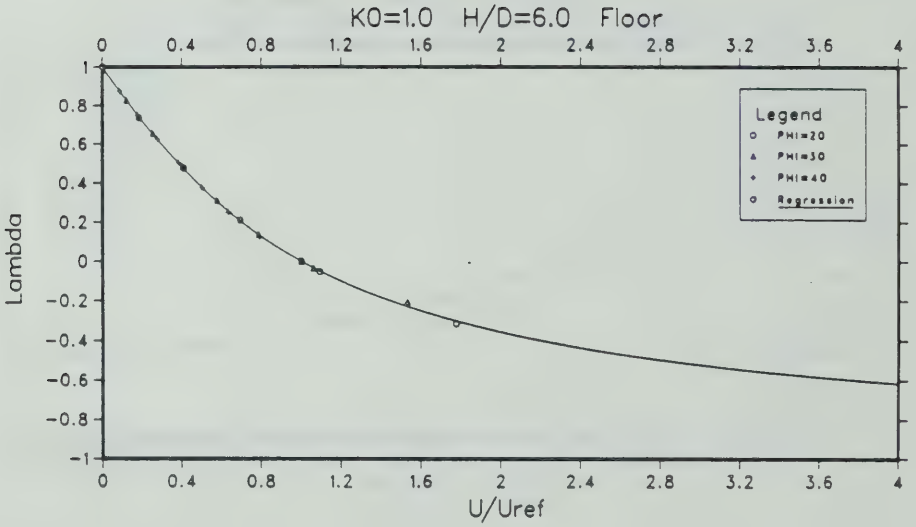

Figure D.25 NNGRC for Floor, K_o= 1.0, H/D=6

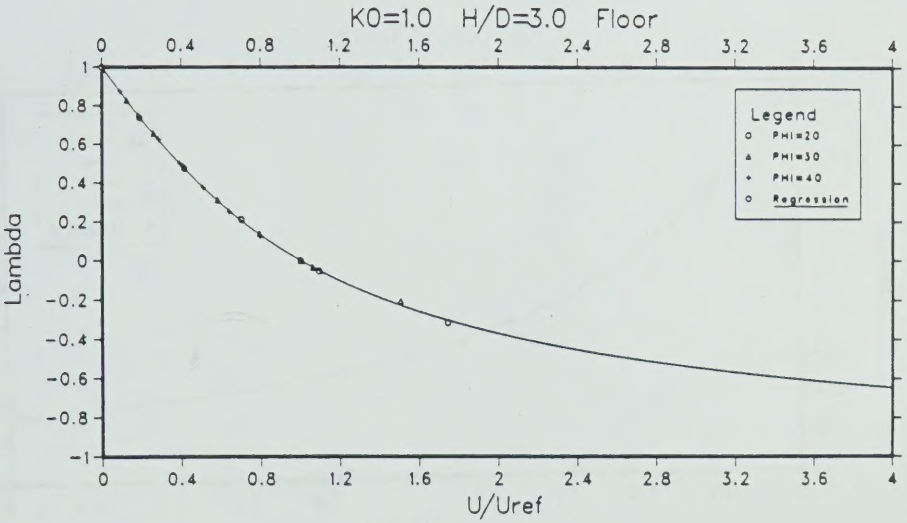

Figure D.26 NNGRC for Floor, K_o= 1.0, H/D=3

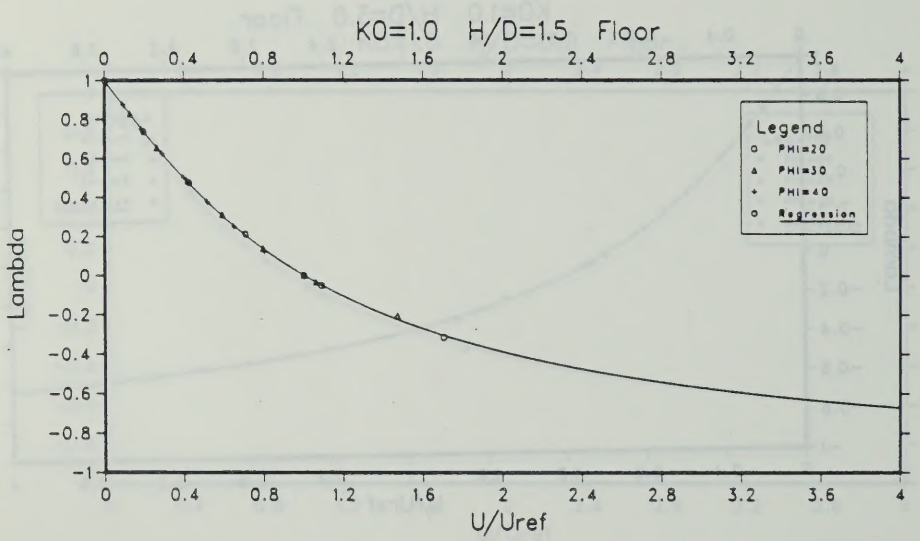

Figure D.27 NNGRC for Floor, K_o= 1.0, H/D=1.5